SYNTHETIC AND BIOLOGICAL STUDIES ON ANALOGUES OF FR901464 AND TMC-205

by

Sami Osman

B.S., Indiana University of Pennsylvania, 2005

Submitted to the Graduate Faculty of

Kenneth P. Dietrich School of Arts and Sciences in partial fulfillment

of the requirements for the degree of

Doctor of Philosophy

University of Pittsburgh

2012

UNIVERSITY OF PITTSBURGH

DIETRICH SCHOOL OF ARTS AND SCIENCES

This dissertation was presented

by

Sami Osman

It was defended on

August 16th, 2012

and approved by

Billy Day, Professor, Departments of Pharmaceutical Sciences and of Chemistry

Paul E. Floreancig, Professor, Department of Chemistry

Peter Wipf, University Professor, Department of Chemistry

Dissertation Advisor: Kazunori Koide, Associate Professor, Department of Chemistry

SYNTHETIC AND BIOLOGICAL STUDIES ON ANALOGUES OF FR901464 AND TMC-205

Sami Osman, PhD

University of Pittsburgh, 2012

FR901464 is a natural product that elicits anticancer activity via inhibition of pre-mRNA splicing, a novel therapeutic approach. Through structure-activity relationship (SAR) studies on FR901464, the Koide group reported a potent stable synthetic analogue of FR901464, meayamycin B (GI_{50} 4 – 211 pM).

An objective of this thesis was to probe electrophilic sites of meayamycin B through SAR anaylsis. This studies in this thesis provided insights into the effects of *cis*-C2′-C3′ enamide and epoxide moieties. A newly synthesized inhibitor, in which the epoxide was replaced with a ketone, exhibited elevated inhibition against cellular proliferation. Cell growth assays illustrated that this analogue inhibited the proliferation of cells in an irreversible manner.

Addtionally, an *in vivo* study led to the development of meayamycin C which, although less potent than meayamycin and meayamycin B, exhibited single digit nanomolar GI_{50} values and selectivity to inhibit the proliferation of certain human cancer cells.

Continuing with the design of pre-mRNA splicing inhibition tools, we also report the preparation and evaluation of two tetraethylene-linked derivatives of meayamycin. These two derivatives inhibited the proliferation of human cell lines and pre-mRNA splicing in cells. Structurally, one of the derivatives is far less complex than tetraethylene glycol-linked meayamycin, though still retained sufficient inhibitory activity towards cell proliferation and pre-

mRNA splicing. These two compounds have the potential serve as starting points for conjugatable FR901464 analogues.

Furthermore, a new synthetic route for meayamycin is described. The new route consists of 8 steps to prepare the western fragment, followed by a final cross metathesis interchange strategy between the right half and FR901464 to yield meayamycin. This is the shortest synthetic approach to prepare meayamycin.

Finally, a study was begun on TMC-205, which was discovered in 2001 in a similar manner to FR901464. The work in this dissertation reports the first synthesis of TMC-205 and developed analogues, including alcohol **3.21**, an eight-fold more potent analogue of TMC-205. Importantly, there is a range of TMC-205 and analogue **3.13** concentrations where the compounds activate an SV40-controlled gene without detectable antiproliferative activity.

TABLE OF CONTENTS

LIST OF TABLES

LIST OF FIGURES

LIST OF SCHEMES

LIST OF EQUATIONS

LIST OF ABBBREVIATIONS

Ac	acetyl
app	apparent
aq	aqueous
ATCC	American Type Culture Collection
Bn	benzyl
Boc	di-*tert*-butyl dicarbonate
Cbz	carbobenzyloxy
CDI	carbonyldiimidazole
Cp	cyclopentadienyl
CSA	camphorsulfonic acid
Cy	cyclohexyl
DBU	1,8-diazabicyclo[5.4.0]undec-7-ene
DCC	dicyclohexyl carbodiimide
DCE	dichloroethane
DHP	dihydropyran
DIBALH	diisobutylaluminum hydride
DIPT	diisopropyl tartarate
DMAP	4-dimethylaminopyridine
DMF	dimethylformamide
DMSO	diethyl sulfoxide
DNA	deoxyribonucleic acid
dr	diastereomeric ratio
EC_{50}	half maximal effective concentration
ee	enantiomeric excess
EI	electron ionization
equiv	equivalent
ESI	electrospray ionization
Et	ethyl
FBS	fetal bovine serum
Fmoc	fluorenylmethoxycarbonyl
GI_{50}	half maximal growth inhibition
h	hour(s)
HATU	*O*-(7-azabenzotriazol-1-yl)-*N*,*N*,*N*',*N*'-tetramethyluronium hexafluorophosphate
HPLC	high performance liquid chromatography
HRMS	high resolution mass spectrometry

IC_{50}	half maximal inhibitory concentration
IR	infrared
J	coupling constant (NMR)
LCMS	low resolution mass spectrometry
LDA	lithium diisopropylamide
M	molar
Me	methyl
m.p.	melting point
MS	mass spectrum
MTS	3-(4,5-dimethylthiazol-2-yl)-5-(3-carboxymethoxyphenyl)-2-(4-sulfophenyl)-2H-tetrazolium salt
^{n}Bu	*n*butyl
NMO	N-methylmorpholine
NMR	nuclear magnetic resonance
PBS	phosphate buffered saline
Ph	phenyl
PMB	para-methoxybenzyl
PMS	phenazine methosulfate
py	pyridine
quant.	quantitative
r.t.	room temperature
R_f	retention factor
RNA	ribonucleic acid
S.D.	standard deviation
SAP	spliceosomal associated protein
SAR	structure-activity relationship
SF3b	splicing factor 3b
snRNP	small nuclear ribonucleoprotein
T	temperature
TBAF	*tetra-n*butylammonium fluoride
TBHP	*t*butylhydroperoxide
^{t}Bu	*t*butyl
TES	triethylsilyl
TFA	trifluoroacetic acid
THF	tetrahydrofuran
THP	tetrahydropyran
TLC	thin-layer chromatography
TPAP	*tetra-n*propylammonium perruthenate
Trt	triphenylmethyl
Ts	*para*-toluenesulfonyl
VEGF	vascular endothelial growth factor

PREFACE

I want to extend my sincerest thanks and appreciation to Professor Kazunori Koide for giving me the opportunity to study in his laboratories and giving me the guidance and rigorous training. I truly appreciate all the time he invested in me during the last six years to develop to the scientist I am today. I would like to thank the members of my dissertation committee, Professor Billy Day, Professor Paul Floreancig and Professor Peter Wipf, and my proposal mentor Professor Michael Trakselis. Their involvement in my training was instrumental toward the development of me as a scientist.

I would like to thank all our collaborators in the University of Pittsburgh and outside the university for being a part of most of the projects I have been involved in. I learned a lot. I would like to thank Apeiron Catalysts and Boehringer-Ingelheim Pharmaceuticals for the gift of Nitro-Grela catalyst, and Matthey Company for the palladium acetate.

I would like to thank all the Koide Group members for all their help and encouragment these past years, and for providing a great atmosphere for learning, inside and outside the lab.

I would like to thank all the friends I have made during my time in Pittsburgh. My exerience in graduate school would not have been the same without all the friends I made in Pittsburgh. Finally, I would like to thank my family for their unwavering love and support. This is for you.

1.0 BACKGROUND

1.1 EUKARYOTIC GENE EXPRESSION

The classic central dogma of molecular biology shows the order of genetic information from DNA → RNA → protein (Figure 1-1). While DNA is being transcribed to produce messenger pre-RNA (pre-mRNA), several essential co-transcriptional processing events take place that ultimately control the localization, stability and translation of mature mRNAs. These events include capping the 5′ end of mRNAs, poly-adenylation of the 3′ end of mRNAs and precursor mRNA (pre-mRNA) splicing. Pre-mRNA splicing is a critical step during the expression of eukaryotic genomes in which the intervening sequences, introns, regions of pre-mRNA that are removed before the mRNA is translated into protein. Removal of intron sequences produces mRNA substrates that are exported to the cytoplasm for subsequent protein translation. Incorrect splicing can be caused by mutations in the pre-mRNA or mutations in *trans*-acting factors, proteins that bind pre-mRNA sequences to control gene expression, and are implicated in an array of human diseases.[1] Recently, it has been shown that small molecules that modulate splicing activity may be effective methods to treat a collection of diseases, such as cancer.[2-7]

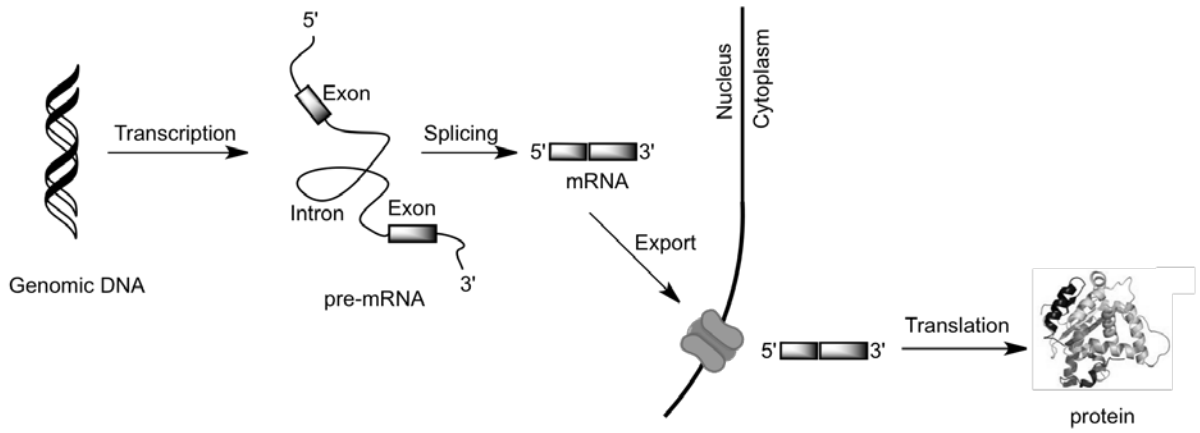

Figure 1-1 Pictorial presentation of eukaryotic gene expression.

The pre-mRNA that results from DNA transcription serves as a binding platform for a highly coordinated series of RNA-RNA and RNA-protein interactions that are critical for the accurate removal of intron sequences. Additionally, conserved *cis*-RNA sequences, DNA sequences in the vicinity of the structural portion of a gene required for gene expression, within the pre-mRNA serve as the biological catalyst of intron removal. Eukaryotic cells have developed an elaborate machinery known as the spliceosome, to facilitate the two chemical steps of the splicing reaction of each intron. Spliceosomes are assembled from key building blocks, which include five uridine-rich snRNP (small nuclear ribonucleoprotein complexes), specifically U1, U2, U4, U5 and U6.[8] Together, these compounds play critical roles in identifying conserved *cis*-RNA sequences, assembling the catalytic spliceosome, and facilitating splicing chemistry.

1.1.1 Chemistry of splicing

RNA transcripts undergo multiple changes before they can be used as templates in protein production. One of the initial steps is the transcription of DNA into pre-mRNA. Pre-

mRNA is composed of introns and exons and approximately 40% of the human genome consists of introns.[9] The removal of introns and the ligation of exons occur through a process of two trans-esterification reactions (Figure 1-2). In the first reaction, the 2'-OH of an adenosine in the intron, termed the branchpoint A, attacks the phosphate bond at the 5' splice site (5' SS). This results in a free 5' exon and the 5' SS is ligated to the branchpoint A, forming a lariat structure. During the second trans-esterification reaction, the 3'-OH of the 5' exon attacks the 3' splice site (3'SS). This nucleophilic attack causes the 5' exon to become ligated with the 3' exon and releases the intervening intron.[8]

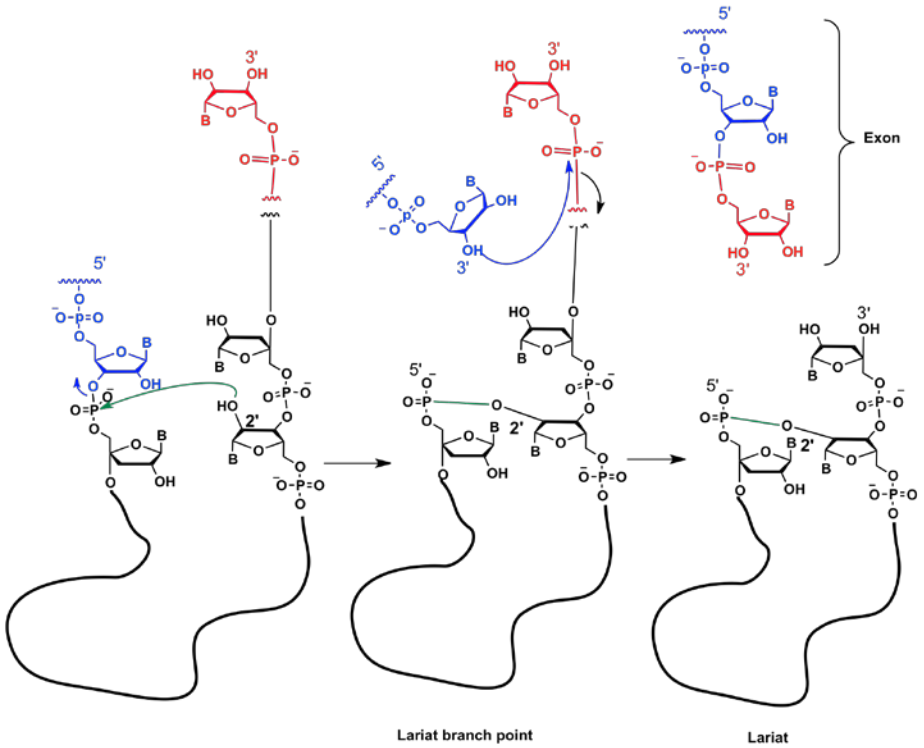

Figure 1-2 Chemical mechanism of the pre-mRNA splicing reaction. Red and blue structures represent exons and black structures represent intron.

1.1.2 Spliceosome components and stepwise recognition of intron

The accurate and efficient catalysis of the two chemical steps in splicing is essential for proper cellular activity. The correct recognition and catalysis of splicing is carried out by the spliceosome, a large protein-RNA complex.[8] The spliceosome is comprised of five snRNPs and each snRNP consists of one snRNA (small nuclear RNAs).

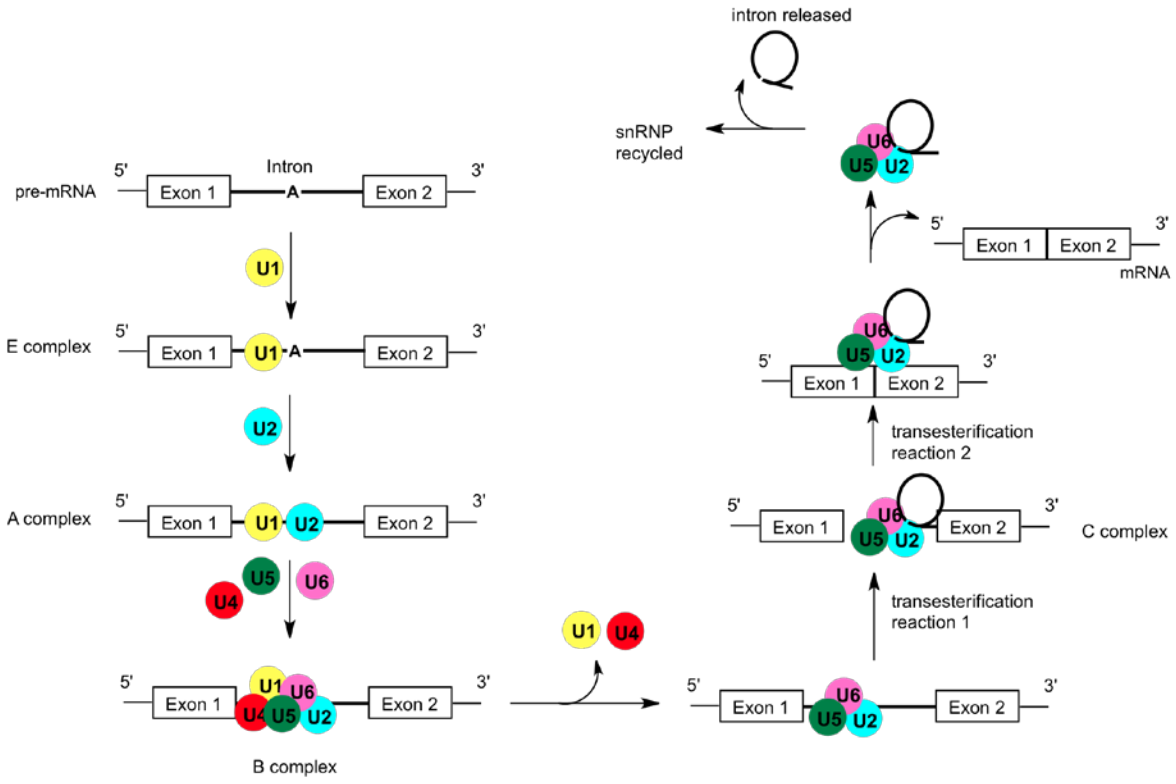

Figure 1-3 Model of human spliceosome assembly.

The snRNAs of the snRNPs play roles in intron recognition and splice site definition and intimately involved in spliceosomal catalysis. The pre-mRNA splicing involves the step-wise assembly of the spliceosome onto the pre-mRNA.[8] There are four main complexes that are

formed, denoted spliceosomal complexes E, A, B, and C, respectively (Figure 1-3).[8] Their involvement is as follows:[8] Complex E, the commitment complex, is created when U1 joins with pre-mRNA, attaching at the 5' intron/exon boundary. Complex A is created when U2 binds to the complex at the branch point adenosine. Complex B is created when the triple complex U5, U4 and U6 assembles onto the pre-mRNA. Complex C, the active spliceosome, is created when U4 dissociates, allowing U6 to base pair with snRNA in U2. Pre-mRNA splicing occurs, resulting in the separation of the 5' exon/intron boundary and formation of the lariat. The joined exons dissociate from the spliceosome/intron complex, leaving the lariat structure behind and the spliceosome dissociates followed by the recycling of snRNPs (Figure 1-3).[8]

1.1.3 Alternative splicing

With the sequencing of a variety of genomes has come the realization that the number of genes does not seem to correlate with the complexity of the organism. One explanation for how these organisms increase in complexity despite a limited genomic set is through the use and regulation of alternative splicing.

Alternative splicing occurs when one pre-mRNA is spliced into multiple mRNAs and, hence, encodes multiple proteins accordingly. There are four patterns of alternative splicing: (1) exon skipping, (2) intron retention, (3) alternate 5'SS, and (4) alternate 3'SS (Figure 1-4). The most common form of alternative splicing in humans is exon skipping.[10] The regulation of alternative splicing occurs through the activity of alternative splicing factors. The presence or absence of these proteins affects the recognition of a particular splice site. If the protein is acting as an enhancer, it will recruit members of the spliceosome to the adjacent splice site. However, if the factor is a splicing silencer, it will inhibit members of the spliceosome from recognizing a

splice site.[10] Alternative splicing of pre-mRNA is a flexible point of gene control in humans. It provides cells with the opportunity to create isoforms of differing, even opposing, functions from a single gene.[10]

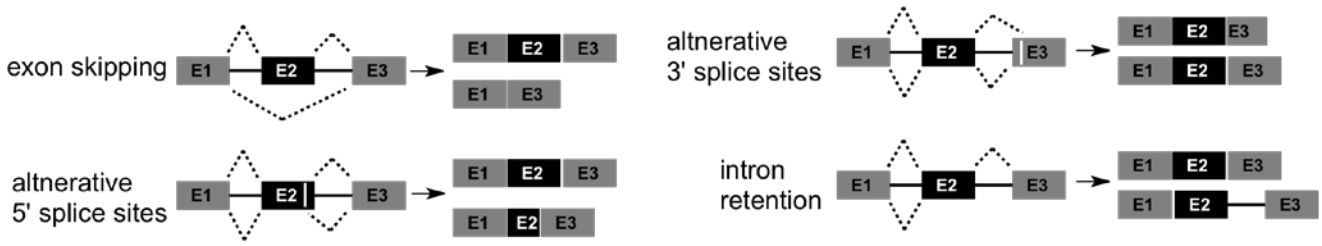

Figure 1-4 Alternative splicing variations.

1.1.4 Splicing and disease

Approximately 15% of single base pair mutations that cause human genetic diseases are linked to pre-mRNA splicing defects. Many of these genetic mutations cause inappropriate exon skipping, which ultimately causes defects in protein expression.[11] Other mutations also lead to alternative splice site selection, thus resulting in inclusion or exclusion of more RNA and longer or shorter exons. This in turn leads to the addition of one or more amino acids, or more commonly reading frame shift.[11] Given that the majority of human genes contain introns, and that most pre-mRNAs undergo alternative splicing, it is not surprising that disruption of normal splicing patterns can cause human diseases such as cancer.[12]

Cancer cells exploit alternative splicing to produce proteins that promote growth and survival.[11,13] Three different approaches could be used to target the pre-mRNA splicing process in cancer. [13]

a. Precisely control alternative pre-mRNA splicing by identifying specific splice sites and block their use.

b. Characterize splice-variant proteins that may be responsible for the malignant phenotype, and identify differences from their normal protein counterpart.

c. Since cancer cells in general have higher metabolic rates than normal cells, and hence increased splicing rates, they are more responsive to pre-mRNA splicing inhibitors.

An example of the second approach was demonstrated by Peter Laverman and coworkers in a strategy to eradicate colon and pancreatic cancer;[14] gastrin, a 33-amino acid peptide hormone, binds to cholecystokinin, a receptor, and participates in gastric motility. Recently, a splice variant of cholecystokinin has been discovered in human colorectal and pancreatic cancer but not in normal tissue. This splice-variant receptor was involved in the development of colorectal and gastric cancer, which makes this receptor a potential therapeutic target. The same group developed a peptide radiolabelled with ^{111}In to target the splice variant of cholecystokinin, although the radiolabelled peptide has some affinity for the normal receptor.

Despite the numerous advances in oncology over the past fifty years, cancer is still the second leading cause of death in the United States.[15] American men and women have a 38 – 44% chance respectively, of developing cancers during their lifetime and, in 2010, more than 500,000 Americans died from cancer.[15] Currently, there is a grave need for new therapies from new sources utilizing novel modes of action to complement already established treatments for cancer. Such approach is targeting the splicing of pre-mRNAs, which is novel and just being recognized as a viable approach to targeting cancer.[13]

Worldwide efforts in the isolation of new natural products have been an important source for novel structures and successful therapeutics.[16] In the search for new small molecules to treat cancer, researchers have begun to investigate new compounds from natural sources with new modes of action. The result of such an investigation is FR901464, an anticancer compound and pre-mRNA splicing inhibitor, and is the motivation for the development of a first in-class of FR901464-like compounds with novel chemotherapeutic effects.

1.2 FR901464

1.2.1 Discovery of FR901464

In the pursuit for natural anticancer therapeutics with new modes of action, researchers at Fujisawa Pharmaceutical Company discovered and isolated FR901463 (512 mg), FR901464 (819 mg), and FR901465 (70 mg) (Figure 1-5) from the fermentation broth of *Pseudonomas sp.* No. 2663 as novel SV40 promoter-dependant transcriptional activators that cause cell cycle arrest at G1 and G2/M phases.[5] All three compounds isolated exhibited potent antitumor activity against a number of human cancer cell lines with IC_{50} (concentration required to inhibit 50% of cell growth) values ranging from 0.2 – 1.7 ng/mL (Table 1-1), in which mouse bone marrow cells, BM, were the least responsive to all three compounds.

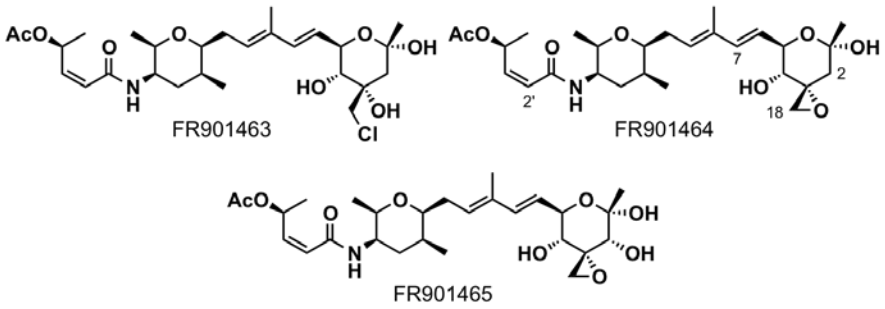

Figure 1-5 Chemical structures of FR901463, FR901464 and FR901465.

Table 1-1 Antiproliferative activity of FR901463, FR901464 and FR901465 in various human cancer cell lines.

	IC_{50} (ng/mL)		
	FR901463	FR901464	FR901465
MCF-7	0.46	0.91	0.59
A549	0.35	0.66	0.44
HCT116	0.22	0.31	0.34
SW480	0.40	0.51	0.53
P388	0.82	1.69	0.48
BM	2.03	5.01	1.91

MCF-7 = human breast adenocarcinoma cells. A549 = human lung adenocarcinoma cells. HCT116 = human colon carcinoma cells. SW480 = human colon adenocarcinoma cells. P388 = lymphocytic leukemia cells. BM = mouse bone marrow cells.

The antitumor activities of the three compounds were then evaluated in mice bearing P388 tumors. The compounds were administered intraperitoneal (ip) once a day for 4 days. Antitumor activity was measured as percentage (%) of median survival time of treated group (T) versus control (C), shown in equation 1.1 (the length of the study was not reported).

Equation 1.1

$$T/C\ (\%) = \frac{\text{median survival of Time (T)}}{\text{median survival of Time (C)}} \times 100\%$$

Of the three compounds, FR901465 was the least effective, T/C(%) of 127 at 0.032 mg/kg. Higher dosages were reported to be toxic. FR901463 displayed a T/C(%) of 160 at 1.0 mg/kg and FR901464 showed T/C(%) of 145 at 0.1 mg/kg. Antitumor effects of FR901463 and FR901464 were then measured in A549 xenografts. The efficacy was determined by a measure of percentage of mean tumor weight of the treated (T) group to that of control (C) group, equation 1.2.

Equation 1.2

$$\text{growth inhibition (GI)\%} = \left(1 - \frac{\text{mean tumor weight (T)}}{\text{mean tumor weight (C)}}\right) \times 100\%$$

FR901464 showed significant GI at dosages of 0.1 to 0.56 mg/kg, GI = 60 – 83%, while FR901463 displayed weaker antitumor effect, a maximum GI of 61%. FR901464 showed prominent antitumor effects against Colon38 and Meth A (3-methylcholanthrene-induced sarcoma) as well, GI = 38 to 86% at dosages between 0.1 to 1.0 mg/kg.[5] These data strongly suggest that FR901464 or its analogues have promising clinical applications. Despite its high potency in inducing SV40 promoter, this compound lowers the mRNA levels of several cancer-related genes, including *p53*, *p21*, *c-myc*, and *E2F-1* in MCF7 cells at 20 nM and induces apoptosis in MCF7 cells at LC_{50} (lethal concentration to kill 50% of the tested population) of 0.5 nM.[5,17,18] Recent work has identified the biosynthetic gene cluster of FR901464, which sets the stage for engineering the pathway for the development of novel analogues.[19] An important final note, however, is that FR901464 is not a compound designed or optimized for clinical use due to its instability (discussed below). It is instead a great lead compound that suggests superior analogues could be developed based on this lead.

Synthetically, the complexity of this compound has led to three total syntheses. The first and only member of the FR90146 family to succumb to synthesis was FR901464, which was

completed by Jacobsen and coworkers in 2001.[20] Kitahara and coworkers completed the second total synthesis of FR901464 in the same year,[21] followed by the Koide group, which completed the most concise synthesis in 2006.[22] These syntheses were each an impressive feat but their lengths make them ineffective in their present form as a source of clinical material.

1.2.2 FR901464 structure activity relationship (SAR) studies by Jacobsen, Kitahara Koide, and Takahashi

Due to FR901464's antiproliferative activity in mammalian cancer cells, medicinal chemistry efforts have been performed to explore the SAR of FR901464. During early synthetic studies undertaken by the Jacobsen group to establish the absolute stereocenters of FR901464, the epoxide moiety was found to be a crucial functional group, most likely acting as a reactive electrophile (Figure 1-6, compound **1.3**, Table 1-2).[20] The epimer of the epoxide, **1.2**, was only 2-fold less active than the natural one (GI_{50} = 400 nM in Tag Jurkat cells), confirming which epimer is the naturally occurring one.[20] Furthermore, Kitahara and coworkers reported one of their synthetic precursors, alkene **1.5**, also exhibited no activity for CMV promoter activation.[23,24] Finally, the Koide group also investigated the epoxide moiety. It was not clear whether the loss of activity of cyclopropane **1.3** and alkene **1.5** was due to loss of oxygen atom or the electrophilicity of the epoxide. To address these questions, Koide and colleagues prepared non-epoxy analogues **1.7**, **1.8** and **1.9**, where the oxygen atom at C3 is retained. All non-epoxy/non-electrophilic analogues were inactive,[23,24] which further supports that the electrophilicity is crucial for the activity of this class of compounds.

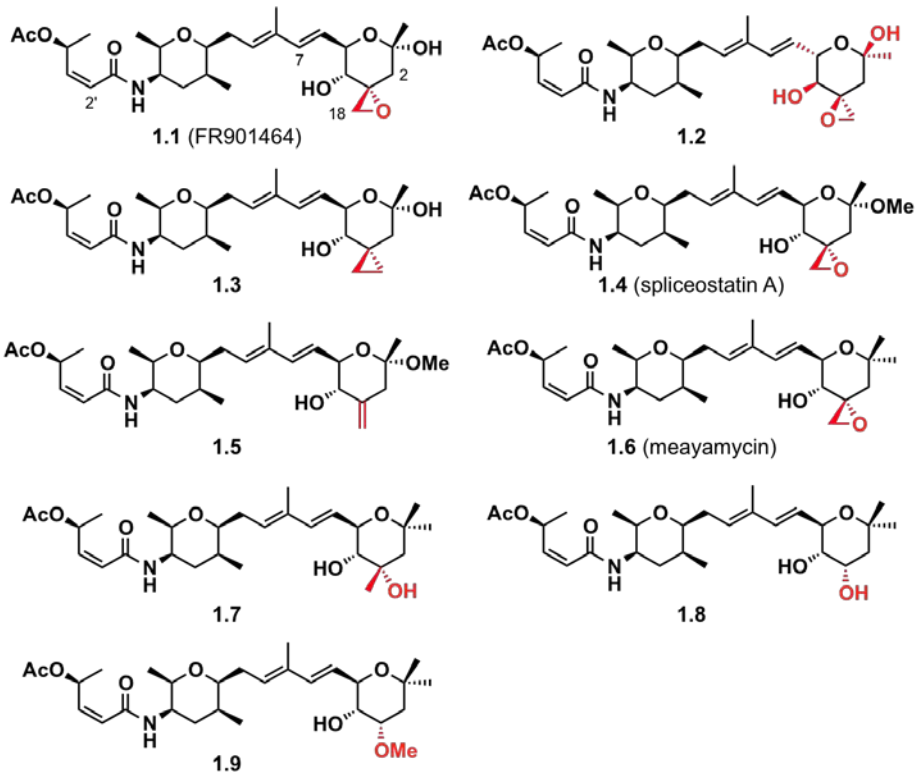

Figure 1-6 Chemical structures of epoxy analogues and their parent compounds (FR901464, spliceostatin A and meayamycin).

Table 1-2 Antiproliferative activity of epoxy-analogues and their parent compounds.

	IC_{50} (nM)		
compound	Tag Jurkat cells	Promoter activation	MCF7 cells
1.1	2	++++	1.1
1.2	400	ND	ND
1.3	>5000	ND	ND
1.4	ND	+++++	ND
1.5	ND	+	ND
1.6	ND	ND	0.01
1.7	ND	ND	>10000
1.8	ND	ND	>10000
1.9	ND	ND	>10000

Tag Jurkat = T lymphocyte cells. MCF7 = human breast adenocarcinoma cell line. ND = not determined. "+" shows relative strength of activity by CMV promoter activation.

The right pyran ring of FR901464 can exist in an open and close form. An initial effort to examine whether the open or cyclic form of the right pyran is the active form of FR901464 was carried out by the Jacobsen group.[20] Substitution of the hydroxy group on C1 with a hydrogen led to an analogue that was equipotent to FR901464 (Figure 1-7, compound **1.10**, Table 1-3),[20] which indicates that the active form of FR901464 is the cyclic structure of the right pyran ring. Furthermore, Kitahara and colleagues efforts were successful after replacing the hydroxy group on C1 with a methoxy group, which led to the birth of spliceostatin A, **1.4** (Figure 1-7), a more stable analogue than FR901464, with enhanced potency in a CMV promoter activation assay, although quantitative data were not available (Table 1-3).[23] Later, the Koide group replaced the hydroxy group on C1 with a methyl group, in effort to further stabilize the right pyran ring and encourage hydrophobic interactions with the target biomolecule.[25] This modification yielded an analogue that was 100 times more potent than FR901464 in MCF-7 cells (GI_{50} = 10 pM), named meayamycin, **1.6** (Figure 1-7). Meayamycin's right pyran unit was indeed more stable than

FR901464's right pyran unit, with an improvement of half-life in phosphate buffers from 4 – 8 h to 48 h.[25]

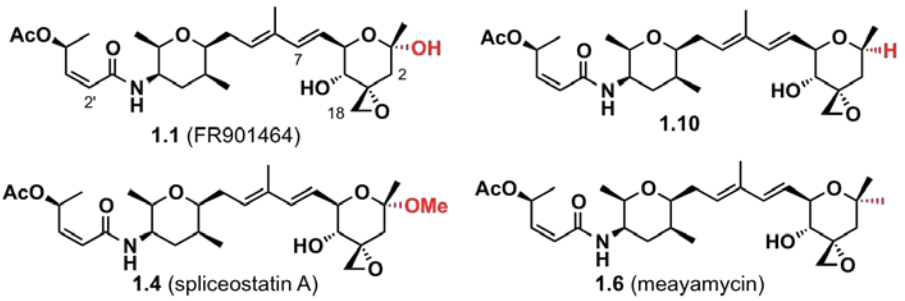

Figure 1-7 Chemical structures of the C1 analogues of FR901464.

Table 1-3 Antiproliferative activity of C1 analogues of FR901464.

	IC_{50} (nM)		
compound	Tag Jurkat cells	Promoter activation	MCF7 cells
1.1	2	++++	1.1
1.10	1.6	+++++	ND
1.4	ND	ND	ND
1.6	ND	ND	0.01

ND = not determined. "+" shows relative strength of activity by CMV promoter activation.

Initial modifications around the C2′ - C4′ unit by the Jacobsen group strongly suggest that the potent anticancer property of FR901464 is not as sensitive to modifications around that unit as compared to the epoxide moiety. More specifically, eliminating the α,β-unsaturated amide moiety in the side chain led to a decrease in activity by 3 orders of magnitude when compared to FR901464 in Tag Jurkat cells, demonstrating the importance of that unit, **1.12** (Figure 1-8, Table 1-4).[20] Furthermore, the epimer on C4′, **1.11** (Figure 1-8), led to a reduction in

potency (15-fold loss).[20] To advance the efforts of the Jacobsen group probing C4′, the Koide group probed this site. Koide group's hypothesis was that due to the 1,3-allylic strain, the hydrogen on C4′ is likely on the same plane as the enamide, and that the epimer of C4′ would place the acetoxy and/or methyl substituent on the wrong face of the molecule, thereby explaining the decrease in activity of the C4′-epimer analogue by Jacobsen and coworkers.[24] To probe this phenomenon, the Koide group prepared 4′-desacetyl-meayamycin **1.13** and *epi*-4′-desacetyl-meayamycin **1.14**. 4′-Desacetyl-meayamycin was 50 times lower in activity relative to meayamycin in MCF-7 cells, while *epi*-4′-desacetyl-meayamycin was 150 times lower in activity, and ~1 order of magnitude less active than 4′-desacetyl-meayamycin, indicating that the acetyl group is important for FR901464's antiproliferative activity (Table 1-4).[24] That was followed by their effort towards functionalizing C4′; the rationale for installing a carbamate group in place of the acetate was because the acetate is prone to esterases-mediated hydrolysis under physiological conditions. Replacement of the methyl group on C2′′ with a morpholine group led to an analogue that was 4 times more active, on the average, than meayamycin, named meayamycin B, **1.15** (Figure 1-8, Table 1-4). As hypothesized, meayamycin B exhibited a prolonged half-life ($t_{1/2}$ = 9 h in mouse serum) compared to meayamycin ($t_{1/2}$ = 2 h in mouse serum).[24]

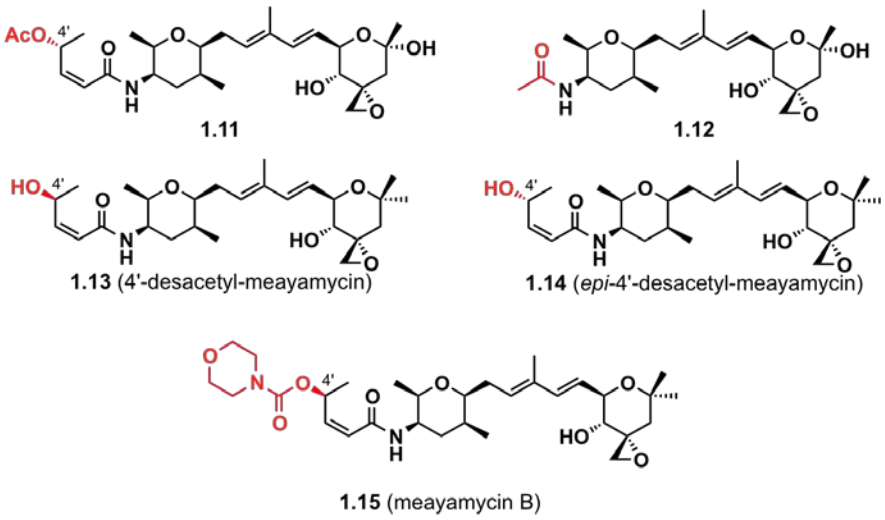

Figure 1-8 Chemical structures of the C2′-C4′ analogues of FR901464.

Table 1-4 Antiproliferative activity of C1 analogues of FR901464.

	IC_{50} (nM)	
compound	Tag Jurkat cells	MCF-7 cells
1.1	2	1.1
1.11	30	ND
1.12	1700	ND
1.6	ND	0.02
1.13	ND	0.48
1.14	ND	4.7
1.15	ND	0.008

ND = not determined.

Takahashi and coworkers prepared FR901464 derivatives to conjugate to affinity nanoparticle beads for biochemical studies. They demonstrated that attaching a long aliphatic carbamate chain on C4′ instead of an acetate led to a 40-fold decrease in activity in EL4 murine lymphoma cells, while the same carbamate group attached on C4 led to a 250-fold reduction in

activity, demonstrating the sensitivity of C4-hydroxy group towards functionalization with large groups (Figure 1-9 and Table 1-5).[26]

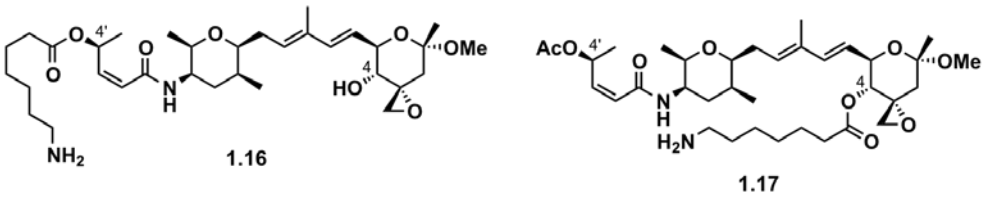

Figure 1-9 Chemical structures of the C4 and C4′ analogues of FR901464.

Table 1-5 Antiproliferative activity of C4 and C4′ analogues of FR901464.

	IC_{50} (nM)	
compound	EL4 cells	MCF7 cells
1.1	2	1
1.16	83	ND
1.17	500	ND

EL4 = mouse lymphoma cells. ND = not determined.

Extensive efforts by the Koide group were devoted towards analogues of the left pyran, in optimism of identifying the ideal conformer of the pyran in cells and also develop an alternative simpler structure to assemble rather than the current left pyran of FR901464. Several acetal derivatives were prepared and tested in MCF-7 cells (Figure 1-10).[24] Their antiproliferative activity (Table 1-6) indicates that the loss of hydrophobicity may be the primary reason for a decrease in potency.[24]

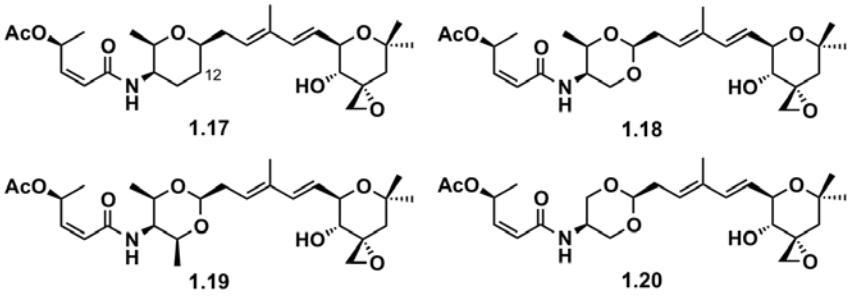

Figure 1-10 Chemical structures of the left pyran analogues of FR901464.

Table 1-6 Antiproliferative activity of C1 analogues of FR901464.

	IC_{50} (nM)
compound	MCF-7 cells
1.6	0.02
1.17	0.3
1.18	2.5
1.19	85
1.20	19

Finally, the Koide group also probed the significance of the diene moiety by preparing two cyclopropyl derivatives, **1.20** and **1.21** (Figure 1-11), due to the encouraging precedence of the use of cyclopropanes as alkene bioisosteres in cancer chemotherapy,[27] and also aiming to decrease the potential of rapid metabolism. The two derivatives were approximately only one order of magnitude lower in potency than the parent compound, which implies that the C8-C9 alkene remains *trans*, though the *cis* geometry needs to be prepared in order to further validate that conclusion. The SAR of FR901464 known at this time is summarized in Figure 1-12.

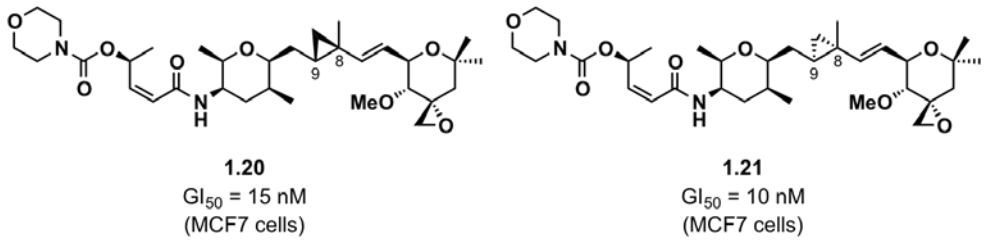

Figure 1-11 Chemical structures and antiproliferative activity of the diene analogues of FR901464.

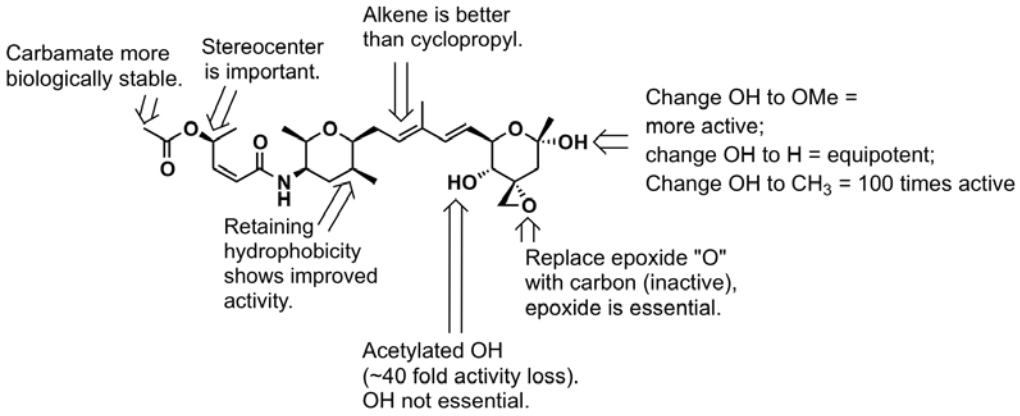

Figure 1-12 Overview of the published data on the SAR for FR901464.

1.2.3 FR901464 targets pre-mRNA splicing

Studies by Minoru Yoshida and coworkers were conducted to identify the molecular target of FR901464 and spliceostatin A, and a biotin derivative was developed for this purpose (Figure 1-13).[7]

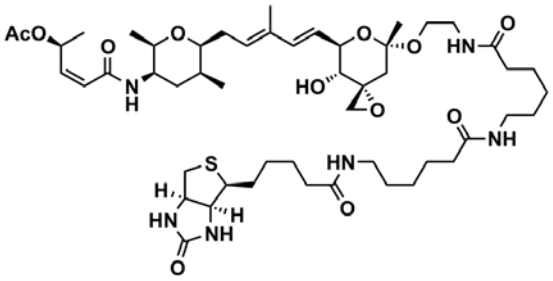

1.22 (biotinylated derivative of spliceostatin A)

Figure 1-13 Chemical structure of the biotin derivative of spliceostatin A.

The biotinylated analogue of spliceostatin A was incubated with HeLa cells and subsequent streptavidin-mediated purification revealed that spliceosome-associated protein 155 (SAP155), SAP145 and SAP130 as candidates, all components of splicing factor (SF) 3b (SF3b is a subunit of U2 snRNP). SiRNA (si = small interfering) experiments did not pin point the exact identity of the target, because siRNA against all three isolated proteins showed similar phenotype to the compound-treated one.[7] However, because SAP155 was the last protein eluted from the streptavidin column, reportedly due to a strong interaction with the biotinylated derivative, it is proposed to be the actual target.[7] Later on, Valcarcel and coworkers showed that SAP155 knockdown in HeLa cells displayed similar alternative splicing patterns to spliceostatin A-treated cells, which indicated that SAP155 might be an actual target.[28] Finally, it was shown that spliceostatin A inhibits pre-mRNA splicing in HeLa cells in a concentration-dependent fashion and causes enlargement of the nuclear speckles, due to the accumulation of unspliced pre-mRNA. Exactly how interfering with pre-mRNA splicing confers to cytotoxicity remains unknown, but it is likely that truncated proteins resulting from the translation of unspliced pre-mRNA or alteration of alterative splicing of apoptosis related genes are the cause. There may be additional cellular targets of FR901464 responsible for the observed cytotoxicity effects.

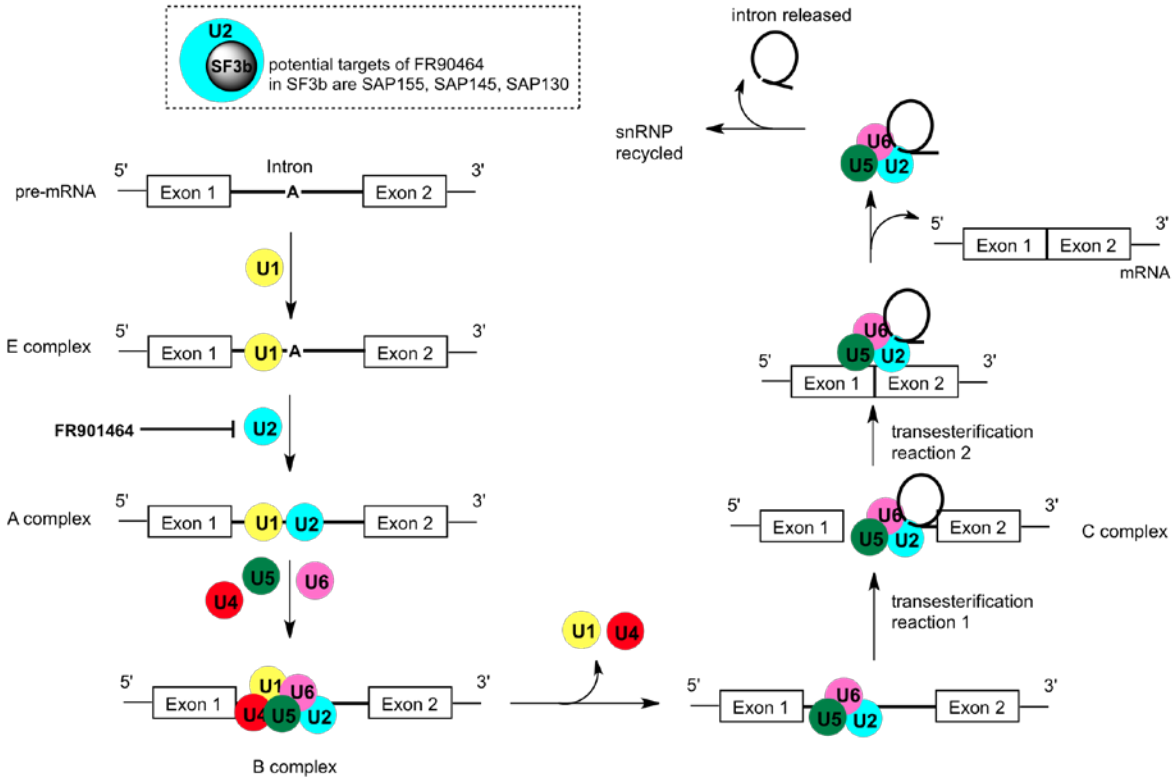

Figure 1-14 The step where FR901464 targets the pre-mRNA splicing process.

1.2.4 Meayamycin's preliminary biological studies by Koide and coworkers

When the Koide group examined the antiproliferative activity of meayamycin B against various human cancer cells, the MDA-MB231 and MCF-7 breast cancer cell lines were among the most responsive (GI_{50} = 8 – 15 pM),[24] in addition to the multidrug resistant (MDR) cell line VCRd5L (DC3F is transformed Chinese hamster cells and VCRd5L is their multidrug-resistant counterpart) being equally responsive (GI_{50} = 0.67 nM, Table 1-7).[29] Additionally, meayamycin did not show significant toxicity against nontumorigenic human lung fibroblasts IMR-90, while toxicity was retained in A549 cells. At the present time, it is not clear whether pre-mRNA splicing inhibition is the reason for this observed specificity.[29] Furthermore, the Koide group

asked whether the electrophilic epoxide present in meayamycin, which has the potential of covalently labeling the biomolecule, manifests reversible or irreversible growth inhibition. The assay designed to address this question was based on transient exposure of meayamycin to cells, and washing away any unbound meayamycin, then allowing the assay to continue for a total of three days. If reversible growth inhibition is the case, cells should begin to grow after removal of meayamycin. Alternatively, if irreversible growth inhibition is the case, cells will remain senescent after removal of meayamycin. They illustrated that meayamycin inhibited the proliferation of A549, MCF-7 and HeLa cells irreversibly, which could mean that meayamycin binds to SF3b irreversibly or induces irreversible cell growth arrest.[29] Finally, the same group demonstrated that meayamycin inhibited pre-mRNA splicing in HEK-293 cells at a concentration-dependant manner, and 50 nM was sufficient for complete inhibition.

Table 1-7 Antiproliferative activity of meayamycin and meayamycin B.

	GI_{50} (nM)	
Cell line	Meayamycin	Meayamycin B
MCF-7	0.020	0.008
MDA-MB231	0.070	0.015
A549	0.26	0.18
DU-145	1.2	0.21
HCT116	0.16	0.004
H1299	0.84	0.15
PC-3	0.2	0.10
VCRd5L	0.67	ND
DC-3F	0.42	ND

MCF-7 = earlier passage of breast cancer cell line, estrogen receptor-positive. MDA-MB231 = breast cancer cell line, estrogen receptor-negative. A549 = lung carcinoma cells, wild-type p53. DU-145 = prostate carcinoma cells. H1299 = lung carcinoma cells, p53-deficient. PC-3 = colon carcinoma cells, p53-deficient. HCT116 = colon carcinoma cells, wild-type p53.

1.2.5 Additional natural products that inhibit pre-mRNA splicing by targeting the spliceosome: pladienolide and herboxidiene (GEX1A)

In 2004, Eisai Corporation discovered seven pladienolides.[30] Their discovery was the result of the development of a cell-based assay designed to identify small molecules that block the hypoxia inducible factor (HIF-1) transcription factor pathway and thus expression of vascular endothelial growth factor (VEGF) genes. This pathway is critical to the growth of tumors in their common low oxygen (hypoxic) environment, because VEGF stimulates the recruitment of new blood vessels to the tumors, a process known as angiogenesis.[31,32] In addition to powerful anti-VEGF activity, the pladienolides displayed a broad range of *in vitro* cytotoxicity against a panel

of 39 tumor cell lines.[31,32] Exposure of colorectal adenocarcinoma WiDr cells to pladienolides resulted in cell cycle arrest at the G1 and G2/M phase, and the cell cycle arrest profile of the pladienolides did not correlate well with 5-fluorouracil, vincristine, or taxol. Thus, the cellular target of these angiogenesis inhibitors was thought to be new for antitumor agent development. Initial *in vivo* activity results were promising; in particular, pladienolide B demonstrated potent activity in six different mouse xenograft models, slowing tumor growth in five and causing complete regression in one.[33] The most important SAR result from the isolation of the pladienolides was the finding that the acetate at C-7 is critical for anti-VEGF activity, while the non-acetylated derivative are much less active. Much of the subsequent semi-synthetic medicinal chemistry on the pladienolides by the Eisai Corporation was done by making various esters and carbamates at C-7 of pladienolide D. These efforts led to a urethane derivative of pladienolide D, with 7-(4-cycloheptylpiperazin-1-yl) substituted for the 7-acetyl group was identified with complete retention of anti-VEGF activity and *in vivo* antitumor activity.[34,35] This derivative, with enhanced *in vivo* potency and pharmacokinetic properties, was denoted E7107 (Figure 1-15) and entered phase I clinical trials for several cancer treatments in 2007.[36] Several chemical biology experiments at the Eisai Corporation were conducted using photoaffinity-labeled probe experiments identified that the molecular target of pladienolide B to be SAP130, a subunit of SF3b.[37] In 2011, the same group used a radiolabeled-probe and pladienolide-resistant cell lines to discover that the compound also binds to SAP155, which led to a proposed model suggesting that the compound binds to an interface between the two proteins (SAP130 and SAP155).[38] E7107 is presumably the first pre-mRNA splicing inhibitor to be clinically tested in humans.[36,39] These data suggest that the pladienolides are members of a new class of spliceosome targeting antitumor agents, including FR901464.

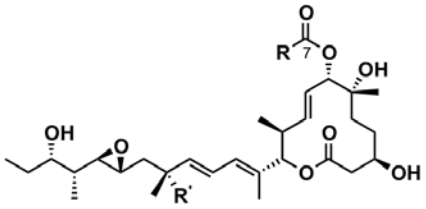

pladienolide D: R = $-CH_3$, R' = OH

pladienolide B: R = $-CH_3$, R' = H

E7107: R = 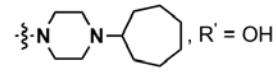 , R' = OH

	Anti-VEGF activity IC_{50} (nM)	Anti-proliferative activity (U-251 cells) IC_{50} (nM)
pladienolide D	5.1 nM	5.0 nM
pladienolide B	1.8 nM	3.5 nM

Figure 1-15 Chemical structures of pladienolides, and their biological activity. U-251 = glioblastoma-derived human cell line.

Another antitumor agent found to be a pre-mRNA splicing inhibitor is herboxidiene/GEX1A (also known as anti-tumor agent TAN-1069), which was originally isolated from a fermentation broth of *Streptomyces* sp. A7847 in 1992 by Isaac and coworkers at Monsanto.[40] In 2002, Yoshida and coworkers, during their screening of natural products that activate luciferase gene under the control of the SV40 promoter (a similar screening method that allowed for the discovery of FR901464), they discovered and re-isolated herboxidiene, termed GEX1A (Figure 1-16).[41,42] This compound was found to be a novel polyketide that exhibited *in vitro* cytotoxicity against several human tumor cell lines, including epidermoid carcinoma A431 cells, human lung carcinoma A549 cells, human colon carcinoma DLD-1 cells, and human normal fibroblast WI-38 cells with IC_{50} values ranging from 3.7 to 51 nM (Figure 1-16). Recently, T. Mizukami and colleagues determined that GEX1A inhibits the splicing of pre-mRNA by targeting a subunit of SF3b, SAP155.[43]

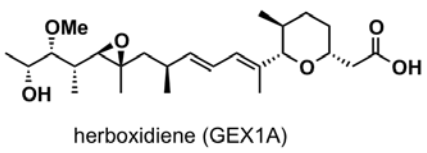

cells	IC_{50} (nM)
A431	3.7
A549	21
DLD-1	51
WI-38	7.6

Figure 1-16 Chemical structure of herboxidiene and its antiproliferative activity.

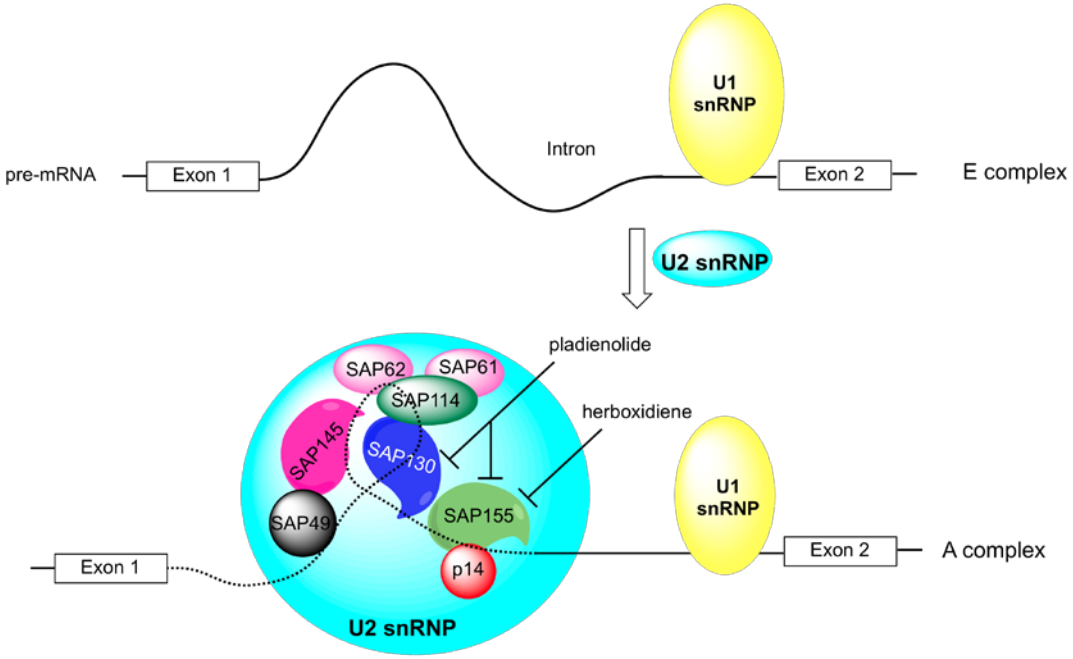

Figure 1-17 Biological targets of pladienolide and herboxidiene (not drawn to scale).

1.2.6 SAR and preliminary biological studies of FR901464-pladienolide type compounds by Webb coworkers

FR901464 and pladienolide B share the same molecular target yet differ in their chemical structure and their ability to inhibit a diverse collection of human tumor lines. It is likely that these molecules share the same mechanism of inhibition given that they share a hypothetical consensus pharmacophore structure as proposed by Webb and coworkers.[44] Based on structural

overlays of features known to be critical for the activity of FR901464 and pladienolide B, Webb and colleagues synthesized lead compounds to try to identify a minimal pharmacophore and assayed the ability of these molecules to inhibit proliferation of cells and pre-mRNA splicing (Figure 1-18 and Table 1-8). Building on the previously SAR data acquired by others, the Webb group proceeded to further reduce the structural complexity of the left tetrahydropyran, the 1,3-conjugated diene, and the right tetrahydropyran by eliminating the C4 hydroxy group.[44]

More specifically, by focusing their efforts on reducing the number of stereocenters on the left pyran, the Webb group developed cyclohexyl **1.23** (Figure 1-18), which exhibits GI_{50} values in the range of 0.1 – 4 μM in various mammalian cancer cell lines, with Jeko-1 and JVM-2 being the most responsive (Table 1-8). They also demonstrated that the diene portion of their scaffold was sensitive to substitution by heteroatoms (carbamate **1.24** and carbonate **1.25**, Table 1-8). Further efforts on **1.23** focused on developing analogues that be both resistant to esterase-mediated hydrolysis and more water-soluble.[4] Analogues **1.27**, **1.28**, **1.29**, **1.30** showed no antiproliferative activity, except for isobutyl ester **1.26**, with GI_{50} values similar to the acetate derivative **1.23** (Table 1-8). According to NCI standards, $T/C \leq 42\%$ is the minimum requirement for activity.[45] The *in vivo* efficacy of **1.26** in mice bearing Jeko-1 was promising ($T/C = 35\%$). In addition, the aqueous solubility of **1.26** was less than 1 μM in phosphate buffered saline (PBS) buffer. To improve the solubility of **1.26**, acetal **1.31** was prepared (Figure 1-18), and had approximately a 50-fold increase solubility in aqueous PBS (47 μM in PBS) and its *in vivo* anticancer activity was comparable to **1.26**. In summary, in addition to being powerful tools to investigate spliceosome mechanics and structure, FR901464 and its derivatives present a unique opportunity to design potential spliceosome-specific cancer therapeutics.

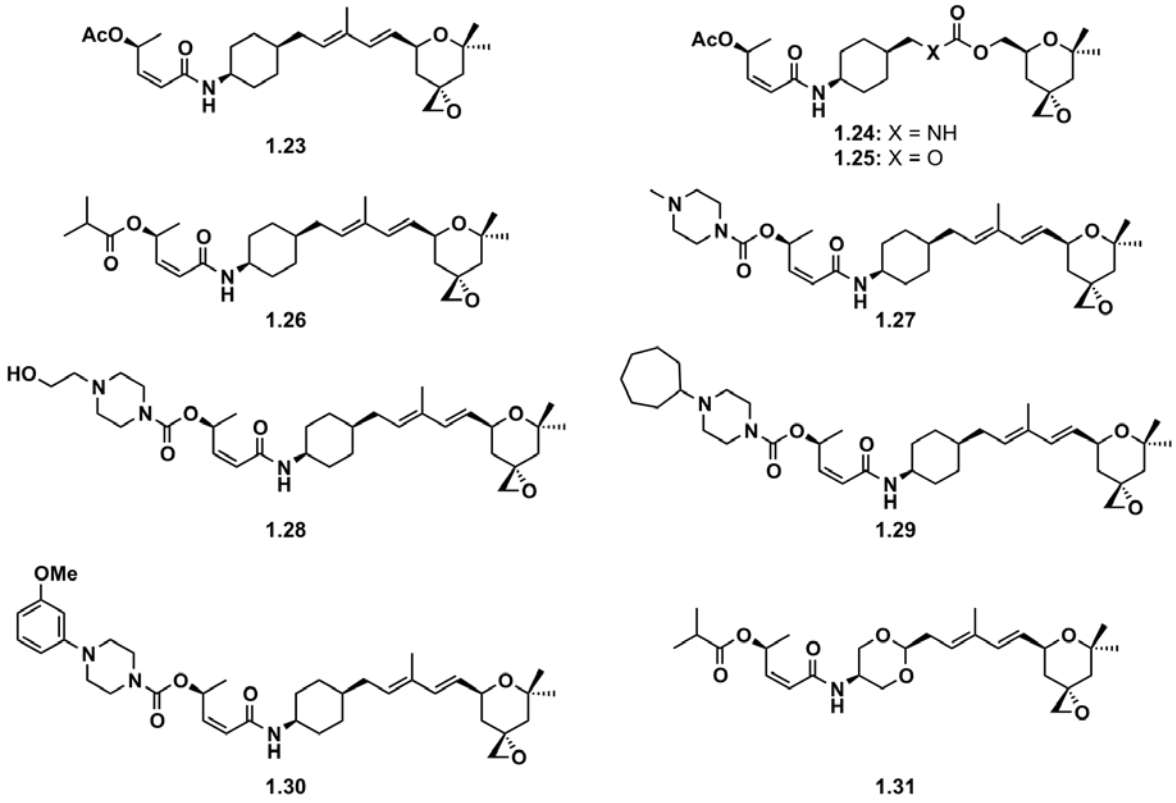

Figure 1-18 Chemical structures of Thomas Webb's analogues.

Table 1-8 Antiproliferative activity of Thomas Webb's analogues.

	IC_{50} (μM)					
compound	JeKo-1	JVM-2	PC-3	WiDr	A549	MCF-7
FR901464	ND	ND	ND	ND	0.0013	0.0018
1.23	0.1	0.13	2.1	2.0	4.65	2.29
1.24	ND	ND	ND	>5.0	>5.0	>5.0
1.25	ND	ND	ND	ND	>5.0	>5.0
1.26	0.12	0.19	2.2	0.91	ND	ND
1.27	>0.5	>0.5	>2.5	>1.25	ND	ND
1.28	>0.5	>0.5	>2.5	>1.25	ND	ND
1.29	ND	>1.0	>5.0	4-5	ND	ND
1.30	>0.5	>0.5	>2.5	>1.25	ND	ND

JeKo-1 and JVM-2 = mantle cell lymphoma cells. ND = not determined.

Later on, a combined effort between T. Webb and P. M. Potter was directed towards further understanding the mode of action of these newly developed simplified FR901464 analogues. Their efforts demonstrated that analogues **1.26** and **1.31** are capable of modulating alternative splicing of *MDM2* and *caspase 2* and *9* in human cells. mRNA levels of alternative splicing were increased in tumor cells relative to normal cells, and these modifications were also observed in human tumor xenografts *in vivo* following exposure of animals to **1.26** and **1.31**. There studies suggest that modulation of alternative splicing may be directly related to the antitumor activity of their FR901464 analogues.

1.2.7 Significance

Targeting the spliceosome and inhibiting pre-mRNA splicing with FR901464 analogues represents a new approach for the treatment of cancer.[46,47] Support of pre-mRNA splicing inhibition as a potential method for cancer therapy has been furthered by the many examples of

cancer-associated alterations in splicing and mutations in the splicing machinery.[13] Two of the most recent examples include mutations of the splicing machinery in myelodysplasia (blood-type cancer)[48] and the development of BRAF splicing variants (BRAF is a kinase involved in the ERK signaling pathway) in mammalian melanomas which are responsible for developed resistance to clinically used vemurafenib (Zelboraf ®).[49]

In the first example, a group led by Seishi Ogawa reported the first results that provide evidence of genetic alterations of the major splicing components in myelodysplasia.[48] Through genome-sequence analysis of 29 patients with myelodysplasia, they discovered mutations in multiple components of the pre-mRNA splicing machinery, including *U2AF25, ZRSR2, SRSF2* and *SF3B1* (one of FR901464's target). These mutations were found in 45 to 85% of patients with myelodysplasia. Most of the reported mutations affect genes involved in splice site recognition during pre-mRNA processing and which eventually lead to human diseases. Subsequently, investigators in the Wellcome Trust Institute in the United Kingdom and the Cleveland Clinic in the United States reported similar findings.[50,51]

In the second example, a group led by David B. Solit at Memorial Sloan-Kettering Cancer Center, discovered that patients with melanoma developed resistance to vemurafenib, is due to aberrantly spliced BRAF.[49] When BRAF is mutated, ERK signaling pathway is hyperactive in melanoma cells. Vemurafenib specifically targets the mutated BRAF form, and account for vemurafenib's remarkable clinical activity. However, an aberrantly spliced version of BRAF that developed after exposure to vemurafenib, also led to accelerated tumor growth, and resistance to vemurafenib therapy quickly developed. This suggests that combination treatment with splicing modulators such as pre-mRNA splicing inhibitors could be tested to overcome BRAF inhibitor-mediated resistance.

Accumulating data shows that these cancer-specific splice variants could be involved in the development of diseases or predict sensitivity to certain drugs. Targeting the pre-mRNA splicing process as an effective approach to combat cancer could be following a similar path to the approach of anticancer drugs targeting microtubules. The successful development of taxane class of antimicrotuble chemotherapy agents represents one of the breakthroughs in cancer chemotherapy.[52] However, it took 16 years after the elucidation of taxol's mode of action in 1979[53] until other compounds acting through a similar mechanism were identified.[54]

As new tools and new information on RNA biology in tumors emerge, scientists expect new and better insights into the still under-explored world of the spliceosome and pre-mRNA splicing and its potential to provide novel avenues for molecular targeted cancer treatment(s). It is evident that FR901464 analogues will bring the potential cures to the treatment of cancer by targeting the pre-mRNA splicing process as supported by the numerous pre-mRNA splicing assays in development to screen and identify new pre-mRNA splicing inhibitors.[55-57]

1.3 TOOLS THAT MODULATE PRE-MRNA SPLICING

1.3.1 Challenges to studying the spliceosome

One challenge in studying the human spliceosome is a lack of tools for arresting the splicing machinery at specific stages during its dynamic assembly pathway. Each spliceosome protein has unique inter-molecular interactions and presumably specific function. A highly coordinated exchange of these factors is essential for spliceosome activity. During spliceosome

assembly, each U snRNA (U1, U2, U4, U5 and U6) interacts with a defined set of proteins and makes critical base pair interactions within and between themselves and pre-mRNA, while undergoing extensive structural rearrangements.[8] The current model of spliceosome assembly suggests that the complex transitions through several stable intermediate assemblies: early complex (E) → pre-spliceosome (A) → fully assembled spliceosome (B) → catalytically active spliceosome (C) (Figure 1-3).[8] Given the dynamic nature of the spliceosome, it is likely that many other assemblies remain to be identified. Therefore, the discovery and characterization of small molecules directed against enzymatic chemistries, targeting crucial protein-protein interactions or disrupting protein-RNA interactions will be instrumental for studying the spliceosome.

The potency of characterized small molecule splicing inhibitors ranges in IC_{50} value from the nanomolar range, for FR901464-like compounds,[6,7,29] to the millimolar range, for the histone deacetylase inhibitor suberoylanilide hydroxamic acid, termed SAHA (to be discussed in the following sections).[58] The molecular targets and direct mechanism of most splicing inhibitors remain to be determined, and many splicing inhibitors may act indirectly. For example, some antibiotics interfere with splicing by sequestering required Mg^{2+} ions while other small molecules interfere with RNA transcription or alter mRNA stability, which would affect events proceeding or following splicing, but not the spliceosome directly.[59,60] To improve the current collection of tools, screening methods to identify novel inhibitors of general splicing events as well as inhibitors of transcript-specific splicing are being developed.[55,56,60,61]

For the purpose of this discussion, pre-mRNA splicing modulators will be classified into three general categories: 1) general splicing inhibitors, 2) intron-specific modulators, i.e.

inhibitors that modulate the splicing of a specific intron, and 3) spliceosome inhibitors, i.e. those which directly interfere with spliceosome assembly.

1.3.2 General splicing inhibitors

1.3.2.1 Antibiotics

Antibiotics have proven to be powerful tools to study the function and structure of macromolecular complexes, such as ribosomes.[62] Furthermore, antibiotics have been shown to play a role in the pre-mRNA splicing process.[59] Splicing activity of a pre-mRNA substrate was potently inhibited when HeLa cells were treated with erythromycin, CI-tetracycline or streptomycin (IC_{50} = 160 mM, 180 mM and 230 mM, respectively). However, given the relatively high concentration of antibiotic needed to inhibit splicing, it is difficult to determine whether the mechanism of inhibition is direct. Cl-tetracycline caused 60% reduction in splicing in addition to a considerable accumulation of pre-mRNA suggesting that this inhibition precedes the first step of splicing. Furthermore, erythromycin (500 μM) inhibited 95% of splicing and a lariat intermediate was accumulated, suggesting that erythromycin inhibits a step between the two steps of trans-esterification. Reactions treated with streptomycin revealed splicing inhibition prior to the first step of the splicing chemistry. However, this inhibition was subsequently shown to be dependent on the concentration of Mg^{2+} ions in the assay suggesting that the observed inhibition might be due to an indirect mechanism. Overall, the use of antibiotics to inhibit splicing chemistry and spliceosome assembly hardly show promise as specific inhibitor tools.

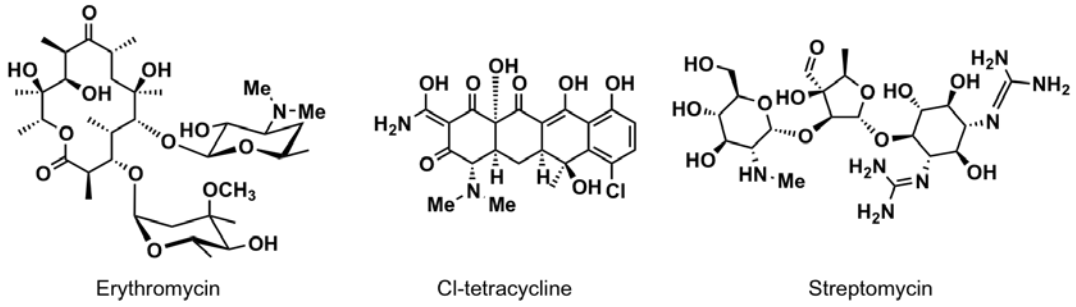

Figure 1-19 Chemical structures of erythromycin, Cl-tetracycline and streptomycin.

1.3.2.2 Inhibitors of histone acetylation

Recently, histone acetyltransferases (HATs) and histone deacetylases (HDACs) were identified as targets of small-molecule splicing inhibitors. In 2008, Kuhn and colleagues investigated the origin of the splicing interference, protein and/or snRNA composition, and blockade of spliceosome assembly of eight small molecule inhibitors of protein acetylation and deacetylation.[58] They found that the compounds SAHA, splitomicin, dihydrocoumarin, and butyrolactone inhibit splicing chemistry, but not the formation of C complex spliceosomes. Two compounds, anacardic acid and garcinal inhibit spliceosome assembly by accumulating an A-like complex. Collectively, anacardic acid and garcinal appear to inhibit the transition of A to B complex spliceosomes. These results suggest a role for acetylation in the stability or assembly of B complex spliceosomes and further support that the current model of spliceosome assembly is incomplete. However, relatively high concentrations of these inhibitors are required for the observed loss of splicing. Additionally, because the targets of acetylation are currently undetermined, it is difficult to identify the mechanism or target of pre-mRNA splicing inhibition. However, blocking post-translation modifiers could be a viable approach to identify the enzymes involved in catalyzing these modifications.

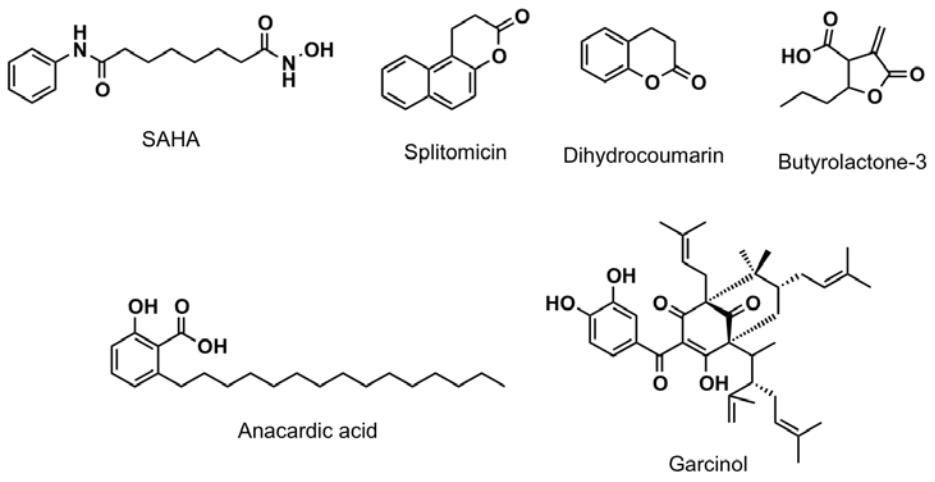

Figure 1-20 Chemical structures of SAHA, splitomicin, dihydrocoumarin, butyrolactone-3, anacardic acid and garcinol.

1.3.2.3 Peptides

The use of peptides designed to bind to specific proteins allows for a more targeted mechanism to isolate stalled mammalian spliceosomes. By interfering with facial interactions, essential rearrangements within the spliceosome can be blocked. Additionally, the use of interfering peptides can inform when a specific interaction is important during spliceosome assembly. For example, Parker and Steitz employed peptides that bind to Ca^{2+}-calmodulin-dependent protein kinase II (CaMK II) in an effort to explore the role of CaMK II-like proteins in spliceosome assembly.[63] Two peptides, one that binds the N-terminus of glycogen synthase (GS) and another that interacts with the calmodulin binding domain (CBD) of CaMK II were identified as inhibitors of *in vitro* splicing and spliceosome assembly. Both peptides blocked splicing chemistry before the first trans-esterification step. Data from Parker and Steitz revealed that while the CBD peptide blocks C complex formation, the GS peptide appears to slow the

transition of B complex to C complex spliceosomes. In addition, splicing reactions complemented with recombinant bovine brain calmodulin (CBD-treated extracts) or with purified rat brain CaMK II (GS-treated extracts) were able to recover some splicing activity. However, reactions extended even to 3 h were unable to overcome inhibition of splicing when no additional protein was added. These findings support a role for CaM kinase in the formation of C complex spliceosomes that is not explained by the current model of spliceosome assembly.

Continuing in the design of peptide-based pre-mRNA splicing inhibitors, Ajuh and Lamond designed peptides derived from the spliceosome proteins CDC5L and one of its interacting partners, PLRG1.[64] CDC5L and PLRG1 are both spliceosomal proteins that are conserved across species, and have shown to be essential for pre-mRNA splicing in humans. A specific domain on PLRG1, termed WD40, and a C-terminal domain on CDC5L, mediates CDC5L and PLRG1 interaction.[64] Peptides were designed to interfere with either the WD40 domains in PLRG1 or the C-terminus of CDC5L. The PLRG1 peptides bound to CDC5L without disrupting the interaction between the two proteins and did not inhibit splicing. A subset of CDC5L-derived peptides bound to PLRG1 and had an inhibitory effect on splicing and spliceosome assembly in a transcript independent manner. Gel analyses of inhibited reactions revealed that there was no inhibition of spliceosome assembly, suggesting that these peptides may interfere with the catalytic activity rather than assembly of spliceosomes. The design of potential peptide inhibitors is complicated by the lack of information concerning the complex architecture and detailed interactions of the spliceosome.

1.3.2.4 Isoginkgetin

A report in 2008 by Moore and coworkers described the design of mammalian cell lines for the identification of small molecule inhibitors of pre-mRNA splicing.[55] This group tested

approximately 8,000 natural compounds and identified the biflavonoid isoginkgetin as a general inhibitor of pre-mRNA splicing (IC_{50} = 30 μM). In addition to its role as an antitumor compound, isoginkgetin was shown to directly inhibit the transition of A complex to B complex spliceosomes. However, its molecular target and mechanism of inhibition were not reported.

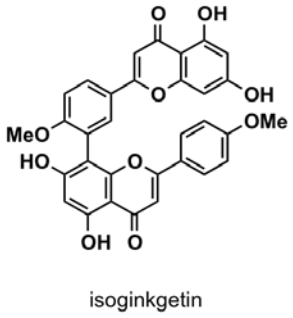

isoginkgetin

Figure 1-21 Chemical structure of isoginkgetin.

1.3.3 Intron specific modulators

1.3.3.1 Small molecules

Borrelidin, a polyketide natural product, is a potent inhibitor of angiogenesis. A group led by B. Wilkinson reported the biosynthesis of a new analogue of borrelidin, **1.32** (Figure 1-22) using genetically engineered bacterial strains of *Streptomyces parvulus*.[65] This analogue was first shown to exhibit anti-bacterial and anti-angiogenic actions. To further clarifying the molecular targets of **1.32**, a biotin derivative was prepared, and, through phage display experiments, the target was found to be splicing factor FB21. Later, Wilkinson and coworkers demonstrated that **1.32** exhibits alternative splicing activity towards the VEGF transcript. Specifically, a C-terminal splicing event in the VEGF mRNA results in production of two VEGF isoforms: $VEGF_{xxx}$, which is pro-angiogenic, and $VEGF_{xxxb}$, which has anti-angiogenic activity. These two isoforms

are formed by the use of alternate 3' splice sites in exons. Concentrations of 0.5 – 5 μM decreased expression of $VEGF_{xxx}$ and increased expression of $VEGF_{xxxb}$, in a manner that was sufficient to completely block angiogenesis.

Later, Younis and colleagues described a high-throughput assay that allowed for rapid detection of potential inhibitors of splicing.[61] From a screen of nearly 23,000 molecules, three splicing inhibitors were identified, namely clotrimazole, chlorhexidine and flunarizine. All three therapeutic agents were shown to alter the splicing and alternative splice site use of specific transcripts rather than to be general inhibitors of splicing chemistry. These findings revealed unexpected activities of clinically used drugs in alternative splicing.

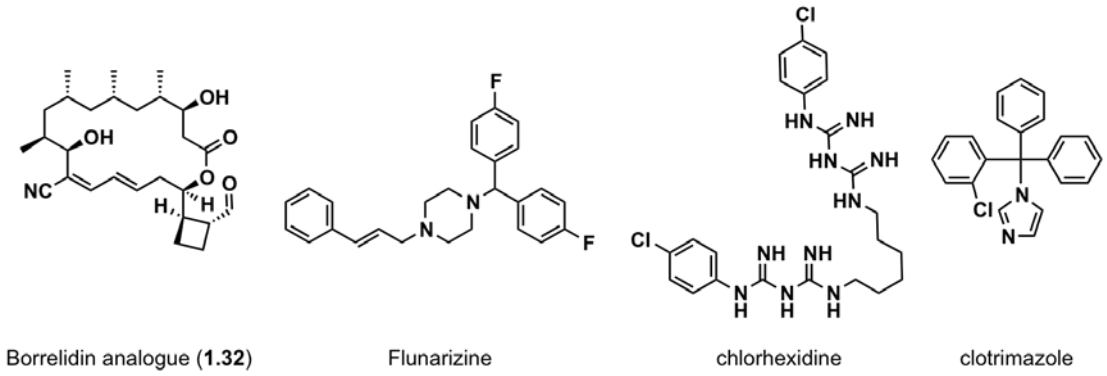

Figure 1-22 Chemical structures of **1.32**, flunarizine, chlorhexidine and clotrimazole.

Along the same lines as Younis's work, Stoilov and colleagues developed a two-color fluorescent reporter construct for high-throughput screens to identify bioactive compounds that modulated alternative splicing.[60] Two libraries were screened which included FDA-approved drugs, enzyme inhibitors and ion-channel antagonists. Neuroblastoma cells treated with Tyrphostin-9, digoxin or 5-iodotubercidin revealed differential alternative pre-mRNA splicing patterns of the experimental substrate, leading this group to propose that each compound modulates splicing via a unique molecular mechanism.

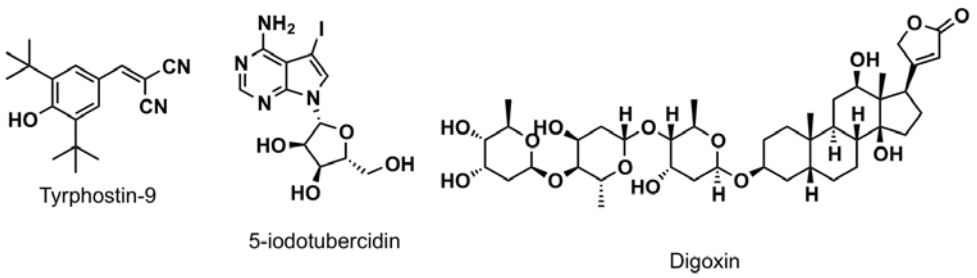

Figure 1-23 Chemical structures of tyrphostin-9, 5-iodotubercidin and digoxin.

From a screen of 220 indole derivatives **1.33**, **1.34** and **1.35** (Figure 1-24) were identified as inhibitors of HIV-1 pre-mRNA splicing *in vivo*.[66] Compound **1.34** led to changes in the alternative splicing of HIV-1 RNA, which resulted in the accumulation of larger transcripts (~800 base pairs) and depletion of smaller ones (~200 base pairs). Similar alternative splicing pattern were observed with **1.33** and **1.35**. This alteration in splicing indicates that the compounds are inhibiting several weak 3' splice sites upstream of key regulators of viral proteins Tat, Rev, Vpu, Env and Nef. Collectively, these studies suggest that targeting of spliceosomal proteins by small molecule inhibitors may be a potential target for anti-HIV therapies. Additionally, because these indole derivatives do not inhibit all splicing events, it is a powerful mechanism to specifically target HIV-infected cells. While these data reveal a promise for targeting specific disease transcripts, their mechanism in general splicing mechanism remains unclear.

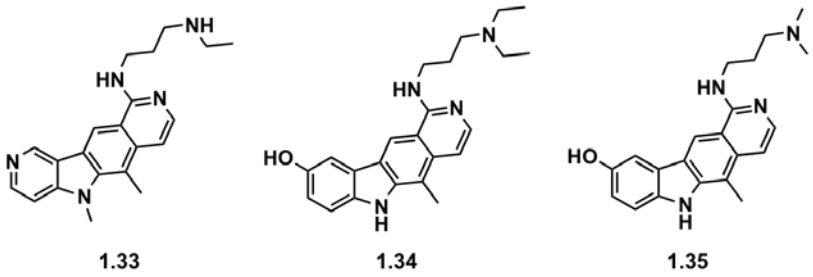

Figure 1-24 Chemical structures of **1.33**, **1.34**, and **1.35**.

1.3.3.2 Antisense Oligonucleotides

Another targeted approach to modulate splicing, in addition to peptides, is through the use of antisense oligonucleotides (AONs). These AONs can be synthesized to complement a specific RNA sequence transcribed from a gene. Designed AONs that bind to specific splice sites or to enhancer or silencer sequences within the pre-mRNA, the splicing mechanism can be altered precisely; i.e. exon skipping or inclusion (Figure 1-25).[67]

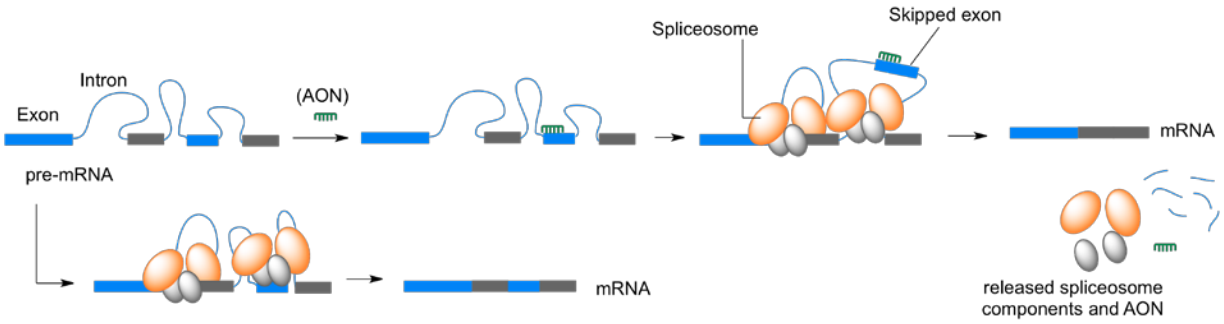

Figure 1-25 Illustration of exon skipping mediated by targeted AON.

An advanced example of using this technology therapeutically was against Duchenne muscular dystrophy (DMD). This disorder is characterized by progressive muscle weakness in childhood and eventually leads to death during early adulthood.[68] The defect is due to DNA mutation of the dystrophin gene, leading to the absence of the functional dystrophin protein. To

restore functional dystrophin, targeted AON were designed and synthesized to inhibit the inclusion of a specific exon during the splicing process.[69] The resulting mRNA, although shorter, retained the functionally important terminal domains.

1.3.4 Spliceosome inhibitors (FR901464, pladienolide and herboxidiene)

The pre-mRNA splicing inhibitors FR901464, pladienolide, and herboxidiene are examples of compounds with known molecular targets.[6,7,43] These compounds were discovered when groups in Japan independently identified natural products from different organisms that inhibited proliferation of cancer cells and pre-mRNA splicing.[5,17,18,31,33,40-42] Modified derivatives of these compounds have since been shown to target the SF3b sub-complex of U2 snRNPs.[6,7,43] SF3b is essential for branch-point adenosine identification and plays an essential role in the assembly of the pre-spliceosome.[70,71] Taken together, these results suggest that SF3b plays a direct role in the anticancer properties of these inhibitors, in addition to its established role in U2 snRNP recruitment to the pre-spliceosome.

1.3.5 Development of future tools

In order to probe the structure and molecular composition of precise intermediates of the spliceosome, it is necessary that preparations of the spliceosomal complex be homogeneous. Therefore, tools must be designed to interfere and arrest spliceosome assembly at a stable and distinct stage. While mutational analysis of pre-mRNA substrates has allowed for the isolation of several now established *bona fide* spliceosome intermediates,[72-76] new tools are being developed

to further elucidate the mechanism of pre-mRNA splicing and the connection to cancer.[7,28,29,37,48,50,77-80]

In the case of the ribosome, another highly complex ribonucleoprotein machinery, the use of antibiotics to capture distinct conformations has been crucial in understanding the dynamics of translation.[62] Similarly, small molecule inhibitors of pre-mRNA splicing will be critical for elucidating spliceosome structure and function. Small molecules can bind to specific targets, thereby allowing for the characterization of a blocked spliceosome complex as well as the investigation of the function of the targeted spliceosome component.

2.0 CHEMICAL AND BIOLOGICAL STUDIES OF FR901464 ANALOGUES

2.1 SIDE CHAIN ANALOGUES

Based on detailed SAR and stability studies, our group recently developed one of the most potent analogues of FR901464, meayamycin B. An interesting feature of the structure of meayamycin B and FR901464 is the presence of a *cis*-enamide at C2′-C3′. This enamide may be prone to nucleophilic addition in biological environments, which is illustrated in selected bioactive natural products with similar electrophilic enamides.[81,82] These electrophilic enamides are critical for the bioactivity of the molecules because this electrophile allows for labeling the target protein. In addition, designed acrylamide-based kinase inhibitors react irreversibly with glutathione,[83] and may react with proteins other than the desired target;[84] such off-target reactions are undesirable. Thus, current drug discovery efforts mostly aim to avoid the formation of irreversible covalent adducts.[85]

With these considerations in mind, we tested whether the electrophilic enamide present in meayamycin B is in fact crucial for its bioactivity. We prepared the *trans*-enamide isomer of meayamycin B to examine the necessity of the *cis*-enamide configuration and the non-enamide analogue of meayamycin B to probe the presence of the electrophilic enamide (Figure 2-1). Although early SAR studies have suggested that eliminating the C1′-C5′ unit is critical for

maintenance of biological activity, certain modifications within this unit have yielded potent analogues (Figure 1-8, 1-9, 1-18).[20,24]

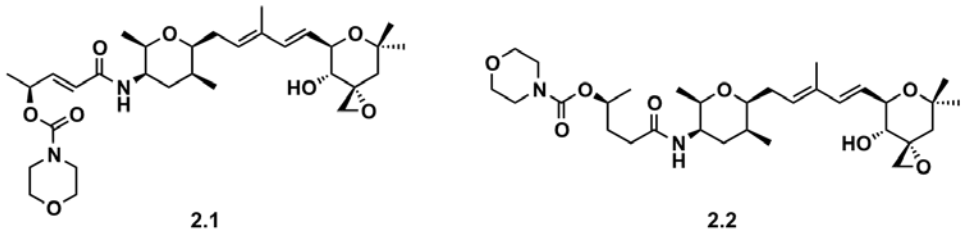

Figure 2-1 Chemical structures of meayamycin B side-chain analogues to be prepared.

2.1.1 *Trans* C2′-C3′ analogue

The synthesis of the C2′-C3′ *trans*-isomer analogue is shown in Scheme 2-1A and Scheme 2-2, with the amide-bond forming reaction as a key step in the synthesis of **2.1**. Although amide-bond forming reactions have been shown to yield both *cis*- and *trans*-isomers,[86] it was applied as a key step here considering the outcome diversity would be beneficial to this project. Specifically, we exploited the facile *cis* to *trans* isomerization of the HATU-activated acid **2.3-I** prior to coupling with the amine resulting from **2.4** (Scheme 2-1). Previously, during this step, in route to preparing meayamycin, minor amounts, approximately 10% of *trans*-isomer **2.6** was obtained.

(A)

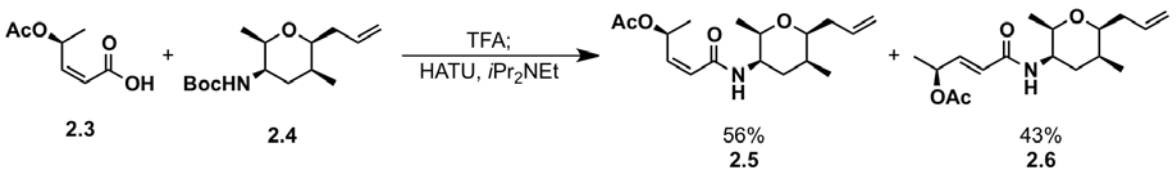

(B)

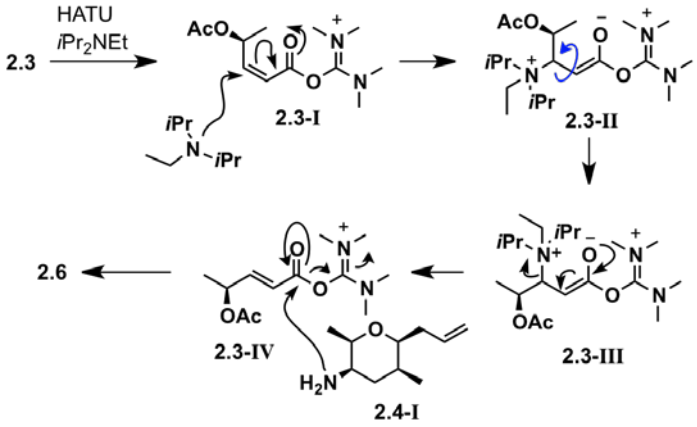

Scheme 2-1 (A) Synthesis of alkene **2.6** through isomerization. (B) Mechanism of isomerization of **2.3** during the amide-bond forming reaction.

To exploit on this observation, acid **2.3** was pre-mixed with HATU and *i*Pr$_2$NEt to deliberately isomerize the HATU-activated acid **2.3-I** to the *trans* form prior to addition of amine **2.4-I** to deliver **2.5** in 56% yield and **2.6** in 43% yield (Scheme 2-1). Transformation of **2.6** into carbamate **2.8** was accomplished through methanolysis of the acetate, and the resulting alcohol was treated with CDI followed by morpholine (Scheme 2-2). The resulting intermediate olefin **2.8** was exposed to methacrolein and ruthenium complex **Ru-1**[87] to furnish aldehyde **2.9** via a cross metathesis reaction. The Wittig reaction was then used to convert aldehyde **2.9** to diene **2.10**. The *trans*-side chain analogue **2.1** was then completed by exposure of diene **2.10** to alkene

2.11 in the presence of pre-catalyst **Ru-1** in 46% yield, after two recycling steps of the starting materials, **2.10** and **2.11**.

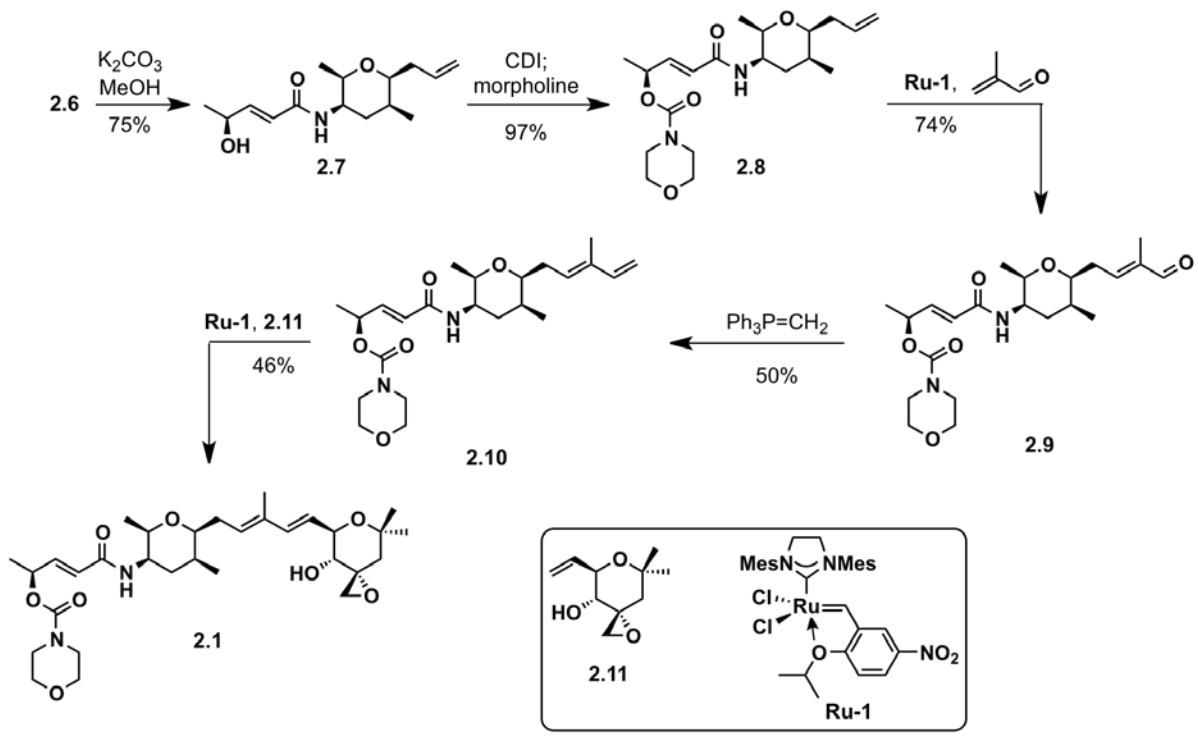

Scheme 2-2 Synthesis of *trans*- C2′-C3′ meayamycin B **2.1**.

2.1.2 Saturated C2′-C3′ analogue

The synthesis of the saturated C2′-C3′ isomer analogue of meayamycin B is illustrated in Scheme 2-3. The synthesis of the key carboxylic acid followed standard procedures, as summarized in Scheme 2-3. Commercially available (*S*)-ethyl lactate was transformed to carbamate **2.13**, followed by reduction to yield the aldehyde derivative. This aldehyde was coupled with $Ph_3P{=}CHCO_2Me$ via a Wittig reaction, followed by palladium-catalyzed

hydrogenation and subsequent hydrolysis to yield the key acid **2.14** in 46% yield over three steps.

Analogue **2.2** was then furnished as follows: protected amine **2.4** was converted to the free amine by exposure to TFA, then further coupled to acid **2.14** in the presence of HATU and *i*Pr_2NEt to yield alkene **2.15**. Treatment of alkene **2.15** with methacrolein and catalyst **Ru-1** afforded aldehyde **2.16**. The diene fragment **2.17**, constructed via the Wittig reaction from **2.16**, was subjected to olefin metathesis reaction with **2.11** and **Ru-1** to afford the saturated C2′-C3′ analogue **2.2** in 36% yield.

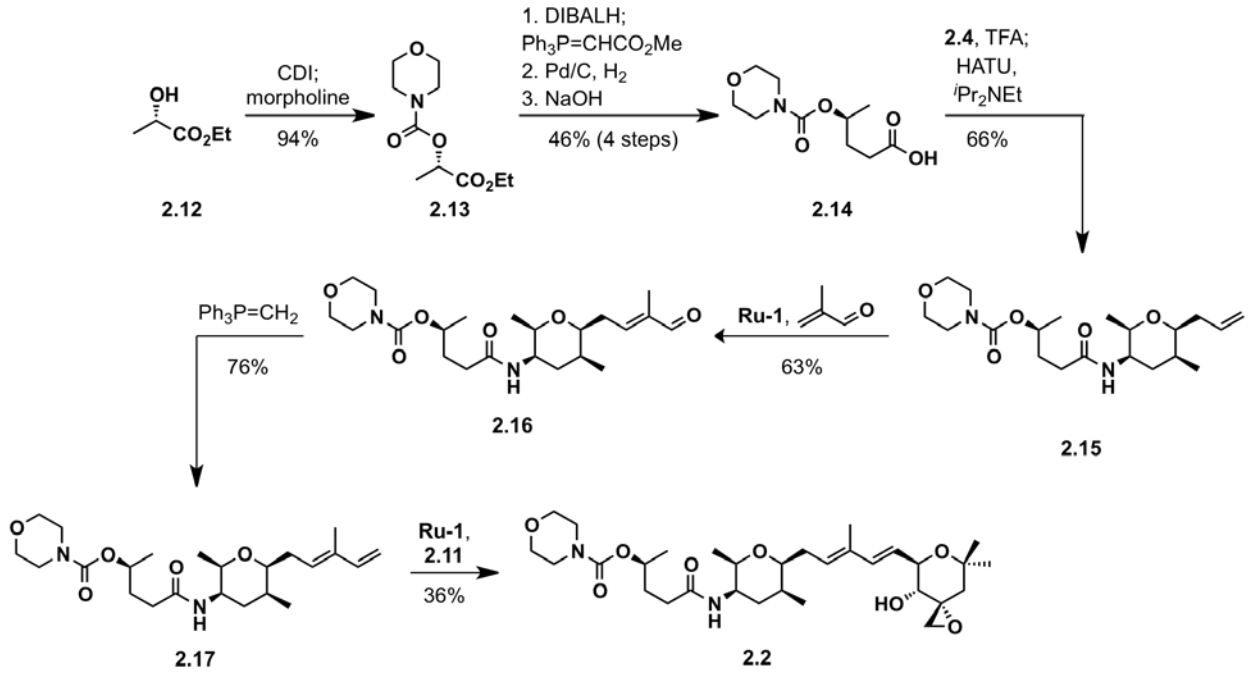

Scheme 2-3 Synthesis of saturated- C2′-C3′ meayamycin B **2.2**.

2.1.3 Antiproliferative evaluation of the *trans* C2′-C3′ and saturated C2′-C3′ analogues

The antiproliferative activities of the *trans* C2′-C3′ isomer **2.1** and saturated C2′-C3′ isomer **2.2** were evaluated in the MCF-7 breast cancer cell line. Growth inhibition was determined with the commercial 3-(4,5-dimethylthiazol-2-yl)-5-(3-carboxymethoxyphenyl)-2-(4-sulfophenyl)-2H-tetrazolium salt (MTS) dye reduction assay at a cell density of 4×10^3 cells per well. It is important to note that this assay involves the ability of these compounds to inhibit the growth of whole cells and that changes in biological activity may be unrelated to the ability of the compounds to interact with the target of FR901464.

We would expect to see a drop in antiproliferative activity of **2.2** to a similar degree as the non-epoxy analogues **1.3**, **1.5**, **1.7**, **1.8**, **1.9** (Figure 1-6, Table 1-2) if the enamide is a crucial electrophile as the epoxide. However, results showed that analogue **2.1** and **2.2** showed 3- and 4-orders of magnitude loss in potency, respectively, when compared to meayamycin B. Comparison of the GI_{50} values between FR901464 and *epi*-C4′-FR901464 (Jacobsen's analogue), show approximately 1-order of magnitude difference in activity, Figure 2-2. Likewise, 4′-desacetyl-meayamycin and *epi*-4′-desacetyl-meayamycin had a 1-order of magnitude difference in activity. Meanwhile, analogues **2.1** and **2.2** were 3- and 4-orders of magnitude difference in activity relative to meayamycin B, respectively. The drastic shift in orientation of C3′-C5′ in analogue **2.1** and the flexible nature of C2′-C5′ in analogue **2.2** is likely to explain the prominently reduced activity when comparing the *epi*-C4′-analogues to their parent derivatives, which are 1-order of magnitude different.

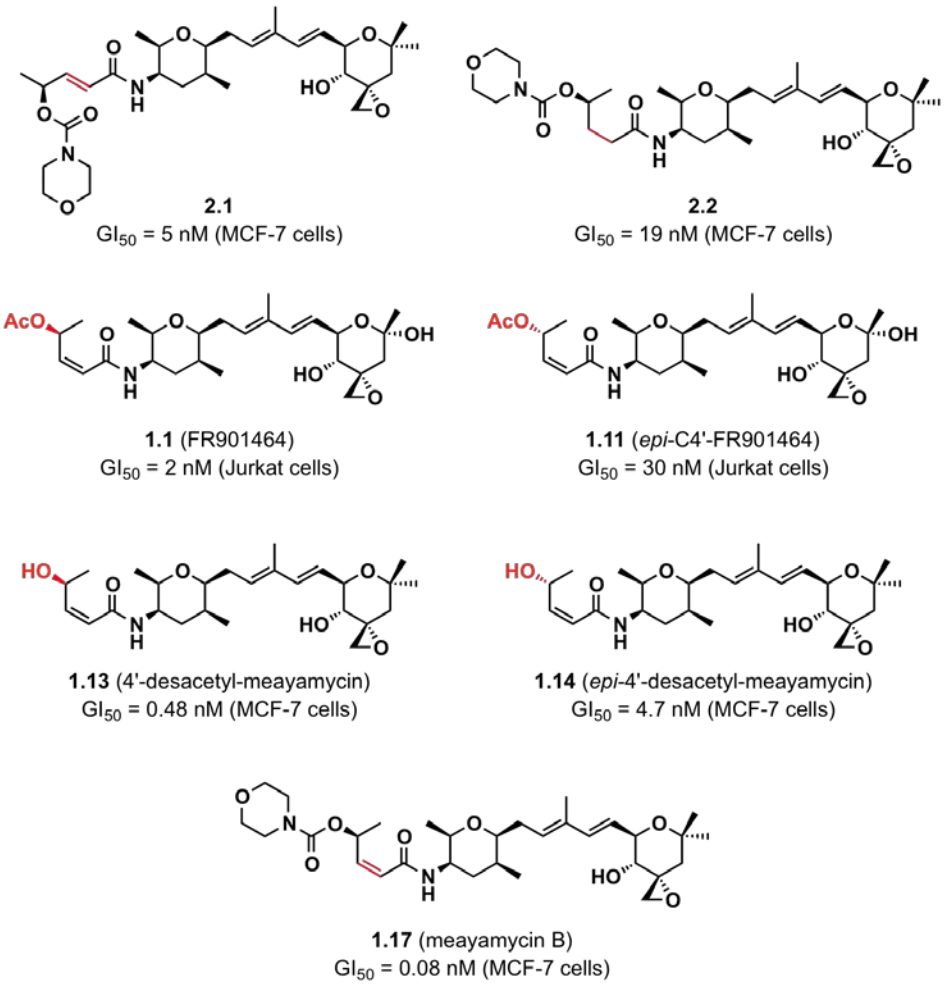

Figure 2-2 Chemical structures of the C2′-C5′ analogues unit of FR901464 and their corresponding antiproliferative activity, GI_{50}, and the cell-type tested.

2.1.4 Summary

The results from these studies, combined with the available SAR data addressing C1′-C5′ unit, strongly indicates that the side chain unit is sensitive to the positioning of the C4′-Me and C4′-H. These results also suggest that the *cis* C2′-C3′ enamide is not an electrophile but, rather, could be a structural requirement for optimum binding to the target biomolecule, though a

spliceosomal-binding assay is necessary to understand if the analogues exhibit strong or weak binding to the spliceosome.

2.2 EVALUATION OF MEAYAMYCIN AND ANALOGUES IN VIVO[1]

Although FR901464 was tested in xenograft models prior to the pladienolides, its progress in terms of drug development lags behind. Studies of FR901464 and its analogues through total chemical syntheses and biological analyses have provided substantial insights into the SAR of FR901464. Here, is reported preliminary studies of meayamycins *in vivo* in collaboration with Southern Research Institute.

2.2.1 Antiproliferative activity of meayamycin and meayamycin B

Working together with Nancy Czaicki, Brian Albert and Dr. Miaosheng Li (previous members of the Koide group), the antiproliferative activities of meayamycin and meayamycin B were determined against various human cell lines. Meayamycin was found to inhibit the growth of all of the tumor cell lines tested, with GI_{50} values ranging from 10 pM to 1230 pM (Table 2-1).[29] The antiproliferative activity of meayamycin was also seen in the nontumorigenic cell lines NHDF, NHFL, HMEC and HUVEC (Table 2-1). On the other hand, the more biologically stable analogue, meayamycin B, was 3.1 ± 1.9 times more potent than meayamycin against MCF-7, MDA-MB231, A549, DU145, HCT-116, H1299, and PC-3 cell lines.[24]

---

[1] This section was published in: S. Osman, W. R. Waud, G. S. Gorman, B. W. Day, K. Koide, *Med. Chem. Commun.* **2011**, *2*, 38.

Table 2-1 Antiproliferative activity of Meayamycin, Meayamycin B, Meayamycin C, Doxorubicin and Bortezomib.

	GI_{50} (nM)				
Cell line	Meayamycin	Meayamycin B	Meayamycin C	Doxorubicin	Bortezomib
MCF-7	0.020	0.0080	0.4	ND	ND
MDA-MB231	0.070	0.015	1.1	ND	ND
A549	0.26	0.18	ND	ND	ND
DU145	1.2	0.2	ND	ND	ND
H1299	0.84	0.15	ND	ND	ND
PC3	0.20	0.10	ND	ND	ND
HCT-116	0.070	0.0040	1.4	70	5
NHDF	0.44	ND	39	462	334
NHLF	0.91	ND	12	223	1.7
HMEC	0.11	ND	9	276	3.5
HUVEC	0.060	ND	4	109	1.1

NHDF = normal human dermal fibroblasts. NHLF = normal human lung fibroblasts. HMEC = human mammary epithelial cells. HUVEC = human vein endothelial cells. ND = not determined.

2.2.2 Evaluation of meayamycins' *in vivo*

Subsequently, an *in vivo* study was initiated with Southern Research Institute to determine whether the compounds could inhibit tumor growth in HCT-116 and PC-3 xenograft models.[88] First, maximum tolerated doses of meayamycin and meayamycin B were determined. Doses for both compounds ranged from 0.03 to 3 mg kg^{-1}/inj administered intravenously on a Q4D×3 schedule (Figure 2-3A and B). The treated animals were monitored for weight loss and mortality. No considerable weight loss or deaths were observed in any of the mice during or after treatment, except that a maximum average body weight loss of 11% was observed with meayamycin B at a dose of 3 mg kg^{-1}/inj (Figure 2-3B). Meayamycin B was also tolerated at a

different dosing schedule, Q1D×5, at doses of 0.5 and 1.0 mg kg^{-1}/inj. A dose of 1.0 mg kg^{-1}/inj led to only a maximum average body weight loss of 10%. Higher doses (1.5–6.0 mg kg^{-1}/inj) were lethal for mice (Figure 2-3C). Webb and coworkers designed structurally simpler analogues that were tolerated at much higher doses (≤50 mg kg^{-1} at a Q1D×5 schedule), but that may be attributed to the lower antiproliferative activity (GI_{50} were at high nM to single-digit μM).[4] These data show that doses of meayamycin and meayamycin B can be administered safely by the intravenous route on Q4D×3 and Q1D×5 schedules.

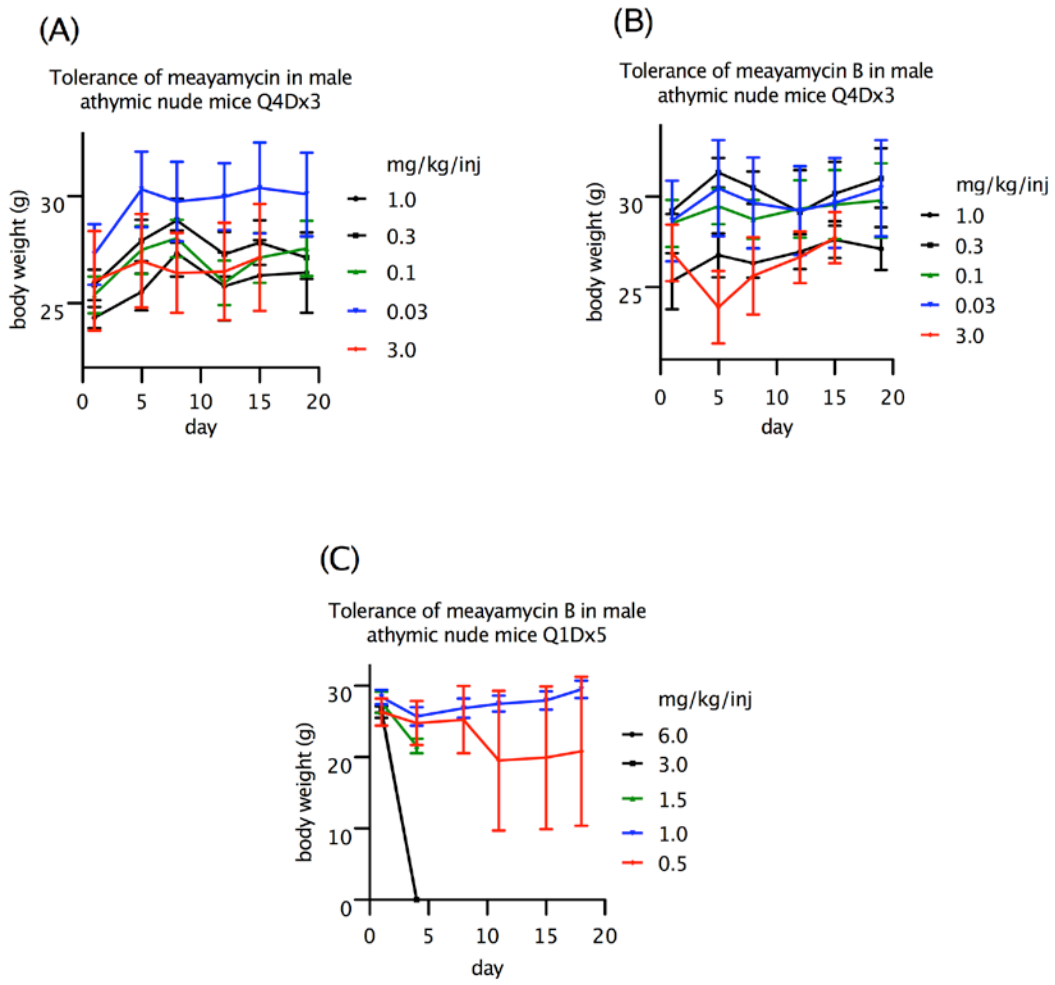

Figure 2-3 Dose tolerance of meayamycin and meayamycin B in mice.

(A) Tolerance of meayamycin in male athymic nude mice Q4D×3. (B) Tolerance of meayamycin B in male athymic nude mice Q4D×3. (C) Tolerance of meayamycin B in male athymic nude mice Q1D×5. n = 3.

The *in vivo* antitumor activity of meayamycin and meayamycin B was initially evaluated in the HCT-116 xenograft model in mice. Dosing schedule studies revealed that intravenously administered meayamycin and meayamycin B achieved inhibition rate (IR = [1-(median tumor

weight treated/median tumor weight control)] × 100%) values of 24% (Day 41) and 41% (Day 41), respectively, using a Q4D×3 dosing schedule (Figure 2-4A and B). With the low IR values of both meayamycin and meayamycin B, we decided to increase the frequency of injections. We chose meayamycin B for this experiment because meayamycin B was more stable than meayamycin in mouse serum ($t_{1/2}$ = 13 h vs. 2 h).[24] Due to the availability of xenograft models at the time, we switched from HCT-116 to PC-3 in the next study. Against the PC-3 tumor xenograft, meayamycin B elicited an IR of 26% on Day 22 using a Q1D×5 dosing schedule (Figure 2-4C). A higher dose was lethal to mice at this injection frequency, which limited our window of optimizations. In HCT-116 tumor xenografts, paclitaxel exhibited an IR of 81% on Days 41 and 44 using a Q1D×5 dosing schedule.

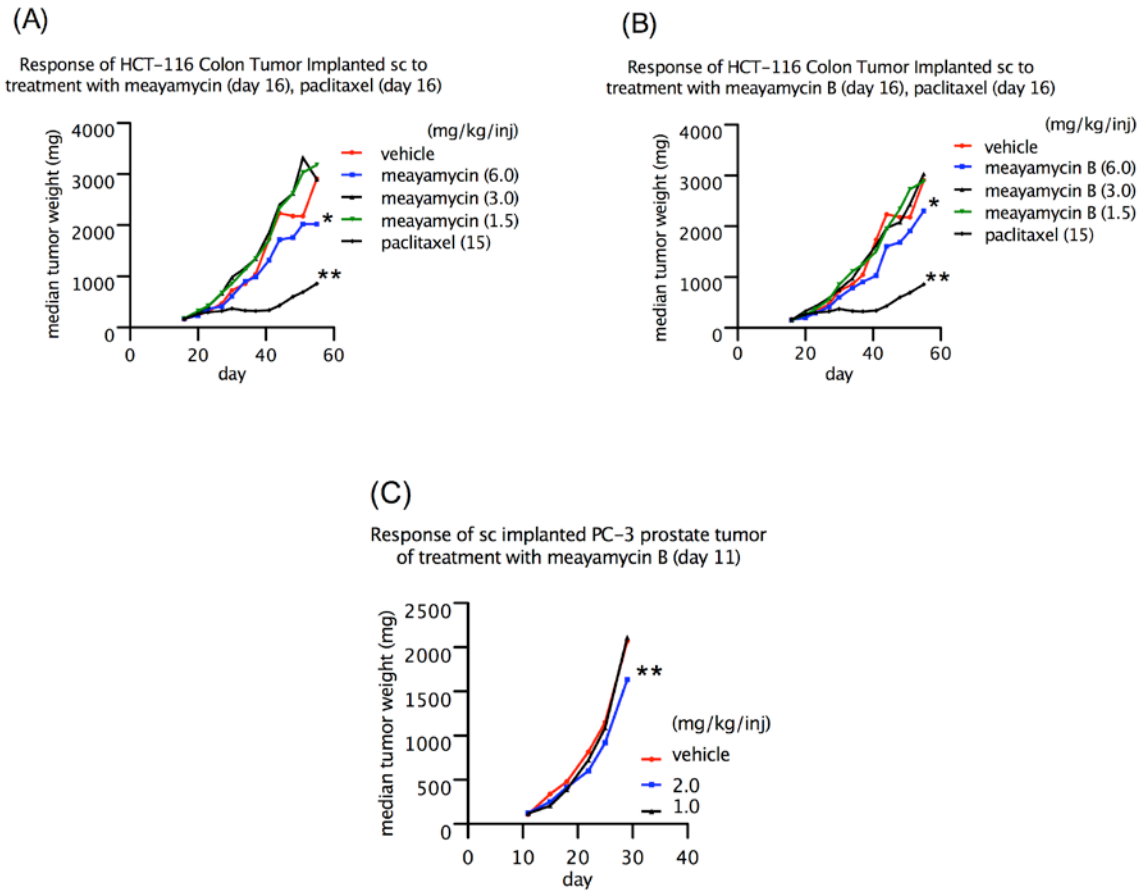

Figure 2-4 Activity of meayamycin, meayamycin B and paclitaxel in human tumor models. (A) Response of HCT-116 tumor implanted subcutaneously to treatment with meayamycin (Day 16) and paclitaxel (Day 16). (B) Response of HCT-116 tumor implanted subcutaneously to treatment with meayamycin B (Day 16) and paclitaxel (Day 16). (C) Response of PC-3 tumor implanted subcutaneously to treatment with meayamycin B (Day 11). Statistical significance was evaluated by comparing the time to 2 tumor mass doubling values of vehicle-treated groups to drug-treated groups. *P* values of less than 0.05 were considered statistically significant. * signifies 0.05<*p*0.8 (statistically not significant), and ** signifies $p<0.05$. n = 10.

Unlike E7107, meayamycin and meayamycin B did not show clear-cut antitumor activity in xenograft models. It was questioned if the compound achieved an adequate plasma concentration in mice. A single dose of meayamycin B (1 mg/kg) was intravenously administered to female non-tumor-bearing athymic nude mice. The study illustrated that less than 1% of the injected meayamycin B was found in plasma within 30 minutes after administration (Figure 2-5). A glucuronidated meayamycin B metabolite exhibited the strongest signal in the mass spectrometric evaluations when compared to other detected metabolites. This result led to the hypothesis that meayamycin C, an alkylated derivative of meayamycin B, might be resistant to glucuronidation.

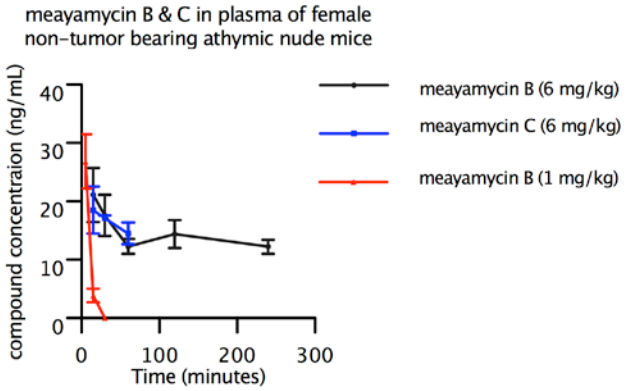

Figure 2-5 Plasma mean concentration time profiles of meayamycin B and meayamycin C in plasma of female non-tumor bearing athymic nude mice. n = 3 for each time point.

2.2.3 Meayamycin C

4-*O*-Alkyl FR901464 analogues were prepared and evaluated by others.[26] However it was not clear whether the loss of activity was due to the large alkyl groups or the loss of a hydrogen bond donor. To answer this question, meayamycin C was synthesized as illustrated in Scheme 2-4. Methylation of alcohol **2.11** followed by cross metathesis yielded meayamycin C. On a side note, it is noteworthy to mention that the olefin cross metathesis of **2.19** with **2.18** was reproducibly higher yielding than that with **2.11**, mostly because **2.18** showed minimal homodimerization while **2.11** always presented substantial homodimerized product. This difference proved to be crucial in the preparation of C8-C9-cyclopropyl analogues by Yangping Wang in our research group.[24]

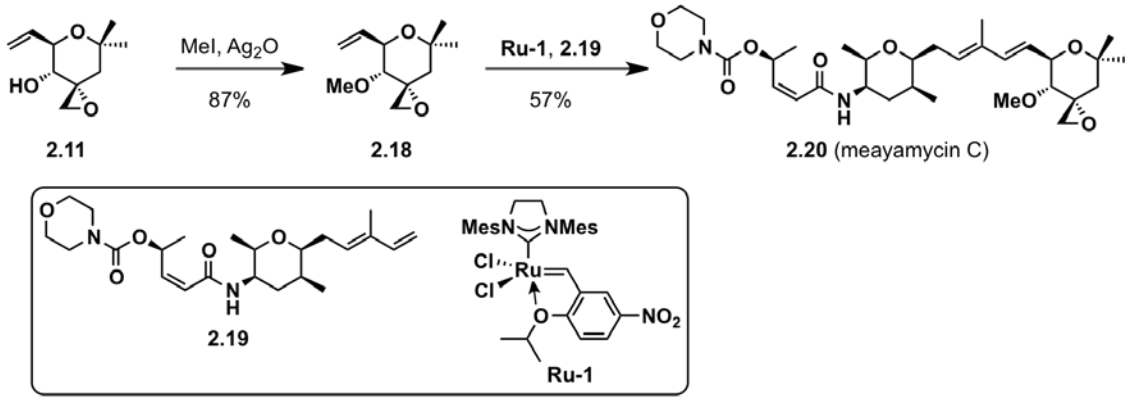

Scheme 2-4 Synthesis of meayamycin C.

Meayamycin C displayed sub- to single-digit nanomolar GI_{50} values against MCF-7, MDA-MB231 and HCT-116 cancer cell lines (Table 2-1). Meayamycin C retained potency to a slightly lesser extent against the normal cell lines NHDF, NHLF, HMEC and HUVEC with GI_{50} values ranging from 4 to 39 nM (Table 2-1). These results, together with previously reported

data, showed that all the FR901464 derivatives used in this study exhibited strong antiproliferative activity against these cell lines. The order of potency was meayamycin B > meayamycin > meayamycin C. Despite the potency of meayamycin and meayamycin C in cancer and non-cancerous cells, the therapeutic index increased from meayamycin to meayamycin C (if, *e.g.*, one compares GI_{50} in the HCT-116 cell line and the non-cancerous cell lines in Table 2-1). The therapeutic index for meayamycin is 6 (NHDF cell line), 2.7 (NHLF cell line), 1.6 (HMEC cell line), and 1 (HUVEC cell line). On the other hand, the therapeutic index for meayamycin C is 15 (NHDF cell line), 4.6 (NHLF cell line), 3.5 (HMEC cell line), and 1.5 (HUVEC cell line). This indicates that there is some degree of selectivity of meayamycin C towards the HCT-116 cancer cell line. This quantitative analysis should be met with caution because the margin of error could be greater when the growth inhibition of nontumorigenic cells was measured. Doxorubicin inhibited HCT-116 cancer cell proliferation with a GI_{50} of 70 nM, while in the normal cell lines NHDF, NHLF, HMEC, and HUVEC, its GI_{50} ranged from 109 to 462 nM (Table 2-1). Velcade displayed single digit nanomolar GI_{50} against these cancer and normal cell lines, except towards NHDF cell line, which was less sensitive (Table 2-1). Taken together, the data from these cell lines demonstrated that all of the meayamycin derivatives retained potent antiproliferative activity in tumor cells derived from a variety of organs and showed similar *in vitro* selectivity to the clinically used anticancer drugs doxorubicin and bortezomib.

Meayamycin C's plasma concentrations were evaluated by Southern Research Institute in female non-tumor-bearing mice after intravenous administration. The plasma concentrations of meayamycin C fell quickly within 1 h after injection and remained below 10 ng/mL for the next 4 h, suggesting that the glucuronidation of meayamycin B was not the major reason for its poor pharmacokinetics and efficacy (Figure 2-5).

2.2.4 Summary

In summary, the meayamycins displayed broad-spectrum antiproliferative activity, and meayamycin B exhibited minimal antitumor efficacy with Q4D×3 and Q1D×5 dosing schedules and no noticeable side effects in the HCT-116 and PC-3 xenograft models. The minimal antitumor efficacy of meayamycin B may be attributed to the poor PK profiles of meayamycin B and C in mice. The mechanism underlying this observation is unclear. Further pharmacokinetics, antitumor efficacy, and toxicological studies are needed to evaluate this promising new avenue in cancer treatment.

2.3 SYNTETHIC EFFORTS TOWARDS A REVERSIBLE GROWTH INHIBITOR BASED OF MEAYAMYCIN B

Splicing inhibitors based on the structure of FR901464, exemplified by meayamycin B (Figure 1-8), are generally believed to exert their biological effects through targeting SF3b. SAR studies on FR901464 have revealed that the presence of the spiroepoxide moiety is required. In addition, the epoxide might be a reactive moiety necessary for covalently modifying irreversibly a nucleophilic residue at the active site of SF3b, but epoxides are also, in general, prone to hydrolysis in a reaction catalyzed by epoxide hydrolases *in vivo*.

The possible irreversible binding of FR901464-type compounds to SF3b could also lead to possible dose-limiting side effects. An example of such a case is an analogue of fumagillin,

TNP-470, that contains a crucial spiroepoxide, which has undergone clinical studies for a variety of cancers.[89] TNP-470 is a type 2-methionine aminopeptidase (MetAP2) inhibitor. Although TNP-470 has shown therapeutic benefits in clinical studies, toxic side effects are a serious limiting factor. It has been reasoned that these unwanted side effects are partly linked to the irreversible character of the inhibition and the presence of reactive groups in the molecule (Figure 2-6).[89] As a result, a MetAP2 reversible inhibitor, fumagalone, was prepared. Through semi-synthesis the spiroepoxide in fumagillin responsible for covalent modification of MetAP2 was converted into an aldehyde, and shown to have antiproliferative properties and reversible MetAP2 inhibition.[89]

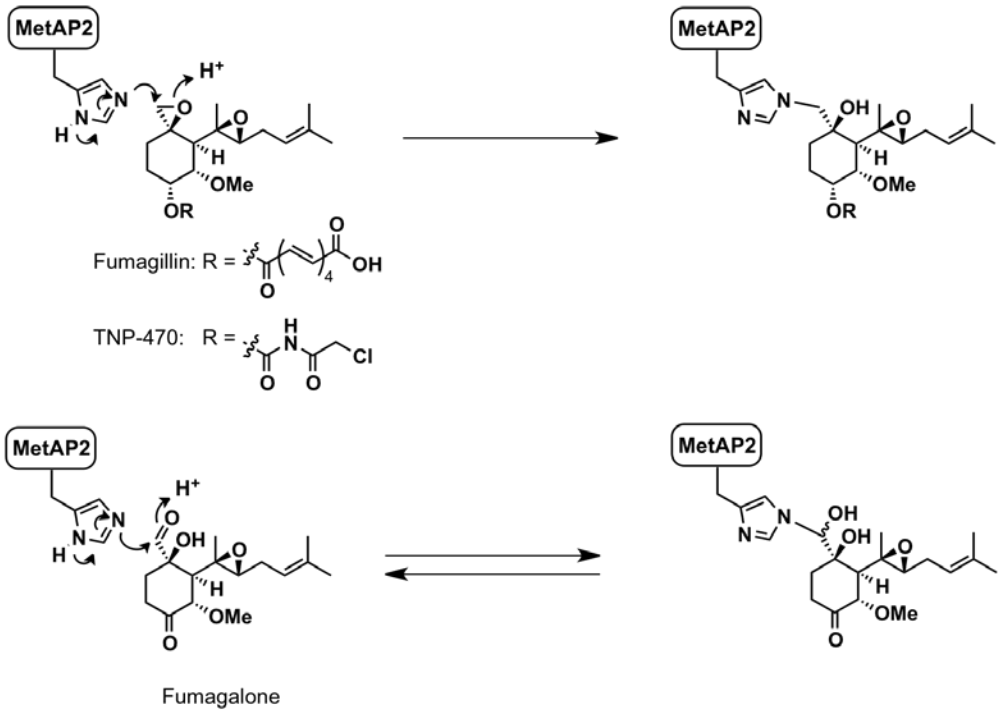

Figure 2-6 General mechanism of MetAP2 with fumagillin and analogues. (**top**) Representation of fumagillin and TNP-470 irreversibly labeling the active site of MetAP2. (**bottom**) Representation of fumagalone reversibly labeling the active site of MetAP2.

As part of an ongoing program aimed at developing new FR901464-based anticancer compounds with pre-mRNA splicing inhibition and different pharmacological properties, a similar approach was used for the medicinal chemistry of fumagillin. The synthetic efforts in this area include a reversible inhibitor of SF3b based on FR901464/meayamycin B, which became not only an interesting intellectual challenge but also a good candidate for developing new pre-mRNA splicing inhibitors that are likely to be less toxic than meayamycin B. As a first step toward a reversible pre-mRNA splicing inhibitor, the spiroepoxide in meayamycin B, presumably responsible for covalent modification of SF3b, was changed to an aldehyde. Because the spiroepoxide group in FR901464 and meayamycin B can react with a nucleophilic residue, it was reasoned that the replacement of the spiroepoxide with an aldehyde would retain the electrophilicity at C18, and it was anticipated that the nucleophilic residue would react with the aldehyde in a reversible fashion.

2.3.1 Efforts towards an aldehyde derivative of meayamycin B

Synthetic efforts began with an epoxide rearrangement to an aldehyde strategy, which was successfully applied to similar spiroepoxides in complex molecules.[90,91] The decision to use a protected derivative of **2.11** was based on the observation that **2.11** would undergo ring contraction in the presence of acid (HF) to yield aldehyde **2.23**, illustrated in Scheme 2-5.

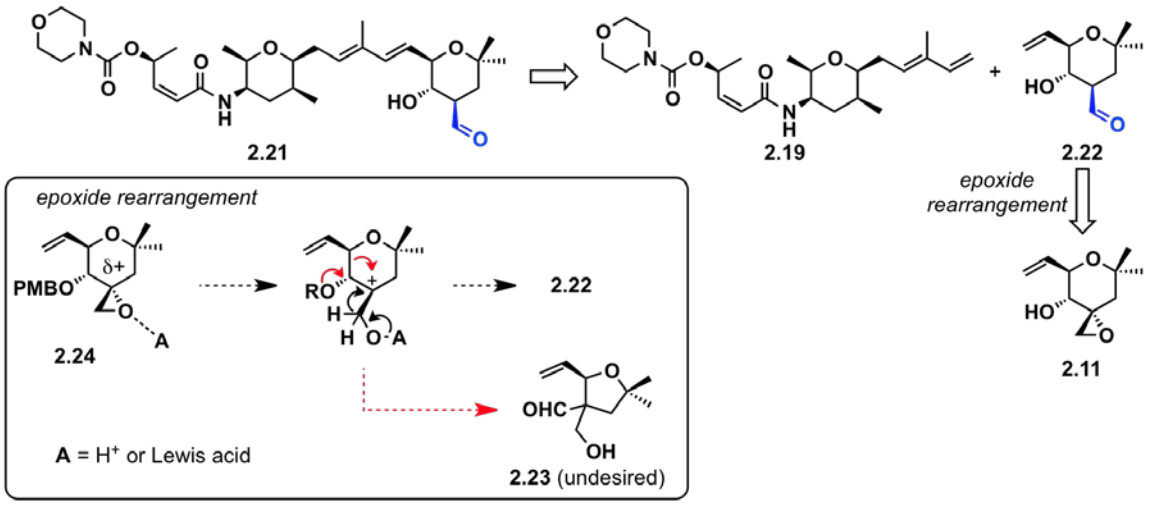

Scheme 2-5 Retrosynthetic approach to prepare the aldehyde derivative of meayamycin B.

Therefore, it was anticipating that **2.24** would not undergo this undesired reaction. A Lewis acid should open epoxide **2.24** to generate a tertiary cation, which could then undergo a 1,2 hydride shift to form aldehyde **2.22**. However, when **2.24** was treated with a variety of Lewis acids, only decomposition or formation of the ring contracted product **2.23** were obtained, and no 1,2-hydride-shift product was isolated (Scheme 2-6, Table 2-2). At this point, we learned that ring contraction was highly favored over the hydride shift, which required for a different strategy to generate the desired aldehyde, or a new compound all together. Further attempting to promote this rearrangement transformation were abandoned, and a new compound was synthesized.

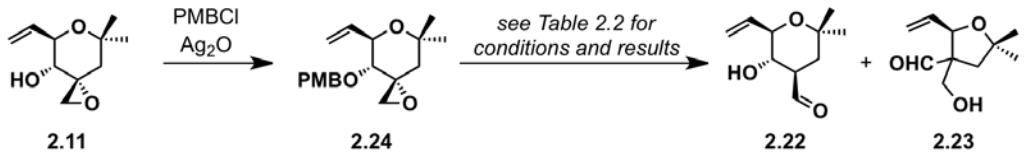

Scheme 2-6 Synthetic efforts to prepare **2.22**.

Table 2-2 Conditions for the rearrangement of **2.24**.

		Yield (%)	
Entry	Conditions	**2.22**	**2.23**
1	BF_3•OEt_2, benzene, 0 °C	not detected	95%
2	BF_3•OEt_2, toluene, -78 °C,	not detected	quantitative
3	Cp_2ZrCl_2, AgOTf, CH_2Cl_2, 25 °C	not detected	50%
4	$TiCl_4$, CH_2Cl_2, -78 °C	not detected	66%

2.3.2 Ketone derivative of meayamycin B

The spiroepoxide was replaced with a carbonyl to yield a ketone derivative of meayamycin B. The rationale was that with this type of replacement, the electrophilicity is retained and that the anticipated nucleophile would react reversibly. It was not certain, however, whether the electrophilic carbon at a different position would diminish the activity. Based on previous SAR data generated by Jacobsen and coworkers,[20] the diastereomeric epoxide was only 2-fold less active than the natural epimer, which indicates that there is no stringent spatial orientation for the electrophilic carbon to label the nucleophilic residue on the biomolecule.

The synthesis of the ketone-variant of meayamycin B, **2.26**, commenced with the preparation of ketone **2.25**. For a detailed discussion of how **2.25** was prepared, please refer to Section 2.5. Cross metathesis of **2.25** with **2.19** delivered **2.26** in 36% yield (Scheme 2-7).

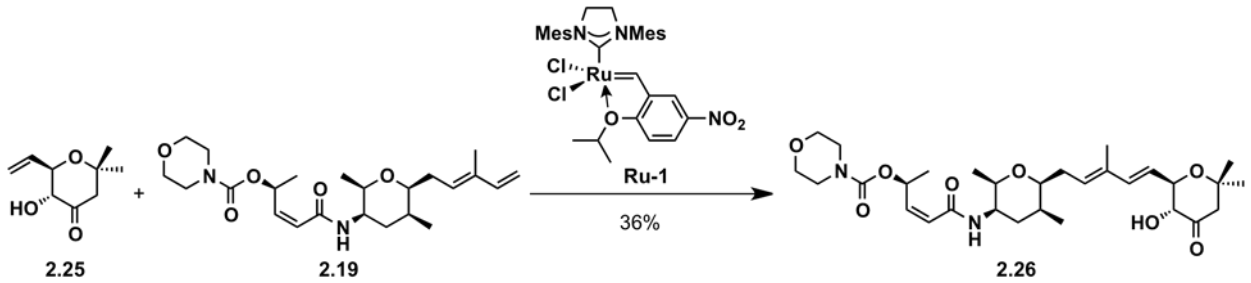

Scheme 2-7 Synthesis of ketone derivative of meayamycin B, **2.26**.

The ability of ketone **2.26** to inhibit the growth of human cancer cells was assessed in a cell-based proliferation assay using MTS as an estimate of relative viable cells. The GI_{50} values were interpolated from 10-point (minimum) dose-response curves. Treatment with ketone **2.26** resulted in GI_{50} values of sub-single digit nM against proliferating A549 and HCT-116 cell lines, and 1 – 20 nM against various human head and neck cancer cell lines, Table 2-3 (the data in Table 2-3 was generated with a combined effort of Ms. Yang Gao - Ph.D. candidate in the Koide group - and myself). Overall, ketone **2.26** is approximately 1 – 2 orders of magnitude less active than meayamycin B.

Table 2-3 Antiproliferative activity of **2.26** and meayamycin B.

Cell line	GI_{50} (nM)	
	2.26	meayamycin B
A549	0.24 ± 1.30	0.18 ± 0.02
HCT-116	0.20 ± 0.10	0.0040 ± 0.0043
UD-SSC2	1.54 ± 0.30	0.23 ± 0.21
UPCI-SSC90	3.2 ± 4.10	0.13 ± 0.11
93-VU-147T	7.3 ± 4.80	0.34 ± 0.26
UM-22B	26.0 ± 26.0	2.9 ± 3.3
UM-SSC47	1.90 ± 1.40	0.15 ± 0.02
PCI-30	20.5 ± 12.1	0.94 ± 1.00
PCI-13	12.1 ± 11.3	≤4.8
JHU-020	11.3 ± 3.00	0.31 ± 0.14

UD-SSC2, UPCI-SSC90, 93-VU-147T, UM-22B, UM-SSC47, PCI-30, PCI-13, JHU-020 are all variants of human head and neck cancer cell lines.

For A549, vincristine displayed GI_{50} = 35 ± 3.2 nM. For HCT-116, cisplatin displayed GI_{50} = 3.9 ± 1.4 μM. For all head and neck cancer cell line, 5-FU displayed GI_{50} in the range between 12 ± 12 μM and 0.15 ± 0.2 μM. All the growth inhibtion assays in the table were performed in parallel.

To determine whether ketone **2.26** reversibly inhibits growth of cancer cells, studies using transient exposure of ketone **2.26** followed by outgrowth in the absence of the compound were performed (Figure 2-7, 2-8).[29,55] Cells were exposed to ketone **2.26** at approximately GI_{90} (10 nM) for the indicated times (Figure 2-7B), followed by outgrowth in the absence of the compound for a total of 5 days. Transient exposure (HeLa cells requires 24 h, A549 and MDA-MB231 cells require 8 h) to 10 nM ketone **2.26** results in complete inhibition of outgrowth of the HeLa, A549 and MDA-MB231 cell poplulation. Additionally, after exposure of ketone **2.26** or vehicle to A549 cells for 8 h then removal of **2.26** or vehicle, followed by continuous monitoring

of cell growth, virtually no cell proliferation was recovered for **2.26**-treated cells (Figure 2-8). These data demonstrate that ketone **2.26** irreversibly inhibits cell proliferation.

(A)

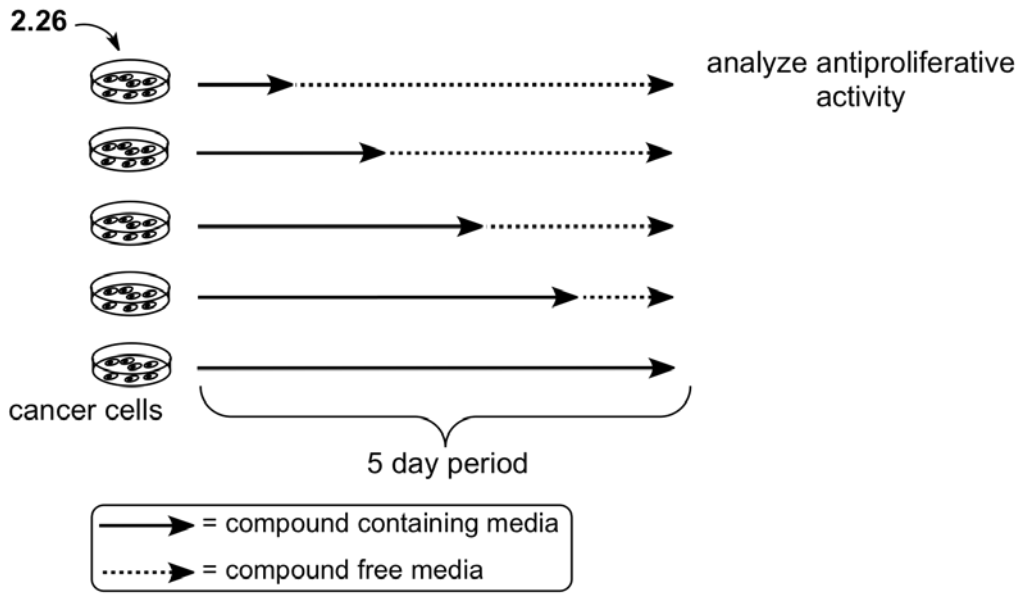

(B)

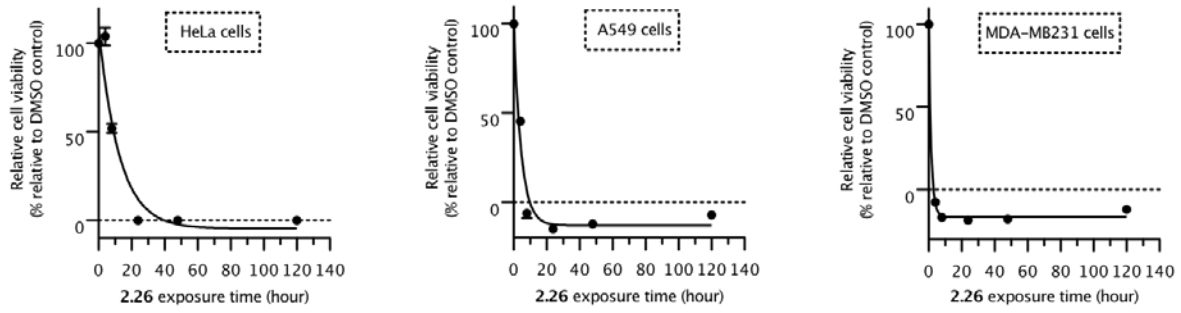

Figure 2-7 Reversibility test.

(A) Representation of growth inhibition reversibility experiment design. (B) Exposure time-dependent growth inhibition of cells (HeLa, A549, and MDA-MB231) in the presence of **2.26** at 10 nM for the indicated periods of time. Cell viability was measured on day 5 by MTS assay.

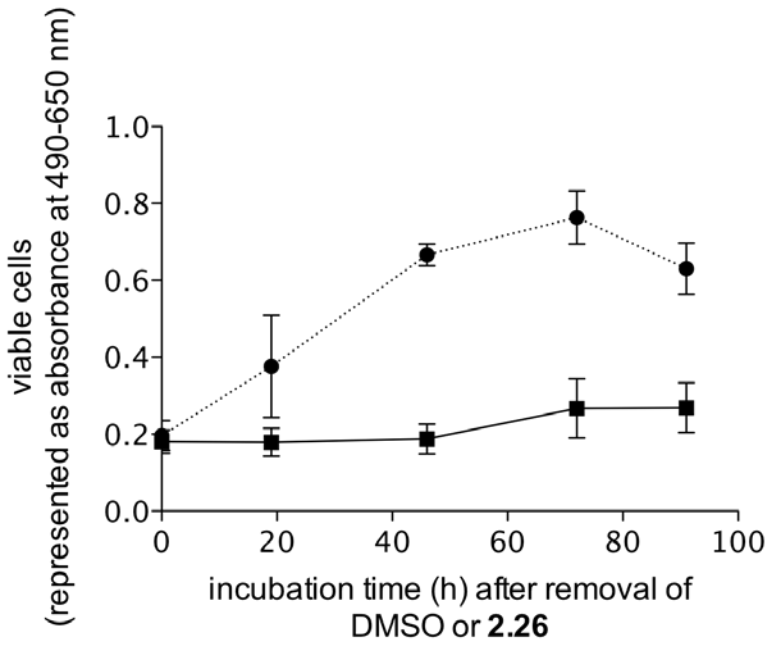

Figure 2-8 A549 cell growth upon treatment with DMSO (*circles*, *dashed line*) or 10 nM **2.26** (*squares*, *solid line*). Number of viable cells was measured by MTS assay.

2.3.3 Summary

Results from this study demonstrate that transient treatment of MDA-MB231, A549 and HeLa cells with ketone **2.26** shows growth inhibition profiles similar to those seen with cells treated with ketone **2.26** for 5 days. These data suggest that in these cell lines, **2.26** might bind irreversibly to its target biomolecule. On the other hand, **2.26** might bind reversibly and induce irreversible cell growth arrest. Detailed binding assay studies are needed to precisely determine the nature of the interaction of **2.26** with its biological target.

While the decrease in potency upon replacement of an epoxide with a ketone, a potentially reversible spliceosome inhibitor, may be an inevitable sacrifice, there is a relatively

large margin to accommodate such a loss in activity, given the extremely high potency of the epoxide-containing precursors. On the basis of the results reported here, we have begun to synthesize the second generation of non-epoxy meayamycin B derivatives to further probe the structure-activity relationship of this new class of pre-mRNA splicing inhibitors. To correlate the effects of ketone **2.26** on cell growth and survival with specific biochemical effects, we began investigating pre-mRNA splicing kinetics interrupted by ketone **2.26**. It will be interesting to determine whether meayamycin B-based none-epoxy containing compounds will have improved pharmacological properties in comparison with meayamycin B.

2.4 TEGYLATED ANALOGUES OF MEAYAMYCIN WITH UNEXPECTED POTENCIES

A long-term goal in the Koide group is to develop FR901464-based probes through conjugation chemistry to study FR901464's biological properties and SF3b. Toward this goal, incorporation of an azide functionality within meayamycin was planned due to the bioorthogonal reactivity of azides with alkynes.

2.4.1 TEGylated meayamycin

These efforts began with trying to install a triethylene glycol containing terminal azide at the C4′-hydroxy group. This site was chosen because the available SAR data indicate this site is more tolerable to large groups relative to the C4-hydroxy group.

Acetate **2.27** was hydrolyzed and then treated with CDI followed by amine **2.29** to deliver azide **2.30**. Cross metathesis between **2.30** and **2.11** failed under various heating and different solvent conditions (Scheme 2-8, Table 2-4). It was not clear from these data whether the azide of the triethylene glycol chain was to blame for this unsuccessful transformation. In order to partially address this concern, azide **2.33** was prepared through exposing allylic alcohol-**2.32** to diphenylphosphorylazide and diisopropylazodicarboxylate. Efforts to couple **2.33** with **2.11** failed to deliver **2.34** (Scheme 2-9A). In the literature there are no examples that illustrate the success of the olefin cross metathesis in the presence of an azide functionality, except for an isolated example by Seeberger and coworkers.[92] Seeberger and coworkers' transformation was successful likely because the azide is relatively hindered, thereby not capable of reaching the ruthenium pre-catalyst (through personal communication, Professor Verdine and coworkers experienced similar difficulties with their olefin cross metathesis in the presence of azide groups). A control experiment (Scheme 2-9B) between alkene **2.35** and acetate **2.36** failed to deliver cross coupled products neither isomerization (91% of the azide was recovered), which indicated that the azide is responsible for the unsuccessful transformation in Scheme 2-8 and Scheme 2-9A.

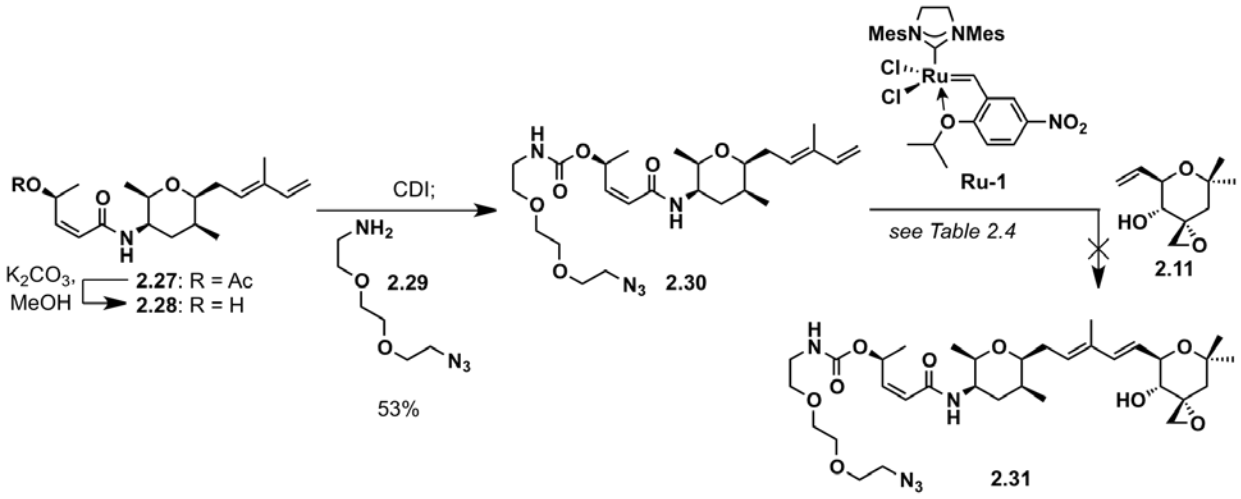

Scheme 2-8 Efforts toward the synthesis of carbamate **2.31**.

Table 2-4 Cross metathesis conditions attempted in efforts to prepare **2.31**.

Additive	Solvent	Temperature (°C)
none	1,2-dichloroethane	50 → 80
$Ti(O^iPr)_4$	1,2-dichloroethane	50 → 70
none	THF	50 → 70
none	MeOH	50 → 70
none	toluene	50 → 90

(A)

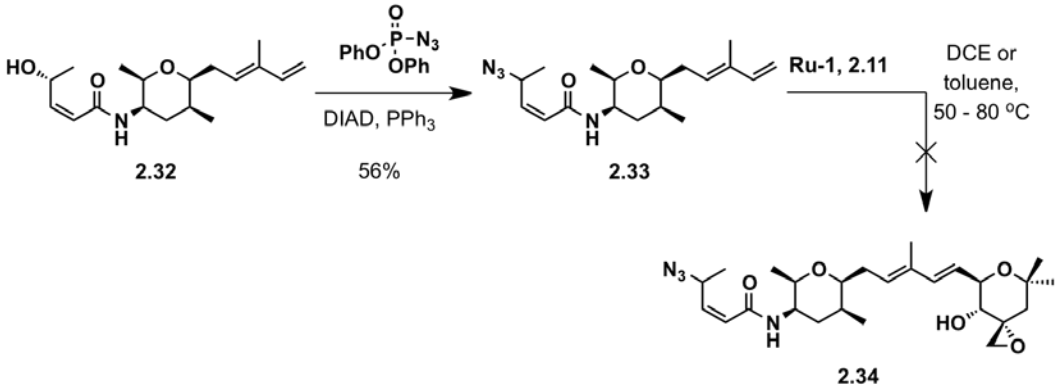

(B)

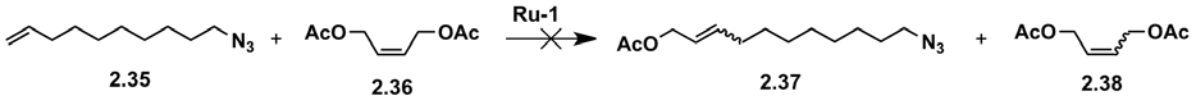

Scheme 2-9 (A) Efforts towards the preparation of azide **2.34**. (B) Control experiment for the effect of the azide group in the cross metathesis reaction.

Based on the above data, a different strategy was taken. It was decided to prepare a derivative of meayamycin C, where the C4-hydroxy group is already protected, and the C4′ is available for functionalization. Methyl ether **2.18** was coupled with allylic alcohol **2.28** to yield desacetyl-meayamycin C **2.39** in 35% yield after 2 recycling steps. Purification of this product was very laborious and yield of this transformation was lower than usual, hence the two recycling rounds. The low yield could be partially attributed to significant amount of *trans*-C2′-C3′ derivative of either **2.28** or **2.39** observed by the ^{1}H NMR spectrum of the crude reaction mixture (Figure 2-9). However, enough amounts of pure **2.39** were isolated in attempts to functionalize C4′-OH. Attempts to functionalize **2.39** either with CDI then amine **2.29**, or isocyanate **2.41** all failed to deliver **2.40** (Scheme 2-10). The results were either no reaction, or

after harsher conditions (i.e., heating) led to numerous by-products as judged by TLC analysis and loss of the epoxide after ^{1}H NMR analysis. Since efforts to install an azide functionality on the 4′-hydroxy group of 4′-desacetyl meayamycin failed, our attention was turned to the 4-hydroxy group. There was skepticism about this approach because the aforementioned SAR data predicted that functionalizing 4-hydroxy group would diminish the potency of meayamycin.[24,26] Nonetheless, meayamycin was treated with NaH and tosylate **2.42** to form tetraethylene glycolated (TEGylated) meayamycin **2.43** (Scheme 2-11). Pleasant surprise was that this new analogue **2.43** was nearly as potent as meayamycin (Table 2-5).

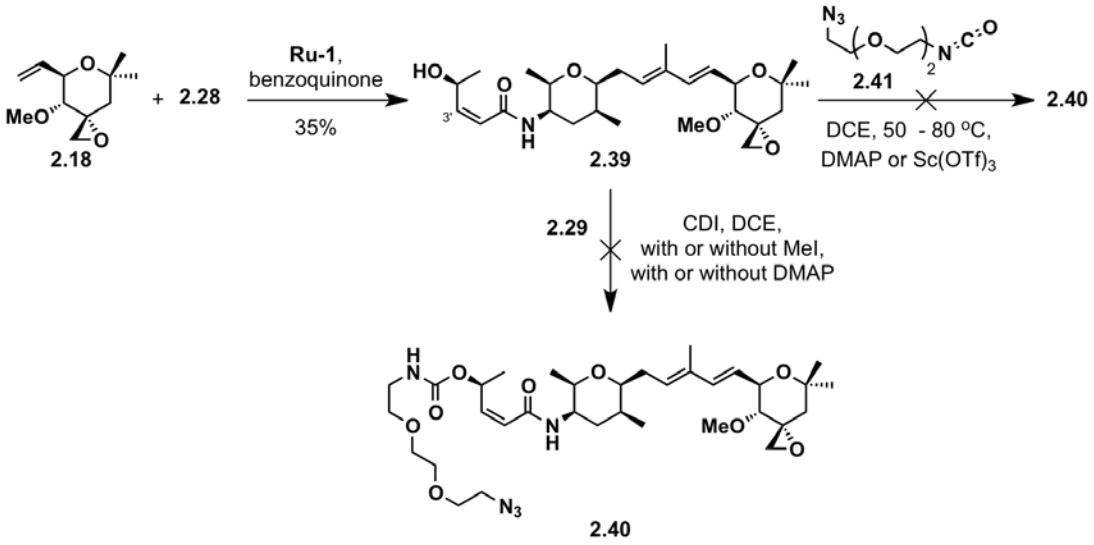

Scheme 2-10 Efforts towards the synthesis of carbamate **2.40**.

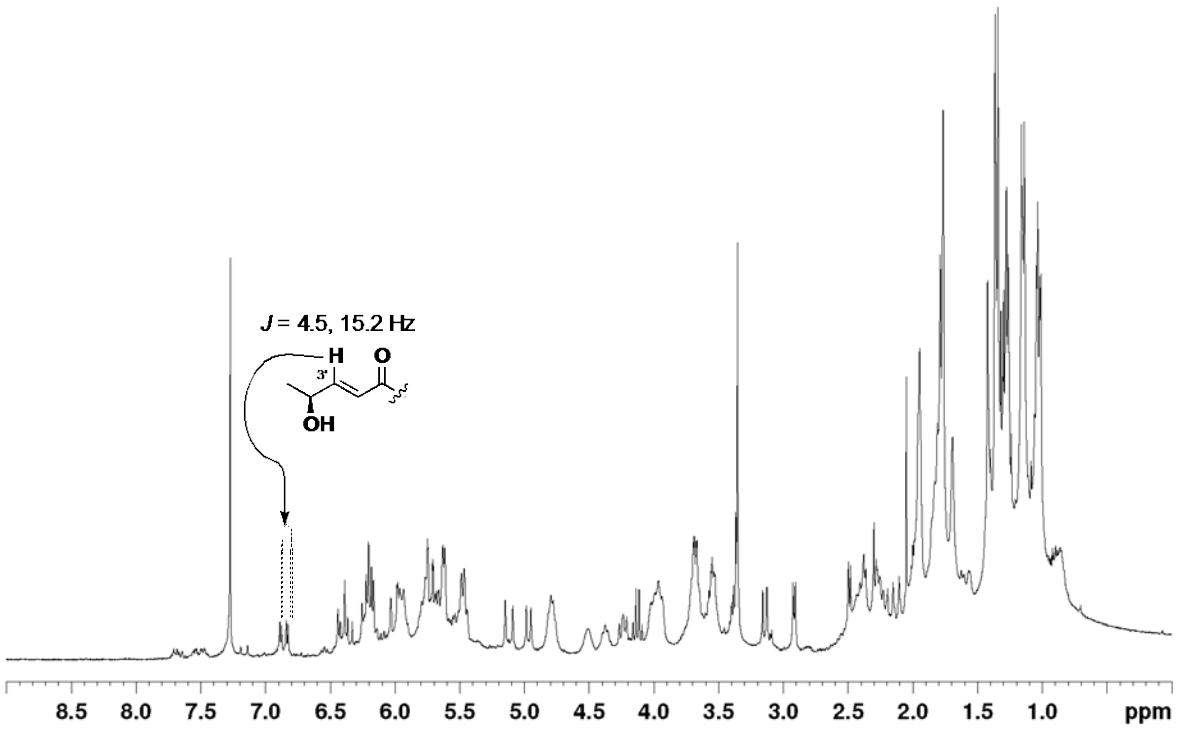

Figure 2-9 ^{1}H NMR spectrum of crude **2.39**.

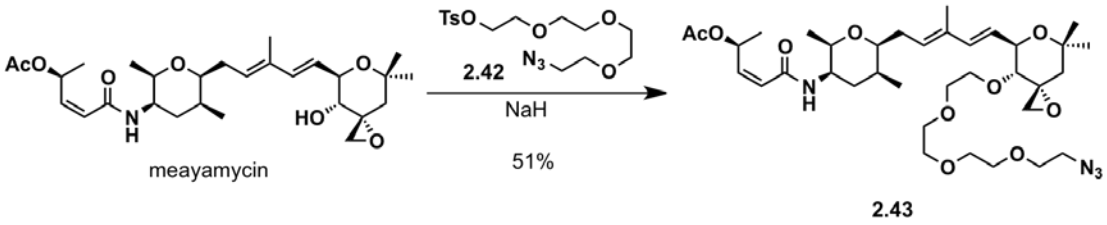

Scheme 2-11 Preparation of TEGylated meayamycin **2.43**.

Splicing inhibition by TEGylated meayamycin **2.43** was evaluated by Ms. Yang Gao in the Koide research group using the published HEK-293-II cell-based assay. In short, luciferase expression increases when pre-mRNA splicing is inhibited.[55] In this assay, TEGylated meayamycin **2.43** exhibited a dose-dependent inhibitory activity towards pre-mRNA splicing after a 16-h treatment (IC_{50} = 2.4 nM; average of three independent experiments). The RT-PCR

analysis of the total RNA extracted from **2.43**-, meayamycin- and DMSO-treated cells further validated that the new analogue **2.43** inhibited pre-mRNA splicing. Pre-mRNA splicing inhibition by **2.43** was examined in HEK-293-II cells over 72 h. The splicing inhibition, in the **2.43**-treated HEK-293-II cells persisted for 48 h, which was different from that in the meayamycin-treated cells (Figure 2-10). Because others have used meayamycin and related compounds to study pre-mRNA splicing over time,[79,93-100] the availability of distinctly temporal splicing inhibitors may prove useful in such mechanistic studies.

2.4.2 Simplified derivatives of TEGylated meayamycin

To further investigate the effect of the TEG-N_3 chain on the 4-hydroxy group of meayamycin, the same TEG-N_3 chain on the corresponding hydroxy group of the right fragment **2.11** (Scheme 2-12A) was installed to form **2.44**. The TEGylated right fragment **2.44** was found to inhibit HCT-116 proliferation with a GI_{50} of 1.5 μM (Table 2-5). The right fragment **2.11** exhibited no antiproliferation activity even at 200 μM. Based on the unexpected antiproliferative activity of **2.44** as well as the SAR data indicating the importance of the epoxide moiety,[20,23-26,29] In collaboration with Mr. Matthew Zhu (a researcher in the Koide laboratory), its simplified derivatives **2.46** and **2.47** (Scheme 2-12B) were prepared. These analogues **2.46** and **2.47** did not exhibit growth inhibition against HCT-116. This indicates that the epoxide coupled to the TEG-N_3 group is not sufficient for antiproliferative activity. The activity of **2.44** could be attributed to the functionalized cyclic pyran necessary for binding of the small molecule to the putative biomolecules(s).

(A)

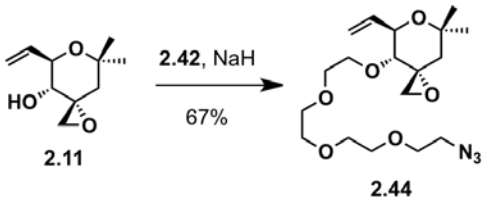

(B)

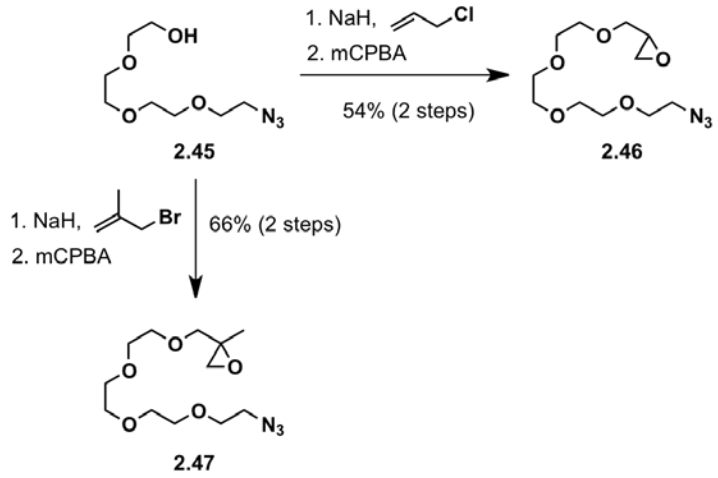

Scheme 2-12 Preparation of (A) TEGylated right fragment **2.44**, (B) TEGylated epoxide **2.46** and **2.47**.

Table 2-5 The Gi_{50} values of meayamycin and analogues.

	GI_{50} (nM)[a]			
Cell line	meayamycin	**2.43**	**2.44**	vincristine
HCT-116	0.038 ± 0.030	0.10 ± 1.4	$1.5 \times 10^3 \pm 0.14 \times 10^3$	0.90 ± 0.3
MCF7*	0.80 ± 1.6	2.4 ± 1.6	ND	1.1 ± 0.5
HEK-293-II	7.8 ± 3.0	46 ± 1.3	$8.9 \times 10^3 \pm 1.2 \times 10^3$	20 ± 0.7
MDA-MB231	0.070 ± 0.06	ND	$1.4 \times 10^3 \pm 1.4 \times 10^3$	3.0 ± 1.2
A549	0.26 ± 0.30	ND	$2.2 \times 10^3 \pm 1.15 \times 10^3$	35.0 ± 1.4
PCI 13	4.8 ± 1.2	ND	$3.7 \times 10^3 \pm 1.1 \times 10^3$	12 ± 5
JHU 012	4.7 ± 1.1	ND	$2.0 \times 10^3 \pm 1.3 \times 10^3$	17.0 ± 3.9

[a] Each experiment consists of twelve data points (twelve different concentrations). ND = not determined. *This MCF7 was a later passage from the American Type Culture Collection.

Growth inhibition assays of **2.43** and meayamycin were always performed in parallel.

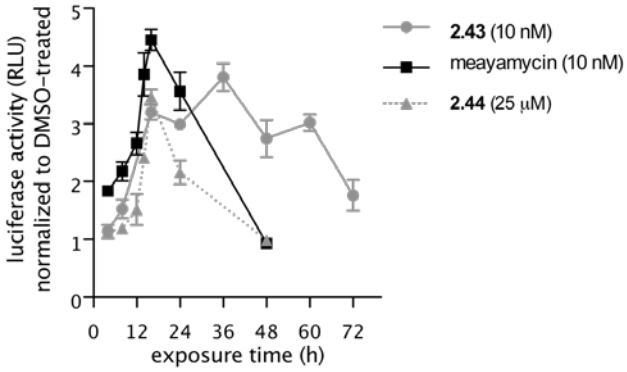

Figure 2-10 Luciferase activity *versus* time for HEK-293-II cells treated with **2.43**, meayamycin, and **2.44**.

The antiproliferative activity of the TEGylated right fragment **2.44** against human cells is shown in Table 2-5. The TEGylated right fragment **2.44** displayed low micromolar GI_{50} values against cancerous cells, while the non-cancerous cell line (HEK-293-II) was less responsive. Consequently, it was determined if **2.44** inhibits pre-mRNA splicing in cells. The pre-mRNA

splicing assays were performed by Ms. Yang Gao. This analogue inhibited pre-mRNA splicing in HEK-293-II cells in a dose-dependant manner (IC_{50} = 3 μM). Pre-mRNA splicing inhibition by the same analogue (25 μM) peaked at 16 h (Figure 2-10). A semi-quantitative RT-PCR experiment showed that unspliced pre-mRNA increased relative to spliced RNA in HEK-293-II cells after a 16-h treatment with the TEGylated right fragment **2.44** at 20 μM (spliced:unspliced = 0.98 ± 0.3 in **2.44**-treated cells and 7.4 ± 1.9 in DMSO-treated).

2.4.3 Summary

In summary, serendipitously discovered new pre-mRNA splicing inhibitor **2.43** and rationally designed **2.44** based on **2.43**. These analogues also exhibited antiproliferative activity towards human tumor cell lines. The TEGylated meayamycin **2.43** represents potential for conjugatable FR901464 analogues, in addition to being used for identifying and studying the elusive target protein(s) of FR901464. The right half of this analogue (i.e., **2.44**) was sufficient for antiproliferative activity and splicing inhibition, potentially facilitating the development of FR901464-based drugs. It is possible that the TEG chain alters the cellular distribution of the meayamycin derivatives, thereby leading to better nuclear entry, or the TEG chain mimics the left part of meayamycin. Based on these considerations, synthesis of modified TEG chains that incorporate various functional groups in order to optimize for potency was begun.

2.5 EFFORTS TOWARDS THE DEVELOPMENT OF A PRACTICAL APPROACH TO SYNTHESIZE MEAYAMYCIN

The potency of meayamycin towards inhibiting pre-mRNA splicing and cancer-cell growth demonstrates that derivatives of this compound can be designed to improve upon or alter its pharmacological properties. In order to ensure a consistent supply of meayamycin and sufficient material for further biological testing, a practical synthesis (i.e. safe, shortened operations, scalable and economical) is required. Such a synthesis is also needed to provide advanced intermediates that could be used to create new analogues of meayamycin.

Meayamycin was initially generated from intermediate **2.11** and diene **2.27**.[25] Modifications of diene **2.27** generated all the nM analogues.[24] In designing a new synthetic scheme, intermediate **2.11** (right fragment) was chosen a target. The previous approach to generate epoxy alcohol **2.11** was 12 steps long and provided sufficient material for biological assays. When performed on the larger scales required for generation of sufficient amounts of **2.11**, several problems were uncovered, which limited the practicality of the synthesis. Notable scale-related difficulties of the route, as described in Scheme 2-13, include the following:

- Aldehyde **2.52** was found to be unstable for storage.
- The alkynalation of **2.52** to form alcohol **2.54** and Mislow-Evans rearrangement using selenide **2.56** to form allylic alcohol **2.57** provided a mixture of diastereomers.
- 2-Nitrophenyl selenocyanate is $70 per gram, and is costly in larger quantities.
- Hg-mediated cyclization of **2.57** to generate geminal-dimethyl **2.58** produced low yields of **2.58** on larger scales, often accompanied by significant amount of unreacted **2.57**.
- Preparation of **2.11** required 12 steps and 10 separate flash chromatographies.
- Preparation of roughly 750 mg of **2.11** costs approximately $2000.

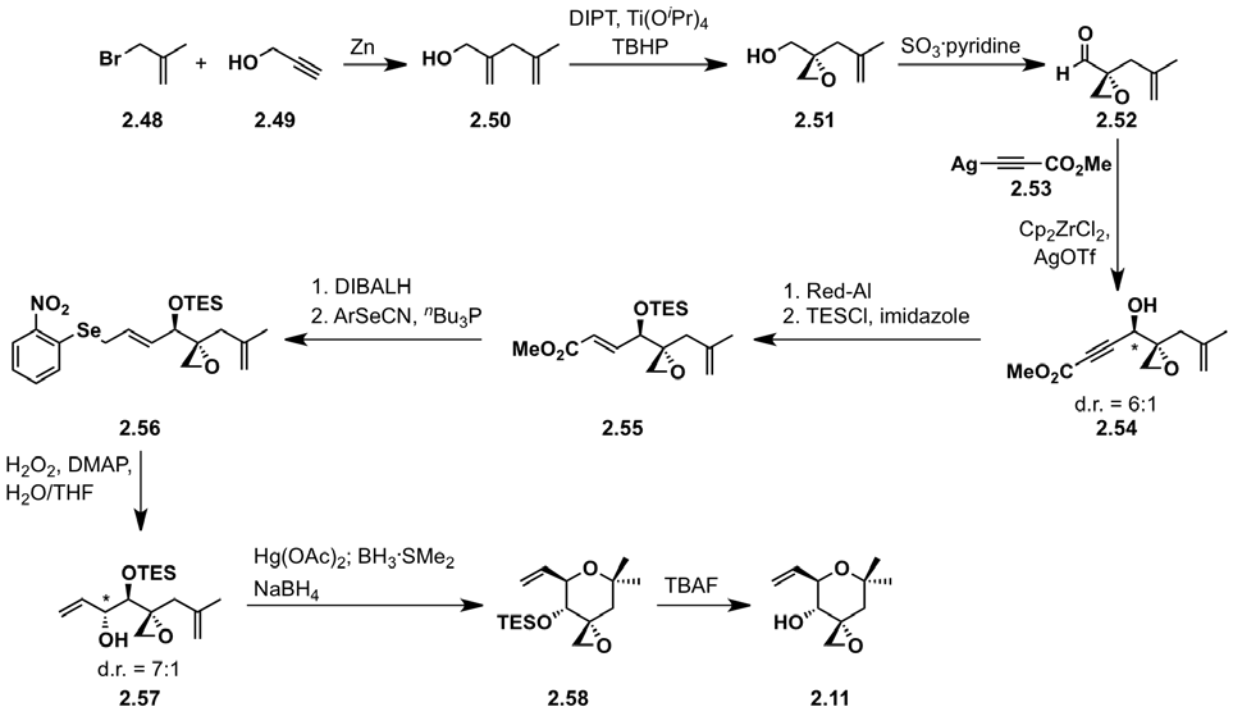

Scheme 2-13 Previous synthetic approach to prepare **2.11**.

Based on the difficulties outlined above, efforts were focused on making the preparation of **2.11** more practical. Because this intermediate is a key fragment of all the Koide group's meayamycin derivatives, and is more stable than FR901464's right fragment, it is important that the production of **2.11** be cost-effective, reproducible and safe.

2.5.1 Preparation of racemic spiroepoxide 2.11

Initial efforts focused on a racemic preparation of **2.11** (referred to as *racemic*-**2.11**). The chosen approach used an acid-mediated endo cyclization of an epoxy-alkene derivative to generate the pyran unit (Scheme 2-14). This approach was inspired by Nicolaou's work on their

synthetic studies towards the pyran units of brevetoxin.[101] This strategy to generate *racemic*-**2.11** required the key intermediate **2.61**.

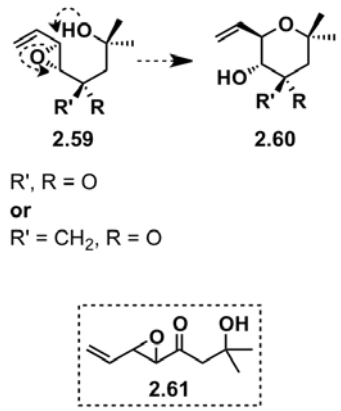

Scheme 2-14 Our new strategy to prepare **2.60**.

Synthesis of **2.61** began with ketone **2.62**. An aldol reaction between acrolein and **2.62** followed by dehydration provided diene **2.64** in approximately 20% yield, with higher yields of the triene **2.65**. Attempts to improve the yield by protecting the tertiary hydroxy on **2.62**, in hopes of reducing the potential retro-aldol reaction, led to no improvement in yield. The use of LDA in the aldol reaction produced large amounts of a polymeric material, believed to be from the use of acrolein, which complicated the workup and purification of diene **2.64**. Unfortunately, other conditions avoiding the use of LDA, illustrated in Table 2-6, resulted in drastically reduced yields of diene **2.64**. As a result, optimization of the aldol reaction was postponed until the success of the synthetic sequence was validated.

Table 2-6 Aldol reaction conditions to prepare **2.63** and **2.64**.

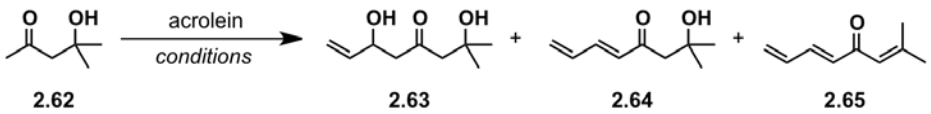

		Yield (%)		
Entry	Conditions	**2.63**	**2.64**	**2.65**
1	1. LDA, -78 °C 2. Ac_2O, NaOAc, r.t.; 100 °C	0	20	35
2	NaOH, THF/H_2O (1:4), 0 to 24 °C	0	12	0
3	NaH, THF, 0 to 24 °C	0	0	0
4	^{t}BuOK, THF, 0 to 24 °C	0	0	0
5	Cs_2CO_3, THF, 0 to 24 °C	0	9	0
6	Bu_2BOTf, $^{i}Pr_2NEt$, CH_2Cl_2, -78 °C	0	trace	0
7	BCl_3, $^{i}Pr_2NEt$, CH_2Cl_2, -78 °C	0	0	81%
8	pyrrolidine, THF or DMSO, 24 to 60 °C	0	trace	0
9	Cy_2BCl, Et_3N, CH_2Cl_2, -78 °C	0	trace	0
10	L-proline, DMSO or DMF	0	0	0

"trace" = less than 5% yield.

Treatment of diene **2.64** with nucleophilic $^{-}$OOH generated epoxy ketone **2.61**, which was cyclized to *racemic*-**2.25** via treatment with CSA. The *anti*-relationship between the hydroxy and vinyl group was confirmed by ^{1}H NMR analysis (*J* value between C4-H and C5-H was 9.9 Hz). Upon treatment of *racemic*-**2.25** with ^{n}BuLi and dibromomethane, the spiroepoxide *racemic*-**2.11** was produced in 73% as a single diastereomer. The rationale for the excellent diastereoselectivity is because one equivalent of ^{n}BuLi will deprotonate the hydroxy group and the lithiated alkoxide can coordinate with the oxygen atom on the carbonyl, thereby, shielding one face of the carbonyl and allowing only the other face prone to attack, thus leading to the epoxide illustrated in Scheme 2-15. Confident with the bond connectivity and relative stereochemistry using our new scheme, we proceeded to optimize the conditions and address the asymmetric variant of this scheme.

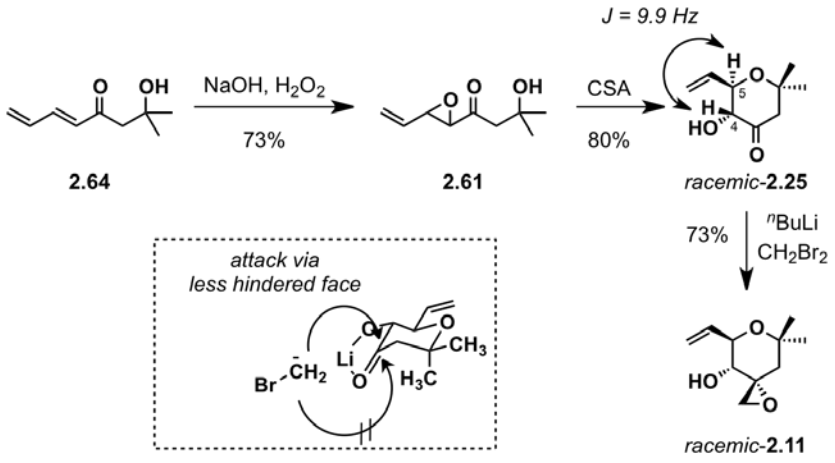

Scheme 2-15 Preparation of *racemic*-**2.11**.

2.5.2 Optimization of the aldol reaction to prepare 2.63

The aldol and dehydration reaction between **2.62** and acrolein to yield diene **2.64** proceeded in poor yield (less than 20%), though the desired material was pure enough for use in subsequent reactions. When the LDA-mediated aldol reaction was attempted using more than 20 grams of ketone **2.62**, several difficulties emerged. In addition, the yield from the reaction decreased and became unpredictable, which was accompanied by the generation of significant amounts of a yellowish polymer by-product. Also, large amounts of LDA were needed for this transformation, in addition to the difficulties associated with maintaining the temperature of the reaction below -70 ºC. Besides the lower and variability of the yields, and increased amount of by-products on larger scale, the reaction did not proceed to completion, despite several hours of incubation and warming. Finally, quenching the reaction is exothermic at larger scales (>10 g), and the formation of polymeric by-products proportionally increases with the scale of the reaction, leading to difficulties purifying the desired product. Furthermore, the magnitude of these difficulties increases with the reaction scale, which makes the reaction difficult to perform

when using more than 20 g of ketone **2.62**. However, the effectiveness of the reaction in producing the desired diene in good purity made the requirements for replacement conditions demanding.

Alternative conditions should provide a good yield of **2.64** (>60%), be operationally simple, and generate material of sufficient purity to be used directly in the subsequent step. With these criteria in mind, an amine-promoted aldol reaction between **2.62** and acrolein was attempted. A variety of reaction conditions were further explored to identify a method for the conversion of **2.62** to **2.64**. The initial screen was carried out on a 96-well plate, using 0.2 M of substrate **2.62**, to provide a qualitative assessment of a few conditions capable of promoting the aldol reaction between **2.62** and acrolein (Figure 2-11). In terms of providing the desired product, as determined by TLC analysis, the most promising conditions was the use of DBU as a base in ^{i}PrOH, EtOH, 1,2-dichloroethane and no solvent at room temperature (Figure 2-11).

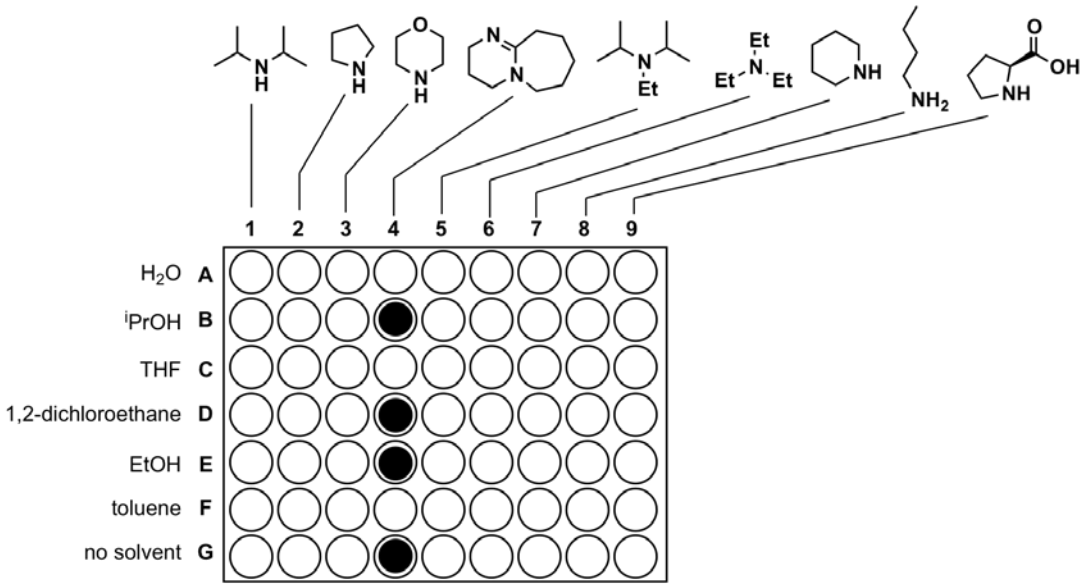

Figure 2-11 Screening results. 1.0 equivalent of acrolein, 2.0 equivalent of **2.62** and greater than 5 equivalent of amines. Black-filled circles indicate presence of product(s) as judged by TLC.

The conditions found in the initial screen were further explored to determine the effects of temperature, time and stochiometry on promoting the aldol reaction between **2.62** and acrolein. However, treatment of **2.62** and acrolein with DBU at -5 ºC deemed ineffective in promoting the reaction, although warming the reaction slowly showed signs of product and also an increase in the presence of polymeric material exponentially. As a result, the desired product was isolated in 8% yield (Scheme 2-16). Varying the solvent did not affect the reaction outcome. Performing the reaction in the absence of solvent led to the formation of a predominantly polymeric material. In a separate experiment, treatment of acrolein with all of the bases mentioned above showed the presence of the same polymeric material I observed during the optimization studies, whereas, the same test with ketone **2.62** was negative. This finding indicates that acrolein is responsible for the formation of the polymeric substance.

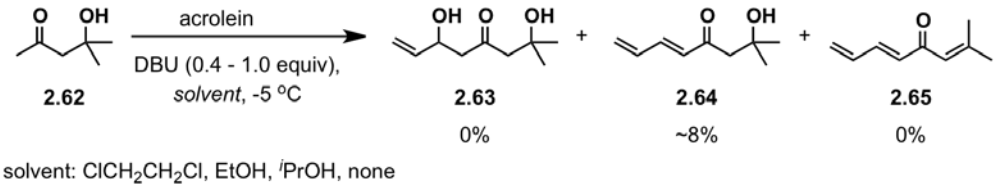

Scheme 2-16 Aldol reaction efforts to prepare **2.64**.

Based on these results, acidic conditions were used to promote the aldol reaction, and a Mukaiyama aldol reaction between derivative of ketone **2.62** and acrolein was attempted. In collaboration with Mr. Alexander Krisko (a researcher in the Koide laboratory), silyl enol ether **2.66** was prepared in two different ways (Table 2-7). The first approach (method A) involved using stoichiometric amounts of NaI, Et_3N, TMSCl in MeCN.[102] Prior to performing this

process, the NaI needed to be dried thoroughly because the process of preparing **2.66** is very water sensitive, most likely because of the hydrolysis of *in situ* generated TMSI. The use of **2.62**, NaI, Et_3N, TMSCl in MeCN yielded **2.66** in 70 – 90% yield. The second approach to prepare **2.66** (method B) involved the replacement of NaI with LiI. The solvent is also switched from MeCN to $CHCl_3$. After rigorously drying LiI, followed by dissolving it in $CHCl_3$ then treatment with **2.62**, Et_3N and TMSCl, the enol ether **2.66** was once again isolated in high yields, listed in Table 2-7. Methods A and B both provided the desired product in excellent yields and no purifications beyond aqueous extractions were required. While both methods (A and B, Table 2-7) to prepare enol **2.66** were very efficient, method B (LiI) was slightly easier to work up due to the reduced volume of water needed at the end, during the workup procedure. However, from a cost-analysis standpoint (cost analysis for chemicals, workup and extraction solvents was performed), the approximate cost to prepare 25 grams of **2.66** using method B is $153, which is reduced to $46 using method A. For that cost saving reason, method A was used. Using method A, prior to starting the reaction, NaI must be dissolve in MeCN, which is time-consuming and requires a large volume of MeCN, e.g. 71 g of NaI needs 800 mL MeCN. Therefore, the quantity of NaI was reduced from 2.7 equivalents to less than 1.0 equivalent. Also, from a mechanistic standpoint, NaI should be catalytic during the process of generating enol **2.66**; the *in situ* generated TMSI activates the carbonyl, followed by deprotonation using Et_3N and generation of TMS-enol ether, and I^- is reformed to regenerate TMSI (Scheme 2-17). Based on this hypothesis, 0.3 equivalent of NaI was used. Performing the reaction with less NaI than the original protocol required drastically reduced the yield to almost half. Therefore, we proceeded with the original protocol and used 2.7 equivalents of NaI. Although this protocol requires careful addition of a

solution of NaI in MeCN and monitoring the temperature, the large scale production of **2.66** yielded more than 80 g in a single transformation without a consequent loss in yield.

Table 2-7 Conditions to prepare silyl enol ether **2.66**.

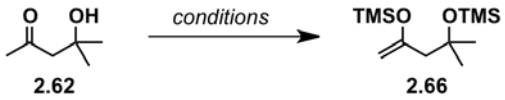

Method	Conditions	Yield (%)
A	TMSCl (2.3 equiv), Et_3N (2.5 equiv), NaI (2.6 equiv), CH_3CN, 40 to 25 °C	86
B	TMSCl (2.7 equiv), LiI (2.7 equiv), Et_3N (2.7 equiv), $CHCl_3$, 25 °C	99

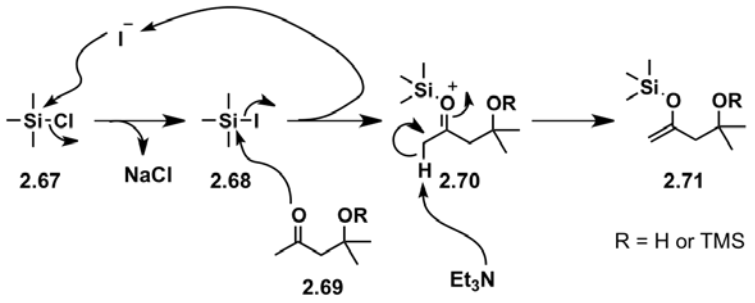

Scheme 2-17 Mechanistic rationale for the use of less NaI towards the preparation of **2.66**.

A variety of reaction conditions have been explored to determine an optimal method for the merge of **2.66** with acrolein. The TMS enol ether **2.66** was prone to desilylation, and formation of undesired ketone **2.62** was often the sole reaction pathway when attempting Mukaiyama aldol reaction[103] with commonly used Lewis acids (such as $SnCl_4$, $AlCl_3$, $Sc(OTf)_3$, BF_3•OEt_2, $MgBr_2$•OEt_2), even when performed under strictly anhydrous conditions (Table 2-8). Although ^{1}H NMR analysis showed the showed the crude silyl enol ether **2.66** was pure, we asked whether impurities not observable by spectroscopic methods could be responsible for the diminished yields for **2.63**. However, applying the conditions of the Mukaiyama aldol (Table 2-

8, entries 1-5) to the distilled batch of **2.66** led no improvement in yield. Therefore, the poor yields of the Mukaiyama aldol reaction were not the result of an impure silyl enol ether **2.66**. The next step, applying Kobayashi conditions[104] with 10 mol% $Yb(OTf)_3$ in 1:10:4 H_2O:EtOH:PhMe generated the corresponding aldol product in ~70% yield. Chromatographic purification was relatively straightforward, even on larger scales (e.g. 30 g), due to the lack of close-running impurities. While the original Kobayashi protocol[104] indicates the possibility of recycling of $Yb(OTf)_3$, this approach was not successful due to the partial solubility of product **2.63** in the aqueous layer.

Table 2-8 Mukaiyama aldol reaction conditions towards the preparation of **2.63**.

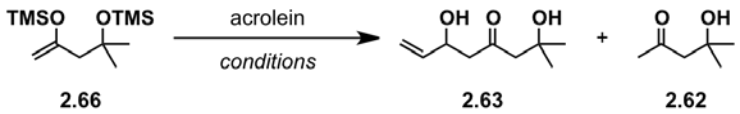

2.66 **2.63** **2.62**

Entry	Conditions	Yield (%)	
		2.63	**2.62**
1	BF_3•OEt_2, CH_2Cl_2, -78 °C	25 – 43	50 – 70
2	$Sc(OTf)_3$, CH_2Cl_2, -78 °C	18	75
3	$MgBr_2$•OEt_2, CH_2Cl_2, -78 °C; 0 °C	0	92
4	$SnCl_4$, CH_2Cl_2, -78 °C	20	68
5	$AlCl_3$, CH_2Cl_2, -78 °C	23	65
6	$Yb(OTf)_3$ (10 mol%), H_2O/EtOH/toluene (1:10:4), 0 °C	72	0

The next step in the preparation of **2.64** was the conversion of the allylic alcohol **2.63** to diene **2.64**. The original protocol to prepare **2.64** described above (Section 2.5.1, Table 2-6, entry 1) specifies mixing the allylic alcohol with sodium acetate and acetic anhydride at room temperature for 12 h then heating to 100 °C for 1 h. Although this protocol is effective on a small scale (e.g. 2 g), we experienced difficulties when we scaled up the reaction to greater than 5 g. Purification of the desired product **2.64** was tedious due to numerous inseparable by-products

during flash chromatography, such as the major by-product triene **2.65**. One additional note is that, during the progress of the reaction, the rate of product formation as determined by TLC analysis varied between experiments, most likely due to the heterogeneous nature of the reaction mixture. The concentration of the reaction was, therefore, decreased to 0.5 M upon addition of solvent, as opposed to the original reaction conditions, which was run without a solvent. We also decreased the prolonged reaction time at room temperature due to the slow reaction progress observed by TLC. As a result, running the reaction in a solvent (0.50 M) such as 1,2-dichloroethane at 50 °C for 6 – 7 h led to reproducible yields (60 – 70%), without any by-product formation.

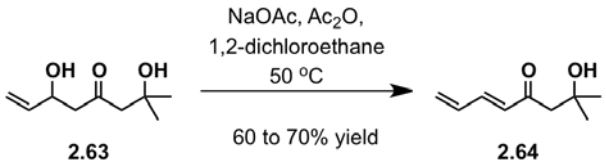

Scheme 2-18 Preparation of **2.64** from **2.63**.

2.5.3 Preparation of chiral 2.11

The above sequence established the relative stereochemistry of **2.11**. Therefore, it was envisioned that possible routes to control the absolute stereochemistry of **2.11** were asymmetric epoxidation of **2.64**, kinetic resolution to cyclize epoxide **2.61** to ketone **2.25**, or enzymatic kinetic resolution of *racemic*-**2.25** or *racemic*-**2.11**. Epoxidation of enone **2.64** was explored as a possible route to prepare chiral variant of **2.61**. As shown in Scheme 2-19, attempts to epoxidize **2.64** using alkaloid **2.73**[105] and cumylydroperoxide did not produce the desired product.

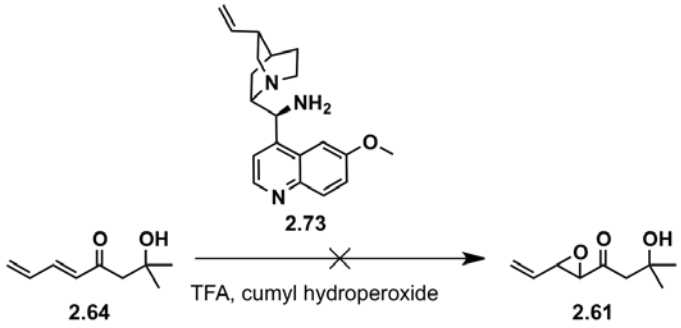

Scheme 2-19 Effort towards the asymmetric synthesis of **2.61** using cinchona alkaloid **2.73**.

Enantioselective epoxidation using metals was tested as an alternative to the organocatalyst procedure. However, treatment of **2.64** with La-BINOL (generated *in situ*), $Ph_3As{=}O$ and *t*-butyl hydrogen peroxide[106] led to no product formation. The possibility of the tertiary hydroxy group in **2.64** to coordinate the $Ph_3As{=}O$-La-BINOL/OO*t*Bu complex is likely to displace $Ph_3As{=}O$, $^{-}$OO*t*Bu or BINOL before the complex can undergo conjugate addition to the enone. This hypothesis is supported by the observation that the reaction provided the desired product with the protected derivative of **2.64**, THP **2.75** (Scheme 2-20). However, after cyclization, the %ee was found to be only 70%. The ee of ketone **2.25** was established upon treatment of **2.25** with (*S*)-(+)-Mosher's acid to afford **2.77**. The diastereomers of this compound were sufficiently resolved in the ^{1}H NMR spectrum to permit analysis. Efforts to apply Deng's method[107] using substrate **2.82** to synthesize **2.83** failed (Scheme 2-23).

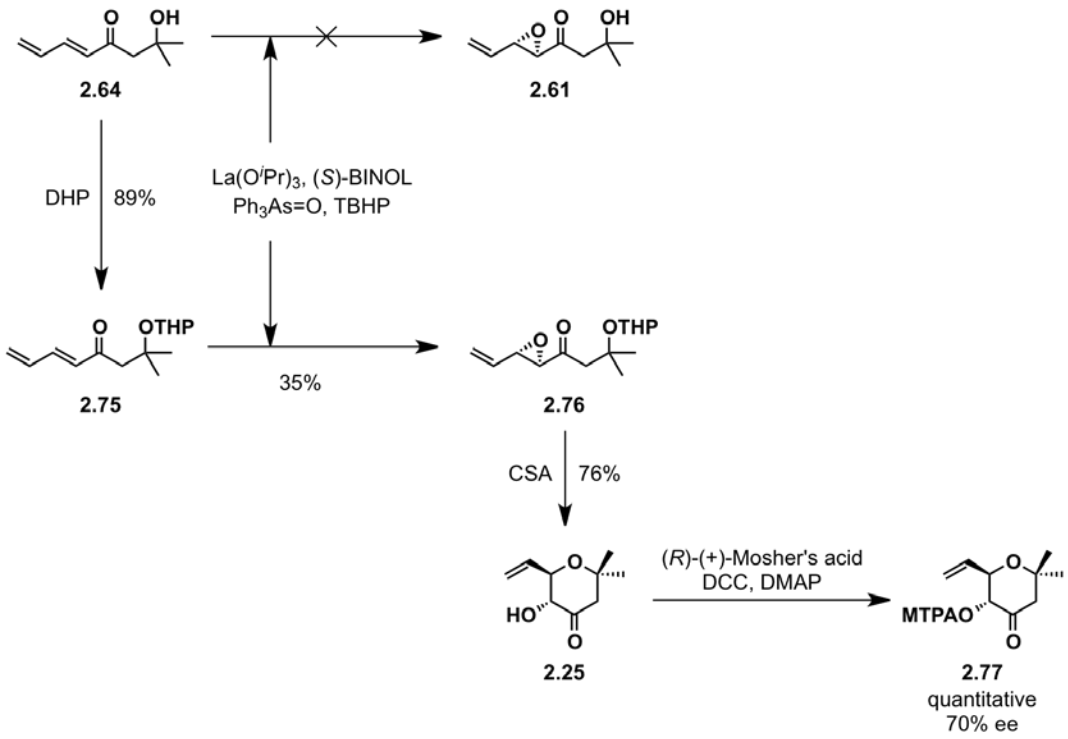

Scheme 2-20 Asymmetric synthesis of ketone **2.25** from **2.75**.

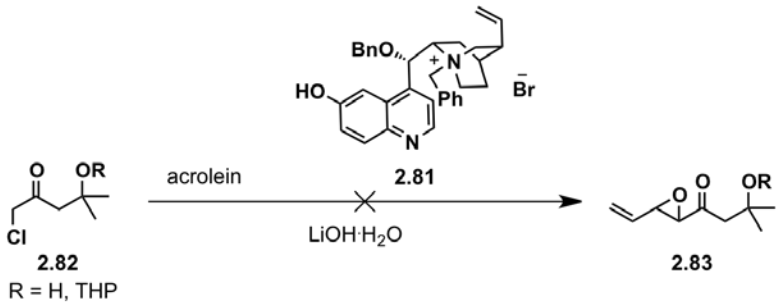

Scheme 2-21 Efforts towards the asymmetric synthesis of **2.83** using chiral phase-transfer catalyst **2.81**.

Enantioselective cyclization of epoxyalcohol **2.61** failed to convert *racemic*-**2.61** to chiral **2.25** under Jacobsen's developed conditions, Scheme 2-22A.[108] Furthermore, Jacobsen's kinetic resolution of racemic epoxides protocol using catalyst **2.87** also failed to open the racemic

spiroepoxide **2.86** (Scheme 2-22 B).[109] These failures prompted exploration of a new area of chiral Brønsted acid catalyzed reactions.[110,111] After preparation and silica gel chromatography purification of chiral phorsphoric acid **2.85**, epoxide **2.61** was converted to ketone **2.25** in ~32% yield with an ee of >90%. However, this transformation was not reproducible, as different batches of phosphoric acid **2.85** produced different results. The poor reproducibility may stem from metal impurities.[112] Specifically, a fraction of the phosphoric acid might be protonated and the remainder is in the phosphoroxide state coordinated to metals. To ensure that we produced the Brønsted acid after chromatography purification, the isolated product was washed with aqueous hydrochloric acid.[112] However, this workup to provide **2.85** did not aid in delivering enantiomerically enriched ketone **2.25**. This poor reproducibility prompted us to prepare a variety of metal-phosphoric Lewis acid compounds (Table 2-9). There is precedence in the literature that the corresponding metal salt of the Brønsted acid is responsible for the asymmetric catalysis.[112] In our studies, the most promising outcome was Mg-**2.88**, though extensive efforts to improve upon 43% ee failed (Table 2-9).

(A)

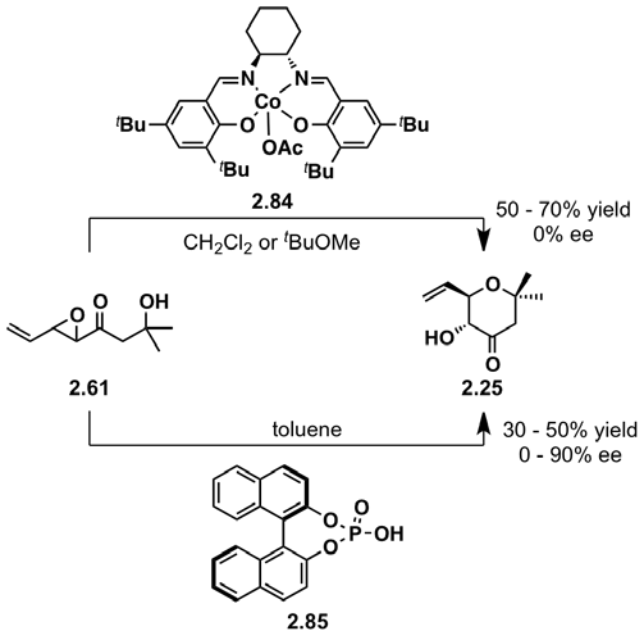

(B)

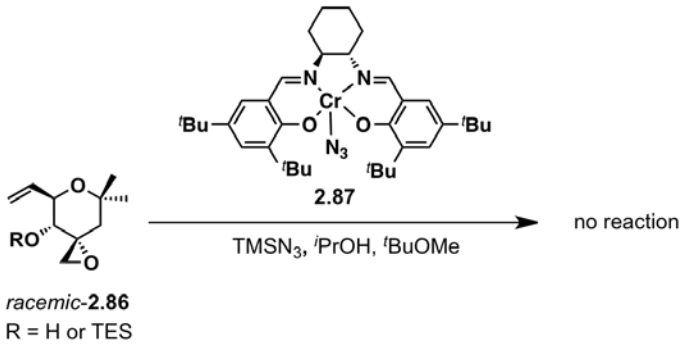

Scheme 2-22 (A) Efforts towards the kinetic resolution of epoxy alcohol **2.61**. (B) Efforts towards the kinetic resolution epoxide opening of epoxide *racemic*-**2.86**.

Table 2-9 Efforts towards the kinetic resolution of **2.61** using phosphoric acid and phosphoric acid salt.

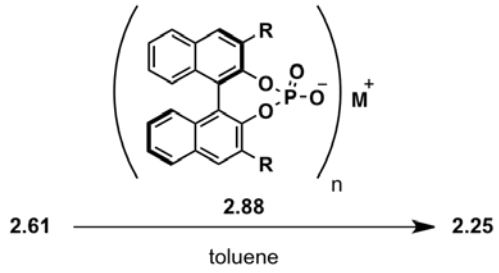

Entry	R	M^+	Yield (%)	% ee (Mosher ester)
1	Ph	H	35	0
2	H	Ba	34	0
3	H	Ca	17	0
4	H	Mg	26	43
5	H	K	9	0
6	H	Na	0	0
7	H	Co	0	0
8	H	Sr	43	0

Since the presented work had already established a protocol to prepare *racemic*-**2.11**, enzymatic kinetic resolution of secondary alcohols **2.25** and **2.11** was explred. The lipase B strain is known to resolve secondary allylic alcohols containing a variety of functional.[113] The other strain, *Candida antarctica* lipase A, also acylates secondary allylic alcohols, but of sterically demanding substrates. Attempts to resolve ketone *racemic*-**2.25** and epoxide *racemic*-**2.11** using both strains of the enzymes failed to produce any acylated product. Additionally, increasing the temperature or prolonging the reaction time failed to afford acylated products.

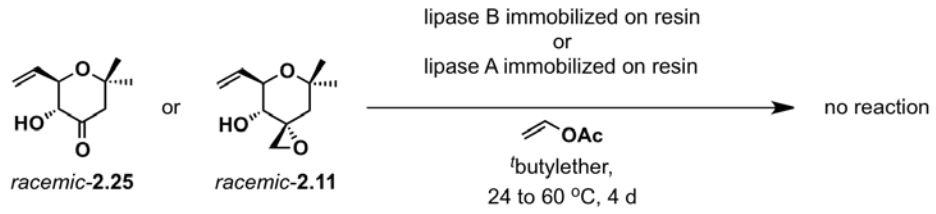

Scheme 2-23 Efforts towards the kinetic resolution of *racemic*-**2.25** and *racemic*-**2.11** using enzymes.

A different strategy to prepare chiral **2.11** was employed, which required additional steps in the synthesis. A 1,2-reduction of ketone **2.64** without $CeCl_3$ provided allylic alcohol **2.89**. We were able to synthesize epoxide **2.61** via a kinetic resolution reaction on **2.89**.[114] However, the product of the Sharpless epoxidation step contained impurity, which was difficult to separate from the desired product. Rigorous purification always resulted in a lower percentage of the isolated product. Therefore, it was more advantageous to avoid the laborious purification and isolation of this substrate, and continue to the oxidation step. Oxidation using catalytic TPAP and stochiometric NMO[115] delivered **2.61** (Scheme 2-24A). Other oxidation methods, e.g. Dess-Martin periodane,[116] Parikh-Doering,[117] Swern oxidation,[118] failed to deliver the desired product. Using the standard workup conditions employed in TPAP/NMO oxidation, filtration and chromatography purification, afforded some loss of product due to decomposition and volatility of **2.61**. To avoid this loss, it was discovered that the reaction mixture could be directly filtered through a short silica gel plug to remove the ruthenium species and any remaining polar impurities from the two prior reactions, allowing the use of impure **2.61** as a starting material without a measurable decrease in yield of **2.25**. The filtrate was directly treated with CSA, then Et_3N to afford ketone **2.25** in greater than 90% ee (Scheme 2-24A).

Due to the rigorous workup needed after the Sharpless epoxidation conditions, attempts were made to use Hisashi Yamamoto's epoxidation method.[119] Treatment of crude allylic alcohol **2.89** with $VO(O^iPr)_3$ and the *N*-hydroxyamide ligand **A** in CH_2Cl_2 formed the desired epoxide. Following the same procedure as reported above: TPAP/NMO mediated oxidation and cyclization using CSA yield ketone **2.25** (Scheme 2-24B). Mosher ester analysis of **2.77** revealed that the epoxidation was not enantioselective. Towards this end, it was opted to proceed with the Sharpless epoxidation protocol.

(A)

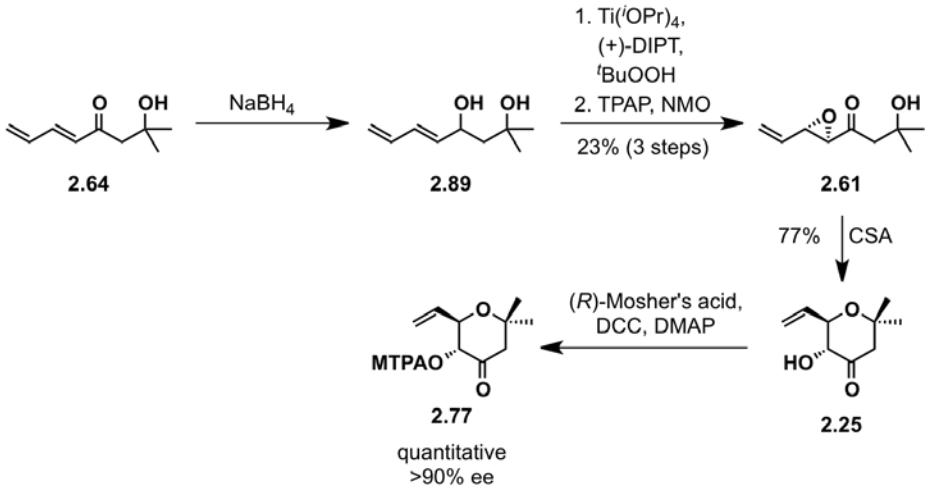

(B)

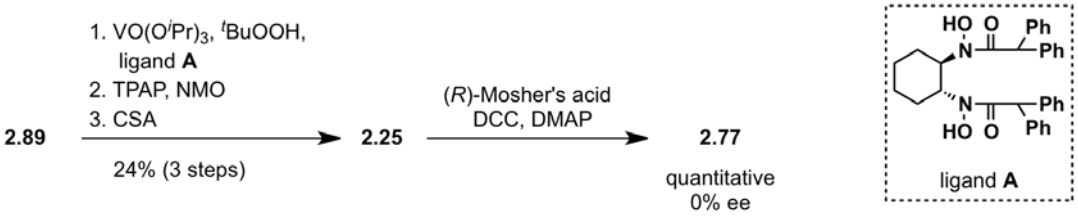

Scheme 2-24 (A) Preparation of chiral **2.25** using Sharpless asymmetric epoxidation kinetic resolution. (B) Preparation of chiral **2.25** using Yamamoto's asymmetric epoxidation kinetic resolution method.

2.5.4 Generation of meayamycin from FR901464

It was realized that meayamycin could be prepared from FR901464 by interchanging the stable fragment of meayamycin, **2.11**, with that of the unstable counter part of FR901464 (Scheme 2-25B, blue fragment). We exploited of the reversibility of the 1,3-diene-ene cross

metathesis using a ruthenium-based catalyst. This was thought to be a viable approach for the two following reasons:

- The reaction of the ruthenium catalyst would preferentially react with **2.91** to form alkylidene **2.94**, followed by formation of **2.95**. This process is reversible.
- Eventually, alkylidene **2.94** would react with the sterically more accessible alkene of diene **2.90** to form alkylidene **2.96**, thereby forming meayamycin.

This fragment interchange strategy was tested by treating FR901464 with excess **2.11** in 1,2-dichloroethane and **Ru-1** in 40 ºC for 14 h to produce meayamycin. Meayamycin formation was validated by the similar retention times to authentic meayamycin and ^{1}H NMR analysis (Figure 2-12B). This is probably the most concise approach to produce meayamycin in a short term as long as FR901464 can be supplied. Another potential use of this interchange strategy, although not tested, is the bubbling of ethylene in a mixture of FR901464 and the ruthenium catalyst to generate the left fragment **2.27**.

(A)

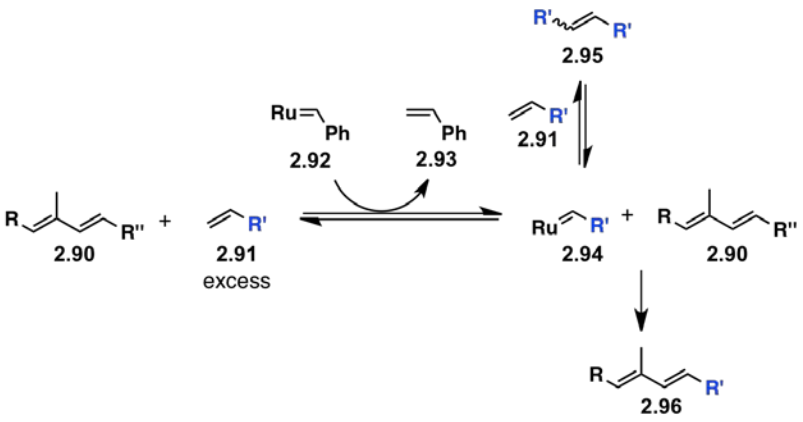

(B)

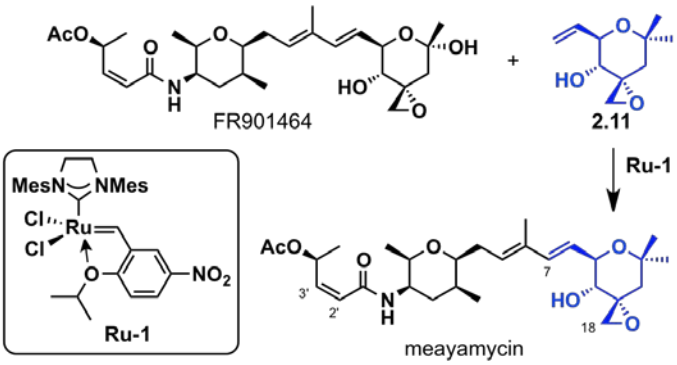

Scheme 2-25 (A) The cross metathesis interchange strategy to prepare meayamycin from FR901464. (B) Preparation of meayamycin from FR901464 using the cross metathesis interchange strategy.

(A)

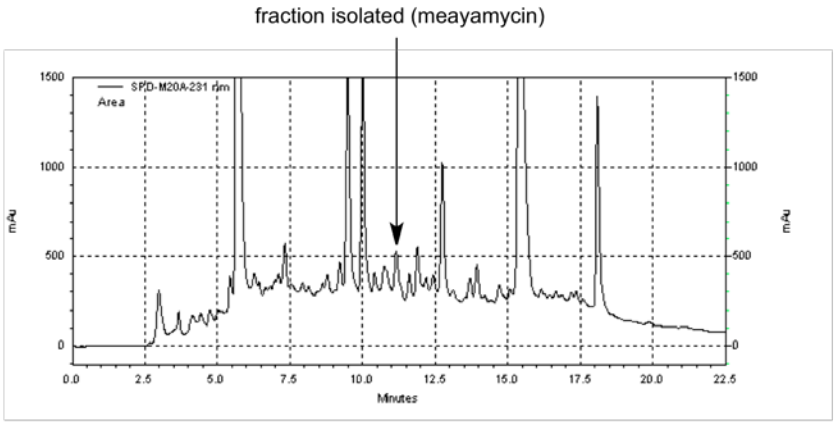
fraction isolated (meayamycin)
SPD-M20A-231 nm
Area
1500
1000
500
0
mAu
0.0
2.5
5.0
7.5
10.0
12.5
15.0
17.5
20.0
22.5
Minutes

(B)

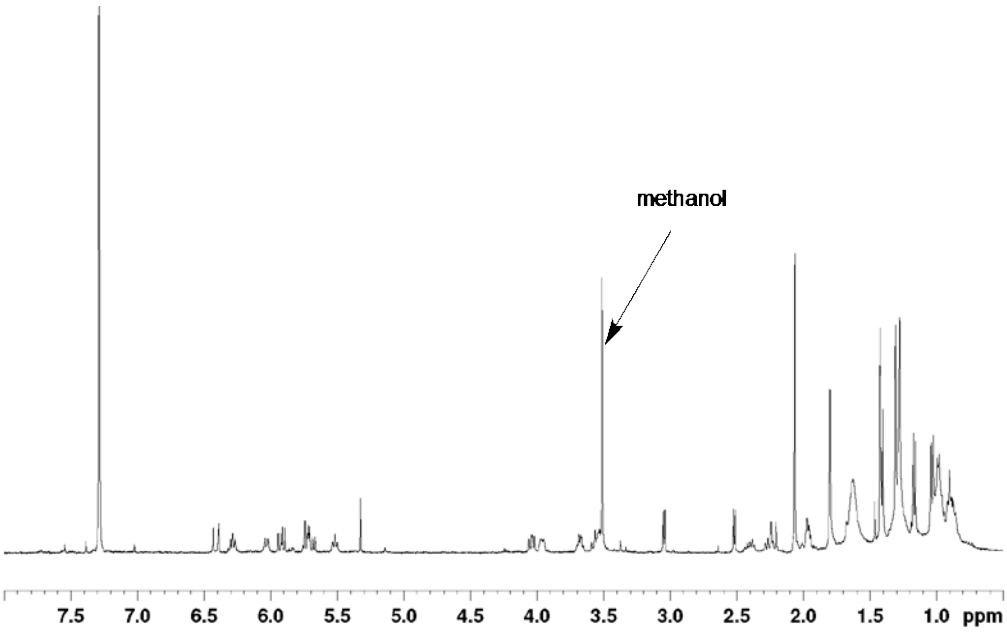
methanol
7.5
7.0
6.5
6.0
5.5
5.0
4.5
4.0
3.5
3.0
2.5
2.0
1.5
1.0
ppm

(C)

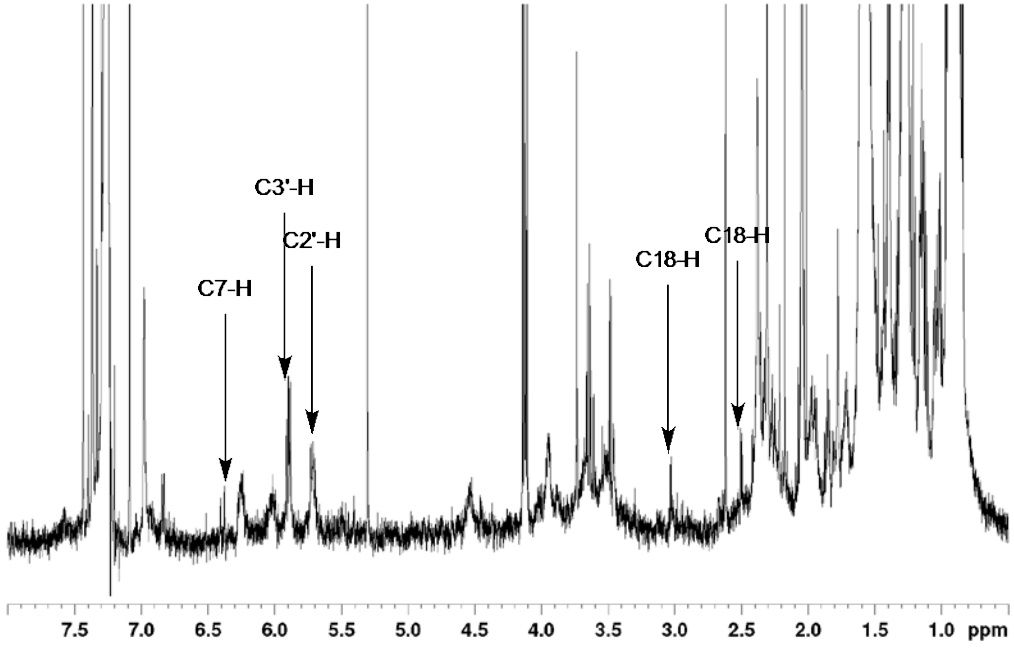

Figure 2-12 (A) HPLC chromatogram of the reaction mixture from Scheme 2-25. (B) ^{1}H NMR of pure meayamycin. (C) ^{1}H NMR of meayamycin from the synthesis using the cross metathesis interchange strategy shown in Scheme 2-25.

The interchange strategy could be a convenient approach to prepare **2.27** and further allow for diversifying C4′. In addition, the process could lead to a cleaner reaction with less by-products formed due to the dramatic reduction of intermediates present in the reaction mixture. A potential disadvantage of this strategy would be the contamination of meayamycin with ruthenium by-products. However, there are many methods for removing ruthenium including activated charcoal,[120] $Ph_3P{=}O$,[121] $Pb(OAc)_4$,[122] and the most convenient method being to use commercial thiol- or thiourea-based resin scavengers.

2.5.5 Summary

The synthetic route to produce intermediate **2.11**, originally developed in the Koide research group, required 12 steps. To improve this approach, using the new scheme, **2.11** was prepared in 8 steps and five separate chromatographic purifications. Furthermore, meayamycin was prepared through one-step reaction from **2.11** and FR901464, contingent on a continuous supply of FR901464 continues. Future improvements directed towards the practical preparation of meayamycin and its derivatives should be focused on identifying alternate coupling strategies to cross metathesis, due to the tedious and rigorous purification efforts continuously invested to yield meayamycin-type compounds. Additionally, it would be advantageous to revisit the chiral Brønsted acid kinetic resolution method to convert **2.61** to **2.25**, which would lead to a 6-step synthesis of intermediate **2.11**.

3.0 CHEMICAL AND BIOLOGICAL STUDIES OF TMC-205 AND ITS ANALOGUES

3.1 BACKGROUND

Irregular gene expression disrupts homeostasis and is often a cause and/or consequence of diseases.[123] Thus, exogenous means to regulate gene expression could be a powerful approach to changing the course of cells' homeostasis. As a research tool, the combination of tetracycline or doxycycline and their responsive promoter has been used successfully *in vitro* and *in vivo* to activate a specific gene.[124,125–126-130] An alternative approach using reporter gene systems has been pursued in the quest for natural products that regulate genes, in which the SV40 promoter was commonly used. These efforts have resulted in the discoveries of natural products such as azelaic bishydroxamic acid,[131] trichostatin A,[132] FR901228,[133] herboxidiene[134,135] and FR901464.[136-138] Mechanistic studies of trichostatin A and FR901464 impacted chemistry, biology, and medicine because these small molecules demonstrated that the inhibitions of histone deacetylases and spliceosome were new approaches to tackle cancer.[7,46,139-142,143] In sum, discoveries and development of small molecules that activate the SV40 promoter is a fruitful area of research.

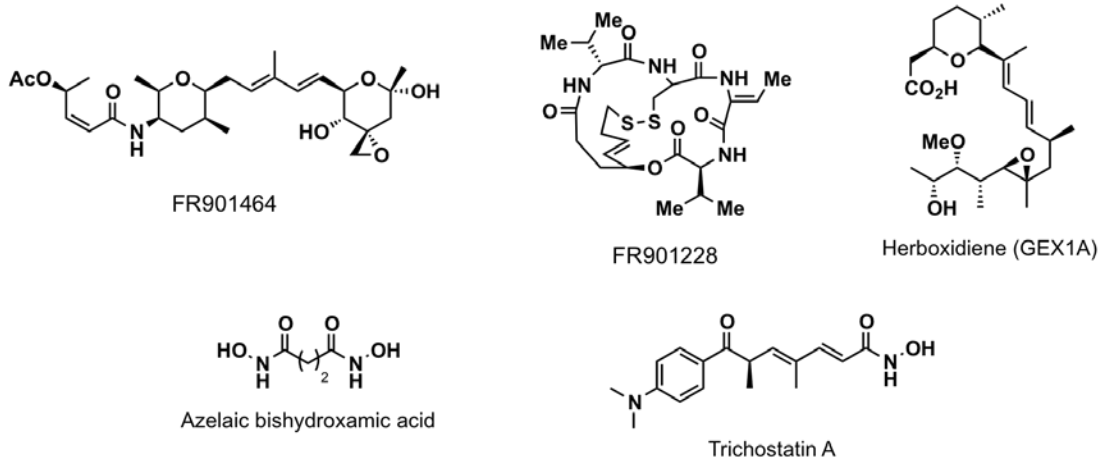

Figure 3-1 Chemical structures of natural products that upregulate the SV40 promoter.

TMC-205 was isolated from a fermentation broth of an unidentified fungal strain TC 1630. The natural product activated an SV40 promoter and was cytotoxic against various human cancer cell lines in the 52–203 μM range as GI_{50} values.[144] Despite the modest potency, TMC-205 may be an attractive lead compound to develop new transcriptional modulators, considering the recent history of the SV40 promoter-activating natural products. Moreover, TMC-205 was found to be light sensitive, and only 3.3 mg of TMC-205 was isolated, necessitating better access to this natural product. Here, we report our synthetic and biological studies of TMC-205 and its analogues.

3.2 SYNTHESIS OF TMC-205

It was important to devise a concise synthesis for subsequent biological studies. An obvious convergent approach was the C6-C9 bond formation toward the end of the synthesis via a cross-coupling reaction (Scheme 3-1). We planned to examine two different strategies:

Stille coupling[145] and Suzuki-Miyaura coupling[146] reactions (Scheme 3-1).

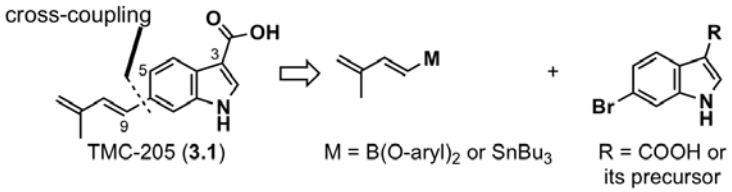

Scheme 3-1 Structure and retrosynthetic analysis of TMC-205.

Treatment of 6-bromoindole (**3.4**) with $(CF_3CO)_2O$ followed by aqueous NaOH afforded carboxylic acid **3.6** in 97% yield over 2 steps (Scheme 3-2A).[147] Boronic ester **3.2** was prepared by the hydroboration of 2-methylbut-1-en-3-yne with catecholborane (Scheme 3-2B).[148,149] Treatment of boronic ester **3.2** with bromide **3.6** in the presence of $Pd(PPh_3)_4$ and Cs_2CO_3 failed to produce the target molecule **3.1** (Scheme 3-2A).[150] With the known organostannane **3.3** prepared from 2-methylbut-1-en-3-yne according to the literature,[151,152] a Stille coupling reaction was examined to convert bromide **3.6** to TMC-205. However, this transformation provided the natural product only in 10% yield, prompting us to seek an alternative approach.

Both of the cross-coupling experiments described above suffered from the poor solubility of carboxylic acid **3.6** in various solvents (THF, MeOH, DMSO, and 1,4-dioxane). The more soluble methyl ester **3.7** was prepared in 65% overall yield from **3.4** (Scheme 3-2C). This ester was subjected to the Suzuki-Miyaura coupling conditions with boronic ester **2** to form methyl ester **3.8** in 98% yield. Finally, treatment of this methyl ester with NaOH followed by acidification with $KHSO_4$ afforded TMC-205 in 88% yield. Therefore, the total synthesis of TMC-205 was accomplished in 5 steps in the longest linear sequence (6 total steps) from the

commercially available bromide **3.4** in 64% overall yield. The GI_{50} value of the synthetic TMC-205 against HCT-116 tumor cells was 68 μM, which is in excellent agreement with the literature.[144]

(A)

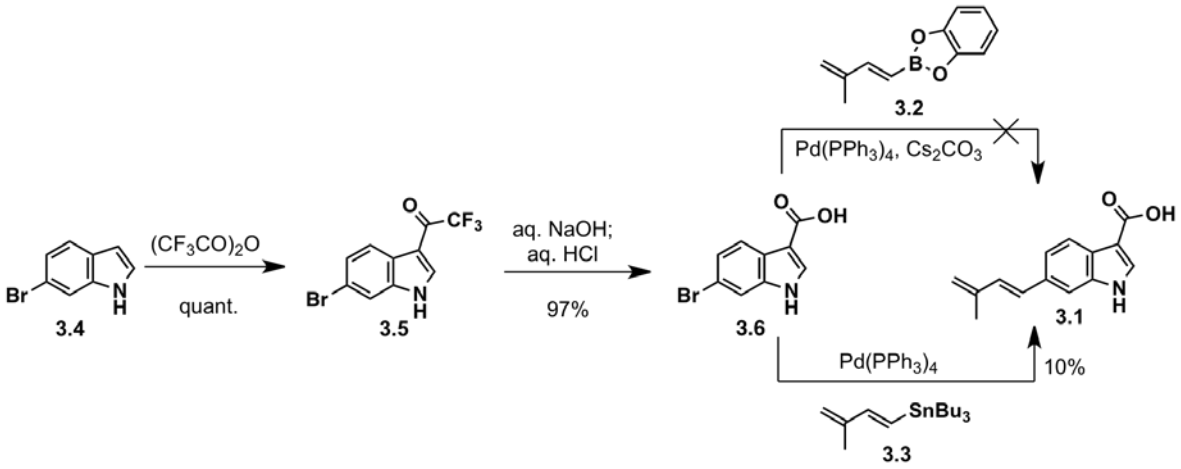

(B)

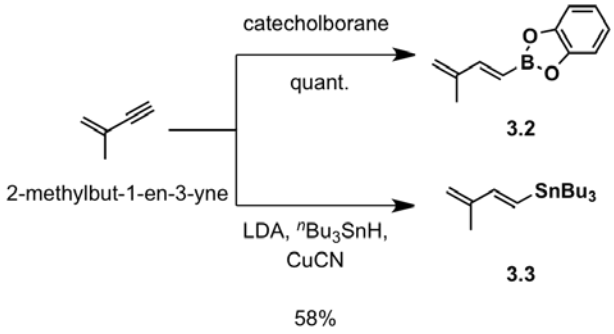

(C)

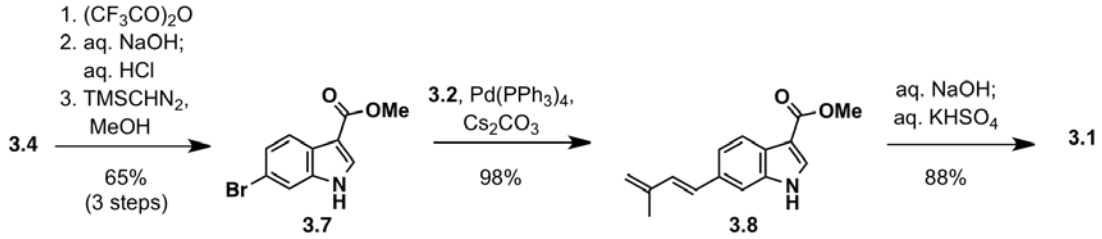

Scheme 3-2 (A) Efforts towards the preparation of TMC-205 using Suzuki-Miyaura and Stille reaction. (B) Preparation of boronic ester **3.2** and organostannane **3.3**. (C) Preparation of **3.1** using Suzuki-Miyaura cross-coupling reaction on ester **3.7**.

3.3 STABILITY OF TMC-205

During our synthesis and structure characterization of TMC-205, this natural product in MeOH and DMSO decomposed noticeably in less than 24 h after being stored under ordinary laboratory visible light and air. HPLC analysis of 16 h-old TMC-205 solutions in MeOH and DMSO showed that the decomposition was not solvent-dependent (Figure 3-2). The ^{1}H NMR spectrum of the CD_3OD solution (Figure 3-3) revealed the presence of an enone group, possibly from enone **3.I** (Figure 3-4) or its derivative in which the indole ring was oxidized (carboxylic acid **3.III**), and a formyl group resulting from either the oxidation of the C9-C10 and/or the C2-C3 bond (carboxylic acid **3.II**, formyl **3.IV**, or formyl **3.V**; Figure 3-4). LC-MS analysis was performed on the decomposed TMC-205 to reveal *m/z* peaks indicating enone **3.I** (*m/z* = 271 $[M+CH_3CN+H]^+$) and formyl **3.V** (m/z = 220 $[M-H]^-$) as major byproducts of TMC-205.

(A) (B)

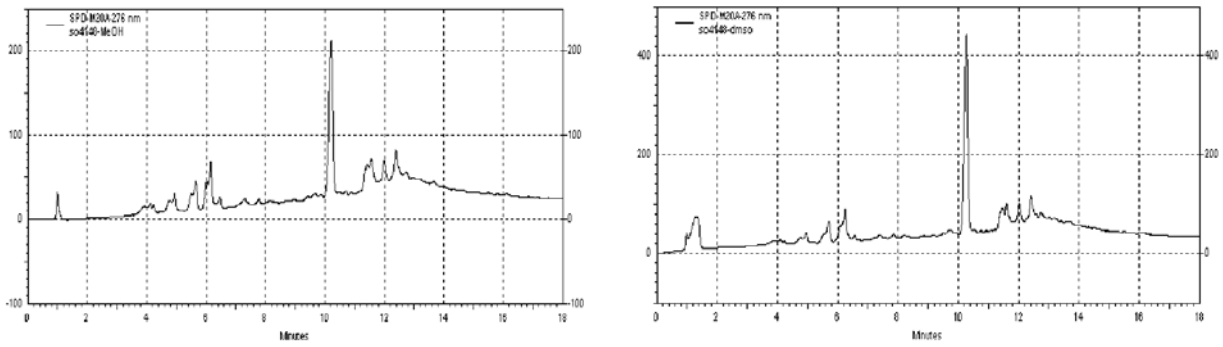

Figure 3-2 HPLC chromatograms of TMC-205 after being exposed to light and air for 16 h. (A) Experiment performed with TMC-205 in MeOH. (B) Experiment performed with TMC-205 in DMSO. (A) and (B): x-axis: elution time (min). y-axis: absorption at 276 nm. Elution conditions: flow rate = 1.0 mL/min. Gradient: 10→95% MeCN in water (containing 0.1% HCOOH) over 20 min. Column: C18 XDB 4.6 mm × 7.5 cm. T = 24 °C.

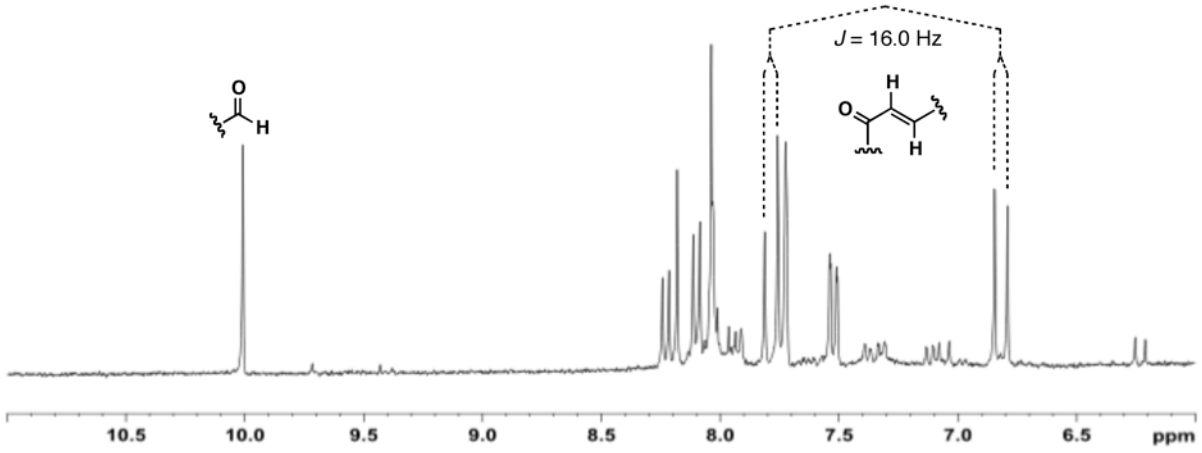

Figure 3-3 ^{1}H NMR spectrum of TMC-205 in CD_3OD after being exposed to light and air for 16 h.

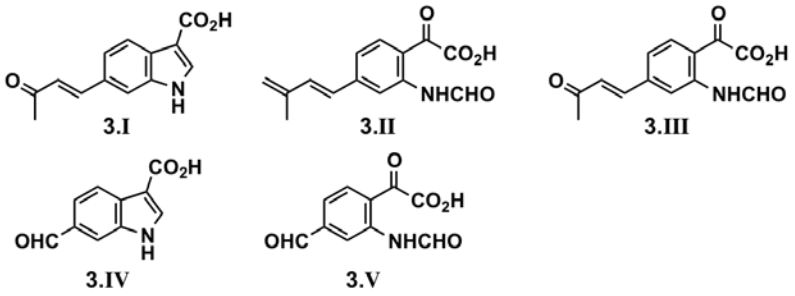

Figure 3-4 (A) Structures of possible byproducts of decomposed TMC-205 (B) Selective oxidation of TMC-205 with singlet oxygen.

Following these analysis, we chose to see which reactive oxygen species (ROS) was responsible for the oxidized by-products of TMC-205. After exposure of synthetic TMC-205 to various cocktails that produce specific ROS (singlet oxygen, superoxide, hydrogen peroxide and hydroxyl radical),[153] we discovered that singlet oxygen was primarily responsible for the decomposition of TMC-205. Treatment with NaN_3, a widely used singlet oxygen scavenger, retarded the decomposition of TMC-205 as determined by HPLC analysis (Figure 3-5).

(A) (B)

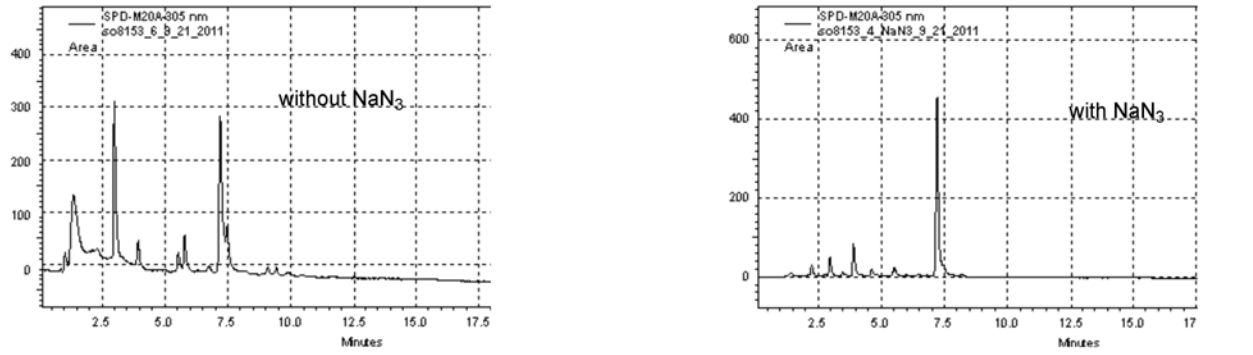

(C) (D)

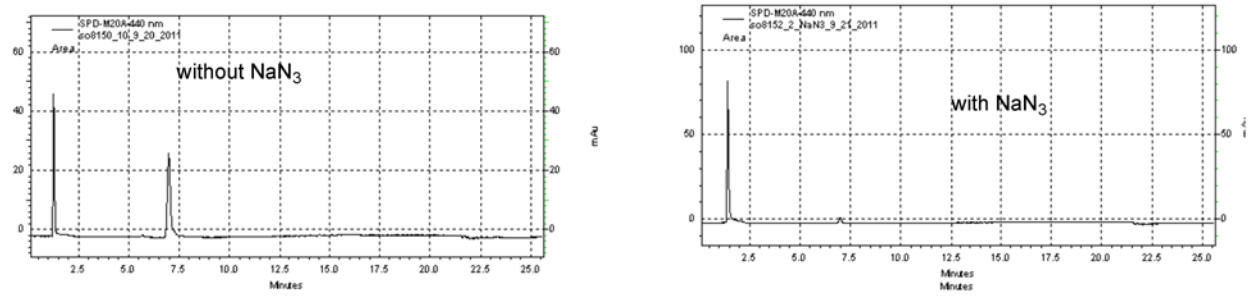

Figure 3-5 HPLC chromatograms (A–D) of the reaction between singlet oxygen and TMC-205 or *N*,*N*-dimethyl nitrosoaniline.

(A) and (B): reaction of TMC-205 (without or with NaN_3) with singlet oxygen. Exposure of TMC-205 to other ROS species (hydroxyl radical, superoxide and hydrogen peroxide) showed no sign of reaction. Exposure of ketone **3.13** to any of the ROS species showed no sign of reaction. (C) and (D): reaction of *N*,*N*-dimethyl nitrosoaniline (without or with NaN_3) with singlet oxygen.

3.4 SYNTHESIS AND ANTIPROLIFERATIVE ACTIVITY OF TMC-205 ANALOGUES

A notable functional group in TMC-205 is the carboxy group. As such, we prepared the decarboxylated analogue **3.9** and alcohol **3.10** (Scheme 3-3A). Alcohol **3.10**, prepared by reducing methyl ester **3.8** using DIBALH, was more sensitive to light, air and heat than TMC-205. The cytotoxicity assay with HCT-116 cells showed that decarboxylated analogue **3.10** was ~3 times less potent than TMC-205 (Table 3-1). Alcohol **3.10** and TMC-205 were equipotent, indicating that the negative charge of the carboxy group is not important.

Next, we addressed the importance of the 1,3-diene moiety by comparing TMC-205 and **3.12** (Scheme 3-3). The alkane analogue **3.12**, assembled by hydrogenation of **3.8** followed by ester hydrolysis, did not show cytotoxicity even at 500 μM, indicating the significance of the diene moiety. On a side note, alkane **3.12** was found to be stable in light and air, unlike TMC-205 or **3.10**, implying that the diene could be a contributing factor to the instability of TMC-205.

(A)

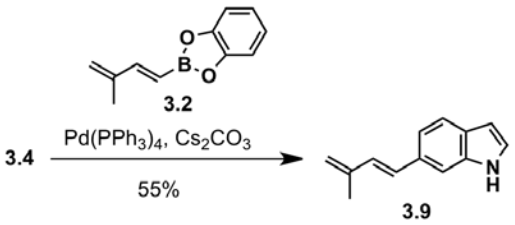

(B)

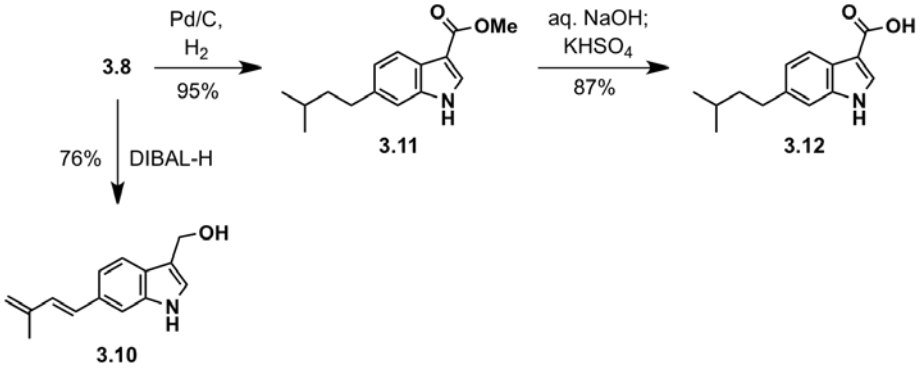

Scheme 3-3 Preparation of analogues **3.9**, **3.10**, and **3.12**.

During these structure-activity relationship studies, it became apparent that the instability of TMC-205 and its analogues could be detrimental to the biological experiments in our research. In order to improve the stability of TMC-205, we decided to introduce an electron-withdrawing group to the natural product, yielding ketone **3.13** (Scheme 3-4). Indeed, this analogue was completely stable under room light and air than TMC-205. Moreover, analogue **3.13** was nearly twice as potent as TMC-205, with a GI_{50} value of 39 μM against HCT-116 cells (Table 3-1).

N-Methylated analogue **3.14** (Scheme 3-4) was less cytotoxic than analogue **3.13**, implying that the N-H group may serve as a hydrogen bonding donor or that a putative binding pocket for this functional group may not tolerate additional steric bulk.

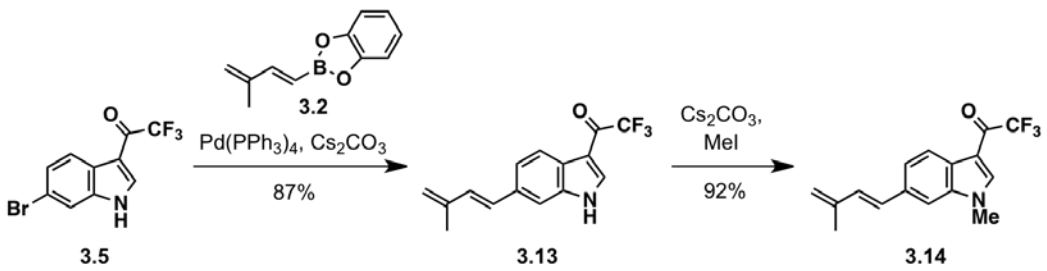

Scheme 3-4 Preparation of analogues **3.13** and **3.14**.

The improved stability of analogue **3.13** enabled us to revisit the question about the 1,3-diene moiety. The air-oxidation of TMC-205 described above might occur in cellular environment to yield an enone functionality that could be the *bona fide* bioactive species.[154] Thus, we asked whether the oxidized product could be relevant to the biological activity of TMC-205. The synthesis of analogue **3.18** began with intermediate **3.5** (Scheme 3-5A). A Heck cross-coupling[155] between **3.5** and methyl vinyl ketone using $Pd(OAc)_2$ and $P(tBu)_3HBF_4$ at 45 °C delivered only the conjugate addition product **3.16**, indicating that the oxidative insertion of Pd(0) into the C-Br bond did not occur. At 100 °C, the Heck reaction of **3.15** proceeded, but concomitant deprotection-conjugate addition at the NH group occurred to give undesired product **3.17** in 50 – 80% yields (Scheme 3-5A). Attempts to convert **3.17** to **3.18** under basic conditions met with no success, resulting in the recovery of the starting material.

These failures prompted us to undertake a different approach towards **3.20**. A Stille coupling between **3.5** and $^{n}Bu_3SnCH{=}CH_2$ yielded C6-vinylated product **3.19** in 72% yield (Scheme 3-5B). Indole **3.19** was treated with methyl vinyl ketone in the presence of **Ru-1** to form the enone analogue **3.20** in 30% yield. Enone **3.20** was 3 and 5 times more potent than 1,3-diene **3.13** and TMC-205, respectively, with a GI_{50} value of 14 μM (Table 3-1). Thus, we asked whether the electrophilicity was of any significance for the activity of this enone. The syntheses of the two allylic alcohols **3.21** and **3.22**, are illustrated in Scheme 3-5B. The secondary allylic alcohol **3.21** was equipotent to enone **3.20** (Table 3-1), suggesting that **3.21** might be oxidized to **3.20**, although this hypothesis warrants further investigation. The tertiary allylic alcohol **3.22** was far less potent, which could imply that the additional methyl group might be too bulky for a putative binding pocket or preventing the alcohol from being oxidized to the enone.

(A)

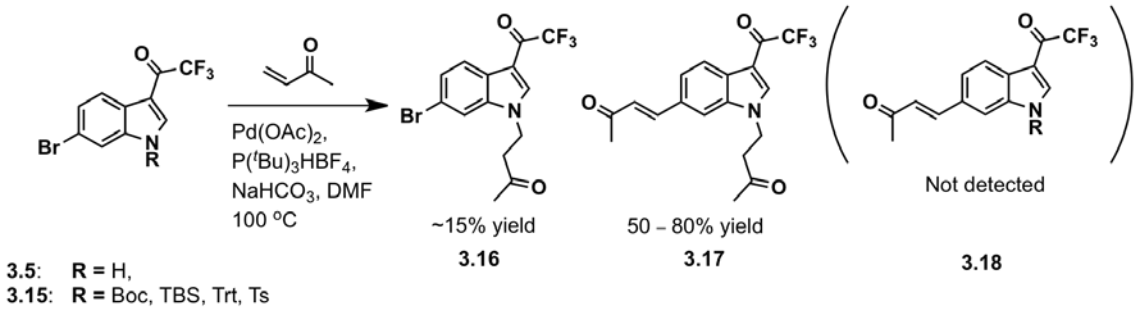

(B)

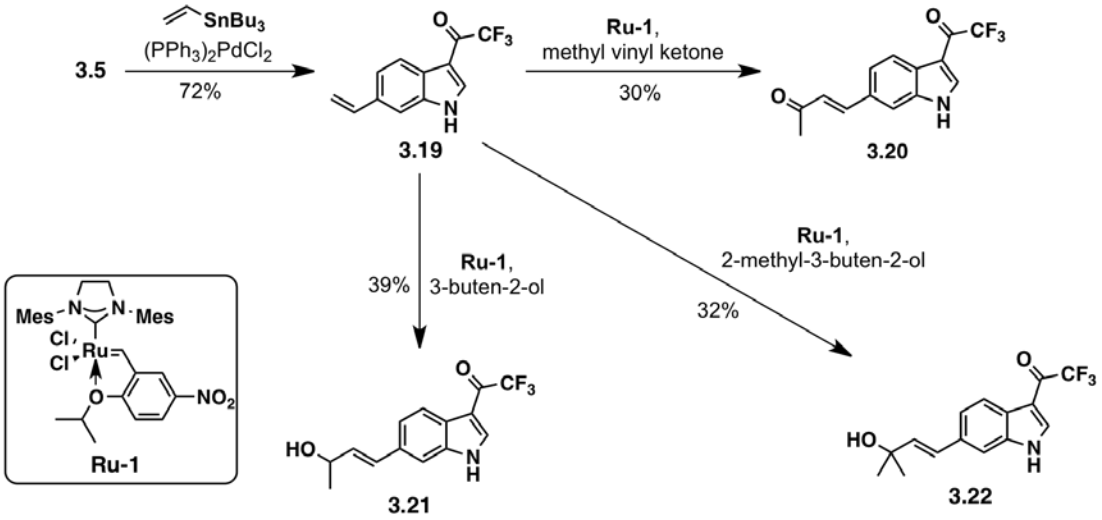

Scheme 3-5 (A) Failed attempts to form enone **3.18**. (B) Preparation of analogues **3.20**, **3.21**, and **3.22**.

After improving the activity of TMC-205 by 8 fold, we prepared readily conjugatable analogues **3.26** and **3.27** (Scheme 3-6) for further studies. These two analogues exhibited significantly reduced antiproliferative activity against HCT-116 cell line (Table 3-1). These

results imply that an aromatic C-H bond may need to be derivatized to insert a handle without loss of activity.

(A)

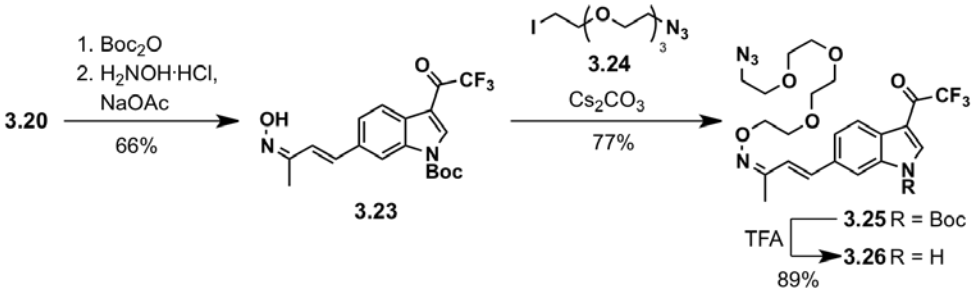

(B)

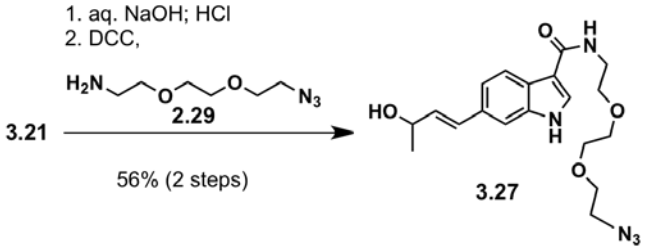

Scheme 3-6 Preparation of analogues (A) **3.26** and (B) **3.27**.

Table 3-1 Antiproliferative activity of TMC-205 and its analogues against HCT-116 cells. Vincrstine was used a control, displayed GI_{50} values between 0.20 ± 0.22 and 0.3 ± 0.1 nM.

Compound	GI_{50} (μM)[a]
3.1	68 ± 3
3.9	147 ± 10
3.10	79 ± 15
3.12	>500
3.13	39 ± 12
3.14	>500
3.20	14 ± 4
3.21	8 ± 6
3.22	>500
3.26	>100
3.27	>99

[a] Each experiment consists of twelve data points (twelve different concentrations).

3.5 GENE EXPRESSION STUDIES OF TMC-205 AND ANALOGUES

Previously, TMC-205 was found to activate *luciferase* gene driven by an SV40 promoter in an SV40 enhancer-dependent manner using the pGL3-control Luciferase Vector® (Promega).[144] The activation of the *luciferase* gene driven by the SV40 promoter without the SV40 enhancer (pGL3-promoter Luciferase Vector®, Promega) was negligible in the presence of TMC-205.[144] Due to the lack of details for dose-dependence, first we determined the TMC-205-concentration dependence with these two commercially available vectors transiently transfected in HeLa cells. All the gene expression experiments were performed by Ms. Yang Gao in our research group. The natural product activated the *luciferase* expression in a dose-dependent manner independent of an SV40 enhancer (Figure 3-6A and 3-6B). A significant and

unexpected discovery from this experiment is that there is a range of concentrations (0.1–1 μM) in which TMC-205 activates the SV40:*luciferase* without inhibiting cell growth (GI_{50} in HeLa cells is 157 μM).[144] Analogue **3.13** and **3.21** also activated the expression of SV40:*luciferase* without inhibiting cell growth (Figure 3-6C and D). RT-PCR analysis of the total RNA extracted from **3.13**-, meayamycin-,[156] and DMSO-treated cells further validated that analogue **3.13** upregulated the expression of luciferase.

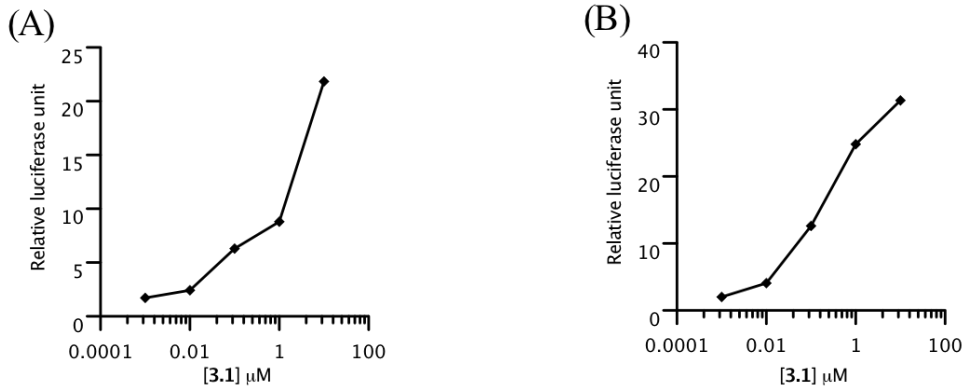

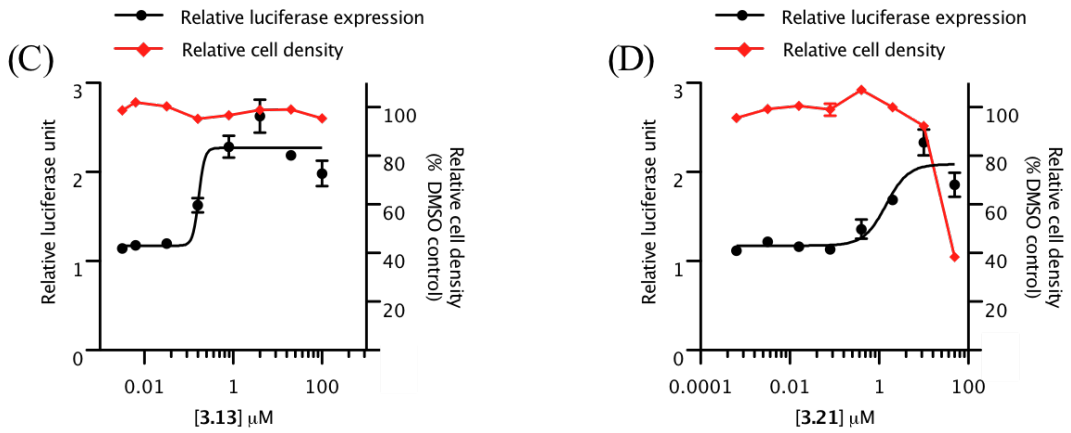

Figure 3-6 Effect of TMC-205, ketone **3.13** and allylic alcohol **3.21** on luciferase expression regulated by an SV40 promoter.

Signals were normalized to the samples treated with vehicle. (A) TMC-205 upregulates expression of luciferase gene under the control of SV40 promoter and enhancer in transiently transfected HeLa cells. (B) TMC-205 upregulates expression of luciferase gene under the control of SV40 promoter without enhancer in transiently transfected HeLa cells. (C) Ketone **3.13** upregulates expression of luciferase gene under the control of SV40 promoter and enhancer in transiently transfected HeLa cells, without loss of cell viability. Data represent mean values ± s.d. (n = 2). (D) Allylic alcohol **3.21** upregulates expression of luciferase gene under the control of SV40 promoter and enhancer in transiently transfected HeLa cells, without loss of cell viability. Data represent mean values ± s.d. (n = 2).

Subsequently, we stably transfected a HeLa cell line with the pGL3-control luciferase vector and were able to observe similar gene activation with TMC-205 at concentrations ranging from 1 to 300 μM without any loss of cell viability (EC_{50} = 6 μM, Figure 3-7). It should be noted

that the cells were treated with TMC-205 and analogues for only 24 h. The more stable and active analogue, **3.13**, also shows a range of concentrations where activation of luciferase gene was observed (EC_{50} = 5 nM) without apparent growth inhibition (Figure 3-7B).

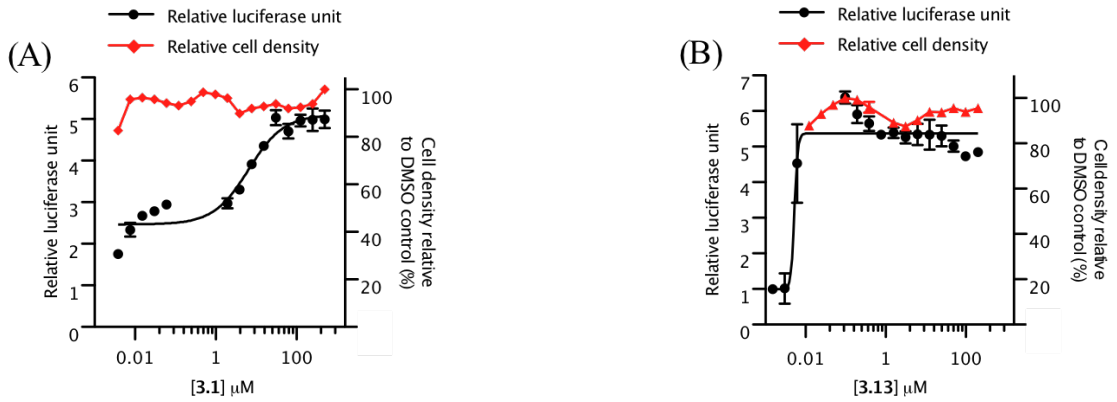

Figure 3-7 Effect of TMC-205 and analogue **3.13** on luciferase expression regulated by an SV40 promoter and enhancer, in stably transfected HeLa cells.

Signals were normalized to the samples treated with vehicle. (A) TMC-205 upregulates expression of luciferase gene, without loss of cell viability. Data represent mean values ± s.d. (*n* = 4). (B) Analogue **3.13** upregulates expression of luciferase gene, without loss of cell viability. Data represent mean values ± s.d. (*n* = 2).

3.6 SUMMARY

In summary, the first total synthesis of TMC-205 has been accomplished. We then developed TMC-205 analogues that include alcohol **3.21**, an eight-fold more potent analogue of TMC-205.

Importantly, there is a range of TMC-205 and analogue **3.13** concentrations where the compounds activate an SV40-controlled gene without apparent antiproliferative activity (e.g., EC_{50} for **3.13** = 5 nM). The SV40 promoter is recognized by human AP-1 and transcription factor Sp-1 (and related transcription factors). These transcription factors are important regulatory proteins in the development of organisms and cancer.[156] While our studies revealed that changes in the expression level of genes regulated by the SV40 promoter were from compound treatment, it could be the outcome of multiple reasons. For instance, one of them being direct influence on transcription factors driving the SV40 promoter, or indirect or non-specific effects could be operative. Further experimentation, beyond the reporter gene assay, to illustrate whether this observed activity is specific or not would be needed. Additionally, TMC-205 (or its derivatives) could be used as a fluorescence quencher, since preliminary experiments revealed that TMC-205 decreases the fluorescence of dichlorofluorescein in a time and concentration dependent manner.

APPENDIX A

EXPERIMENTAL SECTION

General Techniques

All reactions were carried out with freshly distilled solvents under anhydrous conditions, unless otherwise noted. All of the flasks used for carrying out reactions were dried in an oven at 80 °C prior to use. Unless specifically stated, the temperature of a water bath during the evaporation of organic solvents using a rotary evaporator was 47 °C. All of the syringes in this study were dried in an oven at 80 °C and stored in a desiccator over Drierite®. Tetrahydrofuran (THF) was distilled over Na metal and benzophenone. Methylene chloride (CH_2Cl_2) was distilled over calcium hydride. Acetonitrile was distilled from CaH_2 and stored over 3Å molecular sieves. Yields refer to chromatographically and spectroscopically (^{1}H NMR) homogenous materials, unless otherwise stated. All reactions were monitored by thin-layer chromatography (TLC) carried out on 0.25 mm Merck silica gel plates (60F-254) using UV light (254 nm) for visualization or anisaldehyde in ethanol or 0.2% ninhydrin in ethanol as a developing agents and heat for visualization. Silica gel (230-400 mesh) was used for flash column chromatography. A rotary evaporator was connected to a water aspirator that produced a vacuum pressure of approximately 60 mmHg when it was connected to the evaporator. NMR spectra were recorded

on a Bruker Advance spectrometer at 300 MHz, 400 MHz, 500 MHz, 600 MHz or 700 MHz. The chemical shifts are given in parts per million (ppm) on a delta (δ) scale. The solvent peak was used as a reference value, for ^{1}H NMR: $CHCl_3$ = 7.27 ppm, MeOH = 3.31 ppm, DMSO = 2.50 ppm, acetone = 2.05ppm, for ^{13}C NMR: $CDCl_3$ = 77.00 ppm, CD_3OD = 49.00 ppm, DMSO-d_6 = 49.10 ppm and acetone-d_6 = 29.40 ppm. The following abbreviations are used to indicate the multiplicities: s = singlet; d = doublet; t = triplet; q = quartet; m = multiplet; br = broad. High-resolution mass spectra were recorded on a VG 7070 spectrometer. Low-resolution mass spectra [LCMS (ESI)] were recorded on a Shimadzu LCMS-2020. Infrared (IR) spectra were collected on a Mattson Cygnus 100 spectrometer. Samples for acquiring IR spectra were prepared as a thin film on a NaCl plate by dissolving the compound in CH_2Cl_2 and then evaporating the CH_2Cl_2.

Abbreviations

http://pubs.acs.org/paragonplus/submission/joceah/index.html

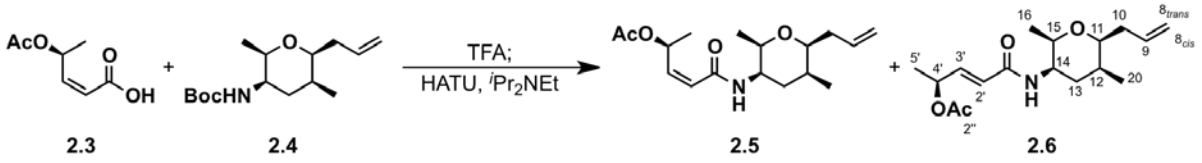

2.3 2.4 2.5 2.6

*Preparation of alkene **2.6**:* To a solution of 5 mL of 10% TFA in CH_2Cl_2 at 0 °C was added the Boc-protected amine **2.4** (81 mg, 0.30 mmol). The reaction was warmed to 23 °C and stirred for 4 h. The solvent was removed *in vacuo*, and the residue was diluted with EtOAc (10 mL) and aqueous saturated $NaHCO_3$ (10 mL). The organic layer was separated, and the aqueous layer was extracted with EtOAc (2 × 10 mL). The combined organic layers were dried over anhydrous Na_2SO_4, filtered, and concentrated *in vacuo*, and the residue was used in the next step without further purification.

To a stirred solution of acid **2.3** (80 mg, 0.50 mmol) in MeCN (1.5 mL) at 23 °C was added *O*-(7-azabenzotriazol-1-yl)-*N,N,N′,N′*-tetramethyluronium hexafluorophosphate (152 mg, 0.40 mmol), followed by *N*,*N*-diisopropylethylamine (194 mg, 1.50 mmol) under a nitrogen atmosphere. The resulting mixture was stirred for 10 min then transferred by cannula to a stirred solution of the amine in MeCN (1.0 mL) at the same temperature. After 15 h at 23 °C, the reaction was quenched with saturated aqueous NH_4Cl (2 mL) and most of the organic solvent was removed *in vacuo*. The aqueous residue was extracted with EtOAc (3 × 10 mL). The combined organic layers were dried over anhydrous Na_2SO_4, filtered, and concentrated *in vacuo*. The crude residue was purified by flash chromatography (7.5 to 50 % EtOAc in hexanes) on silica gel (25 mL) to afford the desired product **2.6** (40 mg, 43% yield) as a clear oil, and the *cis* isomer (**2.5**) (52 mg , 56 % yield) as a clear oil.

*Data for alkene **2.6***: R_f = 0.31 (40% EtOAc in hexanes); IR (film): ν_{max} = 3308, 2974, 2934, 1740 (C=O), 1637 (C=O), 1530, 1446, 1240 cm^{-1}; $[\alpha]_D^{23}$ -1.6 (*c* 1.9, $CHCl_3$); ^1H NMR (300 MHz, 293 K, 1% CD_3OD in $CDCl_3$): δ = 6.75 (dd, *J* = 15.3, 5.4 Hz, 1H, 3′-H), 5.94 (dd, *J* = 15.3, 1.5 Hz, 1H, 2′-H), 5.81–5.73 (m, 1H, 9-H), 5.49 (qdd, *J* = 6.9, 5.4, 1.5 Hz, 1H, 4′-H), 5.14 (dd, *J* = 17.4, 1.5 Hz, 1H, 8_{trans}-H), 5.07 (br d, *J* = 10.2 Hz, 1H, 8_{cis}-H), 4.01–3.97 (m, 1H, 14-H), 3.65 (qd, *J* = 6.3, 2.0 Hz, 1H, 15-H), 3.53 (ddd, *J* = 7.2, 7.2, 2.7 Hz, 1H, 11-H), 2.39–2.30 (m, 1H, 10-H), 2.24–2.13 (m, 1H, 10-H), 2.09 (s, 3H, 2′′-H), 1.95–1.93 (m, 2H, 13-H), 1.82–1.79 (m, 1H, 12-H), 1.37 (d, *J* = 6.9 Hz, 3H, 5′-H), 1.15 (d, *J* = 6.3 Hz, 3H, 16-H), 1.04 (d, *J* = 7.5 Hz, 3H, 20-H); ^{13}C NMR (75 MHz, 293 K, $CDCl_3$): δ = 170.0, 164.6, 142.1, 134.6, 123.5, 116.8, 80.7, 76.0, 69.1, 47.3, 37.3, 35.8, 28.8, 21.2, 19.8, 17.9, 15.2; HRMS (EI+) calcd for $C_{17}H_{27}NO_4Na$ $[M + Na]^+$ 332.1838, found 332.1869.

Data for **2.5**, see: Albert, B. J.; Sivaramakrishnan, A.; Naka, T.; Koide, K. *J. Am. Chem. Soc.* **2006**, *128*, 2792–2793.

2.6 **2.7**

*Preparation of allylic alcohol **2.7***: To a stirred solution of **2.6** (25 mg, 80 μmol) in MeOH (2.5 mL) was added K_2CO_3 (28 mg, 0.20 mmol) at 0 °C under an open atmosphere. After 2 h at the same temperature, the reaction mixture was diluted with saturated aqueous NH_4Cl (3 mL) and H_2O (7 mL), and the resulting solution was extracted with EtOAc (3 × 10 mL). The combined organic layers were dried over anhydrous Na_2SO_4, filtered, and concentrated *in vacuo*. The resulting crude residue was purified by flash chromatography (20 to 90% EtAOc in hexanes) on silica gel (5 mL) to afford **2.7** (16 mg, 75% yield) as a colorles oil.

*Data for allylic alcohol **2.7***: R_f = 0.30 (40% EtOAc in hexanes); IR (film): ν_{max} = 3324 (br), 3076, 2973, 2930, 1671 (C=O), 1625, 1531, 1462, 1362, 1145, 1063 cm^{-1}; $[\alpha]_D^{23}$ -5.2 (*c* 0.8, $CHCl_3$); ^1H NMR (300 MHz, 293 K, 1% CD_3OD in $CDCl_3$): δ = 6.87 (dd, *J* = 15.3, 4.5 Hz, 1H, 3′-H), 5.98 (dd, *J* = 15.3, 1.7 Hz, 1H, 2′-H), 5.87–5.73 (m, 1H, 9-H), 5.15 (dd, *J* = 17.4, 1.5 Hz, 1H, 8′-H), 5.08 (dd, *J* = 10.2, 1.5 Hz, 1H, 8-H), 4.51 (m, 1H, 4′-H), 4.01 (ddd, *J* = 6.9, 2.1, 2.1 Hz, 1H, 14-H), 3.67 (qd, *J* = 6.3, 2.1 Hz, 1H, 15-H), 3.56 (ddd, *J* = 7.2, 7.2, 2.7 Hz, 1H, 11-H), 2.40–2.30 (m, 1H, 10-H), 2.19–2.09 (m, 1H, 10-H), 1.96–1.94 (m, 2H, 13-H), 1.83–1.77 (m, 1H, 12-H), 1.36 (d, *J* = 6.9 Hz, 3H, 5′-H), 1.16 (d, *J* = 6.3 Hz, 3H, 16-H), 1.05 (d, *J* = 7.5 Hz, 3H, 20-H); ^{13}C NMR (75 MHz, 293 K, $CDCl_3$): δ = 165.2, 146.7, 134.7, 121.9, 116.8, 80.8, 76.1,

67.2, 47.3, 37.4, 36.0, 28.9, 23.1, 17.9, 15.1; HRMS (ESI+) calcd for $C_{15}H_{25}NO_3Na$ $[M + Na]^+$ 290.1732, found 290.1712.

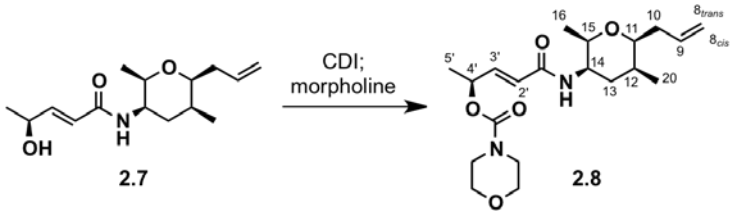

*Preparation of carbamate **2.8***: A stirred solution of **2.7** (24 mg, 90 μmol) in CH_2Cl_2 (0.5 mL) at 23 °C was treated with 1,1'-carbonyldiimidazole (18 mg, 0.11 mmol) under normal atmosphere. After 27 h, morpholine (39.2 mg, 0.450 mmol) was added, and the mixture was stirred at 23 °C for 16 h. The solvent was removed *in vacuo*, and the resulting residue was purified by flash chromatography (20 to 80% EtOAc in hexanes) on silica gel (5 mL) to afford **2.8** (33.0 mg, 97% yield) as a white solid.

*Data for carbamate **2.8***: mp = 161–163 °C ; R_f = 0.35 (60% EtOAc in hexanes); IR (film): ν_{max} = 3304, 2968, 2930, 2858, 1704 (C=O), 1673 (C=O), 1626, 1426, 1241, 1117 cm^{-1}; $[\alpha]_D^{23}$ +3.53 (*c* 1.18, $CHCl_3$); ^1H NMR (300 MHz, 293 K, $CDCl_3$): δ = 6.78 (dd, *J* = 15.3, 5.4 Hz, 1H, 3′-H), 5.96 (dd, *J* = 15.3, 1.5 Hz, 1H, 2′-H), 5.81–5.74 (m, 1H, 9-H), 5.50–5.41 (m, 1H, 4′-H), 5.15 (br d, *J* = 17.1, 1H, 8′-H), 5.08 (br d, *J* = 10.2, 1H, 8-H), 4.01–3.99 (m, 1H, 14-H), 3.68–3.66 (m, 5H, morpholine-C*H*$_2$O, 15-H), 3.56 (ddd, *J* = 6.9, 6.9, 2.4 Hz, 1H, 11-H), 3.48 (t, *J* = 4.7 Hz, 4H, morpholine-C*H*$_2$N), 2.35 (ddd, *J* = 14.1, 6.9, 6.9 Hz, 1H, 10-H), 2.14 (ddd, *J* = 14.1, 6.9, 6.9 Hz, 1H, 10-H), 1.94–1.93 (m, 2H, 13-H), 1.81–1.78 (m, 1H, 12-H), 1.37 (d, *J* = 6.6 Hz, 3H, 5′-H), 1.16 (d, *J* = 6.3 Hz, 3H, 16-H), 1.04 (d, *J* = 7.2 Hz, 3H, 20-H); ^{13}C NMR (75 MHz, 293 K, $CDCl_3$): δ = 164.7, 154.4, 142.8, 134.6,123.4, 116.8, 80.8, 76.1, 70.3, 66.6, 47.3,

44.1, 37.3, 35.9, 28.9, 20.2, 17.9, 15.2; HRMS (ESI+) calcd for $C_{20}H_{32}N_2O_5Na$ $[M + Na]^+$ 403.2209, found 403.2209.

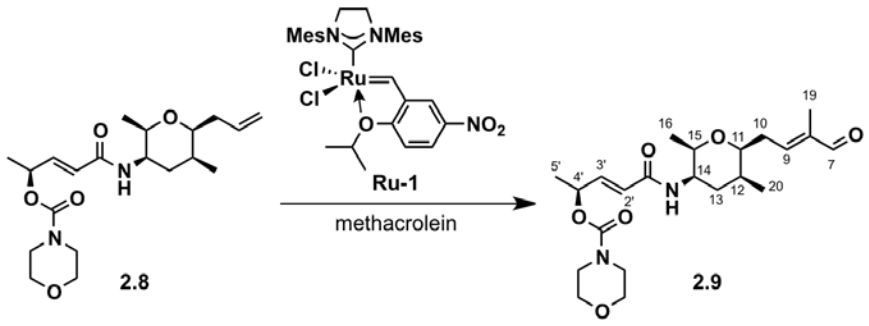

*Preparation of aldehyde **2.9***: To a stirred solution of alkene **2.8** (60 mg, 0.16 mmol) and methacrolein (224 mg, 3.20 mmol) in CH_2Cl_2 (0.3 mL) was added **Ru-1** (2.0 mg, 3.2 μmol), followed by *p*-benzoquinone (2.0 mg, 20 μmol) under open atmosphere. After 12 h at 23 °C, the mixture was concentrated *in vacuo*. The residue was purified by flash chromatography (40 to 100% EtOAc in hexanes) on silica gel (20 mL) to afford aldehyde **2.9** (50 mg, 74% yield) as a dark-grey oil.

*Data for aldehyde **2.9***: R_f = 0.15 (60% EtOAc in hexanes); IR (film): ν_{max} = 3337, 2974, 2926, 2857, 1710 (C=O), 1678 (C=O), 1637 (C=O), 1528, 1459, 1428, 1242, 1117, 1069 cm^{-1}; $[\alpha]_D^{23}$ -6.16 (*c* 1.4, $CHCl_3$) ^1H NMR (300 MHz, 293 K, 1% CD_3OD in $CDCl_3$): δ = 9.43 (s, 1H, 7-H), 6.80 (dd, *J* = 15.3, 5.7 Hz, 1H, 3′-H) 6.54 (ddd, *J* = 7.5, 7.5, 1.2 Hz, 1H, 9-H), 5.94 (dd, *J* = 15.3, 1.2 Hz, 1H, 2′-H), 5.72 (br d, *J* = 9.0 Hz, N-H), 5.46 (dqd, *J* = 5.7, 6.6, 1.2 Hz, 1H, 4′-H), 4.03 (dddd, *J* = 9.0, 6.6, 2.9, 2.9 Hz, 1H, 14-H), 3.74–3.66 (m, 6H, morpholine-CH_2O, 15-H, 11-H), 3.48 (t, *J* = 4.7, 4H, morpholine-CH_2N), 2.63–2.53 (m, 1H, 10-H), 2.47–2.37 (m, 1H, 10-H), 2.00–1.98 (m, 2H, 13-H), 1.87–1.81 (m, 1H, 12-H), 1.77 (s, 3H, 19-H), 1.38 (d, *J* = 6.6 Hz, 3H, 5′-H), 1.17 (d, *J* = 6.6 Hz, 3H, 16-H), 1.09 (d, *J* = 7.5 Hz, 3H, 20-H); ^{13}C NMR (75 MHz,

293 K, $CDCl_3$): δ = 194.9, 164.7, 154.4, 150.1, 143.0, 140.6, 123.2, 79.8, 76.3, 70.3, 66.5, 47.1, 44.1, 35.7, 32.7, 29.5, 20.2, 17.8, 15.3, 14.1; HRMS (ESI+) calcd for $C_{22}H_{34}N_2O_6Na$ $[M + Na]^+$ 445.2315, found 445.2357.

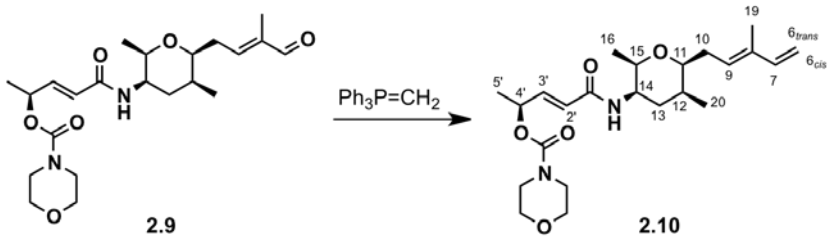

*Preparation of alkene **2.10***: To a stirred suspension of methytriphenylphosphonium bromide (103 mg, 0.290 mmol) in THF (2.0 mL) at 0 °C was added KO^{t}Bu (30.0 mg, 0.270 mmol) under nitrogen atmosphere. After 30 min at 0 °C, aldehyde **2.9** (50.0 mg, 0.120 mmol) in THF (0.2 mL) was added dropwise by cannula at the same temperature and rinsed with additional THF (0.1 mL). After 3 h at the same temperature, the reaction was quenched with saturated aqueous NH_4Cl (5 mL). The mixture was extracted with EtOAc (3 × 10 mL). The combined organic layers were dried over anhydrous Na_2SO_4, filtered, and concentrated *in vacuo*. The crude residue was purified by flash chromatography (30 to 90% EtOAc in heanes) on silica gel (20 mL) to afford the terminal alkene **2.10** (25.0 mg, 50% yield) as a colorless oil.

*Data for alkene **2.10***: R_f = 0.27 (60% EtOAc in hexanes); IR (film): ν_{max} = 3435, 2928, 1707 (C=O), 1640 (C=O), 1456, 1375, 1242, 1118 cm^{-1}; $[\alpha]_D^{23}$ +4.6 (*c* 1.0, $CHCl_3$); ^{1}H NMR (300 MHz, 293 K, $CDCl_3$): δ = 6.79 (dd, *J* = 15.3, 5.4 Hz, 1H, 3′-H), 6.39 (dd, *J* = 17.4, 10.8 Hz, 1H, 7-H), 5.92 (dd, *J* = 15.3, 1.5 Hz, 1H, 2′-H), 5.77 (br d, *J* = 9.0 Hz, 1H, N-H), 5.50 (m, 2H, 4′-H, 9-H), 5.15 (br d, *J* = 17.4 Hz, 1H, 6′-H), 4.99 (br d, *J* = 10.8 Hz, 1H, 6-H), 4.01 (dddd, *J* = 9.0, 6.9, 2.9, 2.9 Hz, 1H, 14-H), 3.70–3.67 (m, 5H, morpholine-C*H*$_2$O, 15-H), 3.57 (ddd, *J* = 7.2, 7.7,

2.7 Hz, 1H, 11-H), 3.49 (t, *J* = 4.8 Hz, 4H, morpholine-CH_2N), 2.46–2.37 (m, 1H, 10-H), 2.32–2.22 (m, 1H, 10-H), 1.95 (ddd, *J* = 0, 3.5, 3.5 Hz, 2H, 13-H), 1.83–1.80 (m, 1H, 12-H), 1.77 (s, 3H, 19-H), 1.40 (d, *J* = 6.9 Hz, 3H, 5′-H), 1.17 (d, *J* = 6.6 Hz, 3H, 16-H), 1.05 (d, *J* = 7.5 Hz, 3H, 20-H); ^{13}C NMR (75 MHz, 293 K, $CDCl_3$): δ = 164.7, 154.4, 142.8, 141.2, 135.8, 127.9, 123.4, 111.2, 80.9, 76.1, 70.3, 65.8, 47.4, 44.0, 35.9, 31.9, 29.0, 20.3, 17.9, 15.3, 12.0; HRMS (ESI+) calcd for $C_{23}H_{36}N_2O_5Na$ $[M + Na]^+$ 443.2522, found 443.2505.

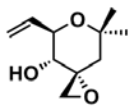

2.11

Synthesis of **2.11**, see: B. J. Albert, A. Sivaramakrishnan, T. Naka, N. L. Czaicki, K. Koide, *J. Am. Chem. Soc.* **2007**, *129*, 2648–2659.

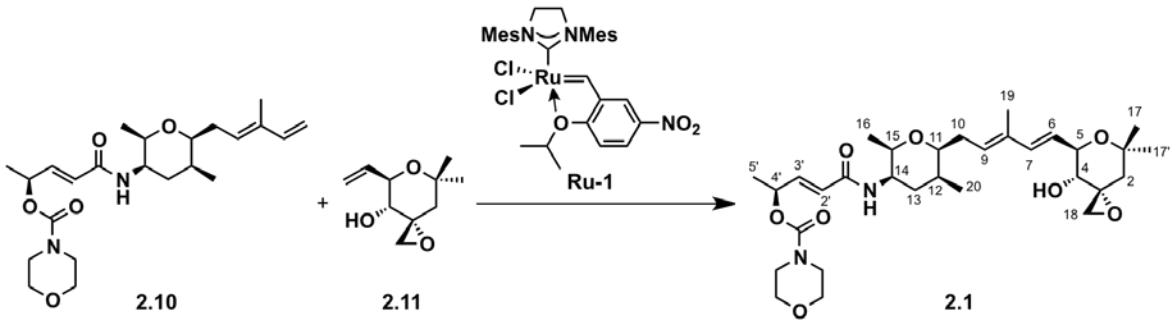

*Preparation of analogue **2.1***: A solution of right fragment **2.11** (14 mg, 80 μmol) was prepared in DCE (0.2 mL) at 23 °C under an open atmosphere. To a stirred solution of **2.10** (25 mg, 60 μmol) in DCE (0.2 mL) was added the solution of **2.11** (0.1 mL), **Ru-1** (1.5 mg, 2.2 μmol), followed by benzoquinone (1.5 mg, 14 μmol) at 23 °C under an open atmosphere. The reaction mixture was then heated to 42 °C. After 2.5 h at the same temperature, additional **Ru-1**

(1.5 mg, 2.2 μmol), benzoquinone (1.5 mg, 14 μmol), and **2.11** (0.1 mL) were added. After 21.5 total hours, the reaction mixture concentrated *in vacuo*. The resulting residue was purified by preparative-TLC (90% EtOAc in hexanes) to afford the desired product (12.0 mg, 35% yield) as a dark thick paste, and a mixture of **2.10** and **2.11** (9.0 mg).

To a stirred solution of recovered **2.11** and **2.10** in DCE (0.4 mL) was added benzoquinone (1.5 mg, 14 μmol) and **Ru-1** (1.5 mg, 2.2 μmol) at 23 °C under an open atmosphere. The reaction mixture was then heated to 42 °C. After an additional 21 h at the same temperature, the reaction was concentrated *in vacuo*. The resulting residue was purified by preparative-TLC (90% EtOAc in hexanes) to afford the desired product (3.9 mg) as a tan thick paste. The combined yield of **2.1** is 16 mg (46% yield).

A portion of this material was re-purified by preparative-TLC (90% EtOAc in hexanes) and used for biological experiments.

*Data for analogue **2.1***: R_f = 0.20 (90% EtOAc in hexanes); IR (film): ν_{max} = 3350 (br), 2924, 2856, 1701 (C=O), 1675 (C=O), 1635, 1527, 1436, 1378, 1276, 1242, 1190, 1118, 1062 cm^{-1}; $[\alpha]_D^{21}$ +0.7 (*c* 1.0, CH_2Cl_2); ^1H NMR (300 MHz, 293 K, 1% CD_3OD in $CDCl_3$): δ = 6.74 (dd, *J* = 15.3, 5.1 Hz, 1H, 3′-H), 6.35 (d, *J* = 15.6 Hz, 1H, 7-H), 5.91 (dd, *J* = 15.3, 1.5 Hz, 1H, 2′-H), 5.76 (br d, *J* = 9.0 Hz, 1H, N-H), 5.66 (dd, *J* = 15.6, 6.6 Hz,1H, 6-H), 5.50 (dd, *J* = 6.9, 6.9 Hz, 1H, 9-H), 5.39 (qdd, *J* = 6.6, 5.1, 1.5 Hz, 1H, 4′-H), 3.97–3.92 (m, 2H, 5-H, 14-H), 3.65–3.60 (m, 5H, 15-H, morpholine-CH_2O), 3.54 (ddd, *J* = 6.3, 6.3, 3.0 Hz, 1H, 11-H), 3.46–3.43 (m, 5H, 4-H, morpholine-CH_2N), 2.94 (d, *J* = 4.7 Hz, 1H, 18-H), 2.45 (dd, *J* = 4.7, 1.5 Hz, 1H, 18-H), 2.38–2.31 (m, 1H, 10-H), 2.26–2.21 (m, 1H, 10-H), 2.17 (d, *J* = 14.4 Hz, 1H, 2_{axial}-H), 1.99–1.95 (m, 2H, 13-H), 1.76 (s, 3H, 19-H), 1.73–1.70 (m, 1H, 12-H), 1.61 (d, *J* = 10.5 Hz, 1H, OH), 1.40 (d, *J* = 14.4 Hz, 1H, $2_{equatorial}$-H), 1.35 (d, *J* = 6.6 Hz, 3H, 5′-H), 1.33 (s, 3H, 17-H),

1.22 (s, 3H, 17′-H), 1.08 (d, J = 6.3 Hz, 3H, 16-H), 1.01 (d, J = 7.2 Hz, 3H, 20-H); ^{13}C NMR (175 MHz, 293 K, $CDCl_3$): δ = 165.3, 155.0, 143.3, 136.4, 134.0, 129.1, 125.6, 121.7, 80.6, 79.4, 76.3, 73.4, 73.0, 72.0, 67.1, 56.9, 46.8, 47.0, 43.0, 36.1, 32.3, 31.3, 29.7, 29.0, 23.8, 20.1, 17.6, 15.4, 12.0; HRMS (ESI+) calcd for $C_{31}H_{48}N_2O_8Na$ $[M + Na]^+$ 599.3308, found 599.3313.

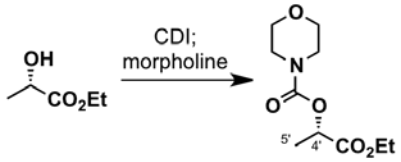

2.12 **2.13**

*Preparation of carbamate **2.13***: To a stirred solution of **2.12** (33.8 g, 0.286 mol) in CH_2Cl_2 (300 mL) was added CDI (48.7 g, 0.300 mol) in portions. The resulting mixture was stirred at 23 °C for 20 h and then cooled to 0 °C. Morpholine (37.4 g, 0.429 mol) was added dropwise. After the addition, the mixture was warmed to 23 °C, stirred for an additional 2 h, and concentrated *in vacuo*. The residue was purified by dry column vacuum chromatography (10 to 70% EtOAc in hexanes) on silica gel (1000 mL) to afford **2.13** (62.1g, 94%) as colorless liquid.

*Data for carbamate **2.13***: R_f = 0.33 (40% EtOAc in hexanes); IR (film): ν_{max} = 3494, 2984, 2859, 1753 (C=O), 1710 (C=O), 1430, 1371, 1302, 1277, 1245, 1203, 1113, 1048, 1021 cm^{-1}; $[\alpha]_D^{22}$ +18.3 (*c* 1.00, $CHCl_3$); ^{1}H NMR (300 MHz, 293K, $CDCl_3$) δ = 5.01 (q, 1H, J = 7.2 Hz, 4′-H), 4.17 (q, 2H, J = 7.2 Hz, CH_2CH$_3$), 3.65 (t, 4H, J = 4.8 Hz, morpholine-CH_2O), 3.48 (br s, 4H, morpholine-CH_2N), 1.45 (d, 3H, J = 6.9 Hz, 5′-H), 1.25 (t, 3H, J = 7.2 Hz, CH$_2$CH_3); ^{13}C NMR (75 MHz, 293K, $CDCl_3$) δ = 171.4, 154.5, 69.5, 66.5, 61.2, 44.3, 17.1, 14.1; HRMS (EI+) calcd. for $C_{10}H_{17}NO_5$ $[M]^+$ 231.1107, found 231.1098.

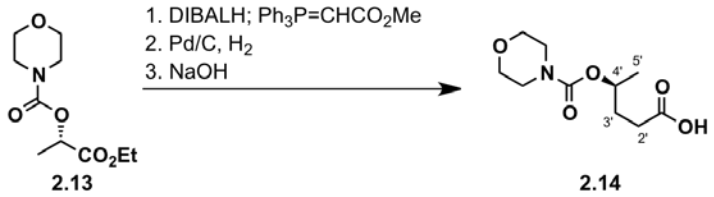

2.13 **2.14**

*Preparation of carboxylic acid **2.14***: To a stirred solution of ester **2.13** (0.99 g, 4.3 mmol) in CH_2Cl_2 (7.4 mL) at -78 °C was added DIBALH (1.0 M in CH_2Cl_2, 4.5 mL) slowly down the flask side under a nitrogen atmosphere. The reaction mixture was stirred for 1 h at -78 °C before adding MeOH (5 mL) slowly. The mixture was stirred at the same temperature for 19 min, followed by the addition of THF (9 mL) and $Ph_3P{=}CHCO_2Me$ (2.16 g, 6.45 mmol). The mixture was then allowed to warm to 23 °C and was stirred for 3.5 h before being quenched with aqueous sodium potassium tartrate (1 M, 20 mL) at the same temperature. After stirring at 23 °C for 27 min, the mixture was extracted with EtOAc (3 × 20 mL). The combined organic layers were washed with brine (10 mL), dried over anhydrous Na_2SO_4, filtered, and concentrated *in vacuo*. The crude mixture was purified by flash chromatography (10% to 30% EtOAc in hexanes) on silica gel (70 mL) to afford a mixture containing the desired product (826 mg) as a clear oil. This mixture was used in the next step without further purification.

To a stirred solution of the product from the first step (826 mg) in EtOAc (10 mL) at 23 °C was added Pd/C (112 mg, 10% wt.%, 0.100 mmol). The flask was flushed with H_2 and kept under hydrogen atmosphere. After stirring for 12.5 h at 23 °C, the reaction mixture was passed through a pad of silica and rinsed with EtOAc (7 mL). The filtrate was concentrated *in vacuo*. The residue was purified by flash chromatography (15% to 40% EtOAc in hexanes) on silica gel (30 mL) to afford a mixture containing the desired product (537 mg) as a clear oil. This mixture was used in the next step without further purification.

To a stirred solution of this mixture (437 mg) in MeOH (8 mL) was added aqueous NaOH (1 M, 9 mL) at 23 °C under an air atmosphere. After 3 h at the same temperature, the reaction mixture was washed with CH_2Cl_2 (7 mL). The aqueous layer was acidified with aqueous HCl (6 M, 10 mL) and extracted with EtOAc (3 × 5 mL). The combined organic layers was dried over anhydrous Na_2SO_4, filtered, and concentrated *in vacuo*. Purification of the residue by flash chromatography (30 to 60% EtOAc in hexanes) on silica gel (50 mL) afforded acid **2.14** (452 mg, 46% yield over 3 steps) as a colorless oil.

*Data for carboxylic acid **2.14***: R_f = 0.26 (40% EtOAc in hexanes); IR (film): ν_{max} = 3455 (br, O-H), 2977, 2929, 2864, 1745 (C=O), 1699 (C=O), 1434, 1248, 1115 cm^{-1}; $[\alpha]_D^{21}$ +25.4 (*c* 1.0, CH_2Cl_2); ^1H NMR (300 MHz, 293 K, 1% CD_3OD in $CDCl_3$): δ = 4.91 (ddq, *J* = 6.3, 6.3, 6.3 Hz, 1H, 4′-H), 3.69–3.61 (m, 4H, morpholine-C*H*$_2$O), 3.48–3.3.42 (m, 4H, morpholine-C*H*$_2$N), 2.43 (dd, *J* = 6.3, 6.3 Hz, 2H, 2′-H), 1.93 (ddd, *J* = 6.3, 6.3, 6.3 Hz, 2H, 3′-H), 1.29 (d, *J* = 6.3 Hz, 3H, 5′-H); ^{13}C NMR (75 MHz, 293 K, $CDCl_3$): δ = 177.7, 155.1, 71.3, 66.6, 44.0, 31.0, 30.0, 20.3; HRMS (ESI+) calcd for $C_{10}H_{17}NO_5Na$ $[M + Na]^+$ 254.1004, found 254.1006.

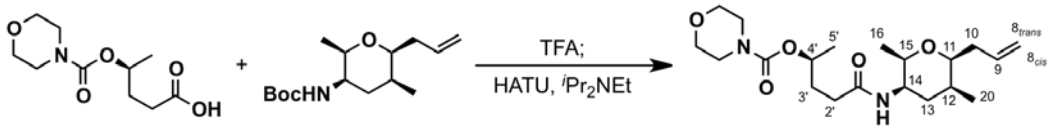

2.14 **2.4** **2.15**

*Preparation of alkene **2.15***: To a solution of 10 mL of 10% TFA in CH_2Cl_2 at 0 °C was added the Boc-protected amine **2.4** (102 mg, 0.380 mmol). The reaction was warmed to 23 °C and stirred for 1 h. The solvent was removed *in vacuo*, and then diluted with EtOAc (5 mL) and saturated aqueous $NaHCO_3$ (5 mL). The layers were separated, and the aqueous layer was

extracted with EtOAc (2 × 5 mL). The combined organic layers were dried over anhydrous Na_2SO_4, filtered, and concentrated *in vacuo* to yield the crude amine.

To a stirred solution of acid **2.14** (11 mg, 0.51 mmol) in MeCN (1.0 mL) at 23 °C was added *O*-(7-azabenzotriazol-1-yl)-*N,N,N′,N′*-tetramethyluronium hexafluorophosphate (173 mg, 0.460 mmol), followed by *N,N*-diisopropylethylamine (172 mg, 1.30 mmol) under a nitrogen atmosphere. To the resulting mixture was added a solution of the amine in MeCN (0.6 mL), and the mixture was stirred at the same temperature for 12 h. The reaction was quenched with saturated aqueous NH_4Cl (10 mL) and most of the organic solvent was removed *in vacuo*. The aqueous residue was extracted with EtOAc (3 × 5 mL). The combined organic layers were dried over anhydrous Na_2SO_4, filtered, and concentrated *in vacuo*. The crude residue was purified by flash chromatography (20 to 100% EtOAc in hexanes) on silica gel (25 mL) to afford amide **2.15** (96 mg, 66% yield) as a colorless oil.

*Data for alkene **2.15***: R_f = 0.26 (70% EtOAc in hexanes); IR (film): ν_{max} = 3342, 2962, 2927, 2856, 1699 (C=O), 1647 (C=O), 1526, 1427, 1243, 1117, 1072 cm^{-1}; $[\alpha]_D^{21}$ +2.23 (*c* 1.0, CH_2Cl_2); ^1H NMR (300 MHz, 293 K, 1% CD_3OD in $CDCl_3$): δ = 5.77 (dddd, *J* = 17.1, 10.2, 7.5, 6.0 Hz, 1H, 9-H), 5.15 (dd, *J* = 17.1, 1.5 Hz, 1H, 8_{trans}-H), 5.08 (br d, *J* = 10.2 Hz, 1H, 8_{cis}-H), 4.85 (app qt, *J* = 6.3, 6.3 Hz, 1H, 4′-H), 3.92 (m, 1H, 14-H), 3.65–3.61 (m, 5H, morpholine-C*H*$_2$O, 15-H), 3.54 (ddd, *J* = 7.5, 7.5, 2.7 Hz, 1H, 11-H), 3.46 (t, *J* = 4.5 Hz, 4H, morpholine-C*H*$_2$N), 2.40–2.26 (m, 3H, 10-H, 2′-H), 2.24–2.10 (m, 3H, 10-H, 3′-H), 1.95–1.1.87 (m, 2H, 13-H), 1.84–1.73 (m, 1H, 12-H), 1.27 (d, *J* = 6.3 Hz, 3H, 5′-H), 1.14 (d, *J* = 6.3 Hz, 3H, 16-H), 1.04 (d, *J* = 7.5 Hz, 3H, 20-H); ^{13}C NMR (75 MHz, 293 K, $CDCl_3$): δ = 171.7, 155.1, 134.6, 116.8, 80.7, 76.0, 71.5, 66.6, 47.1, 44.0, 37.3, 35.9, 32.9, 32.0, 28.4, 20.4, 17.8, 15.1; HRMS (ESI+) calcd for $C_{20}H_{34}N_2O_5Na$ $[M + Na]^+$ 405.2365, found 405.2346.

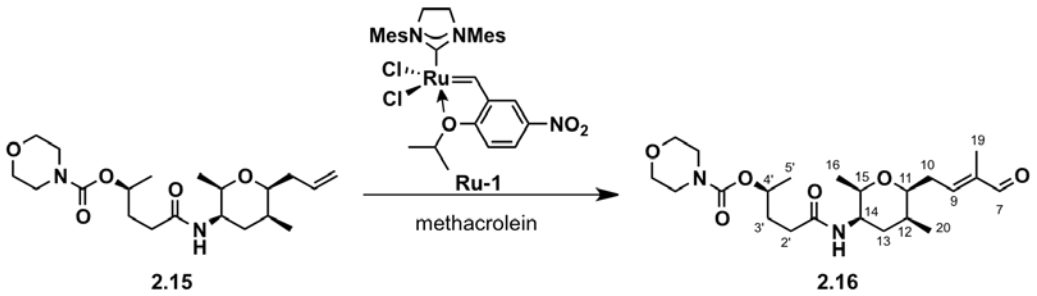

*Preparation of aldehyde **2.16***: To a stirred solution of alkene **2.15** (75 mg, 0.20 mmol) in benzene (0.4 mL) was added methacrolein (178 mg, 2.50 mmol) and **Ru-1** (3.3 mg, 0.0040 mmol) under an open atmosphere. The mixture was heated to 50 °C. After 12 h, the mixture was concentrated *in vacuo*. The residue was purified by flash chromatography (70% to 100% EtOAc in hexanes) on silica gel (25 mL) to afford aldehyde **2.16** (53 mg, 63% yield) as a colorless oil.

*Data for aldehyde **2.16***: R_f = 0.20 (EtOAc); IR (film): ν_{max} = 3349, 2926, 2856, 1691 (C=O), 1640 (C=O), 1525, 1426, 1243, 1117, 1072 cm^{-1}; $[\alpha]_D^{23}$ -2.34 (*c* 1.1, CH_2Cl_2); ^1H NMR (500 MHz, 293 K, $CDCl_3$): δ = 9.44 (s, 1H, 7-H), 6.54 (ddd, *J* = 7.5, 7.5, 1.0 Hz, 1H, 9-H), 5.71 (br d, *J* = 9.0 Hz, 1H, N-H), 4.87 (qdd, *J* = 6.5, 6.5, 6.5 Hz, 1H, 4′-H), 3.96 (dddd, *J* = 9.0, 6.0, 2.5, 2.5 Hz, 1H, 14-H), 3.68 (m, 6H, morpholine-C*H*$_2$O, 15-H, 11-H), 3.46 (m, 4H, morpholine-C*H*$_2$N), 2.58 (ddd, *J* = 15.5, 7.5, 7.5 Hz, 1H, 10-H), 2.43 (ddd, *J* = 15.5, 7.5, 6.0 Hz, 1H, 10-H), 2.32 (ddd, *J* = 15.0, 9.0, 7.0 Hz, 1H, 2′-H), 2.27 (ddd, *J* = 15.0, 9.0, 7.0 Hz, 1H, 2′-H), 2.22 (dddd, *J* = 16.0, 9.0, 9.0, 6.5 Hz, 1H, 3′-H), 2.18 (dddd, *J* = 16.0, 9.0, 6.5, 5.0 Hz, 1H, 3′-H), 1.97–1.95 (m, 1H, 13-H), 1.94–1.90 (m, 1H, 13-H), 1.85–1.81 (m, 1H, 12-H), 1.78 (s, 3H, 19-H), 1.28 (d, *J* = 6.5 Hz, 3H, 5′-H), 1.16 (d, *J* = 6.5 Hz, 3H, 16-H), 1.08 (d, *J* = 7.5 Hz, 3H, 20-H); ^{13}C NMR (75 MHz, 293 K, $CDCl_3$): δ = 195.0, 171.6, 155.2, 150.2, 140.8, 79.8, 76.2, 71.5, 66.6, 46.9, 44.1, 35.8, 33.0, 32.8, 32.0, 29.5, 20.5, 17.8, 15.3, 9.5; HRMS (EI+) calcd for $C_{22}H_{36}N_2O_6$ $[M]^+$ 424.2573, found 424.2566.

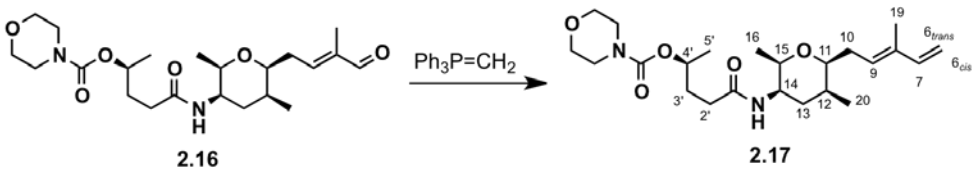

*Preparation of alkene **2.17***: To a stirred suspension of methytriphenylphosphonium bromide (67 mg, 0.19 mmol) in THF (0.3 mL) at 0 °C was added KO^{t}Bu (20 mg, 0.18 mmol) under a nitrogen atmosphere. After 8 min at 0 °C, aldehyde **2.16** (32 mg, 0.075 mmol) in THF (0.7 mL) was added at the same temperature. The reaction mixture was stirred at the same temperature for 43 min, then quenched with saturated aqueous NH_4Cl (2 mL). The mixture was extracted with EtOAc (3 × 5 mL). The combined organic layers were dried over anhydrous Na_2SO_4, filtered and concentrated *in vacuo*. The crude residue was purified by flash chromatography (50% to 100% EtOAc in hexanes) on silica gel (5 mL) to afford terminal alkene **2.17** (24 mg, 76% yield) as a colorless oil.

*Data for alkene **2.17***: R_f = 0.27 (EtOAc); IR (film): ν_{max} = 3361, 2973, 2926, 2856, 1698 (C=O), 1647 (C=O), 1527, 1427, 1244, 1117, 1072 cm^{-1}; $[\alpha]_D^{22}$ -1.43 (*c* 1.0, CH_2Cl_2); ^{1}H NMR (500 MHz, 293 K, $CDCl_3$): δ = 6.38 (dd, *J* = 17.5, 10.5 Hz, 1H, 7-H), 5.70 (br d, *J* = 9.0 Hz, 1H, N-H), 5.46 (dd, *J* = 6.5, 6.5 Hz, 1H, 9-H), 5.14 (d, *J* = 17.5 Hz, 1H, 6_{trans}-H), 4.98 (d, *J* = 10.5 Hz, 1H, 6_{cis}-H), 4.86 (qdd, *J* = 6.0, 6.0, 6.0 Hz, 1H, 4′-H), 3.93 (dddd, *J* = 9.0, 5.5, 2.5, 2.5 Hz, 1H, 14-H), 3.69–3.63 (m, 5H, morpholine-CH_2O, 15-H), 3.54 (ddd, *J* = 7.5, 7.5, 3.0 Hz, 1H, 11-H), 3.51–3.43 (m, 4H, morpholine-CH_2N), 2.42 (ddd, *J* = 14.5, 6.5, 6.5 Hz, 1H, 10-H), 2.32–2.25 (m, 3H, 10-H, 2′-H), 2.21 (ddd, *J* = 16.0, 9.5, 9.5, 7.0 Hz, 1H, 3′-H), 2.17 (ddd, *J* = 16.0, 9.5, 6.0, 5.0 Hz, 1H, 3′-H), 1.95–1.89 (m, 2H, 13-H), 1.81–1.79 (m, 1H, 12-H), 1.77 (s, 3H, 19-H), 1.28 (d, *J* = 6.0 Hz, 3H, 5′-H), 1.15 (d, *J* = 6.5 Hz, 3H, 16-H), 1.04 (d, *J* = 7.0 Hz,

3H, 20-H); ^{13}C NMR (75 MHz, 293 K, $CDCl_3$): δ = 171.6, 155.1, 141.2, 135.7, 128.0, 111.2, 80.8, 76.0, 71.5, 66.9, 66.6, 51.9, 47.1, 35.8, 33.0, 32.2, 28.8, 20.5, 17.9, 15.2, 12.0; HRMS (EI+) calcd for $C_{23}H_{38}N_2O_5$ $[M]^+$ 422.2781, found 422.2778.

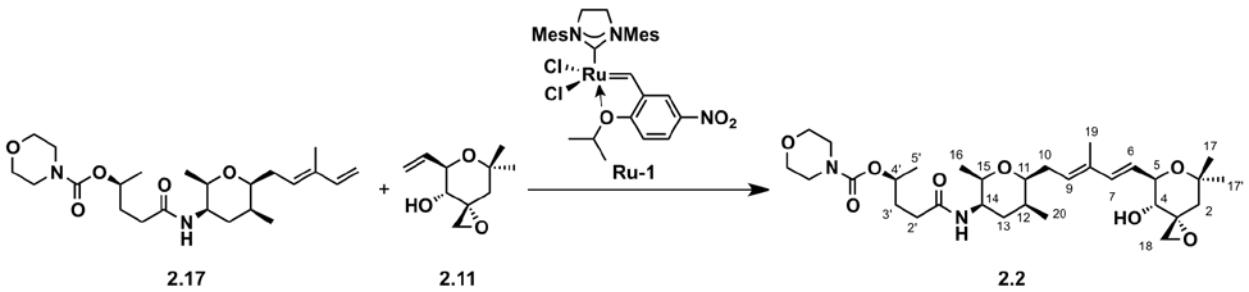

*Preparation of analogue **2.2***: A solution of right fragment **2.11** (10 mg, 0.056 mmol) was prepared in DCE (0.2 mL) at 23 °C under an open atmosphere. To a stirred solution of **2.17** (18 mg, 0.043 mmol) in DCE (0.1 mL) was added the solution of **2.11** (0.1 mL), benzoquinone (1.0 mg, 0.0086 mmol), followed by **Ru-1** (3.0 mg, 0.0045 mmol) at 23 °C under an open atmosphere. The reaction mixture was then heated to 50 °C. After 1.5 h at the same temperature, additional **Ru-1** (2.8 mg, 0.0042 mmol) and **2.11** (0.1 mL) were added. After 18 total hours, the reaction mixture was concentrated *in vacuo*. The resulting residue was purified by flash chromatography (50% to 100% EtOAc in hexanes) on silica gel (5 mL) to afford the desired product (7 mg, 28% yield) as a tan oil, and a mixture of **2.11** and **2.17** (20.3 mg).

To a stirred solution of recovered **2.11** and **2.17** in DCE (0.2 mL) was added benzoquinone (2.0 mg, 0.020 mmol) and **Ru-1** (4.0 mg, 0.0060 mmol) at 23 °C under an open atmosphere. The reaction mixture was then heated to 50 °C. After an additional 18 h at the same temperature, the reaction mixture was concentrated *in vacuo*. The resulting residue as purified by flash chromatography (50% to 100% EtOAc in hexanes) on silica gel (5 mL) to afford the desired product (2.5 mg). The combined yield of **2.2** is 9.5 mg (36% yield).

A portion of this material was purified by preparative-TLC (EtOAc) and used for biological experiments.

*Data for analogue **2.2***: R_f = 0.17 (EtOAc); IR (film): ν_{max} = 3393 (br), 2924, 2854, 1696 (C=O), 1673 (C=O), 1529, 1460, 1380, 1244, 1116 cm^{-1}; $[\alpha]_D^{22}$ +0.15 (*c* 0.95, CH_2Cl_2); ^1H NMR (700 MHz, 293 K, 1% CD_3OD in $CDCl_3$): δ = 6.41 (d, *J* = 15.0 Hz, 1H, 7-H), 5.70 (dd, *J* = 15.0, 7.0 Hz, 1H, 6-H), 5.69 (br d, *J* = 9.1 Hz, 1H, N-H), 5.51 (dd, *J* = 7.0, 7.0 Hz, 1H, 9-H), 4.88–4.86 (m, 1H, 4′-H), 4.03 (dd, *J* = 10.5, 7.0 Hz, 1H, 5-H), 3.95–3.92 (m, 1H, 14-H), 3.77–3.75 (m, 1H, 15-H), 3.67–3.63 (m, 4H, morpholine-C*H*$_2$O), 3.55 (dd, *J* = 10.5, 10.5 Hz, 1H, 4-H), 3.52 (ddd, *J* = 7.0, 7.0, 2.8 Hz, 1H, 11-H), 3.48–3.44 (m, 4H, morpholine-C*H*$_2$N), 3.04 (d, *J* = 4.9 Hz, 1H, 18-H), 2.51 (d, *J* = 4.9 Hz, 1H, 18-H), 2.44–2.37 (m, 1H, 10-H), 2.32–2.29 (m, 3H, 10-H, 2′-H), 2.78 (ddd, *J* = 15.4, 9.8, 9.8, 6.3 Hz, 1H, 3′-H), 2.25–2.23 (m, 1H, 3′-H), 2.22 (d, *J* = 14.0 Hz, 1H, 2_{axial}-H),1.96–1.91 (m, 2H, 13-H), 1.81–1.77 (m, 1H, 12-H), 1.79 (s, 3H, 19-H), 1.44 (d, *J* = 14.0 Hz, 1H, $2_{equatorial}$-H), 1.41 (s, 3H, 17-H), 1.32 (d, *J* = 7.0 Hz, 3H, 5′-H), 1.27 (s, 3H, 17′-H), 1.14 (d, *J* = 6.3 Hz, 3H, 16-H), 1.08 (d, *J* = 7.7 Hz, 3H, 20-H); ^{13}C NMR (150 MHz, 293 K, $CDCl_3$): δ = 171.7, 155.1, 138.1, 128.8, 128.3, 124.9, 80.8, 76.0, 74.7, 73.1, 71.5, 68.1, 66.7, 57.7, 47.8, 47.1, 42.8, 35.8, 33.0, 32.0, 31.2, 29.7, 28.5, 23.6, 20.5, 17.9, 15.3, 14.3, 12.6; HRMS (EI+) calcd for $C_{31}H_{50}N_2O_8$ $[M]^+$ 578.3553, found 578.3559.

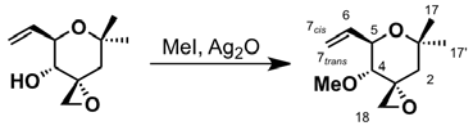

2.11 **2.18**

*Preparation of epoxide **2.18***: To a light-protected, stirred solution of alcohol **2.11** (20 mg, 0.11 mmol) and MeI (78 mg, 0.55 mmol) in DMF (0.2 mL) was added Ag_2O (51 mg, 0.22

mmol) at 23 °C under an open atmosphere. The resulting mixture was stirred at the same temperature for 17 h, after which the reaction mixture was poured into H_2O (5 mL), and the resulting mixture was extracted with Et_2O (3 × 10 mL). The combined organic layers were dried over anhydrous Na_2SO_4, filtered, and concentrated *in vacuo*. Purification of the residue by flash chromatography (10 to 30% EtOAc in hexanes) on silica gel (20 mL) afforded **2.18** (19 mg, 87% yield) as a pale yellow oil.

*Data for epoxide **2.18***: R_f = 0.3 (20% EtOAc in hexanes); IR (film): ν_{max} = 2974, 2926, 1465, 1370, 1126, 1195, 1127, 1060, 1026 cm^{-1}; $[\alpha]_D^{21}$ +42.7 (*c* 1.13, CH_2Cl_2); ^1H NMR (300 MHz, 293 K, $CDCl_3$): δ = 5.93 (ddd, *J* = 17.1, 10.2, 6.6 Hz, 1H, 6-H), 5.46 (ddd, *J* = 17.1, 1.5, 1.5 Hz, 1H, 7_{trans}-H), 5.28 (ddd, *J* = 10.2, 1.5, 0.6 Hz, 1H, 7_{cis}-H), 4.17 (dd, *J* = 9.9, 6.6 Hz, 1H, 5-H), 3.38 (s, 3H, OCH_3), 3.14 (d, *J* = 9.9 Hz, 1H, 4-H), 2.91 (d, *J* = 4.8 Hz, 1H, 18-H), 2.49 (d, *J* = 4.8 Hz, 1H, 18-H), 2.13 (d, *J* = 14.1 Hz, 1H, 2_{axial}-H), 1.40 (s, 3H, 17-H), 1.38 (d, *J* = 14.1 Hz, 1H, $2_{equatorial}$-H), 1.26 (s, 3H, 17′-H); ^{13}C NMR (175 MHz, 293 K, $CDCl_3$): δ = 136.4, 118.0, 78.5, 73.2, 73.1, 61.0, 56.8, 47.5, 43.2, 31.0, 23.7; HRMS (EI+) calcd for $C_{10}H_{15}O_3$ $[M - CH_3]^+$ 183.1021, found 183.1023.

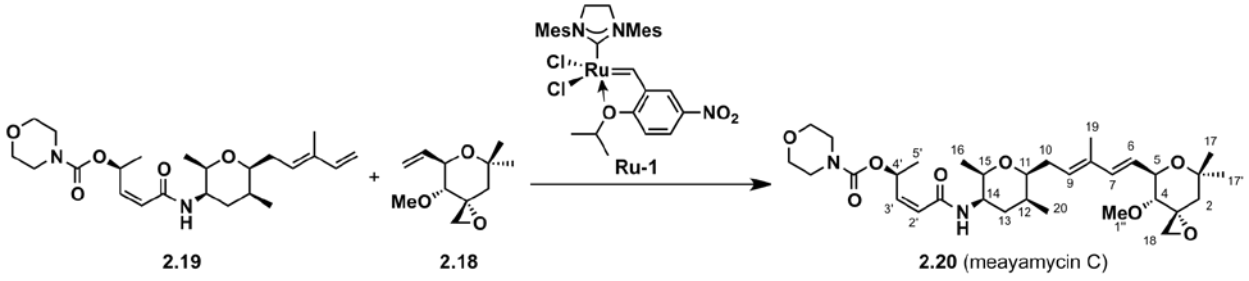

*Preparation of meayamycin C (**2.20**)*: A solution of **2.18** (18 mg, 0.091 mmol) was prepared in DCE (0.2 mL) at 23 °C under an open atmosphere. A stirred solution of **2.19** (26 mg, 0.062 mmol) in DCE (0.2 mL) was treated with an aliquot of solution of **2.18** (0.1 mL), benzoquinone

(1.5 mg, 0.014 mmol), followed by **Ru-1** (1.5 mg, 2.2 μmol) at 23 °C under an open atmosphere. The reaction mixture was then heated to 42 °C. After 2.5 h at the same temperature, additional **Ru-1** (1.5 mg, 2.2 μmol) and remaining aliquot of solution of **2.18** (0.1 mL) were added. After 17 total hours, the reaction was concentrated *in vacuo*. The resulting residue was purified by flash chromatography (10 to 100% EtOAc in hexanes) on silica gel (5 mL) to afford the desired product (16 mg, 44% yield), and a mixture of **2.18** and **2.19** (14 mg).

To a stirred solution of recovered **2.18** and **2.19** in DCE (0.2 mL) was added benzoquinone (1.0 mg, 9.3 μmol) and **Ru-1** (2.0 mg, 3.0 μmol) at 23 °C under an open atmosphere. The reaction mixture was then heated to 42 °C. After an additional 22 h at the same temperature, the reaction was concentrated *in vacuo*. The resulting residue was purified by flash chromatography (10 to 100% EtOAc in hexanes) on silica gel (5 mL) to afford the desired product (5.0 mg) as a clear oil. The combined yield of **2.20** is 21 mg (57%).

A portion of this material was purified by preparative-TLC (80% EtOAc in hexanes) and used for biological experiments.

*Data for meayamycin C (**2.20**)*: R_f = 0.20 (80% EtOAc in hexanes); IR (film): ν_{max} = 3366, 2925, 2855, 1700 (C=O), 1632 (C=O), 1515, 1426, 1277, 1241, 1119, 1071 cm^{-1}; $[\alpha]_D^{21}$ +1.5 (*c* 1.04, CH_2Cl_2); ^1H NMR (700 MHz, 293 K, CD_2Cl_2): δ = 6.35 (d, *J* = 16.1 Hz, 1H, 7-H), 6.14–6.10 (m, 2H, 4′-H, N-H), 5.89 (dd, *J* = 11.9, 7.7 Hz, 1H, 3′-H), 5.68 (dd, *J* = 11.9, 1.4 Hz, 1H, 2′-H), 5.61 (dd, *J* = 16.1, 7.0 Hz, 1H, 6-H), 5.51 (br t, *J* = 7.0, 1H, 9-H), 4.11 (dd, *J* = 9.1, 7.0 Hz, 1H, 5-H), 3.89–3.87 (m, 1H, 14-H), 3.65 (qd, *J* = 7.0, 2.1 Hz, 1H, 15-H), 3.60–3.57 (m, 4H, morpholine-C*H*$_2$O), 3.51 (ddd, *J* = 7.7, 7.7, 2.8 Hz, 1H, 11-H), 3.42–3.38 (m, 4H, morpholine-C*H*$_2$N), 3.28 (s, 3H, OC*H*$_3$), 3.08 (d, *J* = 9.1 Hz, 1H, 4-H), 2.80 (d, *J* = 4.9 Hz, 1H, 18-H), 2.39 (d, *J* = 4.9 Hz, 1H, 18-H), 2.37–2.33 (m, 1H, 10-H), 2.21–2.17 (m, 1H, 10-H), 2.07

(d, J = 14.0 Hz, 1H, 2_{axial}-H), 1.94–1.90 (m, 2H, 13-H), 1.76 (s, 3H, 19-H), 1.77–1.74 (m, 1H, 12-H), 1.33 (s, 3H, 17-H), 1.32 (d, J = 6.3 Hz, 3H, 5′-H), 1.30 (d, J = 14.0 Hz, 1H, $2_{equatorial}$-H), 1.20 (s, 3H, 17′-H), 1.10 (d, J = 7.0 Hz, 3H, 16-H), 1.00 (d, J = 7.7 Hz, 3H, 20-H); ^{13}C NMR (175 MHz, 293 K, CD_2Cl_2): δ = 164.7, 154.8, 143.9, 137.1, 134.7, 128.9, 125.3, 122.2, 80.8, 79.0, 75.9, 73.1, 73.0, 69.5, 66.5, 60.6, 56.6, 47.2, 47.0, 43.3, 35.8, 33.3, 32.0, 30.8, 29.4, 23.6, 20.1, 17.6, 14.8, 12.4; HRMS (ESI+) calcd for $C_{32}H_{50}N_2O_8Na$ $[M + Na]^+$ 613.3465, found 613.3448.

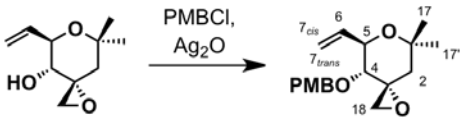

2.11 **2.24**

*Preparation of epoxide **2.24***: To a light-protected, stirred solution of alcohol **2.11** (92.6 mg, 0.503 mmol) and PMBCl (200 μL, 1.47 mmol) in DMF (1.0 mL) was added Ag_2O (174 mg, 0.751 mmol) at 23 °C under a nitrogen atmosphere. The resulting mixture was stirred at 60 °C for 43 h, after which the reaction mixture was poured into H_2O (25 mL), and the resulting mixture was extracted with Et_2O (2 × 15 mL). The combined organic layers were dried over anhydrous Na_2SO_4, filtered, and concentrated *in vacuo*. Purification of the residue by flash chromatography (10 to 30% EtOAc in hexanes) on silica gel (8 mL) afforded PMB ether **2.24** (113 mg, 74%) as a colorless oil.

*Data for epoxide **2.24***: R_f = 0.26 (30% EtOAc in hexanes); IR (film): ν_{max} = 2973, 1612, 1514, 1466, 1249, 1115, 1033, 822 cm^{-1}; $[\alpha]_D^{25}$ +40.2 (*c* 0.75, $CHCl_3$); ^{1}H NMR (300 MHz, 293K, $CDCl_3$) δ = 7.21 (br d, 2H, J = 8.4 Hz, Ar-H), 6.86 (br d, 2H, J = 8.4 Hz, Ar-H), 5.95 (ddd, 1H, J = 17.3, 10.4, 6.8 Hz, 6-H), 5.47 (br d, 1H, J = 17.3 Hz, 7_{trans}-H), 5.29 (br d, 1H, J =

10.4 Hz, 7_{cis}-H), 4.57 (d, 1H, J = 11.1 Hz, ArCH_2), 4.36 (d, 1H, J = 11.1 Hz, ArCH_2), 4.26 (dd, 1H, J = 9.6, 6.8 Hz, 5-H), 3.81 (s, 3H, OCH_3), 3.40 (d, 1H, J = 9.6 Hz, 4-H), 2.85 (d, 1H, J = 4.9 Hz, 18-H), 2.41 (d, 1H, J = 4.9 Hz, 18-H), 2.10 (d, 1H, J = 14.1 Hz, 2_{axial}-H), 1.43 (s, 3H, 17-H), 1.36 (d, 1H, J = 14.1 Hz, $2_{equatorial}$-H), 1.27 (s, 3H, 17′-H); ^{13}C NMR (75 MHz, 293K, $CDCl_3$) δ = 159.4, 136.5, 130.0, 129.6, 118.1, 113.8, 75.8, 74.3, 73.5, 73.2, 57.0, 55.2, 47.5, 43.4, 31.0, 23.7; HRMS (EI+) calcd. for $C_{18}H_{24}O_4Na$ $[M + Na]^+$ 327.1572, found 327.1556.

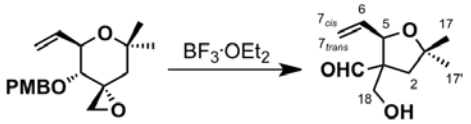

2.24 **2.23**

*Preparation of aldehyde **2.23***: A 10-mL round-bottomed flask equipped with a Teflon-coated magnetic stir bar containing alkene **2.24** (7.0 mg, 0.023 mmol) was purged with N_2. The flask was charged with PhH (3 mL), cooled in an ice-water bath (0 °C external temperature), then BF_3•OEt_2 (1 μL, 0.0037 mmol) was added. The mixture was stirred for 10 min, then diluted with H_2O (0.5 mL). The mixture was extracted with EtOAc (3 × 2 mL), and the combined organic layer was dried over Na_2SO_4, filtered and concentrated *in vacuo*. The crude residue was purified by flash chromatography (10→30% EtOAc in hexanes) on silica gel (2 mL) to afford aldehyde **2.23** as a clear oil (4 mg, 95% yield).

*Data for aldehyde **2.23***: R_f = 0.22 (30% EtOAc in hexanes); IR (film): ν_{max} = 3430 (br, O-H), 2972, 1721 (C=O), 1370, 1170, 1077, 999, 930 cm^{-1}; ^{1}H NMR (300 MHz, 293K, $CDCl_3$): δ = 9.62 (s, 1H), 5.94 (ddd, J = 17.1, 10.5, 6.2 Hz, 1H), 5.48 (ddd, J = 17.1, 1.5, 1.5 Hz, 1H), 5.31 (ddd, J = 10.5, 1.5, 1.5 Hz, 1H), 4.51 (br ddd, J = 6.2, 1.5, 1.5 Hz, 1H), 3.91 (br d, J = 11.1 Hz, 1H), 3.84 (br d, J = 11.1 Hz, 1H), 2.19 (d, J = 13.7 Hz, 1H), 1.97 (d, J = 13.7 Hz, 1H), 1.45 (s,

3H), 1.37 (s, 3H); ^{13}C NMR (75 MHz, $CDCl_3$, 293 K): δ = 204.2, 133.4, 118.1, 82.8, 80.9, 64.4, 63.1, 43.6, 29.6, 28.1; HRMS (EI+) calcd. for $C_{10}H_{16}O_3$ $[M]^+$ 184.1099, found 184.1094.

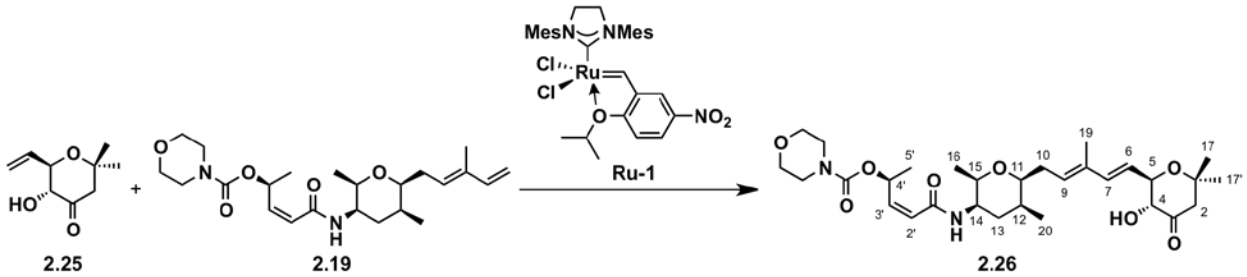

*Preparation of ketone **2.26***: A 10-mL round-bottomed flask equipped with equipped with a Teflon-coated magnetic stir bar containing diene **2.19** (18 mg, 0.04 mmol) and alkene **2.25** (9.1 mg, 0.05 mmol) was charged with DCE (0.3 mL), **Ru-1** (3.2 mg, 0048 mmol). The mixture was stirred in an oil bath for 2 h at 40 °C, then additional **Ru-1** (2.1 mg, 0.0031 mmol) was added, and the mixture was stirred for an additional 14 h, then concentrated *in vacuo*. The crude residue was purified by flash chromatography (10→100% EtOAc in hexanes) on silica gel (5 mL) to afford **2.26** as an oil (8.1 mg, 36% yield).

Some of this material was purified by preparative-TLC (EtOAc) and used for biological experiments.

*Data for ketone **2.26**:* R_f = 0.26 (70% EtOAc in hexanes); IR (film): ν_{max} = 3341 (br, O-H), 2973, 2923, 1734 (C=O), 1668 (C=O), 1526, 1372, 1243, 1130, 1 cm^{-1}; $[\alpha]_D^{19}$ +2.16 (*c* 0.74, CH_2Cl_2); ^{1}H NMR (500 MHz, 1% CD_3OD in $CDCl_3$, 293 K): δ = 6.43 (d, *J* = 16.0 Hz, 1, 7-H), 6.20 (br d, *J* = 9.0 Hz, 1H, N-H), 6.17–6.13 (m, 1H, 4′-H), 5.94 (dd, *J* = 12.0, 7.5 Hz, 1H, 3′-H), 5.74 (dd, *J* = 12.0, 1.0 Hz, 1H, 2′-H), 5.58 (dd, *J* = 16.0, 9.0 Hz, 1H, 6-H), 5.36–5.30 (m, 1H, 9-H), 4.16 (dd, *J* = 9.0, 9.0 Hz, 1H, 4-H), 3.97–3.95 (m, 2H, 5-H, 14-H), 3.68–3.65 (m, 4H, C*H*$_2$O), 3.60–3.52 (m, 2H, 15-H, 11-H), 3.50–3.48 (m, 4H, C*H*$_2$N), 2.42–2.38 (m, 2H, 10-H, 2_{axial}-H), 2.26–2.23 (m, 1H, 10-H), 1.98–1.93 (m, 2H, 13-H), 1.88 (d, *J* = 14.0 Hz, 1H, $2_{equatorial}$-

H), 1.80 (s, 3H, 19-H), 1.78–1.76 (m, 1H, 12-H), 1.48 (s, 3H, 17-H), 1.43 (d, J = 6.5 Hz, 3H, 4′-H), 1.28 (s, 3H, 17′-H), 1.17 (d, J = 6.5 Hz, 3H, 16-H), 1.04 (d, J = 7.5 Hz, 3H, 20-H); ^{13}C NMR (100 MHz, CD_2Cl_2, 293 K): δ = 208.2, 164.4, 154.3, 142.7, 136.5, 135.0, 131.5, 125.1, 123.2, 83.6, 75.7, 73.8, 70.1, 66.6, 57.3, 47.0, 44.4, 35.8, 34.6, 31.6, 29.7, 22.7, 20.0, 17.4, 15.2, 13.9; HRMS (ESI+) calcd. for $C_{30}H_{46}N_2O_8Na$ $[M + Na]^+$ 585.3152, found 585.3157.

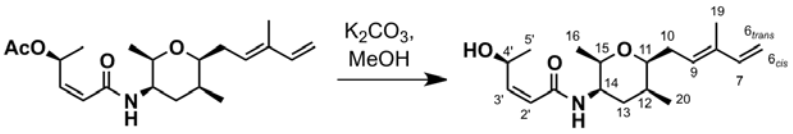

2.27 **2.28**

*Preparation of allylic alcohol **2.28***: To a stirred solution of **2.27** (26.5 mg, 75.8 μmol) in MeOH (0.38 mL) was added K_2CO_3 (26.3 mg, 0.190 mmol) at 0 °C under an open atmosphere. After 2 h at the same temperature the reaction was diluted with saturated aqueous NH_4Cl (60 μL), and the resulting mixture was stirred for 5 min. The resulting reaction mixture was dried over anhydrous Na_2SO_4, filtered, and concentrated *in vacuo*. The resulting residue was purified by flash chromatography (20 to 50% EtOAc in hexanes) on silica gel (3 mL) to give **2.28** (19.2 mg, 82%) as a colorless oil.

*Data for allylic alcohol **2.28***: R_f = 0.21 (50% EtOAc in hexanes); IR (film): ν_{max} = 3325, 2975, 1655 (C=O), 1621, 1522, 1456, 1116, 1062, 894 cm^{-1}; $[\alpha]_D^{26}$ +10.0 (*c* 0.95, $CHCl_3$); ^{1}H NMR (300 MHz, 293K, 1% CD_3OD in $CDCl_3$) δ = 6.36 (dd, 1H, J = 17.4, 10.8 Hz, 7-H), 6.16 (dd, 1H, J = 11.9, 5.6 Hz, 3′-H), 5.74 (dd, 1H, J = 11.9, 1.3 Hz, 2′-H), 5.44 (br app t, 1H, J = 8.1 Hz, 9-H), 5.11 (d, 1H, J = 17.4 Hz, 6_{trans}-H), 4.96 (d, 1H, J = 10.8 Hz, 6_{cis}-H), 4.83–4.73 (m, 1H, 4′-H), 3.97–3.93 (m, 1H, 14-H), 3.68 (qd, 1H, J = 6.6, 2.1 Hz, 15-H), 3.55 (qd, 1H, J = 7.1, 2.5 Hz, 11-H), 2.48–2.31 (m, 1H, 10-H), 2.31–2.13 (m, 1H, 10-H), 1.95–1.92 (m, 2H, 13-H), 1.76

(br s, 3H, 19-H), 1.34 (d, 3H, *J* = 6.6 Hz, 5′-H), 1.14 (d, 3H, *J* = 6.6 Hz, 16-H), 1.01 (d, 3H, *J* = 7.1 Hz, 20-H); ^{13}C NMR (125 MHz, 293K, $CDCl_3$) δ = 166.1, 150.8, 141.2, 135.7, 127.9, 122.5, 111.2, 80.8, 75.8, 64.6, 47.5, 35.7, 31.8, 28.8, 22.7, 17.9, 15.2, 11.9; HRMS (EI+) calcd. for $C_{18}H_{29}NO_3$ $[M]^+$ 307.2147, found 307.2148.

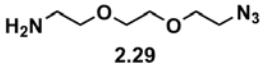

2.29

Synthesis of **2.29**, see: E. Klein, S. DeBonis, B. Theide, D. A. Skoufias, F. Kozielski, L. Frank, *Bioorg. Med. Chem.,* **2007**, *15*, 6474–6488.

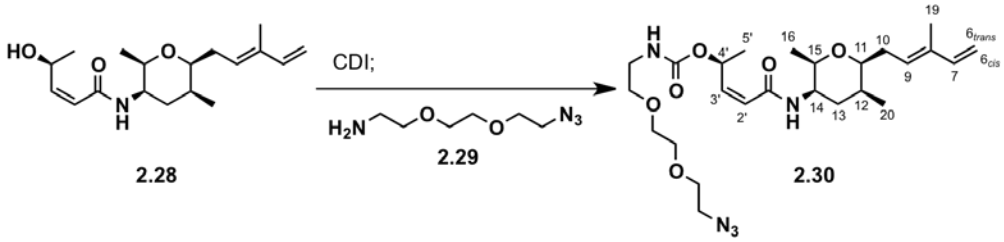

*Preparation of carbamate **2.30**:* A 25-mL round-bottomed flask equipped with a Teflon-coated magnetic stir bar containing alcohol **2.28** (55 mg, 0.18 mmol) was charged with CH_2Cl_2 (1.0 mL). The reaction flask was cooled in an ice-water bath (0 °C external temperature), and 1,1′-carbonyldiimidazole (35.0 mg, 0.22 mmol) was added to the mixture. The mixture was stirred for 4.75 h as the ice-water bath was left to warm to 23 °C. Then a solution of amine **2.29** (157 mg, 0.900 mmol) in CH_2Cl_2 (0.2 mL) was added to the mixture at 23 °C under an open atmosphere. The mixture was stirred for 17 h, and then the solvent was removed *in vacuo*. The residue was purified by flash chromatography (10→80% EtOAc in hexanes) on silica gel (5 mL) to afford carbamate **2.30** as a clear oil (53 mg, 58% yield).

*Data for carbamate **2.30***: R_f = 0.25 (60% EtOAc in hexanes); IR (film): ν_{max} = 3340, 2927, 2108 (N_3), 1708 (C=O), 1666 (C=O), 1515, 1252 cm^{-1}; $[\alpha]_D^{24}$ –14.4 (*c* 1.3, $CHCl_3$); ^1H NMR (500 MHz, 1% CD_3OD in $CDCl_3$, 293 K): δ = 6.38 (dd, *J* = 17.5, 11.0 Hz, 1H, 7-H), 6.18 (br d, *J* = 9.0 Hz, 1H, N-H), 6.10 (dq, *J* = 7.0, 7.0 Hz, 1H, 4′-H), 5.93 (dd, *J* = 11.5, 7.0 Hz, 1H, 3′-H), 5.71 (br d, *J* = 11.5 Hz, 1H, 2′-H), 5.47 (br t, *J* = 7.0 Hz, 1H, 9-H), 5.25–5.17 (m 1H, N-H), 5.13 (d, *J* = 17.5 Hz, 1H, 6_{trans}-H), 4.97 (d, *J* = 11.0 Hz, 1H, 6_{cis}-H), 3.95 (m, 1H, 14-H), 3.71–3.34 (m, 14H, 15-H, 11-H, triethylene glycol-*H*′s), 2.42–2.37 (ddd, *J* = 14.8, 7.0, 7.0 Hz, 1H, 10-H), 2.28–2.22 (ddd, *J* = 14.8, 7.0, 7.0 Hz, 1H, 10-H), 1.99–1.95 (m, 1H, 13-H), 1.95–1.91 (m, 1H, 13-H), 1.80–1.78 (m, 1H, 12-H), 1.76 (s, 3H, 19-H), 1.38 (d, *J* = 7.0 Hz, 3H, 5′-H), 1.17 (d, *J* = 6.0 Hz, 3H, 16-H), 1.04 (d, *J* = 7.5 Hz, 3H, 20-H); ^{13}C NMR (75 MHz, $CDCl_3$, 293 K): δ = 165.0, 156.0, 144.1, 141.3, 135.6, 128.2, 122.2, 111.1, 80.8, 76.0, 70.6, 70.1, 69.3, 50.6, 47.0, 40.7, 35.9, 31.9, 30.3, 29.7, 28.9, 20.2, 17.8, 15.0, 11.9; HRMS (ESI+) calcd. for $C_{25}H_{41}N_5O_6Na$ $[M + Na]^+$ 530.2955, found 530.2943.

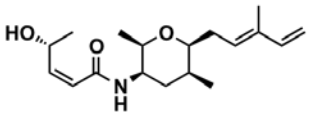

2.32

Synthesis of **2.32**, see: S. Osman, B. J. Albert, Y. Wang, M. Li, N. L. Czaicki, K. Koide, *Chem. – Eur. J.* **2011**, *17*, 895–904.

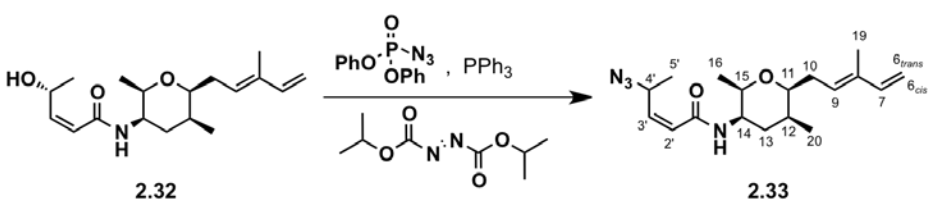

*Preparation of azide **2.33**:* A 10-mL round-bottomed flask equipped with a Teflon-coated magnetic stir bar containing alcohol **2.32** (10 mg, 0.033 mmol) was evacuated and backfilled with nitrogen. The flask was cooled in an ice-water bath (0 °C external temperature), then THF (1 mL), PPh_3 (26 mg, 0.099 mmol), diisopropylazodicarboxylate (20 mg, 0.099 mmol) and diphenylphosphorylazide (27 mg, 0.099 mmol) were added. The mixture was stirred for 16 min, then diluted with saturated aqueous $NaHCO_3$ (8 mL). The mixture was concentrated *in vacuo*, and then extracted with Et_2O (10 mL). The organic layer was dried over Na_2SO_4, filtered and concentrated *in vacuo*. The crude residue was purified by flash chromatography (5→30% EtOAc in hexanes) on silica gel (5 mL) to afford azide **2.33** as a clear oil (5.6 mg, 56% yield).

*Data for azide **2.33***: R_f = 0.25 (20% EtOAc in hexanes); IR (film): ν_{max} = 3397, 2924, 2110 (N_3), 1727 (C=O), 1509, 1463, 1113 cm^{-1}; ^1H NMR (500 MHz, $CDCl_3$, 293 K): δ = 6.38 (dd, *J* = 17.0, 10.5 Hz, 1H, 7-H), 5.90 (dd, *J* = 11.0, 9.0 Hz, 1H, 3′-H), 5.79 (d, *J* = 11.0 Hz, 1H, 2′-H), 5.53–5.51 (m, 1H, 4′-H), 5.47 (br t, *J* = 7.0 Hz, 1H, 9-H), 5.12 (d, *J* = 17.0 Hz, 1H, 6_{trans}-H), 4.97 (d, *J* = 10.5 Hz, 1H, 6_{cis}-H), 3.96–3.93 (m, 1H, 14-H), 3.68 (qd, *J* = 6.5, 2.0 Hz, 1H, 15-H), 3.56 (ddd, *J* = 7.0, 7.0, 3.0 Hz, 1H, 11-H), 2.44–2.38 (m, 1H, 10-H), 2.30–2.24 (m, 1H, 10-H), 1.96–1.95 (m, 2H, 13-H), 1.84–1.80 (m, 1H, 12-H), 1.77 (s, 3H, 19-H), 1.31 (d, *J* = 6.5 Hz, 3H, 5′-H), 1.16 (d, *J* = 6.5 Hz, 3H, 16-H), 1.04 (d, *J* = 7.0 Hz, 3H, 20-H); ^{13}C NMR (150 MHz, $CDCl_3$, 293 K): δ = 164.6, 143.4, 141.2, 135.8, 128.0, 123.4, 111.2, 79.7, 76.0, 57.6, 54.2, 47.4, 35.8, 31.9, 28.9, 19.5, 17.9, 15.3, 12.0; HRMS (EI+) calcd. for $C_{18}H_{28}N_4O_2$ $[M]^+$ 332.2212, found 332.2199.

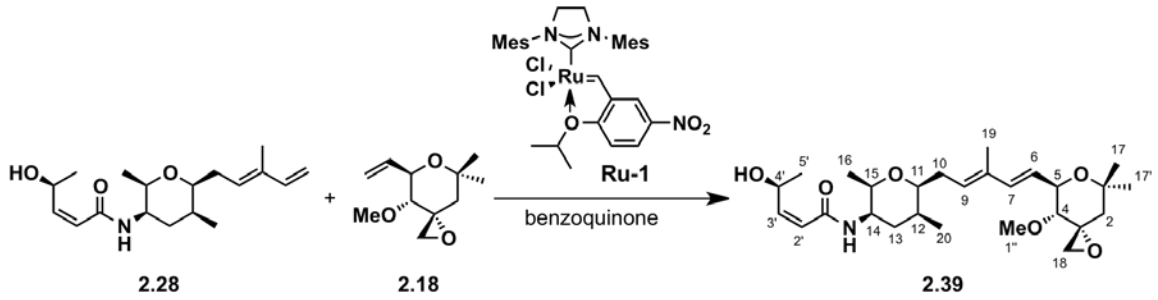

*Preparation of 4'-desacetyl meayamycin C **2.39**:* A 10-mL round-bottomed flask equipped with a Teflon-coated magnetic stir bar containing diene **2.28** (30 mg, 0.10 mmol) and alkene **2.18** (25 mg, 0.14 mmol) was charged with toluene (0.3 mL), **Ru-1** (5.0 mg, 0.0074 mmol) and benzoquinone (4.0 mg, 0.0040 mmol). The mixture was stirred in an oil bath for 22 h at 40 °C, then concentrated *in vacuo*. The crude residue was purified by flash chromatography (10→100% EtOAc in hexanes) on silica gel (5 mL) to afford 4′-desacetyl meayamycin C **2.39** as a dark-grey oil (11 mg). The recovered starting materials (**2.28** and **2.18**) were dissolved in DCE (0.2 mL), followed by addition of **Ru-1** (4 mg, 0.006 mmol) and benzoquinone (3 mg, 0.03 mmol). The reaction mixture was stirred in a 40 °C oil bath for 21 h, then concentrated *in vacuo*. The crude residue was purified by flash chromatography (10→100% EtOAc in hexanes) on silica gel (5 mL) to afford 4′-desacetyl meayamycin C **2.39** as a dark-grey oil (3.7 mg). The recovered starting materials (**2.28** and **2.18**) were dissolved in DCE (0.2 mL), followed by addition of **Ru-1** (3 mg, 0.004 mmol) and benzoquinone (3 mg, 0.03 mmol). The reaction mixture was stirred in an oil bath for 17 h at 40 °C, then concentrated *in vacuo*. The crude residue was purified by flash chromatography (10→100% EtOAc in hexanes) on silica gel (5 mL) to afford 4′-desacetyl meayamycin C **2.39** as a dark oil (2 mg). The total mass of 4′-desacetyl meayamycin C **2.39** is 16.7 mg (35% yield).

Data for 4'-desacetyl meayamycin C ***2.39***: R_f = 0.3 (70% EtOAc in hexanes); IR (film): ν_{max} = 3323 (br, O-H), 2975, 2930, 1656 (C=O), 1526, 1444, 1116 cm^{-1}; $[\alpha]_D^{22}$ –5.7 (*c* 0.8, CH_2Cl_2); ^1H NMR (500 MHz, 1% CD_3OD in $CDCl_3$, 293 K): δ = 6.42 (d, *J* = 15.5 Hz, 1H, 7-H), 6.19 (dd, *J* = 11.5, 5.8 Hz, 1H, 3′-H), 5.93 (br d, *J* = 9.0 Hz, 1H, N-H), 5.72 (d, *J* = 11.5 Hz, 1H, 2′-H), 5.66 (dd, *J* = 15.5, 7.0 Hz, 1H, 6-H), 5.49 (br t, *J* = 7.0 Hz, 1H, 9-H), 4.82–4.75 (m, 1H, 4′-H), 4.24 (dd, *J* = 9.5, 7.0 Hz, 1H, 5-H), 3.96–3.94 (m, 1H, 14-H), 3.68 (qd, *J* = 6.3, 1.8 Hz, 1H, 15-H), 3.54 (ddd, *J* = 7.0, 7.0, 2.5 Hz, 1H, 11-H), 3.36 (s, 3H, 1′′-H), 3.15 (d, *J* = 9.5 Hz, 1H, 4-H), 2.92 (d, *J* = 5.0 Hz, 1H, 18-H), 2.49 (d, *J* = 5.0 Hz, 1H, 18-H), 2.44–2.37 (m, 1H, 10-H), 2.26–2.22 (m, 1H, 10-H), 2.13 (d, *J* = 14.0 Hz, 1H, 2_{axial}-H), 1.99–1.92 (m, 2H, 13-H), 1.79 (s, 3H, 19-H), 1.63–1.59 (m, 1H, 12-H), 1.43 (s, 3H, 17-H), 1.41 (d, *J* = 14.0 Hz, 1H, $2_{equatorial}$-H), 1.36 (d, *J* = 6.5 Hz, 3H, 5′-H), 1.28 (s, 3H, 17′-H), 1.15 (d, *J* = 6.3 Hz, 3H, 16-H), 1.03 (d, *J* = 7.0 Hz, 3H, 20-H); ^{13}C NMR (150 MHz, $CDCl_3$, 293 K): δ = 166.1, 150.8, 137.7, 134.9, 128.4, 125.0, 122.6, 80.9, 78.8, 75.8, 73.3, 64.6, 60.9, 56.8, 47.5, 43.3, 35.7, 31.9, 31.1, 29.6, 28.8, 23.8, 22.7, 17.9, 15.3, 12.7; HRMS (ESI+) calcd. for $C_{27}H_{43}NO_6Na$ $[M + Na]^+$ 500.2988, found 500.2995.

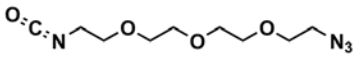

2.41

Synthesis of **2.41**, see: K. Breitenkamp, K. N. Sill, H. Skaff, *PCT Int. Appl.,* **2007**, WO 2007127473 A2 20071108.

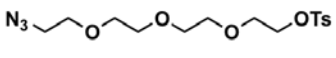

2.42

Synthesis of **2.42**, see: H. S. Gill, et. al. *J. Med. Chem.*, **2009**, *52*, 5816–5825.

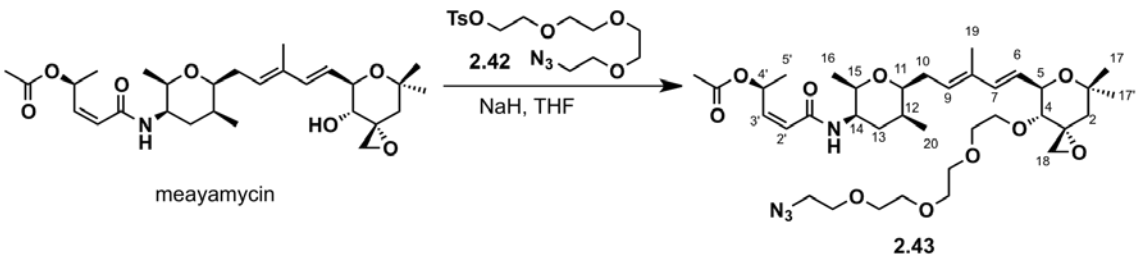

*Preparation of 4-TEGylated meayamycin **2.43***: A 10-mL round-bottomed flask equipped with a Teflon-coated magnetic stir bar containing meayamycin (3.3 mg, 0.0065 mmol) was added THF (0.1 mL) and tosylate **2.42** (7.1 mg, 2.8 mmol). The flask was cooled in an ice-water bath (0 °C external temperature), then NaH (5.3 mg, 0.13 mmol) was added to the flask. The mixture was stirred for 7 h as the ice-water bath was left to warm to 23 °C. The mixture was diluted with saturated aqueous NH_4Cl (2 mL), and THF was removed *in vacuo*. The resulting mixture was extracted with EtOAc (6 × 5 mL). The combined organic layers were dried over Na_2SO_4, filtered and concentrated *in vacuo*. The residue was purified by preparative-TLC (80% EtOAc in hexanes) to afford 4-TEGylated meayamycin **2.43** as a colorless oil (2.3 mg, 51% yield).

*Data for 4-TEGylated meayamycin **2.43***: R_f = 0.23 (80% EtOAc in hexanes); IR (film): ν_{max} = 3391, 2922, 2854, 2106 (N_3), 1779 (C=O), 1598 (C=O), 1459, 1178, 1017 cm^{-1}; $[\alpha]_D^{22}$ +10.2 (*c* 0.23, CH_2Cl_2); ^1H NMR (500 MHz, $CDCl_3$, 293 K): δ = 6.40 (d, *J* = 15.5 Hz, 1H, 7-H), 6.27 (m, 4′-H), 5.99 (br d, *J* = 9.0 Hz, 1H, N-H), 5.90 (dd, *J* = 11.5, 7.5 Hz, 1H, 3′-H), 5.71 (dd, *J* = 11.5, 1.5 Hz, 1H, 2′-H), 5.64 (dd, *J* = 15.5, 7.5 Hz, 1H, 6-H), 5.48 (br t, *J* = 7.5 Hz, 1H, 9-H), 4.26 (dd, *J* = 9.0, 7.5 Hz, 1H, 5-H), 3.97–3.93 (m, 1H, 14-H), 3.72–3.48 (m, 16H, tetraethylene glycol-*H*'s, 15-H, 11-H), 3.42–3.39 (m, 2H, N_3CH_2), 3.32 (d, *J* = 9.0 Hz, 1H, 4-H), 3.12 (d, *J* = 5.5 Hz, 1H, 18-H), 2.45 (d, *J* = 5.5 Hz, 1H, 18-H), 2.42–2.39 (m, 1H, 10-H), 2.24–2.21 (m, 1H, 10-H), 2.13 (d, *J* = 14.0 Hz, 1H, 2_{axial}-H), 2.07 (s, 3H, 2′′-H), 1.99–1.94 (m, 2H, 13-H), 1.78 (s,

3H, 19-H), 1.62–1.59 (m, 1H, 12-H), 1.43 (s, 3H, 17-H), 1.40 (d, J = 6.5 Hz, 3H, 5′-H), 1.39 (d, J = 14.0 Hz, 1H, $2_{equatorial}$-H), 1.28 (s, 3H, 17′-H), 1.16 (d, J = 6.5 Hz, 3H, 16-H), 1.02 (d, J = 7.5 Hz, 3H, 20-H); ^{13}C NMR (125 MHz, $CDCl_3$, 293 K): δ = 170.4, 164.8, 143.5, 138.1, 134.7, 125.0, 122.5, 80.8, 77.5, 75.9, 74.6, 72.9, 70.7, 70.6, 70.1, 68.9, 68.1, 57.5, 50.7, 47.6, 47.1, 42.8, 35.8, 31.9, 31.0, 28.9, 23.6, 21.3, 20.0, 17.8, 15.4, 12.8; HRMS (ESI+) calcd. for $C_{36}H_{58}N_4O_{10}Na$ $[M + Na]^+$ 729.4051, found 729.4031.

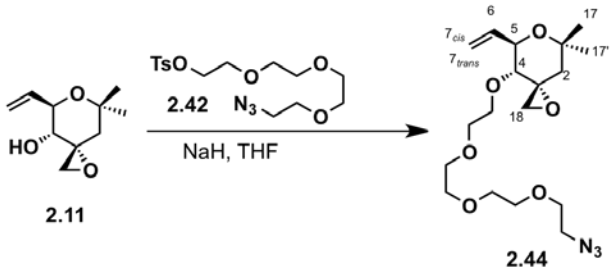

*Preparation of TEGylated right fragment **2.44**:* A 25-mL round-bottomed flask equipped with a Teflon-coated magnetic stir bar containing right fragment **2.11** (15 mg, 0.080 mmol) was added THF (0.6 mL) and tosylate **2.42** (45 mg, 0.12 mmol). The flask was cooled in an ice-water bath (0 °C external temperature) and NaH (8.2 mg, 0.32 mmol) was added to the flask. The mixture was stirred for 9 h as the ice-water bath was left to warm to 23 °C. The mixture was diluted with saturated aqueous NH_4Cl (1 mL), and THF was removed *in vacuo*. The resulting mixture was extracted with EtOAc (3 × 5 mL). The combined organic layers were dried over Na_2SO_4, filtered and concentrated *in vacuo*. The residue was purified by flash chromatography (10→70% EtOAc in hexanes) on silica gel (20 mL) to afford TEGylated right fragment **2.44** as a colorless oil (20 mg, 67% yield).

*Data for TEGylated right fragment **2.44**:* R_f = 0.3 (70% EtOAc in hexanes); IR (film): ν_{max} = 2919, 2970, 2104 (N_3), 1457, 1299, 1123 cm^{-1}; $[\alpha]_D^{22}$ +42.9 (*c* 1.0, CH_2Cl_2); ^1H NMR (400 MHz, $CDCl_3$, 293 K): δ = 5.95 (ddd, *J* = 17.2, 10.4, 6.4 Hz, 1H, 6-H), 5.43 (ddd, *J* = 17.2, 2.8, 1.2 Hz, 1H, 7_{trans}-H), 5.25 (ddd, *J* = 10.4, 2.8, 1.2 Hz, 1H, 7_{cis}-H), 4.21 (dd, *J* = 9.6, 6.4 Hz, 1H, 5-H), 3.77–3.51 (m, 14H, tetraethylene glycol-*H*'s), 3.40 (t, *J* = 5.2 Hz, 2H, N_3CH_2), 3.31 (d, *J* = 9.6 Hz, 1H, 4-H), 3.11 (d, *J* = 5.2 Hz, 1H, 18-H), 2.45 (d, *J* = 5.2 Hz, 1H, 18-H), 2.12 (d, *J* = 14.0 Hz, 1H, 2_{axial}-H), 1.42 (s, 3H, 17-H), 1.37 (d, *J* = 14.0 Hz, 1H, $2_{equatorial}$-H), 1.27 (s, 3H, 17′-H); ^{13}C NMR (100 MHz, $CDCl_3$, 293 K): δ = 136.5, 117.8, 77.6, 73.3, 73.2, 72.3, 70.7, 70.6, 70.5, 70.0, 57.0, 50.7, 47.3, 43.4, 31.1, 23.7; HRMS (ESI+) calcd. for $C_{18}H_{31}N_3O_6Na$ $[M + Na]^+$ 408.2111, found 408.2120.

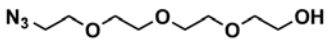

2.45

Synthesis of **2.45**, see: Y. Gong, Y. Luo, D. Bong, *J. Am. Chem. Soc.*, **2006**, *128*, 14430–14431.

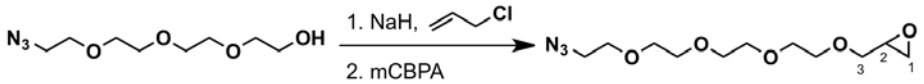

2.45 **2.46**

*Preparation of epoxide **2.46**:* A 100-mL round-bottomed flask equipped with a Teflon-coated magnetic stir bar containing alcohol **2.45** (666 mg, 3.04 mmol) was added THF (10 mL). The flask was cooled in an ice-water bath (0 °C external temperature), then NaH (243 mg, 6.08 mmol) and allyl chloride (349 mg, 4.56 mmol) were added to the flask. The mixture was stirred for 23 h as the ice-water bath was left to warm to 23 °C. The mixture was diluted with saturated

aqueous NH_4Cl (2 mL) and H_2O (10 mL), then THF was removed *in vacuo*. The resulting mixture was extracted with EtOAc (3 × 50 mL). The combined organic layers were dried over Na_2SO_4, filtered and concentrated *in vacuo*. The crude alkene was used directly in the next step.

A 100-mL round-bottomed flask equipped with a Teflon-coated magnetic stir bar containing the crude alkene, was diluted with CH_2Cl_2 (5 mL) then cooled in an ice-water bath (0 °C external temperature). Meta-chloroperoxybenzoic acid (454 mg, 2.63 mmol) was added, and the mixture was stirred for 17 h as the ice-water bath was left to warm to 23 °C. 2-methyl-2-butene (172 mg, 2.46 mmol) was added followed by saturated aqueous $NaHCO_3$ (5 mL). The organic layer was separated, and the aqueous layer was extracted with EtOAc (3 × 10 mL). The combined organic layers were washed with brine (10 mL), dried over Na_2SO_4, filtered and concentrated *in vacuo*. The residue was purified by flash chromatography (70→100% EtOAc in hexanes) on silica gel (50 mL) to afford epoxide **2.46** as a colorless oil (182 mg, 54% yield over 2 steps).

*Data for epoxide **2.46***: R_f = 0.22 (60% EtOAc in hexanes); IR (film): ν_{max} = 2871, 2108 (N_3), 1298, 1110 cm^{-1}; ^1H NMR (300 MHz, $CDCl_3$, 293 K): δ = 3.79 (dd, *J* = 11.4, 3.0 Hz, 1H, 3-H), 3.72–3.64 (m, 14H, tetraethylene glycol-*H*'s), 3.43 (dd, *J* = 11.4, 6.0 Hz, 1H, 3-H), 3.39 (t, *J* = 5.1 Hz, C*H*$_2$N$_3$), 3.19–3.14 (m, 1H, 2H), 2.79 (dd, *J* = 5.1, 5.1 Hz, 1H, 1-H), 2.61 (dd, *J* = 5.1, 3.0 Hz, 1, 1-H); ^{13}C NMR (100 MHz, $CDCl_3$, 293 K): δ = 72.0, 70.7, 70.6, 70.0, 50.8, 50.7, 44.3, 40.9; HRMS (ESI+) calcd. for $C_{11}H_{21}N_3O_5Na$ $[M+Na]^+$ 298.1379, found 298.1415.

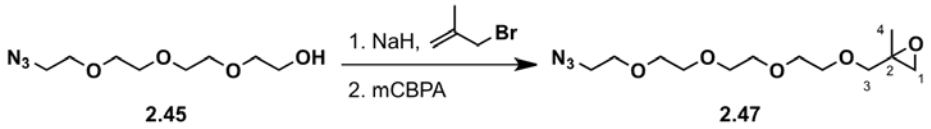

*Preparation of epoxide **2.47**:* A 100-mL round-bottomed flask equipped with a Teflon-coated magnetic stir bar containing alcohol **2.45** (809 mg, 3.69 mmol) was added THF (12 mL). The flask was cooled in an ice-water bath (0 °C external temperature), then NaH (295 mg, 7.38 mmol) and methallyl bromide (747 mg, 5.54 mmol) were added to the flask. The mixture was stirred for 20 h as the ice-water bath was left to warm to 23 °C. The mixture was diluted with saturated aqueous NH_4Cl (2 mL) and H_2O (20 mL), then THF was removed *in vacuo*. The resulting mixture was extracted with EtOAc (3 × 50 mL). The combined organic layers were dried over Na_2SO_4, filtered and concentrated *in vacuo*. The crude residue was purified by flash chromatography (20→40% EtOAc in hexanes) on silica gel (50 mL) to afford the alkene as a colorless oil (979 mg, 97% yield).

A 100-mL round-bottomed flask equipped with a Teflon-coated magnetic stir bar containing the alkene (461 mg, 1.69 mmol), was diluted with CH_2Cl_2 (6 mL) then cooled in an ice-water bath (0 °C external temperature). Meta-chloroperoxybenzoic acid (437 mg, 2.53 mmol) was added, and the mixture was stirred for 17 h as the ice-water bath was left to warm to 23 °C. 2-methyl-2-butene (236 mg, 3.38 mmol) was added followed by saturated aqueous $NaHCO_3$ (5 mL). The organic layer was separated, and the aqueous layer was extracted with EtOAc (3 × 20 mL). The combined organic layers were washed with brine (10 mL), dried over Na_2SO_4, filtered and concentrated *in vacuo*. The residue was purified by flash chromatography (40→80% EtOAc in hexanes) on silica gel (50 mL) to afford epoxide **2.47** as a colorless oil (332 mg, 66% yield over 2 steps).

*Data for epoxide **2.47***: R_f = 0.23 (70% EtOAc in hexanes); IR (film): ν_{max} = 2870, 2107 (N_3), 1289, 1117 cm^{-1}; ^1H NMR (400 MHz, $CDCl_3$, 293 K): δ = 3.69–3.64 (m, 14H, tetraethylene glycol-*H*'s), 3.61 (d, *J* = 11.2 Hz, 1H, 3-H), 3.44 (d, *J* = 11.2 Hz, 1H, 3-H), 3.39 (t, *J* = 4.8,

C$H_2$$N_3$), 2.74 (d, J = 4.8 Hz, 1H, 1-H), 2.62 (d, J = 4.8 Hz, 1H, 1-H), 1.37 (s, 3H, 4-H); ^{13}C NMR (100 MHz, $CDCl_3$, 293 K): δ = 74.3, 70.5, 70.4, 69.9, 55.9, 51.3, 50.5, 18.2; HRMS (ESI+) calcd. for $C_{12}H_{23}N_3O_5Na$ $[M+Na]^+$ 312.1535, found 312.1562.

Cells and reagents: HCT-116 cells were obtained as a gift from Professor Andreas Vogt (University of Pittsburgh), the MCF7 cells were a gift from Professor Paul Robbins (University of Pittsburgh), the MDA-MB231, MCF-7, DU145, H1299 and A549 cells were a gift from Professor Billy Day (University of Pittsburgh), the HEK-293-II cells were a gift from Professor Melissa Moore (University of Massachusetts), and the PCI-13, PCI-30, UD-SSC90, 93-VU-147T, UM-22B, UMSSC47, JHU-020 and JHU-012 cells were from Professor Robert Ferris (University of Pittsburgh). All cell culture media were supplemented with 10% fetal bovine serum, 1% L-glutamine and 1% penicillin/streptomycin. MCF7, MCF-7, DU145, H1299, MDA-MB231 and A549 were grown in RPMI 1640 media. HCT-116 cells were grown in McCoy's 5A media. HEK-293-II, PCI-13, PCI-30, UD-SSC90, 93-VU-147T, UM-22B, UMSSC47, JHU-020 and JHU-012 were grown in DMEM media. All synthetic compounds were dissolved in dimethyl sulfoxide (DMSO) as stock solutions and stored at -20 °C.

Antiproliferative activity assays: Cells were plated in a 96-well plate at an initial density of approximately 4×10^3 cells per well in 100 μL of cell culture medium and were incubated in an incubator of 37 °C in an atmosphere containing 5% carbon dioxide for 24 h prior to compound addition. One plate of cells was used for a time zero cell number determination, and cells in other plates were treated with either DMSO or a range of concentrations, in triplicate, of test agents. Serial three-fold dilutions were used in this experiment for the indicated ranges. The compound was added to the cells at the desired concentration in 100 mL medium (containing 2% DMSO).

Cell viability was measured spectrophotometrically using the commercial 3-(4,5-dimethylthiazol-2-yl)-5-(3-carboxymethoxyphenyl)-2-(4-sulfophenyl)-2H-tetrazolium, inner salt (MTS) dye reduction assay with phenazine methosulfate (PMS) as the electron acceptor (20 μL per well). The absorbance (at 490 nm minus that at 650 nm) was measured using a Modulus II Microplate Multimode Reader (Turner BioSystem). Evaluation of analogues was performed in triplicate at each concentration, and the final numbers were averaged. GraphPad Prism 5.0© was used to generate dose-response curves and calculate GI_{50} values. Growth inhibition is calculated as defined by the National Cancer Institute [$GI_{50} = 100 \times (T - T_0)/(C - T_0)$; T_0 = cell density at time zero; T = cell density of the test well after period of exposure to test compound; C = cell density of the vehicle treated] (see: http://www.dtp.nci.nih.gov/branches/btb/ivclsp.html). Vincristine was used as a positive control.

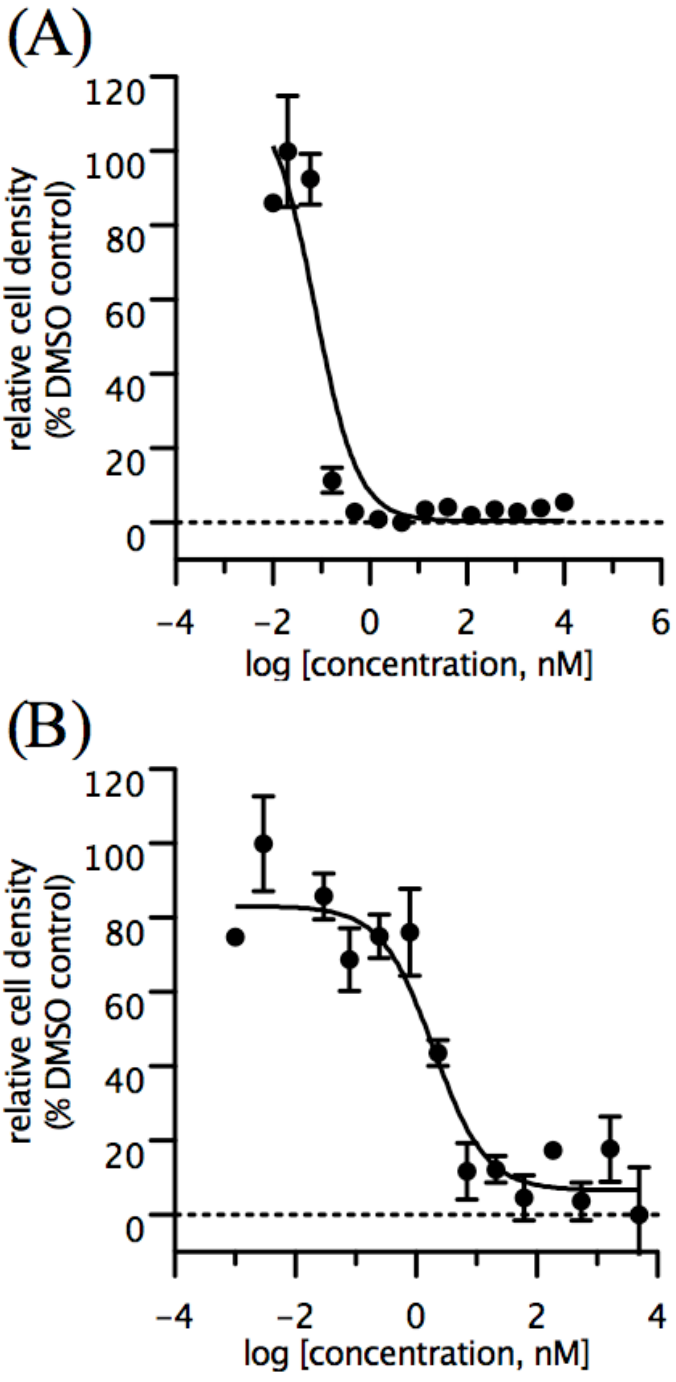
(A)
relative cell density
(% DMSO control)
120
100
80
60
40
20
0
−4
−2
0
2
4
6
log [concentration, nM]
(B)
relative cell density
(% DMSO control)
120
100
80
60
40
20
0
−4
−2
0
2
4
log [concentration, nM]

(C)

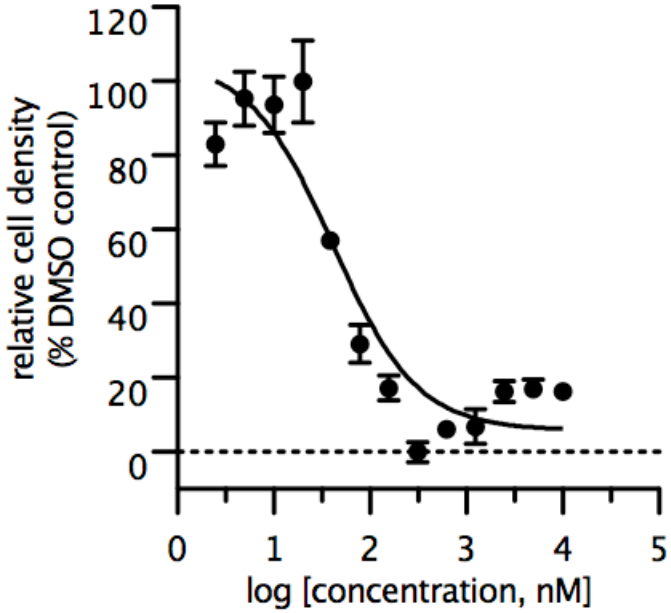
relative cell density
(% DMSO control)
120
100
80
60
40
20
0
0
1
2
3
4
5
log [concentration, nM]

(D)

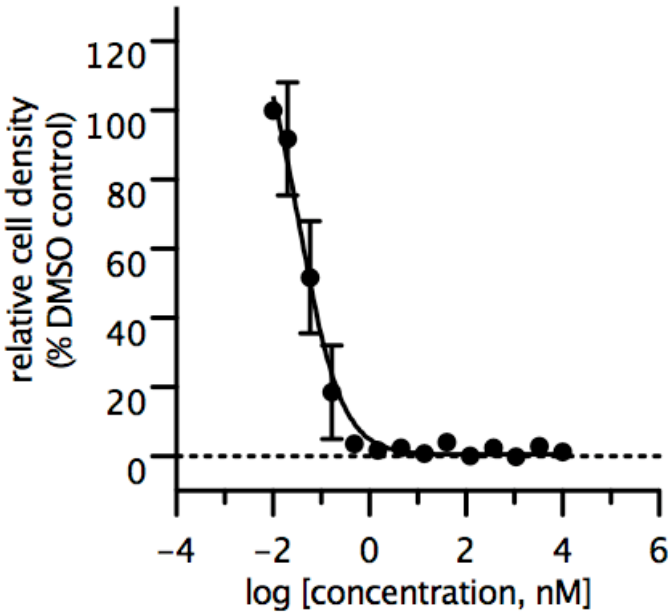
relative cell density
(% DMSO control)
120
100
80
60
40
20
0
−4
−2
0
2
4
6
log [concentration, nM]

(E)

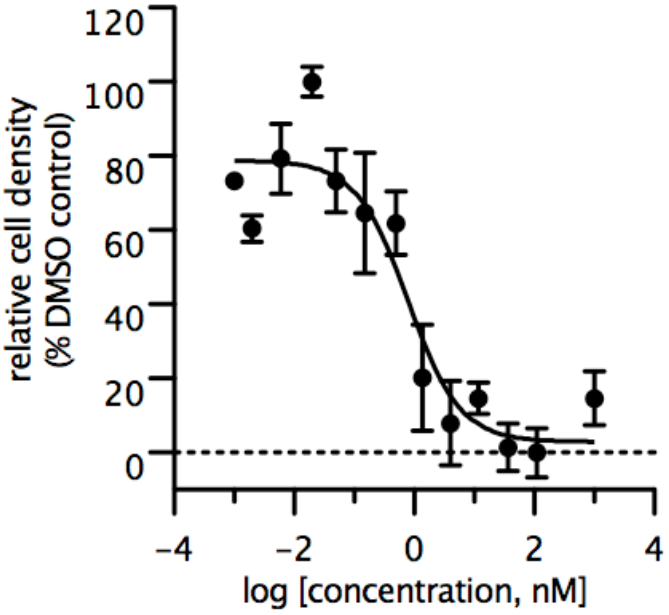
120
100
80
60
40
20
0
relative cell density
(% DMSO control)
−4
−2
0
2
4
log [concentration, nM]

(F)

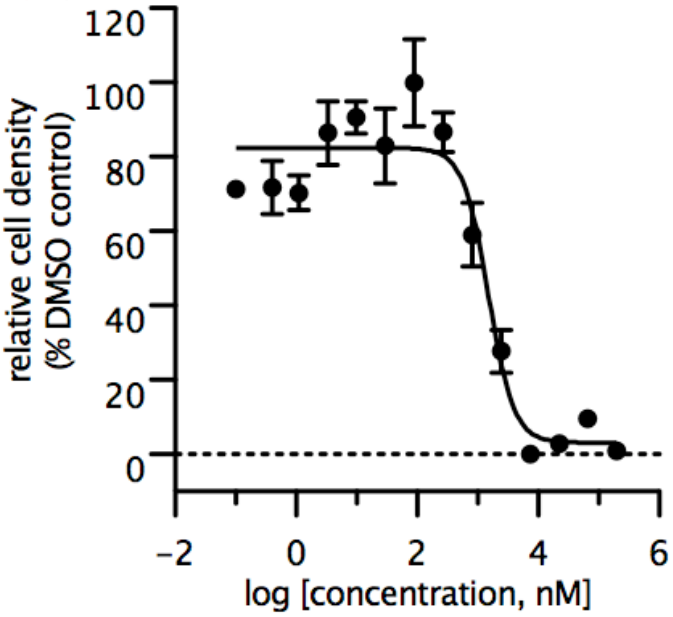
120
100
80
60
40
20
0
relative cell density
(% DMSO control)
−2
0
2
4
6
log [concentration, nM]

(G)

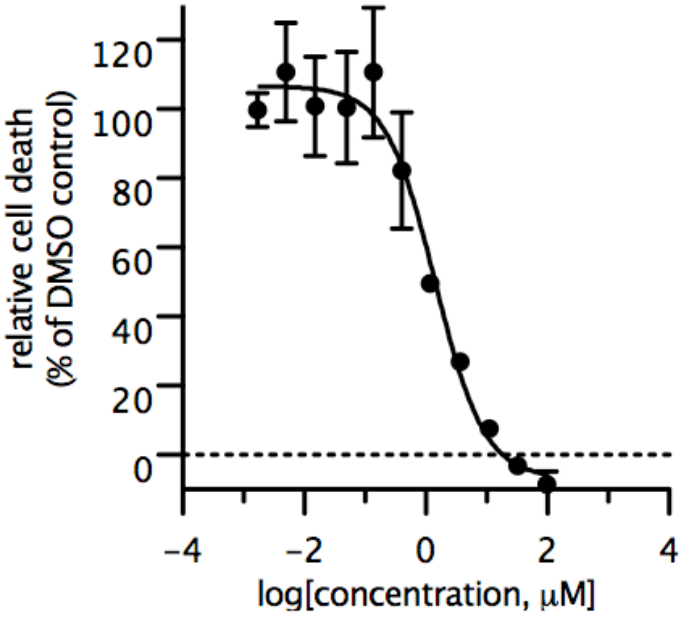
relative cell death
(% of DMSO control)
120
100
80
60
40
20
0
−4
−2
0
2
4
log[concentration, μM]

(H)

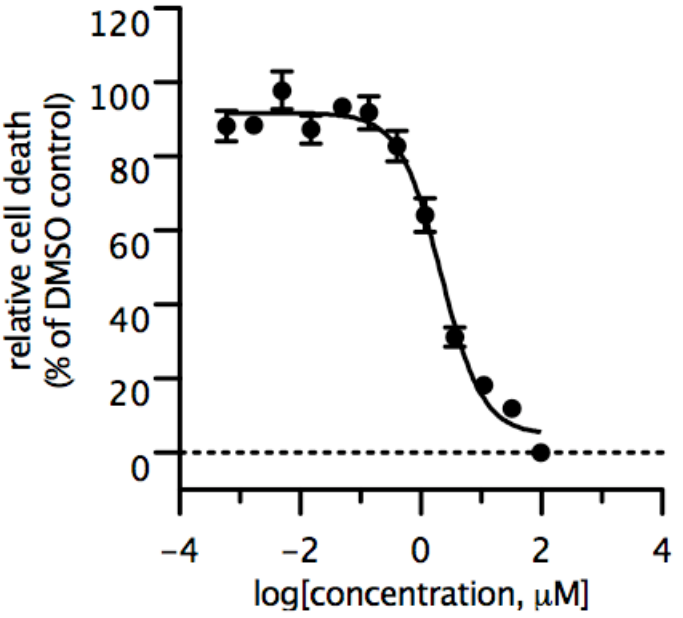
relative cell death
(% of DMSO control)
120
100
80
60
40
20
0
−4
−2
0
2
4
log[concentration, μM]

(I)

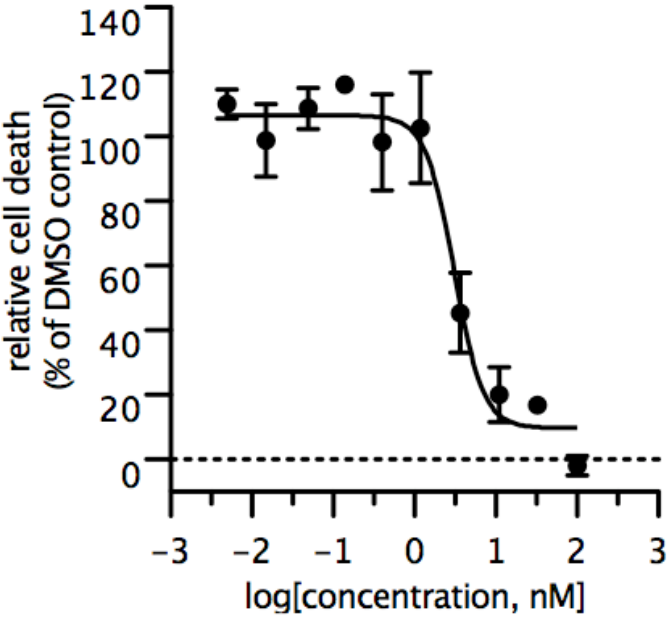
relative cell death
(% of DMSO control)
140
120
100
80
60
40
20
0
−3
−2
−1
0
1
2
3
log[concentration, nM]

(J)

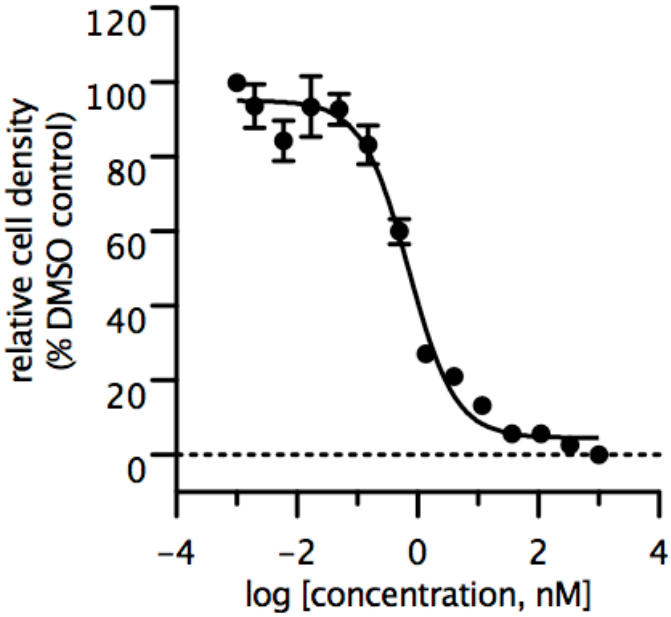
relative cell density
(% DMSO control)
120
100
80
60
40
20
0
−4
−2
0
2
4
log [concentration, nM]

(K)

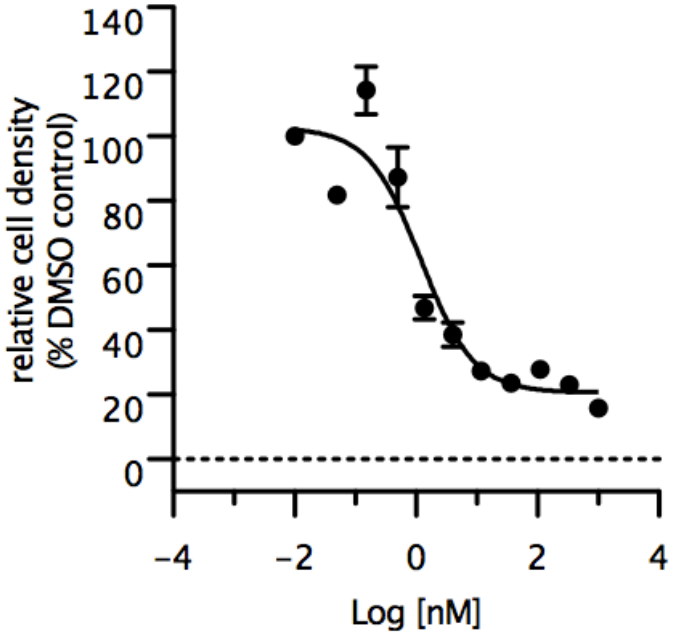
relative cell density
(% DMSO control)
140
120
100
80
60
40
20
0
-4
-2
0
2
4
Log [nM]

(L)

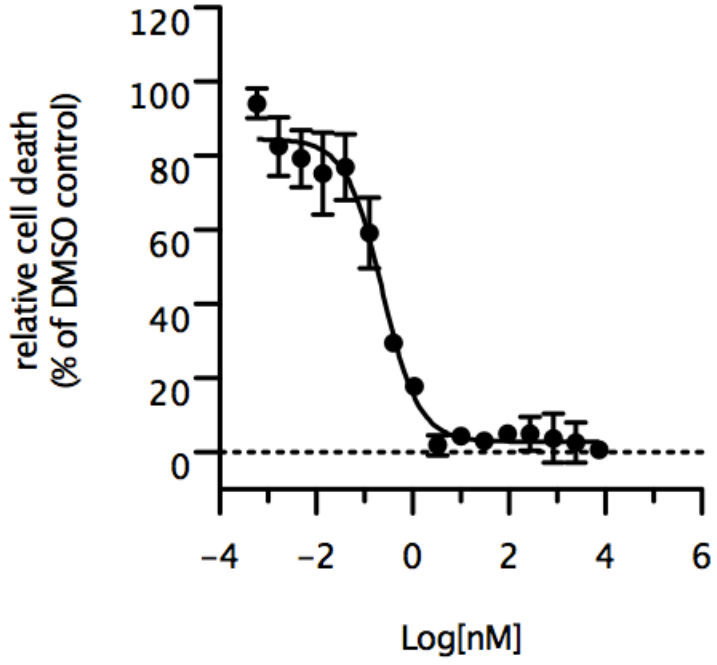
relative cell death
(% of DMSO control)
120
100
80
60
40
20
0
-4
-2
0
2
4
6
Log[nM]

(M)

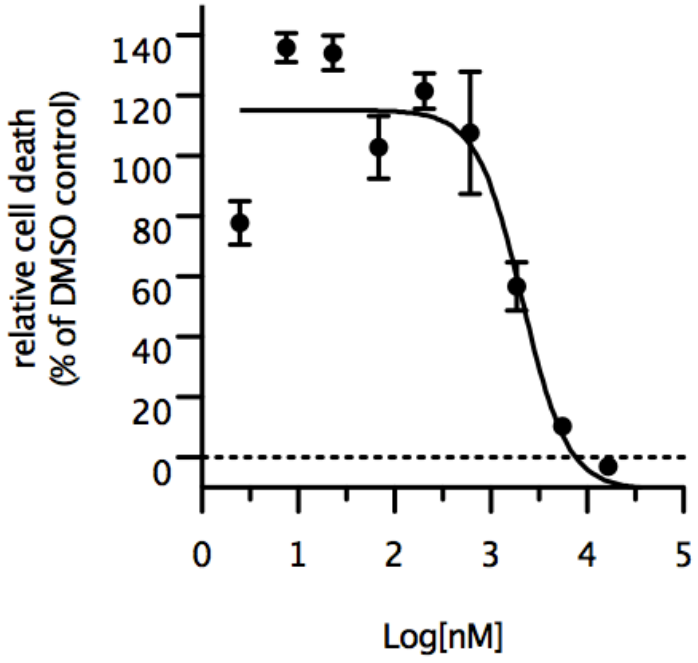
relative cell death
(% of DMSO control)
140
120
100
80
60
40
20
0
0
1
2
3
4
5
Log[nM]

(N)

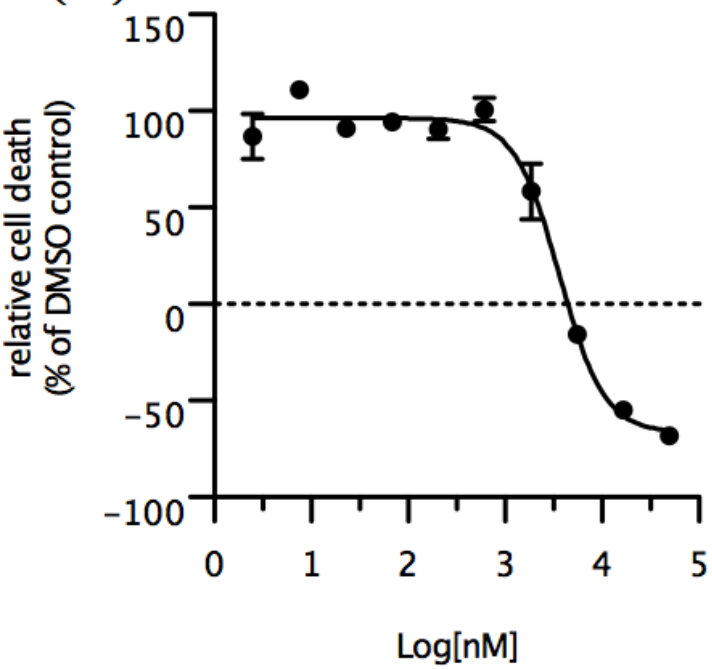
relative cell death
(% of DMSO control)
150
100
50
0
-50
-100
0
1
2
3
4
5
Log[nM]

(O)

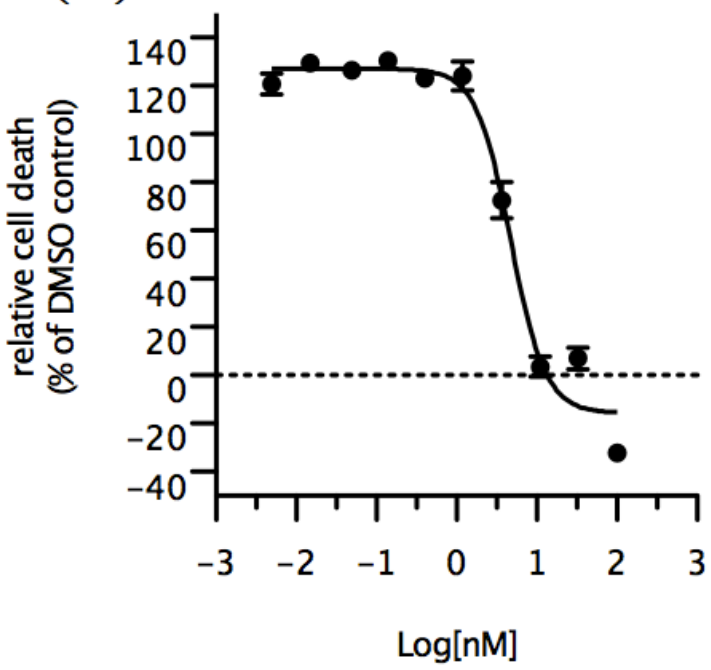
relative cell death
(% of DMSO control)
140
120
100
80
60
40
20
0
-20
-40
-3
-2
-1
0
1
2
3
Log[nM]

(P)

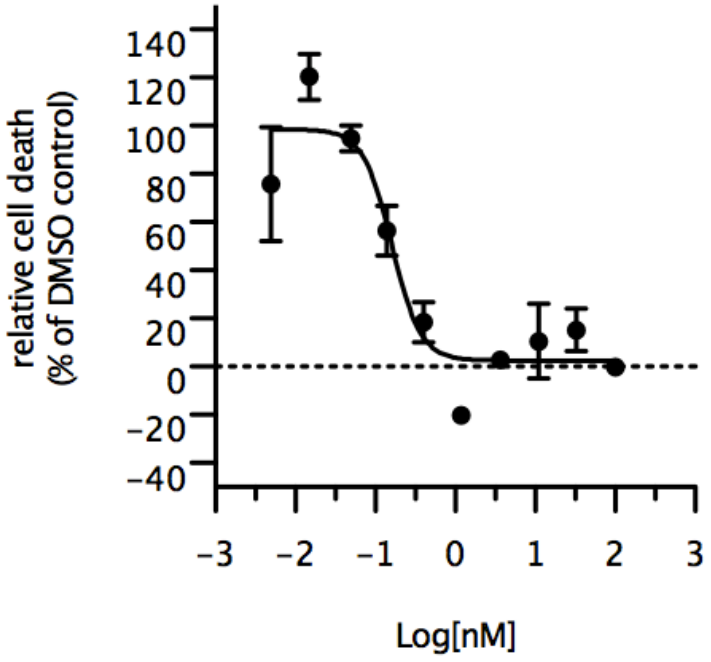
relative cell death
(% of DMSO control)
140
120
100
80
60
40
20
0
-20
-40
-3
-2
-1
0
1
2
3
Log[nM]

(Q)

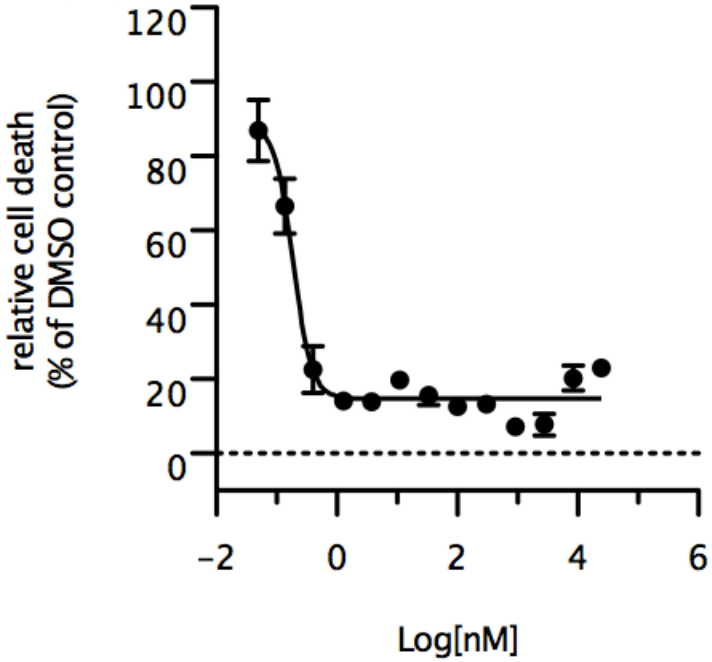
relative cell death
(% of DMSO control)
120
100
80
60
40
20
0
−2
0
2
4
6
Log[nM]

(R)

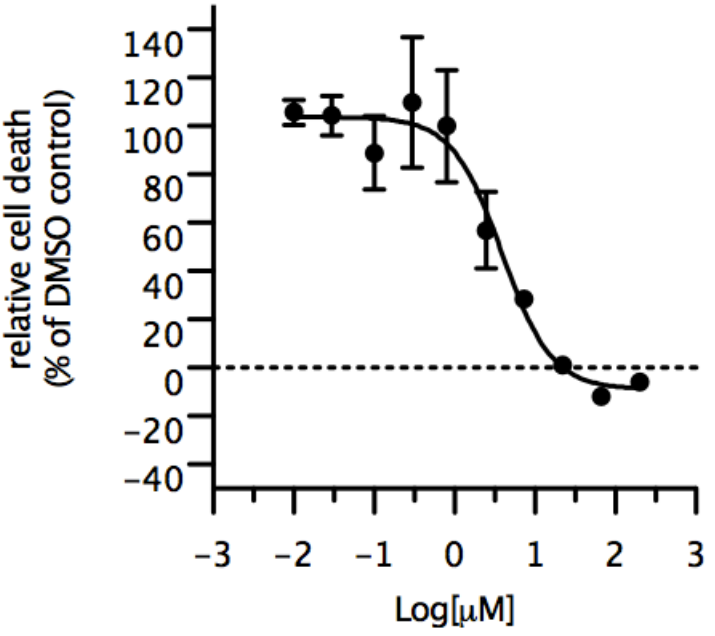
relative cell death
(% of DMSO control)
140
120
100
80
60
40
20
0
−20
−40
−3
−2
−1
0
1
2
3
Log[μM]

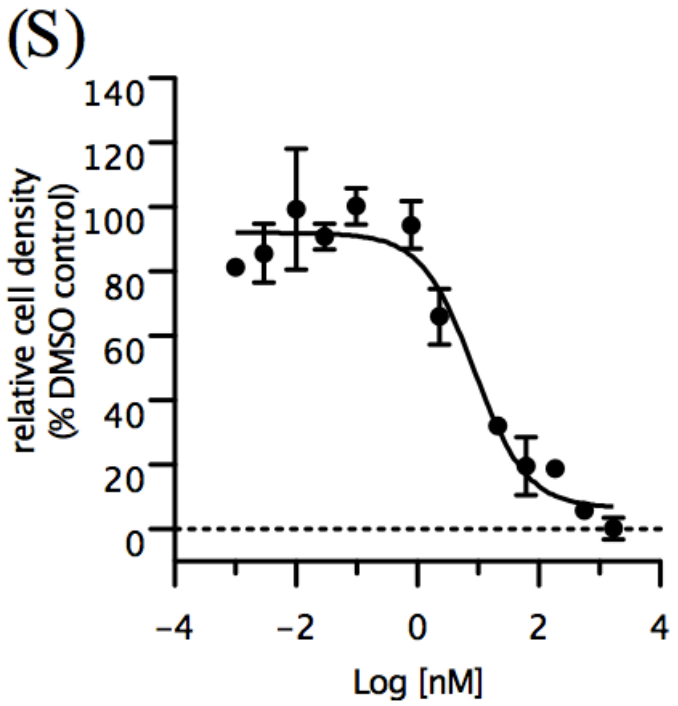

Figure A1. A representative example of the antiproliferative dose-dependant activity of meayamycin and analogues in cells.

(**A**) **2.43**-treated HCT-116 cells (**B**) **2.43**-treated MCF7 cells (**C**) **2.43**-treated HEK-293-II cells (**D**) meayamycin-treated HCT-116 cells (**E**) meayamycin-treated MCF7 cells (**F**) **2.44**-treated HCT-116 cells (**G**) **2.44**-treated MDA-MB231 cells (**H**) **2.44**-treated A549 cells (**I**) vincristine-treated MDA-MB231 cells (**J**) vincristine-treated A549 cells. (**K**) vincristine-treated HCT-116 cells. (**L**) **2.26**-treated A549 cells. (**M**) **2.44**-treated JHU 012 cells. (**N**) **2.44**-treated PCI 13 cells. (**O**) meayamycin-treated PCI 13 cells. (**P**) meayamycin B-treated JHU 020 cells. (**Q**) **2.26**-treated HCT-116 cells. (**R**) cisplatin-treated HCT-116 cells. (**S**) vincristine-treated HEK-293-II cells.

Antiproliferative reversibility test: Cells were plated in a 96-well plate at an initial density of approximately 4×10^3 cells per well in 100 µL of medium and were incubated for 24 h prior

to the addition of the compound. One concentration was used in each experiment for all times examined. The compound was added to the cells at twice the desired concentration in 100 µL cell culture medium. At the desired time intervals, the medium containing the compound was revmoved, the wells were washed three times with new medium and 200 µL of new medium containing 1% DMSO was added. At the last time interval, after washing and replacing the medium, cell proliferation was measured using the commercial MTS solution (20 µL/well) as described above for the antiproliferative activity assay.

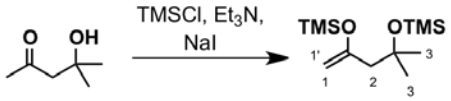

2.62 **2.66**

*Preparation of silyl enol ether **2.66**:* A 1-L round-bottomed flask equipped with a Teflon-coated magnetic stir bar containing 4-hydroxy-4-methyl-2-pentanone (22 g, 189 mmol) was purged with argon. Et_3N (66 mL, 435 mmol) and TMSCl (55 mL, 491 mmol) were added to the flask at 23 °C and the mixture was stirred at the same temperature for 30 min. A solution of NaI (75 g, 500 mmol) in MeCN (850 mL) was added to the reaction mixture over 1 h at the same temperature. The mixture was stirred for an additional 3.5 h, then diluted with ice/cold H_2O (1.5 L). The mixture was extracted with EtOAc (5 × 500 mL). The combined organic layers were dried over Na_2SO_4, filtered and concentrated *in vacuo*. The resulting crude residue of **2.66** (34 g, 70% yield) was <90% pure by ^1H NMR, and used directly in the next step without further purification.

*Data for silyl enol ether **2.66**:* IR (film): ν_{max} = 2961, 1620, 1321, 1251, 1042 cm^{-1}; ^1H NMR (300 MHz, $CDCl_3$, 293 K): δ = 4.08 (d, *J* = 3.3 Hz, 2H, 1′-, 1-H), 2.21 (s, 2H, 2-H), 1.28 (s, 6H,

3-H), 0.23 (s, 9H, TMS), 0.12 (s, 9H, TMS); ^{13}C NMR (100 MHz, $CDCl_3$, 293 K): δ = 157.0, 92.7, 73.8, 51.8, 29.9, 2.7, 0.04;

HRMS of compound **2.66** was not obtainable.

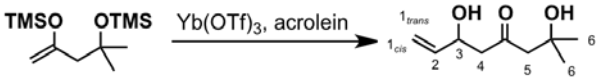

2.66 **2.63**

*Preparation of allylic alcohol **2.63**:* To a 1-L round-bottomed flask equipped with a Teflon-coated magnetic stir bar containing **2.66** (1.9 g, 7.3 mmol), was added toluene (15 mL) and acrolein (11.6 mL, 174 mmol). The flask was cooled in an ice-water bath (0 °C external temperature), then a solution of $Yb(OTf)_3$ (533 mg, 0.86 mmol) in H_2O:EtOH (1:10, 4.1 mL) was added. The mixture was stirred at the same temperature for 24 h, then diluted with brine (30 mL). The organic solvents were removed *in vacuo*, then the resulting mixture was extracted with EtOAc (3 × 20 mL). The combined organic layers were dried over Na_2SO_4, filtered and concentrated *in vacuo*. The crude residue was purified by flash chromatography (10→80% EtOAc in hexanes) on silica gel (100 mL) to afford **2.63** as a clear oil (903 mg, 72% yield).

*Data for allylic alcohol **2.63**:* R_f = 0.18 (40% EtOAc in hexanes); IR (film): ν_{max} = 3410 (br O-H), 2974, 2932, 1701 (C=O), 1378, 1144 cm^{-1}; ^{1}H NMR (300 MHz, 1% CD_3OD in $CDCl_3$, 293 K): δ = 5.87 (ddd, *J* = 5.6, 10.4, 16.8 Hz, 1H, 2-H), 5.31 (ddd, *J* = 16.8, 1.2, 1.2 Hz, 1H, 1_{trans}-H), 5.16 (ddd, *J* = 10.4, 1.2, 1.2 Hz, 1H, 1_{cis}-H), 4.61 (ddddd, *J* = 8.8, 6.0, 6.0, 1.2, 1.2 Hz, 1H, 3-H), 2.73–2.63 (m, 4H, 2-H, 5-H), 1.25 (s, 6H, 6-H); ^{13}C NMR (100 MHz, $CDCl_3$, 293 K): δ = 212.5, 138.8, 115.3, 69.8, 68.6, 54.2, 50.5, 29.4; HRMS (ESI+) calcd. for $C_9H_{17}O_3$ $[M + H]^+$ 173.1178, found 173.1184.

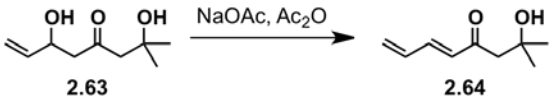

2.63 **2.64**

*Preparation of diene **2.64**:* To a 250-mL round-bottomed flask equipped with a Teflon-coated magnetic stir bar was added **2.63** (10.7 g, 62.2 mmol), DCE (40 mL), Ac_2O (6.20 mL, 62.2 mmol) and NaOAc (1.50 g, 18.7 mmol). The mixture was stirred in a 60 °C oil bath for 24 h. The mixture was cool to 23 °C, then diluted with EtOAc (150 mL) and saturated aqueous sodium bicarbonate (200 mL). The organic layer was separated, dried over Na_2SO_4, filtered and concentrated *in vacuo*. The crude residue was purified by flash chromatography (10→50% EtOAc in hexanes) on silica gel (100 mL) to afford **2.64** as a clear oil (6.7 g, 70% yield).

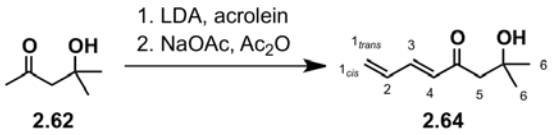

2.62 **2.64**

*Preparation of diene **2.64**:* A 250-mL round-bottomed flask equipped with a Teflon-coated magnetic stir bar containing diisopropylamine (9.1 g, 90 mmol) was purged with N_2. The flask was cooled in an ice-water bath (0 °C external temperature). ^{n}BuLi (55 mL, 90 mmol) was added slowly, while the mixture got viscous. THF (42 mL) was added, then the homogenous mixture was cooled to -78 °C. A solution of 4-hydroxy-4-methyl-2-pentanone (5.0 g, 43 mmol) in THF (17 mL) was added and the mixture was stirred for 50 min at the same temperature. A solution of acrolein (2.7 g, 47 mmol) in THF (38 mL) was added and the mixture was stirred for 1 h. The reaction mixture was then quenched with saturated aqueous NH_4Cl (200 mL), then diluted with H_2O (100 mL). THF was removed *in vacuo*, then the resulting mixture was extracted with Et_2O (3 × 25 mL). The combined organic layers were washed with brine (20 mL), dried over Na_2SO_4, filtered and concentrated *in vacuo*. To the crude residue was added Ac_2O (4.8 g, 47 mmol) and

NaOAc (2.3 g, 28 mmol). The mixture was stirred at 23 °C for 22 h, then heated to 100 °C, and stirred for 2 h. The mixture was cooled to 23 °C, diluted with saturated aqueous $NaHCO_3$ (100 mL) and extracted with Et_2O (3 × 70 mL). The combined organic layers were dried over Na_2SO_4, filtered and concentrated *in vacuo*. The crude residue was purified by flash chromatography (5→30% EtOAc in hexanes) on silica gel (200 mL) to afford **2.64** as a clear oil (2.78 g, 42% yield).

*Data for diene **2.64**:* R_f = 0.33 (40% EtOAc in hexanes); IR (film): ν_{max} = 3437 (br O-H), 2973, 1678 (C=O), 1204, 1110 cm^{-1}; ^1H NMR (300 MHz, 1% CD_3OD in $CDCl_3$, 293 K): δ = 7.16 (dd, *J* = 15.6 Hz, 10.8 Hz, 1H, 3-H), 6.48 (ddd, *J* = 16.8, 10.8, 10.8 Hz, 1H, 2-H), 6.18 (d, *J* = 15.6 Hz, 1H, 4-H), 5.72 (d, *J* = 16.8 Hz, 1H, 1_{trans}-H), 5.60 (d, *J* = 10.8 Hz, 1H, 1_{cis}-H), 2.77 (s, 2H, 5-H), 1.29 (s, 6H, 6-H); ^{13}C NMR (75 MHz, $CDCl_3$, 293 K): δ = 202.0, 143.6, 135.0, 131.0, 127.4, 69.9, 50.5, 29.4; HRMS (EI+) calcd. for $C_9H_{14}O_2$ $[M\text{-}CH_3]^+$ 139.0759, found 139.0756.

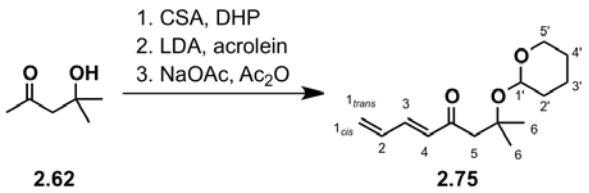

2.62 **2.75**

*Preparation of diene **2.75**:* A 250-mL round-bottomed flask equipped with a Teflon-coated magnetic stir bar containing 4-hydroxy-4-methyl-2-pentanone (10 g, 86 mmol) was cool in an ice-water bath (0 °C external temperature). 3,4-Dihydro-2H-pyran (14.5 g, 172 mmol) was added followed by CSA (200 mg, 0.860 mmol). The mixture was stirred for 1 h while slowly warming the cooling bath to 23 °C. The mixture was diluted with saturated aqueous $NaHCO_3$ (70 mL) and extracted with Et_2O (3 × 70 mL). The combined organic layers were dried over Na_2SO_4, filtered and concentrated *in vacuo*. The residue was purified by flash chromatography (10→30% EtOAc

in hexanes) on silica gel (200 mL) to afford THP-protected derivative of **2.62** as a clear liquid (16.4 g, 96% yield).

A 500-mL round-bottomed flask equipped with a Teflon-coated magnetic stir bar containing diisopropylamine (4.2 g, 42 mmol) was purged with N_2. The flask was cooled in an ice-water bath (0 °C external temperature). ^{n}BuLi (26.3 mL, 42 mmol) was added slowly, while the mixture got viscous. THF (35 mL) was added, then the homogenous mixture was cooled to -78 °C. A solution of the THP-protected derivative of **2.62** (7 g, 35 mmol) in THF (17 mL) was added and the mixture was stirred for 50 min at the same temperature. A solution of acrolein (2.4 g, 42 mmol) in THF (18 mL) was added and the mixture was stirred for 1 h. The reaction mixture was then quenched with saturated aqueous NH_4Cl (100 mL), then diluted with H_2O (100 mL). THF was removed *in vacuo*, then the resulted mixture was extracted with Et_2O (3 × 70 mL). The combined organic layers were washed with brine (50 mL), dried over Na_2SO_4, filtered and concentrated *in vacuo*. To the crude residue was added Ac_2O (4 g, 39 mmol) and NaOAc (1.7 g, 21 mmol). The mixture was stirred at 23 °C for 21 h, then heated to 100 °C, and stirred for 2 h. The mixture was cooled to 23 °C, diluted with saturated aqueous sodium bicarbonate (100 mL) and extracted with Et_2O (3 × 70 mL). The combined organic layers were dried over Na_2SO_4, filtered and concentrated *in vacuo*. The crude residue was purified by flash chromatography (2→10% EtOAc in hexanes) on silica gel (200 mL) to afford **2.75** as a clear oil (2 g, 24% yield).

*Data for diene **2.75**:* R_f = 0.25 (20% EtOAc in hexanes); IR (film): ν_{max} = 2942, 2870, 1683 (C=O), 1590, 1128, 1023 cm^{-1}; ^{1}H NMR (300 MHz, $CDCl_3$, 293 K): δ = 7.15 (dddd, *J* = 15.3, 11.7, 0.6, 0.6 Hz, 1H, 3-H), 6.30 (d, *J* = 15.3 Hz, 1H, 4-H), 5.65 (dddd, *J* = 17.1, 1.2, 0.6, 0.6 Hz,

1H, 1_{trans}-H), 5.52 (dddd, *J* = 10, 1.2, 0.6, 0.6 Hz, 1H, 1_{cis}-H), 4.81 (dd, *J* = 2.4, 2.4 Hz, 1H, 1′-H), 3.94–3.87 (m, 1H, 5′-H), 3.48–3.40 (m, 1H, 5′-H), 2.84 (d, *J* = 13.5 Hz, 1H, 5-H), 2.73 (d, *J* = 13.5 Hz, 1H, 5-H), 1.85–1.40 (m, 6H, 4′-, 3′-, 2′-H), 1.37 (s, 3H, 6-H), 1.32 (s, 3H, 6-H); ^{13}C NMR (75 MHz, $CDCl_3$, 293 K): δ = 199.3, 142.4, 135.4, 131.9, 126.1, 93.8, 75.8, 63.0, 53.0, 32.1, 27.2, 26.2, 25.4, 20.4; HRMS (EI+) calcd. for $C_{14}H_{22}O_3$ $[M]^+$ 238.1569, found 238.1562.

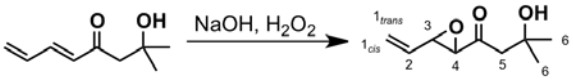

2.64 **2.61**

*Preparation of epoxide **2.61**:* A 50-mL round-bottomed flask equipped with a Teflon-coated magnetic stir bar containing **2.64** (390 mg, 2.50 mmol) was charged with MeOH (13 mL). The flask was cooled in an ice-water bath (0 °C external temperature). H_2O_2 (30% aqueous solution, 1 mL, 12.5 mmol) and aqueous 1M NaOH (0.46 mL, 0.5 mmol) were added to the reaction mixture at the same temperature. The mixture was stirred at the same temperature for 3.5 h, then diluted with saturated aqueous NH_4Cl (10 mL). The mixture was extracted with Et_2O (3 × 10 mL). The combined organic layers were dried over Na_2SO_4, filtered and concentrated *in vacuo*. The crude residue was purified by flash chromatography (5→30% EtOAc in hexanes) on silica gel (25 mL) to afford **2.61** as a clear oil (309 mg, 73% yield).

*Data for epoxide **2.61**:* R_f = 0.33 (40% EtOAc in hexanes); IR (film): ν_{max} = 3403 (br, O-H), 2974, 2930, 1709 (C=O), 1442, 1199, 1135 cm^{-1}; ^{1}H NMR (300 MHz, $CDCl_3$, 293 K): δ = 5.56 (ddd, *J* = 17, 11, 6 Hz, 1H, 2-H), 5.55 (dd, *J* = 17, 2.5 Hz, 1H, 1_{trans}-H), 5.41 (dd, *J* = 11, 2.5 Hz, 1H, 1_{cis}-H), 3.49 (dd, *J* = 6, 2.1 Hz, 1H, 3-H), 3.38 (d, *J* = 2.1 Hz, 1H, 4-H), 2.67 (d, *J* = 17.1 Hz, 1H, 5-H), 2.50 (d, *J* = 17.1 Hz, 1H, 5-H), 1.28 (s, 3H, 6-H), 1.27 (s, 3H, 6-H); ^{13}C NMR (175

MHz, $CDCl_3$, 293 K): δ = 207.9, 133.0, 121.8, 69.8, 61.2, 57.9, 47.9, 29.5, 29.4; HRMS (EI+) calcd. for $C_9H_{13}O_2$ $[M\text{-}OH]^+$ 153.0916, found 153.0910.

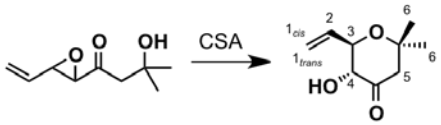

2.61 **2.25**

*Preparation of ketone **2.25**:* A 100-mL round-bottomed flask equipped with a Teflon-coated magnetic stir bar containing **2.61** (633 mg, 3.7 mmol) was charged with CH_2Cl_2 (20 mL). The flask was cooled in an ice-water bath (0 °C external temperature). CSA (860 mg, 3.7 mmol) was added, and the mixture was stirred for 19 h, while the cooling bath was left to warm to 23 °C. Et_3N (1 mL) was added, then the mixture was concentrated *in vauo*. The crude residue was purified by flash chromatography (10→30% EtOAc in hexanes) on silica gel (50 mL) to afford **2.25** as a clear oil (512 mg, 80% yield).

*Data for ketone **2.25**:* R_f = 0.35 (30% EtOAc in hexanes); IR (film): ν_{max} = 3474 (br, O-H), 2975, 2934, 1723 (C=O), 1374, 1240, 1107, 1080 cm^{-1}; ^1H NMR (300 MHz, 1% CD_3OD in C_6D_6, 293 K): δ = 6.16 (ddd, *J* = 17.1, 10.5, 4.8 Hz, 1H, 2-H), 5.53 (ddd, *J* = 17.1, 1.8, 1.8 Hz, 1H, 1_{trans}-H), 5.17 (ddd, *J* = 10.5, 1.8, 1.8 Hz, 1H, 1_{cis}-H), 3.86 (dd, *J* = 9.0, 6.8 Hz, 1H, 3-H), 3.63 (d, *J* = 9.0 Hz, 1H, 4-H), 1.00 (s, 3H, 6-H), 0.75 (s, 3H, 6-H); ^{13}C NMR (75 MHz, $CDCl_3$, 293 K): δ = 207.4, 135.5, 118.0, 77.9, 76.7, 76.4, 51.5, 30.8, 23.6; HRMS (ESI+) calcd. for $C_9H_{15}O_3$ $[M + H]^+$ 171.1021, found 171.1006.

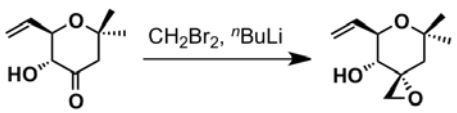

2.25 *racemic*-**2.11**

*Preparation of epoxide racemic-**2.11**:* A 25-mL round-bottomed flask equipped with a Teflon-coated magnetic stir bar containing **2.25** (200 mg, 1.18 mmol) was purged with N_2. To the flask was added THF (12 mL) and CH_2Br_2 (246 mg, 1.42 mmol). The flask was cooled to -78 °C, then ^{n}BuLi (1.6 mL, 2.6 mmol) was added. The mixture was stirred for 7 h, while warming the cooling bath to 20 °C. The reaction mixture was quenched with saturated aqueous NH_4Cl (15 mL), and THF was removed *in vacuo*. The resulting mixture was extracted with Et_2O (3 × 15 mL). The combined organic layers were dried over Na_2SO_4, filtered and concentrated *in vacuo*. The crude residue was purified by flash chromatography (5→30% EtOAc in hexanes) on silica gel (40 mL) to afford *racemic*-**2.11** as a clear oil (157 mg, 73% yield).

Spectroscopic data for *racemic*-**2.11** matches B. J. Albert, A. Sivaramakrishnan, T. Naka, N. L. Czaicki, K. Koide, *J. Am. Chem. Soc.* **2007**, *129*, 2648–2659.

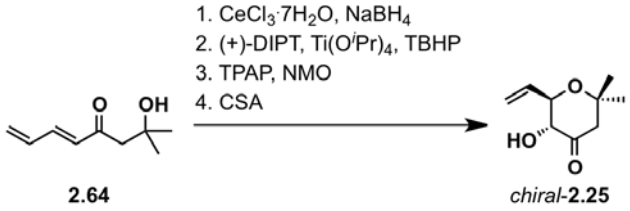

2.64 *chiral*-**2.25**

*Preparation of ketone chiral-**2.25**:* A 500-mL round-bottomed flask equipped with a Teflon-coated magnetic stir bar was added **2.64** (2.4 g, 15.4 mmol) and MeOH (60 mL). The mixture was cooled to 0 °C, then $CeCl_3$•$7H_2O$ (11.6 g, 30.8 mmol) was added in one portion, followed by addition of $NaBH_4$ (1.16 g, 30.8 mmol) added over 15 min. The mixture was stirred at the same temperature for 30 min, then diluted with saturated aqueous NH_4Cl (50 mL). MeOH was removed *in vacuo*, then the resulting mixture was extracted with EtOAc (3 × 20 mL). The combined organic layers were dried over Na_2SO_4, filtered and concentrated *in vacuo*. The crude alcohol was used directly in the next step.

A 250-mL round-bottomed flask equipped with a Teflon-coated magnetic stir bar containing the crude alcohol was purged with argon. CH_2Cl_2 (60 mL) and 4Å M.S. (3.1 g) were added to the flask. The mixture was cooled to -20 °C (external temperature), then $Ti(O^iPr)_4$ (0.38 g, 1.34 mmol), (+)-DIPT (0.5 g, 2.1 mmol) and *t*BuOOH solution in isoocatane (1.4 mL, 8.0 mmol) were added sequentially at the same temperature. The mixture was stirred at the same temperature for 13 h, then diluted with 1 M NaOH (50 mL), Celite ® (3.0 g), Na_2SO_4 (3.0 g), NaCl (3.0 g). The mixture was stirred for 40 min, then filtered through a pad of Celite® and florisil mixture. The filtrate was concentrated *in vacuo*, and the resulting crude residue was purified by flash chromatography (10→70% EtOAc in hexanes) on silica gel (200 mL) to afford the epoxyalcohol as a clear oil (0.8 g) with impurities of titantium and tartarate. The impure epoxide was used in the next step without further purification.

To a 1-L round-bottomed flask equipped with a Teflon-coated magnetic stir bar containing the epoxy-alcohol (0.8 g) was added CH_2Cl_2 (200 mL), 4Å molecular sieves (3.3 g), TPAP (101 mg,0.29 mmol) and NMO (2.5 g, 18.4 mmol) at 23 °C. The mixture was stirred at the same temperature for 40 min, then filtered through a plug of silica. The filtrate was concentrated to approximately 200 mL of CH_2Cl_2 remained in the flask. To the flask was added CSA (860 mg, 3.7 mmol) at 23 °C. The mixture was stirred at the same temperature for 19 h, then Et_3N (1 mL) was added. The mixture was concentrated *in vacuo*, and the crude residue was purified by flash chromatography (10→30% EtOAc in hexanes) on silica gel (50 mL) to afford *chiral*-**2.25** as a clear oil (512 g, 20% yield, over 4 steps). The optical rotation of *chiral*-**2.25** is $[\alpha]_D^{20}$ +28.1 (*c* 1.0, CH_2Cl_2).

The optical rotation of the chiral variant of **2.11** prepared from *chiral*-**2.25** is $[\alpha]_D^{20}$ +68.3 (*c* 1.2, CH_2Cl_2).

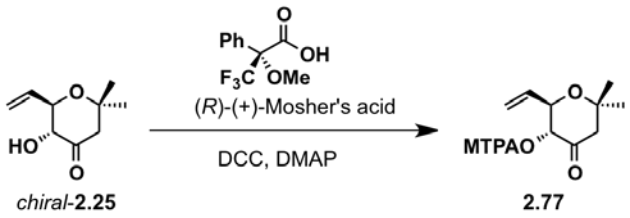

*Preparation of Mosher ester derivative **2.77***: A 10-mL round-bottomed flask was charged with ketone *chiral*-**2.25** (5.2 mg, 0.030 mmol) and CH_2Cl_2 (0.13 mL). The flask was cooled on an ice-water bath (0 °C external temperature), then (*R*)-(+)-Mosher's acid (11.3 mg, 0.046 mmol), DCC (19.1 mg, 0.090 mmol) and DMAP (4.5 mg, 0.036 mmol) were added at the same temperature under an open atmosphere to the flask containing the mixture. The reaction mixture was stirred, while warming slowly to 25 °C, for 3.5 h. The mixture was filtered through a plug of silica gel, and the filter cake was rinsed with CH_2Cl_2 (20 mL). The filtrate was concentrated *in vacuo*, and the crude residue was used without purification for analysis. The diastereomers were sufficiently separated in the ^{1}H NMR spectrum such that integration could be performed. *Peaks used for analysis*: ^{1}H NMR (300 MHz, 293K, $CDCl_3$): δ = 5.90 (ddd, *J* = 17.1, 10.2, 6.6 Hz, 1H), 5.68 (ddd, *J* = 17.1, 10.5, 6.3 Hz, 1H).

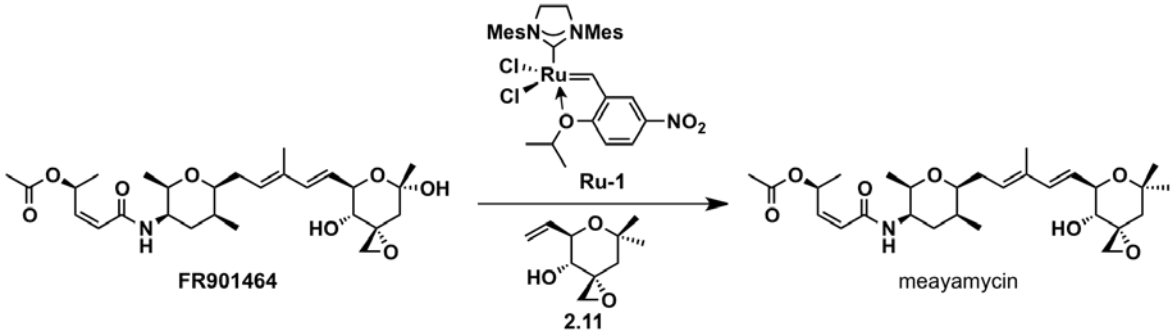

Preparation of meayamycin: A 10-mL round-bottomed flask was charged with FR901464 (3.1 mg, 0.006 mmol), **2.11** (6.2 mg, 0.034 mmol), **Ru-1** (2.2 mg, 0.0030 mmol), benzoquinone (2.1 mg, 0.020 mmol), and DCE (0.15 mL). The flask was stirred in a 40 °C oil bath for 14 h, then concentrated *in vacuo*. The crude residue was purified by preparative TLC (70% EtOAc in hexanes), then the isolated semipure product was further purified by preparative HPLC (Absorption at 232 nm. Elution conditions: flow rate = 10.0 mL/min, gradient: 40→100% MeCN in water over 15 min, then 15-25 min 100% MeCN. Column: Agilent Prep-C18 column 21.2 × 150 mm, 5 μm. T = 24 °C. Retention time = 10.5 min).

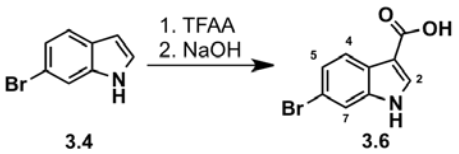

3.4 3.6

*Preparation of carboxylic acid **3.6**:* A 10-mL round-bottomed flask was charged with **3.4** (100 mg, 0.510 mmol) and DMF (2 mL). The flask was cooled on an ice-water bath (0 °C external temperature), then TFAA (118 mg, 0.561 mmol) was added at the same temperature under an open atmosphere to the flask containing the mixture. The reaction mixture was stirred, while warming slowly to 23 °C, for 15 h. The mixture was then poured into a seperatory funnel containing H_2O (50 mL) and extracted with Et_2O (2 × 20 mL). The combined organic extracts were dried over Na_2SO_4 and concentrated under reduced pressure using a rotary evaporator to yield a pale yellow solid. The crude solid was transferred to a 50-mL round-bottomed flask equipped with a Teflon-coated magnetic stir bar, then aqueous NaOH (4 M, 4 mL) was added to

the flask. The mixture was refluxed under an open atmosphere for 23 h, then cooled to 23 °C, and washed with CH_2Cl_2 (2 × 25 mL). The aqueous layer was then acidified with aqueous HCl (6 M, 3 mL), and the resulting precipitate was isolated by vacuum filtration to give carboxylic acid **3.6** as a pale yellow solid (119 mg, 97% yield) with >95% purity.

*Data for carboxylic acid **3.6**:* ^{1}H NMR (300 MHz, 293K, DMSO-d_6): δ = 12.07 (br s, 1H, OH), 11.88 (br s, 1H, N-H), 8.01 (d, J = 3.0 Hz, 1H, 2-H), 7.92 (d, J = 8.6 Hz, 1H, 4-H), 7.64 (d, J = 1.7 Hz, 1H, 7-H), 7.28 (dd, J = 8.6, 1.7 Hz, 1H, 5-H); HRMS (EI+) calcd for $C_9H_6NO_2Br$ $[M]^+$ 238.9582, found 238.9585. These spectroscopic data for carboxylic acid **3.6** were consistent with the literature: *J. Nat. Prod.* **1993**, *56,* 1553.

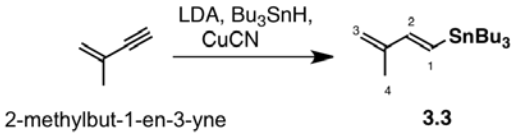

*Preparation of alkenyl stannane **3.3**:* A 50-mL round-bottomed flask equipped with a Teflon-coated magnetic stir bar was evacuated and backfilled with nitrogen. The flask was cooled on an ice-water bath and diisopropylamine (0.24 g, 2.4 mmol) was added via syringe. ^{n}BuLi (1.6 M in hexanes, 1.5 mL, 2.4 mmol) was slowly added using a syringe, at the same temperature under a nitrogen atmosphere. The mixture was stirred for 3 min, resulting in the development of a viscous liquid, an indication of LDA formation. The mixture was cooled to -40 °C (external temperature), and then THF (5 mL) followed by Bu_3SnH (670 mg, 2.30 mmol) were added. The resulting mixture was treated with CuCN (191 mg, 2.10 mmol) via opening and closing the round-bottomed flask's septa at the same temperature. A solution of 2-methylbut-1-en-3-yene (132 mg, 2.00 mmol) in THF (1 mL) was added to the reaction flask at the same temperature using a syringe. The reaction mixture was stirred at the same temperature under a nitrogen

atmosphere for 3 h, and then quenched with MeOH (2 mL) at the same temperature to result in a dark brown liquid mixture. The reaction mixture was diluted with Et_2O (20 mL) and washed with saturated aqueous NH_4Cl (2 × 20 mL) and brine (2 × 20 mL). The organic layer was dried over Na_2SO_4, filtered, and concentrated under reduced pressure using a rotary evaporator. The crude residue was dissolved in EtOAc (10 mL) in a 50-mL oven-dried round-bottomed flask, then AgOAc (1 g) was added at 23 °C under an open atmosphere. The mixture was stirred for 1 h at 23 °C, filtered through Celite®, and concentrated under reduced pressure using a rotary evaporator. The resulting residue was purified by flash chromatography (3% Et_3N in hexanes) on silica gel (50 mL) to afford alkenyl stannane **3.3** as a colorless oil (414 mg, 58% yield).

*Data for alkenyl stannane **3.3**:* ^{1}H NMR (300 MHz, 293K, $CDCl_3$): δ = 6.64 (d, *J* = 19.2 Hz, 1H, 2-H), 6.21 (d, *J* = 19.2 Hz, 1H, 1-H), 5.01 (br s, 1H, 3-H), 4.96 (br s, 1H, 3-H), 1.86 (s, 3H, 4-H), 1.64–1.48 (m, 6H, butyl), 1.39–1.25 (m, 12H, butyl), 1.01–0.82 (m, 9H, butyl); ^{13}C NMR (75 MHz, 293 K, $CDCl_3$): δ = 149.0, 143.7, 135.7, 115.6, 29.1, 27.7, 27.0, 18.5, 17.8, 13.6, 9.4. These spectroscopic data for *alkenyl stannane* **3.3** were consistent with literature: *Tetrahedron* **1991**, *47*, 1163.

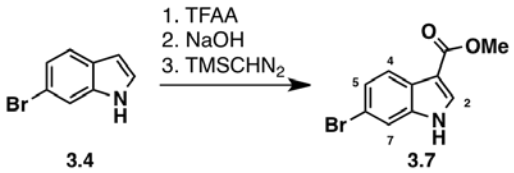

3.4 3.7

*Preparation of methyl ester **3.7**:* Indole **3.4** (400 mg, 2.00 mmol) was dissolved in DMF (6 mL) in a 50-mL round-bottomed flask. The mixture was cooled in an ice-water bath (0 °C), then TFAA (882 mg, 4.20 mmol) was added at the same temperature under an open atmosphere. The reaction mixture was stirred, while warming the cooling bath slowly to 23 °C, for 1 h. The reaction mixture was then poured into a separatory funnel containing H_2O (100 mL) and extracted with Et_2O (2 × 20 mL). The combined organic layers were concentrated under reduced pressure using a rotary evaporator to yield a pale yellow solid. The crude solid was transferred to a 50-mL round-bottomed flask and aqueous NaOH (4 M, 8 mL) was added. The mixture was stirred in a 100 °C oil bath for 19 h under an open atmosphere. The reaction mixture was then cooled to 23 °C and washed with CH_2Cl_2 (2 × 10 mL). The aqueous layer was acidified with 6 M aqueous HCl, and the resulting precipitate was isolated by vacuum filtration. The resulting solid was added to MeOH (4 mL) in a 50-mL oven-dried round-bottomed flask equipped with a Teflon-coated magnetic stir bar. $TMSCHN_2$ (2 M in Et_2O, 4.1 mL, 8.2 mmol) was added slowly over 7 min to the flask containing the mixture, using a syringe, at 23 °C under an open atmosphere. The reaction mixture was stirred for 23 min at the same temperature, after which it was concentrated under reduced pressure using a rotary evaporator, to afford methyl ester **3.7** as a pale yellow solid (330 mg, 65% yield over 3 steps) with >95% purity.

*Data for methyl ester **3.7**:* R_f = 0.34 (40% EtOAc in hexanes); ^{1}H NMR (300 MHz, 293K, CD_3OD): δ = 7.96 (d, J = 8.7 Hz, 1H, 4-H), 7.95 (s, 1H, 2-H), 7.61 (d, J = 1.8 Hz, 1H, 7-H), 7.29 (dd, J = 8.7, 1.8 Hz, 1H, 5-H), 3.87 (s, 3H, OMe); HRMS (EI+) calcd for $C_{10}H_8NO_2Br$ $[M]^+$

252.9738, found 252.9740. These spectroscopic data for methyl ester **3.7** were consistent with the literature: *J. Nat. Prod.* **2005**, *68*, 1484.

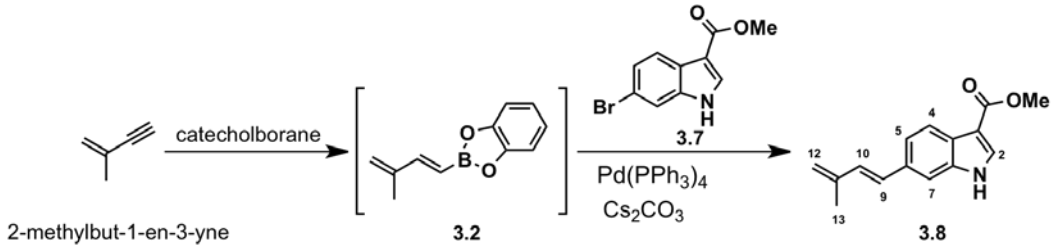

*Preparation of methyl ester **3.8**:* A 10-mL sealed tube equipped with a Teflon-coated magnetic stir bar was evacuated and backfilled with nitrogen. To the sealed tube was added catecholborane (1.05 g, 8.80 mmol) and then 2-methylbut-1-en-3-yene (1.50 g, 22.0 mmol) via a syringe at 23 °C. The resulting mixture was stirred for 2 h in an 80 °C oil bath. The mixture was then cooled to 23 °C and an aliquot (1 drop) of the mixture was analyzed by ^{1}H NMR to confirm the formation of **3.2**. The mixture was then transferred, via a syringe, to a 250-mL round-bottomed flask equipped with a Teflon-coated magnetic stir bar that had been purged with nitrogen before. THF (60 mL), MeOH (15 mL), $Pd(PPh_3)_4$ (173 mg, 0.0150 mmol), **3.7** (760 mg, 3.00 mmol), and Cs_2CO_3 (3.0 g, 9.0 mmol) were added to the flask by opening and closing the round-bottomed flask's septa at 23 °C. The resulting mixture was refluxed for 21 h under a nitrogen atmosphere. The reaction mixture was then cooled to 23 °C, filtered through a silica plug, and the filter cake was rinsed with EtOAc (200 mL). The resulting filtrate was concentrated under reduced pressure using a rotary evaporator. The crude residue was purified by flash chromatography (10→40% EtOAc in hexanes) on silica gel (100 mL) to afford methyl ester **3.8** as a pale yellow solid (670 mg, 93% yield).

*Data for methyl ester **3.8**:* m.p. = 89–90 °C; R_f = 0.37 (40% EtOAc in hexanes); IR (film): ν_{max} = 3274 (N-H), 2947, 1678 (C=O), 1531, 1444, 1417, 1198, 1136, 1051 cm^{-1}; ^1H NMR (300 MHz, 293K, CD_3OD): δ = 7.97 (d, *J* = 8.0 Hz, 1H, 4-H), 7.93 (s, 1H, 2-H), 7.47 (br s, 1H, 7-H), 7.35 (dd, *J* = 8.0, 1.2 Hz, 1H, 5-H), 6.93 (d, *J* = 16.0 Hz, 1H, 10-H), 6.65 (d, *J* = 16.0 Hz, 1H, 9-H), 5.10 (br s, 1H, 12-H), 5.03 (br s, 1H, 12-H), 3.87 (s, 3H, O*Me*), 1.98 (s, 3H, 13-H); ^{13}C NMR (75 MHz, 293 K, CD_3OD): δ = 167.8, 143.8, 134.0, 133.9, 133.3, 132.3, 131.5, 127.1, 122.1, 121.5, 117.0, 111.3, 108.7, 51.6, 19.0; HRMS (EI+) calcd for $C_{15}H_{15}NO_2$ $[M]^+$ 241.1103, found 241.1107.

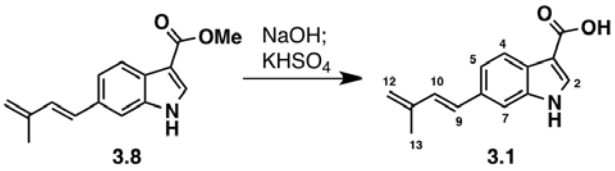

*Preparation of TMC-205 (**3.1**):* MeOH (1.5 mL) and aqueous NaOH (4 M, 2.5 mL) were added to a 25-mL oven-dried round-bottomed flask containing **3.8** (20 mg, 0.080 mmol) under an open atmosphere at 23 °C. The resulting solution was covered from light and stirred in an 80 °C oil bath for 2.25 h. The solution was then cooled to 23 °C and steps subsequent to cooling were performed in a dark environment. The solution was washed with CH_2Cl_2 (1 mL) and then the aqueous layer was acidified with aqueous 3 M $KHSO_4$ (10 mL). The aqueous layer was extracted with EtOAc (3 × 10 mL). The combined organic layers were dried over Na_2SO_4, filtered, and concentrated under reduced pressure using a rotary evaporator ($T_{water\ bath}$ = 30 °C) to afford 16 mg of TMC-205 (**3.1**) as a pale yellow solid (88% yield, >95% purity).

*Data for TMC-205 (**3.1**):* R_f = 0.24 (40% EtOAc in hexanes); IR (film): ν_{max} = 3432 (broad, O-H), 2920, 2851,1644 (C=O), 1528, 1451, 1349 cm^{-1}; ^1H NMR (500 MHz, 293K, CD_3OD): δ =

7.99 (d, J = 8.3 Hz, 1H, 4-H), 7.92 (s, 1H, 2-H), 7.48 (br s, 1H, 7-H), 7.35 (dd, J = 8.3, 1.5 Hz, 1H, 5-H), 6.94 (d, J = 16 Hz, 1H, 10-H), 6.67 (d, J = 16 Hz, 1H, 9-H), 5.10 (br s, 1H, 12-H), 5.03 (br s, 1H, 12-H), 1.98 (s, 3H, 13-H); ^{13}C NMR (75 MHz, 293 K, CD_3OD): δ = 169.0, 143.7, 139.0, 134.0, 133.8, 131.3, 130.7, 127.3, 122.1, 121.3, 116.7, 111.1, 109.9, 18.8; HRMS (EI+) calcd for $C_{14}H_{13}NO_2$ [M^+] 227.0946, found 227.0936.

Table A1. Comparison of the spectral data of natural and synthetic TMC-205. δC and δH (the number of protons, multiplicity, J in Hz).

Position	TMC-205 $^{13}C^{a}$	TMC-205 $^{1}H^{a}$	TMC-205 (synthetic) $^{13}C^{b}$	TMC-205 (synthetic) $^{1}H^{b}$
2	132.8 (d)	7.98 (1H, d, 2.7)	132.7	7.98 (1H, br s)
3	107.6		107.5	
3a	125.8		125.5	
4	120.6	7.94 (1H, d, 8.5)	120.4	7.94 (1H, d, 8.4)
5	119.5	7.39 (1H, dd, 8.5, 1.2)	119.3	7.39 (1H, d, 8.4)
6	131.2		131.1	
7	110.5	7.52 (1H, br s)	110.4	7.52 (1H, br s)
7a	136.8		136.6	
8	165.6		165.6	
9	129.6	6.69 (1H, d, 16.1)	129.4	6.69 (1H, 16.1)
10	129.7	6.96 (1H, d, 16.1)	129.5	6.97 (1H, 16.1)
11	141.7		141.6	
12_{cis}	116.6	5.16 (1H, br s)	116.4	5.16 (1H, br s)
12_{trans}		5.05 (1H, br s)		5.05 (1H, br s)
13	18.4	1.95 (3H, s)	18.3	1.93 (3H, s)
1-NH		11.82 (1H, br s)		11.85 (1H, br s)
COOH		11.88 (1H, br s)		11.96 (1H, br s)

[a] M. Sakurai, J. Kohno, M. Nishio, K. Yamamoto, T. Okuda, K. Kawano, N. Nakanishi, *J. Antibiot.* **2001**, *54*, 628–634.

[b] Deuterated solvent used is DMSO-d_6, ^{1}H NMR in 700 MHz, ^{13}C NMR in 175 MHz.

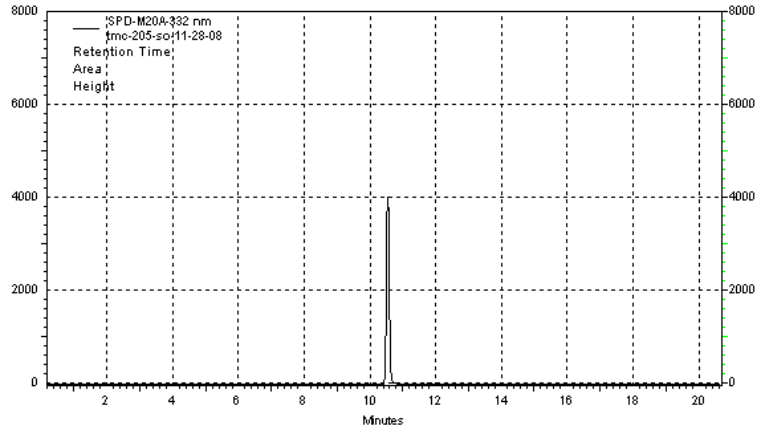

Figure A2. HPLC chromatogram of synthetic TMC-205.

y-axis: Absorption at 276 nm. Elution conditions: flow rate = 1.0 mL/min, gradient: 10→95% MeCN in water (containing 0.1% HCOOH) over 20 min. Column: C18 XDB 4.6 mm × 7.5 cm. *T* = 24 °C.

TMC-205 and Reactive Oxygen Species[c]

Solution **A**: [TMC-205 (**3.1**)] = 1 mM in MeOH; solution **B**: [NaN_3] = 20 mM in pH 10 buffer; solution **C**: [*N*, *N*-dimethyl nitrosoaniline[d]] = 50 mM in DMSO; solution **D**: [**13**] =1 mM in MeOH; solution **E**: [$NaMoO_4$•$2H_2O$] = 100 mM in pH 10 buffer; solution **F**: [KO_2] = 100 mM in DMSO; solution **G**: [$FeSO_4$•$7H_2O$] = 100 mM in pH 7 buffer. These solutions were used immediately after preparation.

Singlet oxygen: Solution of **A** or **C** or **D** ([reagent]$_{final}$ = 15.0 μM) with or without solution **B** [NaN_3]$_{final}$ = 15 μM or 1 mM), solution **E** (40.0 μL, [$NaMoO_4$•$2H_2O$]$_{final}$ = 1.0 mM) and 30% H_2O_2 (10.0 μL, [H_2O_2]$_{final}$ = 25.0 mM) were added to a mixture of MeOH/pH 10 buffer (5:95) (4.0 mL), and the samples were incubated for 60 min at 37 °C.

Superoxide: Solution of **A** or **D** ([reagent]$_{final}$ = 15.0 μM) with solution **F** (10.0 μL, [KO_2]$_{final}$ = 250 μM) were added to a mixture of MeOH/pH 7 buffer solution (5:95) (4.0 mL), and the samples were incubated for 60 min at 37 °C.

Hydrogen peroxide: Solution of **A** or **D** ([reagent]$_{final}$ = 15.0 μM) and 30% H_2O_2 (10 μL, [H_2O_2]$_{final}$ = 25.0 mM) were added to a mixture of MeOH/pH 7 buffer solution (5:95) (4.0 mL), and the samples were incubated for 60 min at 37 °C.

Hydroxyl radical: Solution of **A** or **D** ([reagent]$_{final}$ = 15.0 μM), solution **G** (10.0 μL, [$FeSO_4$•$7H_2O$]$_{final}$ = 250 μM) and 30% H_2O_2 ([H_2O_2]$_{final}$ = 250 μM) were added to a mixture of MeOH/pH 7 buffer solution (5:95) (4.0 mL), and the samples were incubated for 60 min at 37 °C.

After incubations, samples were analyzed by HPLC and low-resolution mass spectra [LC-MS (APCI)]. HPLC monitoring was performed on a Zorbax XDB-C_{18} column, 4.6 min × 7.5 cm, 1.0 mL/min, 20% MeCN in H_2O (containing 0.1% HCOOH) to 100% MeCN linear gradient elution from 0.5 to 20 min, followed by 100% MeCN from 20 to 25 min, followed by 100% MeCN to 20% MeCN in H_2O (containing 0.1% HCOOH) linear gradient from 25 to 30 min.

[c]A. L. Garner, C. M. St. Croix, B. R. Pitt, G. D. Leikauf, S. Ando, K. Koide, *Nat. Chem.* **2009**, *1*, 316.

[d]*N*, *N*-Dimethyl nitrosoaniline was used to ensure singlet oxygen was efficiently generated: Shio Y. Wang, H. Jiao, *J. Agric. Food Chem.* **2000**, *48*, 5677.

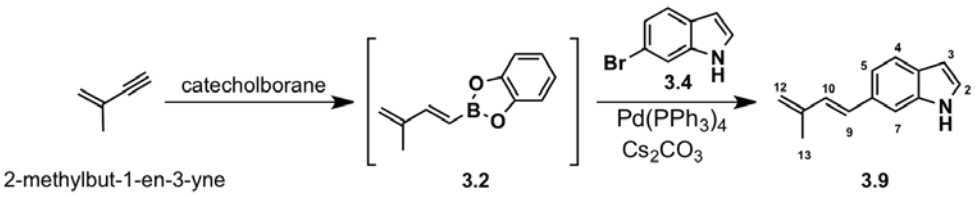

*Preparation of decarboxylated analogue **3.9**:* A 10-mL sealed tube equipped with a Teflon-coated magnetic stir bar was evacuated and backfilled with nitrogen. To the sealed tube was added catecholborane (363 mg, 3.00 mmol) then 2-methylbut-1-en-3-yene (485 mg, 7.40 mmol) via a syringe at 23 °C. The resulting solution was stirred for 4.75 h in an 85 °C oil bath. The mixture was then cooled to 23 °C, and an aliquot (1 drop) of the solution was analyzed by ^{1}H NMR spectroscopy to confirm the formation of **3.2**. The mixture was then transferred, via a syringe, to a 50-mL round-bottomed flask equipped with a Teflon-coated magnetic stir bar that had been purged with nitrogen before. THF (4 mL), MeOH (1 mL), $Pd(PPh_3)_4$ (69 mg, 0.060 mmol), **3.4** (118 mg, 0.600 mmol), and Cs_2CO_3 (586 mg, 1.80 mmol) were added to the 50-mL round-bottomed flask at 23 °C by opening and closing the round-bottomed flask's septa. The resulting mixture was stirred in a 70 °C oil bath for 23 h under a nitrogen atmosphere. The reaction mixture was then cooled to 23 °C and filtered through a silica plug. The filter cake was rinsed with EtOAc (200 mL) and Et_2O (200 mL), and the resulting filtrate was concentrated under reduced pressure using a rotary evaporator. The crude residue was purified by flash chromatography (0→20% EtOAc in hexanes) on silica gel (180 mL) to afford the decarboxylated analogue **3.9** as a pale yellow solid (60 mg, 55% yield).

*Data for decarboxylated analogue **3.9**:* m.p. = 104–106 °C; R_f = 0.32 (20% EtOAc in hexanes); IR (film): ν_{max} = 3222 (N-H), 3053, 2930, 1617, 1453, 1335, 1264, 1092 cm^{-1}; ^{1}H NMR (300 MHz, 293K, CD_3OD): δ = 7.49 (br d, *J* = 8.1 Hz, 1H, 4-H), 7.43 (s, 1H, 7-H),

7.23–7.18 (m, 2H, 5-H, 2-H), 6.91 (d, *J* = 16.0 Hz, 1H, 10-H), 6.67 (d, *J* = 16.0 Hz, 1H, 9-H), 6.41 (br d, *J* = 2.1 Hz, 1H, 3-H), 5.07 (br s, 1H, 12-H), 5.00 (br s, 1H, 12-H), 1.99 (s, 3H, 13-H); ^{13}C NMR (75 MHz, 293 K, CD_3OD): δ = 144.3, 138.6, 132.7, 132.0, 130.6, 129.9, 126.9, 121.7, 119.4, 116.5, 111.1, 103.0, 19.4; ESI-MS calcd for $C_{14}H_{17}NO$ $[M + MeOH]^+$ 215.13, found 215.10. These spectroscopic data for decarboxylated analogue **3.9** were consistent with literature: H. Ishii, Y. Murakami, T. Furuse, H. Takeda, N. Ikeda, *Tetrahedron Lett*. **1973**, *14*, 355.

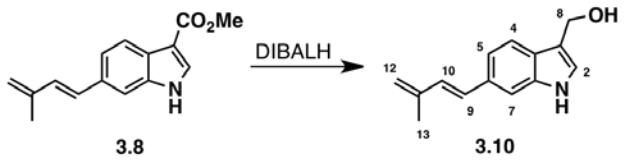

*Preparation of alcohol **3.10**:* A 10-mL round-bottomed flask was charged with **3.8** (20 mg, 0.080 mmol) at 23 °C under an open atmosphere. The flask was evacuated and backfilled with nitrogen. THF (1.3 mL) was added to the flask via a syringe, and the flask was cooled to -78 °C (external temperature). DIBALH (1 M in hexanes, 0.48 mL, 0.48 mmol) was added at -78 °C, by a syringe and then the mixture was stirred for 30 min at the same temperature. H_2O (0.9 mL) was added to the reaction mixture at -78 °C, then warmed to 23 °C, filtered through Celite®, and the filtrate was concentrated under reduced pressure using a rotary evaporator. The crude residue was purified by flash chromatography (10→60% EtOAc in hexanes) on silica gel (25 mL) to afford alcohol **3.10** as a pale yellow solid (13 mg, 76% yield).

*Data for alcohol **3.10**:* m.p. = 91–92 °C; R_f = 0.36 (50% EtOAc in hexanes); IR (film): ν_{max} = 3370 (broad, O-H), 2923, 2854, 1724, 1457, 1377, 1073 cm^{-1}; ^{1}H NMR (300 MHz, 293K, CD_3OD): δ = 7.59 (d, *J* = 8.0 Hz, 1H, 4-H), 7.40 (br s, 1H, 2-H), 7.22 (d, *J* = 8.0 Hz, 1H, 5-H), 7.21 (s, 1H, 7-H), 6.90 (d, *J* = 15.9 Hz, 1H, 10-H), 6.65 (d, *J* = 15.9 Hz, 1H, 9-H), 5.06 (br s, 1H,

12-H), 4.99 (br s, 1H, 12-H), 4.82 (s, 2H, 8-H), 1.98 (s, 3H, 13-H); ^{13}C NMR (75 MHz, 293 K, CD_3OD): δ = 143.8, 138.7, 132.6, 131.3, 130.3, 125.5, 119.8, 119.1, 118.9, 116.7, 116.1, 110.7, 57.2, 18.9; HRMS (EI+) calcd for $C_{14}H_{15}NO$ $[M]^+$ 213.1154, found 213.1155.

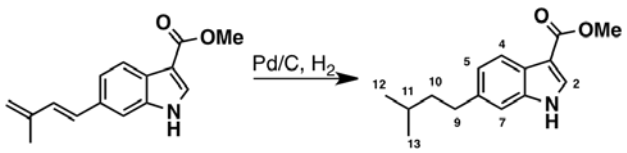

3.8 **3.11**

*Preparation of **3.11**:* MeOH (5 mL) and Pd/C (10% wt., 17 mg, 0.015 mmol) were added to a 25 mL oven-dried round-bottomed flask containing **3.8** (73 mg, 0.30 mmol) at 23 °C under an open atmosphere. The flask was evacuated and backfilled with a hydrogen atmosphere using a balloon filled with hydrogen gas. The mixture was stirred under the hydrogen atmosphere for 12.5 h at 23 °C, and then filtered through a plug of Celite, followed by solvent removal under reduced pressure using a rotary evaporator. The resulting crude residue was purified by flash chromatography (5→30% EtOAc in hexanes) on silica gel (40 mL) to afford **3.11** as a pale yellow solid (70 mg, 95% yield).

*Data for **3.11**:* m.p. = 97–98 °C; R_f = 0.23 (20% EtOAc in hexanes); IR (film): ν_{max} = 3266 (N-H), 2953, 2869, 1627 (C=O), 1534, 1446, 1369, 1200, 1149, 1051 cm^{-1}; ^{1}H NMR (300 MHz, 293K, CD_3OD): δ = 7.92 (d, *J* = 8.4 Hz, 1H, 4-H), 7.87 (d, *J* = 3.0 Hz, 1H, 2-H), 7.22 (d, *J* = 1.2 Hz, 1H, 7-H), 7.01 (dd, *J* = 8.4, 1.2 Hz, 1H, 5-H), 3.85 (s, 3H, O*Me*), 2.68 (t, *J* = 7.8 Hz, 2H, 9-H), 1.62–1.48 (m, 3H, 10-H, 11-H), 0.93 (d, *J* = 6.3 Hz, 6H, 12-H, 13-H); ^{13}C NMR (75 MHz, 293 K, CD_3OD): δ = 168.1, 139.2, 138.6, 132.9, 125.4, 123.8, 121.8, 112.3, 108.3, 51.5, 42.8, 35.1, 28.9, 23.1; HRMS (EI+) calcd for $C_{15}H_{19}NO_2$ $[M]^+$ 245.1416, found 245.1406.

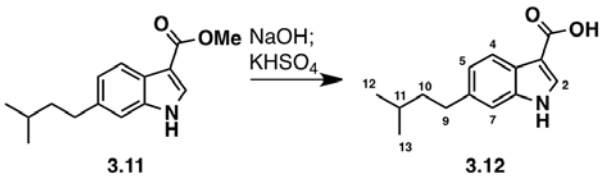

*Preparation of alkane analogue **3.12**:* MeOH (1.5 mL) and aqueous NaOH (6 M, 2.5 mL) were added to a 10-mL round-bottomed flask containing **3.11** (23 mg, 0.090 mmol) at 23 °C under an open atmosphere. The mixture was stirred in a 50 °C oil bath for 3.5 h and then cooled to 23 °C. The reaction mixture was washed with CH_2Cl_2 (10 mL). The aqueous layer was acidified with $KHSO_4$ (3 M, 10 mL) and extracted with EtOAc (2 × 20 mL). The combined organic extracts were dried over Na_2SO_4, filtered, and concentrated under reduced pressure using a rotary evaporator. The resulting residue was purified by flash chromatography (20→50% EtOAc in hexanes with 1% acetic acid) on silica gel (5 mL) to afford the alkane analogue **3.12** as a pale yellow solid (18 mg, 87% yield).

*Data for alkane analogue **3.12**:* m.p. = 127–129 °C; R_f = 0.33 (50% EtOAc in hexanes); IR (film): ν_{max} = 3431 (broad, O-H), 3138, 2954, 2927, 1682 (C=O), 1535, 1453, 1358, 1195, 1141 cm^{-1}; ^1H NMR (300 MHz, 293K, CD_3OD): δ = 7.94 (d, *J* = 8.1 Hz, 1H, 4-H), 7.87 (s, 1H, 2-H), 7.22 (br s, 1H, 7-H), 7.01 (dd, *J* = 8.1, 1.2 Hz, 1H, 5-H), 2.69 (t, *J* = 7.7 Hz, 2H, 9-H), 1.63–1.49 (m, 3H, 10-H, 11-H), 0.93 (d, *J* = 6.3 Hz, 6H, 12-H, 13-H); ^{13}C NMR (75 MHz, 293 K, CD_3OD): δ = 169.5, 139.0, 138.7, 133.1, 125.8, 123.7, 121.9, 112.2, 108.8, 42.8, 35.2, 28.9, 23.1; HRMS (EI+) calcd for $C_{14}H_{17}NO_2$ $[M]^+$ 231.1259, found 231.1257.

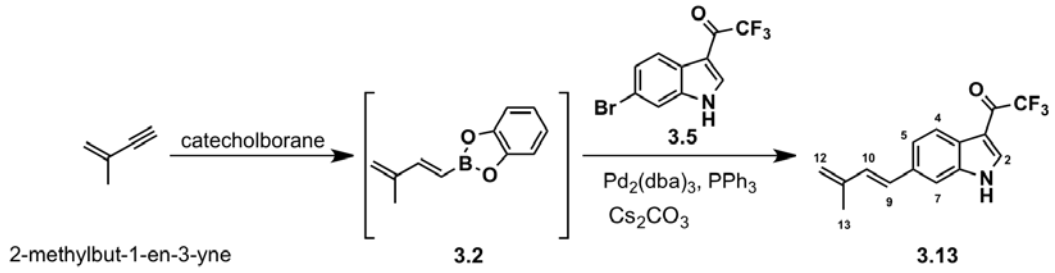

*Preparation of ketone **3.13**:* An oven-dried 10-mL sealed tube equipped with a Teflon-coated magnetic stir bar was evacuated and backfilled with nitrogen. To the sealed tube was added catecholborane (1.05 g, 8.80 mmol) and then 2-methylbut-1-en-3-yne (1.50 g, 22.0 mmol) via a syringe at 23 °C. The resulting solution was stirred for 2 h in an 80 °C oil bath. The mixture was then cooled to 23 °C and an aliquot (1 drop) of the mixture was analyzed by ^{1}H NMR spectroscopy to confirm the formation of **3.2**. The mixture was then transferred, by a syringe, to a 100-mL round-bottomed flask equipped with a Teflon-coated magnetic stir bar that had been previously purged with nitrogen. Toluene (5 mL), EtOH (5 mL), $Pd_2(dba)_3$ (192 mg, 0.21 mmol), PPh_3 (110 mg, 0.42 mmol), **3.5** (500 mg, 1.7 mmol), and Cs_2CO_3 (2.0 g, 6.3 mmol) were added in this order to the flask by opening and closing the round-bottomed flask's septa at 23 °C. The resulting mixture was stirred in a 90 °C oil bath for 9 h under a nitrogen atmosphere. The reaction mixture was then cooled to 23 °C, filtered through a silica plug, and the filter cake was rinsed with EtOAc. The resulting filtrate was concentrated under reduced pressure using a rotary evaporator. The crude residue was purified by flash chromatography (2.5→20% EtOAc in hexanes) on silica gel (40 mL) to afford ketone **3.13** as a pale yellow solid (413 mg, 87% yield).

*Data for ketone **3.13**:* m.p. = 76–77 °C; R_f = 0.18 (30 % EtOAc in hexanes); IR (film): ν_{max} = 3217 (N-H), 3094, 1635 (C=O), 1525, 1497, 1426, 1393, 1241, 1184, 1136 cm^{-1}; ^{1}H NMR (300 MHz, 293K, CD_3OD): δ = 8.22 (d, *J* = 1.8 Hz, 1H, 2-H), 8.19 (d, *J* = 8.4 Hz, 1H, 4-H), 7.57 (br s, 1H, 7-H), 7.48 (dd, *J* = 8.4, 0.9 Hz, 1H, 5-H), 6.99 (d, *J* = 16.1 Hz, 1H, 10-H), 6.68 (d, *J* =

16.1 Hz, 1H, 9-H), 5.14 (br s, 1H, 12-H), 5.07 (br s, 1H, 12-H), 1.99 (s, 3H, 13-H); ^{13}C NMR (175 MHz, 293 K, CD_3OD): δ = 174.7, 142.1, 137.7, 136.8, 134.3, 131.0, 128.7, 126.2, 125.0, 122.7, 121.3, 117.3, 115.1, 109.7, 17.4; HRMS (EI+) calcd for $C_{15}H_{12}NOF_3$ $[M]^+$ 279. 0871, found 279.0880.

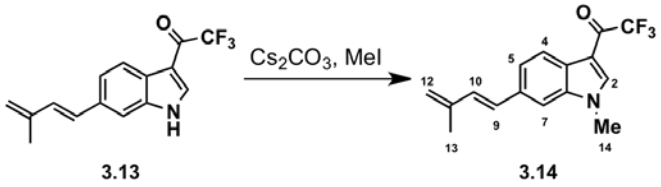

3.13 3.14

*Preparation of N-methylated analogue **3.14**:* To a 25-mL round-bottomed flask equipped with a Teflon-coated magnetic stir bar was added **3.13** (90 mg, 0.32 mmol), MeI (227 mg, 1.60 mmol), DMF (1.5 mL) and Cs_2CO_3 (208 mg, 0.64 mmol). The mixture was stirred at 23 °C for 1.5 h, then diluted with H_2O (30 mL) and extracted with Et_2O (2 × 10 mL). The combined organic extracts were dried over Na_2SO_4, filtered, and concentrated under reduced pressure using a rotary evaporator. The crude residue was purified by flash chromatography (2.5→20% EtOAc in hexanes) on silica gel (40 mL) to afford *N*-methylated analogue **3.14** as a pale yellow oil (86 mg, 92% yield).

*Data for N-methylated analogue **3.14**:* R_f = 0.29 (30 % EtOAc in hexanes); IR (film): ν_{max} = 3030, 2922, 2853, 1663 (C=O), 1530, 1466, 1376, 1289, 1177, 1135 cm^{-1}; ^{1}H NMR (300 MHz, 293K, CD_3OD): δ = 8.22 (d, *J* = 1.8 Hz, 1H, 2-H), 8.19 (d, *J* = 8.1 Hz, 1H, 4-H), 7.62 (br s, 1H, 7-H), 7.51 (dd, *J* = 8.4, 1.2 Hz, 1H, 5-H), 7.04 (d, *J* = 15.9 Hz, 1H, 10-H), 6.73 (d, *J* = 15.9 Hz, 1H, 9-H), 5.15 (br s, 1H, 12-H), 5.08 (br s, 1H, 12-H), 3.95 (s, 3H, 14-H), 2.00 (s, 3H, 13-H); ^{13}C NMR (150 MHz, 293 K, CD_3OD): δ = 174.3, 142.1, 140.1, 138.3, 134.5, 131.2, 128.6, 126.1,

122.2, 121.6, 118.1, 116.3, 108.8, 108.4, 32.7, 17.4; HRMS (EI+) calcd for $C_{16}H_{14}NOF_3$ $[M]^+$ 293.1027, found 293.1015.

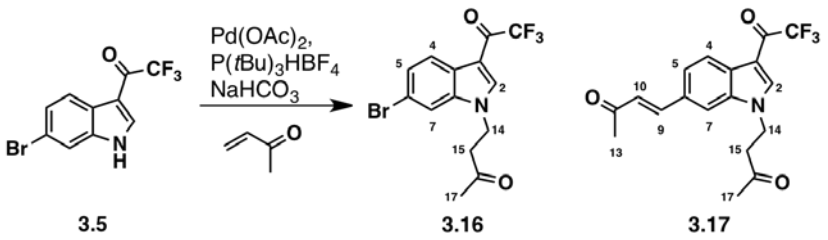

*Preparation of **3.16** and **3.17**:* An oven-dried 10-mL sealed tube purged with nitrogen was charged with DMF (1 mL), $Pd(OAc)_2$ (2.000 mg, 0.007 mmol), $P(tBu)_3HBF_4$ (4.000 mg, 0.014 mmol). The mixture was stirred in a 100 °C oil bath for 25 min, then cooled to 23 °C. To the mixture was added **3.5** (20 mg, 0.07 mmol), $NaHCO_3$ (11 mg, 0.13 mmol) and methylvinyl ketone (49 mg, 0.70 mmol) then stirred in a 100 °C oil for an additional 25 h. The mixture was filtered through a pad of silica, rinsed with EtOAc, and the filtrate was concentrated under reduced pressure using a rotary evaporator. The crude residue was purified by flash chromatography (10→70% EtOAc in hexanes) on silica gel (10 mL) to afford **3.16** as a pale yellow viscous oil (4 mg, 15% yield) and **3.17** as a pale yellow paste (17 mg, 69% yield).

*Data for **3.16**:* R_f = 0.23 (20 % EtOAc in hexanes); IR (film): ν_{max} = 3124, 2924, 1718 (C=O), 1668 (C=O), 1527, 1394, 1288, 1183, 1144, 882 cm^{-1}; ^1H NMR (300 MHz, 293K, CD_3OD): δ = 8.30 (d, *J* = 1.8 Hz, 1H, 2-H), 8.16 (d, *J* = 8.7 Hz, 1H, 4-H), 7.87 (d, *J* = 1.8 Hz, 1H, 7-H), 7.46 (dd, *J* = 8.7, 1.8 Hz, 1H, 5-H), 4.52 (t, *J* = 6.6 Hz, 2H, 14-H), 3.11 (t, *J* = 6.6 Hz, 2H, 15-H), 2.13 (s, 3H, 17-H); ^{13}C NMR (175 MHz, 293 K, CD_3OD): δ = 206.6, 174.3, 140.0, 137.6, 126.6, 125.6, 123.0, 117.6, 116.1, 113.9, 108.8, 41.8, 41.5, 28.5; HRMS (EI+) calcd for $C_{14}H_{11}NO_2F_3Br[M]^+$ 360.9925, found 360.9919.

*Data for **3.17**:* R_f = 0.30 (50 % EtOAc in hexanes); IR (film): ν_{max} = 3121, 2925, 2851, 1714 (C=O), 1668 (C=O), 1604, 1527, 1371, 1289, 1256, 1182, 1142, 1156, 1045 cm^{-1}; ^1H NMR (700 MHz, 293K, CD_3OD): δ = 8.39 (d, *J* = 2.1 Hz, 1H, 2-H), 8.29 (d, *J* = 8.4 Hz, 1H, 4-H), 7.95 (br s, 1H, 7-H), 7.81 (d, *J* = 16.1 Hz, 1H, 9-H), 7.67 (dd, *J* = 8.4, 1.4 Hz, 1H, 5-H), 6.93 (d, *J* = 16.1 Hz, 1H, 10-H), 4.60 (t, *J* = 6.3 Hz, 2H, 14-H), 3.15 (t, *J* = 6.3 Hz, 2H, 15-H), 2.41 (s, 3H, 13-H), 2.14 (s, 3H, 17-H); ^{13}C NMR (175 MHz, 293 K, CD_3OD): δ = 206.4, 199.8, 174.2, 144.7, 137.0, 131.2, 128.7, 126.2, 123.7, 123.3, 122.1, 117.8, 116.2 111.6, 41.9, 41.5, 28.5, 26.0; HRMS (EI+) calcd for $C_{18}H_{16}NO_3F_3$ $[M]^+$ 351.1082, found 351.1078.

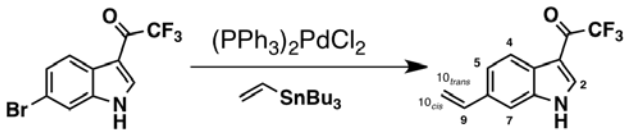

*Preparation of alkene **3.19**:* A 25-mL round-bottomed flask purged with argon was charged with **3.5** (406 mg, 1.40 mmol), DMF (7 mL), $(PPh_3)_2PdCl_2$ (29.3 mg, 42.0 μmol), and vinylstannane (666 mg, 2.10 mmol) at 23 °C. The mixture was stirred in a 50 °C oil bath for 17.5 h, then filtered through a pad of silica and rinsed with a solution of 70% EtOAc in hexanes. The filtrate was diluted with H_2O (100 mL) and the organic layer was separated. The aqueous layer was extracted with a solution of 70% EtOAc in hexanes (2 ×10 mL), then the combined organic layers were dried over Na_2SO_4, filtered, and concentrated under reduced pressure using a rotary evaporator. The crude residue was purified by flash chromatography (10→50% EtOAc in hexanes) on silica gel (15 mL) to afford **3.19** as a pale yellow solid (242 mg, 72% yield).

*Data for alkene **3.19**:* m.p. = 153–154 °C; R_f = 0.20 (30 % EtOAc in hexanes); IR (film): ν_{max} = 3221 (N-H), 2927, 1636 (C=O), 1498, 1430, 1270, 1185, 1135 cm^{-1}; ^1H NMR (400 MHz,

293K, 1% CD_3OD in acetone-d_6): δ = 8.41 (d, *J* = 2.0 Hz, 1H, 7-H), 8.25 (d, *J* = 8.0 Hz, 1H, 4-H), 7.67 (br s, 1H, 2-H), 7.54 (dd, *J* = 8.0, 1.2 Hz, 1H, 5-H), 6.88 (dd, *J* = 18.0, 11.0 Hz, 1H, 9-H), 5.86 (d, *J* = 18.0 Hz, 1H, 10-H_{trans}), 5.26 (d, *J* = 11.0 Hz, 1H, 10-H_{cis}); ^{13}C NMR (100 MHz, 293 K, acetone-d_6): δ = 174.3, 137.2, 137.0, 134.5, 125.9, 121.7, 121.6, 118.6, 115.8, 112.9, 110.6, 110.0; ESI-MS calcd for $C_{14}H_{12}F_3N_2O$ $[M + CH_3CN]^+$ 281.09, found 281.05. ESI-MS calcd for $C_{12}H_9F_3NO$ $[M + H]^+$ 240.06, found 240.05.

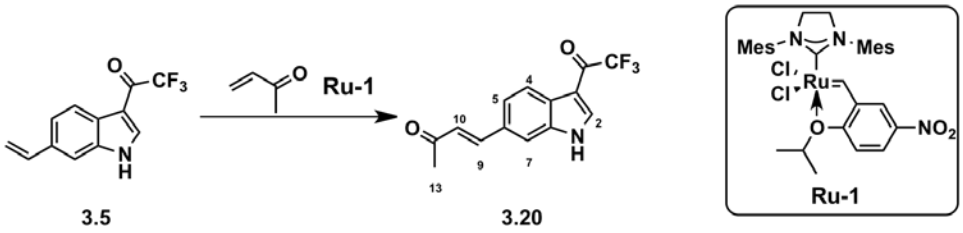

*Preparation of enone **3.20**:* A 25-mL round-bottomed flask was charged with **3.5** (150 mg, 0.63 mmol), PhH (2 mL), **Ru-1** (21.5 mg, 0.0320 mmol), and methylvinyl ketone (218 mg, 3.12 mmol) at 23 °C. The mixture was stirred at 23 °C for 26 h then concentrated under reduced pressure using a rotary evaporator. The crude residue was purified by flash chromatography (10→80% EtOAc in hexanes) on silica gel (30 mL) to afford enone **3.20** as a white solid (53.3 mg, 30% yield).

*Data for enone **3.20**:* m.p. = >200 °C; R_f = 0.28 (50 % EtOAc in hexanes); IR (film): ν_{max} = 3212 (N-H), 2922, 1662 (C=O), 1635 (C=O), 1499, 1429, 1265, 1185, 1136 cm^{-1}; ^1H NMR (300 MHz, 293K, CD_3OD): δ = 8.33 (d, *J* = 1.8 Hz, 1H, 2-H), 8.30 (d, *J* = 8.4 Hz, 1H, 4-H), 7.82 (br s, 1H, 7-H), 7.79 (d, *J* = 16.5 Hz, 1H, 9-H), 7.65 (dd, *J* = 8.4, 0.9 Hz, 1H, 5-H), 6.86 (d, *J* = 16.5 Hz, 1H, 10-H), 2.40 (s, 3H, 13-H); ^{13}C NMR (175 MHz, 293 K, CD_3OD): δ = 199.9, 174.7, 144.8, 137.8, 137.1, 131.0, 128.1, 125.9, 123.0, 121.8, 117.9, 116.2, 109.9, 26.0; HRMS (EI+) calcd for $C_{14}H_{10}NO_2F_3$ $[M]^+$ 281.0664, found 281.0662.

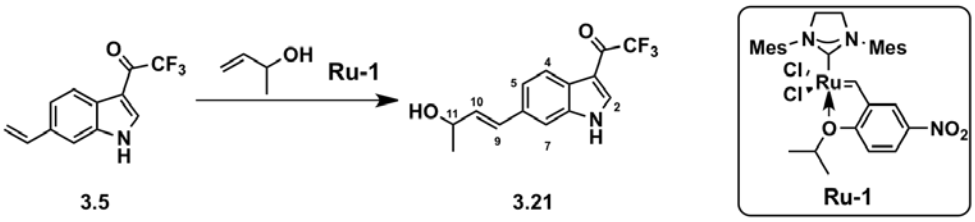

3.5 3.21 Ru-1

*Preparation of allylic alcohol **3.21**:* A 25-mL pear-shaped flask was charged with **3.5** (82 mg, 0.34 mmol), DCE (0.4 mL), 3-buten-2-ol (123 mg, 1.70 mmol), and **Ru-1** (18 mg, 0.027 mmol) at 23 °C. The mixture was stirred in a 50 °C oil bath for 22 h, then concentrated under reduced pressure using a rotary evaporator. The crude residue was purified by flash chromatography (10→60% EtOAc in hexanes) on silica gel (30 mL) to afford allylic alcohol **3.21** as a pale yellow oil (38 mg, 39% yield).

*Data for allylic alcohol **3.21**:* R_f = 0.25 (60 % EtOAc in hexanes); IR (film): ν_{max} = 3218 (broad, O-H), 2970, 2927, 1633 (C=O), 1498, 1443, 1265, 1185, 1134, 1091 cm^{-1}; ^1H NMR (300 MHz, 293K, CD_3OD): δ = 8.21 (d, *J* = 1.5 Hz, 1H, 2-H), 8.18 (d, *J* = 8.4 Hz, 1H, 4-H), 7.52 (br s, 1H, 7-H), 7.43 (dd, *J* = 8.4, 1.5 Hz, 1H, 5-H), 6.68 (d, *J* = 15.9 Hz, 1H, 9-H), 6.33 (dd, *J* = 15.9, 6.3 Hz, 1H, 10-H), 4.44 (qd, *J* = 6.6, 6.3 Hz, 1H, 11-H), 1.34 (d, *J* = 6.6 Hz, 3H, 13-H); ^{13}C NMR (75 MHz, 293 K, CD_3OD): δ = 176.5, 138.8, 138.2, 135.5, 134.7, 130.5, 127.1, 123.3, 122.9, 120.6, 116.8, 111.5, 69.6, 23.9; HRMS (ES+) calcd for $C_{14}H_{12}NO_2F_3Na$ $[M + Na]^+$ 306.0718, found 306.0730.

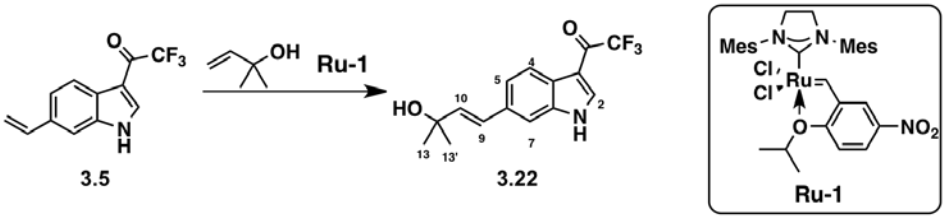

*Preparation of allylic alcohol **3.22**:* A 25-mL round-bottomed flask was charged with **3.5** (75 mg, 0.31 mmol), DCE (0.4 mL), 2-methyl-3-buten-2-ol (135 mg, 1.57 mmol), and **Ru-1** (16 mg, 0.024 mmol) at 23 °C. The mixture was stirred in a 40 °C oil bath for 22 h, then concentrated under reduced pressure using a rotary evaporator. The crude residue was purified by flash chromatography (20→80% EtOAc in hexanes) on silica gel (25 mL) to afford allylic alcohol **3.22** as a pale yellow oil (29 mg, 32% yield).

*Data for allylic alcohol **3.22**:* R_f = 0.21 (50 % EtOAc in hexanes); IR (film): ν_{max} = 3224 (broad, O-H), 2923, 2853, 1633 (C=O), 1461, 1426, 1265, 1184, 1133, 1089 cm^{-1}; ^1H NMR (300 MHz, 293K, 1% CD_3OD in acetone-d_6): δ = 8.37 (br s, 1H, 7-H), 8.21 (d, *J* = 8.1 Hz, 1H, 4-H), 7.61 (d, *J* = 1.2 Hz, 1H, 2-H), 7.48 (dd, *J* = 8.1, 1.2 Hz, 1H, 5-H), 6.73 (d, *J* = 15.9 Hz, 1H, 9-H), 6.49 (d, *J* = 15.9 Hz, 1H, 10-H), 1.38 (s, 6H, 13, 13'-H); ^{13}C NMR (75 MHz, 293 K, acetone-d_6): δ = 175.1, 139.6, 138.4, 137.7, 135.5, 126.6, 126.3, 122.9, 122.5, 120.1, 116.2, 111.4, 110.8, 70.7; HRMS (EI+) calcd for $C_{15}H_{14}NO_2F_3$ $[M]^+$ 297.0977, found 297.0978.

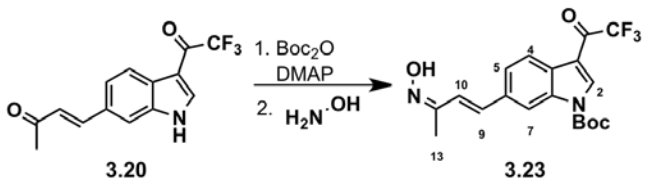

*Preparation of oxime **3.23**:* A 25-mL round-bottomed flask was charged with **3.20** (31 mg, 0.11 mmol), Boc_2O (37 mg, 0.13 mmol), CH_2Cl_2 (0.6 mL), and DMAP (7.5 mg, 0.060 mmol) at 23 °C. The mixture was stirred at 23 °C for 1 h, then concentrated under reduced pressure. The

crude residue was purified by flash chromatography (2.5→30% EtOAc in hexanes) on silica gel (10 mL) to afford Boc-protected **3.20** (40 mg, 95% yield).

To a 25-mL round-bottomed flask containing the Boc-protected **3.20** (40 mg, 0.10 mmol) was added MeOH (0.7 mL), $HONH_2$•HCl (14 mg, 0.20 mmol), and NaOAc (21 mg, 0.25 mmol) at 23 °C. The mixture was stirred in a 50 °C oil bath for 19 h and then diluted with H_2O (15 mL). The mixture was extracted with CH_2Cl_2 (2 × 3 mL), and the combined organic extracts were dried over Na_2SO_4, filtered and concentrated under reduced pressure. The crude residue was purified by flash chromatography (5→30% EtOAc in hexanes) on silica gel (10 mL) to afford oxime **3.23** as a pale yellow viscous oil (27 mg, 66% yield over two steps).

*Data for oxime **3.23**:* R_f = 0.32 (30 % EtOAc in hexanes); IR (film): ν_{max} = 3306 (broad, O-H), 2925, 2854, 1745 (C=O), 1698 (C=O), 1441, 1373, 1319, 1255, 1150, 1103 cm^{-1}; ^1H NMR (300 MHz, 293K, 1% CD_3OD in acetone-d_6): δ = 8.53 (d, *J* = 1.8 Hz, 1H, 7-H), 8.38 (d, *J* = 1.5 Hz, 1H, 2-H), 8.25 (d, *J* = 8.4 Hz, 1H, 4-H), 7.70 (dd, *J* = 8.4, 1.8 Hz, 1H, 5-H), 7.16 (d, *J* = 16.5 Hz, 1H, 9-H), 6.96 (d, *J* = 16.5 Hz, 1H, 10-H), 2.12 (s, 3H, 13-H), 1.76 (s, 9H, Boc); ^{13}C NMR (100 MHz, 293 K, acetone-d_6): δ = 174.1, 156.8, 155.0, 136.6, 135.4, 134.3, 132.1, 127.9, 126.8, 124.5, 121.8, 113.6, 107.4, 98.9, 85.0, 27.3, 13.5; HRMS (EI+) calcd for $C_{19}H_{19}N_2O_4F_3$ $[M]^+$ 396.1297, found 396.1290.

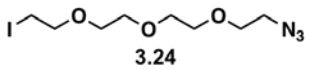

3.24

Synthesis of **3.24**, see: X. Qiu, G. Li, G. Wu, J. Zhu, L. Zhou, P. Chen, A. R. Chamberlin, W. Lee, *J. Med. Chem.* **2009**, *52*, 1757.

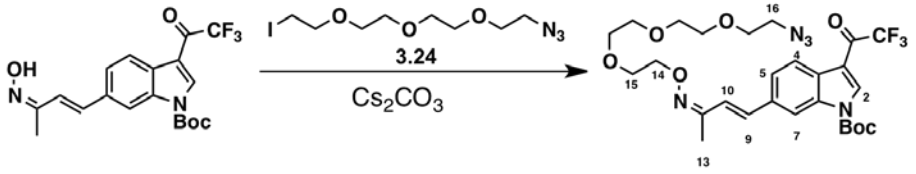

*Preparation of **3.25**:* A 10-mL round-bottomed flask was charged **3.23** (21 mg, 0.050 mmol), DMF (0.6 mL), **3.24** (26 mg, 0.080 mmol), and Cs_2CO_3 (17 mg, 0.050 mmol) at 23 °C. The mixture was stirred for 4 h at 23 °C, then diluted with saturated aqueous NH_4Cl (7 mL) and H_2O (10 mL), and the mixture was extracted with EtOAc (3 × 5 mL). The combined organic extracts were dried over Na_2SO_4, filtered, and concentrated under reduced pressure using a rotary evaporator. The crude residue was purified by flash chromatography (10→70% EtOAc in hexanes) on silica gel (8 mL) to afford **3.25** as a colorless oil (23 mg, 77% yield).

*Data for **3.25**:* R_f = 0.32 (70 % EtOAc in hexanes); IR (film): ν_{max} = 3128, 2926, 2872, 2109 (N_3), 1767 (C=O), 1669 (C=O), 1527, 1453, 1289, 1191, 1152 cm^{-1}; ^1H NMR (300 MHz, 293K, acetone-d_6): δ = 8.44 (d, *J* = 1.8 Hz, 1H, 7-H), 8.30 (d, *J* = 8.1 Hz, 1H, 4-H), 8.11 (br s, 1H, 2-H), 7.64 (dd, *J* = 8.1, 1.8 Hz, 1H, 5-H), 7.43 (d, *J* = 16.5 Hz, 1H, 9-H), 7.04 (d, *J* = 16.5 Hz, 1H, 10-H), 4.69 (t, *J* = 5.1 Hz, 2H, 14-H), 3.98 (t, *J* = 5.1 Hz, 2H, 15-H), 3.63–3.58 (m, 5H, tetraethylene glycol-*H*'s), 3.55–3.48 (m, 5H, tetraethylene glycol-*H*'s), 3.32 (t, *J* = 5.1 Hz, 2H, 16-H), 2.23 (s, 3H, 13-H), 1.54 (s, 9H, Boc); ^{13}C NMR (100 MHz, 293 K, acetone-d_6): δ = 174.6, 162.1, 151.8, 141.5, 138.2, 137.8, 133.1, 128.1, 124.1, 122.4, 119.2, 116.2, 110.4, 109.3, 82.9, 71.0, 70.9, 70.8, 70.7, 70.2, 69.6, 50.9, 47.7, 27.4, 10.9; HRMS (ES+) calcd for $C_{27}H_{34}N_5O_7F_3Na$ $[M + Na]^+$ 620.2308, found 620.2292.

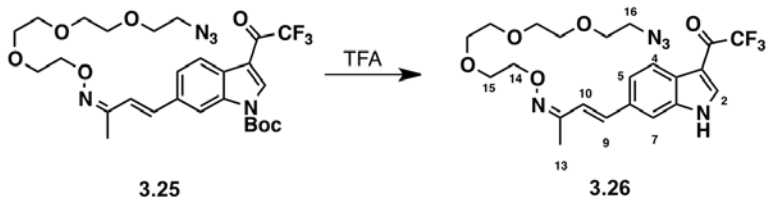

*Preparation of **3.26**:* A 10-mL round-bottomed flask was charged with **3.25** (17 mg, 0.03 mmol) then cooled in an ice-water bath mixture. A solution of 1:9 v/v TFA in CH_2Cl_2 (1 mL) was added to **3.25** at the same temperature, then the resulting solution was stirred at the same temperature for 45 min, then warmed to 23 °C, and stirred for an additional 22.5 h. The mixture was diluted with saturated aqueous $NaHCO_3$ (5 mL) and then the organic layer was separated. The aqueous layer was extracted with CH_2Cl_2 (3 × 5 mL). The combined organic extracts were dried over Na_2SO_4, filtered and concentrated under reduced pressure using a rotary evaporator. The crude residue was purified by flash chromatography (30→80% EtOAc in benzene) on silica gel (5 mL) to afford **3.26** as a pale yellow oil (13 mg, 89% yield).

*Data for **3.26**:* R_f = 0.27 (60 % EtOAc in hexanes); IR (film): ν_{max} = 3396 (N-H), 2922, 2872, 2108 (N_3), 1669 (C=O), 1527, 1444, 1291, 1190, 1142 cm^{-1}; ^1H NMR (300 MHz, 293K, 1% CD_3OD in acetone-d_6): δ = 8.40 (br s, 1H, 7-H), 8.26 (d, *J* = 8.1 Hz, 1H, 4-H), 7.95 (br s, 1H, 2-H), 7.59 (d, *J* = 8.1 Hz, 1H, 5-H), 7.12 (d, *J* = 16.5 Hz, 1H, 9-H), 6.97 (d, *J* = 16.5 Hz, 1H, 10-H), 4.66 (t, *J* = 4.8 Hz, 2H, 14-H), 3.97 (t, *J* = 4.8 Hz, 2H, 15-H), 3.61–3.53 (m, 4H, tetraethylene glycol-*H*'s), 3.55–3.50 (m, 6H, tetraethylene glycol-*H*'s), 3.32 (t, *J* = 4.8 Hz, 2H, 16-H), 2.10 (s, 3H, 13-H); ^{13}C NMR (100 MHz, 293 K, acetone-d_6): δ = 174.2, 155.4, 141.0, 138.2, 134.2, 132.4, 127.1 123.4, 122.3, 119.3, 116.3, 110.1, 109.4, 71.0, 70.9, 70.8, 70.7, 70.2, 69.6, 50.9, 47.7, 9.0; HRSM (ES+) calcd for $C_{22}H_{26}N_5O_5F_3Na$ $[M + Na]^+$ 520.1784, found 520.1768.

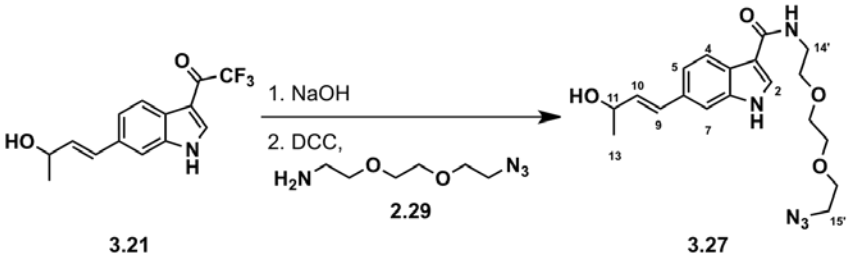

*Preparation of **3.27**:* A 10-mL round-bottomed flask was charged with **3.21** (21 mg, 0.070 mmol), MeOH (0.5 mL) and aqueous NaOH (4 M, 0.2 mL) at 23 °C. The resulting solution was stirred in a 40 °C oil bath for 9 h. After cooling to 24 °C, the solution was concentrated to remove MeOH, then the aqueous mixture was washed with CH_2Cl_2 (3 × 2 mL). The aqueous layer was acidified with aqueous HCl (4 M, 5 mL) and the aqueous layer was extracted with CH_2Cl_2 (2 × 5 mL). The combined organic extracts were dried over Na_2SO_4, filtered, and concentrated to yield the crude carboxylic acid (15.3 mg). A majority of this acid was used without further purification.

A 25-mL round-bottomed flask was charged with the crude carboxylic acid (14.2 mg, 0.06 mmol), amine **2.29** (16.9 mg, 0.090 mmol), CH_2Cl_2 (1 mL) and *N*,*N*'-dicyclohexylcarbodiimide (25 mg, 0.12 mmol) at 23 °C. The mixture was stirred at the same temperature for 4 h, then diluted with H_2O (7 mL). The organic layer was separated and the aqueous layer was extracted with CH_2Cl_2 (5 × 5 mL). The combined organic extracts were dried over Na_2SO_4, filtered, and concentrated under reduced pressure using a rotary evaporator. The crude residue was purified by flash chromatography (40→100% EtOAc in hexanes) on silica gel (10 mL) to afford **3.27** as a pale yellow viscous oil (13 mg, 56% yield over 2 steps).

*Data for **3.27**:* R_f = 0.28 (100 % EtOAc); IR (film): ν_{max} = 3233 (broad, O-H), 2926, 2106 (N_3), 1622 (C=O), 1544, 1452, 1305, 1110 cm^{-1}; ^1H NMR (300 MHz, 293K, 1% CD_3OD in acetone-d_6): δ = 8.18 (d, *J* = 8.4 Hz, 1H, 4-H), 7.96 (d, *J* = 1.2 Hz, 1H, 7-H), 7.50 (br s, 1H, 2-

H), 7.33 (dd, *J* = 8.4, 1.2 Hz, 1H, 5-H), 6.66 (d, *J* = 15.9 Hz, 1H, 9-H), 6.10 (dd, *J* = 15.9, 7.5 Hz, 1H, 10-H), 3.89 (dq, *J* = 7.5, 6.3 Hz, 1H, 11-H), 3.70–3.62 (m, 8H, triethylene glycol-*H*'s), 3.58 (t, *J* = 5.1 Hz, 2H, 14'-H), 3.36 (t, *J* = 5.1 Hz, 2H, 15'-H), 1.27 (d, *J* = 6.3 Hz, 3H, 13-H); ^{13}C NMR (100 MHz, 293 K, acetone-d_6): δ = 164.5, 137.0, 132.0, 131.4, 129.9, 127.8, 126.1, 121.2, 119.3, 112.1, 110.0, 77.9, 70.2, 69.9, 69.8, 55.0, 50.5, 38.8, 21.0; ESI-MS calcd for $C_{21}H_{28}N_6O_4$ $[M + CH_3CN]^+$ 428.22, found 428.20.

Procedure for Pd removal: A Deloxan® MP metal scavenger (30 mg) was washed with EtOH (20 mL) over a C_{18} octadecyl column. The washed metal scavenger was added to a 10-mL round-bottomed flask equipped with a Teflon-coated magnetic stir bar containing TMC-205 (12.0 mg). To the flask was added toluene (0.7 mL), using a syringe, under an open atmosphere at 23 °C. The mixture was shielded from light and stirred in an 80 °C oil bath for 2 h, then cooled to 23 °C. All steps subsequent to cooling were performed in a dark environment. The flask was cooled on an ice-water bath for 7 min and then the cold mixture was filtered through a filter paper. The filtrate was concentrated under reduced pressure using a rotary evaporator ($T_{water\ bath}$ = 30 °C). The crude residue was purified by preparative TLC (60% EtOAc in hexanes) to give TMC-205 (**3.1**, 11.4 mg) as a pale yellow solid. This product was used for the antiproliferative activity assay. All the TMC-205 analogues were purified by the same procedure prior to biological experiments.

I thank Amanda L Garner in our group for analyzing the palladium content of **3.8**. See: A. L. Garner, F. Song, K. Koide, *J. Am. Chem. Soc.* **2009**, *131*, 5163.

Cells and reagents: HCT-116 cells was gifts from Professor Andreas Vogt (University of Pittsburgh. HCT-116 cells were maintained at 37 °C in an atmosphere containing 5% carbon dioxide in Corning cell culture dishes (75 mm) in McCoy's 5A cell culture medium containing 10% fetal bovine serum, 1% L-glutamine, and 1% penicillin-streptomycin solution (Invitrogen). All synthetic compounds were dissolved in DMSO as stock solutions and stored at -20 °C. For the experiments, aliquots were thawed at room temperature in a dark environment, and diluted solutions were prepared in McCoy's 5A medium containing 1% DMSO prior to addition to the cell culture media.

Antiproliferative activity assay: HCT-116 cells were plated in a 96-well plate at an initial density of approximately 1×10^4 cells per well in McCoy's 5A cell culture medium (135 μL) and were incubated in an incubator at 37 °C in an atmosphere containing 5% carbon dioxide for 24 h prior to compound addition. One plate of cells was used for a time zero cell number determination, and cells in other plates were treated for 72 h with either DMSO or a range of concentrations, in triplicate, of test agents. Serial two-fold dilutions were used in this experiment. The test compounds was added to the cells at the desired concentration in 15 μL medium (containing 1% DMSO). Cell proliferation was measured spectrophotometrically using the commercial 3-(4,5-dimethylthiazol-2-yl)-5-(3-carboxymethoxyphenyl)-2-(4-sulfophenyl)-2H-tetrazolium, inner salt (MTS) dye reduction assay with phenazine methosulfate (PMS) as the electron acceptor (20 μL per well). The absorbance (at 490 nm minus that at 630 nm) was measured by a Spectromax M5 plate reader (Molecular Devices) or Modulus II Microplate Multimode Reader (Turner BioSystem). Evaluation of test compounds was performed in triplicate at each concentration, and the final numbers were averaged. Microsoft Excel and GraphPad Prism 5.0© were used to generate dose-response curves and calculate GI_{50} values.

Growth inhibition was calculated as defined by the National Cancer Institute [$GI_{50} = 100 \times (T - T_0)/(C - T_0)$; T_0 = cell density at time zero; T = cell density of the test well after period of exposure to test compound; C = cell density of the vehicle treated] (see: http://www.dtp.nci.nih.gov/branches/btb/ivclsp.html). Vincristine was used as a positive control.

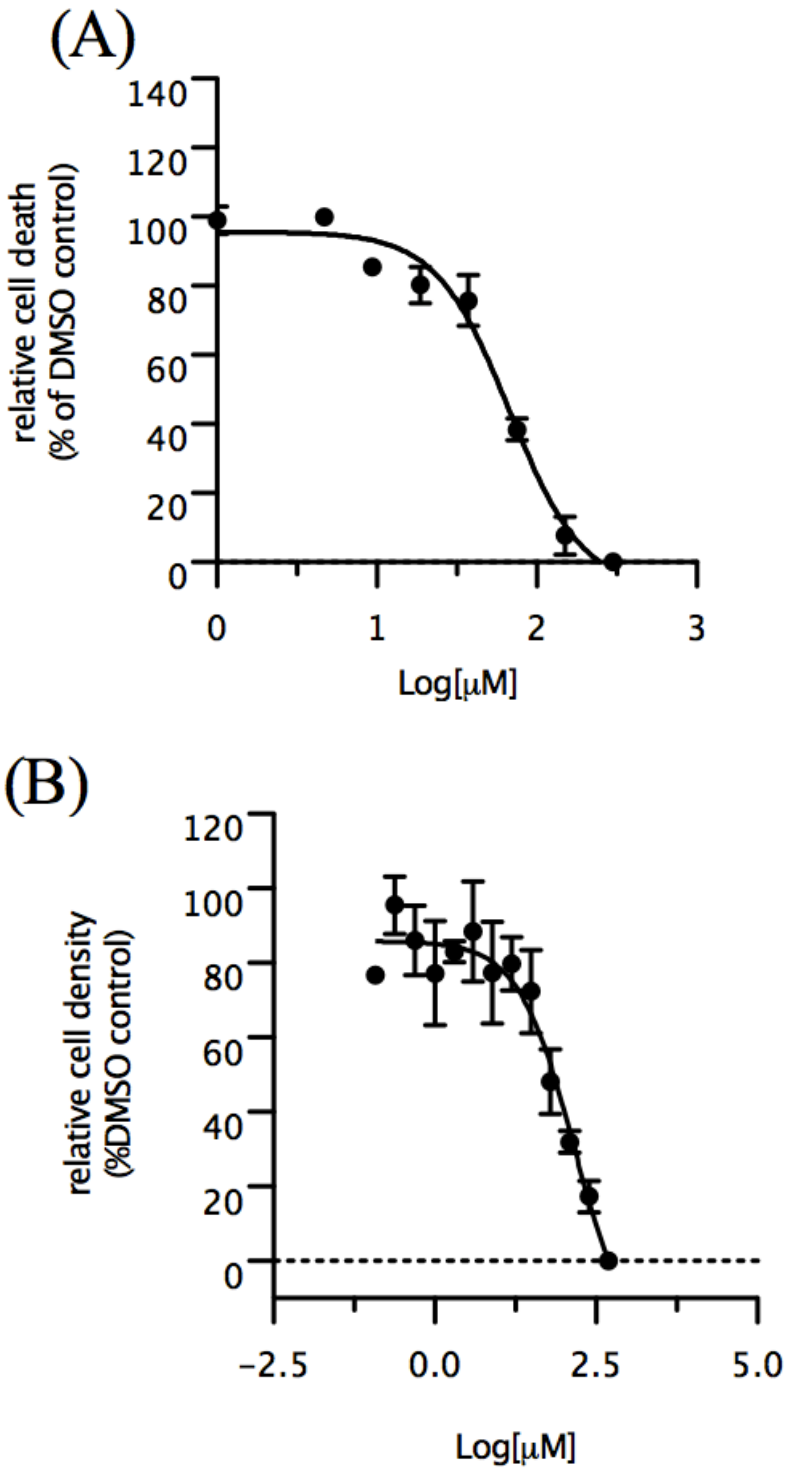
(A)
relative cell death
(% of DMSO control)
140
120
100
80
60
40
20
0
0
1
2
3
Log[μM]
(B)
relative cell density
(%DMSO control)
120
100
80
60
40
20
0
-2.5
0.0
2.5
5.0
Log[μM]

(C)

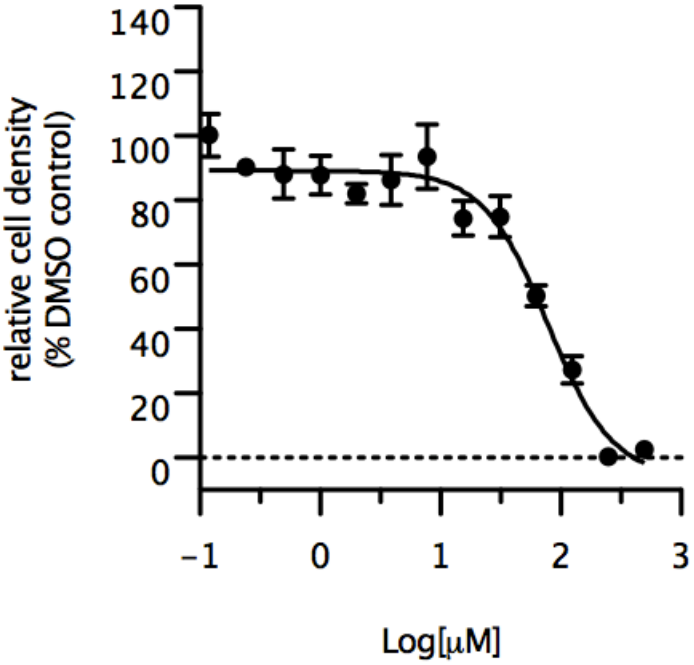
140
120
100
80
60
40
20
0
relative cell density
(% DMSO control)
−1
0
1
2
3
Log[μM]

(D)

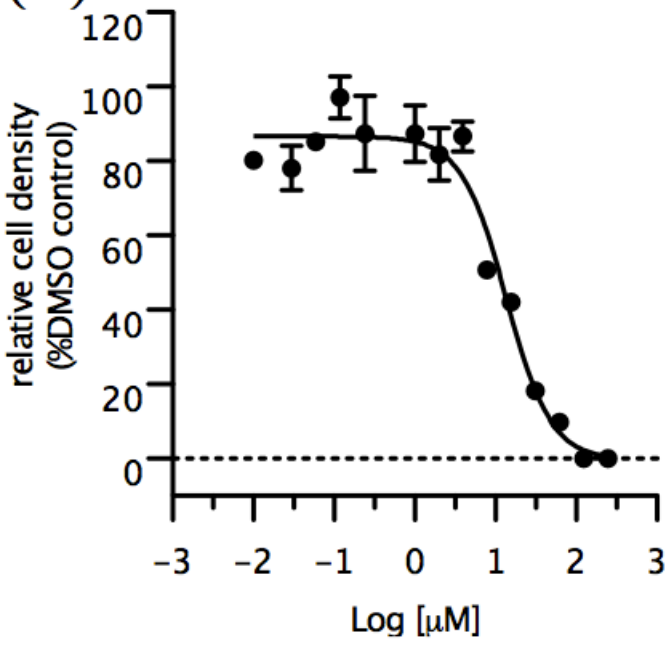
120
100
80
60
40
20
0
relative cell density
(%DMSO control)
−3
−2
−1
0
1
2
3
Log [μM]

(E)

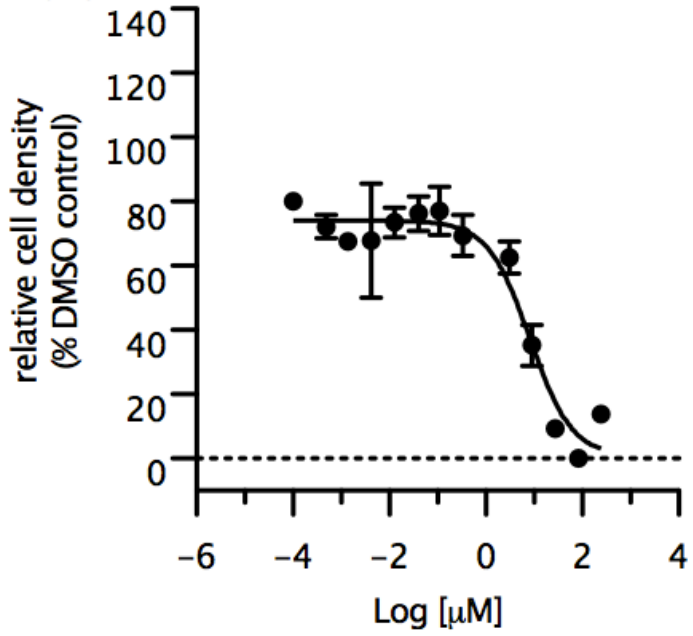
140
120
100
80
60
40
20
0
relative cell density
(% DMSO control)
−6
−4
−2
0
2
4
Log [μM]

(F)

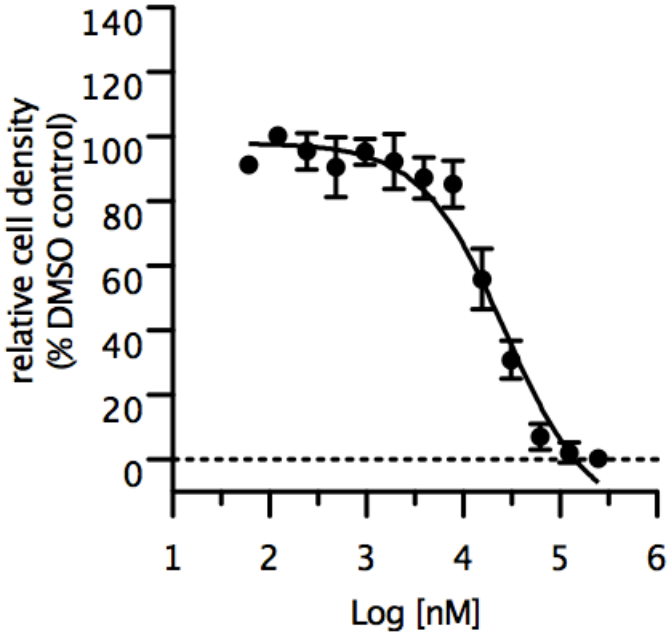
140
120
100
80
60
40
20
0
relative cell density
(% DMSO control)
1
2
3
4
5
6
Log [nM]

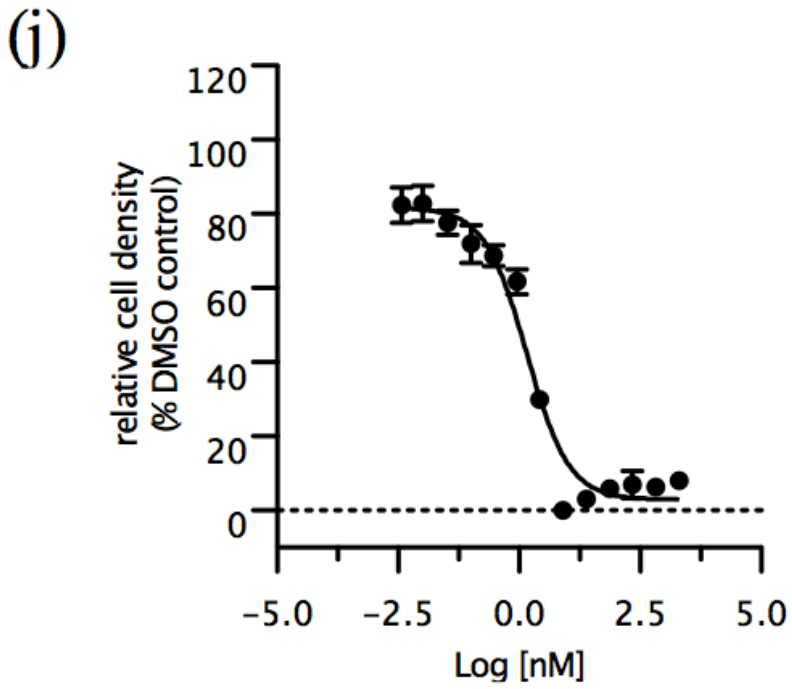

Figure A3. A representative example of the antiproliferative dose-dependant activity of TMC-205 and analogues in cells.

(**A**) **2.43**-treated HCT-116 cells. (**B**) **3.9**-treated HCT-116 cells. (**C**) **3.10**-treated HCT-116 cells. (**D**) **3.20**-treated HCT-116 cells. (**E**) **3.21**-treated HCT-116 cells. (**J**) vincristine-treated HCT-116 cells.

APPENDIX B

^{1}H AND ^{13}C SPECTRA

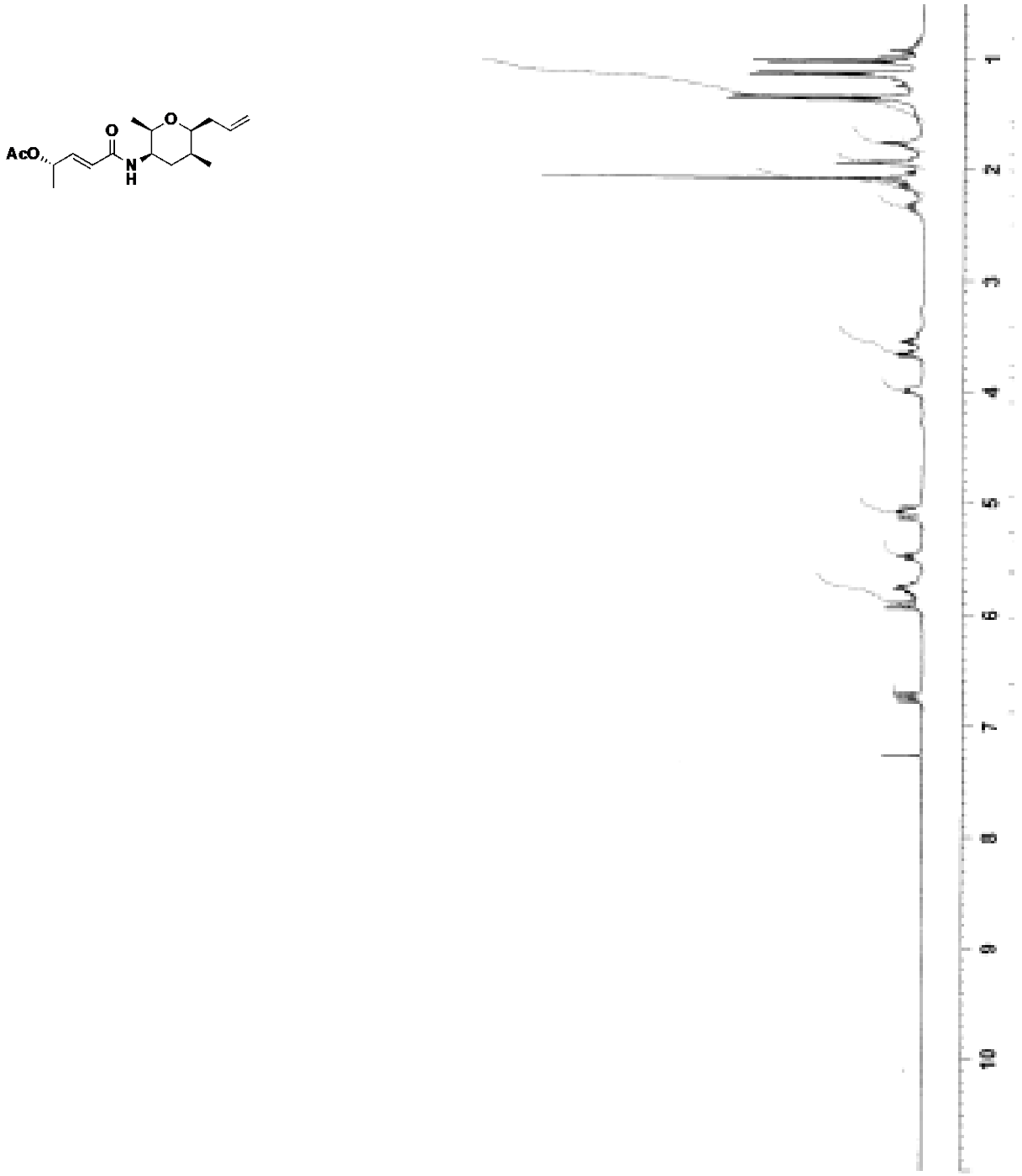

Spectrum 1. ^{1}H NMR spectrum of alkene **2.6** (300 MHz, 1% CD_3OD in $CDCl_3$, 293K)

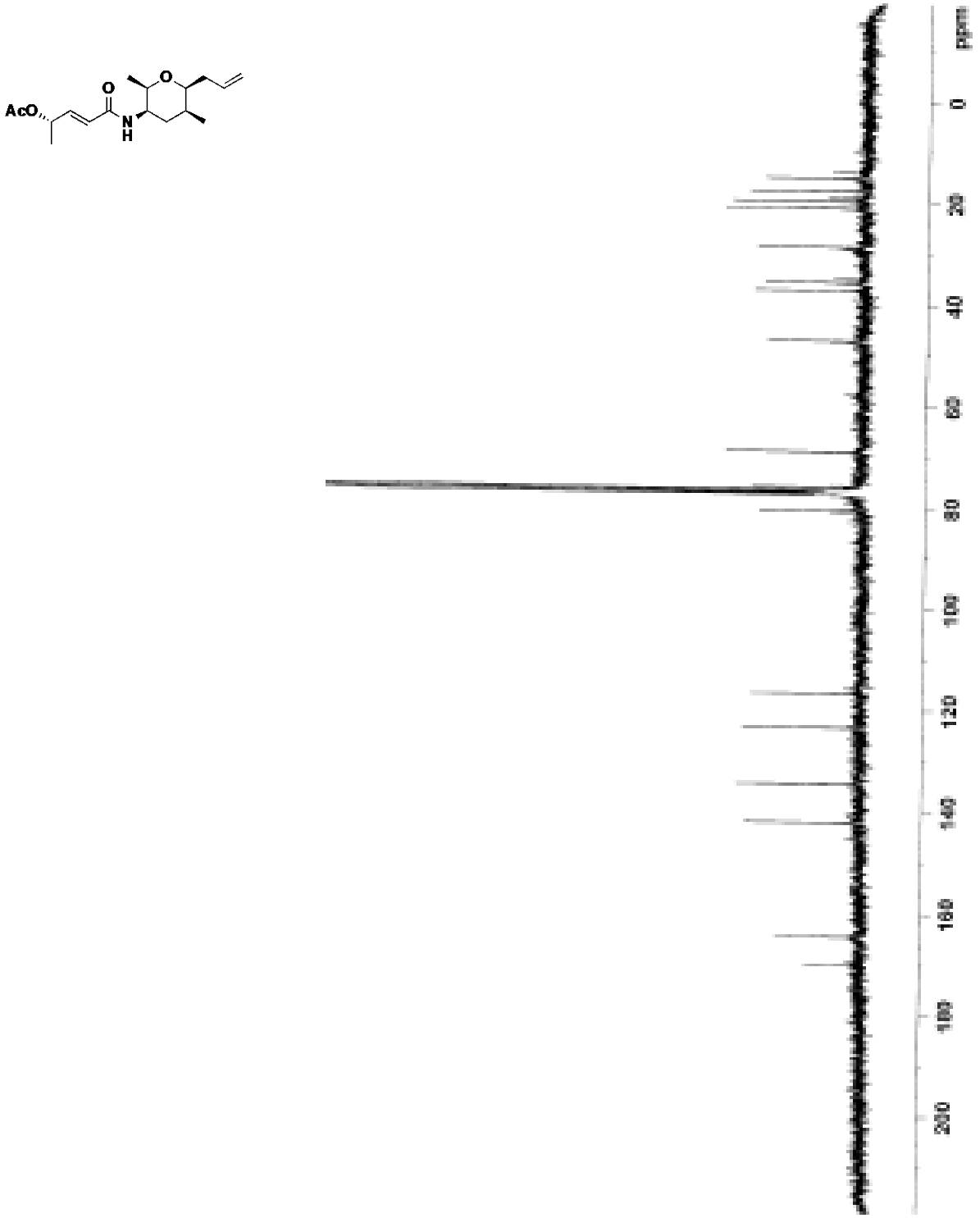

Spectrum 2. ^{13}C NMR spectrum of alkene **2.6** (75 MHz, $CDCl_3$, 293K)

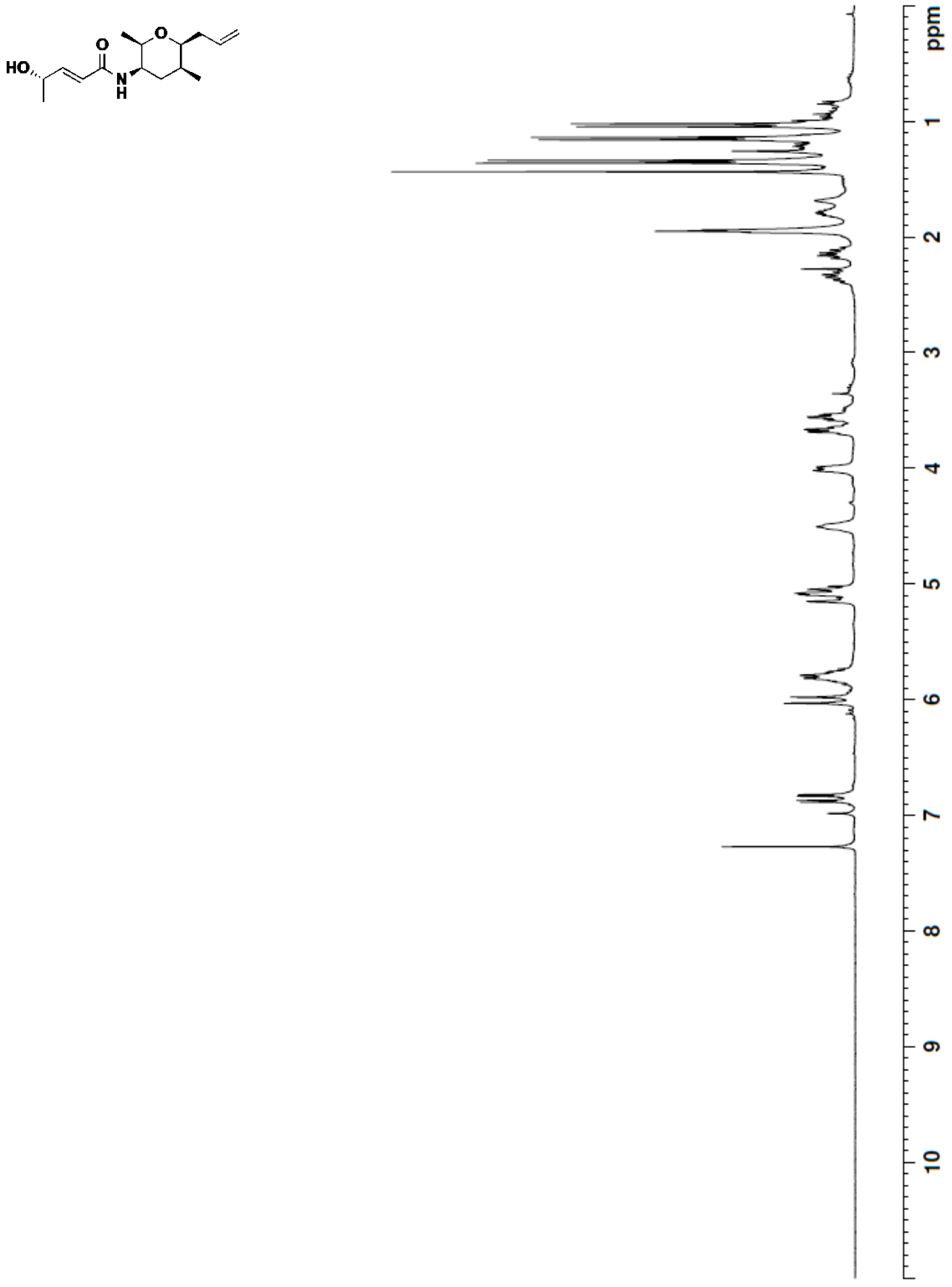

Spectrum 3. ^{1}H NMR spectrum of allylic alcohol **2.7** (300 MHz, 1% CD_3OD in $CDCl_3$, 293K)

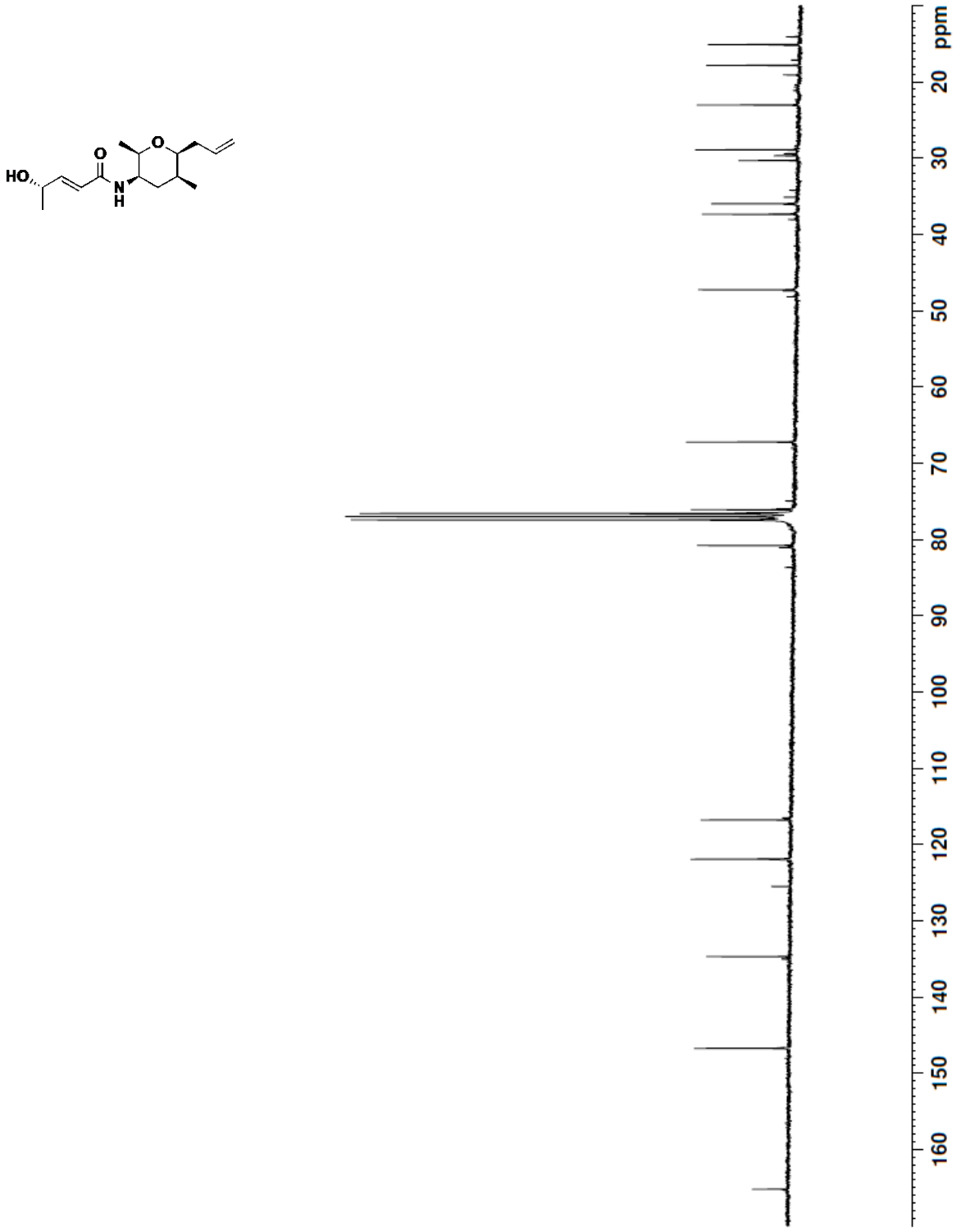

Spectrum 4. ^{13}C NMR spectrum of allylic alcohol **2.7** (75 MHz, $CDCl_3$, 293K)

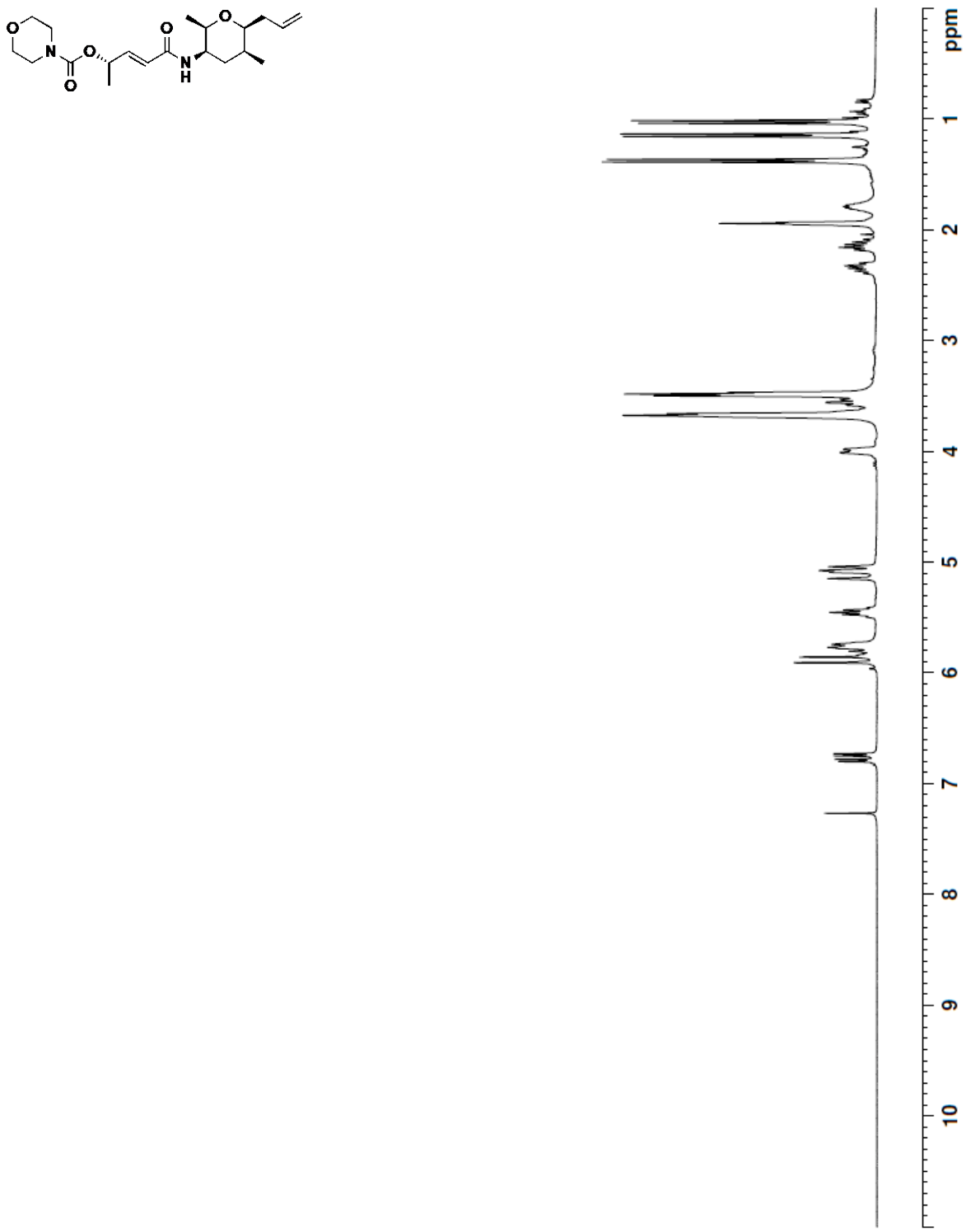

Spectrum 5. ^{1}H NMR spectrum of carbamate **2.8** (300 MHz, $CDCl_3$, 293K)

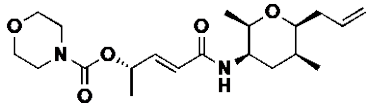

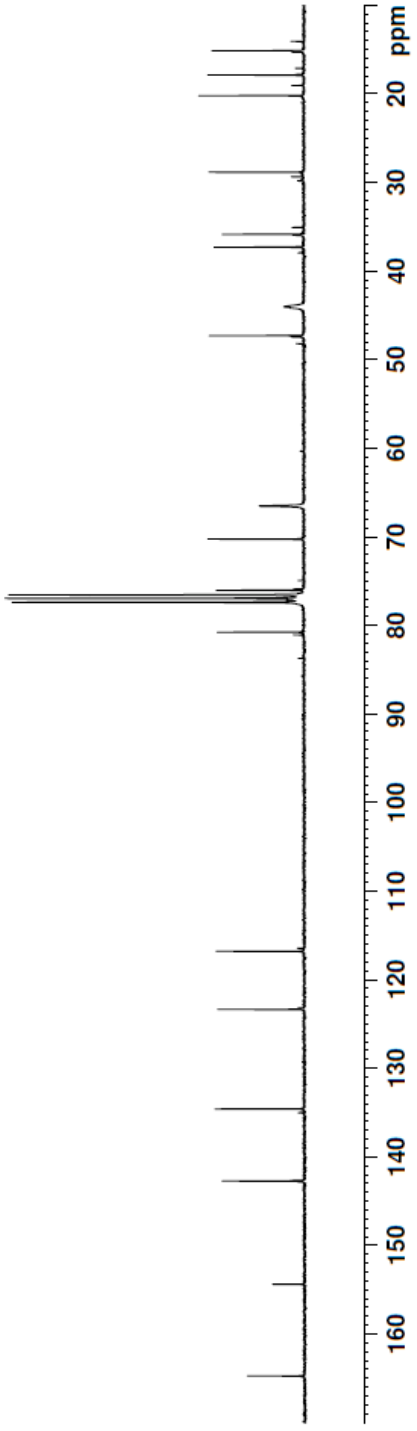

Spectrum 6. ^{13}C NMR spectrum of carbamate **2.8** (75 MHz, $CDCl_3$, 293K)

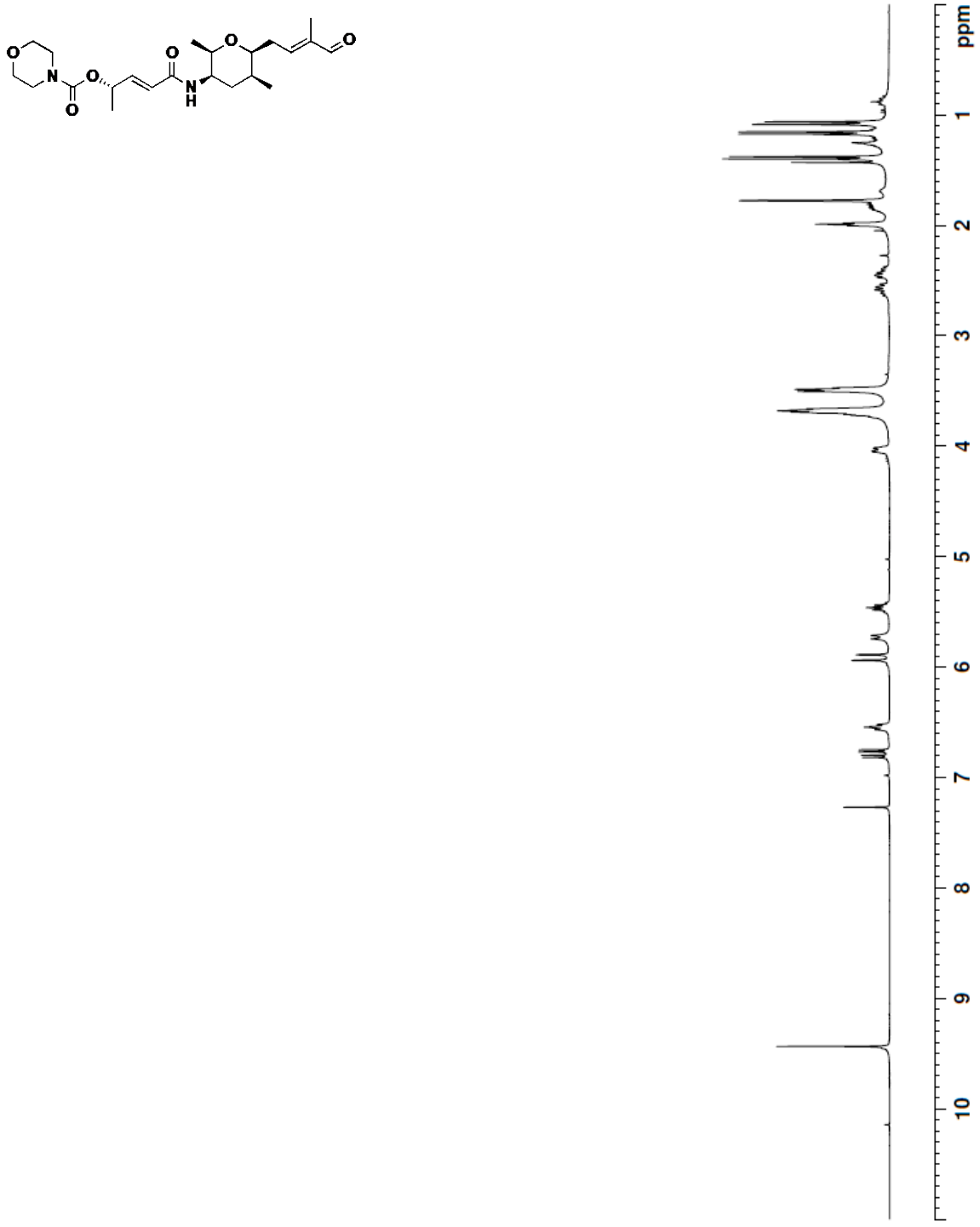

Spectrum 7. ^{1}H NMR spectrum of aldehyde **2.9** (300 MHz, 1% CD_3OD in $CDCl_3$, 293K)

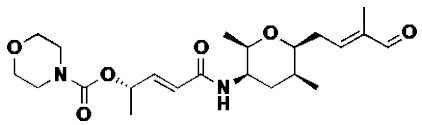

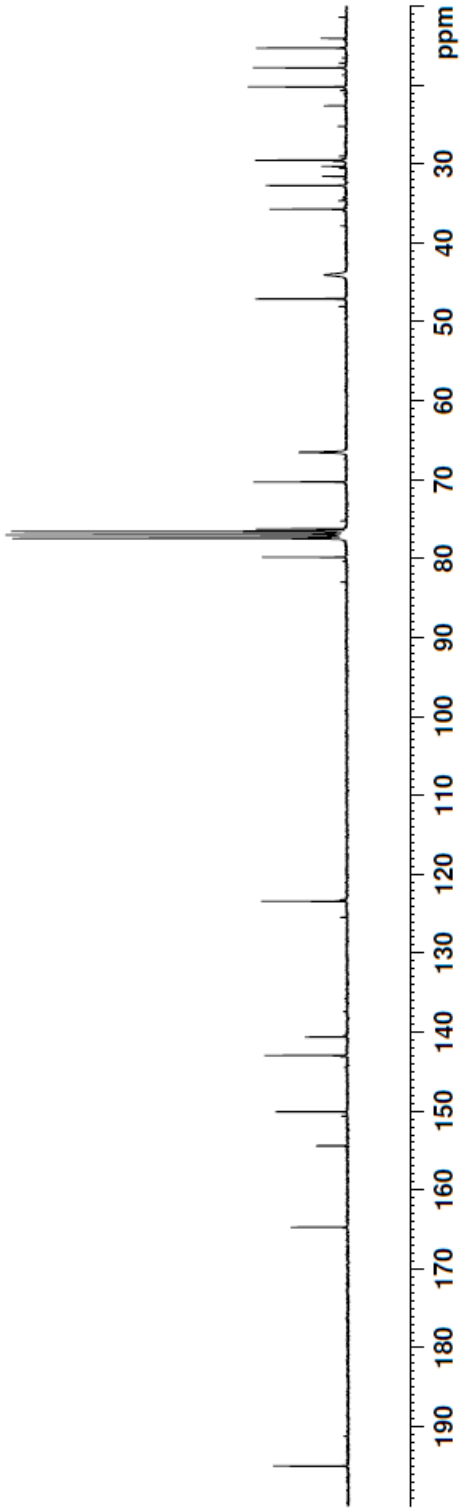

Spectrum 8. ^{13}C NMR spectrum of aldehyde **2.9** (75 MHz, $CDCl_3$, 293K)

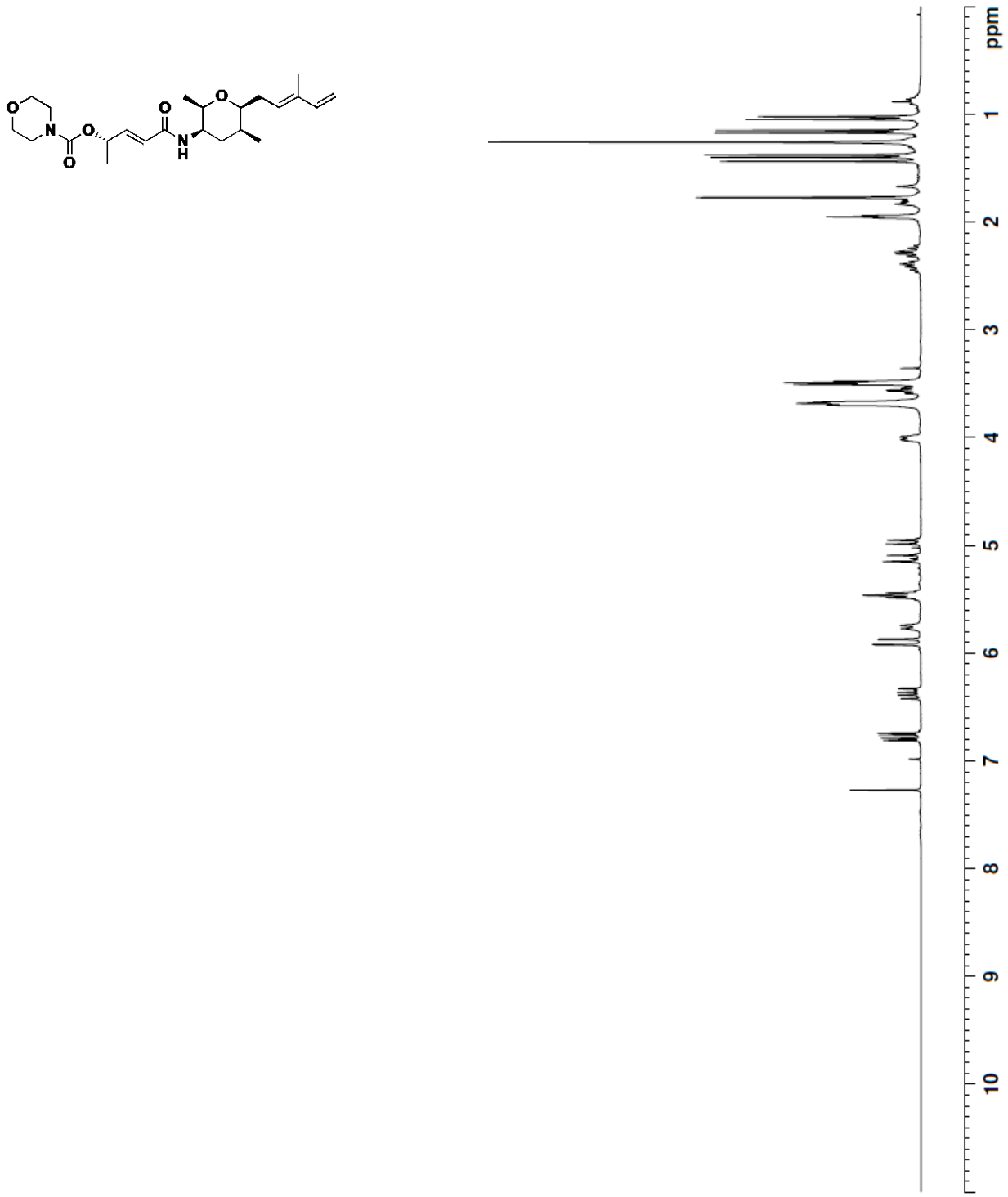

Spectrum 9. ^{1}H NMR spectrum of alkene **2.10** (300 MHz, $CDCl_3$, 293K)

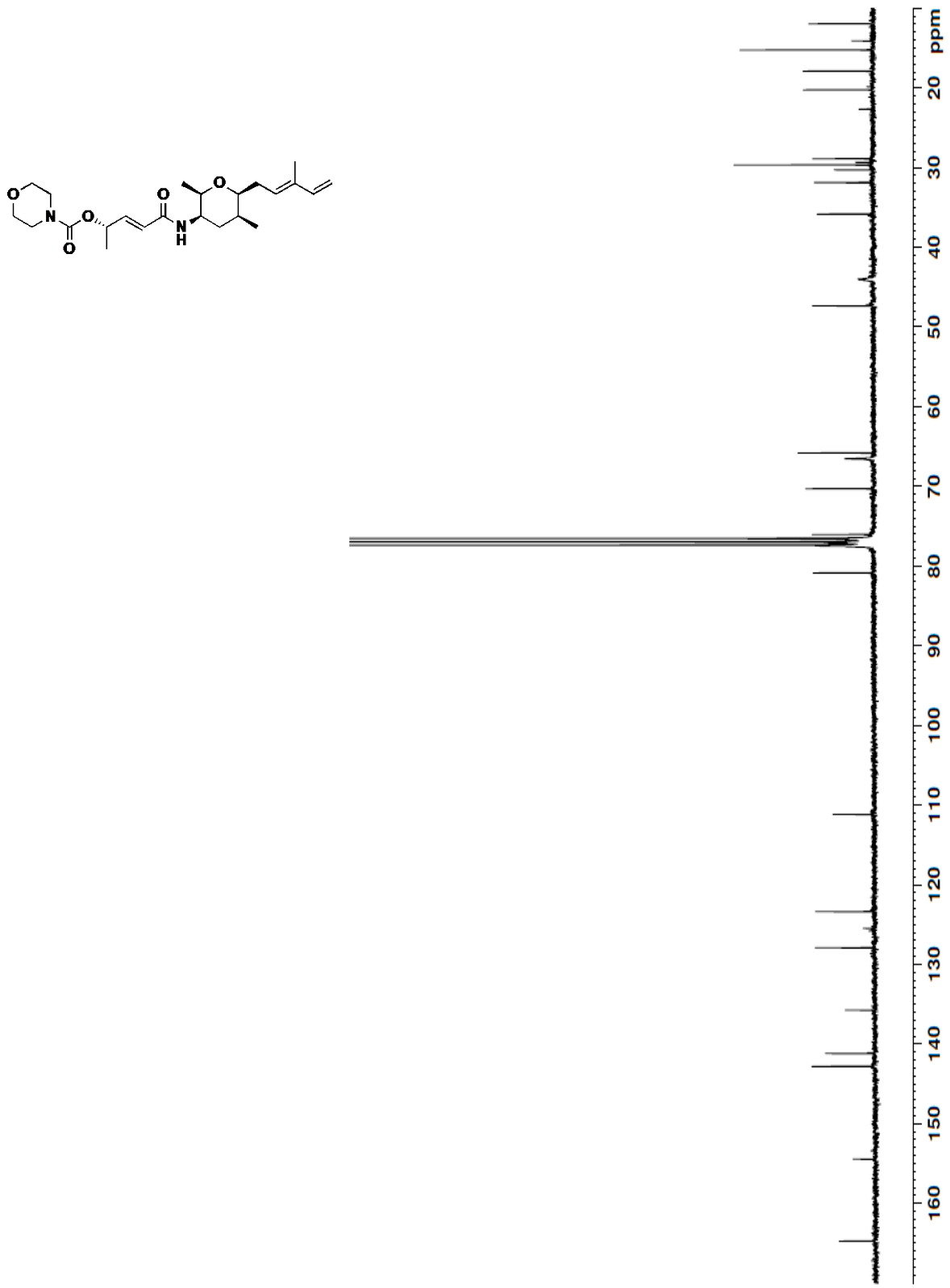

Spectrum 10. ^{13}C NMR spectrum of alkene **2.10** (75 MHz, $CDCl_3$, 293K)

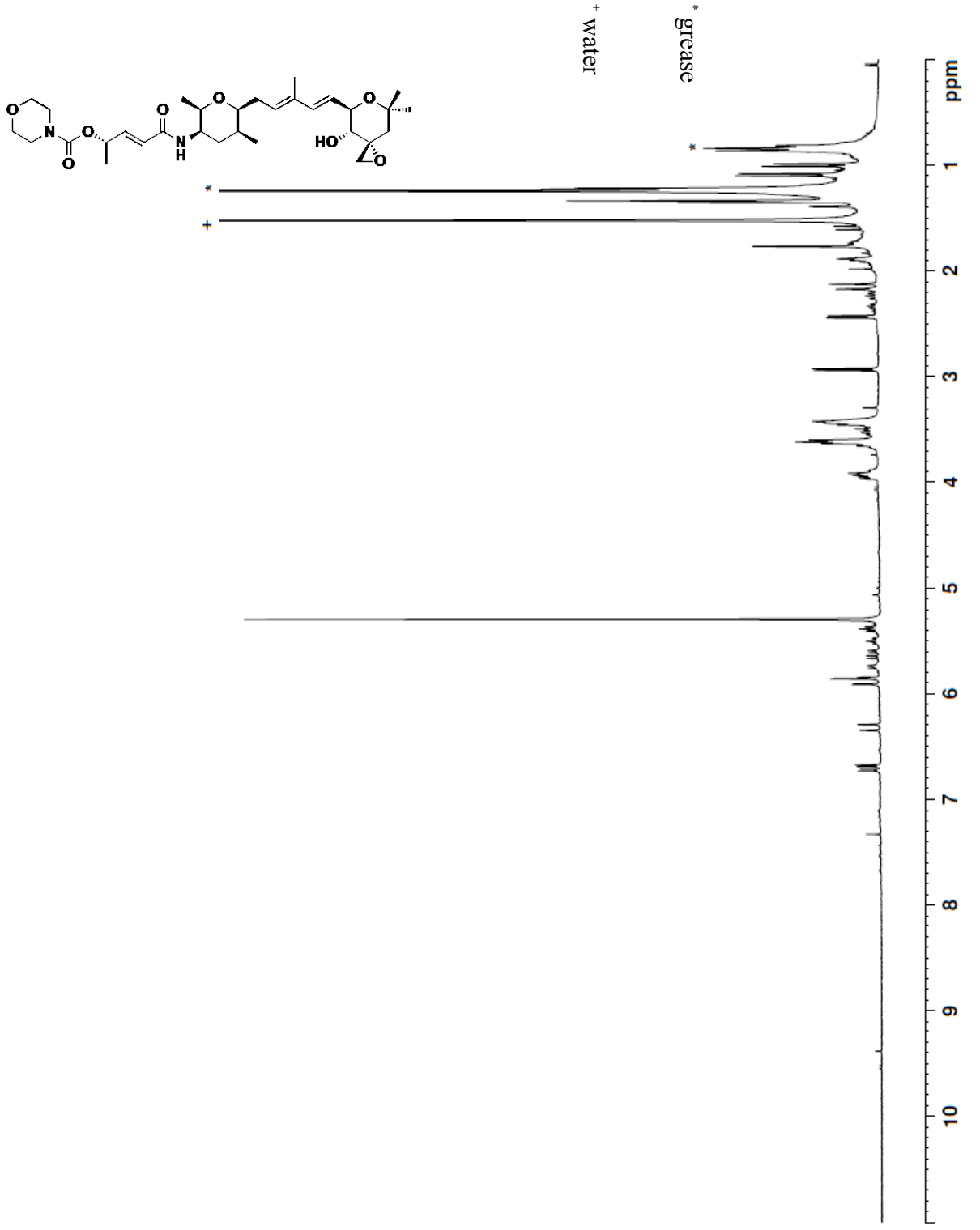

Spectrum 11. ^{1}H NMR spectrum of analogue **2.1** (300 MHz, 1% CD_3OD in CD_2Cl_2, 293K)

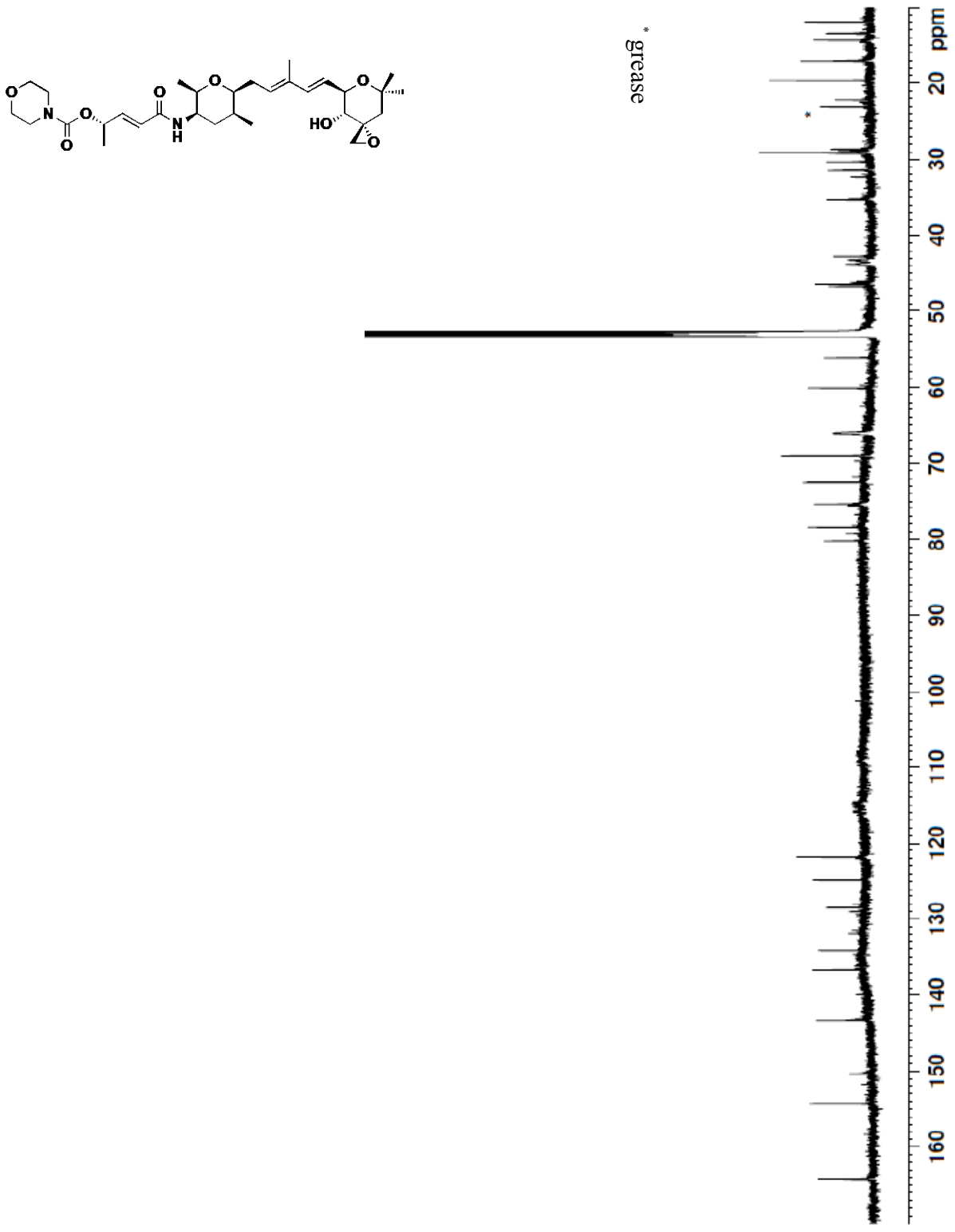

Spectrum 12. ^{13}C NMR spectrum of analogue **2.1** (175 MHz, $CDCl_3$, 293K)

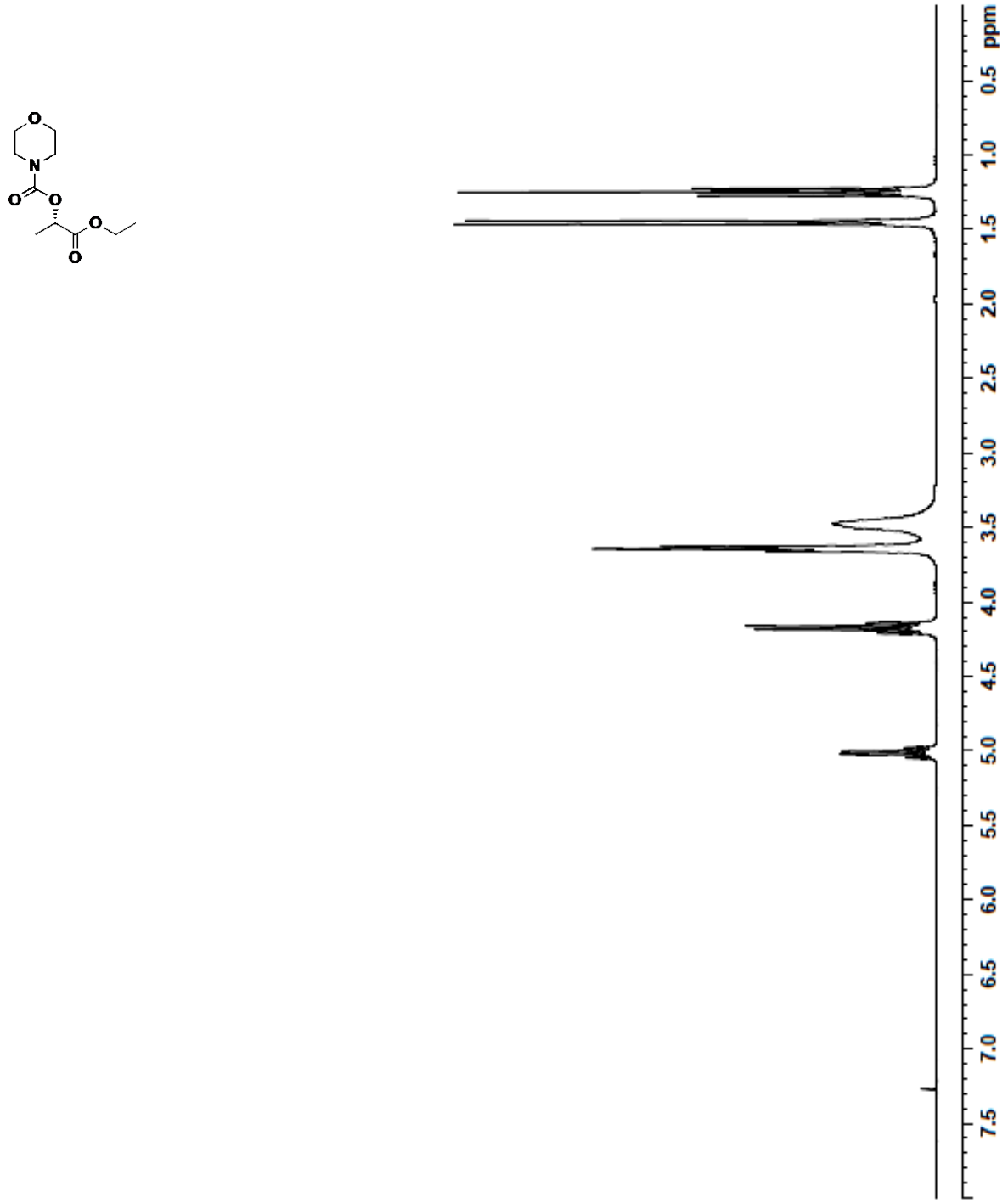

Spectrum 13. ^{1}H NMR spectrum of carbamate **2.13** (300 MHz, $CDCl_3$, 293K)

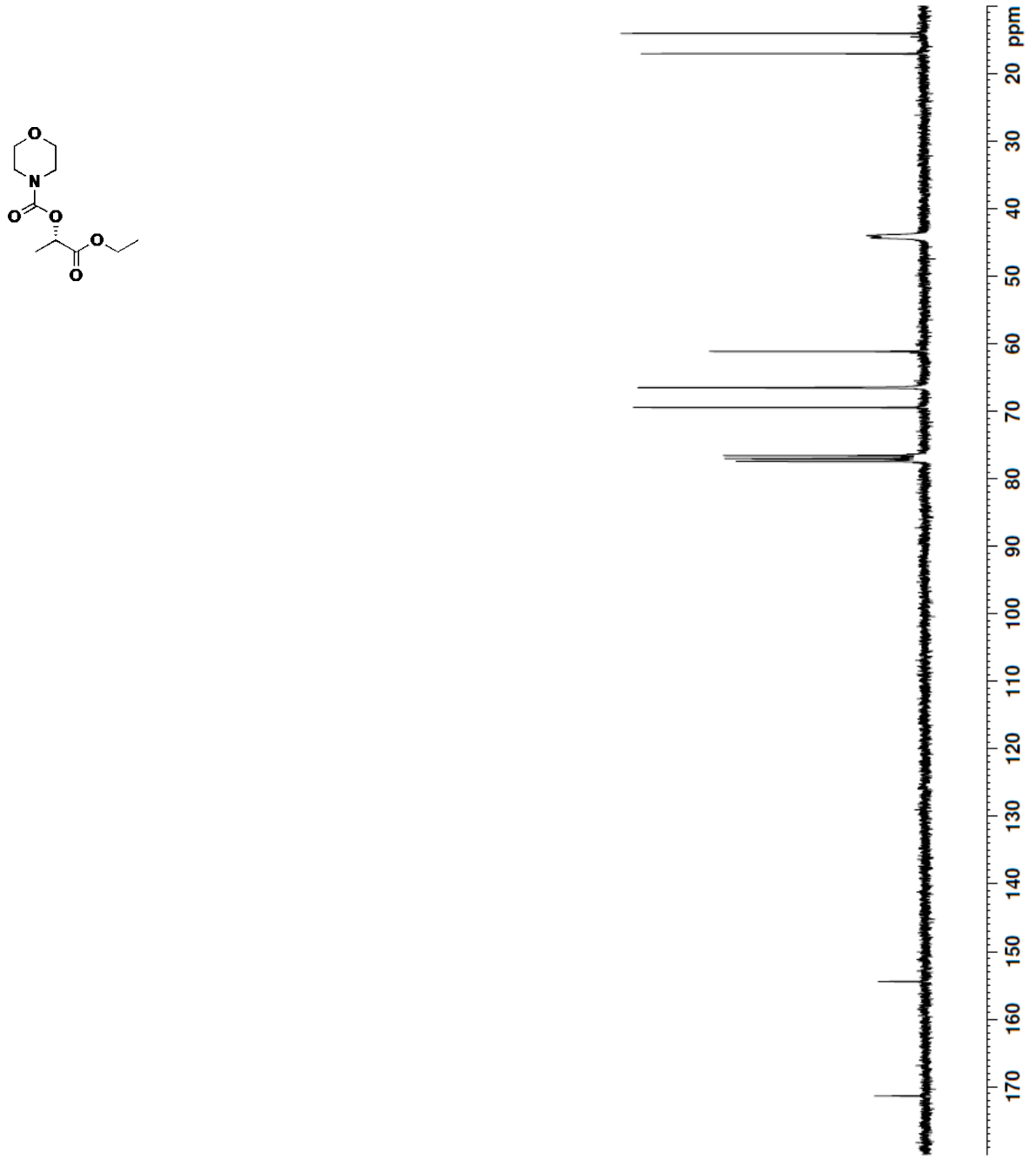

Spectrum 14. ^{13}C NMR spectrum of carbamate **2.13** (75 MHz, $CDCl_3$, 293K)

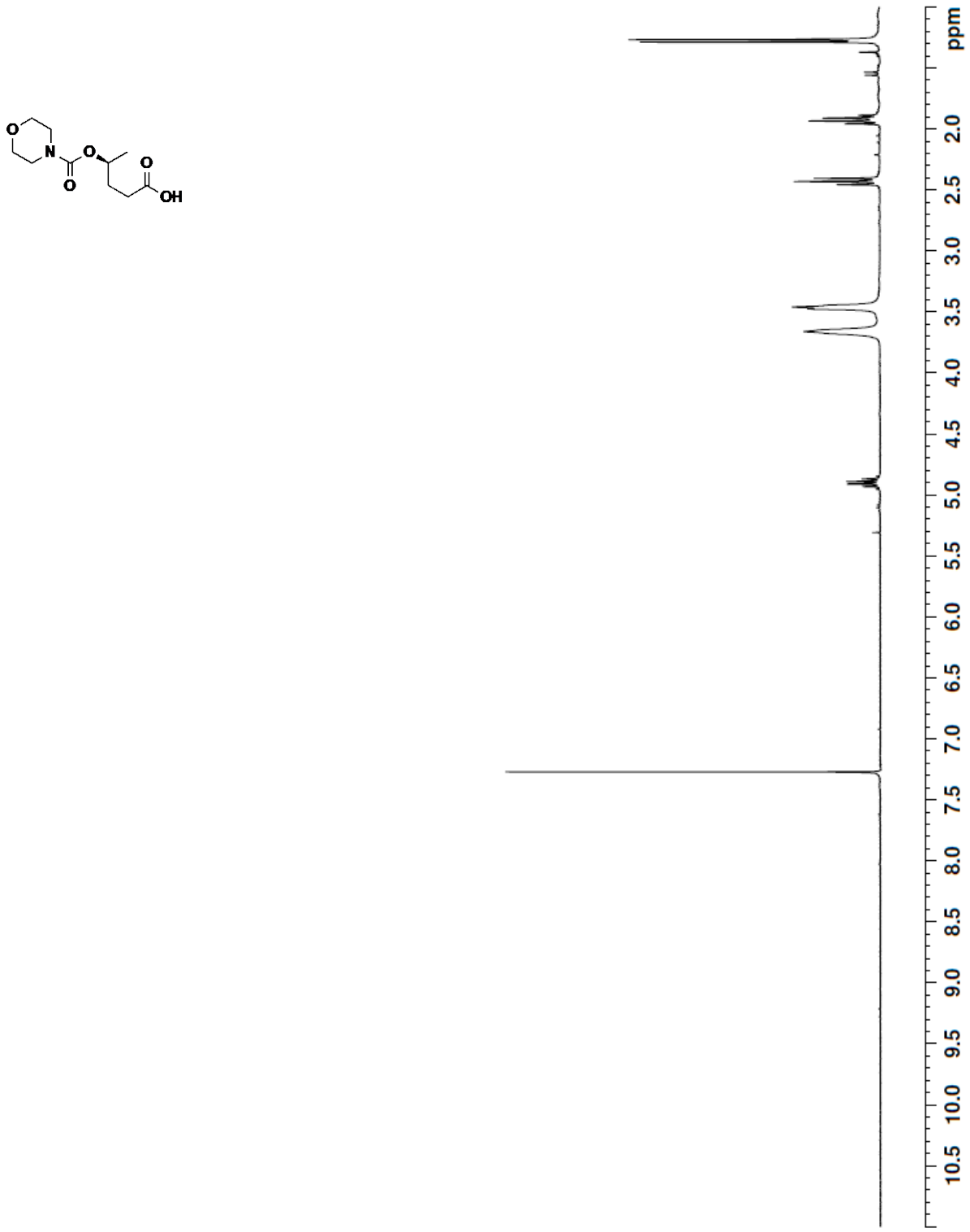

Spectrum 15. ^{1}H NMR spectrum of carboxylic acid **2.14** (300 MHz, 1% CD_3OD in $CDCl_3$, 293K)

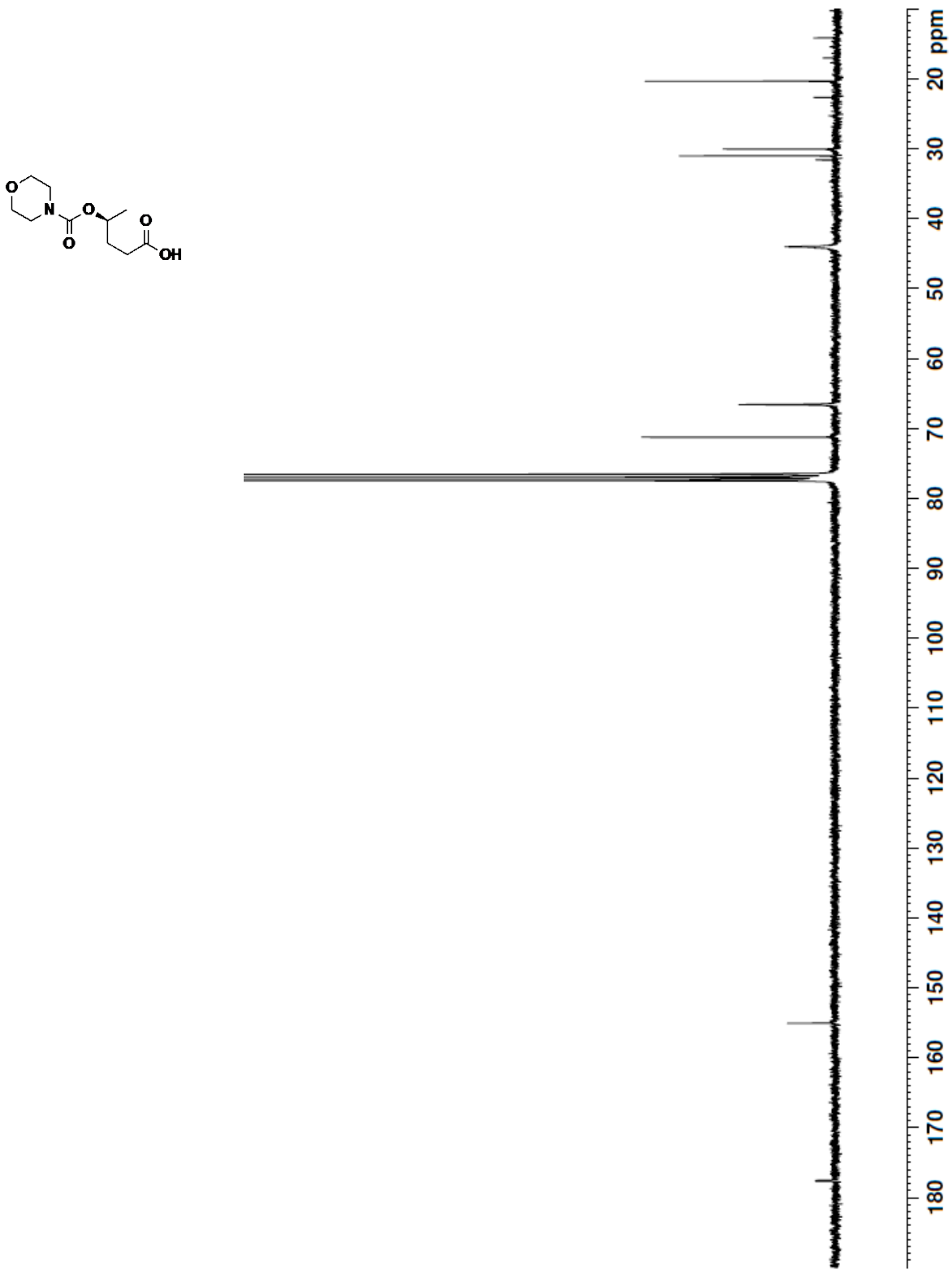

Spectrum 16. ^{13}C NMR spectrum of carboxylic acid **2.14** (75 MHz, $CDCl_3$, 293K)

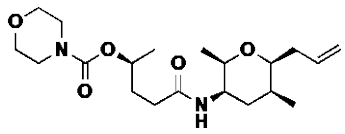

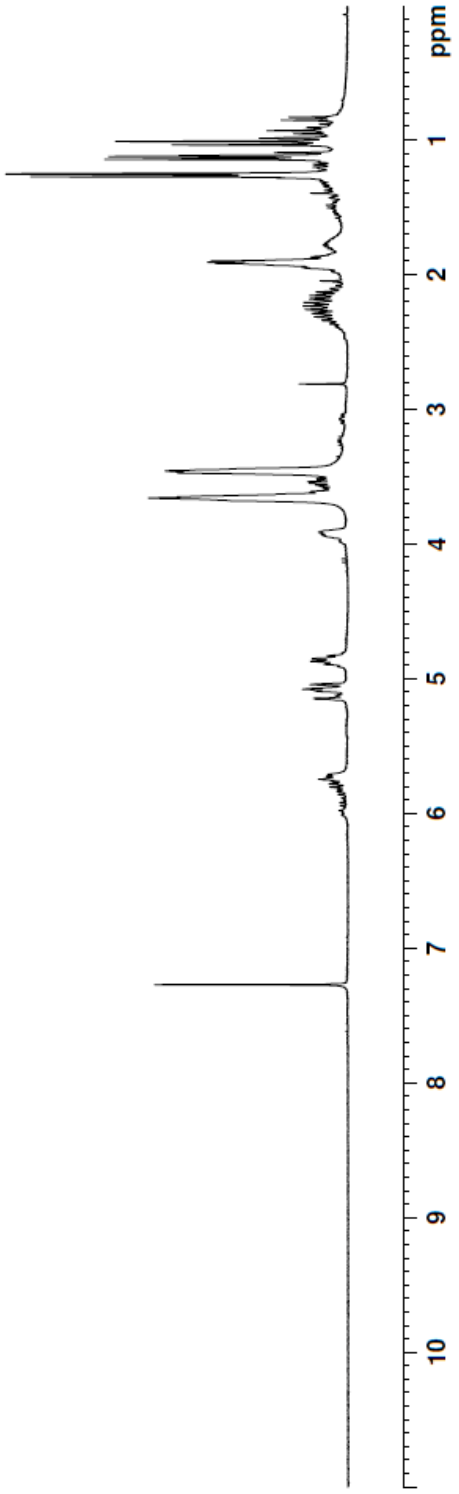

Spectrum 17. ^{1}H NMR spectrum of alkene **2.15** (300 MHz, 1% CD_3OD in $CDCl_3$, 293K)

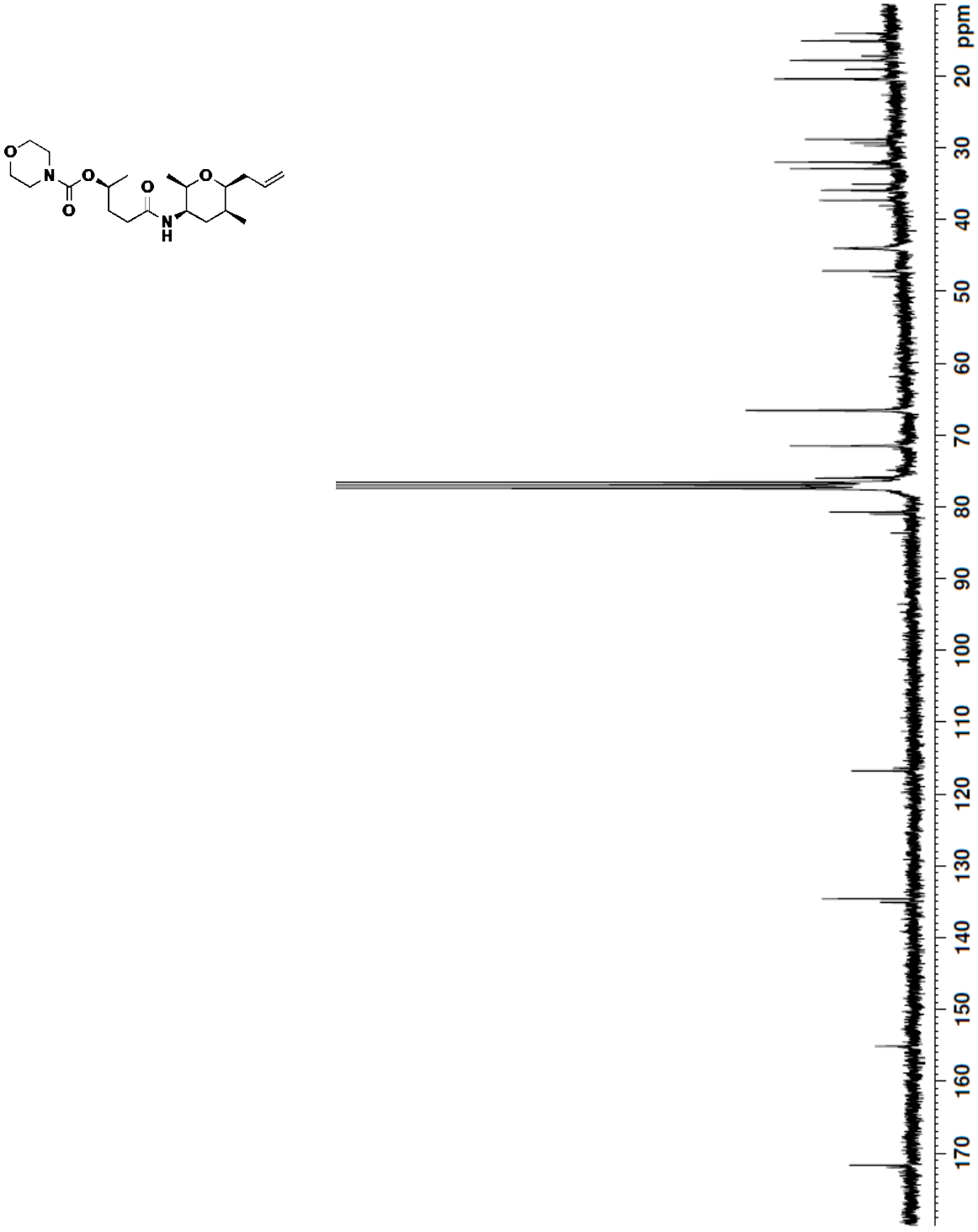

Spectrum 18. ^{13}C NMR spectrum of alkene **2.15** (75 MHz, $CDCl_3$, 293K)

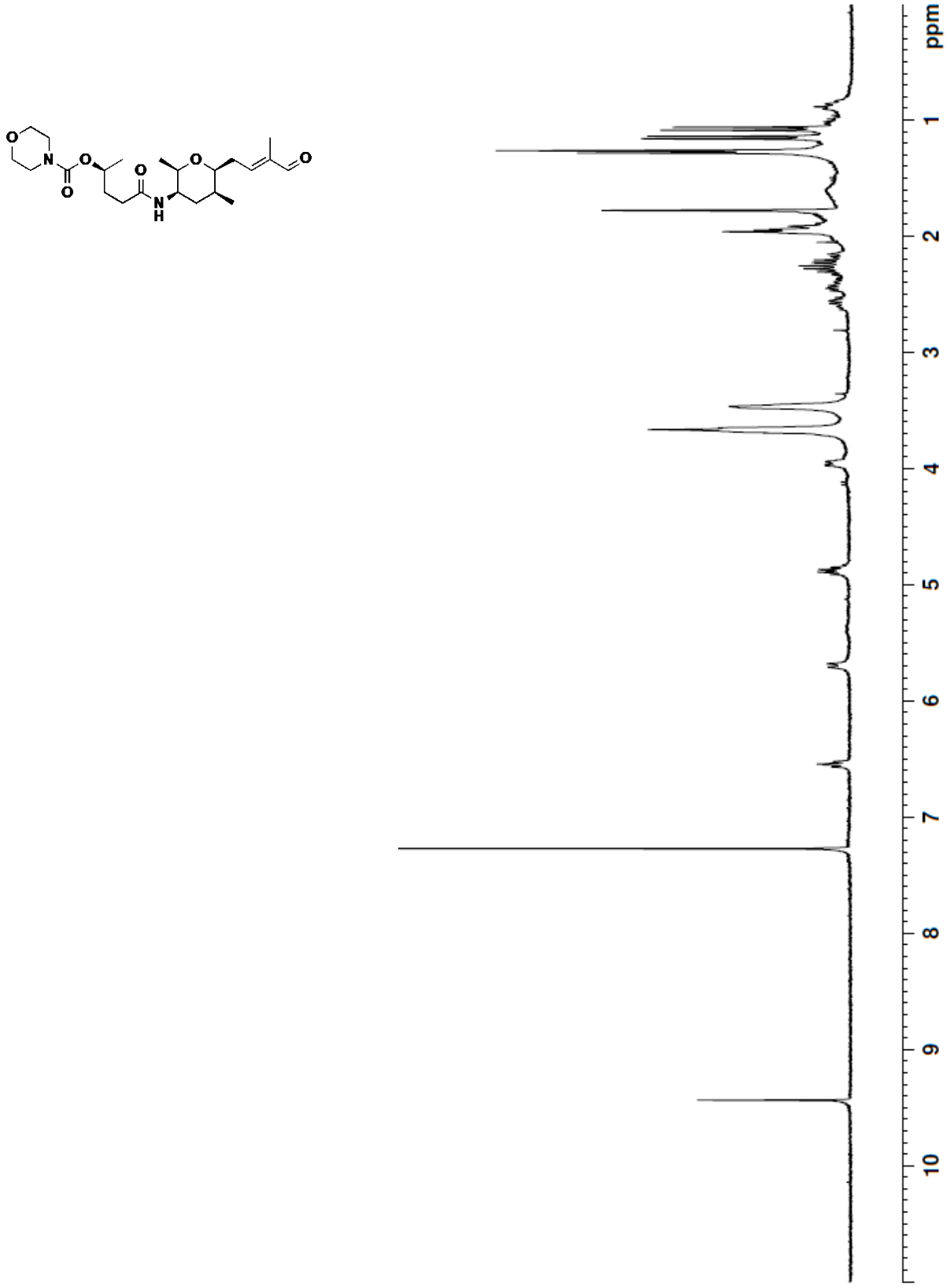

Spectrum 19. ^{1}H NMR spectrum of aldehyde **2.16** (300 MHz, $CDCl_3$, 293K)

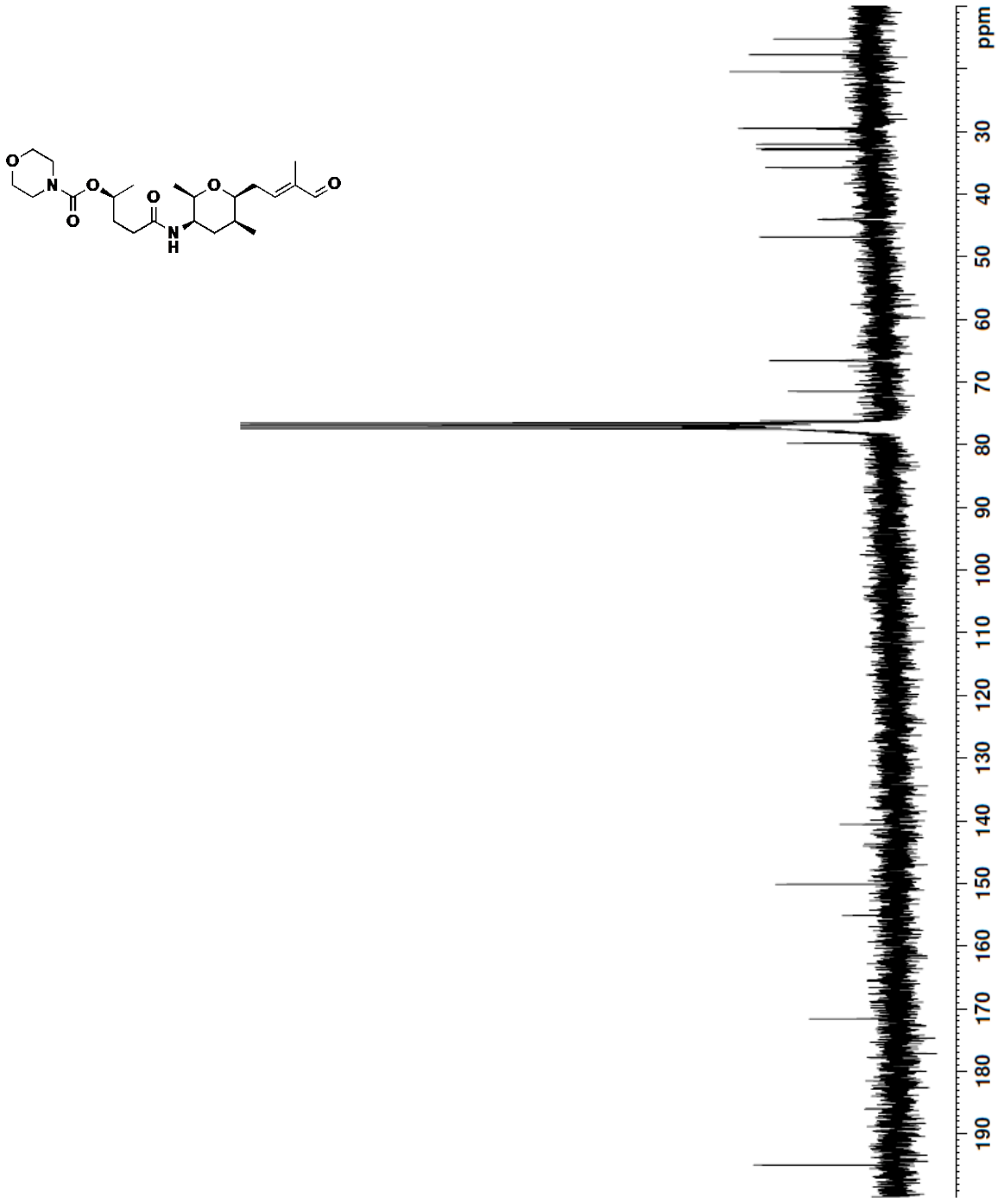

Spectrum 20. ^{13}C NMR spectrum of aldehyde **2.16** (75 MHz, $CDCl_3$, 293K)

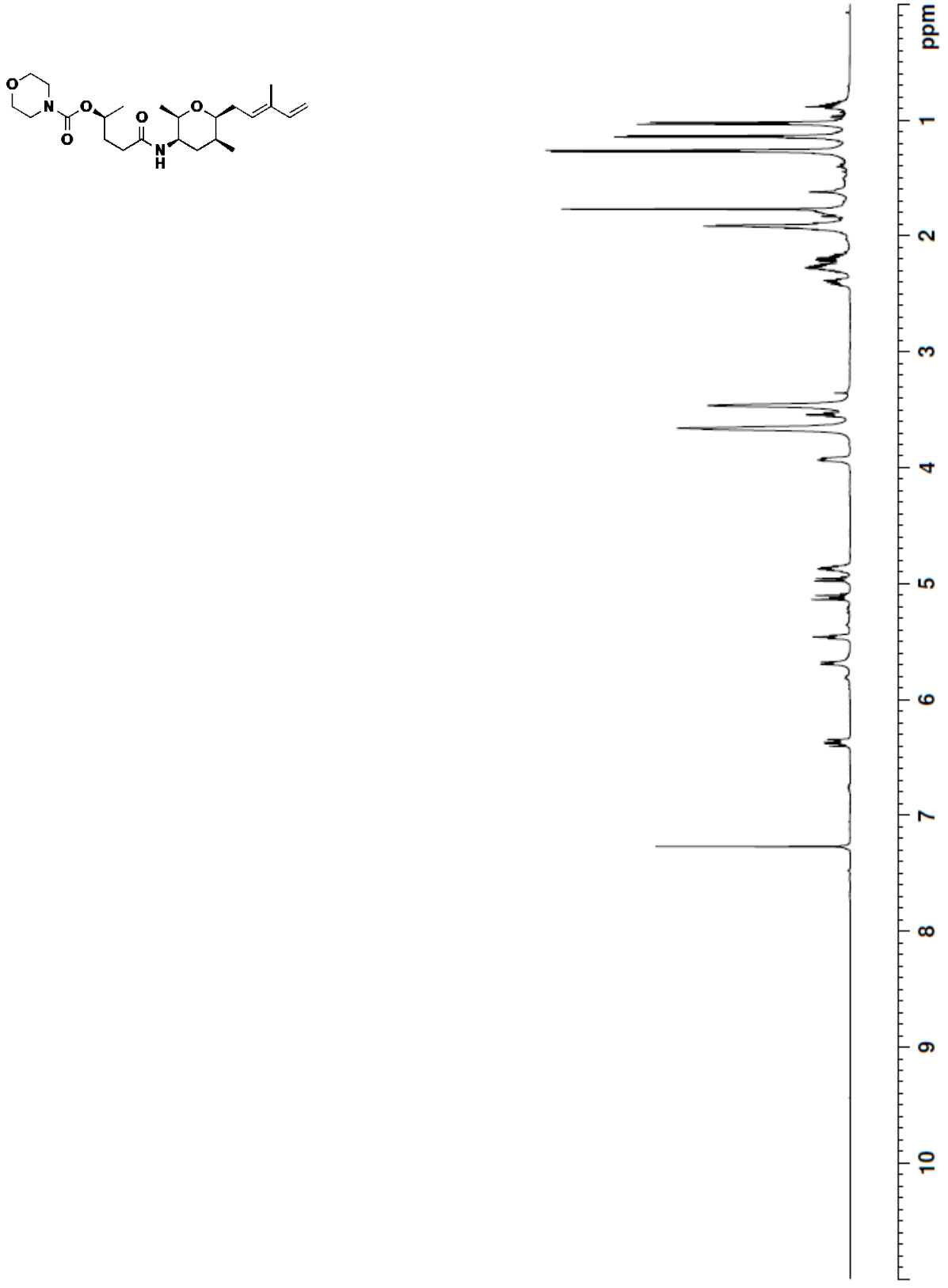

Spectrum 21. ^{1}H NMR spectrum of alkene **2.17** (300 MHz, $CDCl_3$, 293K)

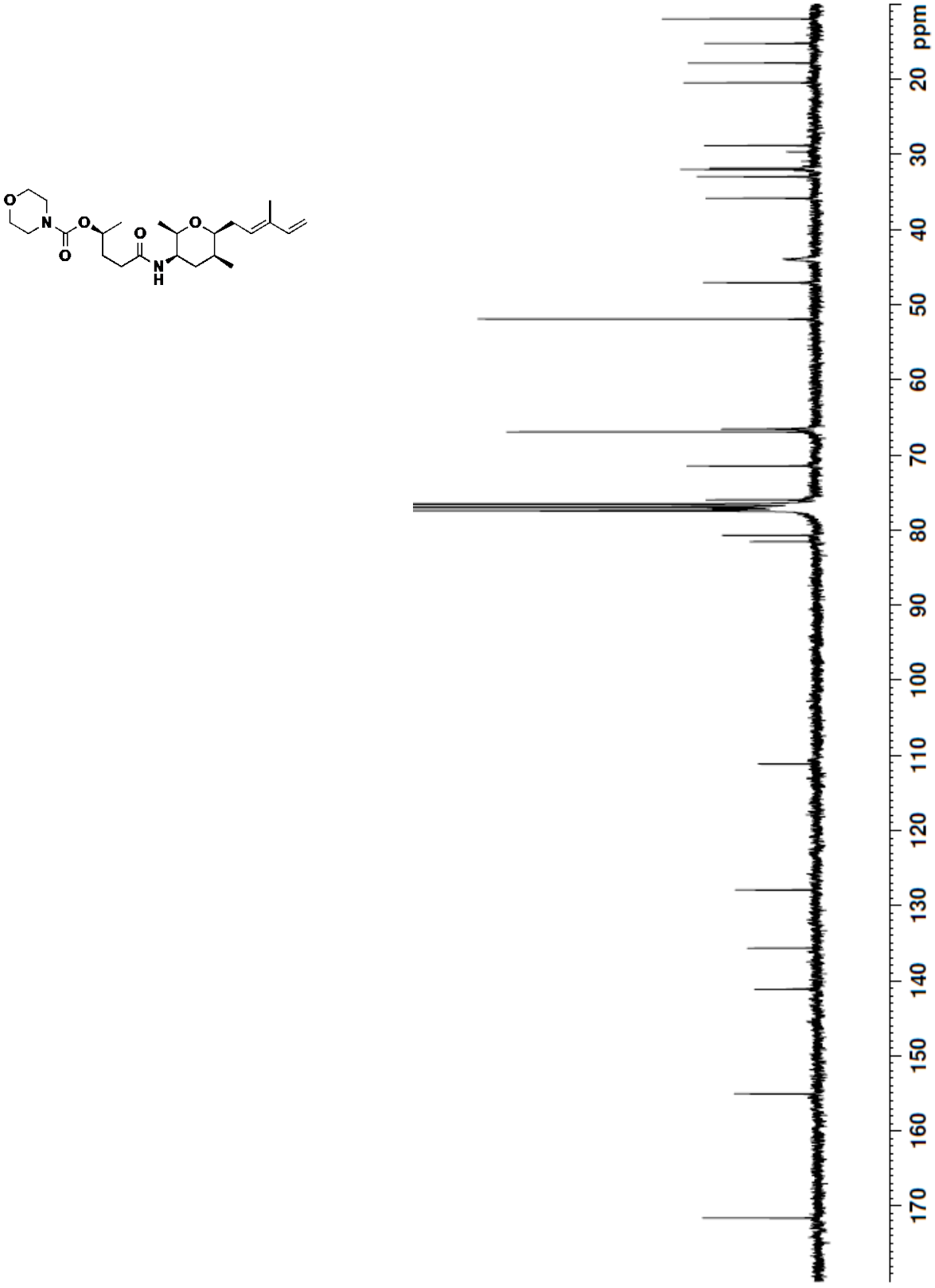

Spectrum 22. ^{13}C NMR spectrum of alkene **2.17** (75 MHz, $CDCl_3$, 293K)

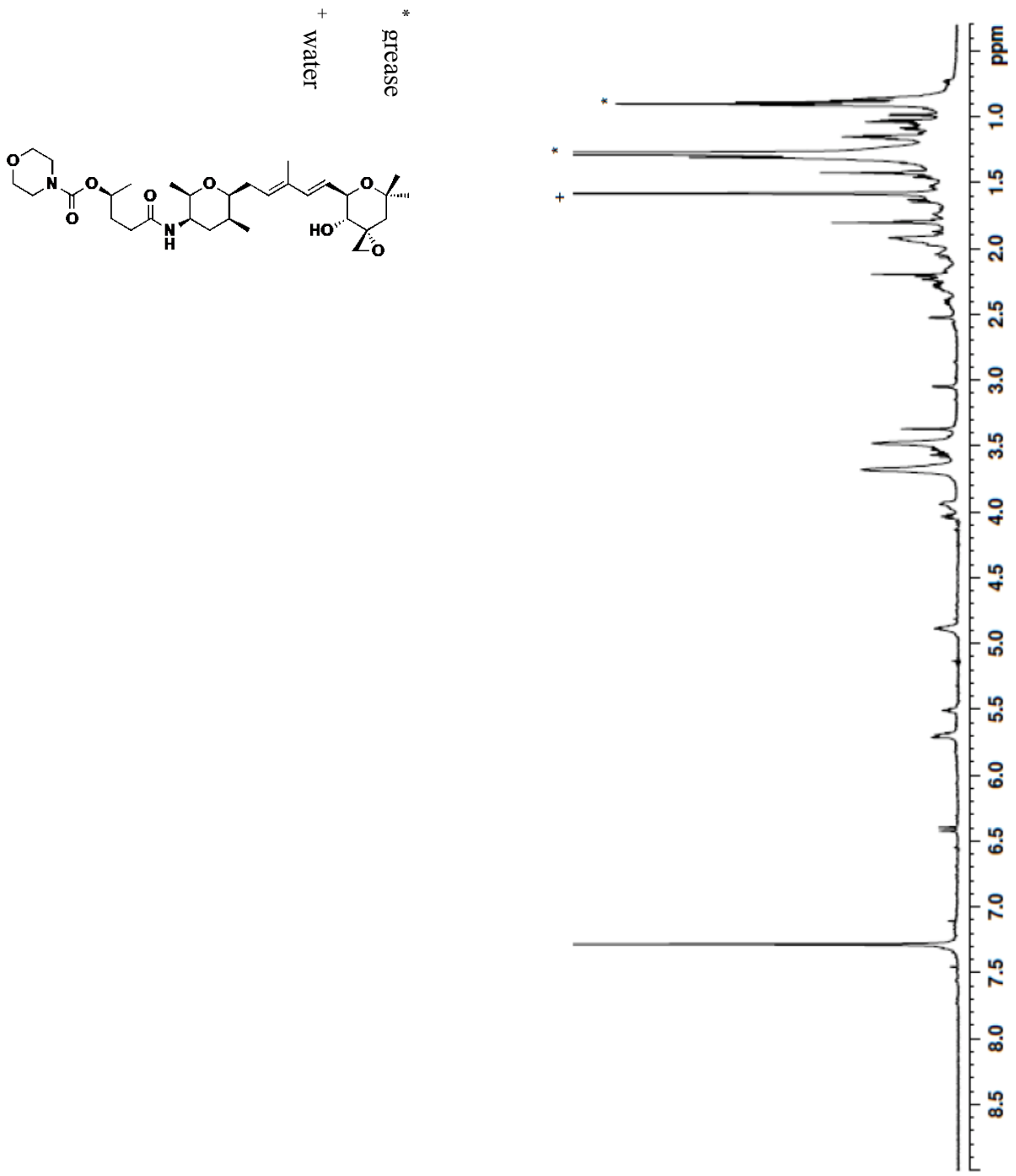

Spectrum 23. ^{1}H NMR spectrum of analogue **2.2** (700 MHz, 1% CD_3OD in $CDCl_3$, 293K)

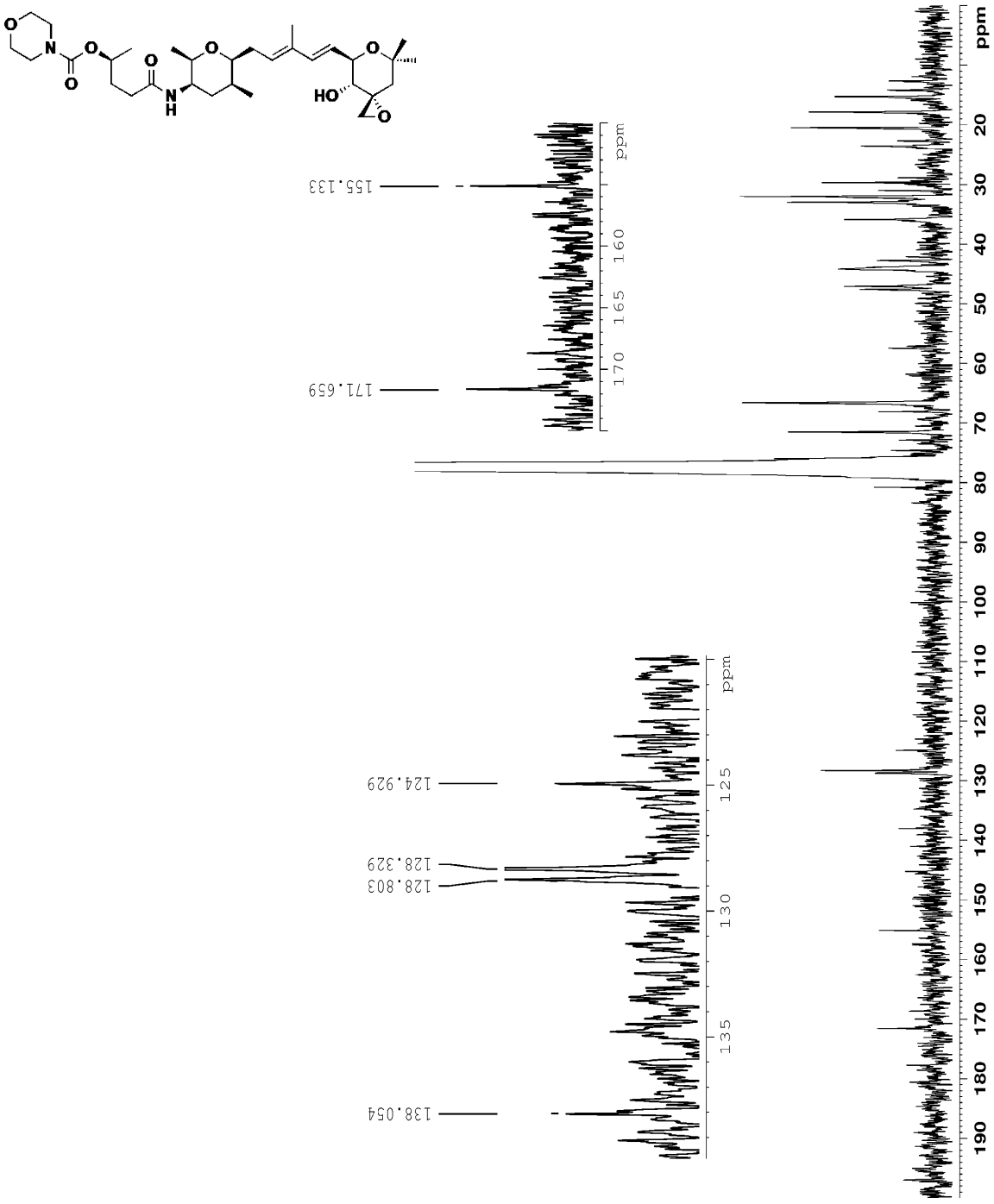

Spectrum 24. ^{13}C NMR spectrum of analogue **2.2** (150 MHz, $CDCl_3$, 293K)

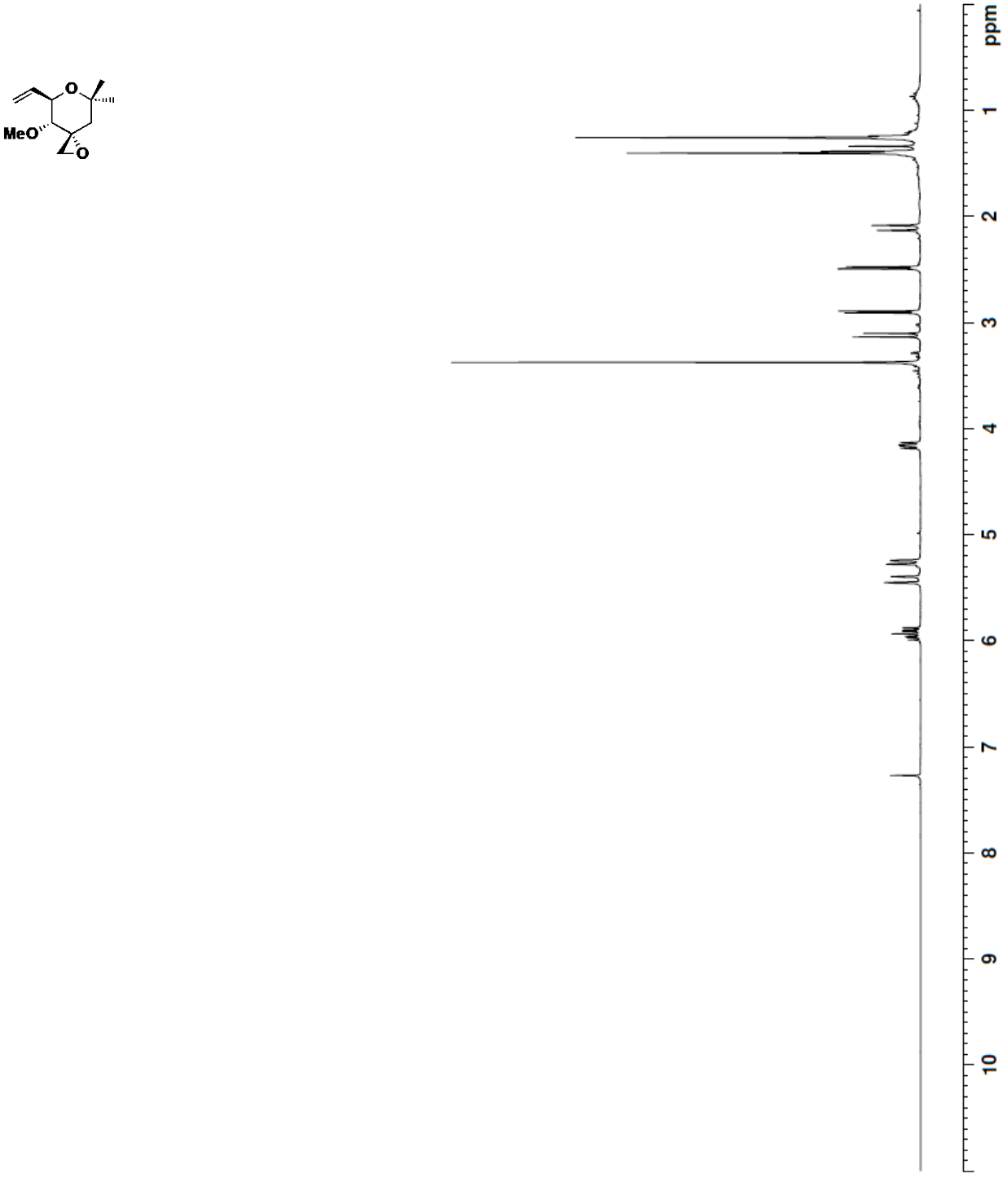

Spectrum 25. ^{1}H NMR spectrum of epoxide **2.18** (300 MHz, $CDCl_3$, 293K)

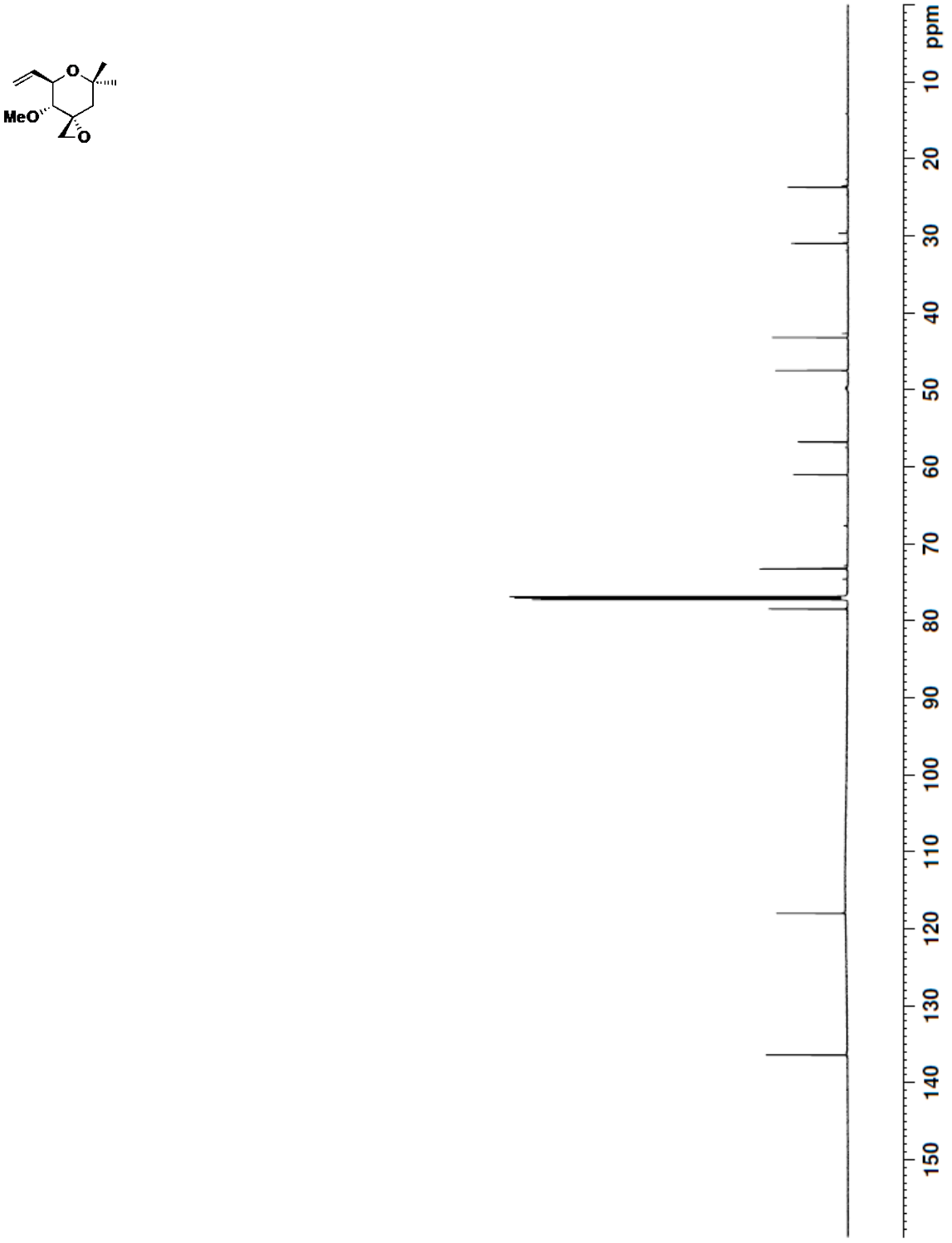

Spectrum 26. ^{13}C NMR spectrum of epoxide **2.18** (175 MHz, $CDCl_3$, 293K)

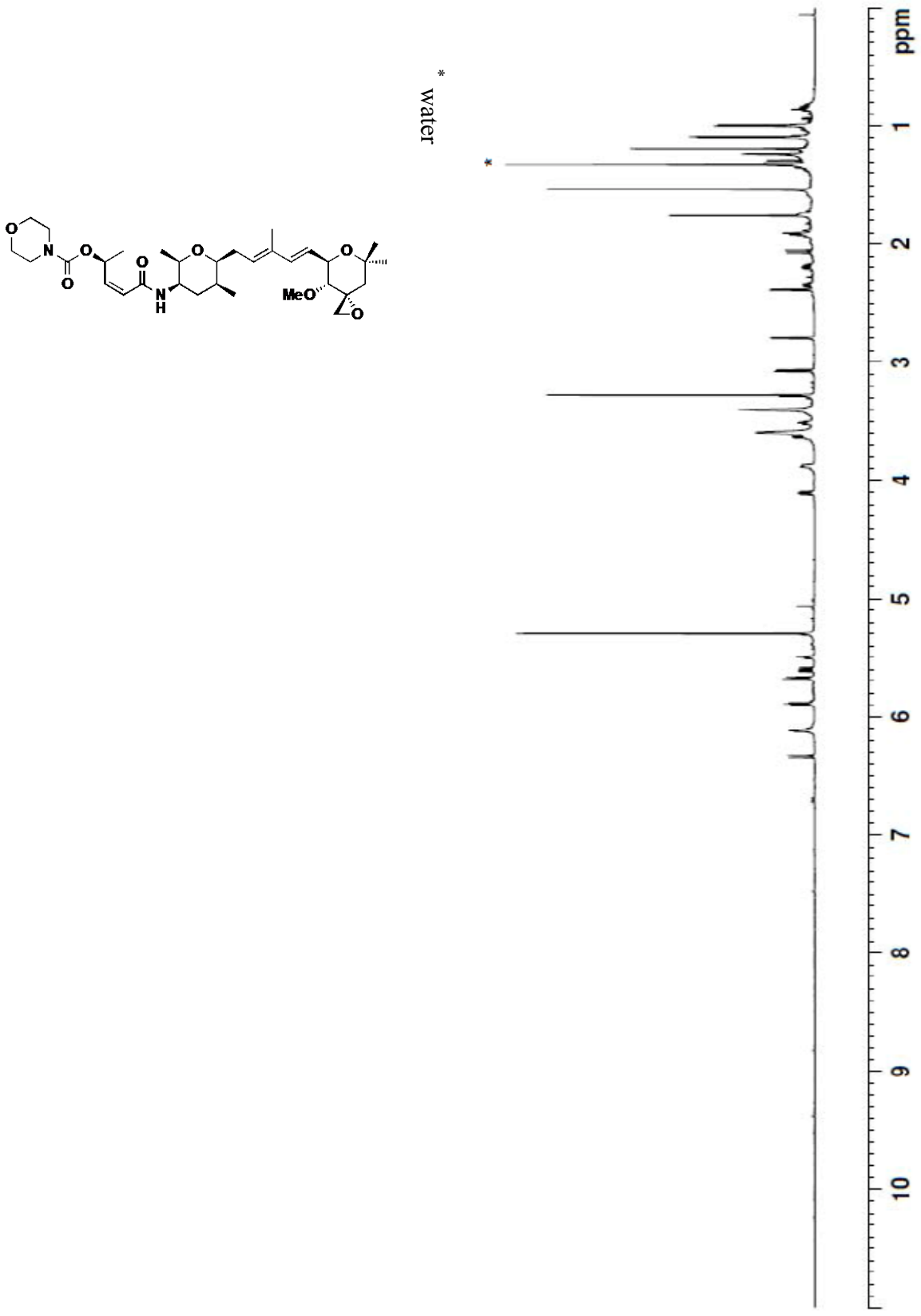

Spectrum 27. ^{1}H NMR spectrum of meayamycin C (**2.20**) (700 MHz, CD_2Cl_2, 293K)

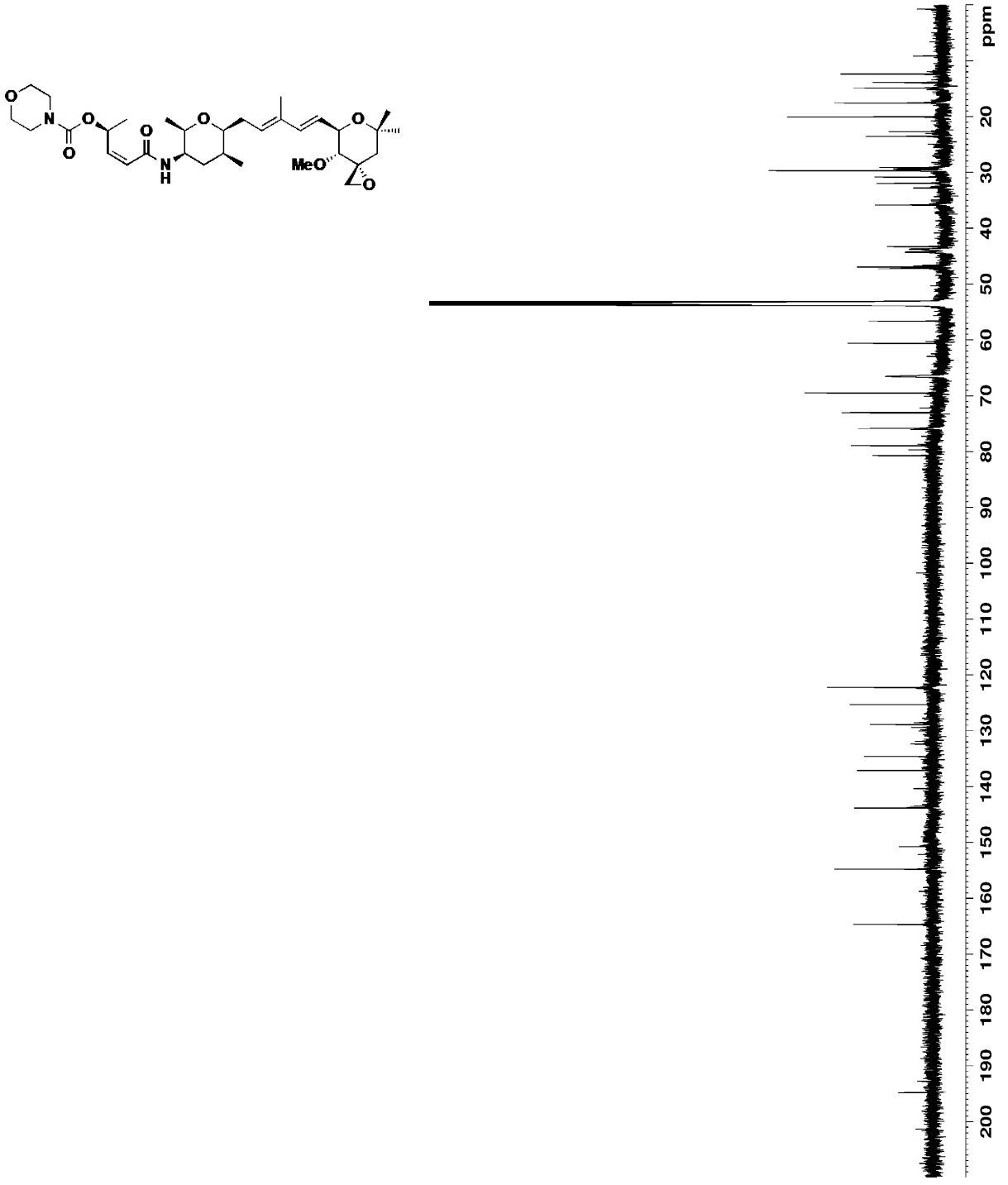

Spectrum 28. ^{13}C NMR spectrum of meayamycin C (**2.20**) (175 MHz, CD_2Cl_2, 293K)

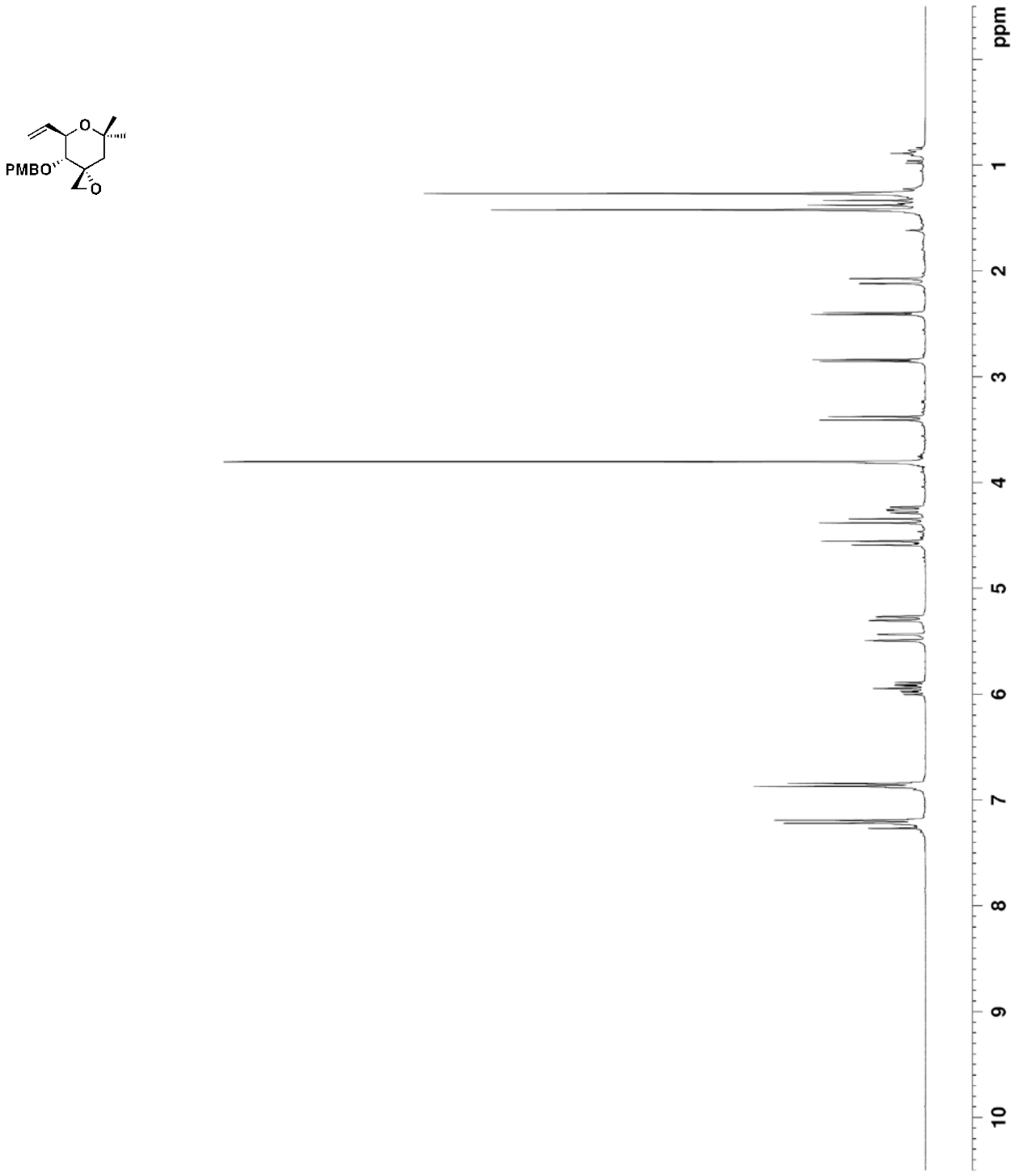

Spectrum 29. ^{1}H NMR spectrum of epoxide **2.24** (300 MHz, $CDCl_3$, 293K)

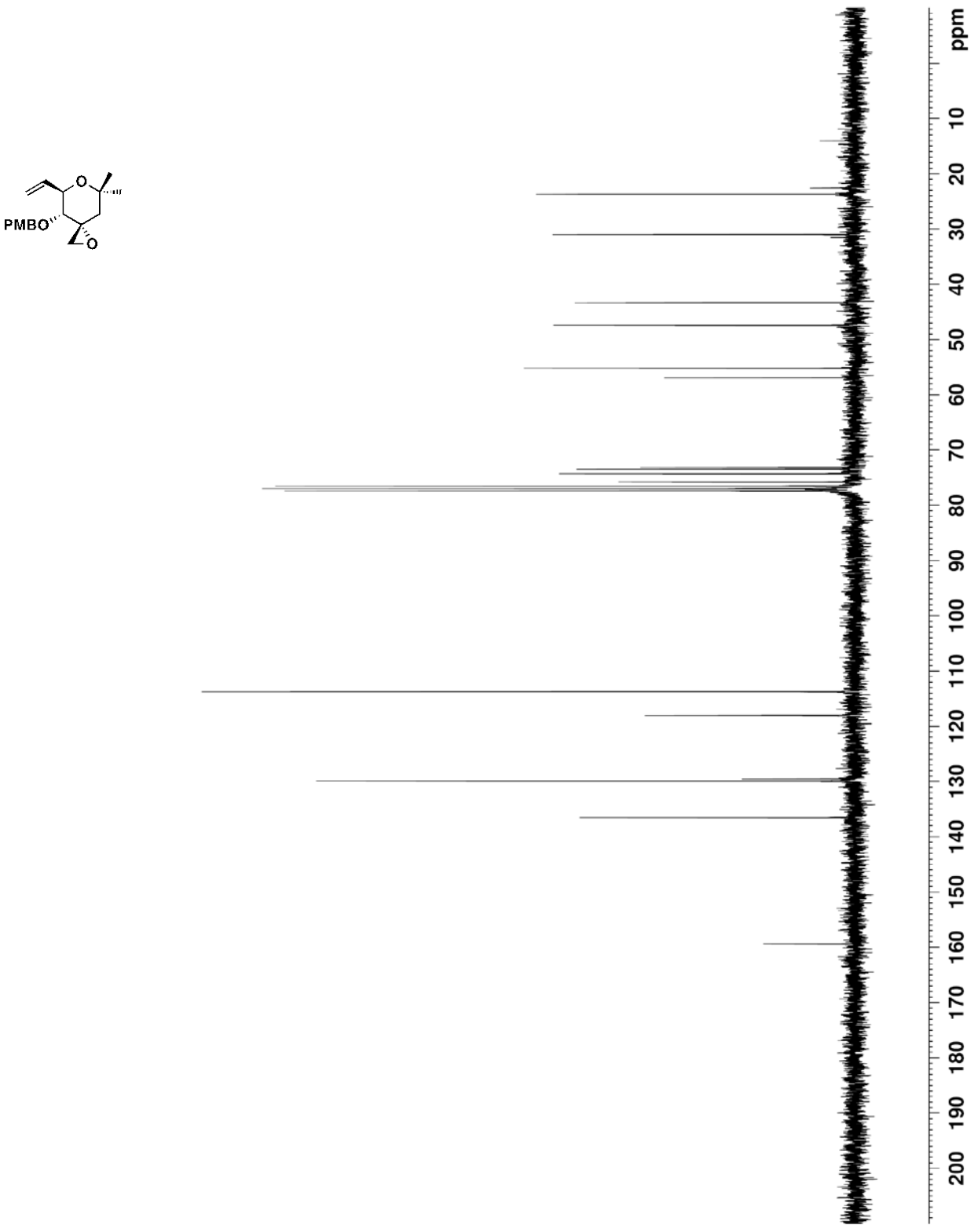

Spectrum 30. ^{13}C NMR spectrum of epoxide **2.24** (75 MHz, $CDCl_3$, 293K)

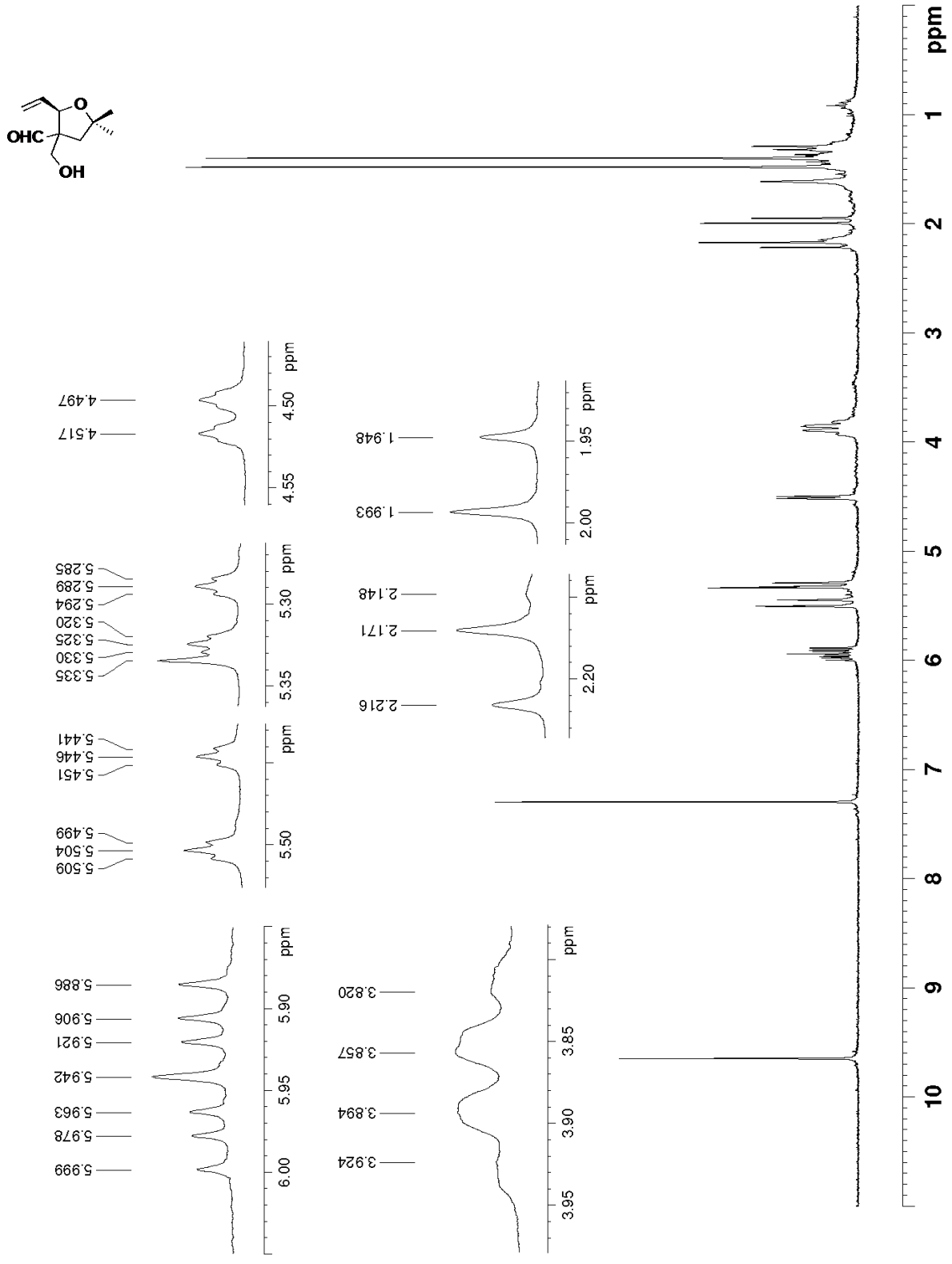

Spectrum 31. ^{1}H NMR spectrum of aldehyde **2.23** (300 MHz, $CDCl_3$, 293K)

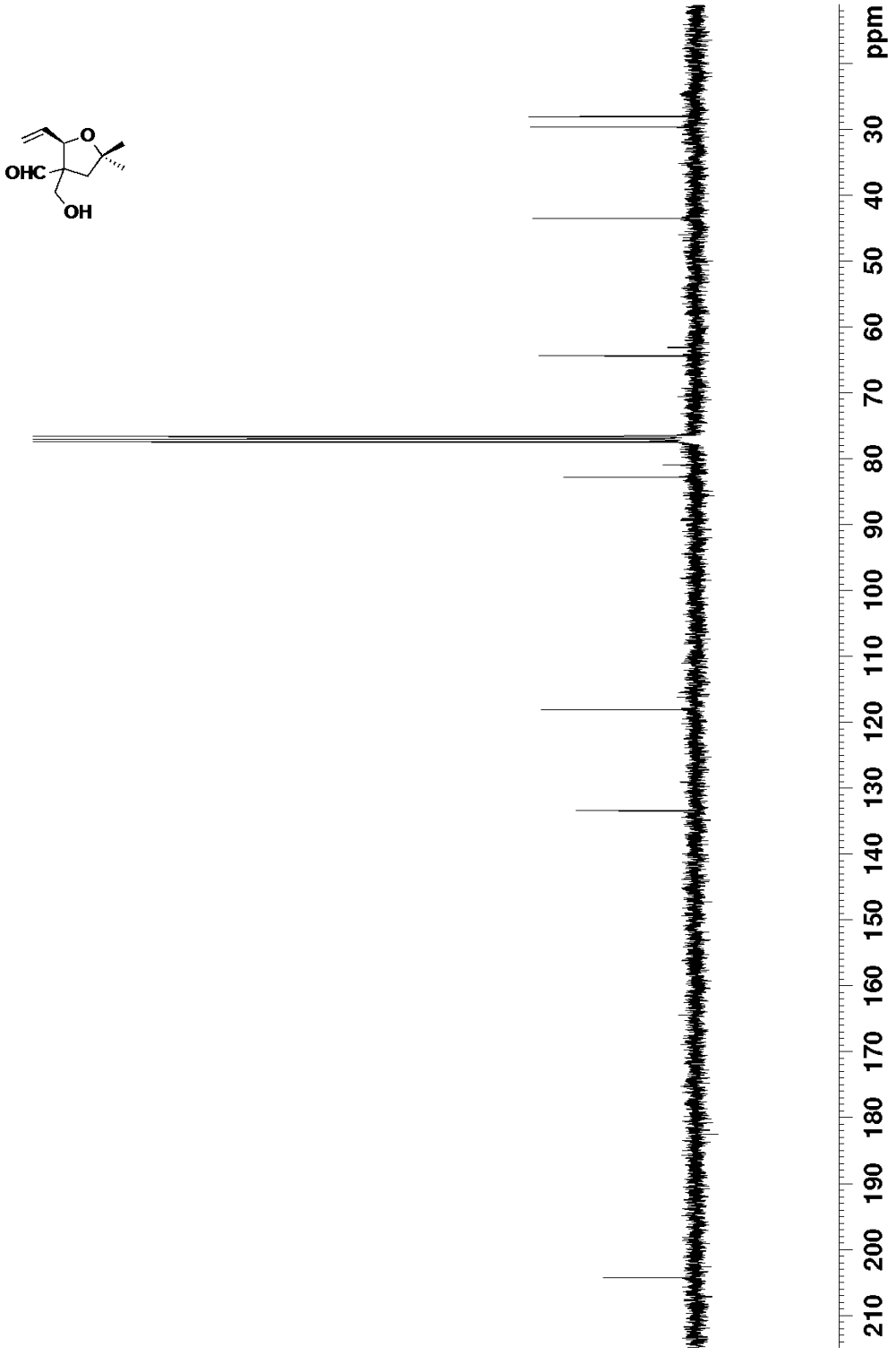

Spectrum 32. ^{13}C NMR spectrum of aldehyde **2.23** (75 MHz, $CDCl_3$, 293K)

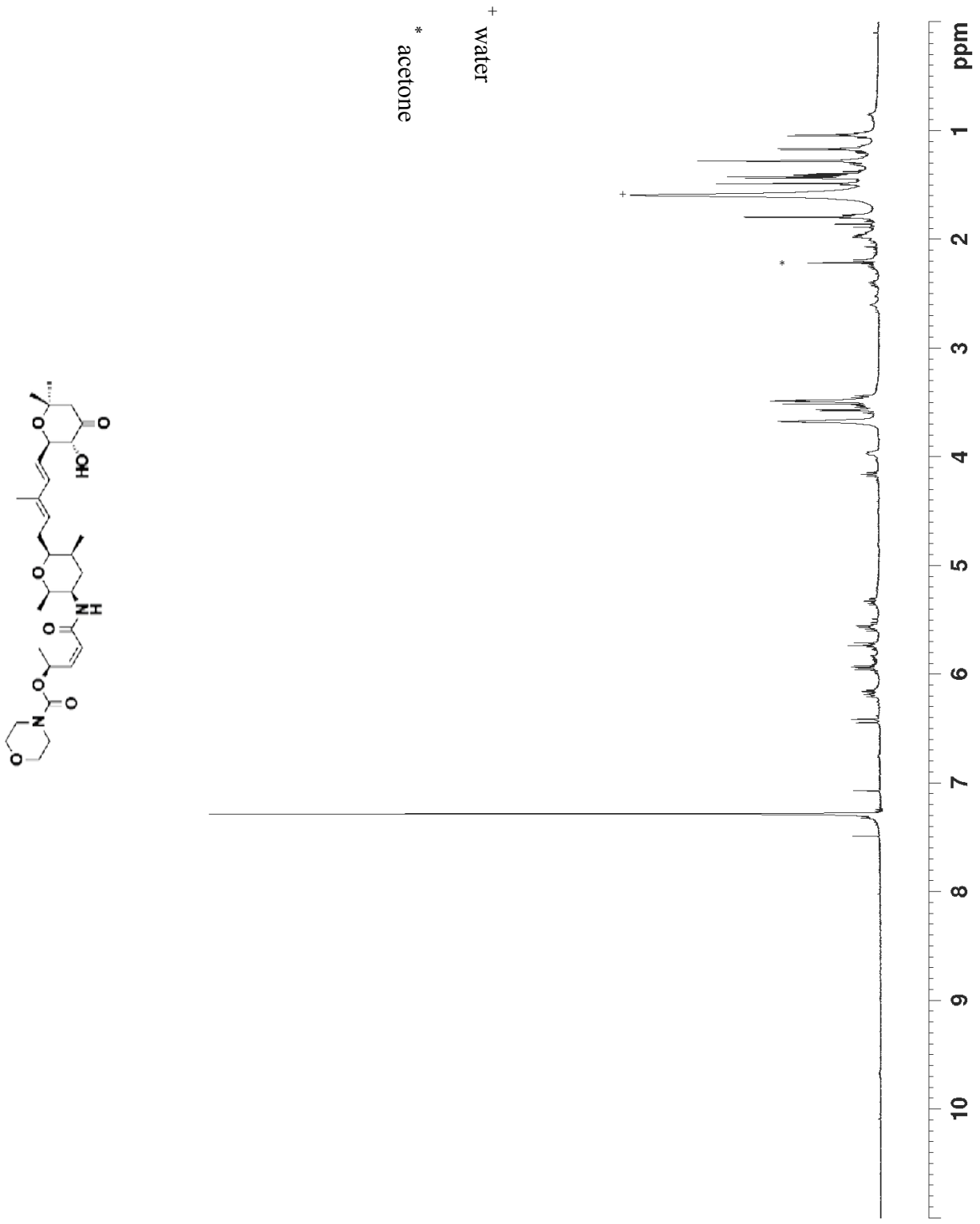

Spectrum 33. ^{1}H NMR spectrum of ketone **2.26** (500 MHz, 1% CD_3OD in $CDCl_3$, 293K)

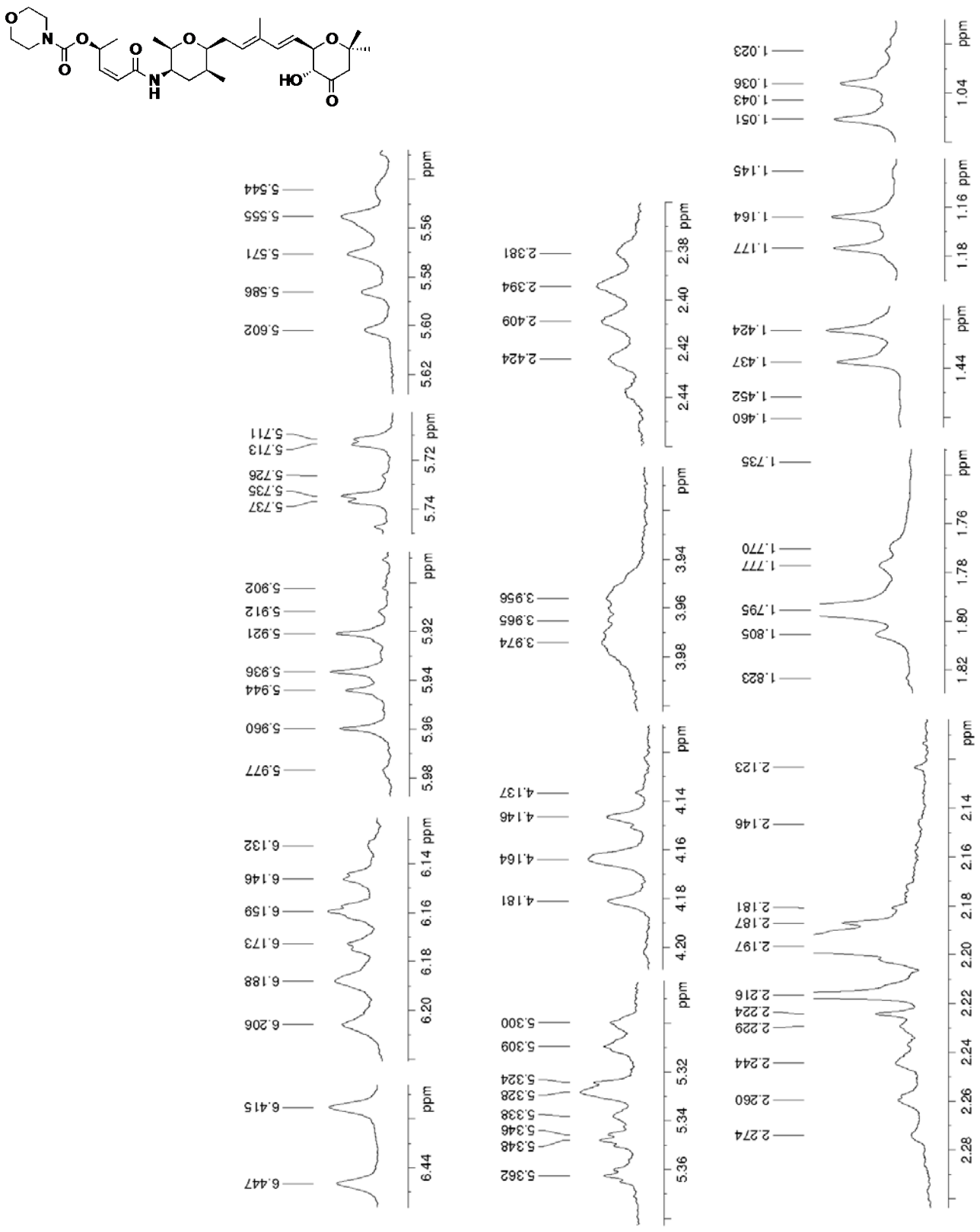

Spectrum 34. ^{1}H NMR spectrum of ketone **2.26** (500 MHz, 1% CD_3OD in $CDCl_3$, 293K)

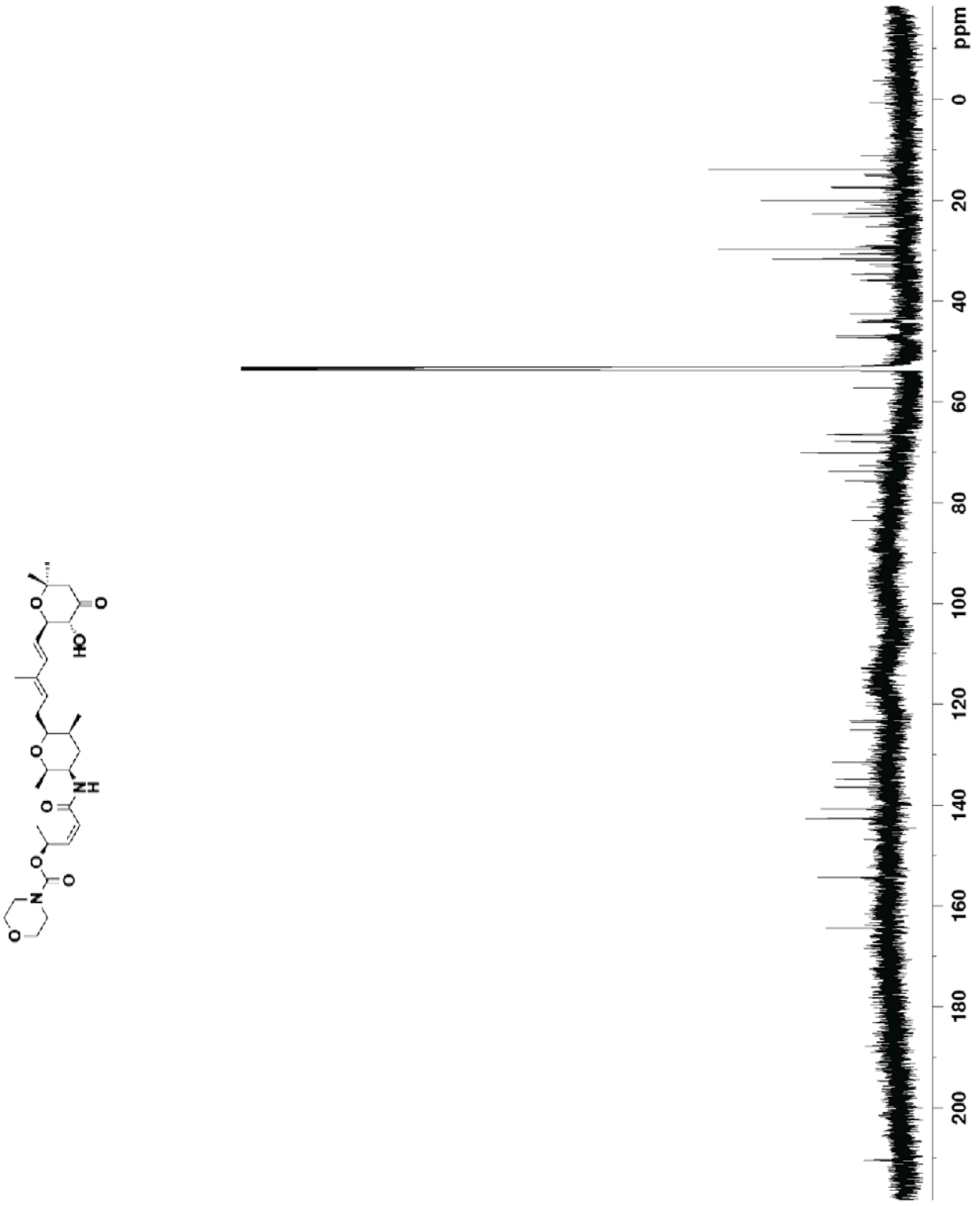

Spectrum 35. ^{13}C NMR spectrum of ketone **2.26** (100 MHz, CD_2Cl_2, 293K)

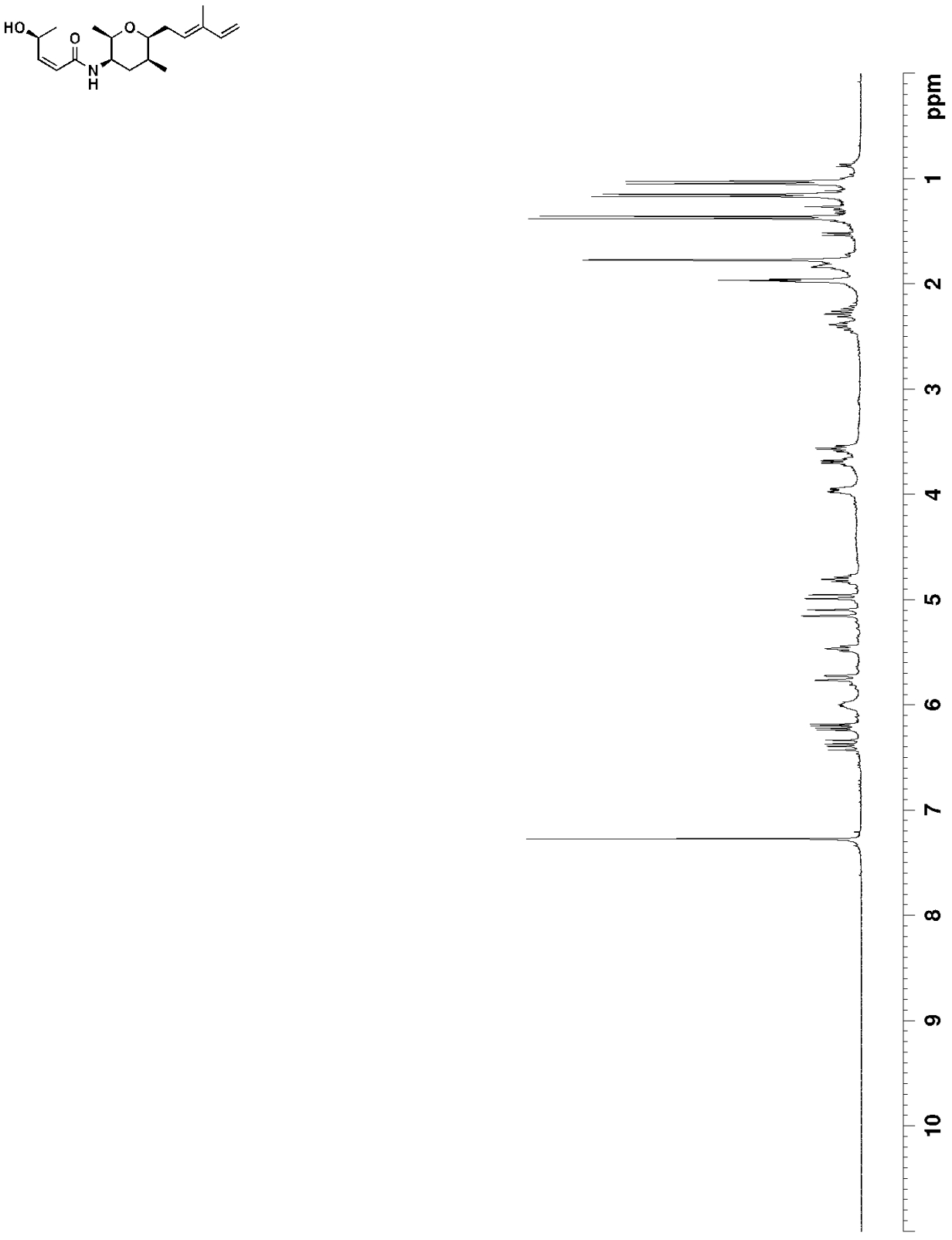

Spectrum 36. ^{1}H NMR spectrum of allylic alcohol **2.28** (500 MHz, $CDCl_3$, 293K)

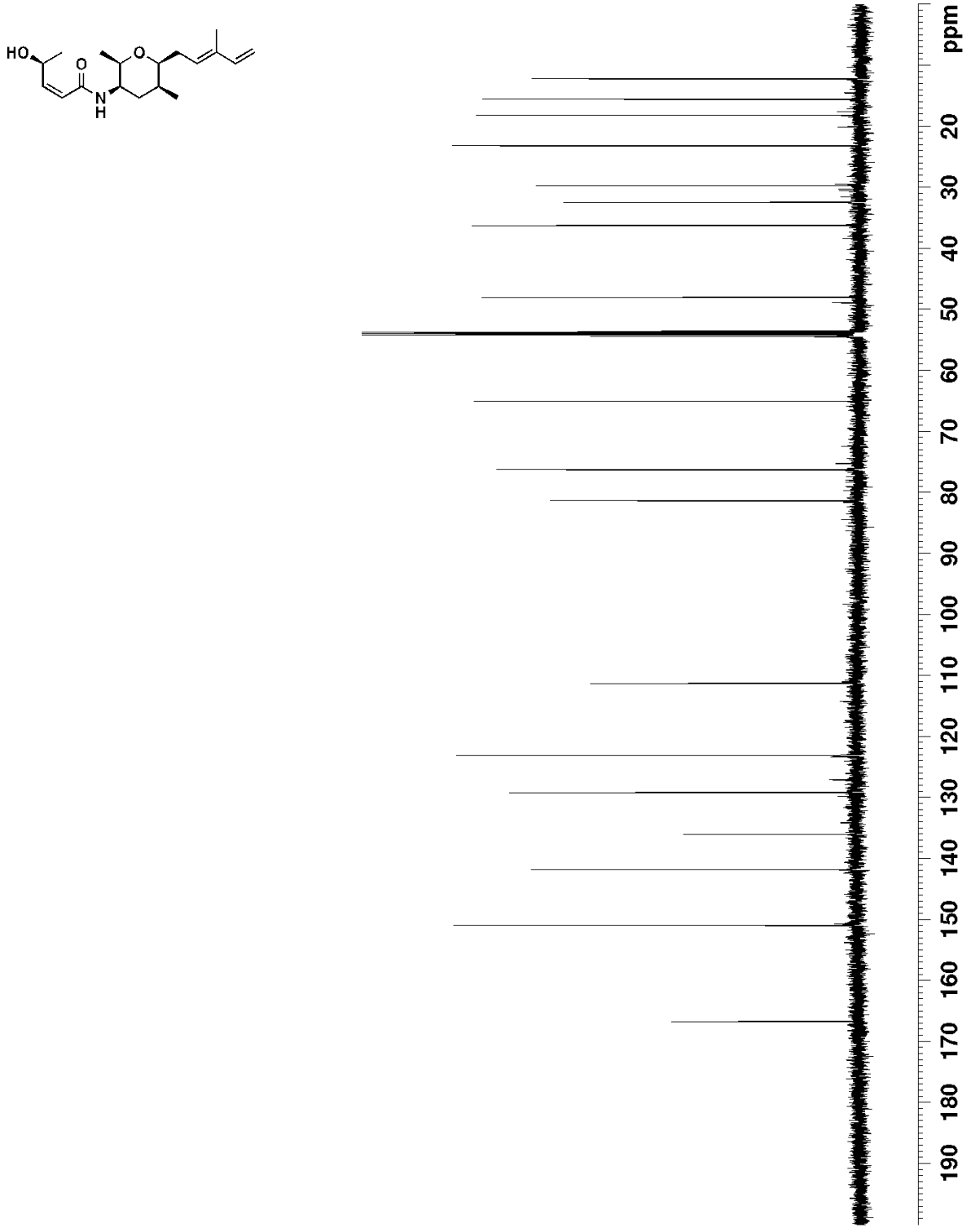

Spectrum 37. ^{13}C NMR spectrum of allylic alcohol **2.28** (125 MHz, CD_2Cl_2, 293K)

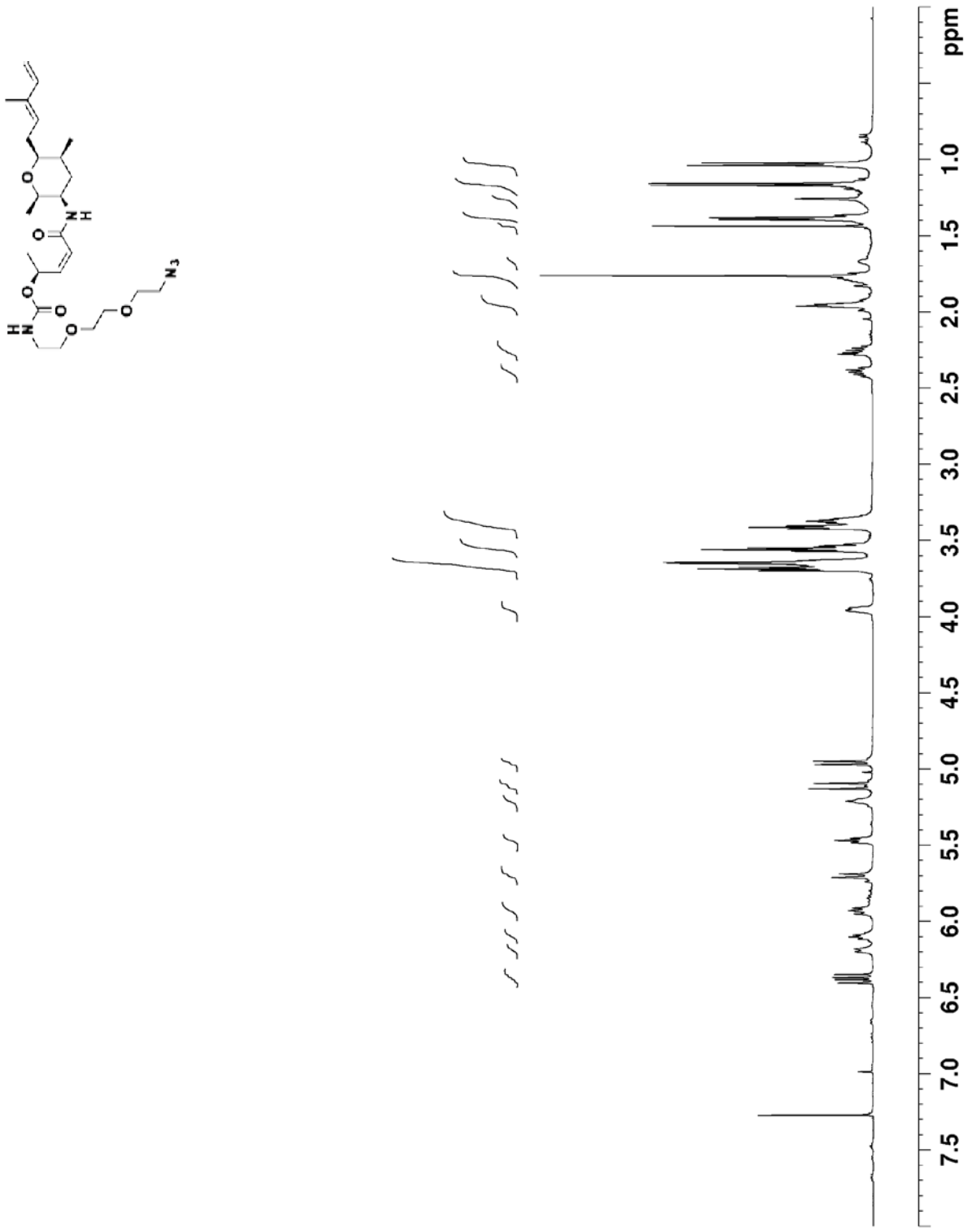

Spectrum 38. ^{1}H NMR spectrum of carbamate **2.30** (500 MHz, 1% CD_3OD in $CDCl_3$, 293K)

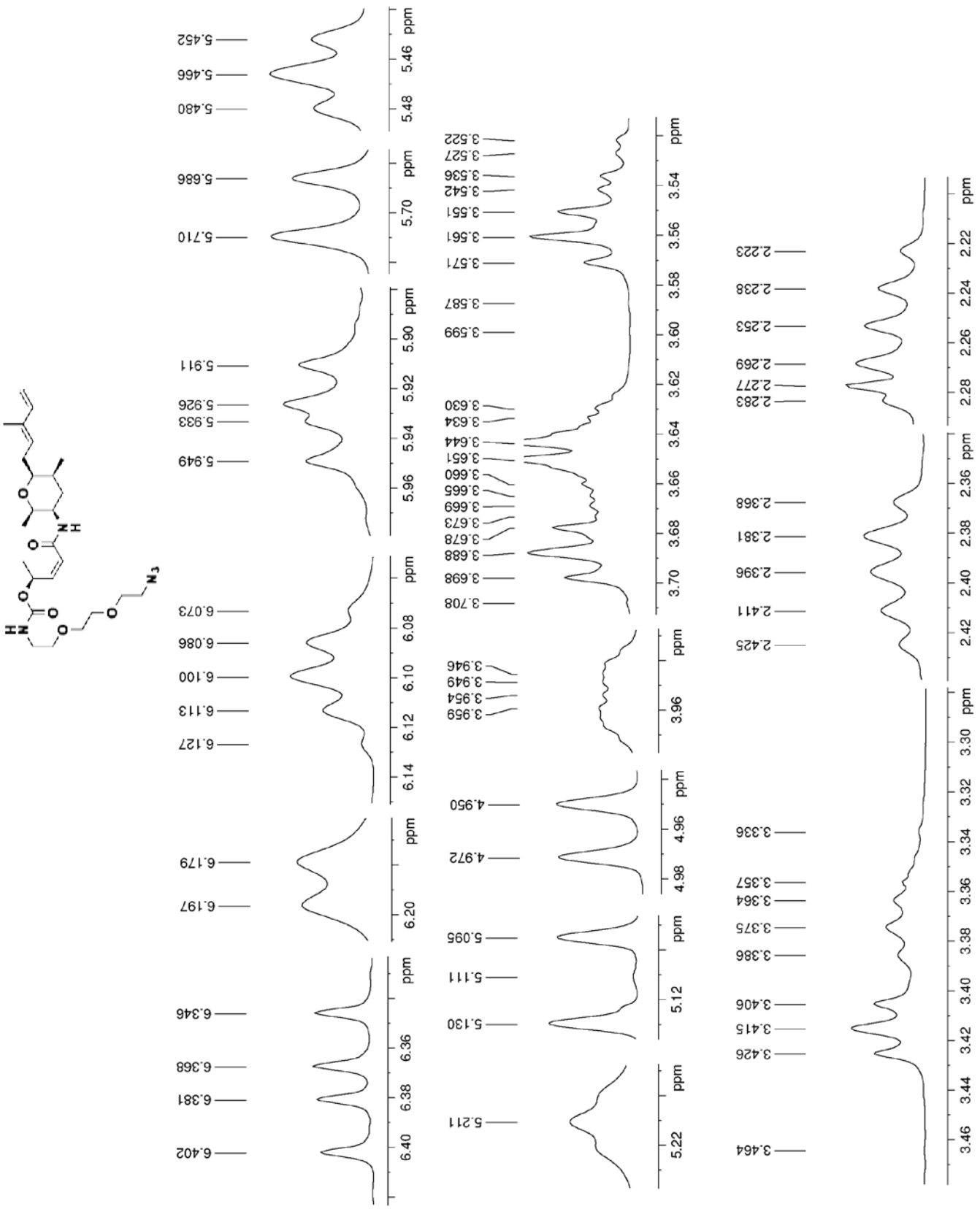

Spectrum 39. ^{1}H NMR spectrum of carbamate **2.30** (500 MHz, 1% CD_3OD in $CDCl_3$, 293K)

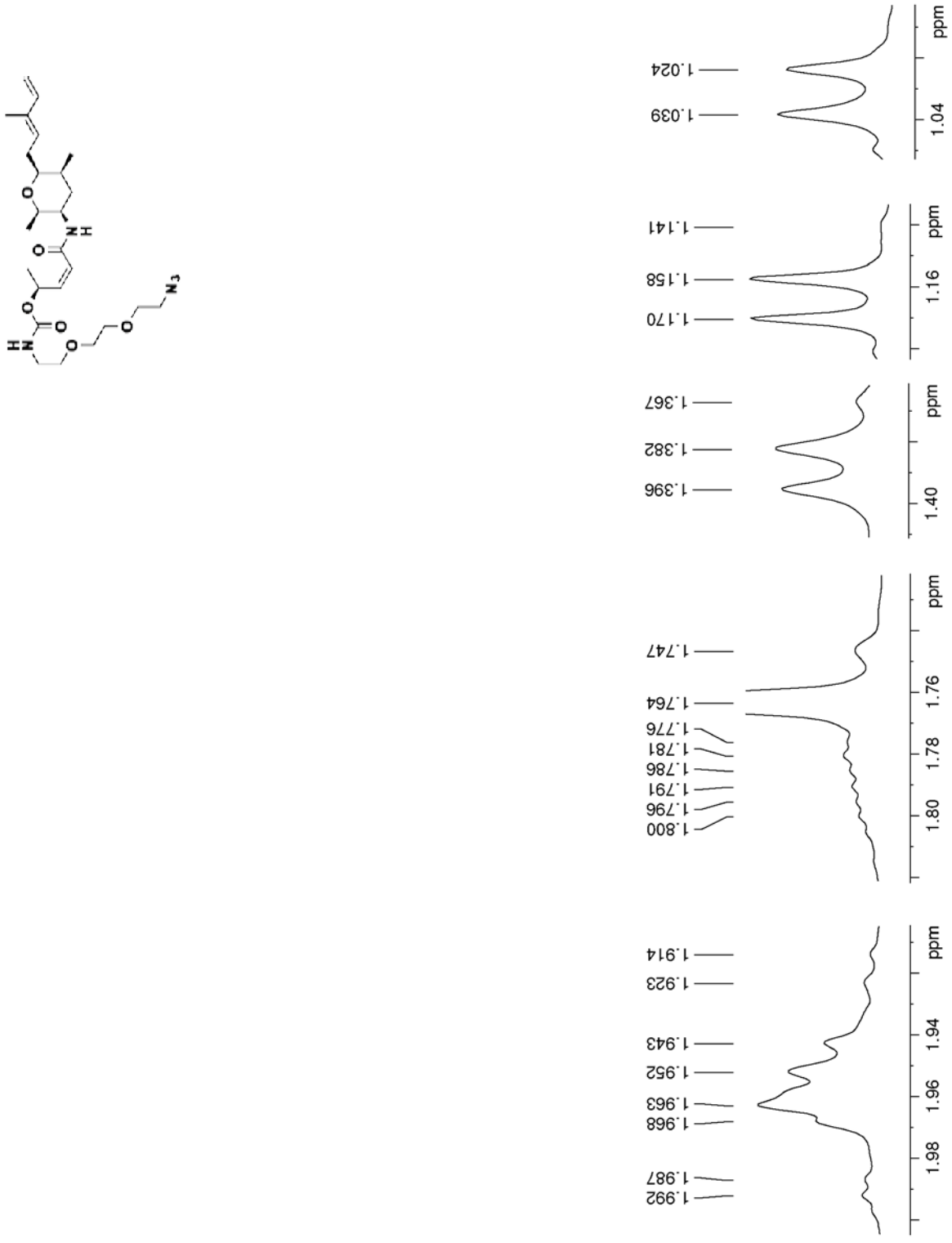

Spectrum 40. ^{1}H NMR spectrum of carbamate **2.30** (500 MHz, 1% CD_3OD in $CDCl_3$, 293K)

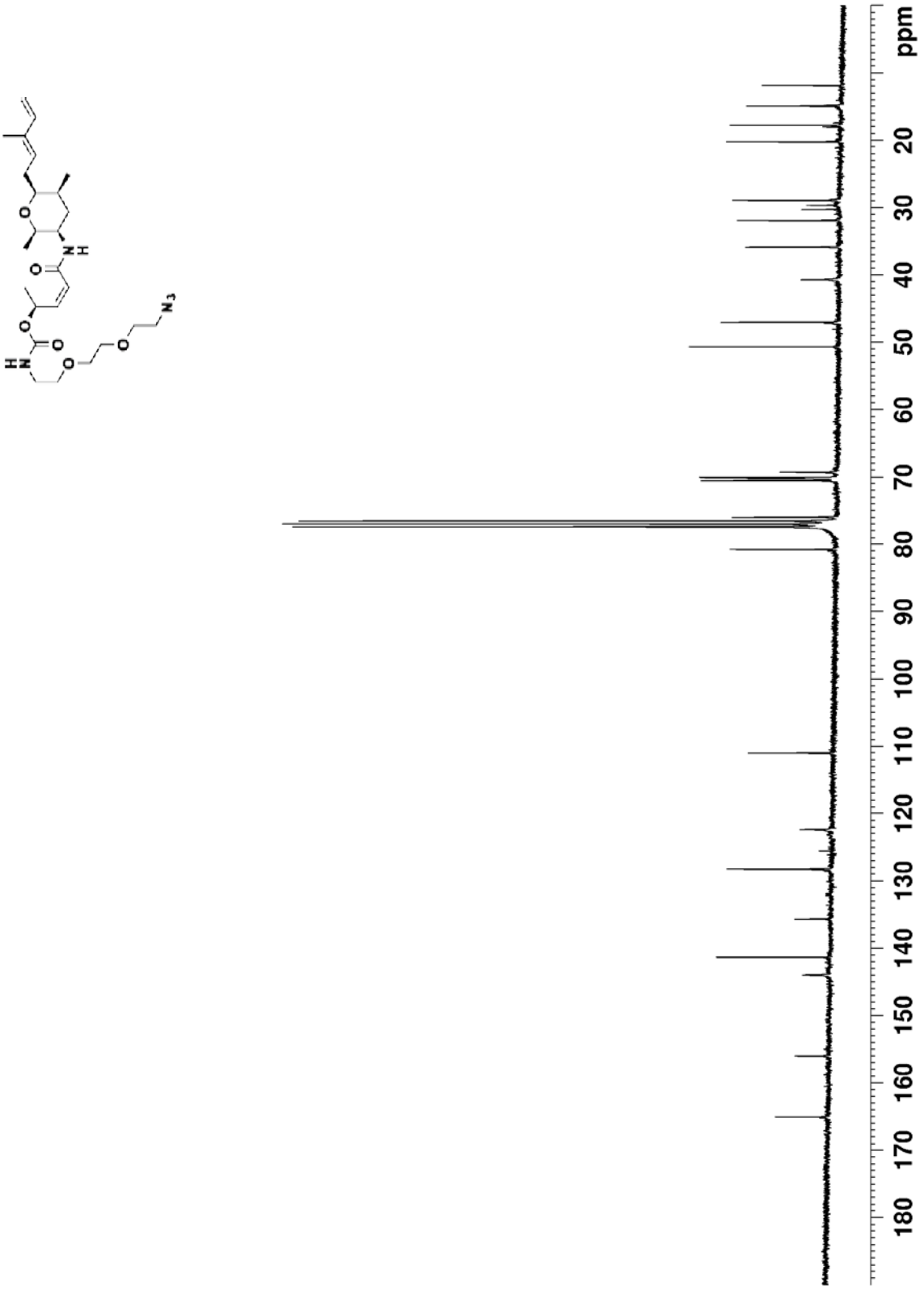

Spectrum 41. ^{13}C NMR spectrum of carbamate **2.30** (75 MHz, $CDCl_3$, 293K)

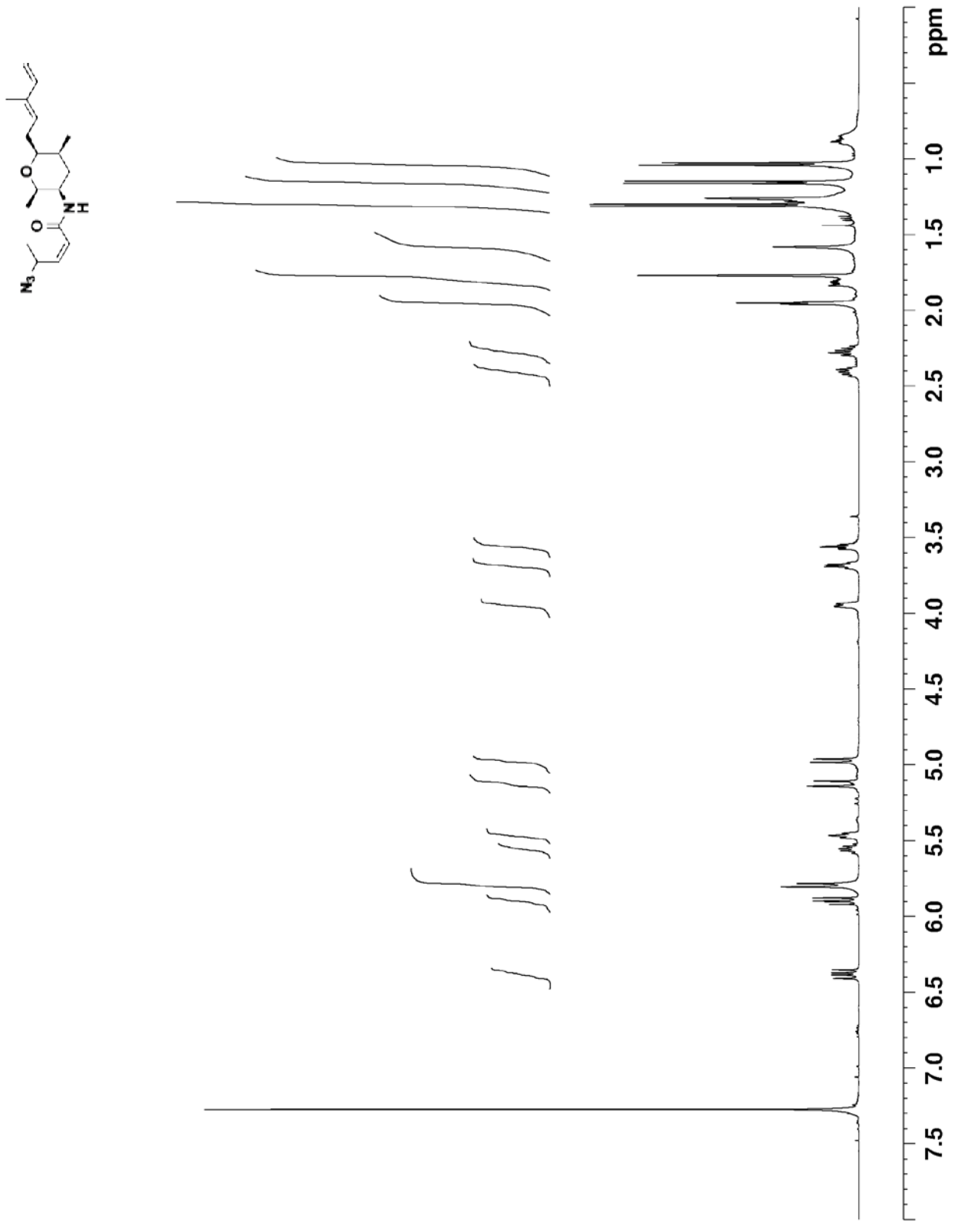

Spectrum 42. ^{1}H NMR spectrum of azide **2.33** (500 MHz, $CDCl_3$, 293K)

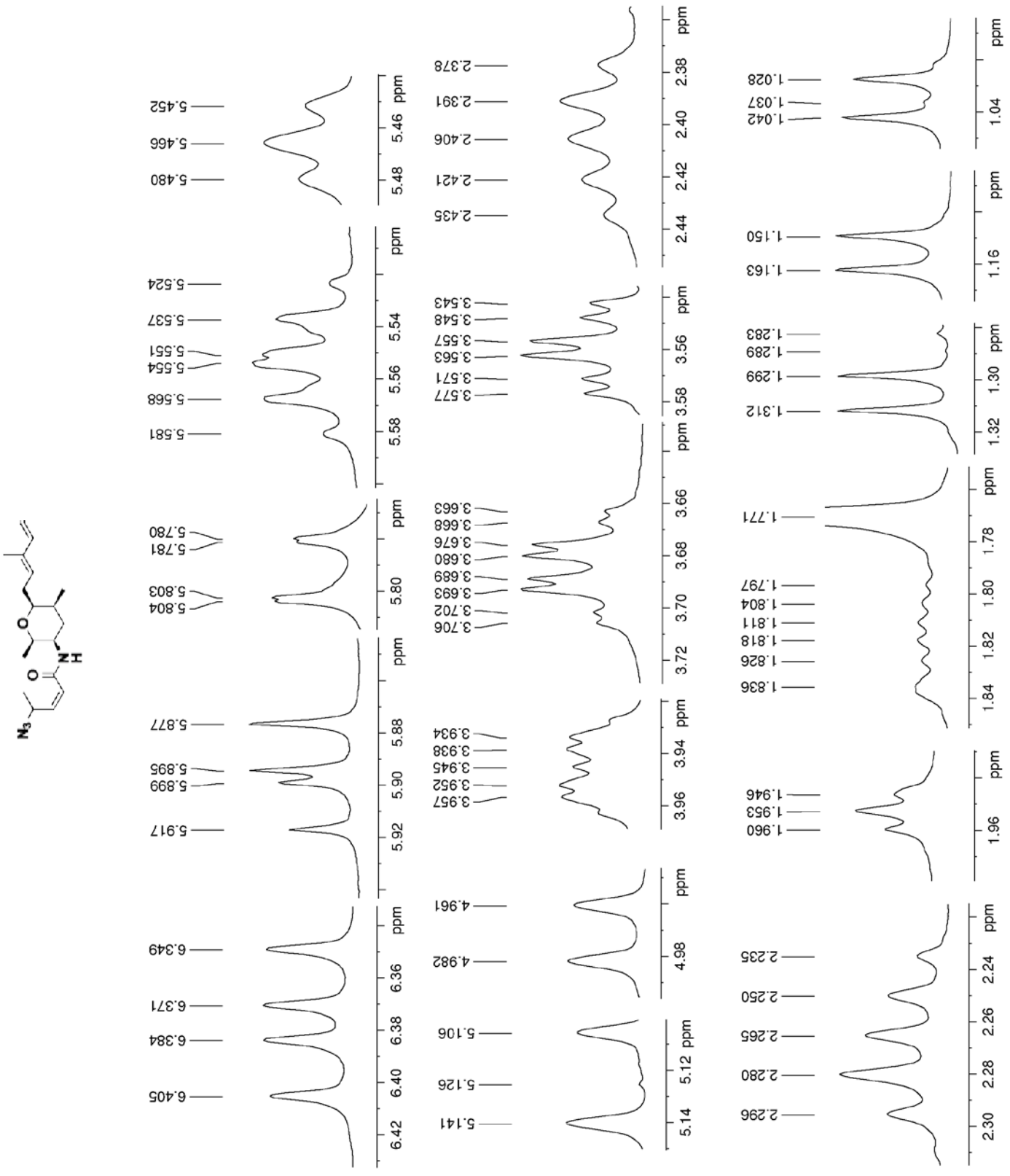

Spectrum 43. ^{1}H NMR spectrum of azide **2.33** (500 MHz, $CDCl_3$, 293K)

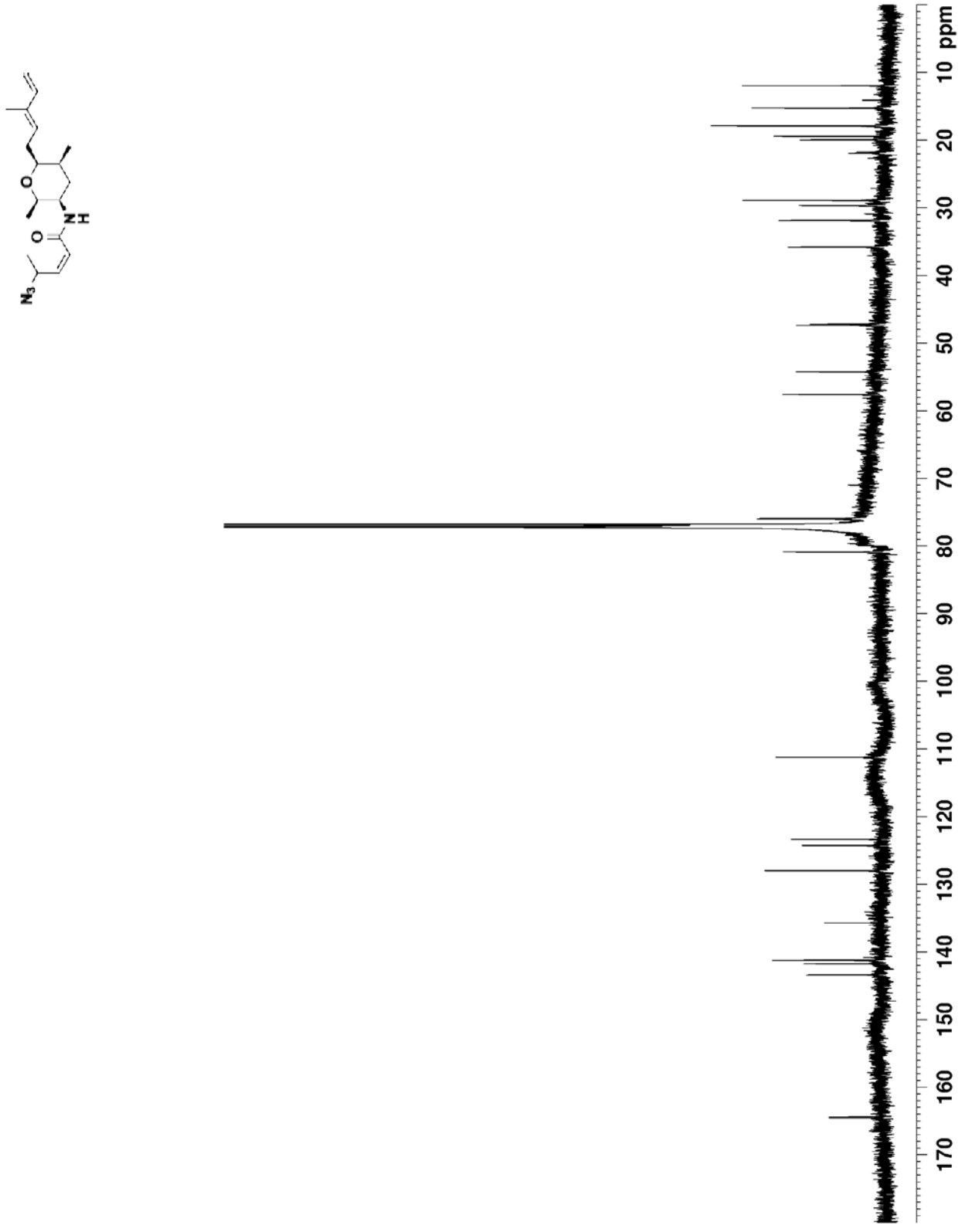

Spectrum 44. ^{13}C NMR spectrum of azide **2.33** (150 MHz, $CDCl_3$, 293K)

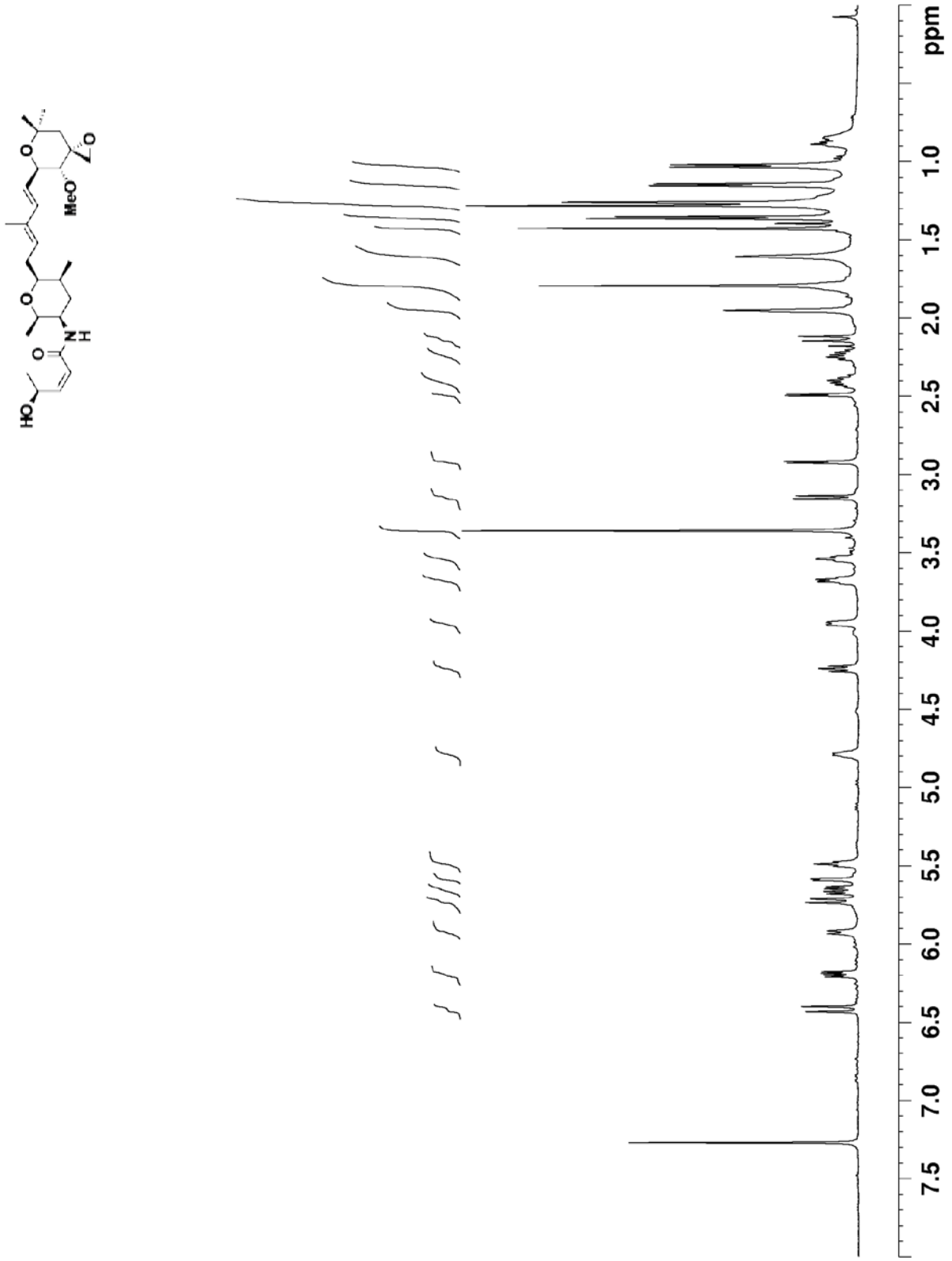

Spectrum 45. ^{1}H NMR spectrum of 4'-desacetyl meayamycin C **2.39** (500 MHz, 1% CD_3OD in $CDCl_3$, 293K)

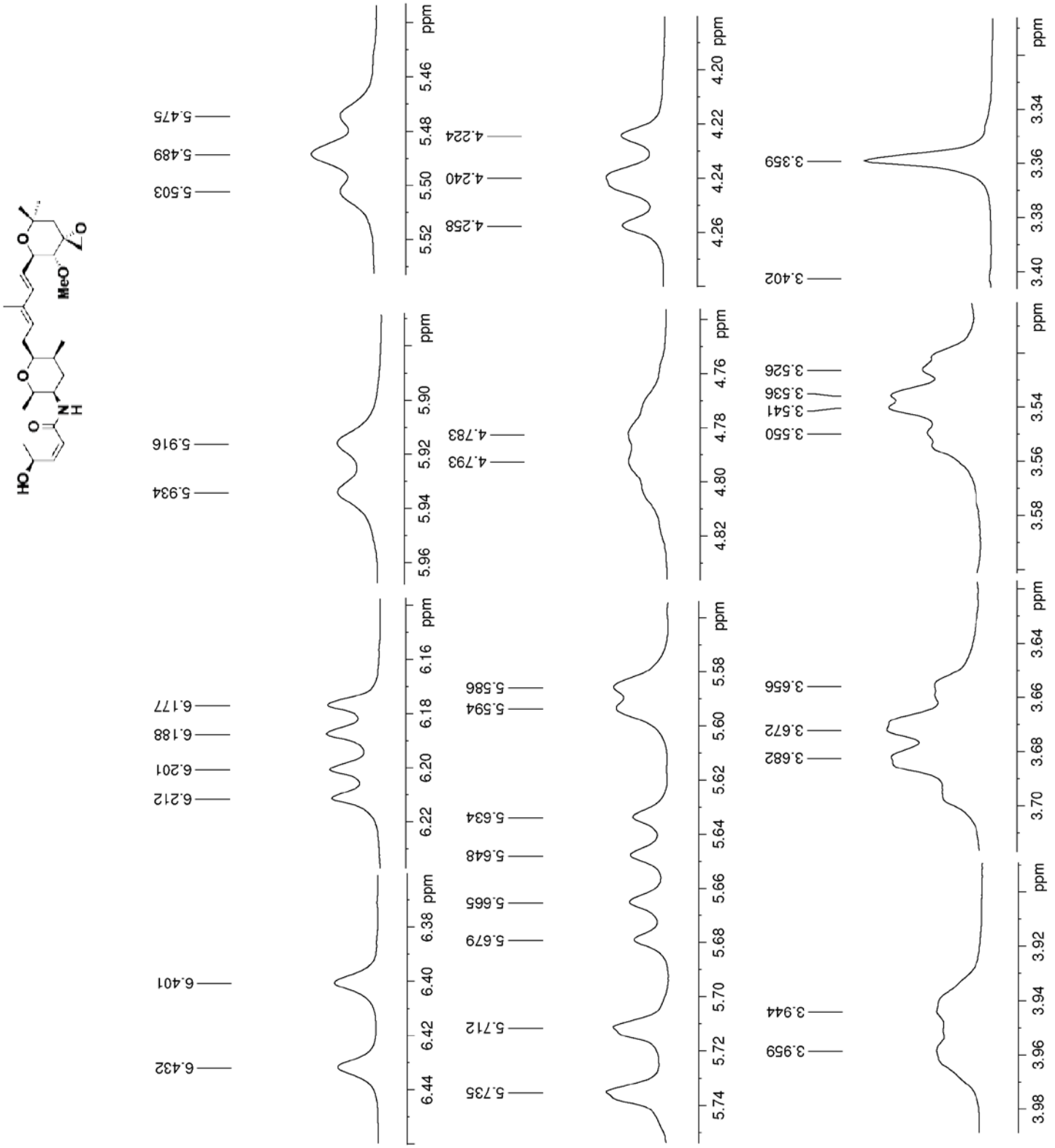

Spectrum 46. ^{1}H NMR spectrum of 4'-desacetyl meayamycin C **2.39** (500 MHz, 1% CD_3OD in $CDCl_3$, 293K)

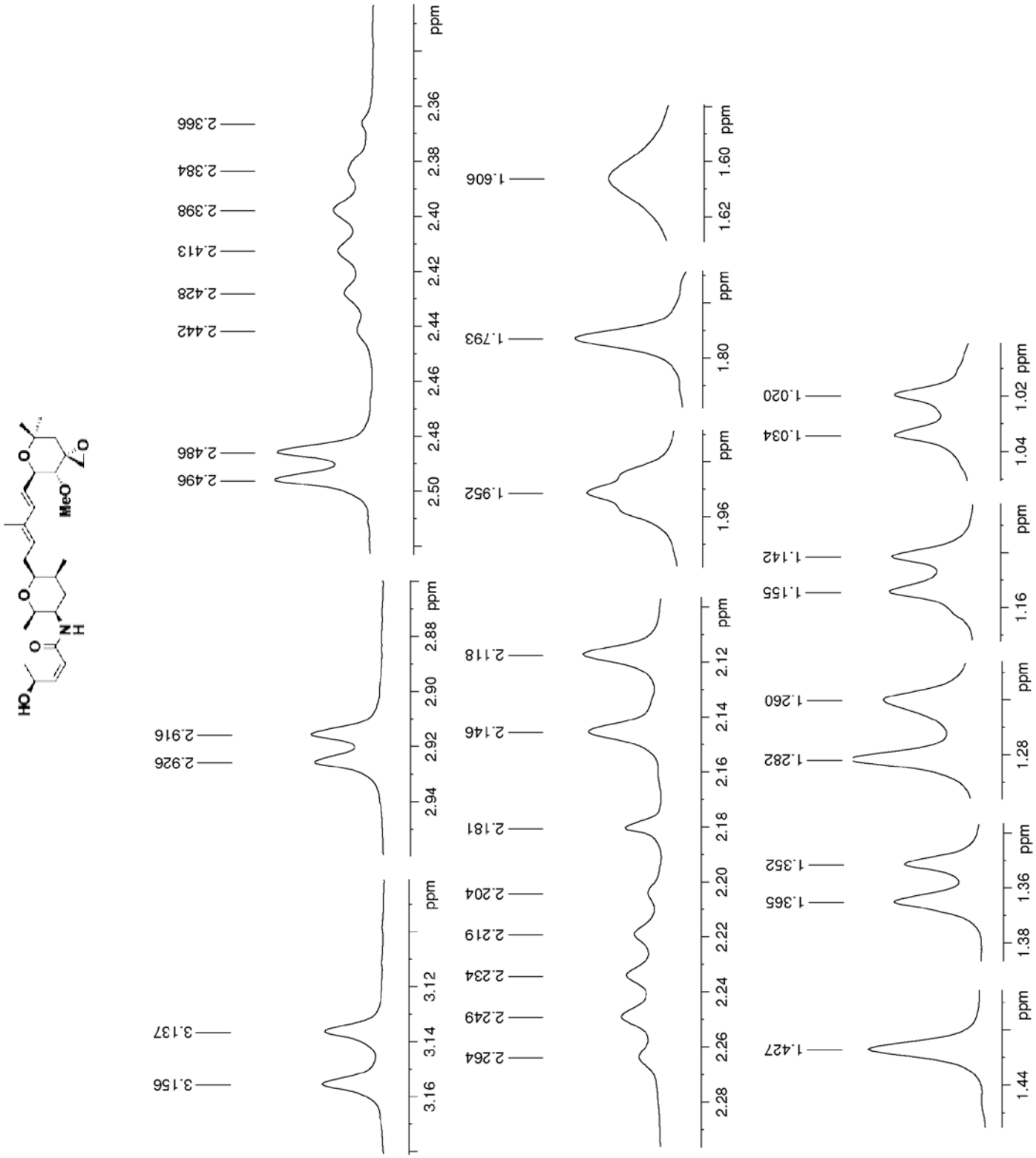

Spectrum 47. ^{1}H NMR spectrum of 4'-desacetyl meayamycin C **2.39** (500 MHz, 1% CD_3OD in $CDCl_3$, 293K)

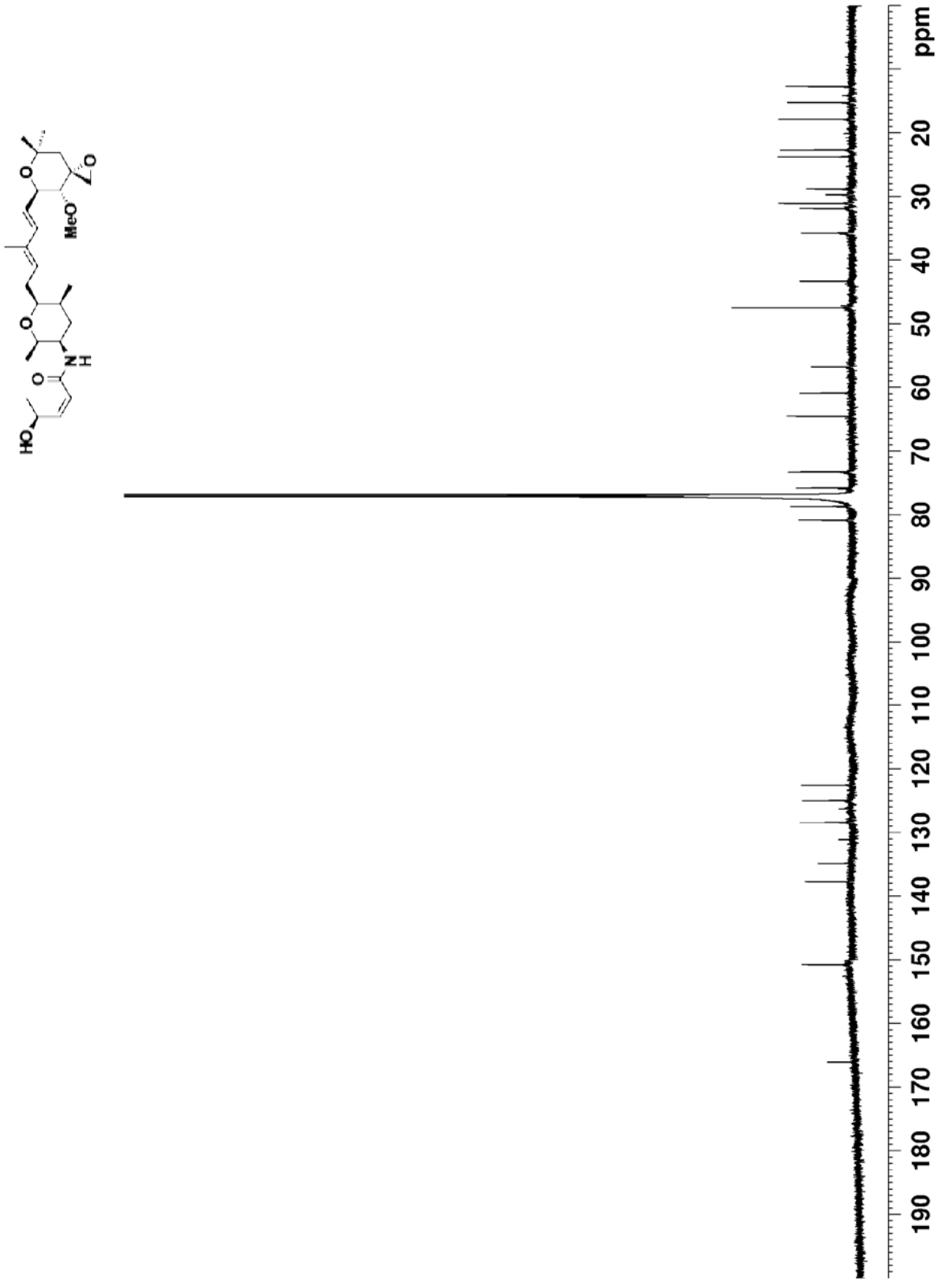

Spectrum 48. ^{13}C NMR spectrum of 4'-desacetyl meayamycin C **2.39** (150 MHz, $CDCl_3$, 293K)

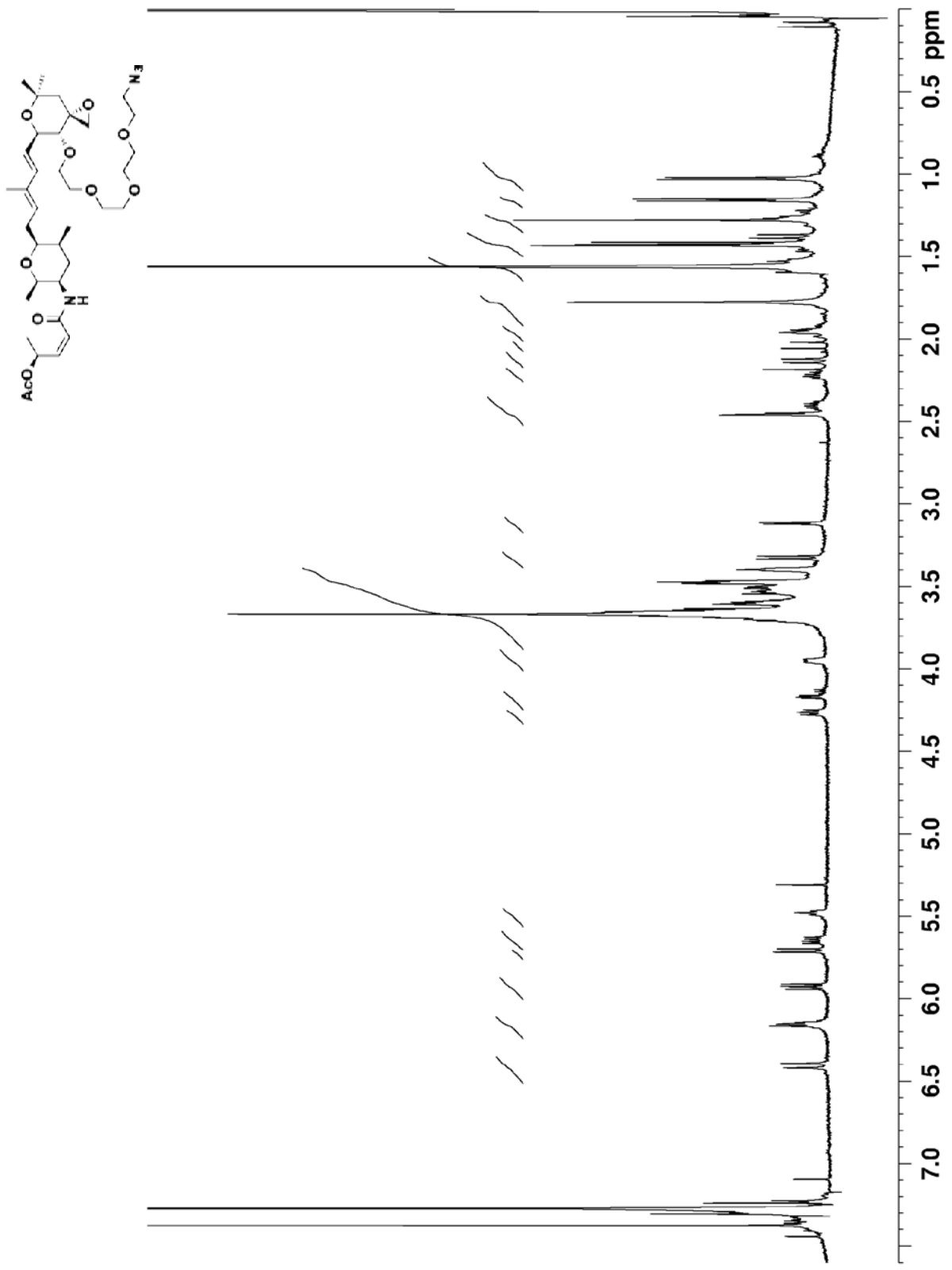

Spectrum 49. ^{1}H NMR spectrum of 4-TEGylated meayamycin **2.43** (500 MHz, $CDCl_3$, 293K)

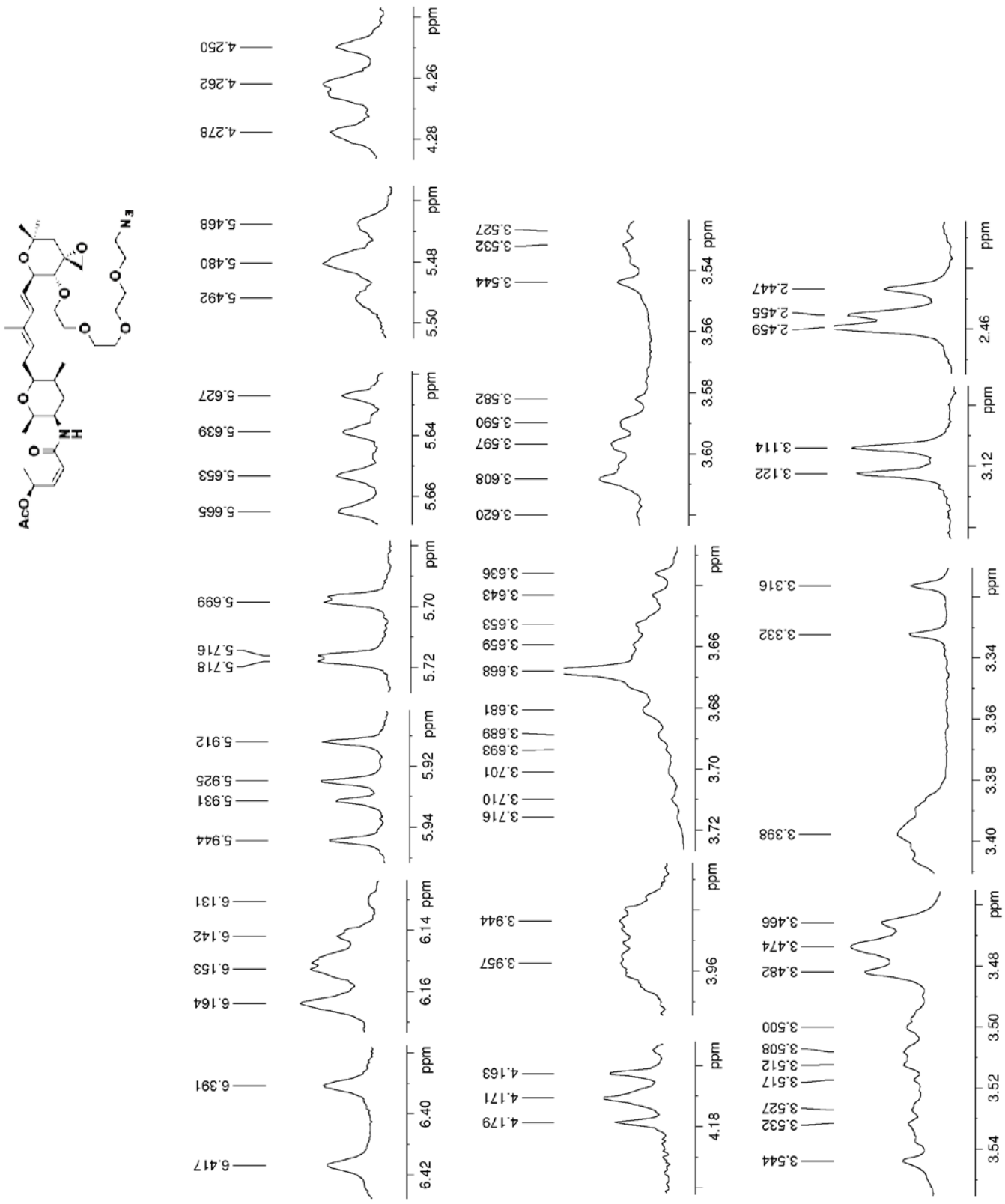

Spectrum 50. ^{1}H NMR spectrum of 4-TEGylated meayamycin **2.43** (500 MHz, $CDCl_3$, 293K)

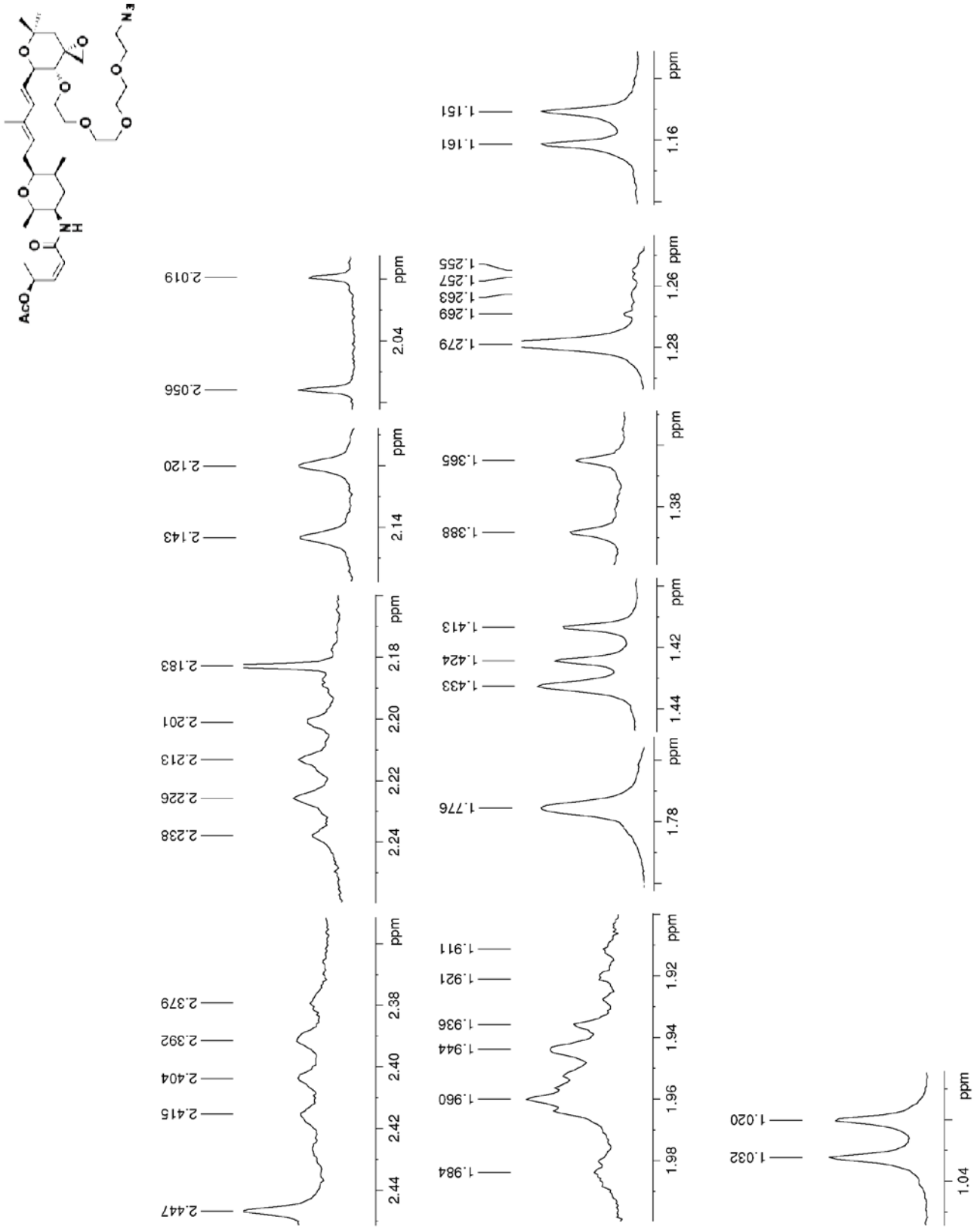

Spectrum 51. ^{1}H NMR spectrum of 4-TEGylated meayamycin **2.43** (500 MHz, $CDCl_3$, 293K)

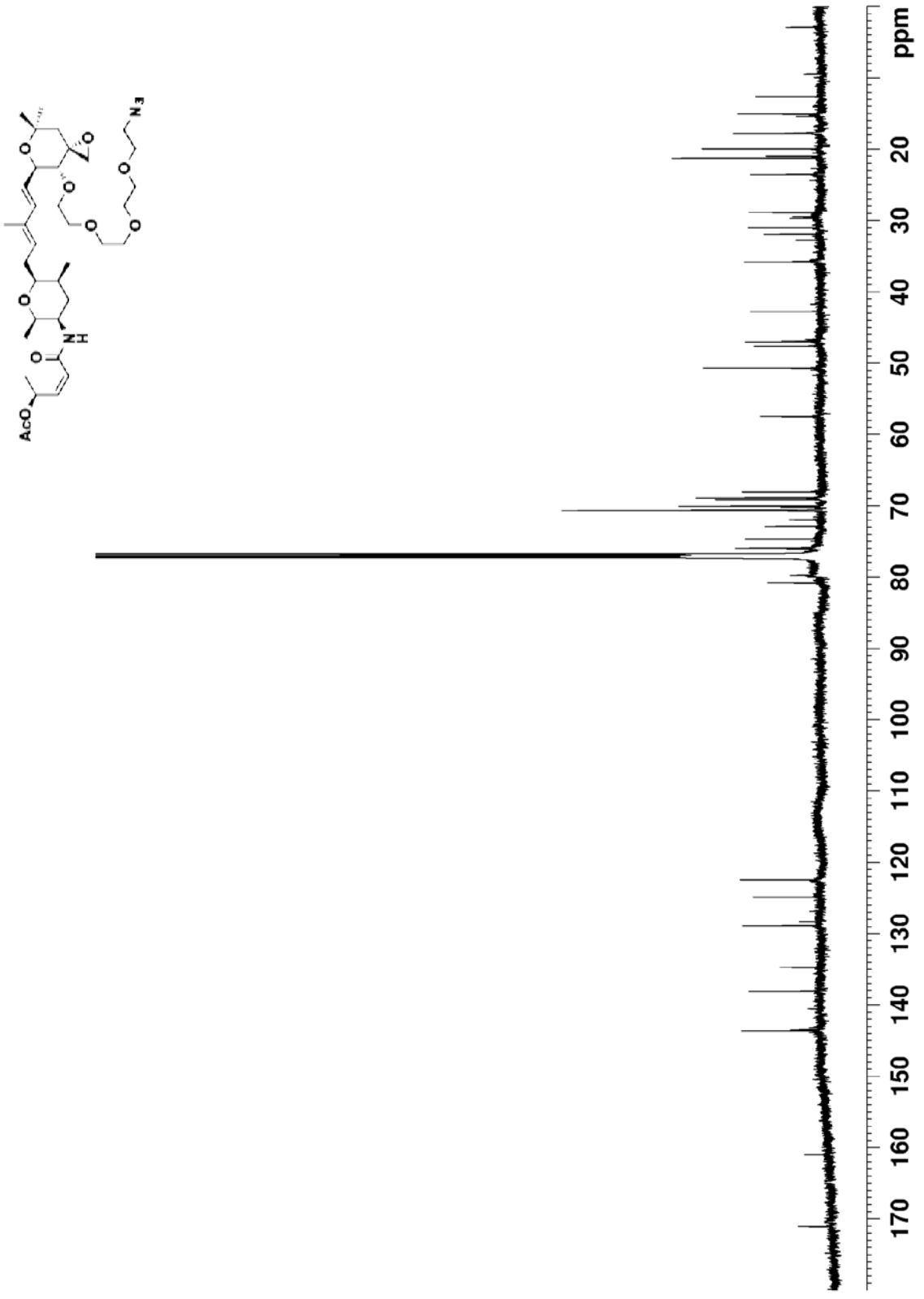

Spectrum 52. ^{13}C NMR spectrum of 4-TEGylated meayamycin **2.43** (125 MHz, $CDCl_3$, 293K)

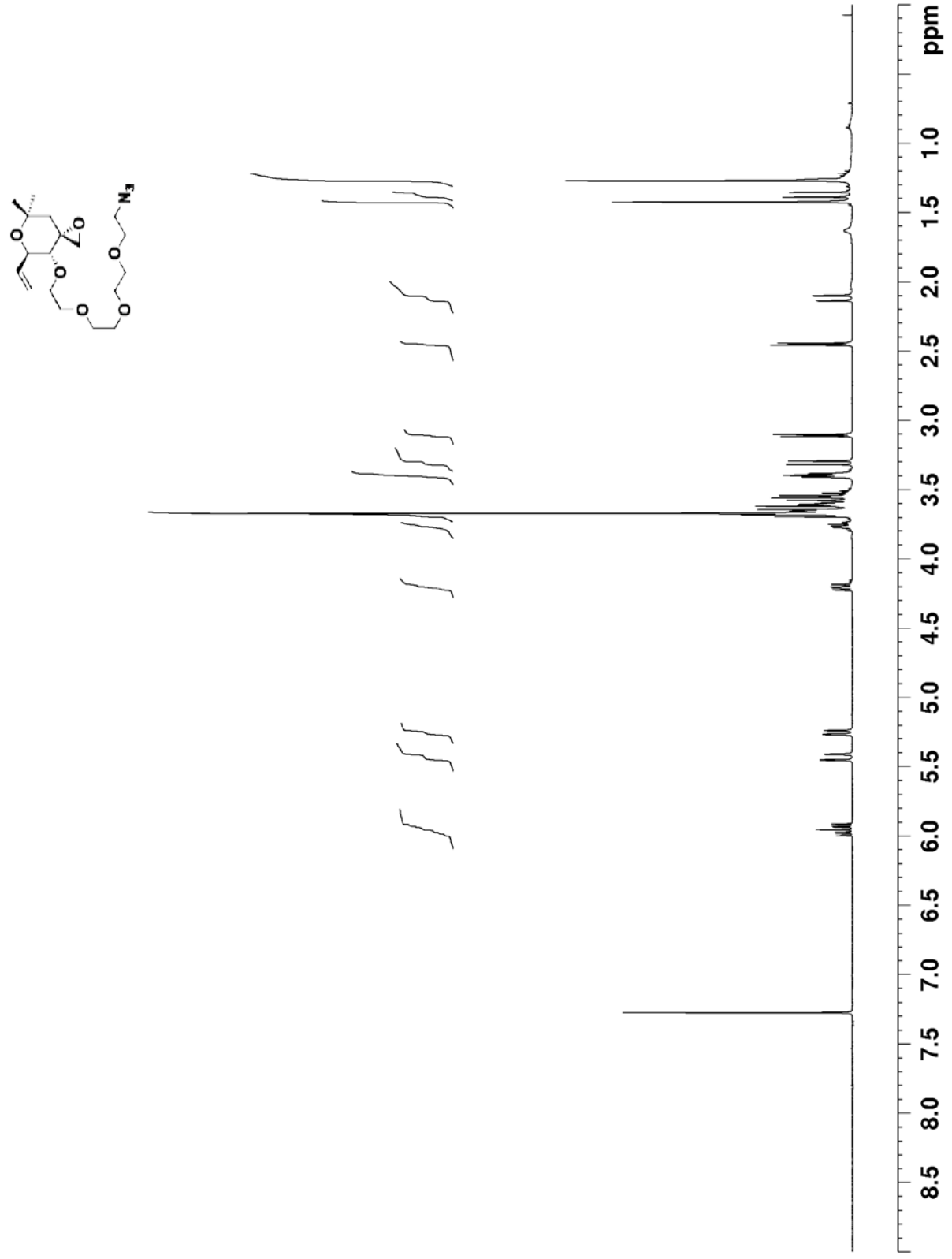

Spectrum 53. ^{1}H NMR spectrum of TEGylated right fragment **2.44** (400 MHz, $CDCl_3$, 293K)

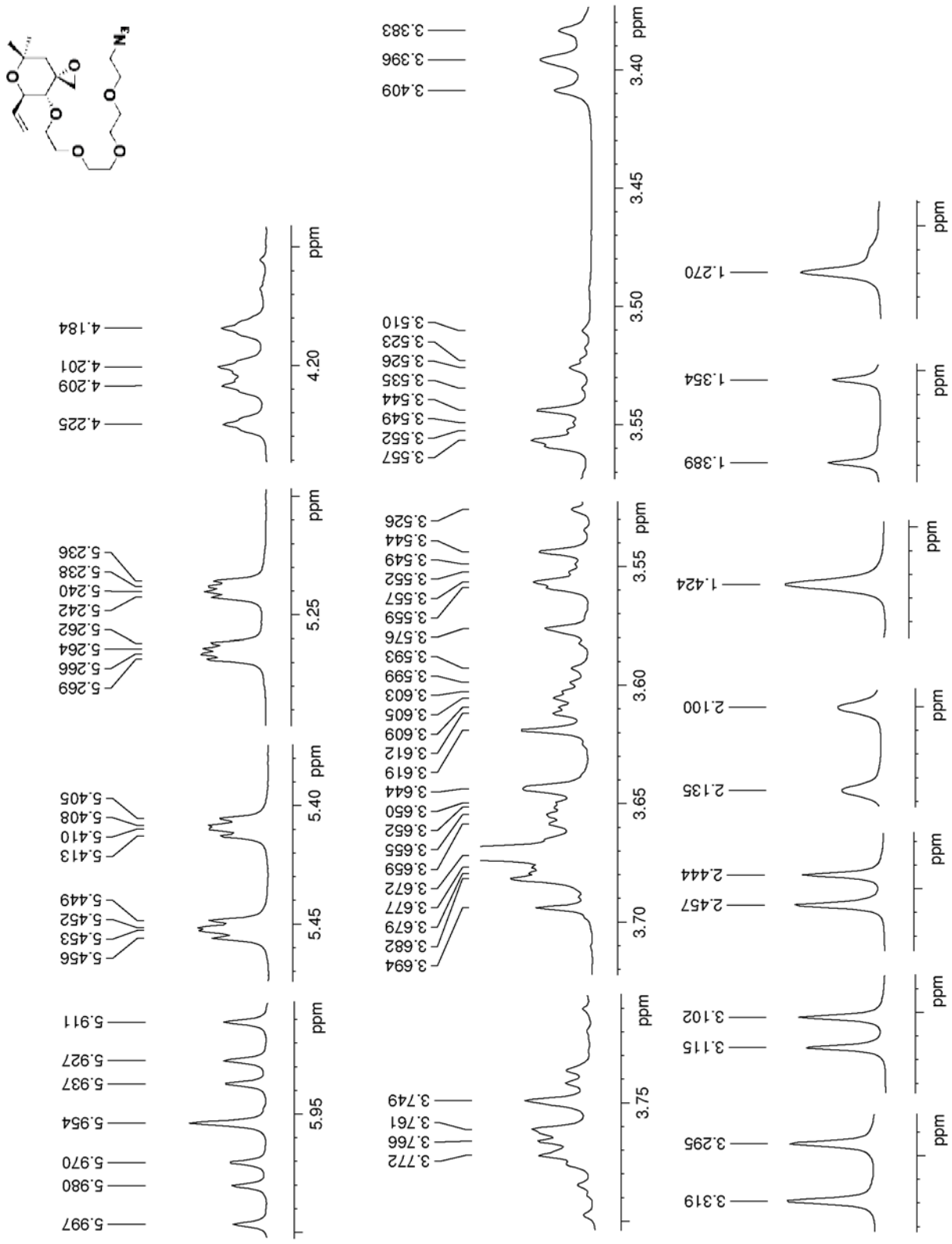

Spectrum 54. ^{1}H NMR spectrum of TEGylated right fragment **2.44** (400 MHz, $CDCl_3$, 293K)

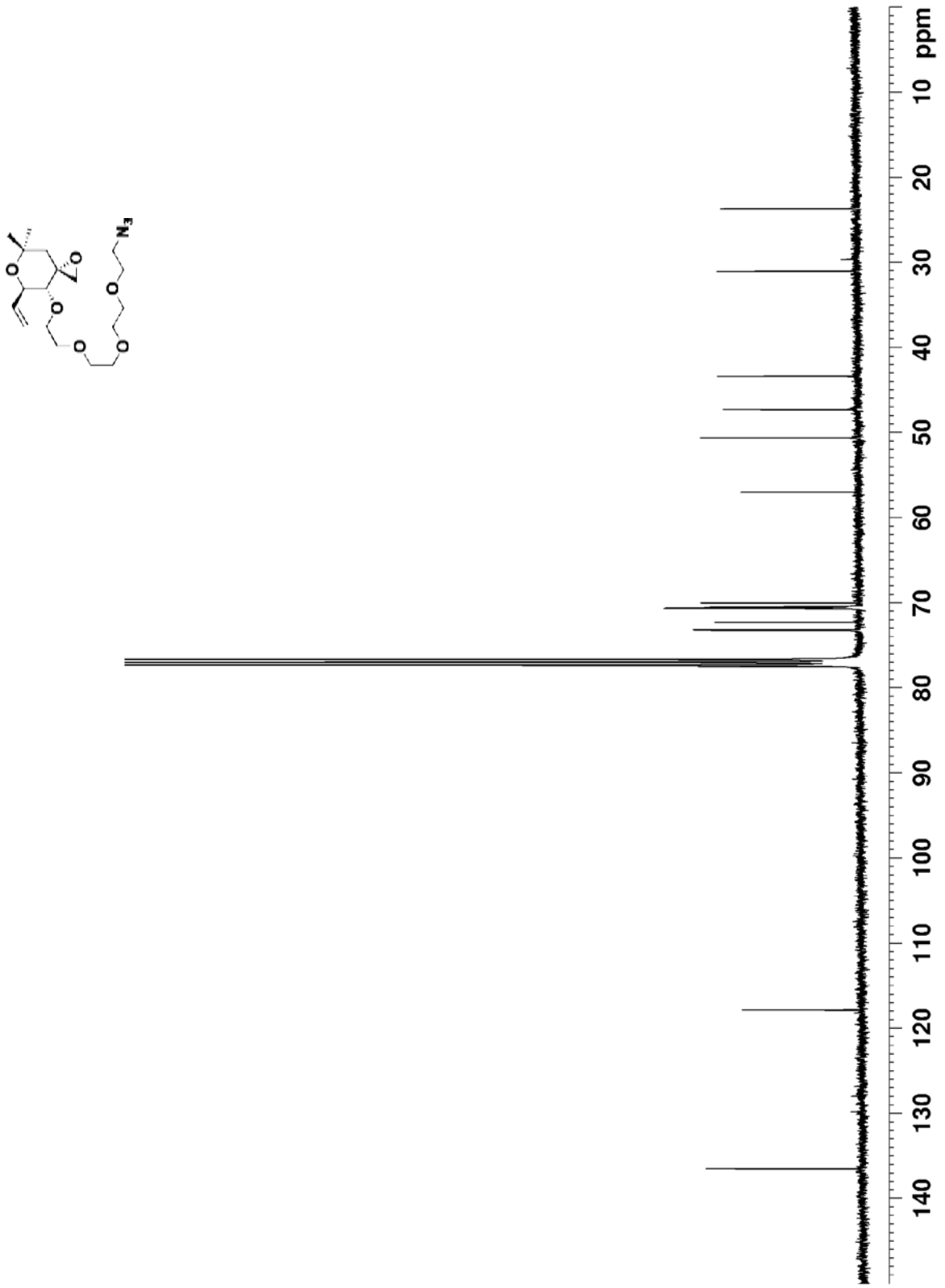

Spectrum 55. ^{13}C NMR spectrum of TEGylated right fragment **2.44** (100 MHz, $CDCl_3$, 293K)

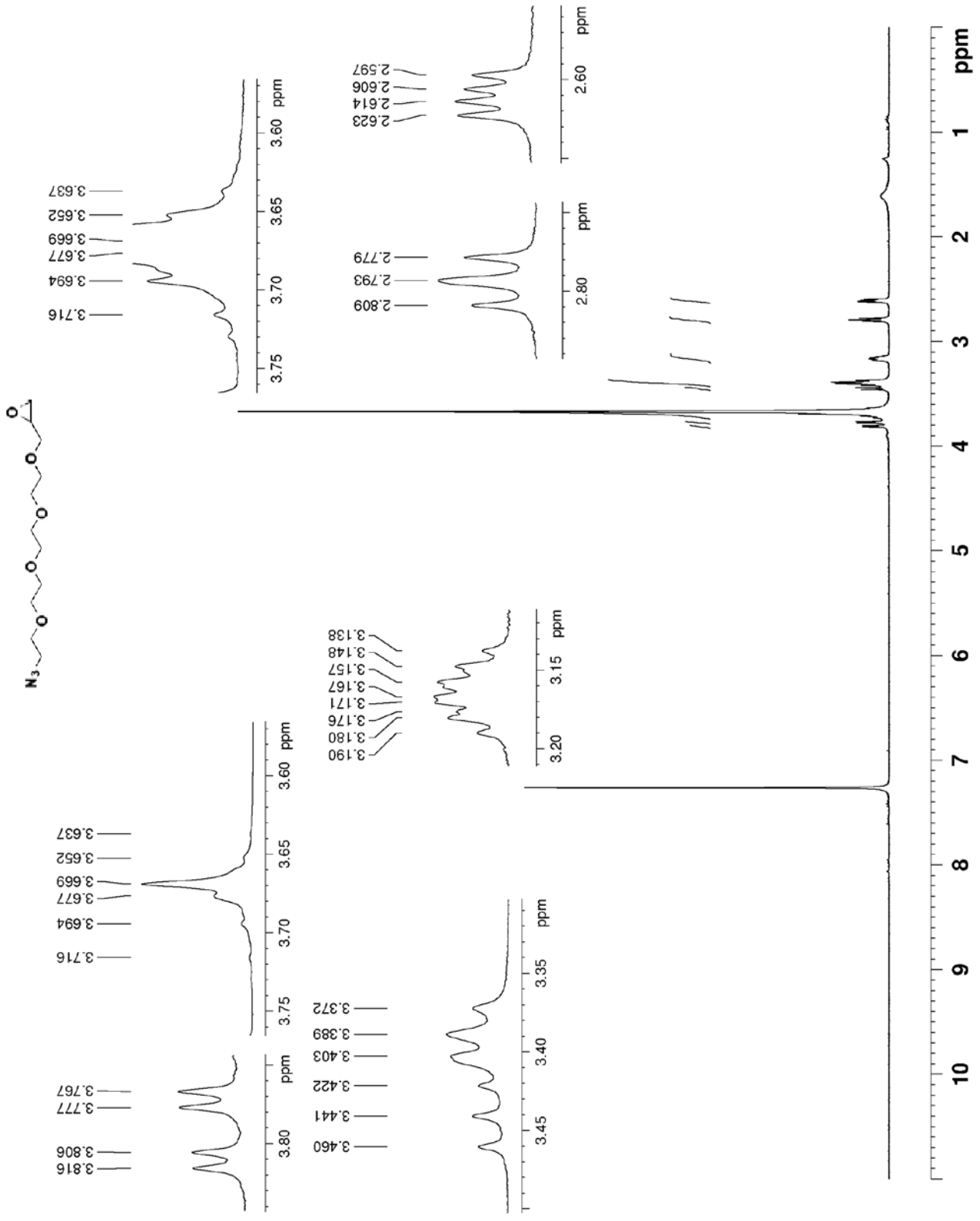

Spectrum 56. ^{1}H NMR spectrum of epoxide **2.46** (300 MHz, $CDCl_3$, 293K)

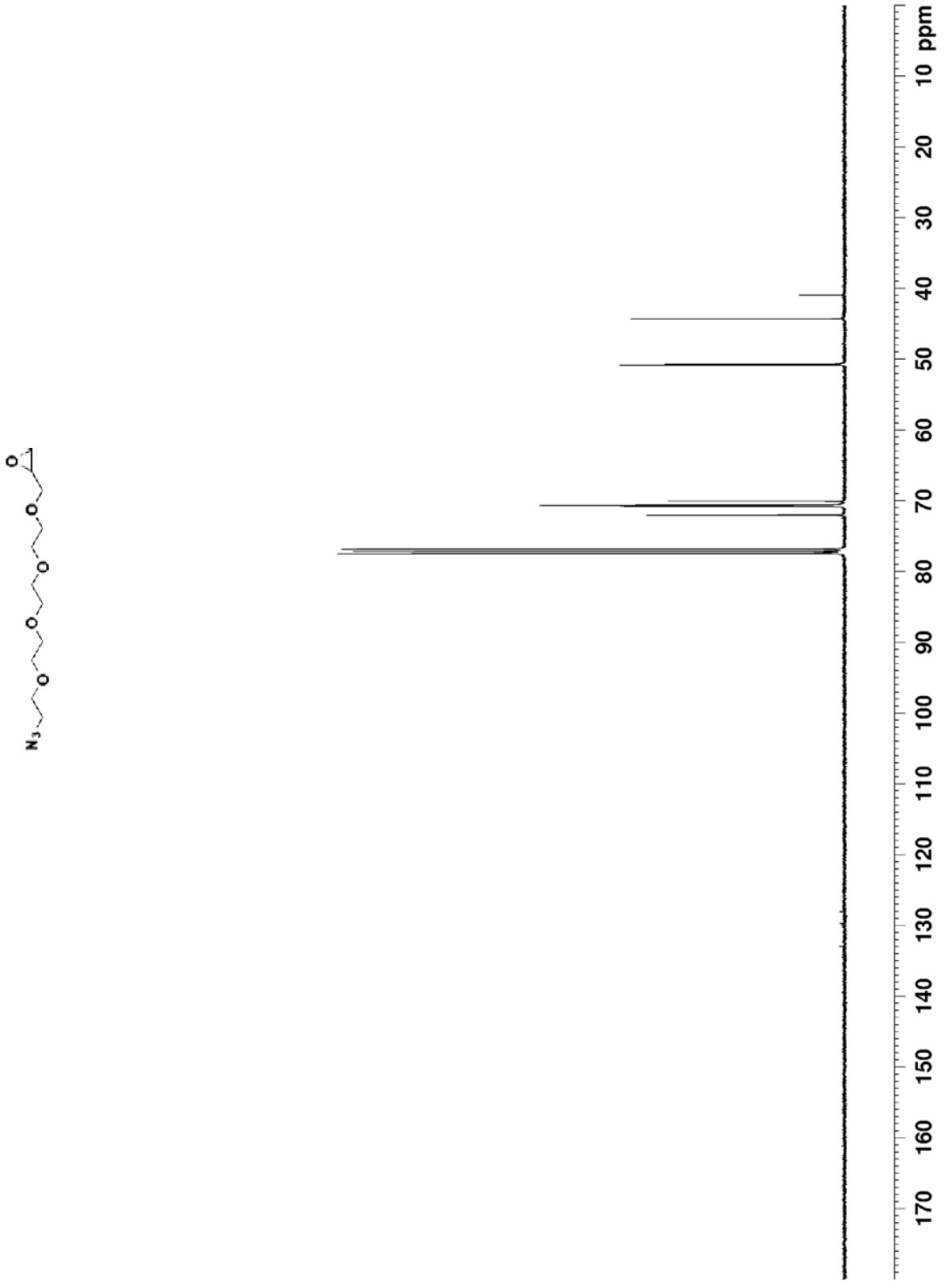

Spectrum 57. ^{13}C NMR spectrum of epoxide **2.46** (100 MHz, $CDCl_3$, 293K)

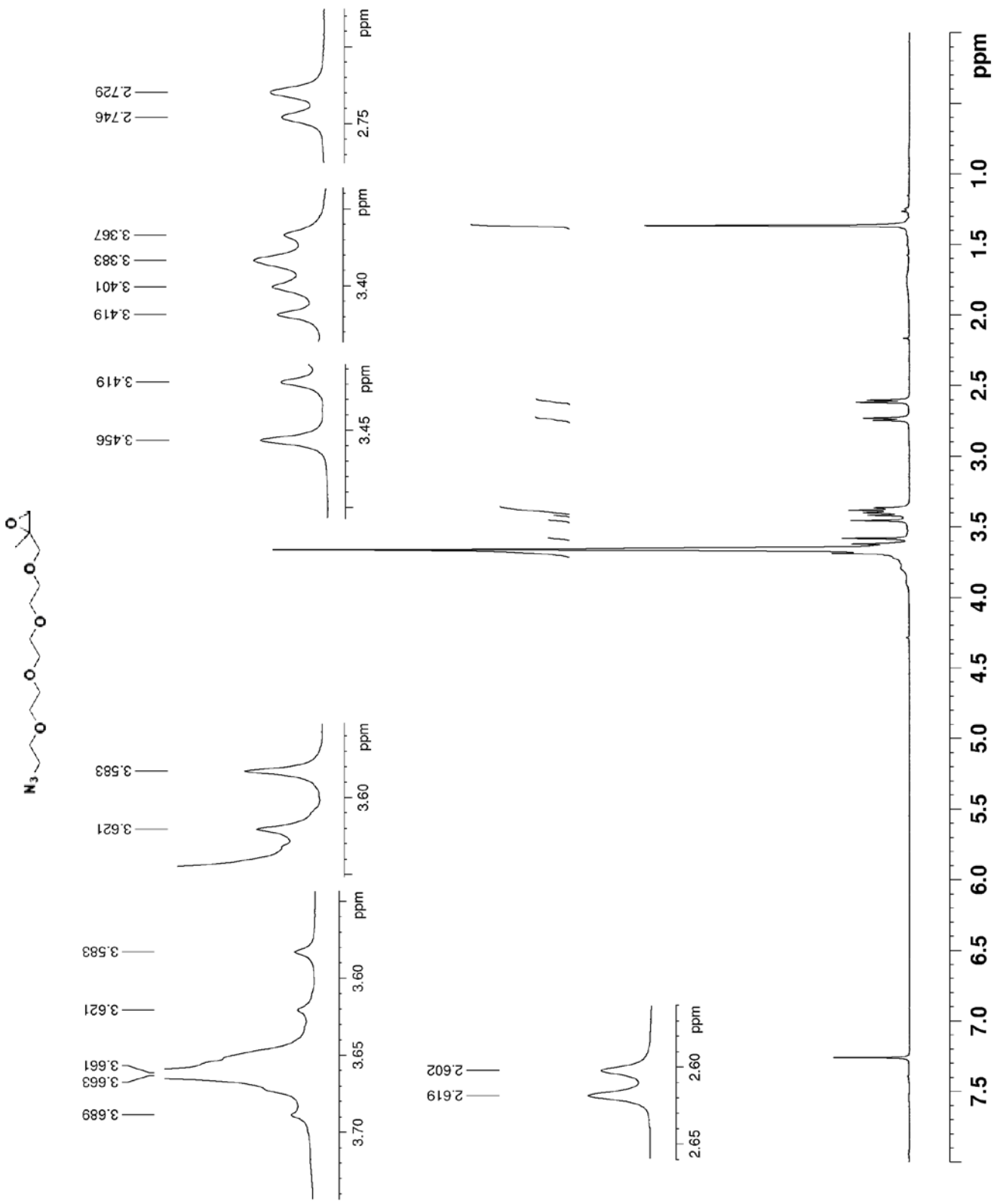

Spectrum 58. ^{1}H NMR spectrum of epoxide **2.47** (400 MHz, $CDCl_3$, 293K)

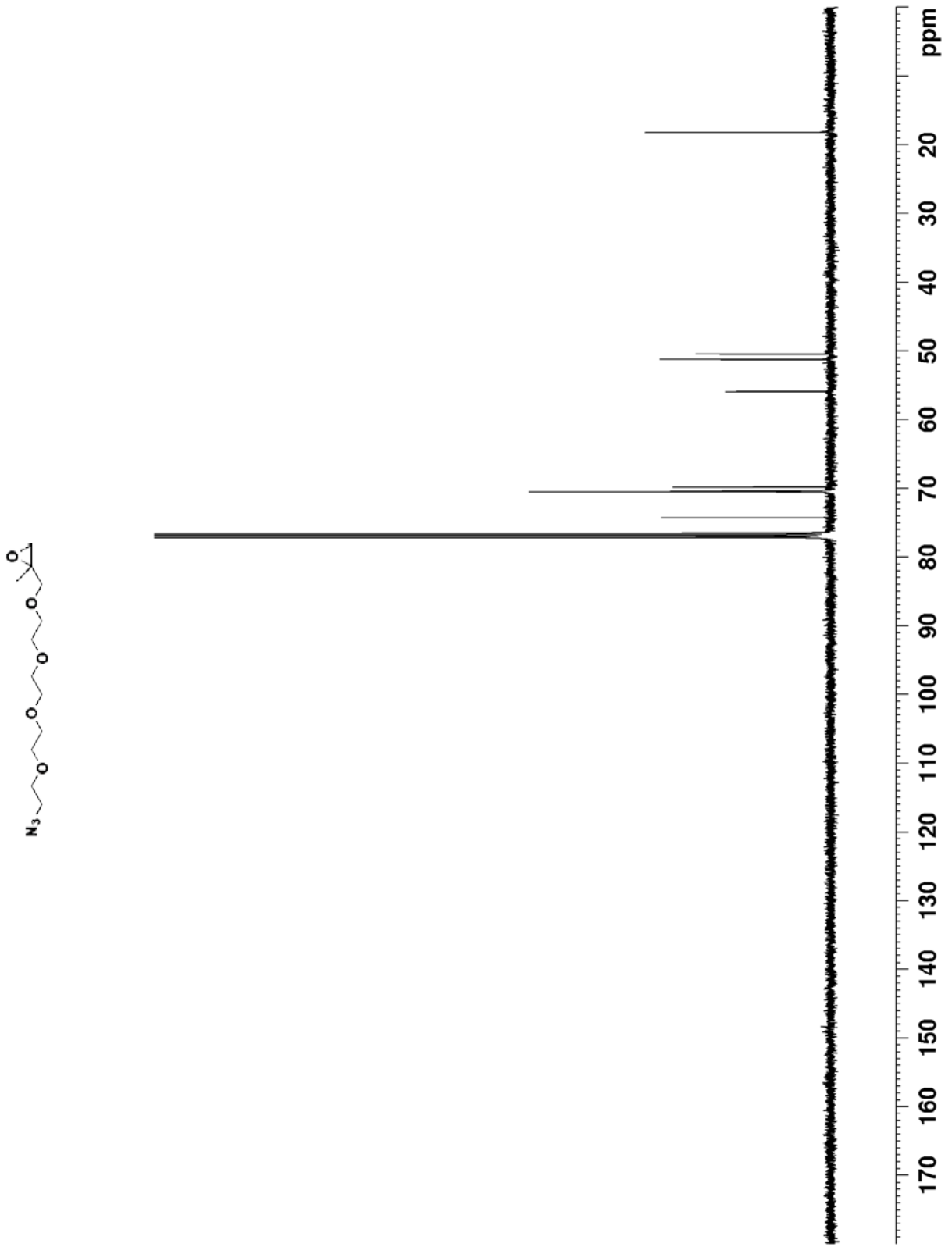

Spectrum 59. ^{13}C NMR spectrum of epoxide **2.47** (100 MHz, $CDCl_3$, 293K)

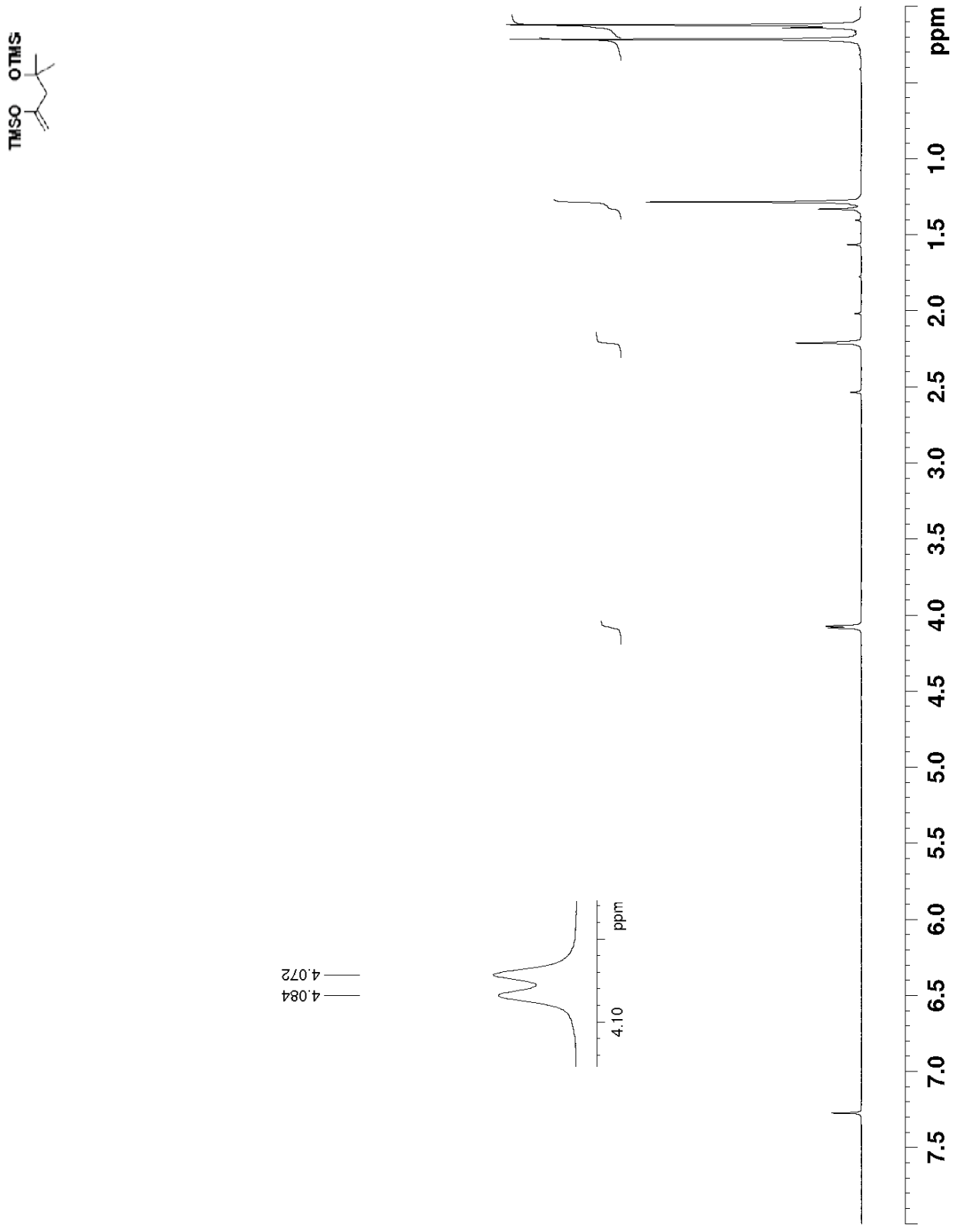

Spectrum 60. ^{1}H NMR spectrum of silyl enol ether **2.66** (300 MHz, $CDCl_3$, 293K)

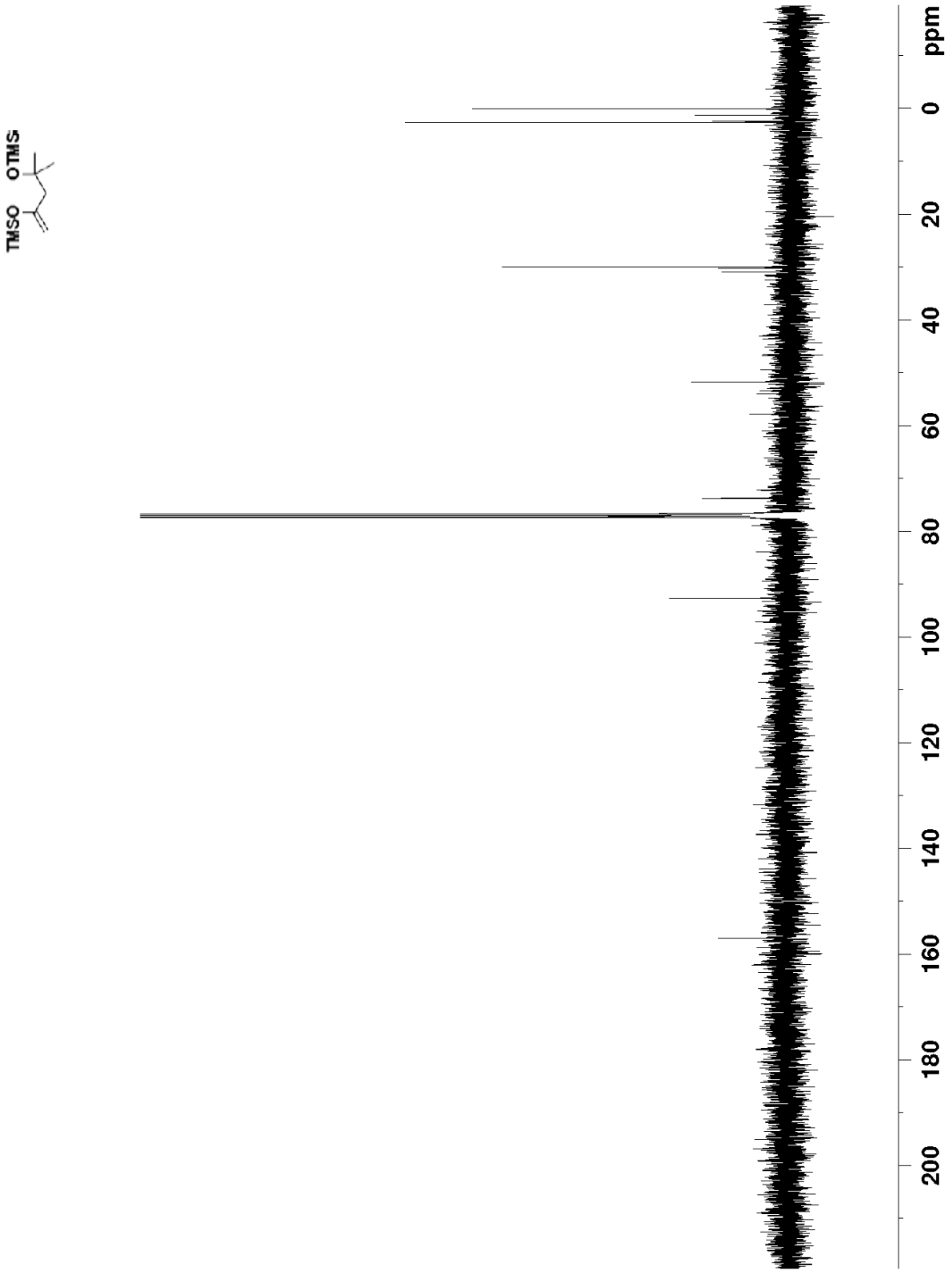

Spectrum 61. ^{13}C NMR spectrum of silyl enol ether **2.66** (100 MHz, $CDCl_3$, 293K)

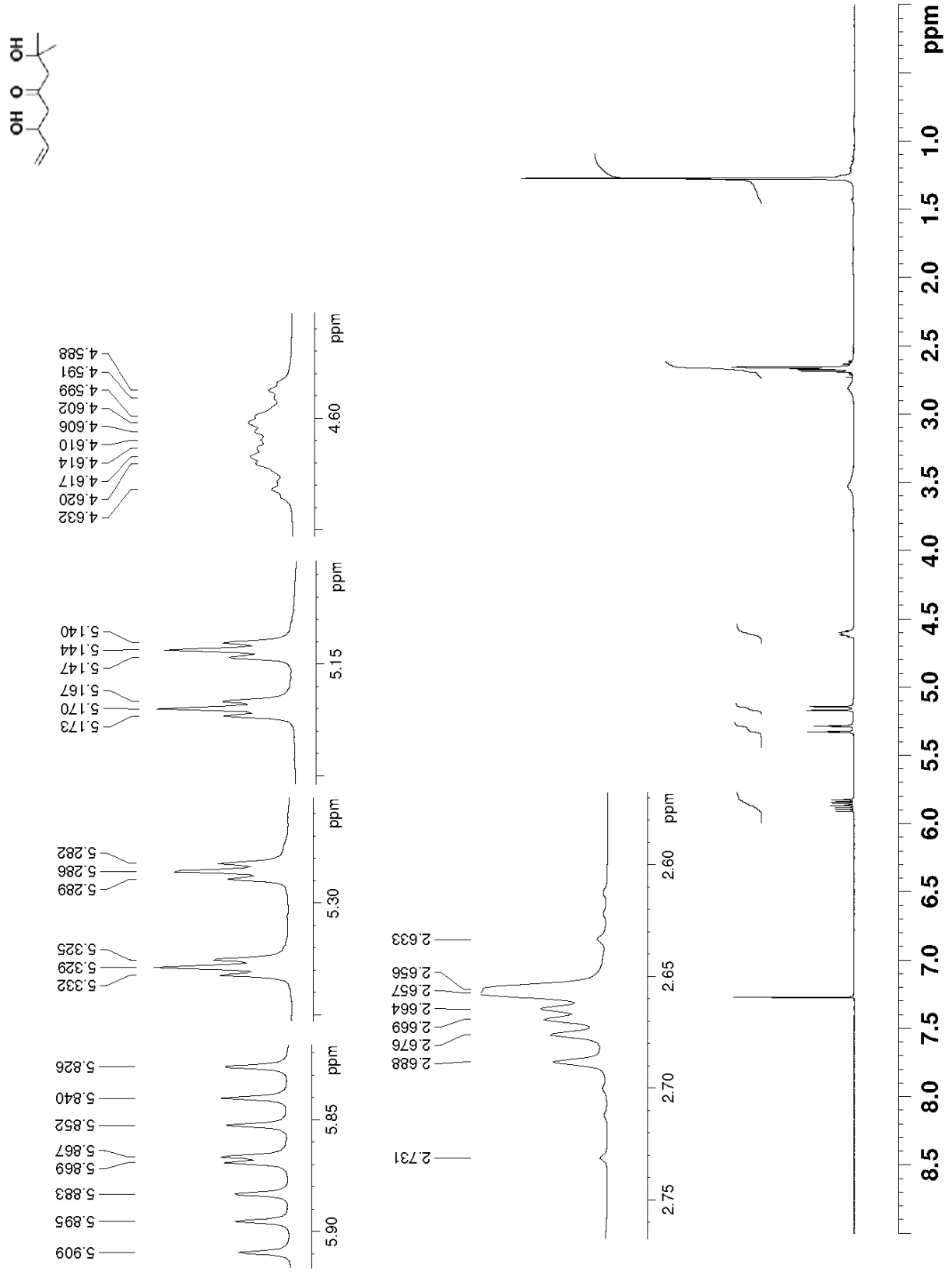

Spectrum 62. ^{1}H NMR spectrum of allylic alcohol **2.63** (300 MHz, 1% CD_3OD in $CDCl_3$, 293K)

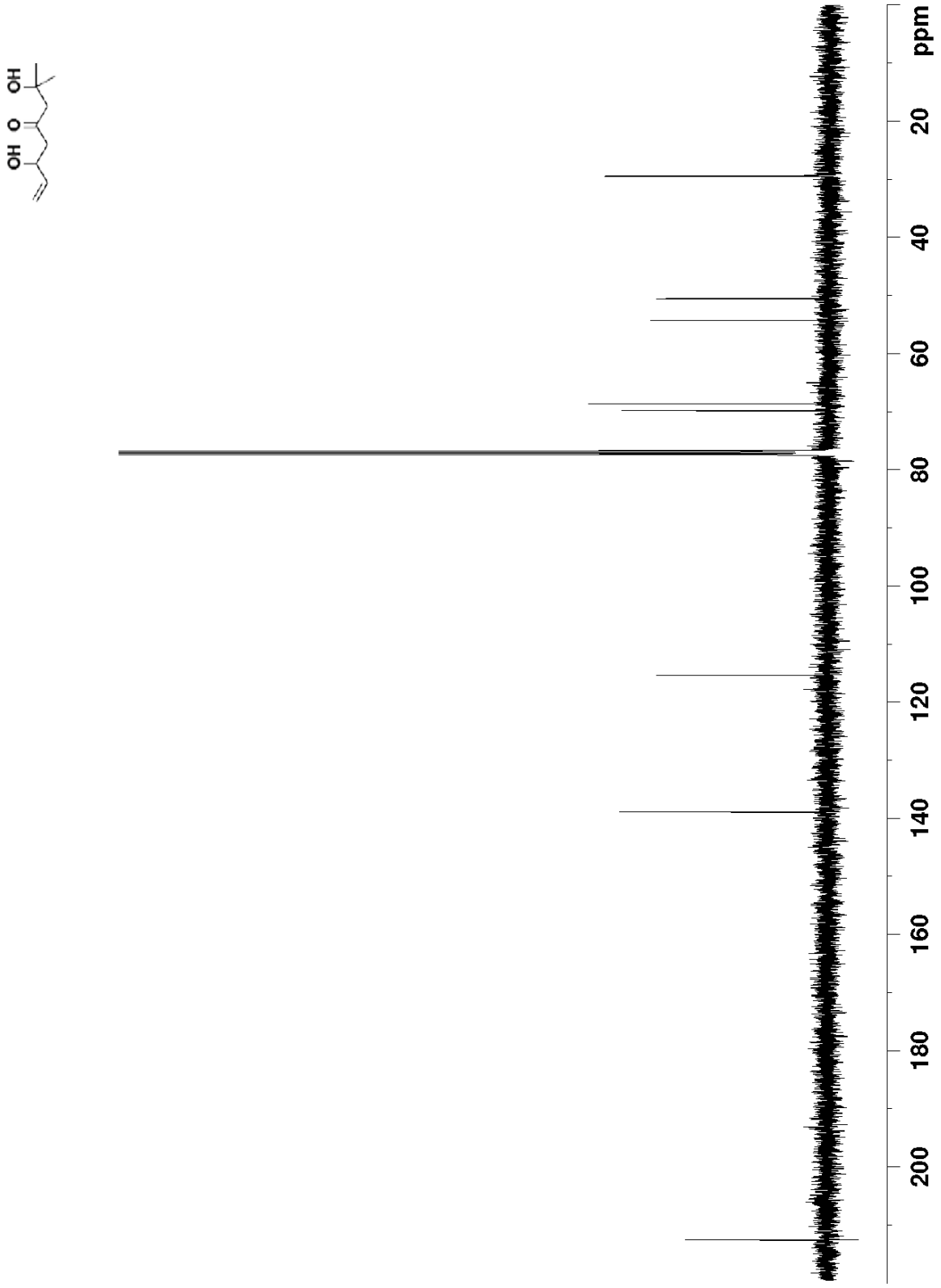

Spectrum 63. ^{1}H NMR spectrum of allylic alcohol **2.63** (100 MHz, $CDCl_3$, 293K)

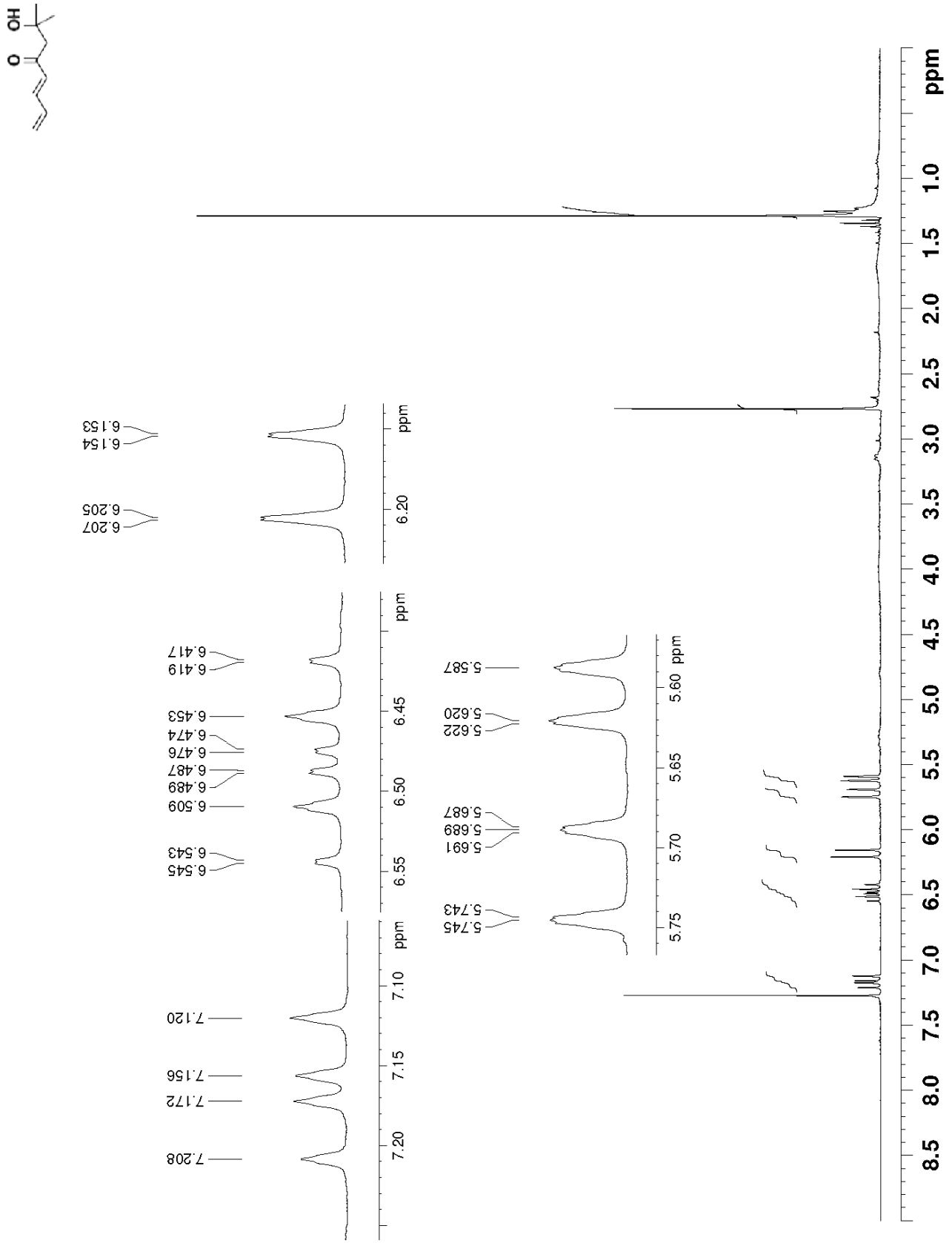

Spectrum 64. ^{1}H NMR spectrum of diene **2.64** (300 MHz, 1% CD_3OD in $CDCl_3$, 293K)

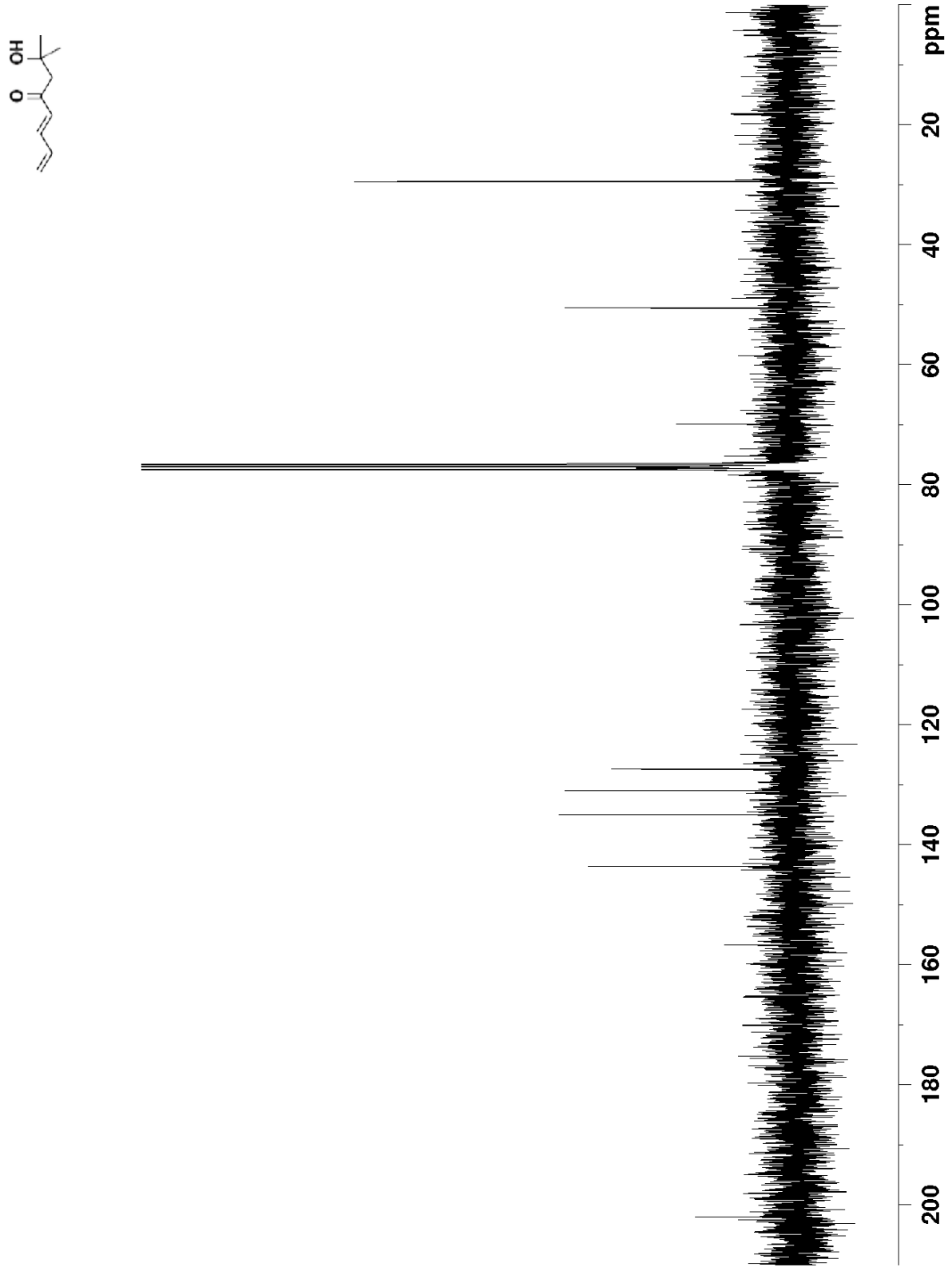

Spectrum 65. ^{13}C NMR spectrum of diene **2.64** (75 MHz, $CDCl_3$, 293K)

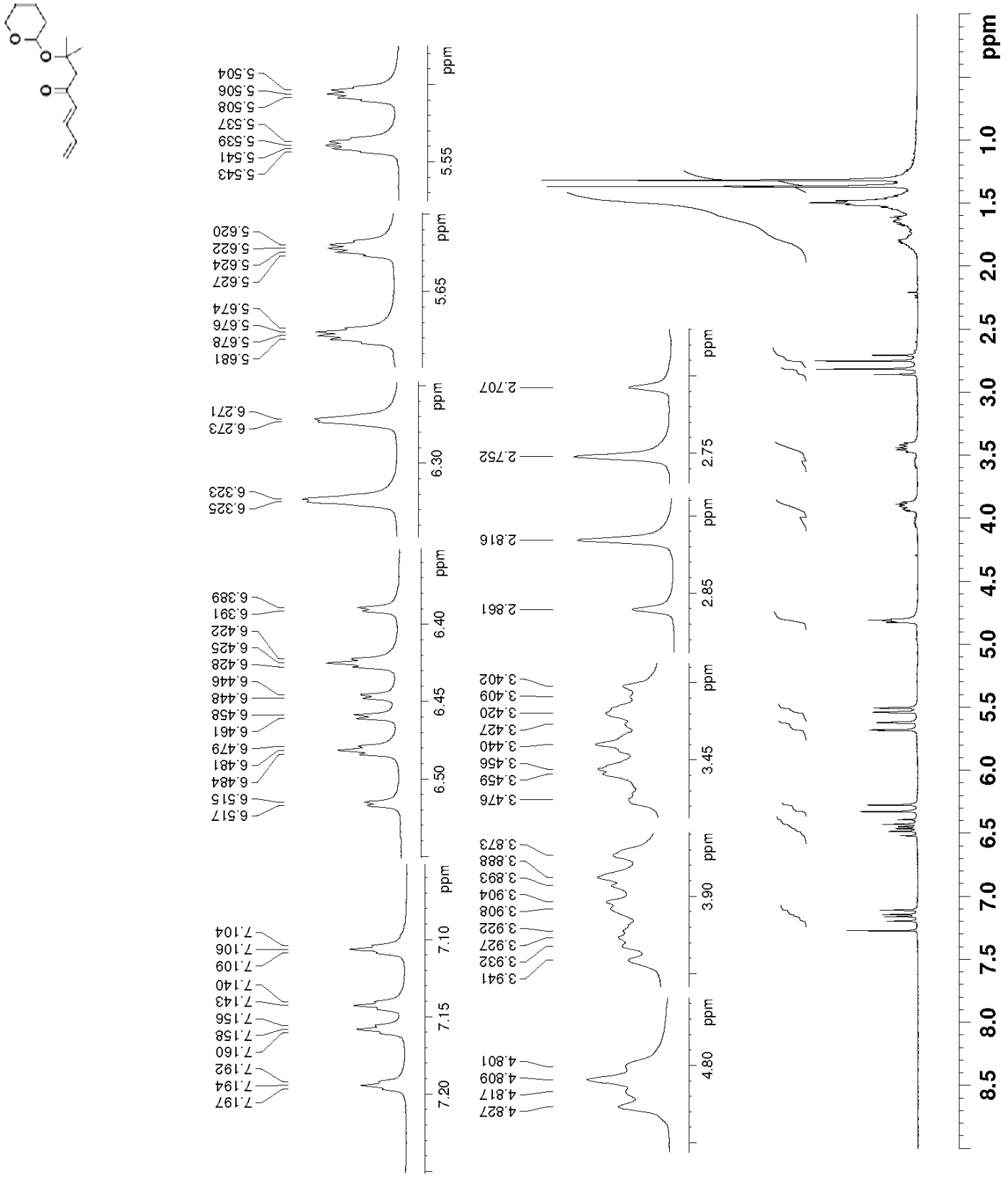

Spectrum 66. ^{1}H NMR spectrum of diene **2.76** (300 MHz, $CDCl_3$, 293K)

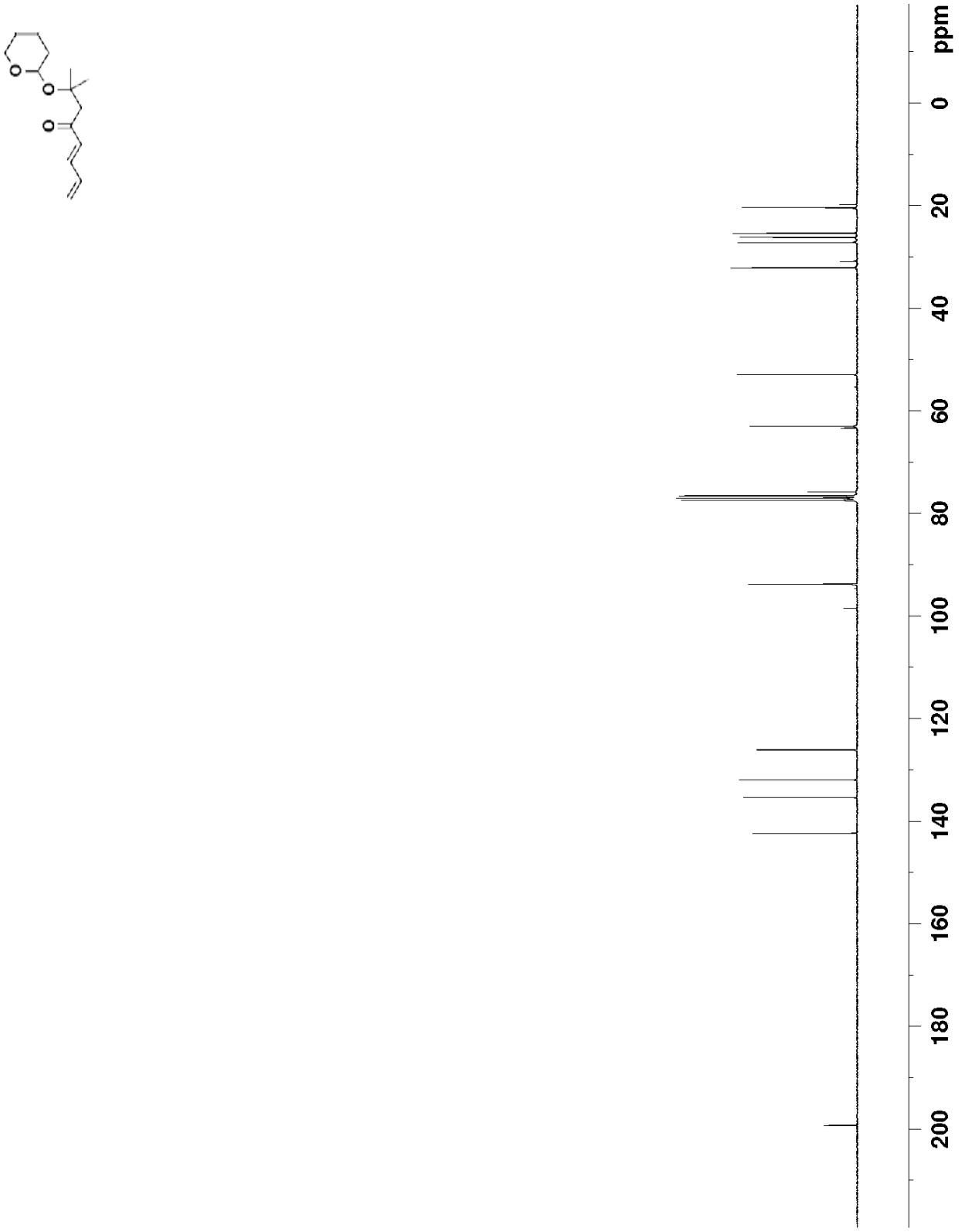

Spectrum 67. ^{13}C NMR spectrum of diene **2.76** (75 MHz, $CDCl_3$, 293K)

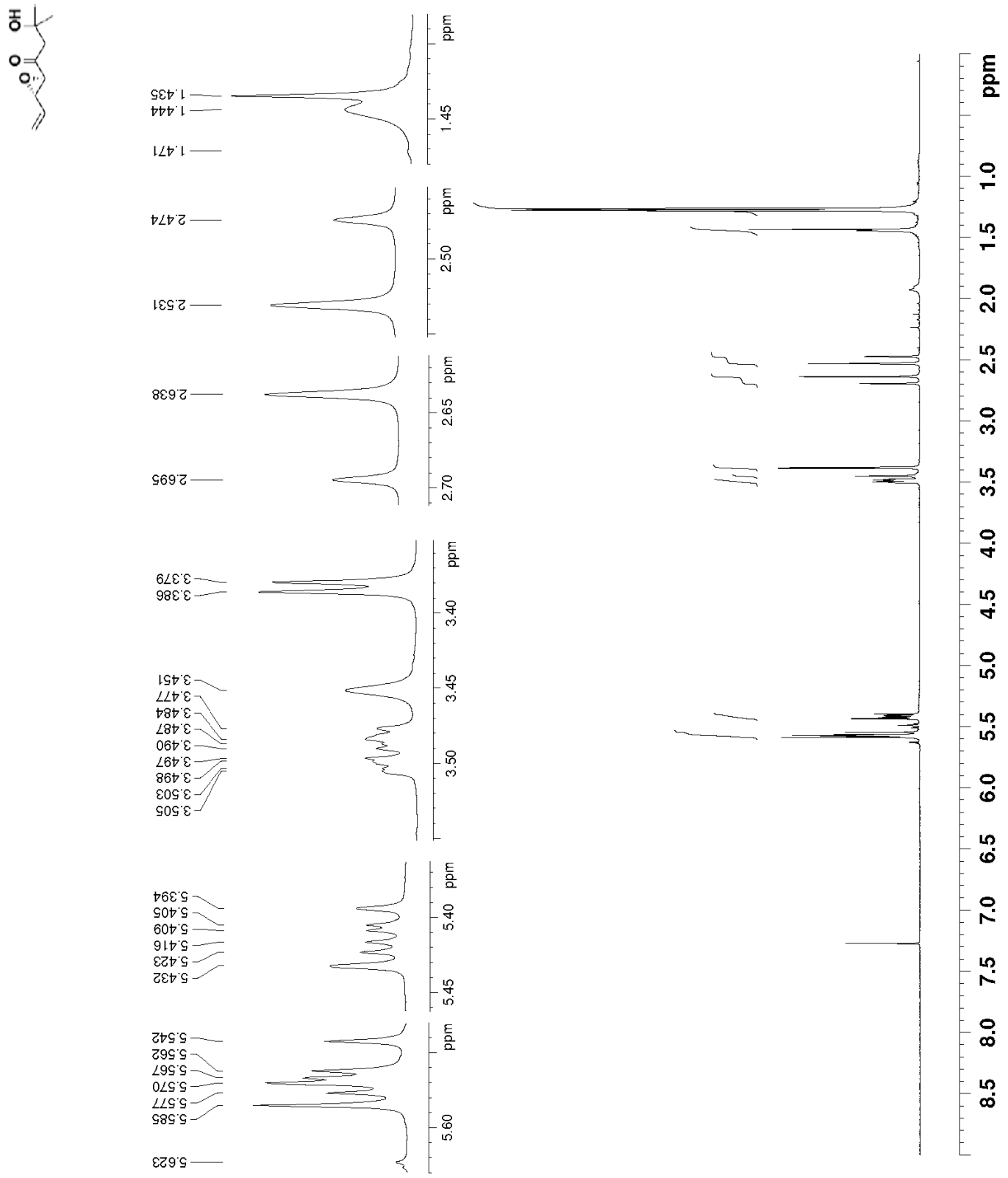

Spectrum 68. ^{1}H NMR spectrum of epoxide **2.61** (300 MHz, $CDCl_3$, 293K)

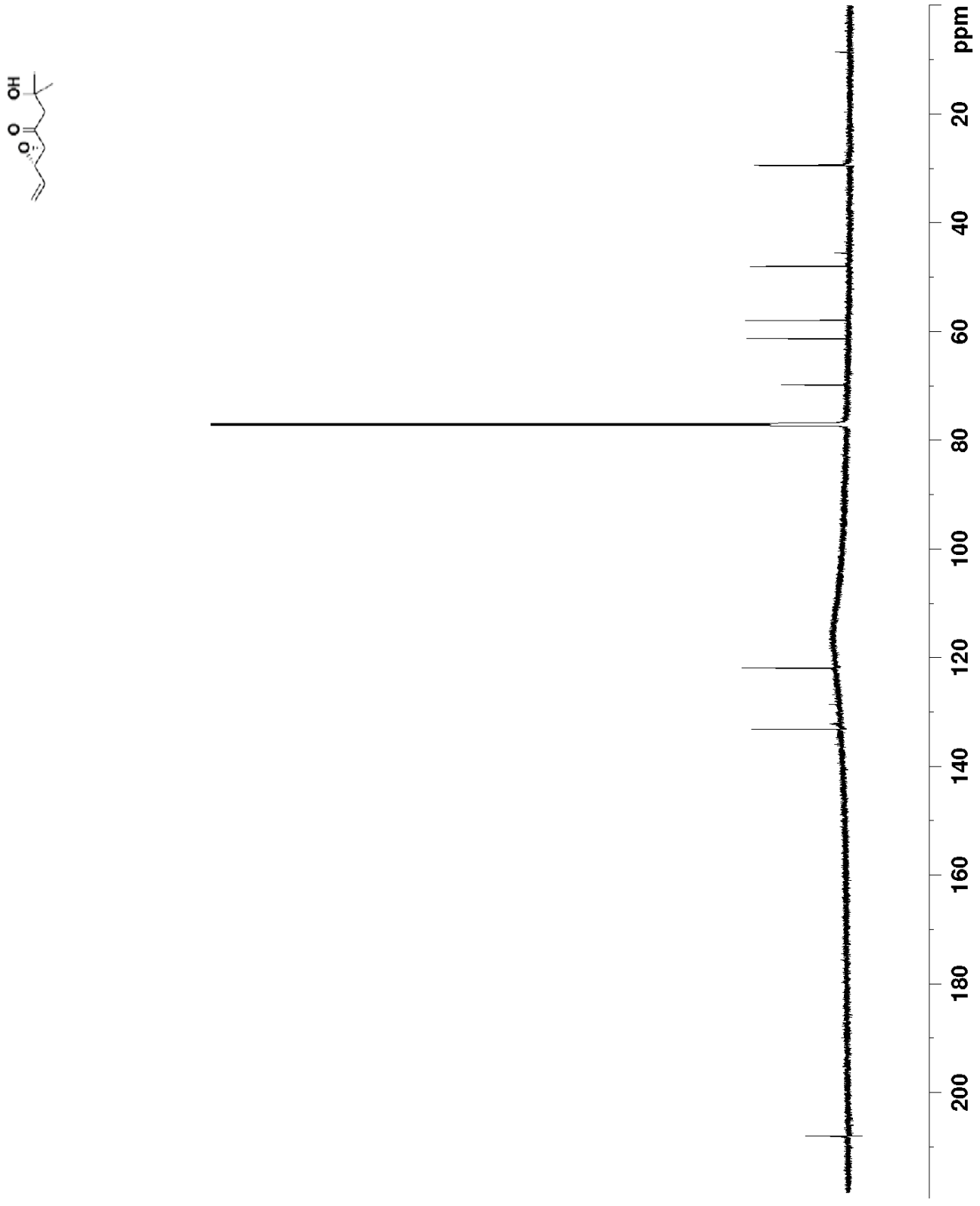

Spectrum 69. ^{13}C NMR spectrum of epoxide **2.61** (175 MHz, $CDCl_3$, 293K)

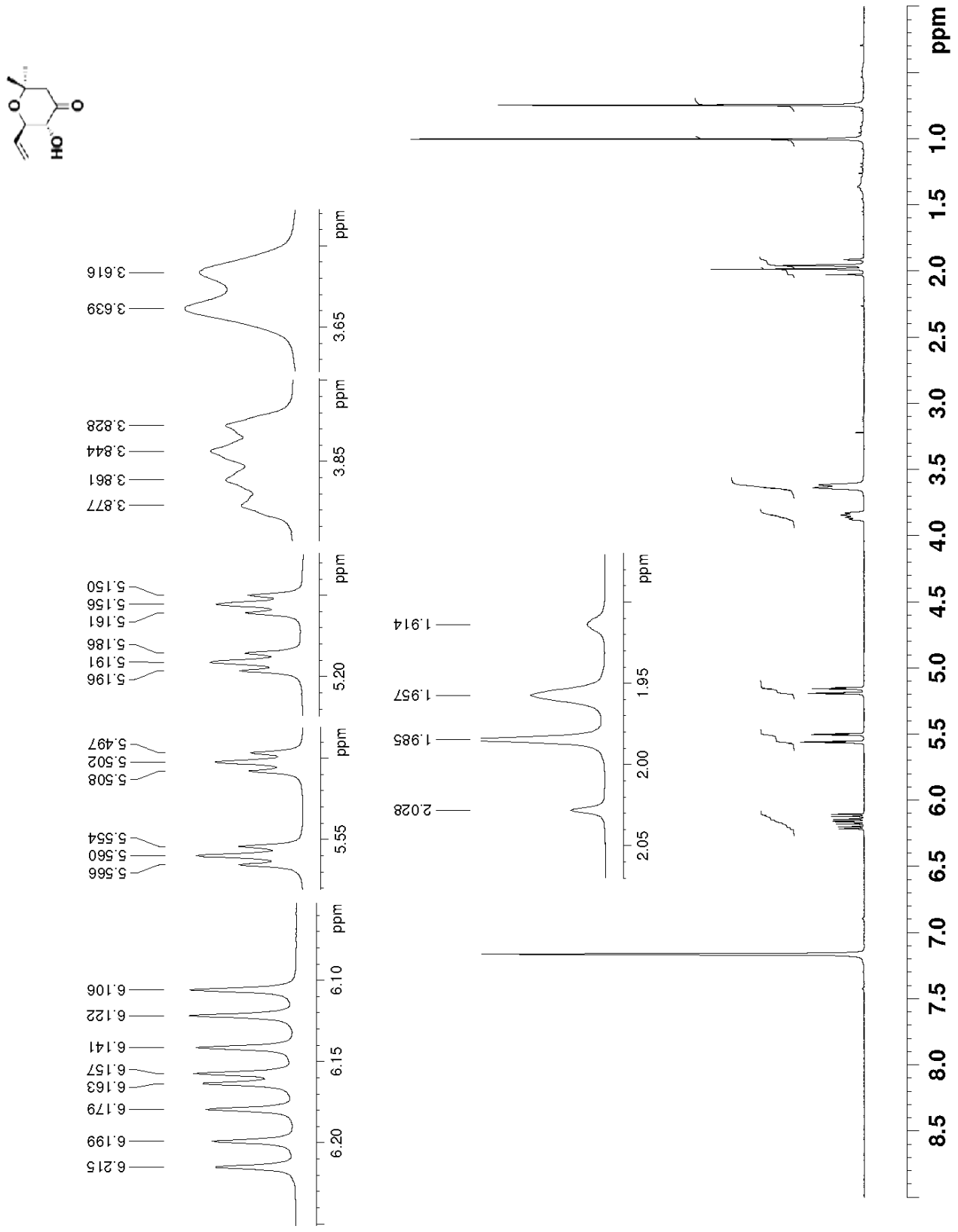

Spectrum 70. ^{1}H NMR spectrum of ketone **2.25** (300 MHz, 1% CD_3OD in C_6D_6, 293K)

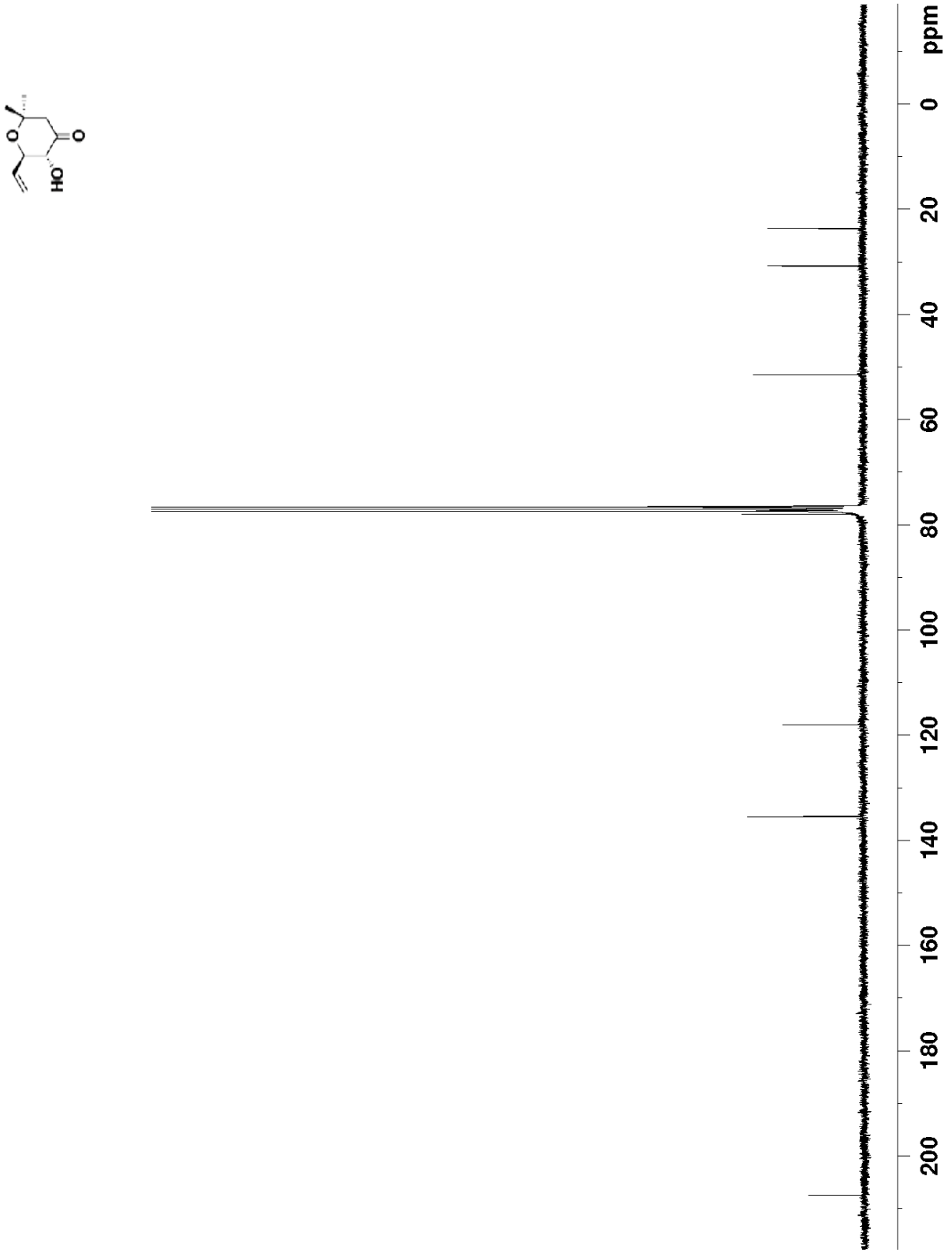

Spectrum 71. ^{13}C NMR spectrum of ketone **2.25** (75 MHz, $CDCl_3$, 293K)

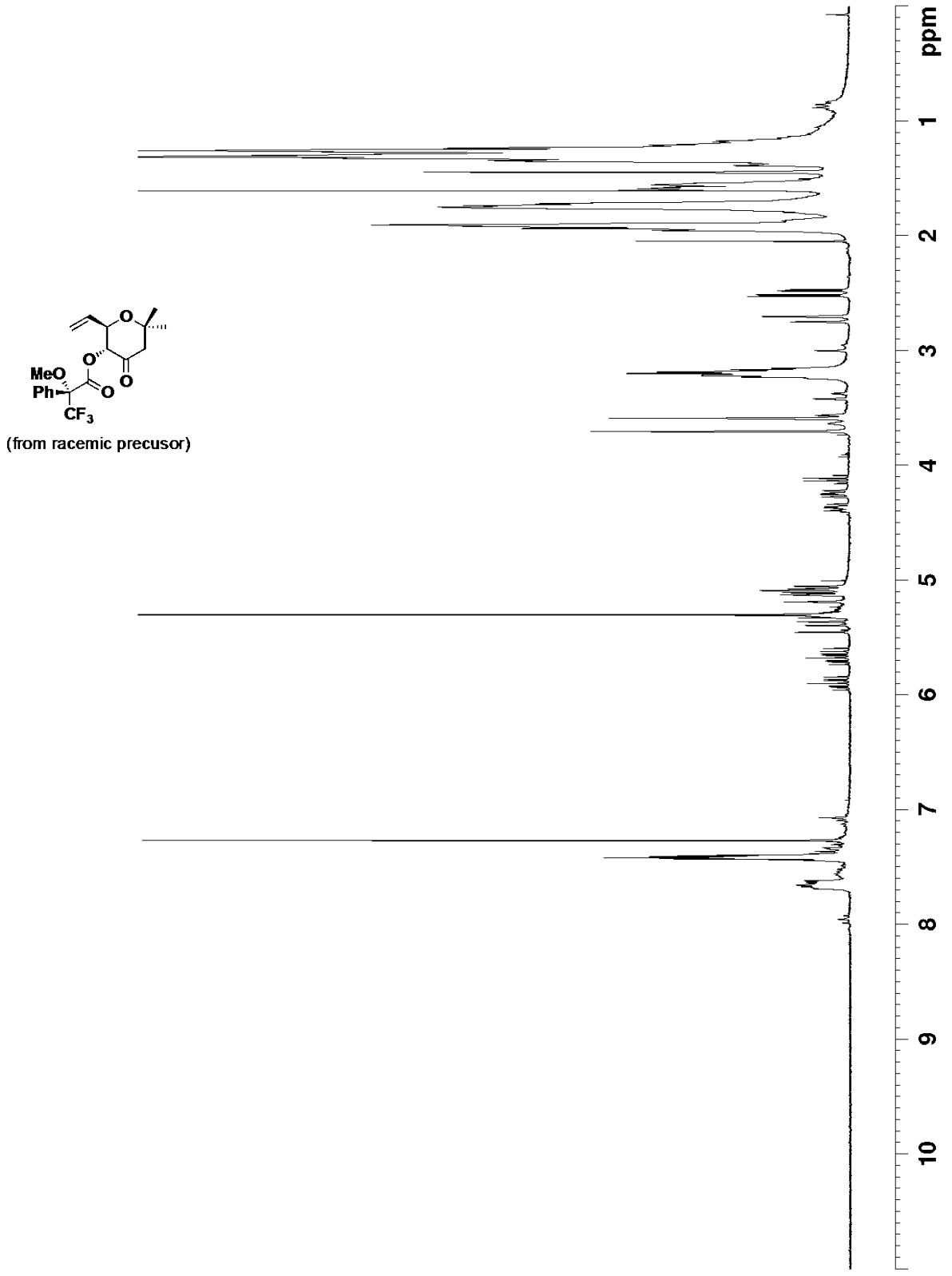

Spectrum 72. ^{1}H NMR spectrum of Mosher ester derivative **2.77** (400 MHz, $CDCl_3$, 293K)

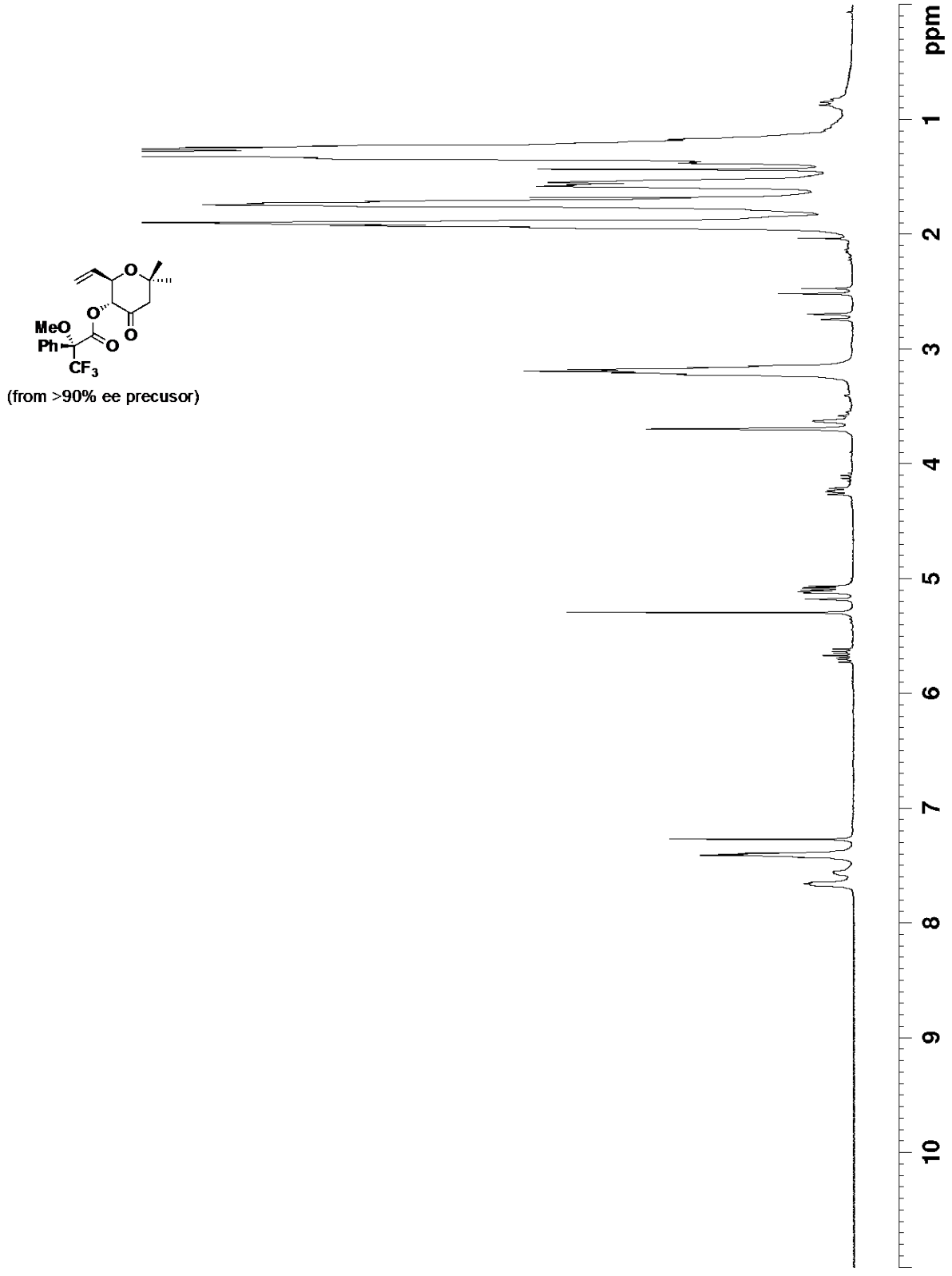

Spectrum 73. ^{1}H NMR spectrum of Mosher ester derivative **2.77** (400 MHz, $CDCl_3$, 293K)

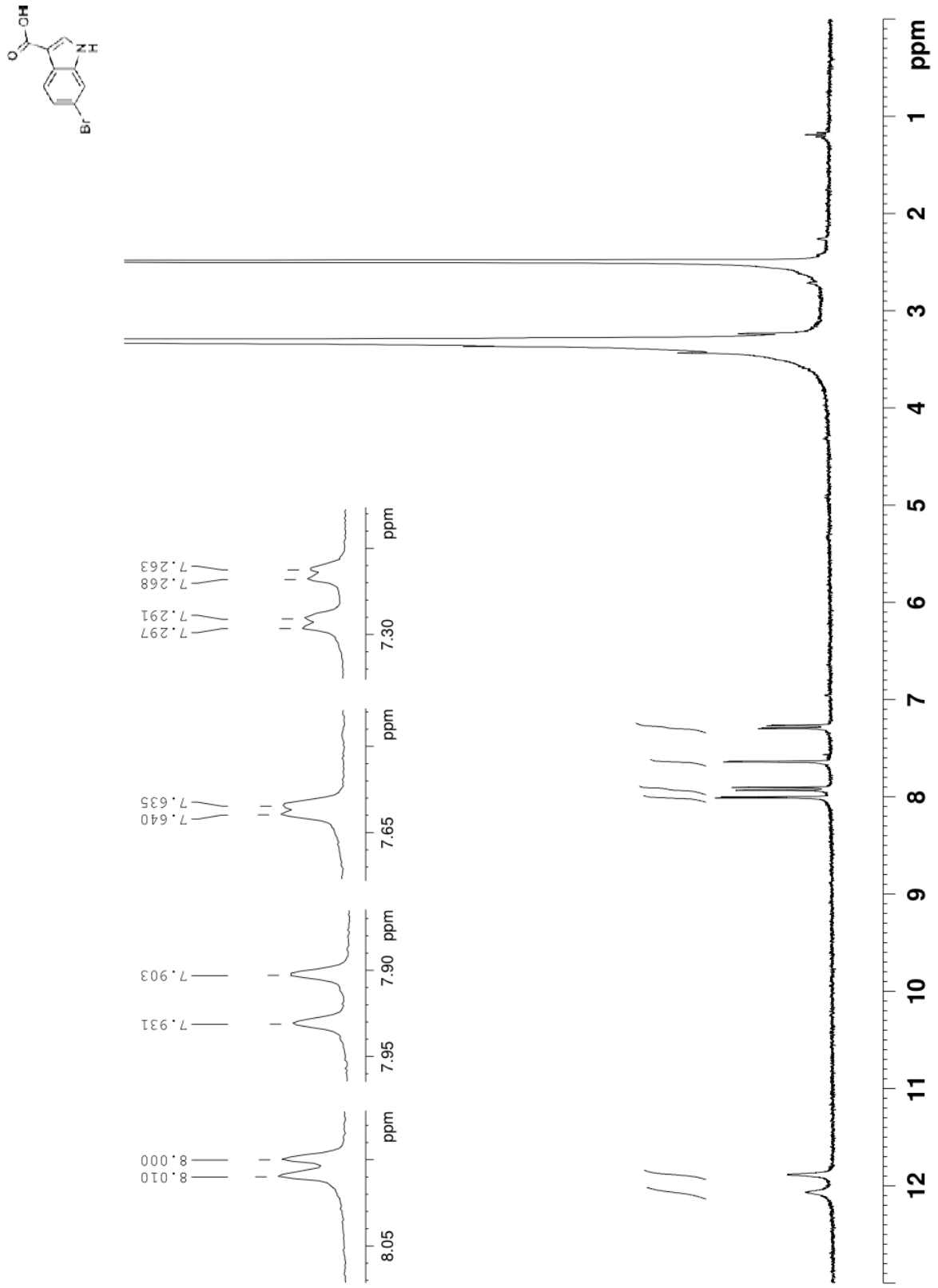

Spectrum 74. ^{1}H NMR spectrum of carboxylic acid **3.6** (300 MHz, DMSO-d_6, 293K)

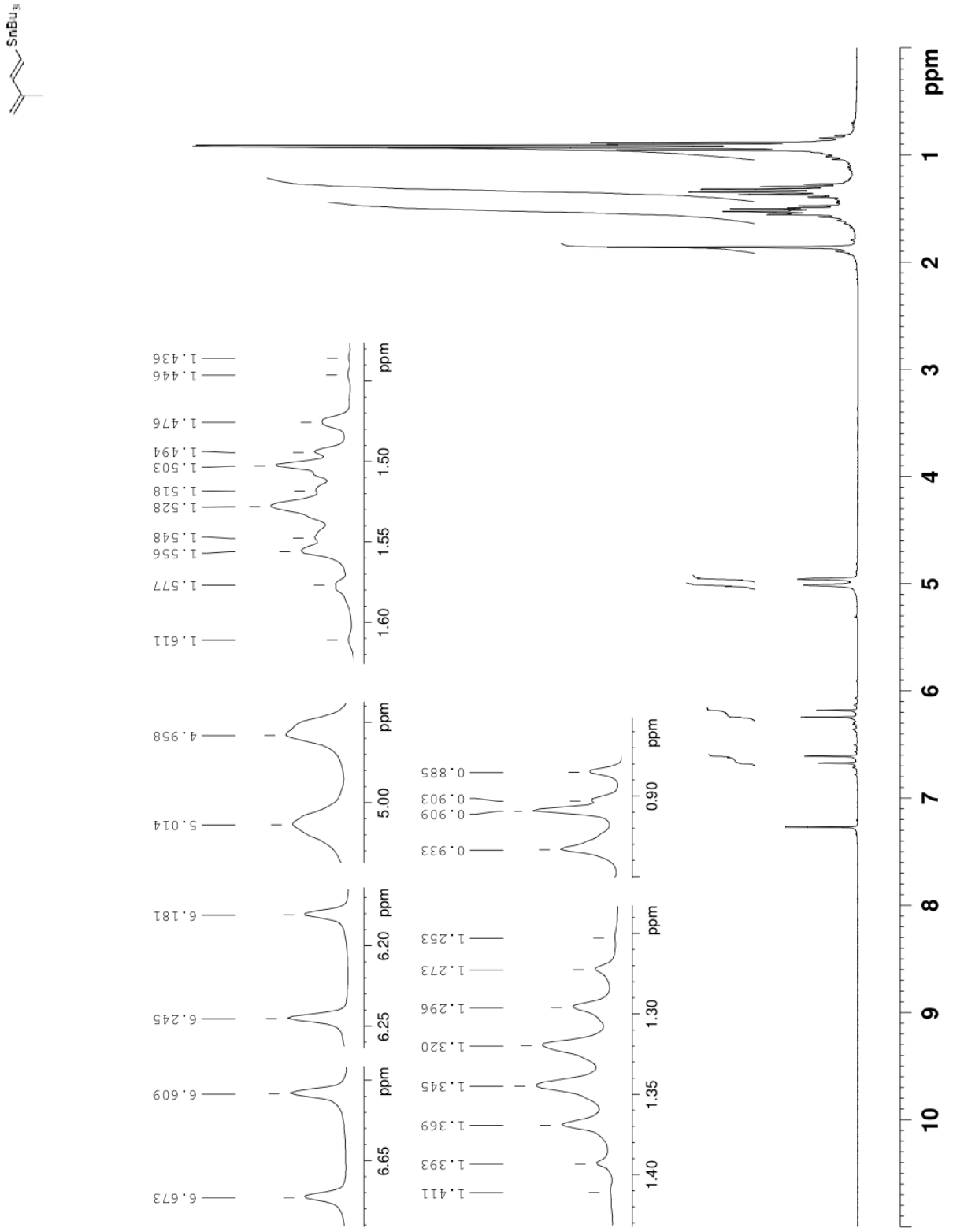

Spectrum 75. ^{1}H NMR spectrum of alkenyl stannane **3.3** (300 MHz, $CDCl_3$, 293K)

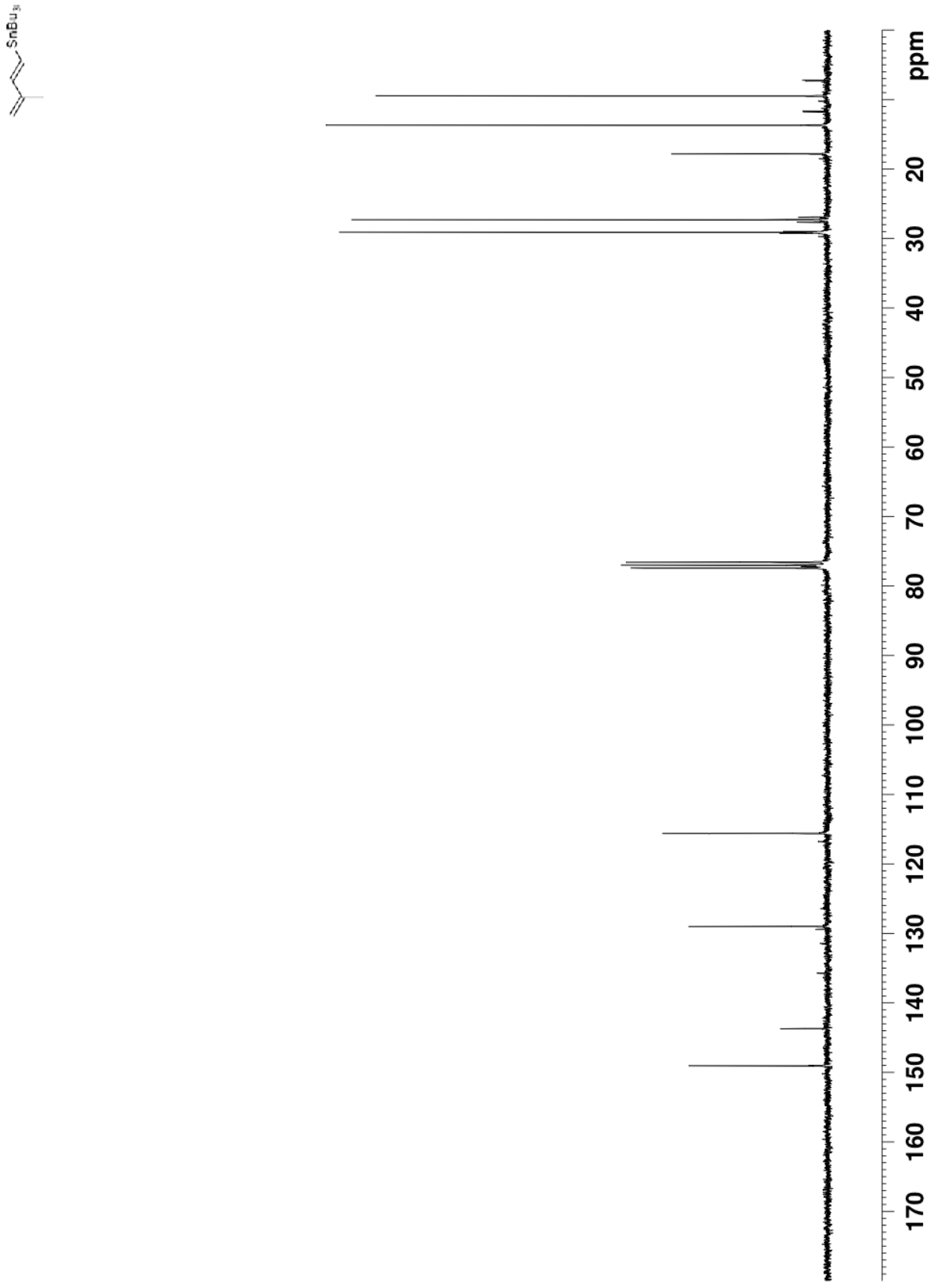

Spectrum 76. ^{13}C NMR spectrum of alkenyl stannane **3.3** (75 MHz, $CDCl_3$, 293K)

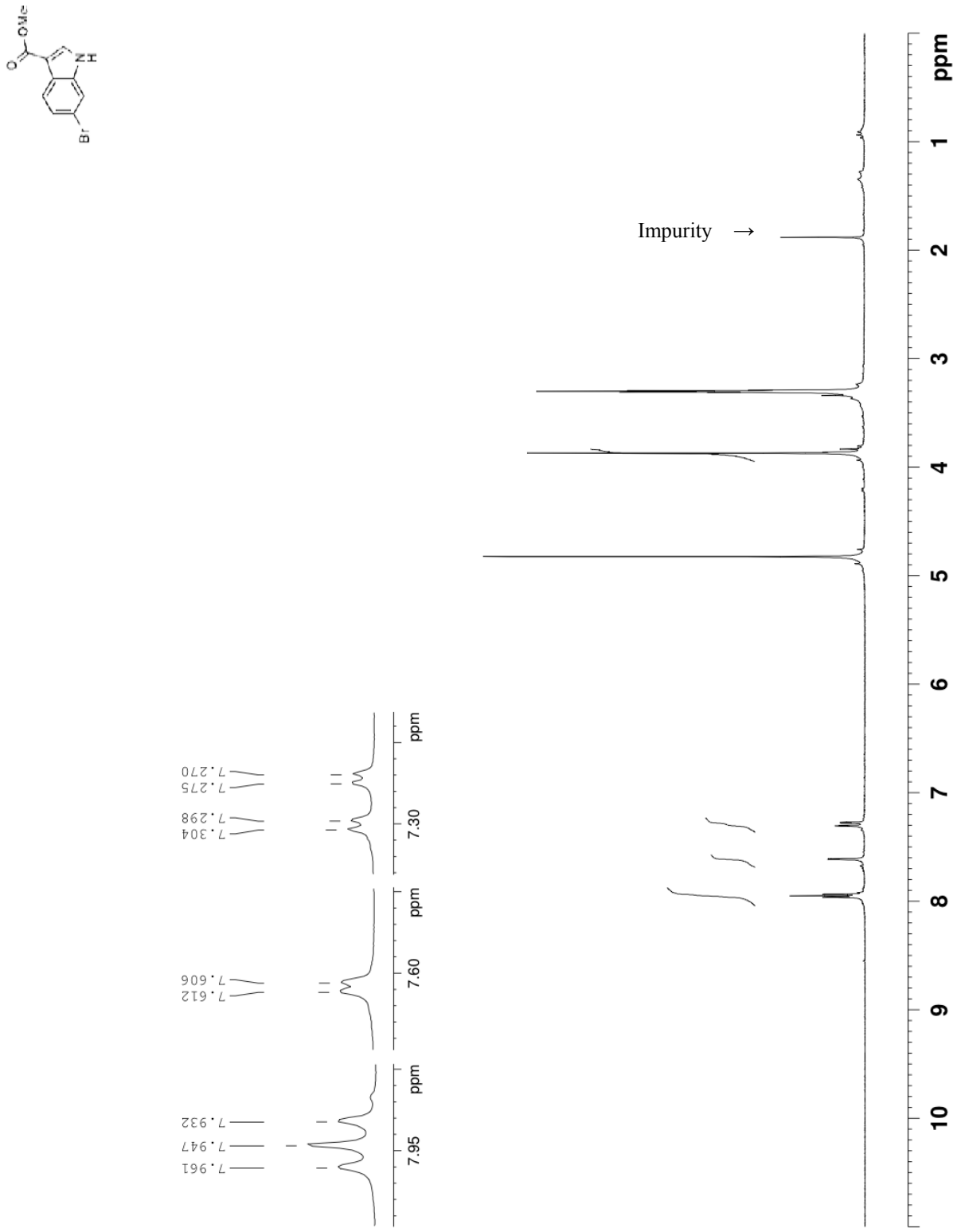

Spectrum 77. ^{1}H NMR spectrum of methyl ester **3.7** (300 MHz, CD_3OD, 293K)

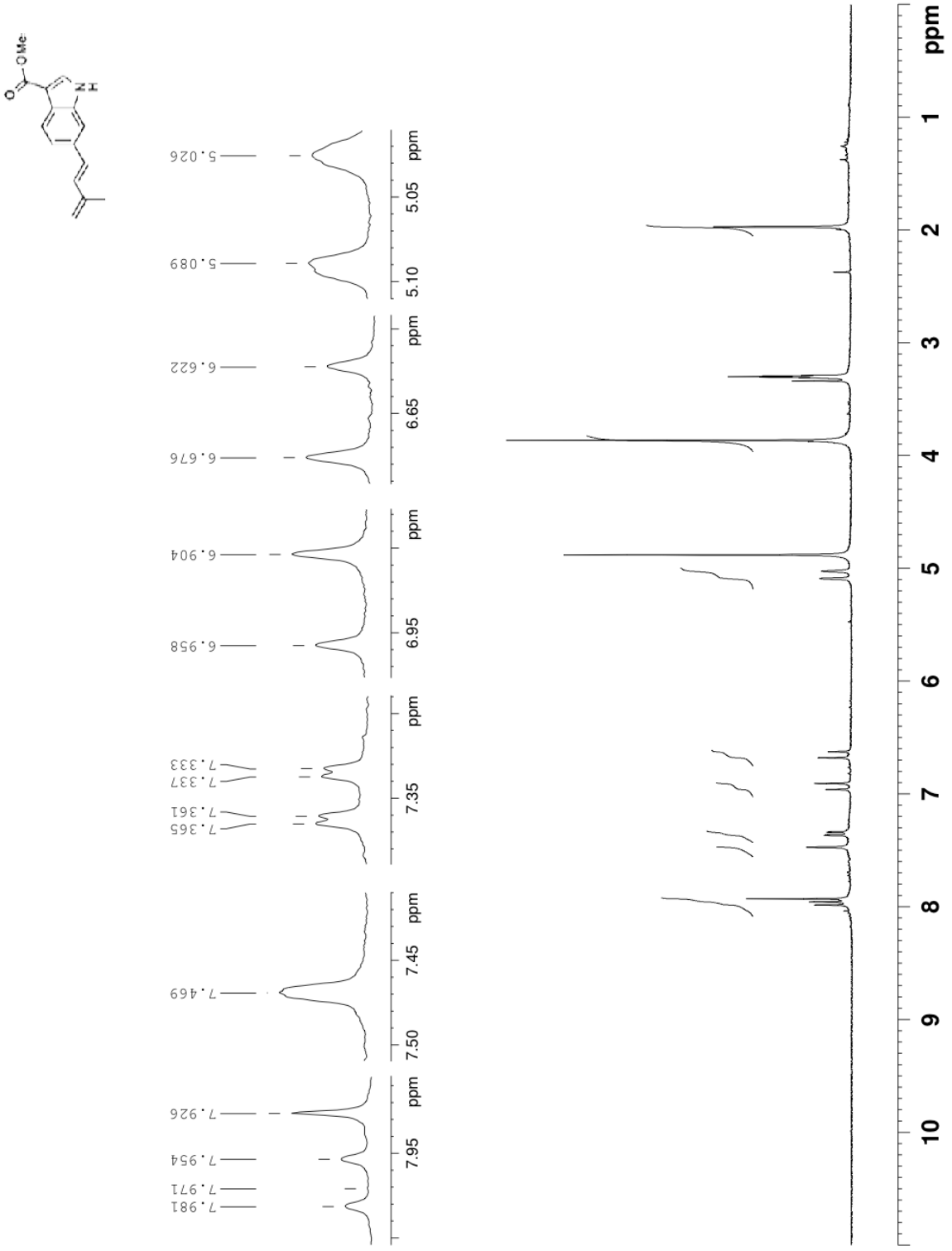

Spectrum 78. ^{1}H NMR spectrum of methyl ester **3.8** (300 MHz, CD_3OD, 293K)

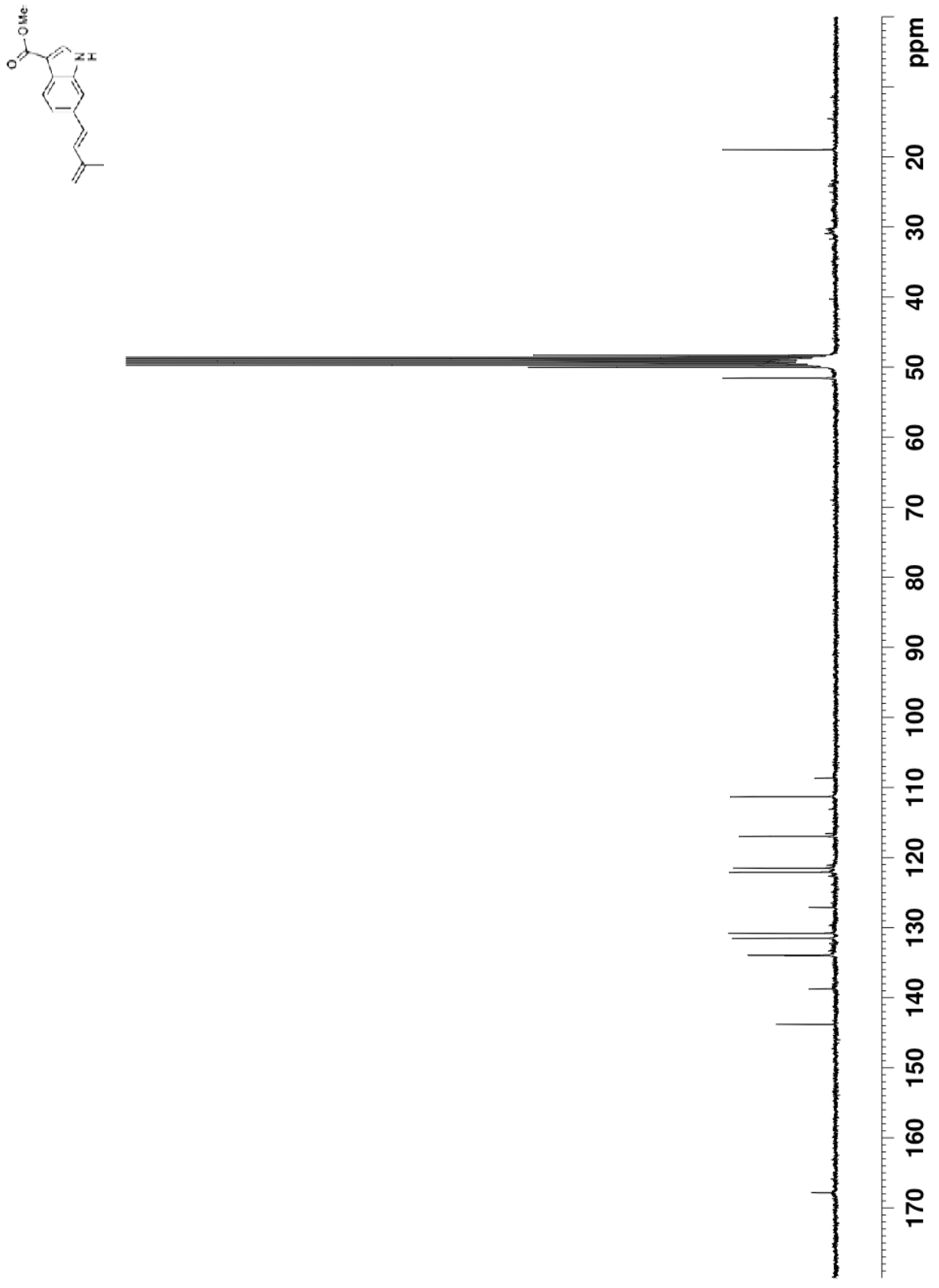

Spectrum 79. ^{13}C NMR spectrum of methyl ester **3.8** (75 MHz, CD_3OD, 293K)

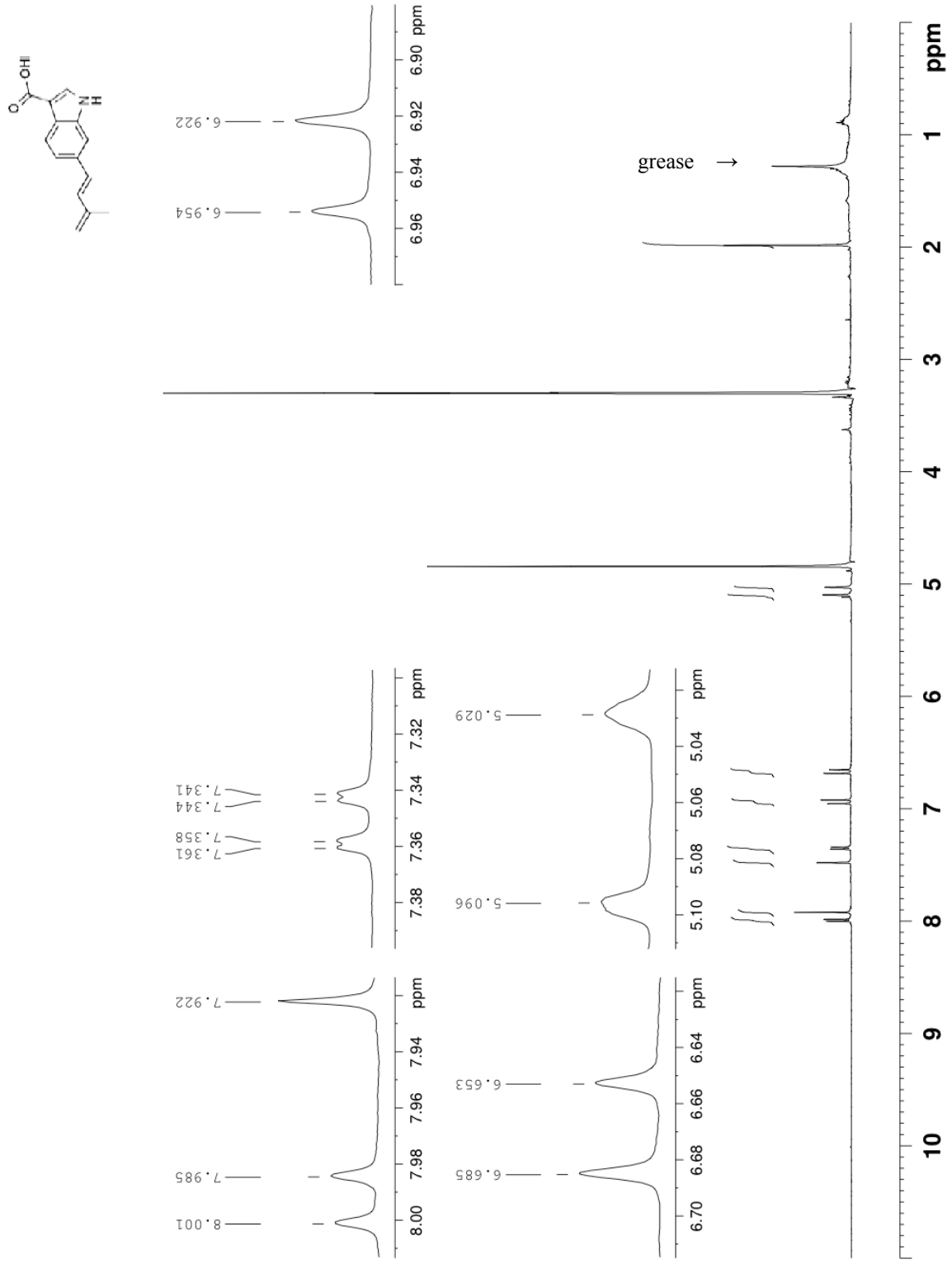

Spectrum 80. ^{1}H NMR spectrum of TMC-205 (**3.1**) (500 MHz, CD_3OD, 293K)

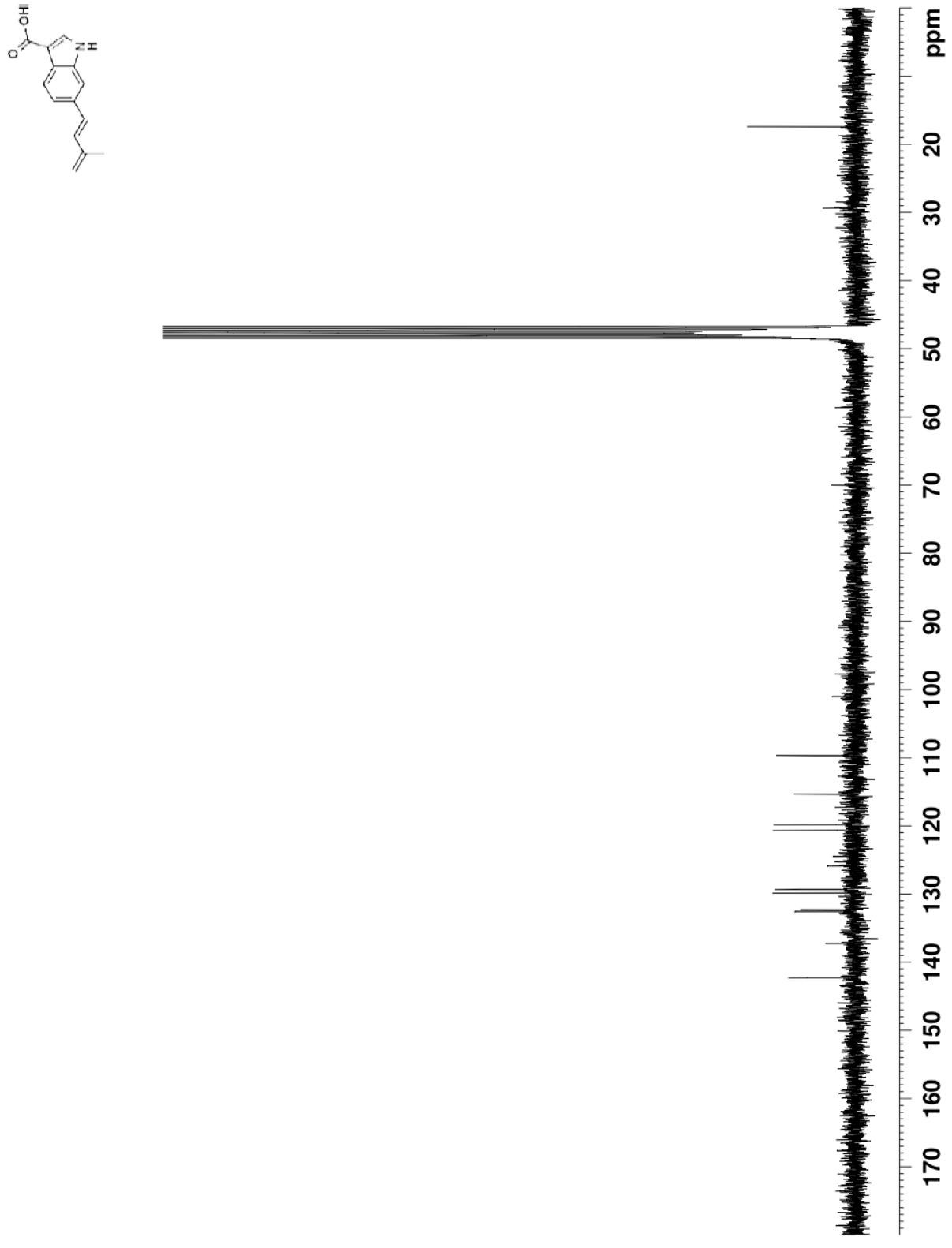

Spectrum 81. ^{13}C NMR spectrum of TMC-205 (**3.1**) (75 MHz, CD_3OD, 293K)

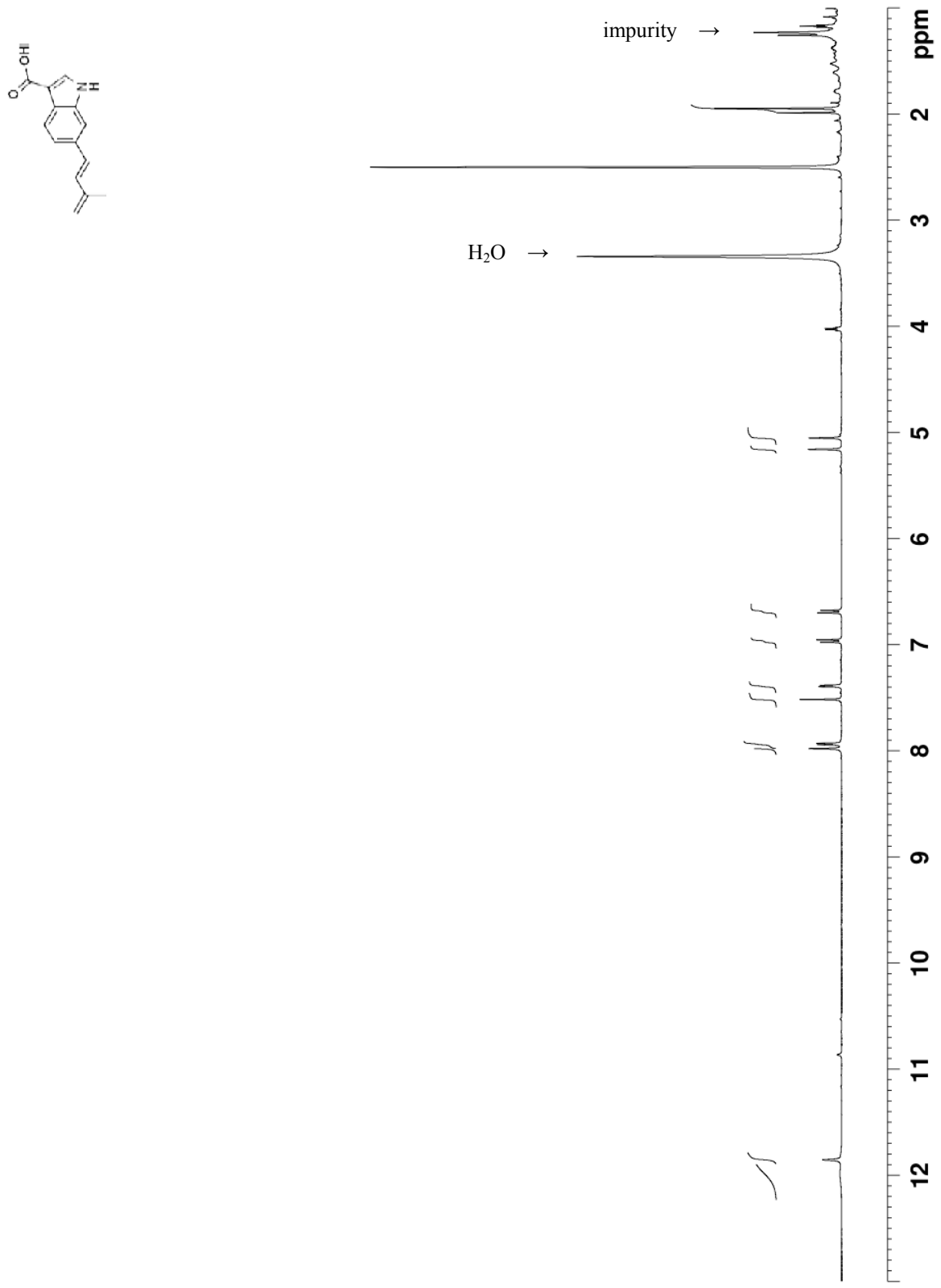

Spectrum 82. ^{1}H NMR spectrum of TMC-205 (**3.1**) (700 MHz, DMSO-d_6, 293K)

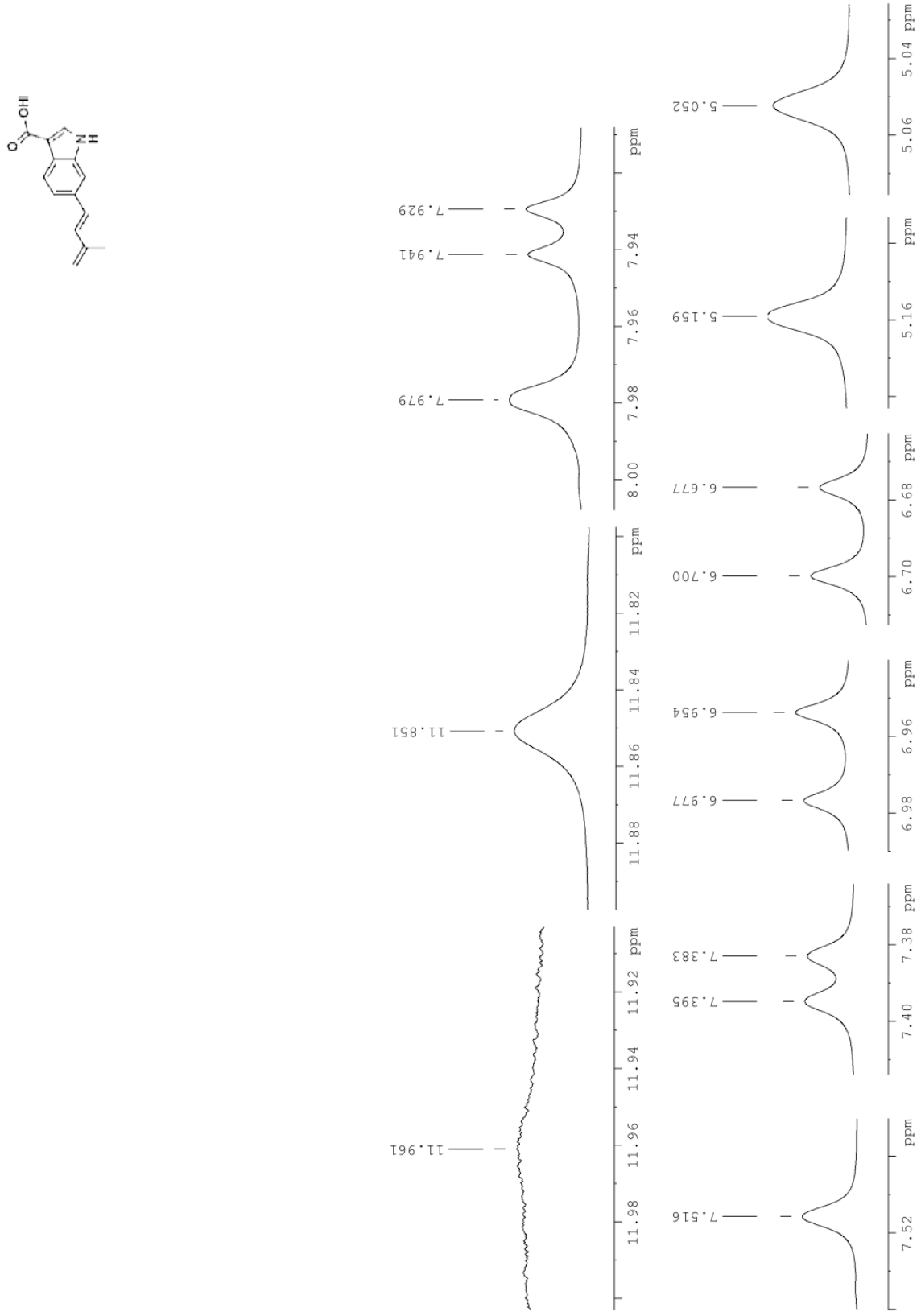

Spectrum 83. ^{1}H NMR spectrum of TMC-205 (**3.1**) (700 MHz, DMSO-d_6, 293K)

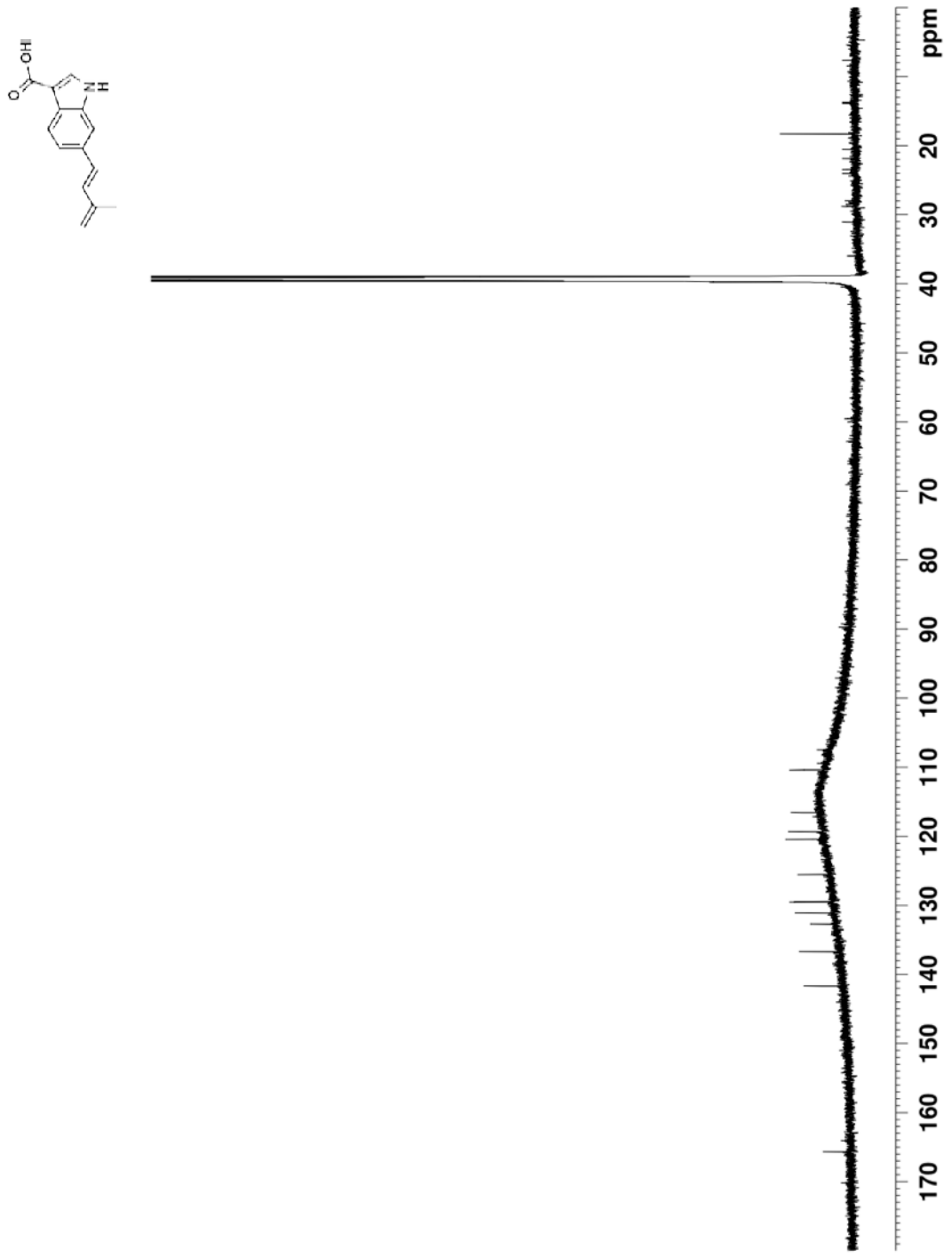

Spectrum 84. ^{13}C NMR spectrum of TMC-205 (**3.1**) (175 MHz, DMSO-d_6, 293K)

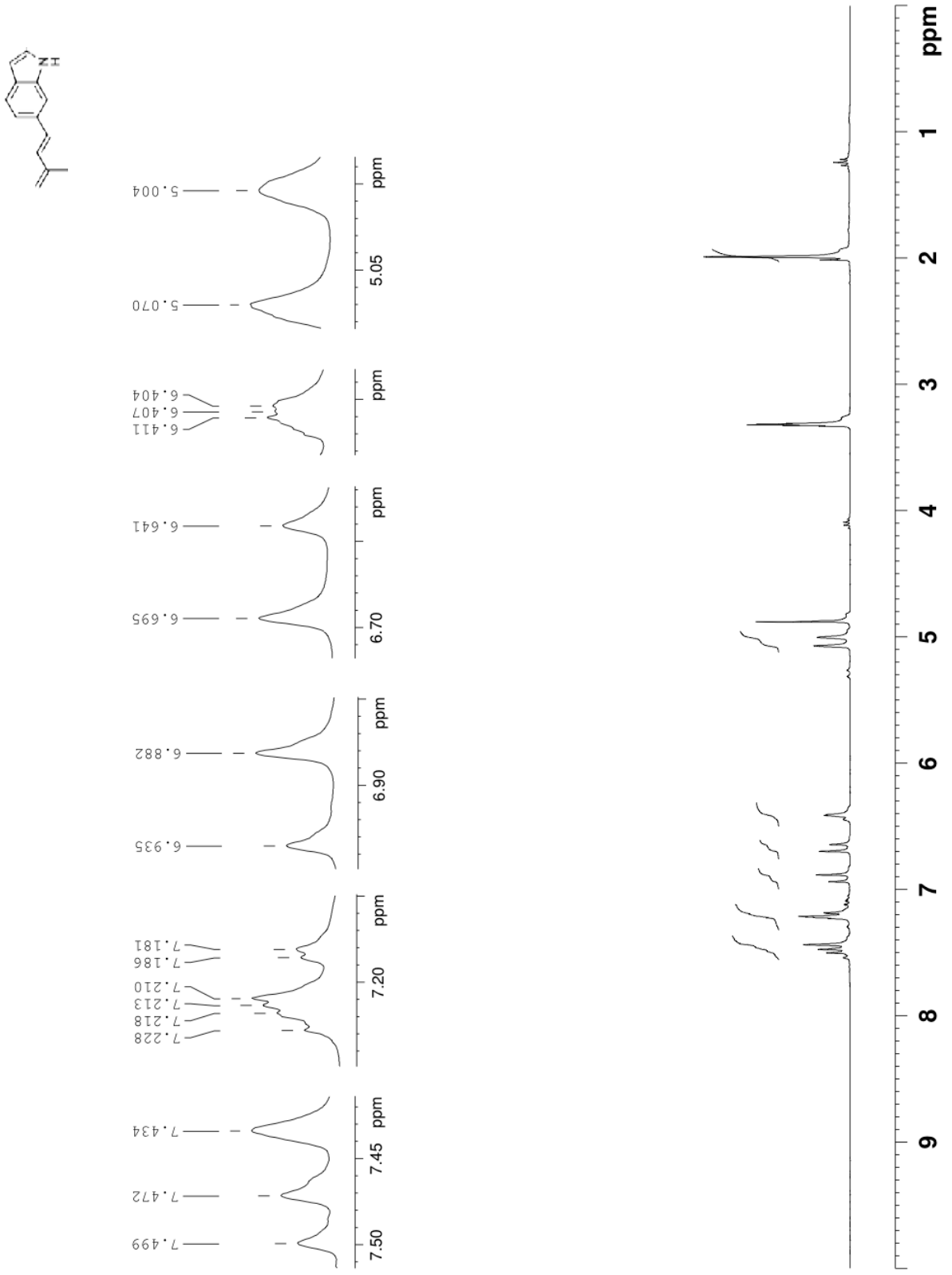

Spectrum 85. ^{1}H NMR spectrum of decarboxylated analogue **3.9** (300 MHz, CD_3OD, 293K)

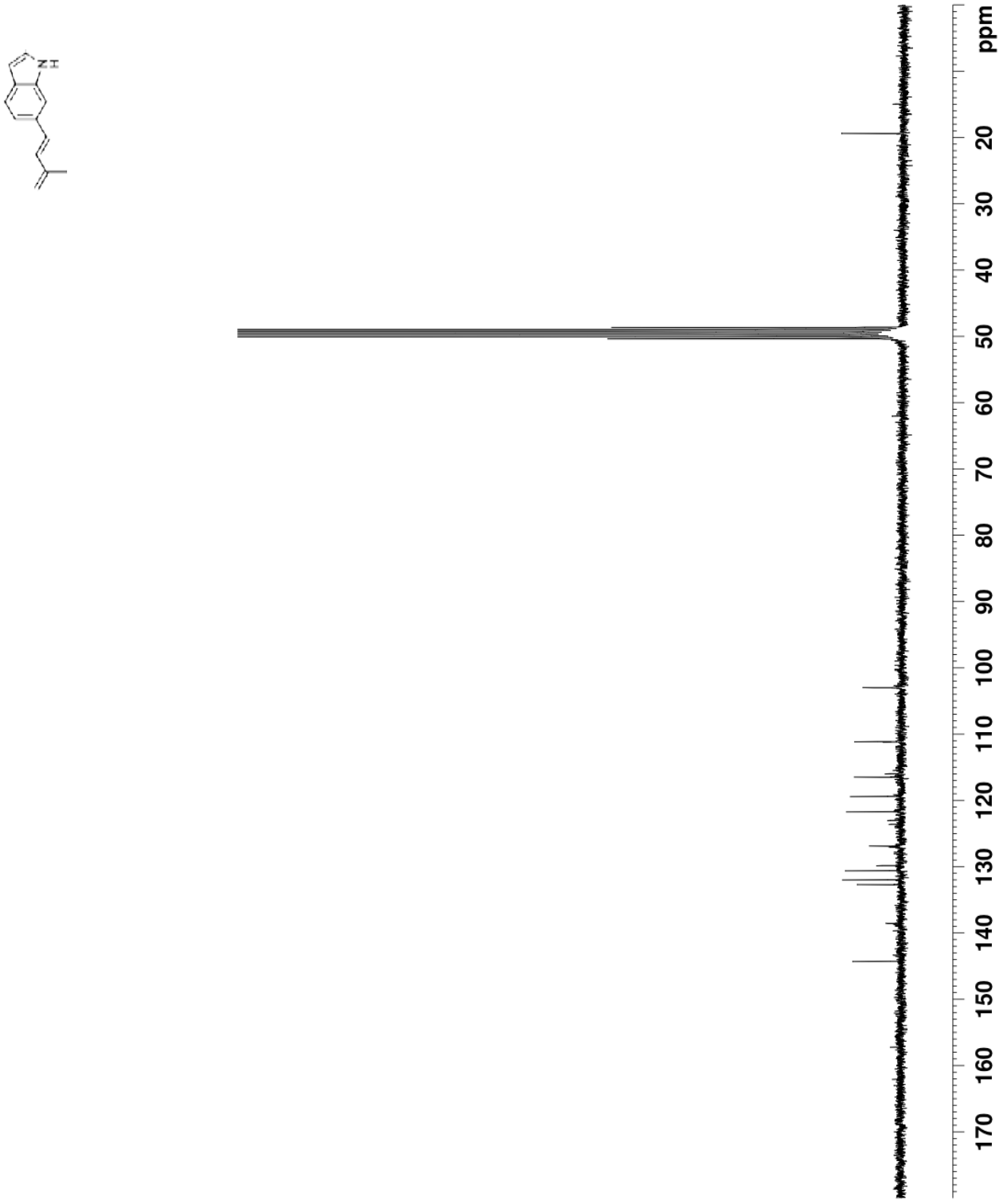

Spectrum 86. ^{13}C NMR spectrum of decarboxylated analogue **3.9** (75 MHz, CD_3OD, 293K)

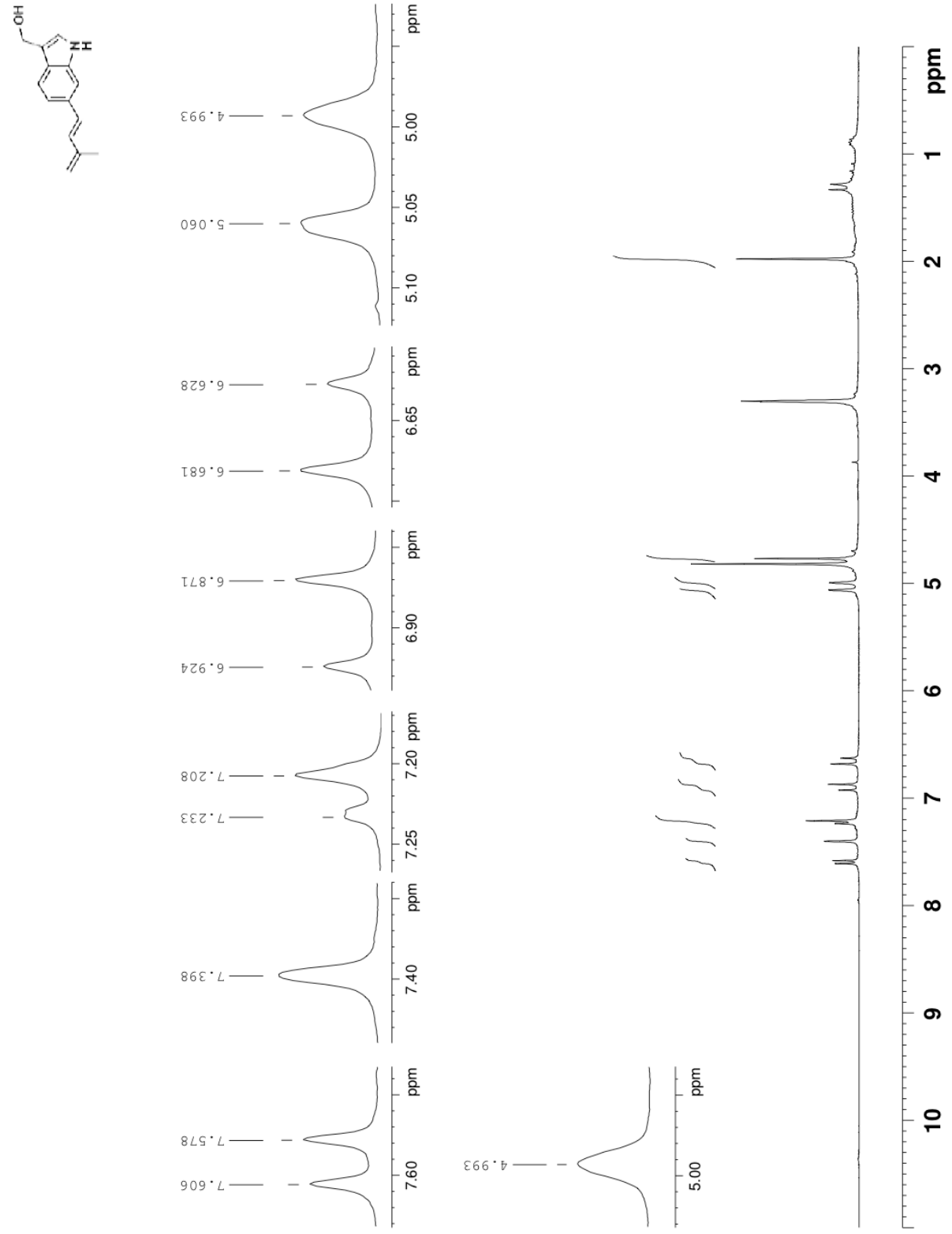

Spectrum 87. ^{1}H NMR spectrum of alcohol **3.10** (300 MHz, CD_3OD, 293K)

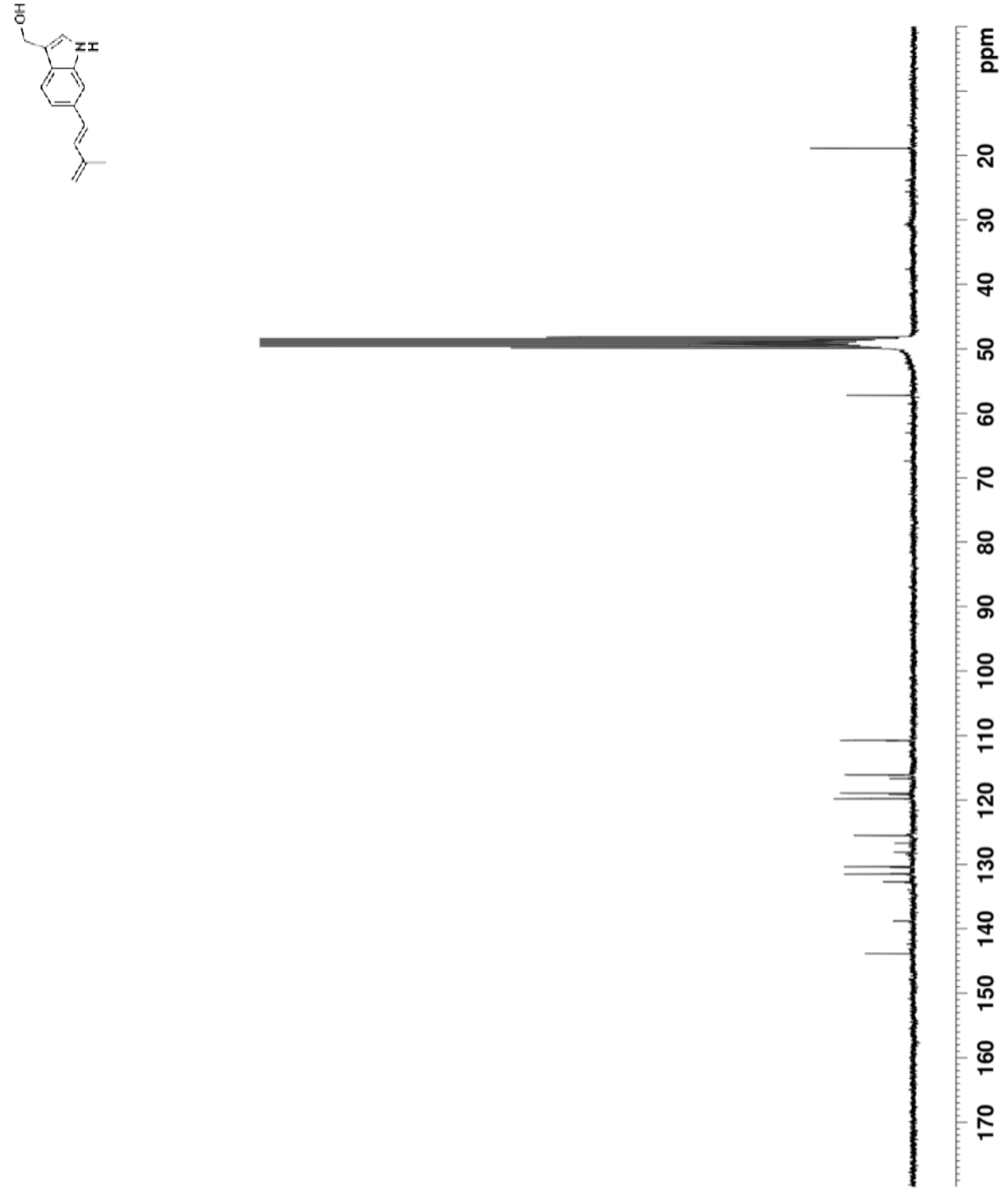

Spectrum 88. ^{13}C NMR spectrum of alcohol **3.10** (75 MHz, CD_3OD, 293K)

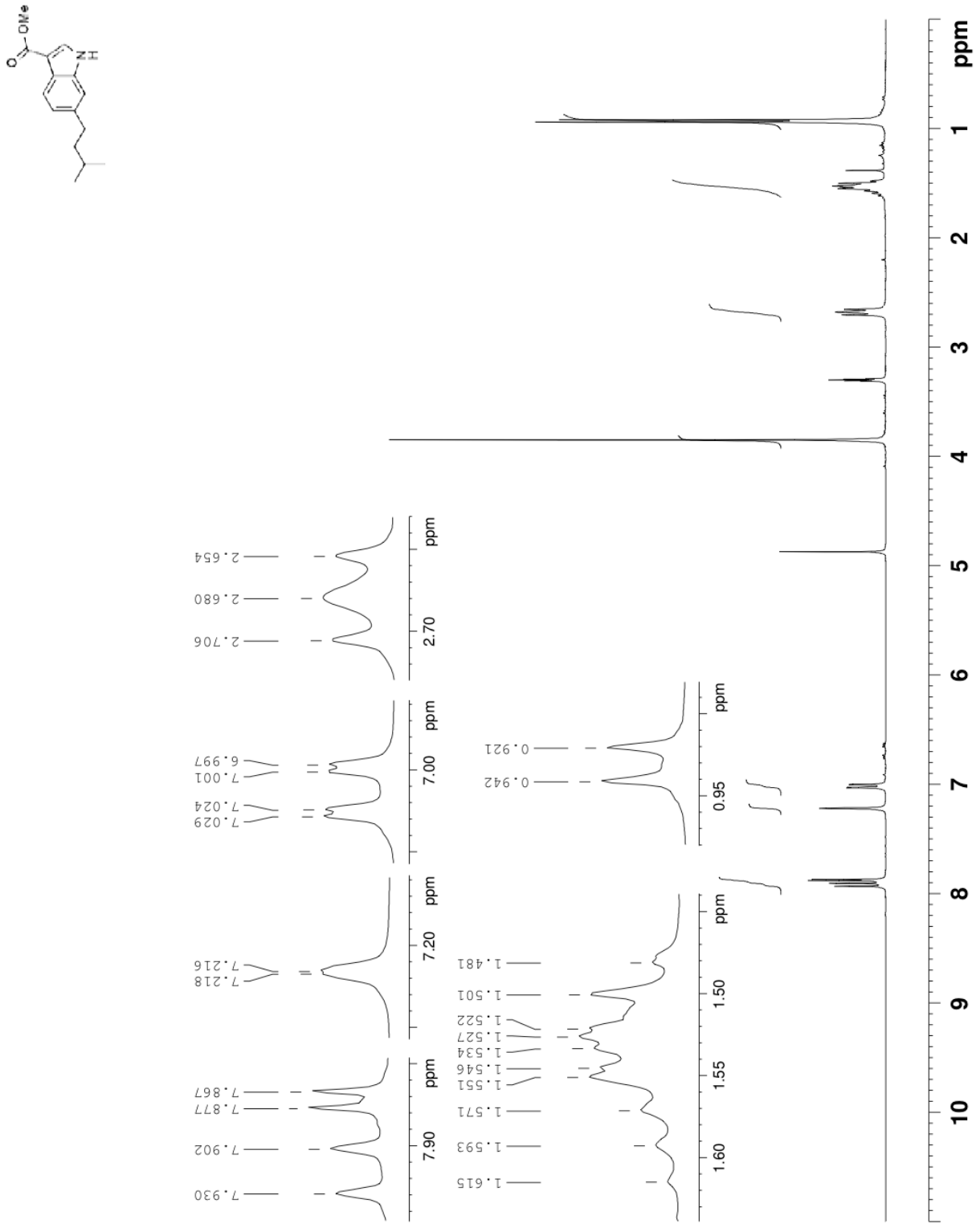

Spectrum 89. ^{1}H NMR spectrum of **3.11** (300 MHz, CD_3OD, 293K)

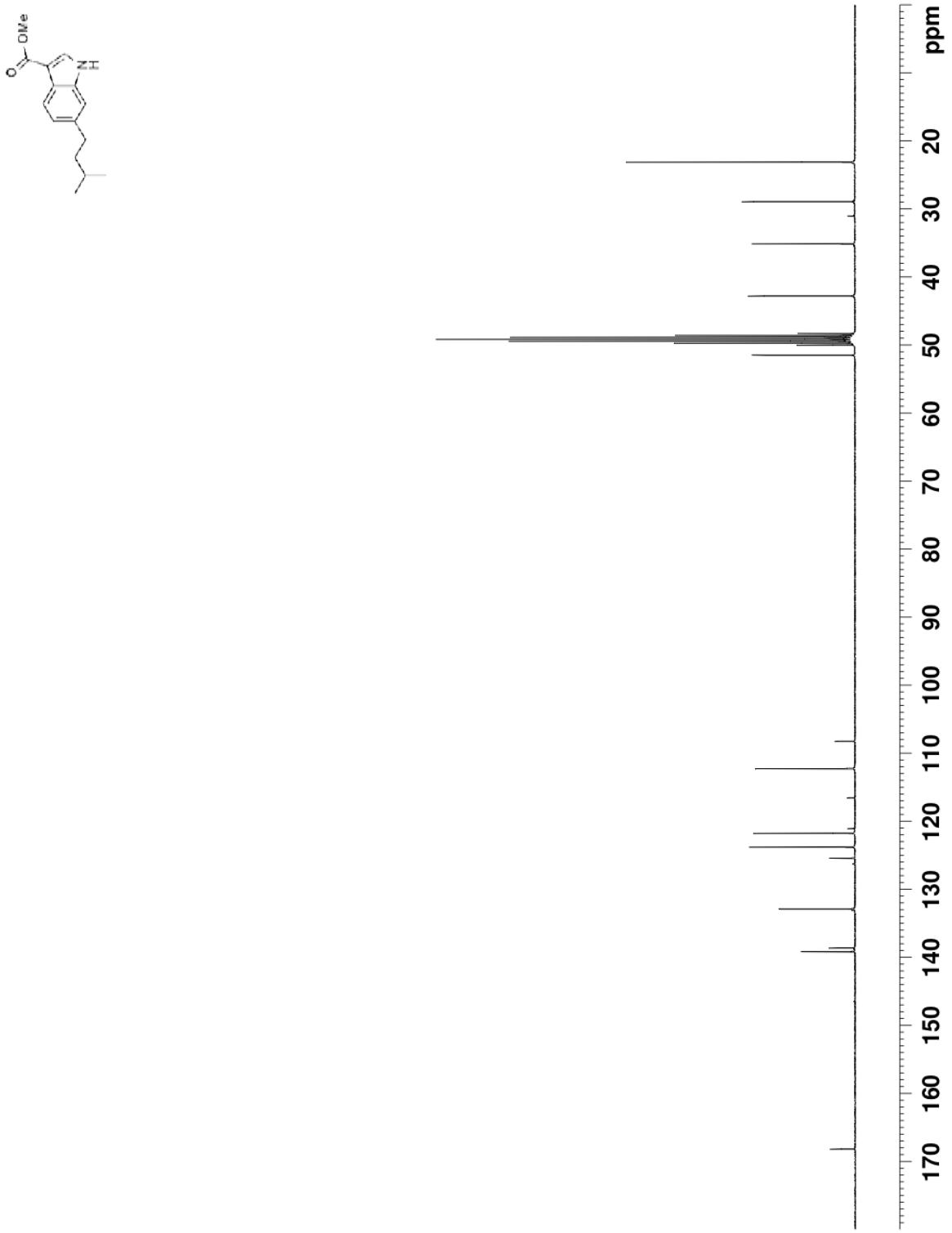

Spectrum 90. ^{13}C NMR spectrum of **3.11** (75 MHz, CD_3OD, 293K)

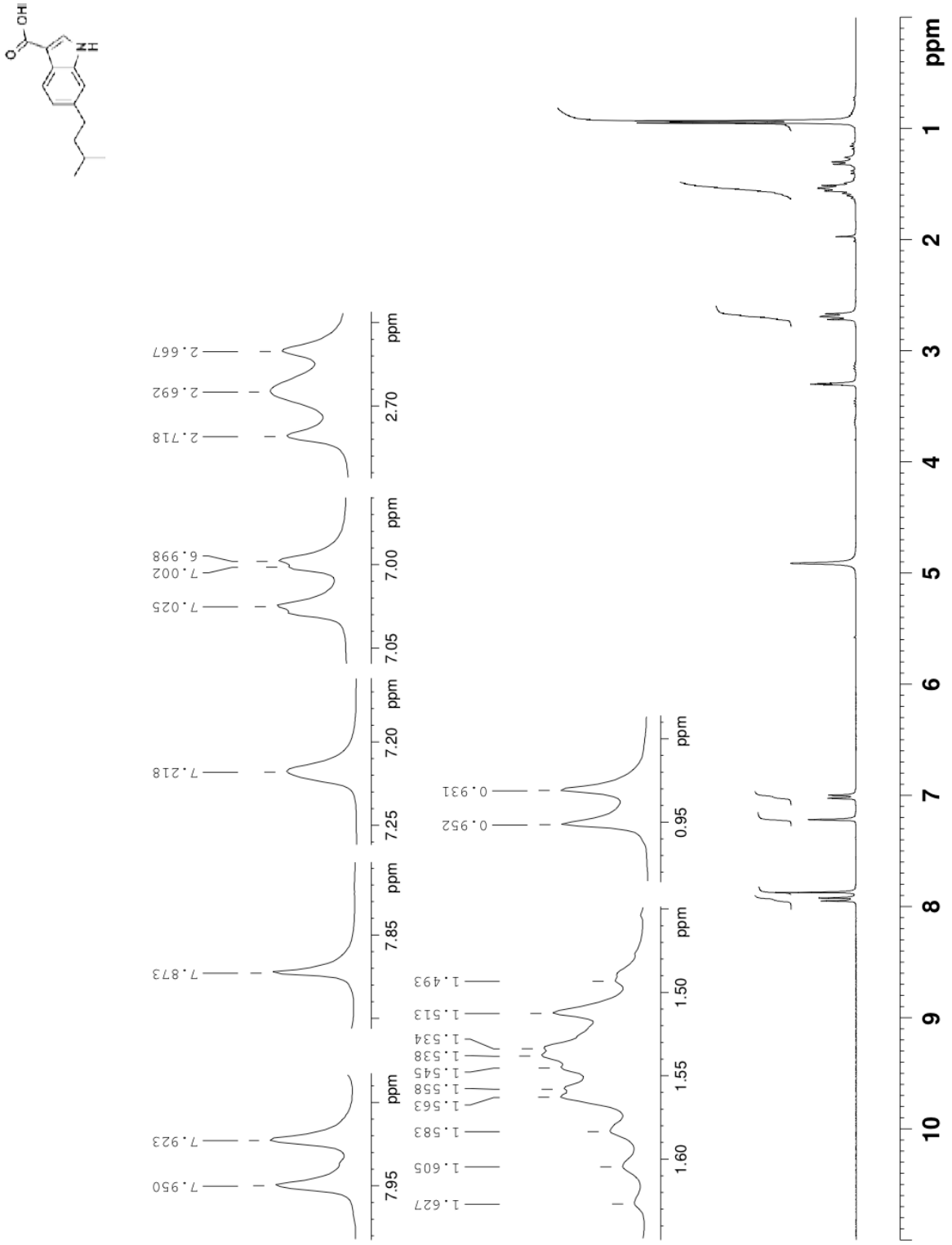

Spectrum 91. ^{1}H NMR spectrum of alkane analogue **3.12** (300 MHz, CD_3OD, 293K)

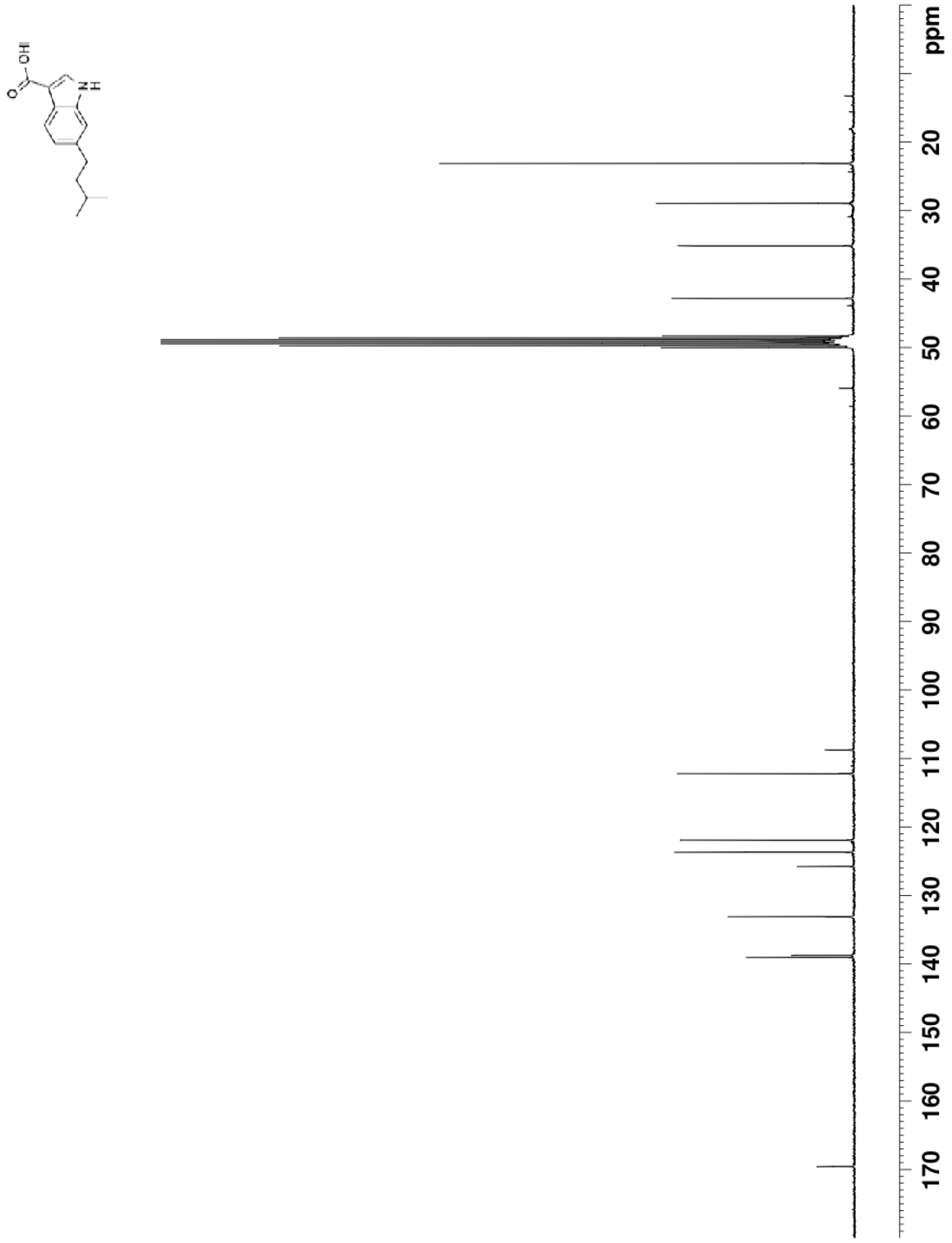

Spectrum 92. ^{13}C NMR spectrum of alkane analogue **3.12** (75 MHz, CD_3OD, 293K)

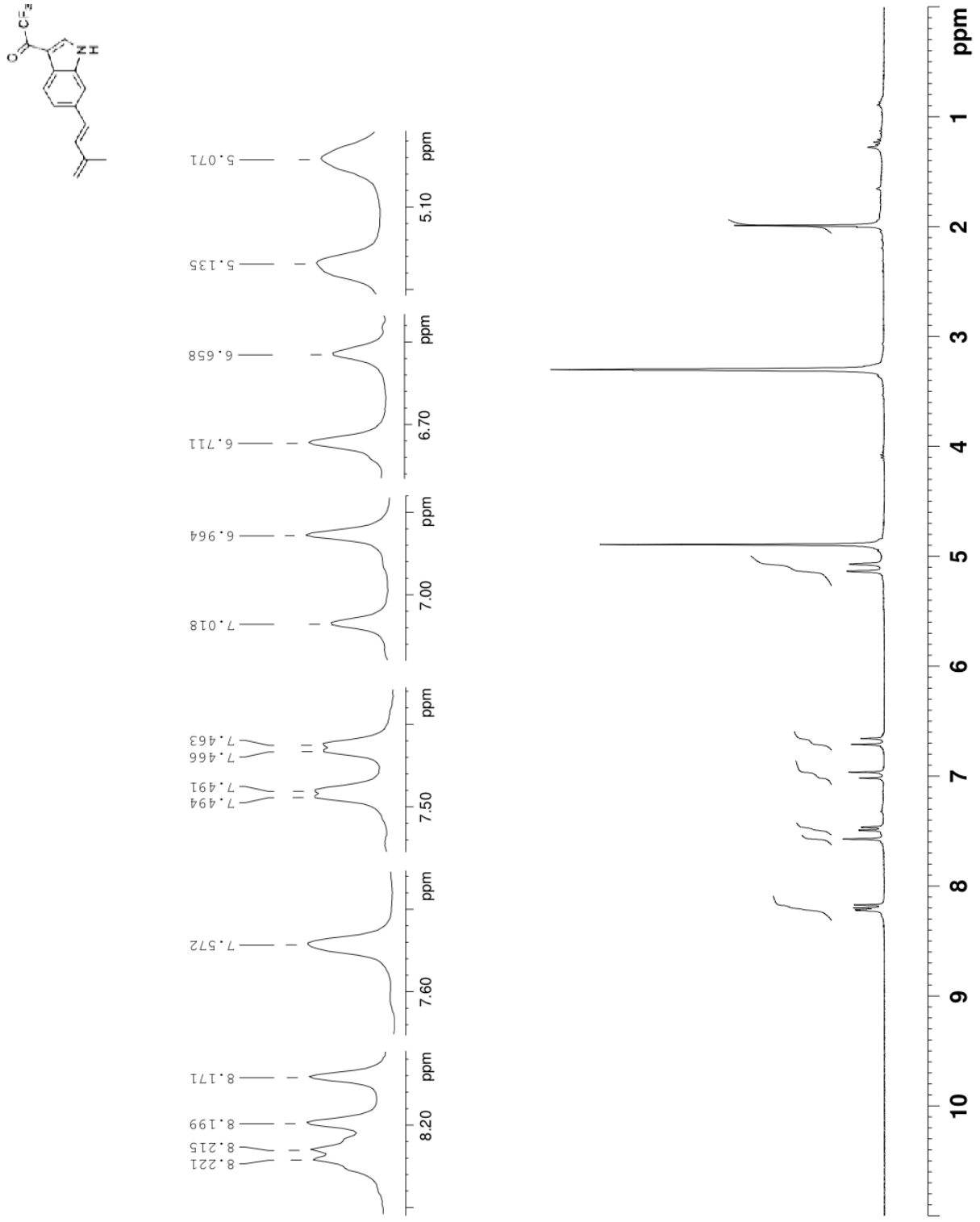

Spectrum 93. ^{1}H NMR spectrum of ketone **3.13** (300 MHz, CD_3OD, 293K)

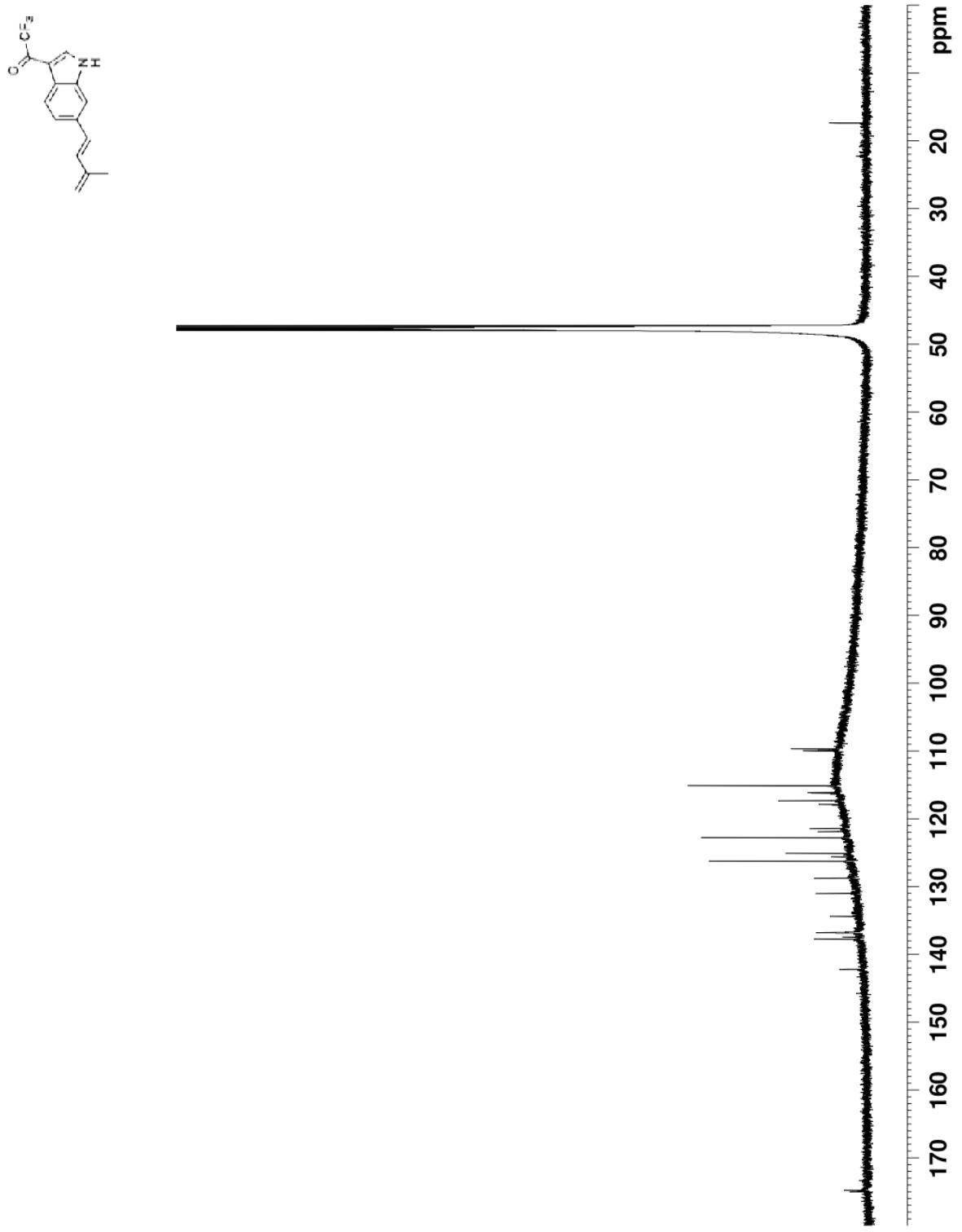

Spectrum 94. ^{13}C NMR spectrum of ketone **3.13** (175 MHz, CD_3OD, 293K)

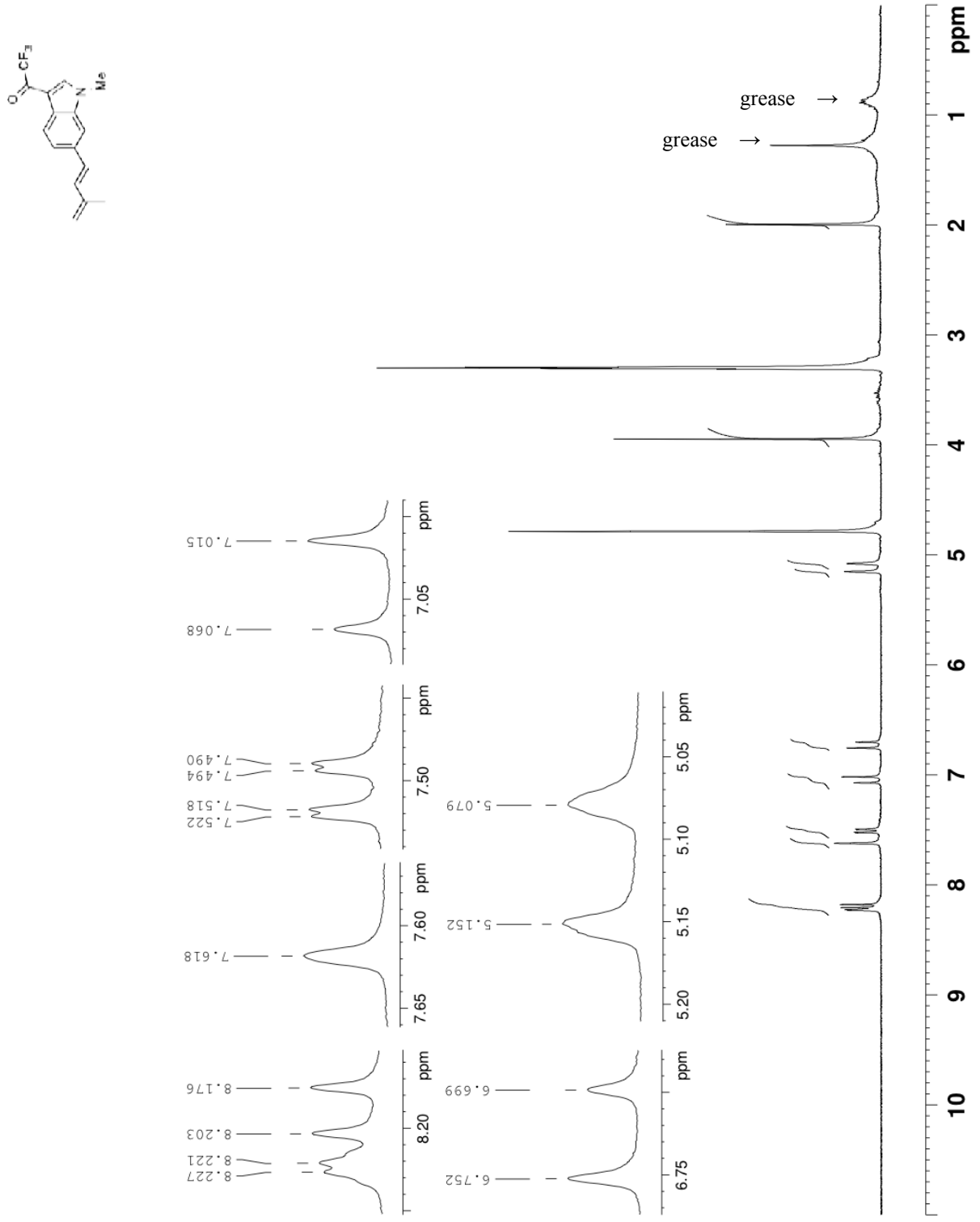

Spectrum 95. ^{1}H NMR spectrum of *N*-methylated analogue **3.14** (300 MHz, CD_3OD, 293K)

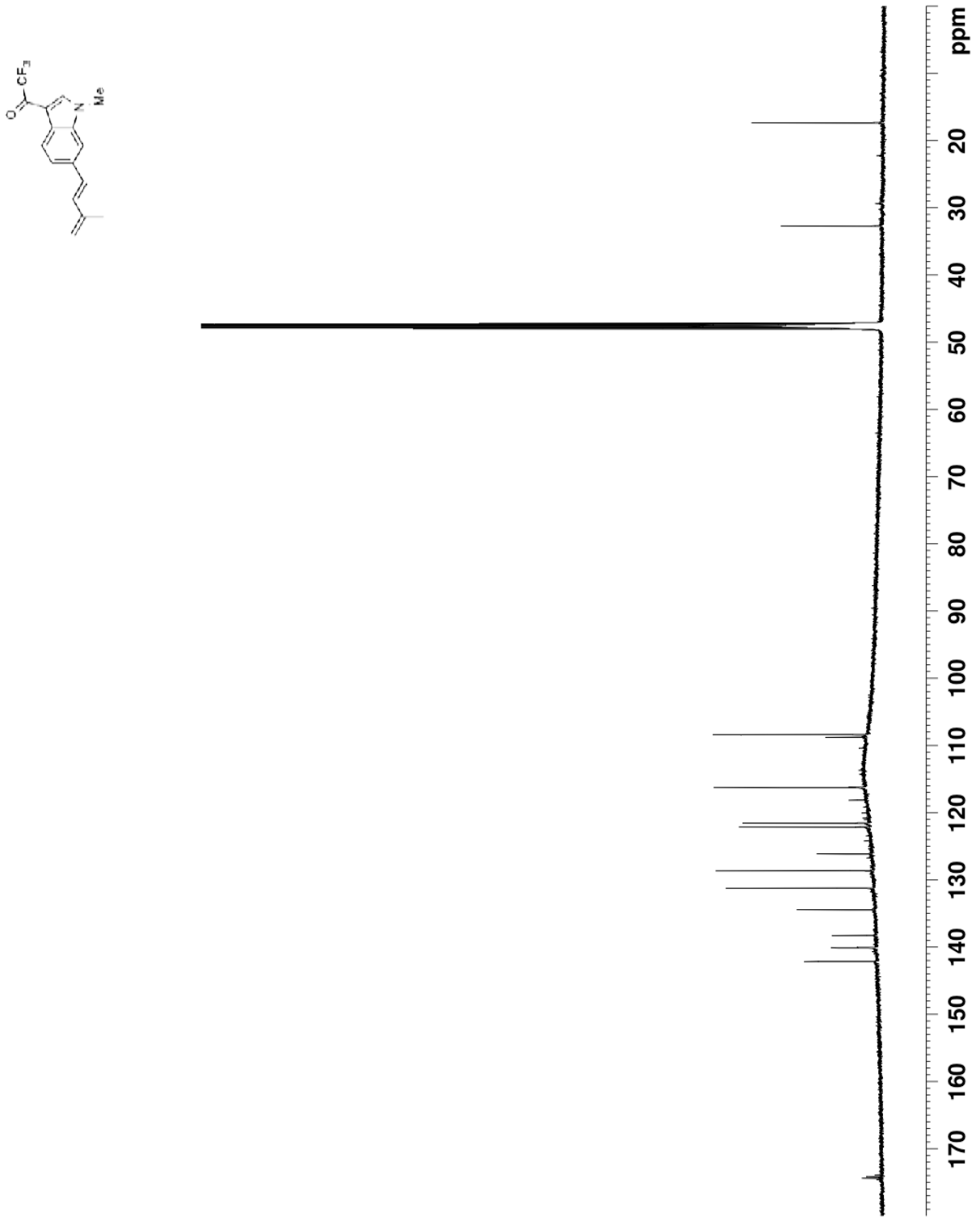

Spectrum 96. ^{13}C NMR spectrum of *N*-methylated analogue **3.14** (150 MHz, CD_3OD, 293K)

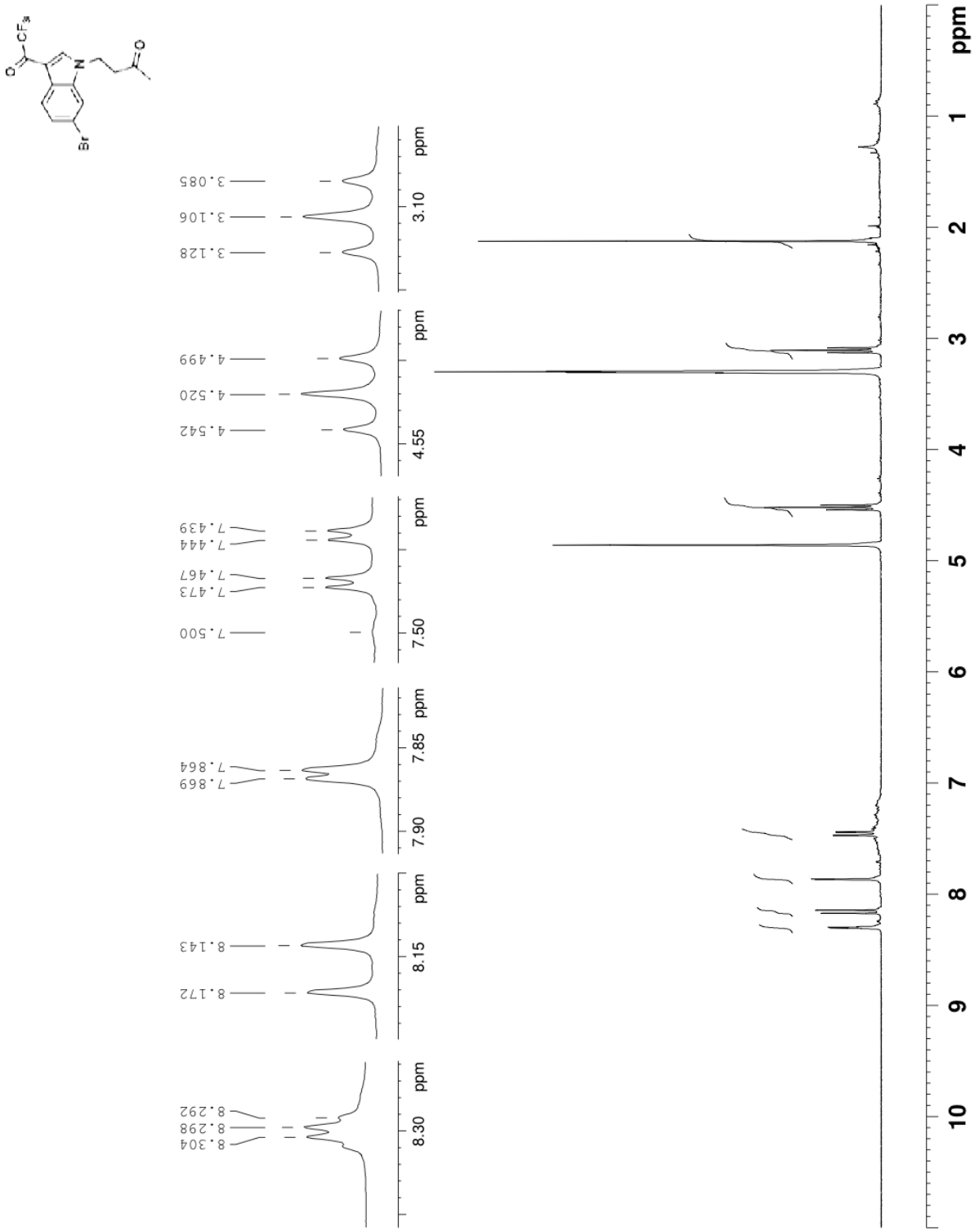

Spectrum 97. ^{1}H NMR spectrum of **3.16** (300 MHz, CD_3OD, 293K)

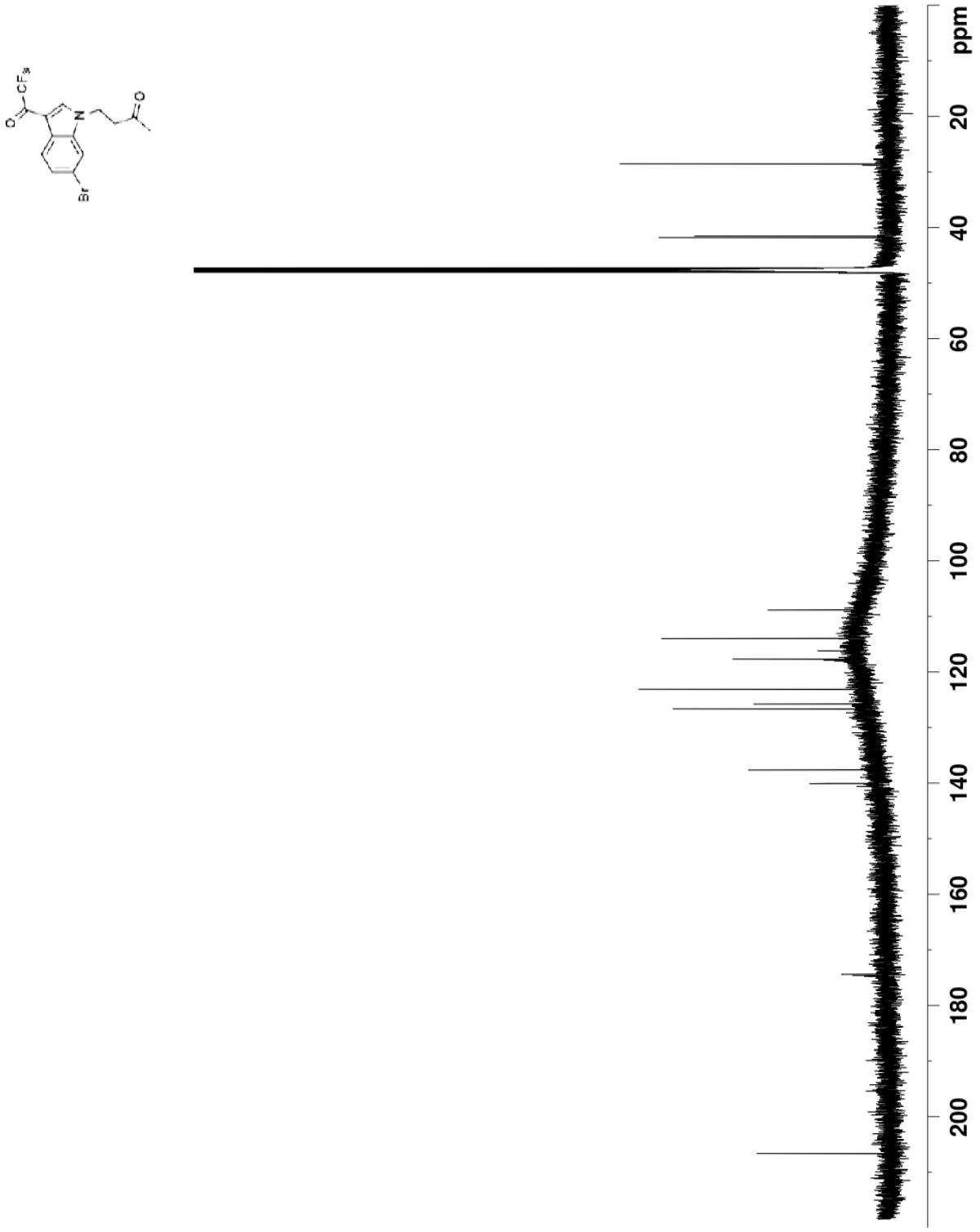

Spectrum 98. ^{13}C NMR spectrum of **3.16** (175 MHz, CD_3OD, 293K)

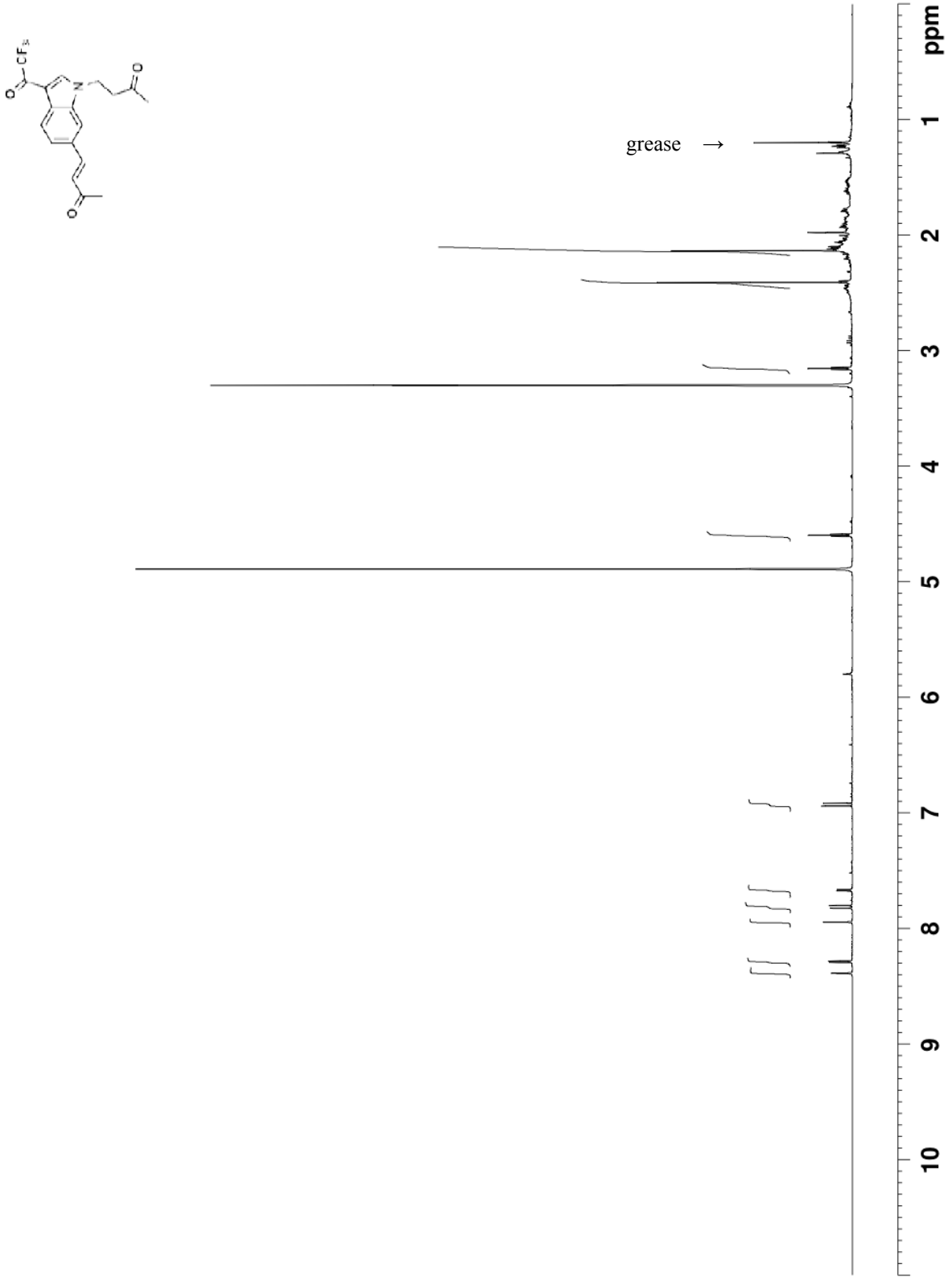

Spectrum 99. ^{1}H NMR spectrum of **3.17** (700 MHz, CD_3OD, 293K)

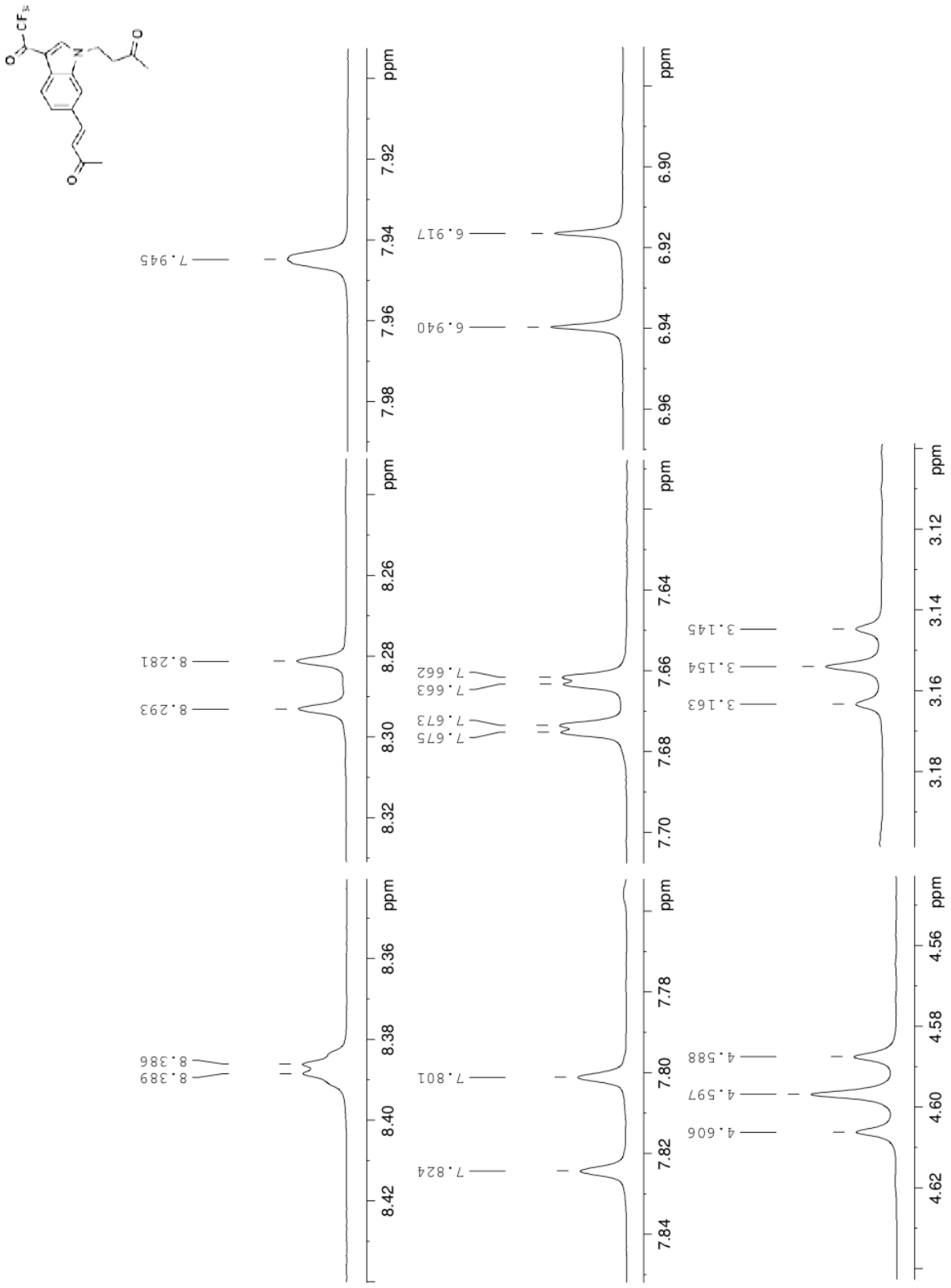

Spectrum 100. ^{1}H NMR spectrum of **3.17** (700 MHz, CD_3OD, 293K)

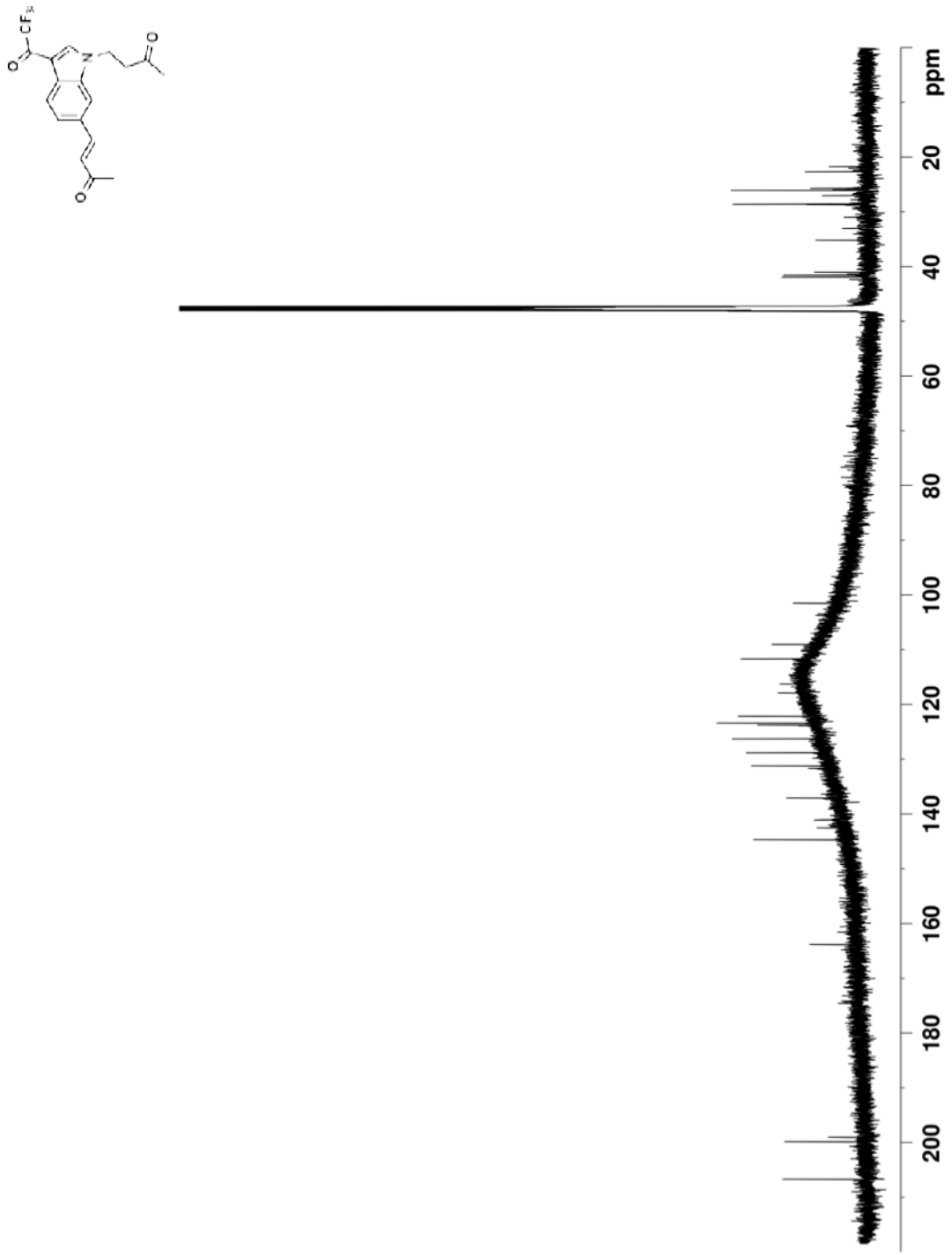

Spectrum 101. ^{13}C NMR spectrum of **3.17** (175 MHz, CD_3OD, 293K)

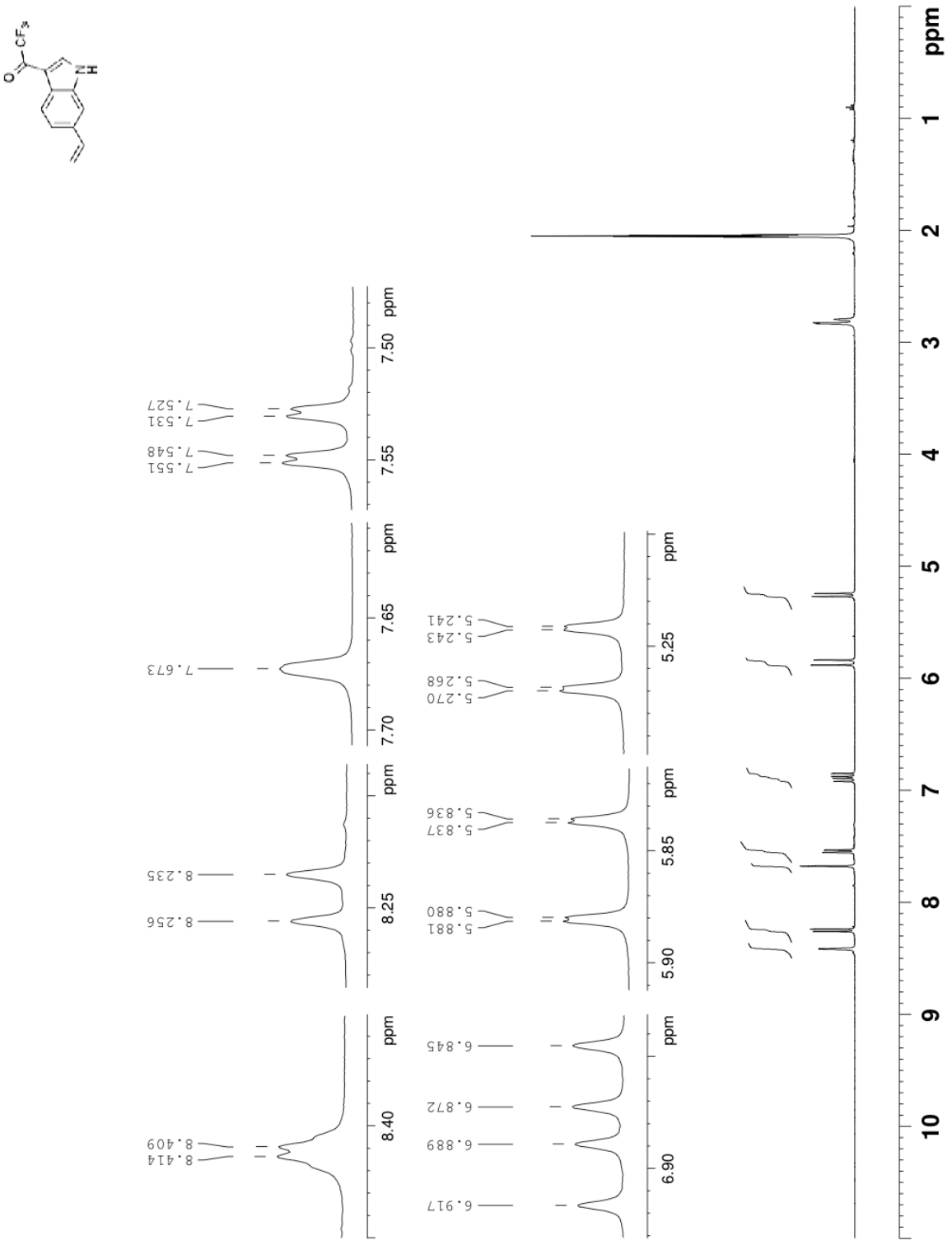

Spectrum 102. ^{1}H NMR spectrum of alkene **3.19** (400 MHz, 1%CD_3OD in acetone-d_6 293K)

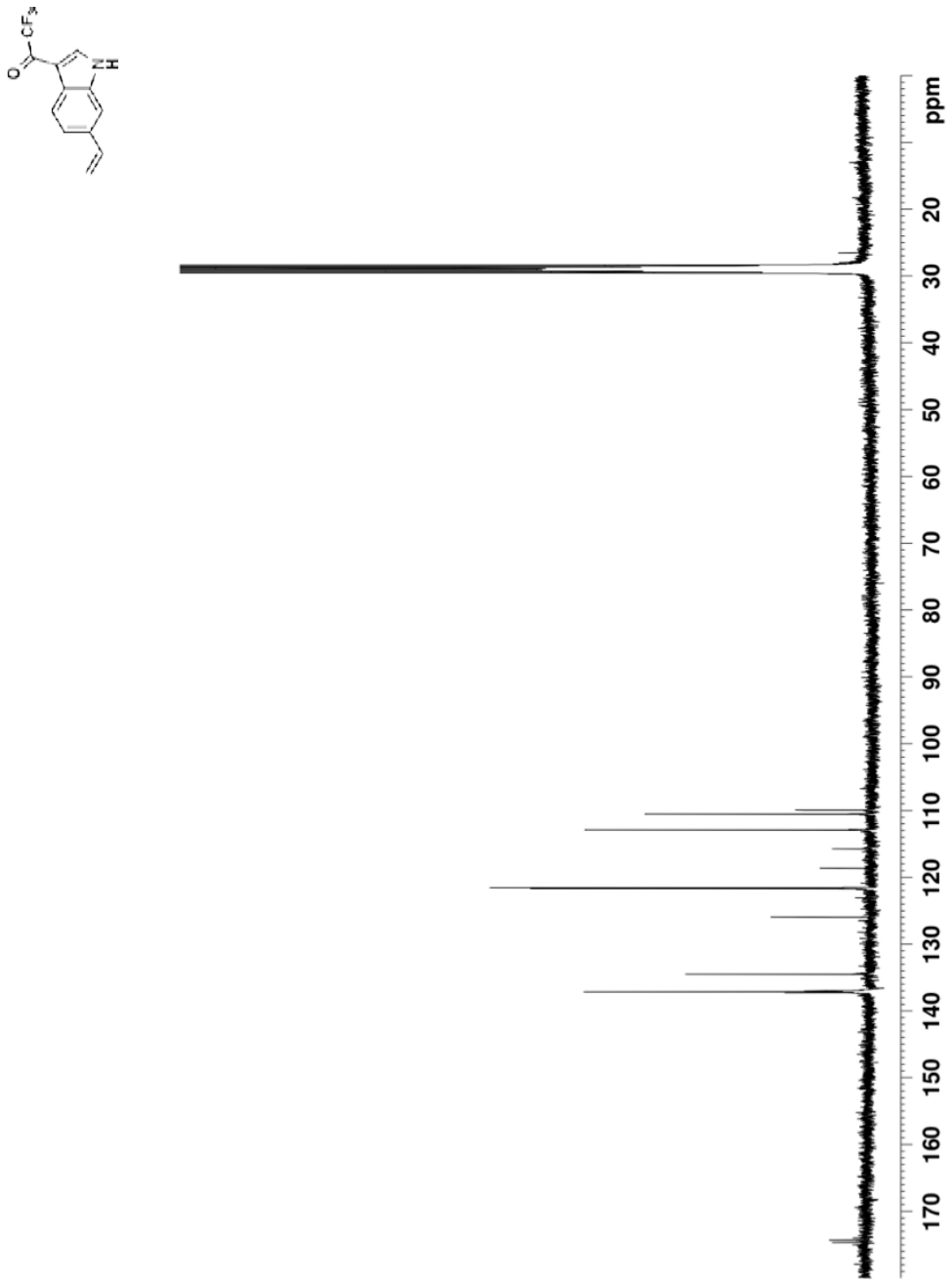

Spectrum 103. ^{13}C NMR spectrum of alkene **3.19** (100 MHz, acetone-d_6, 293K)

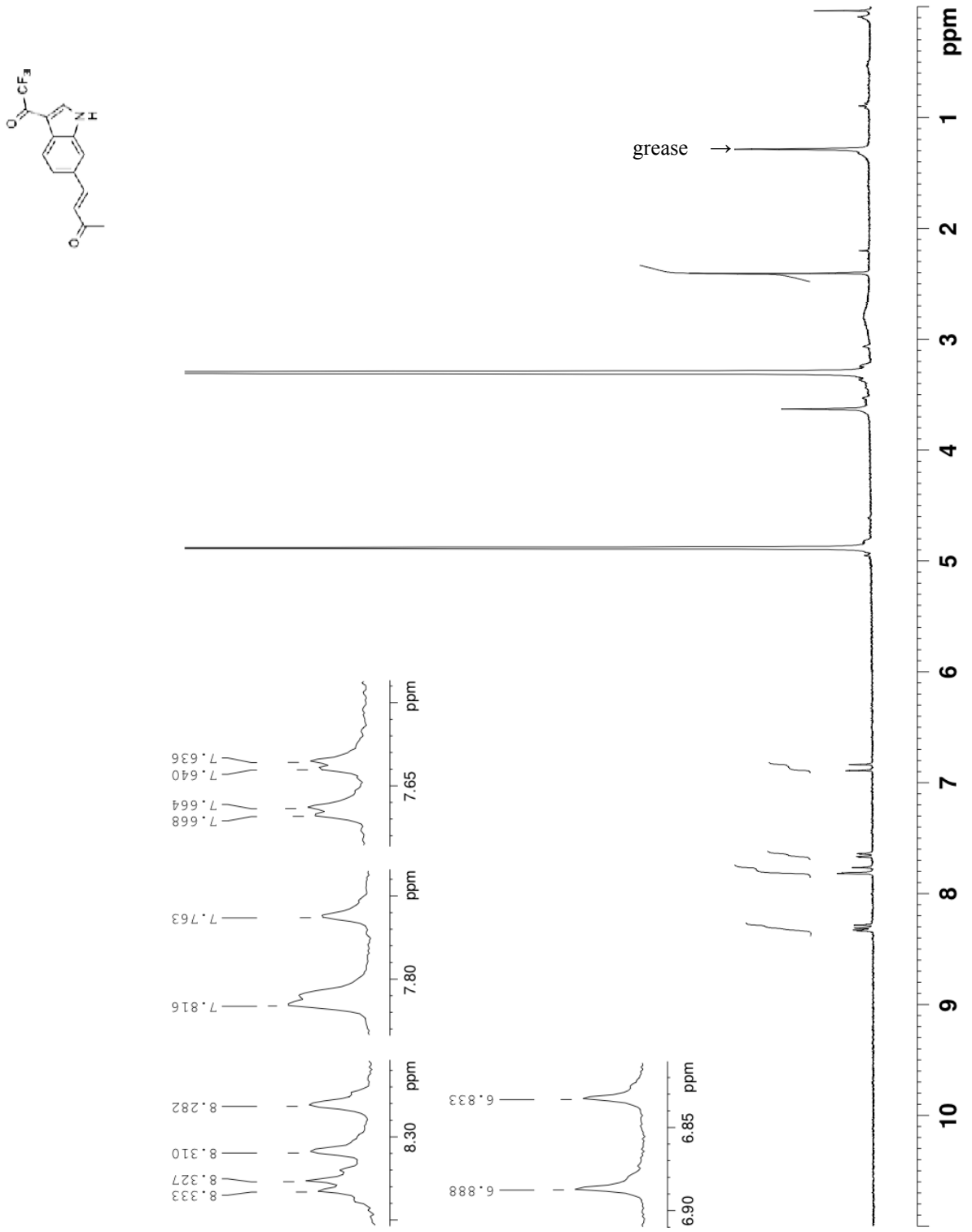

Spectrum 104. ^{1}H NMR spectrum of enone **3.20** (300 MHz, CD_3OD, 293K)

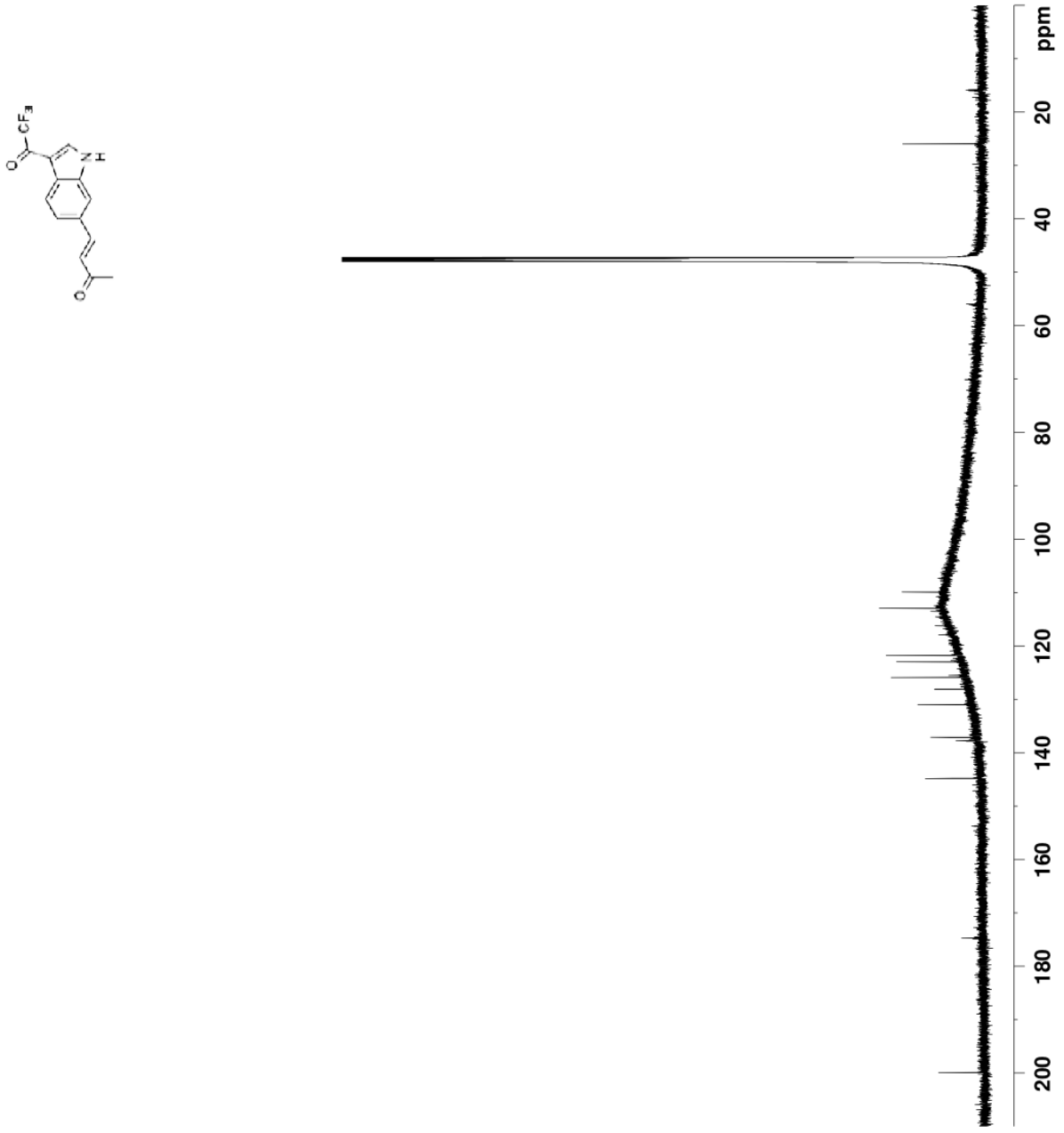

Spectrum 105. ^{13}C NMR spectrum of enone **3.20** (175 MHz, CD_3OD, 293K)

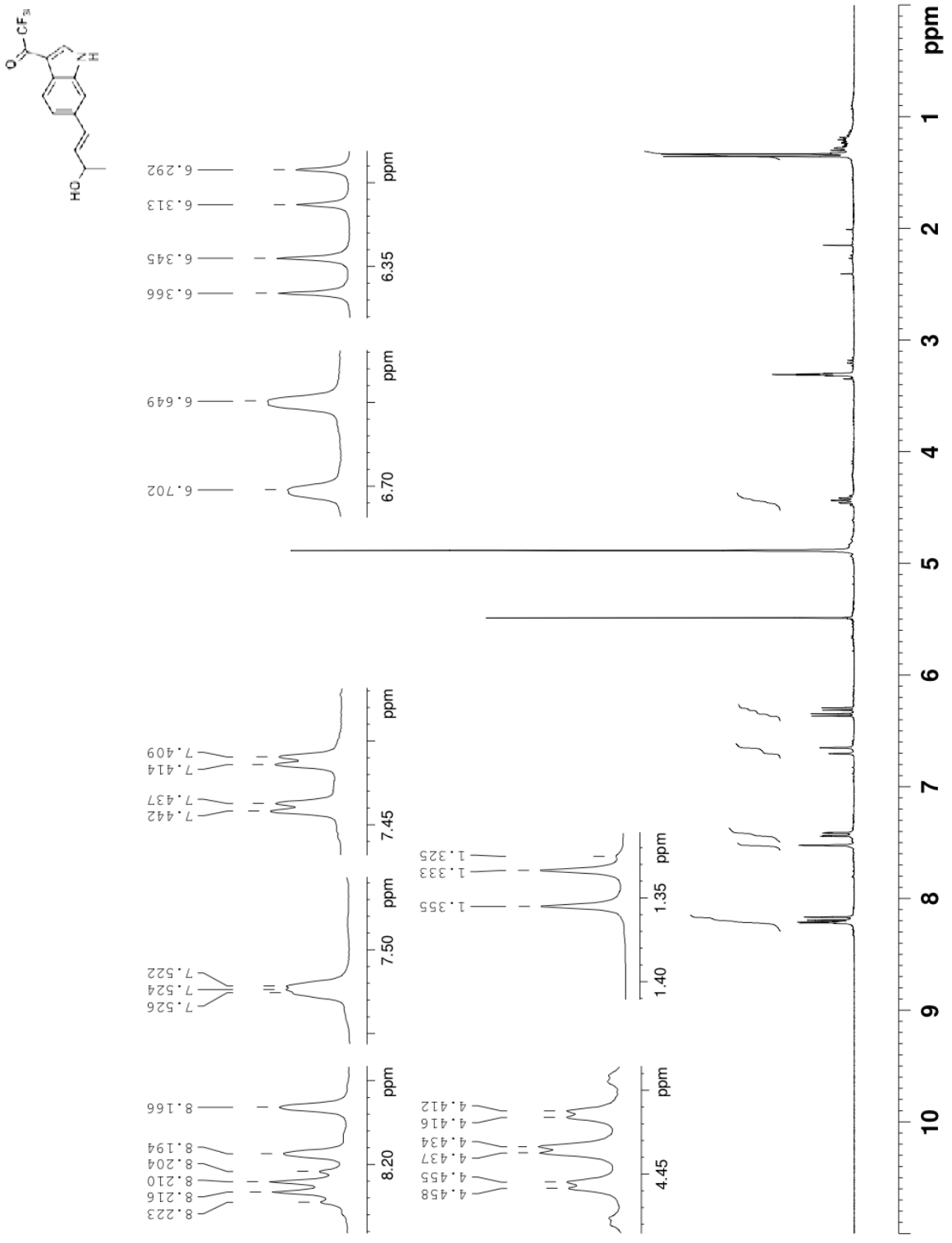

Spectrum 106. ^{1}H NMR spectrum of allylic alcohol **3.21** (300 MHz, CD_3OD, 293K)

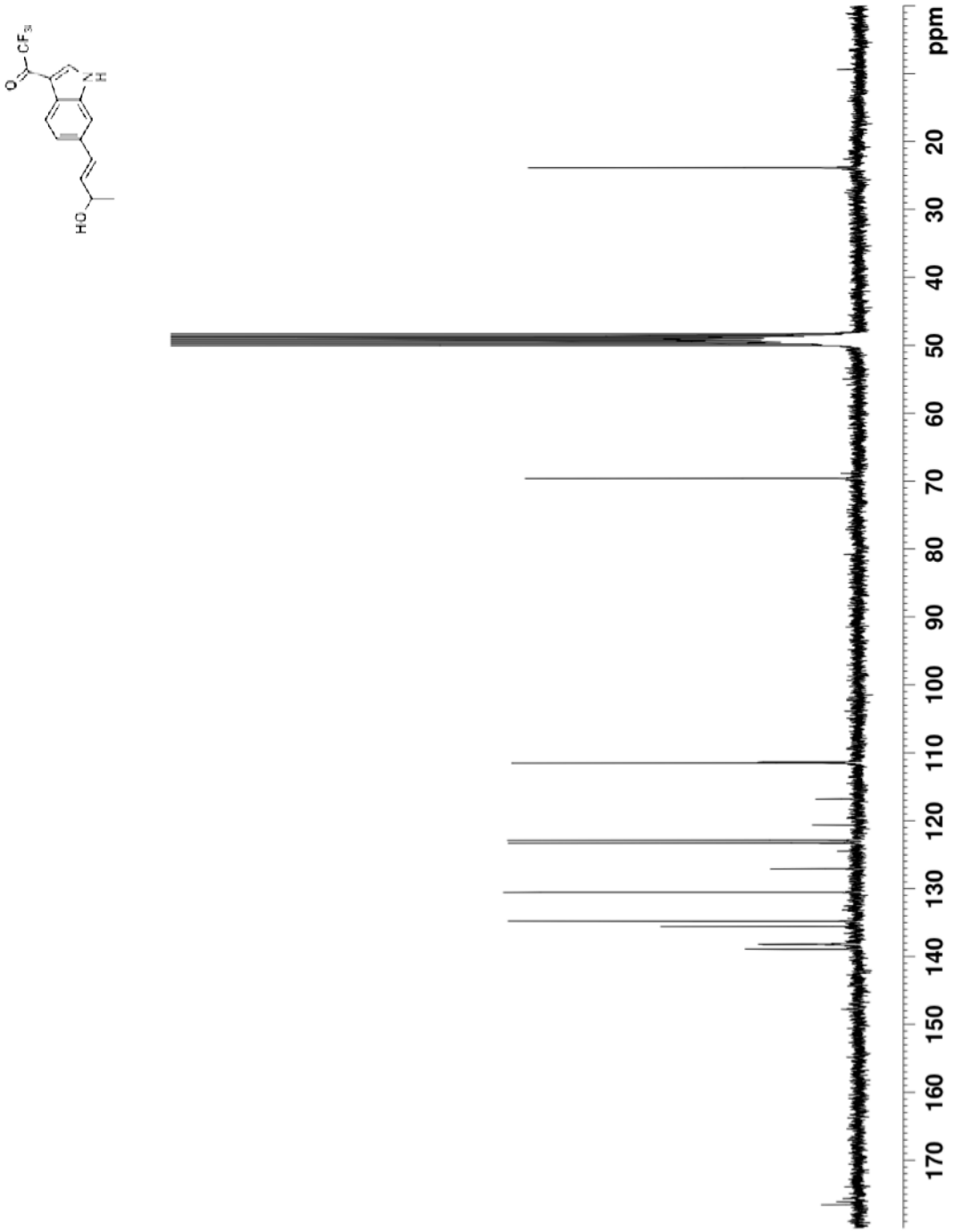

Spectrum 107. ^{13}C NMR spectrum of allylic alcohol **3.21** (75 MHz, CD_3OD, 293K)

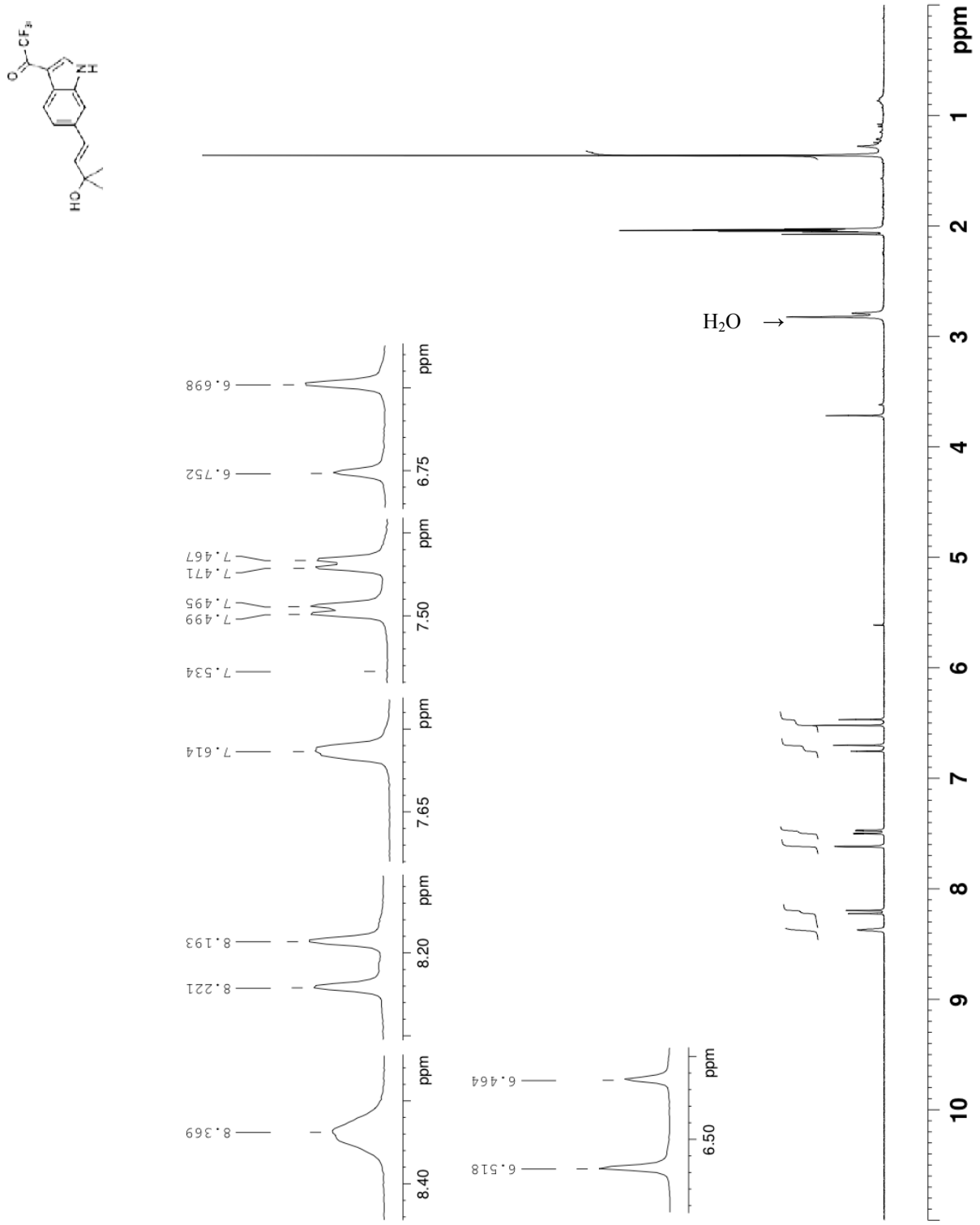

Spectrum 108. ^{1}H NMR spectrum of allylic alcohol **3.22** (300 MHz, 1%CD_3OD in acetone-d_6 293K)

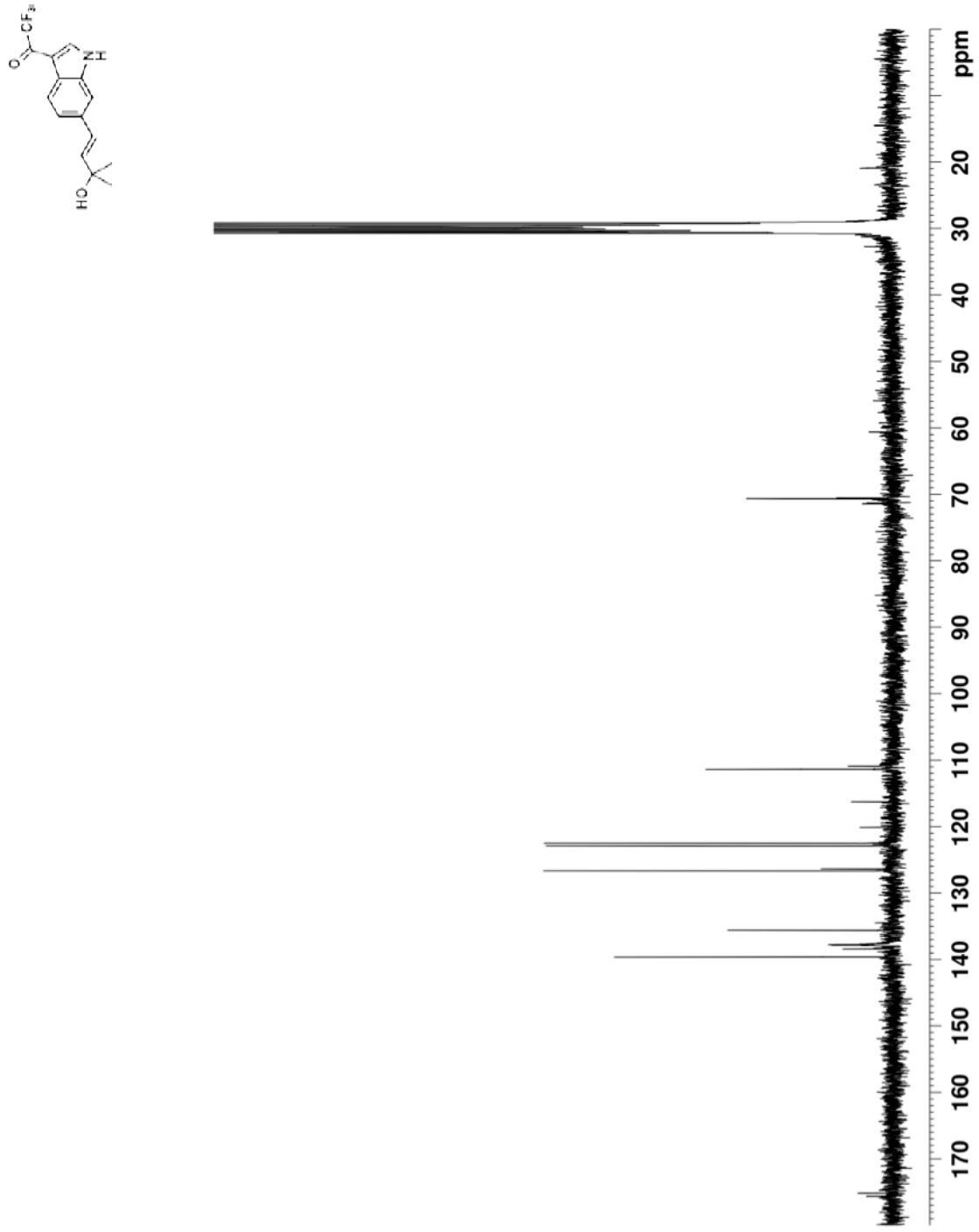

Spectrum 109. ^{13}C NMR spectrum of allylic alcohol **3.22** (75 MHz, acetone-d_6, 293K)

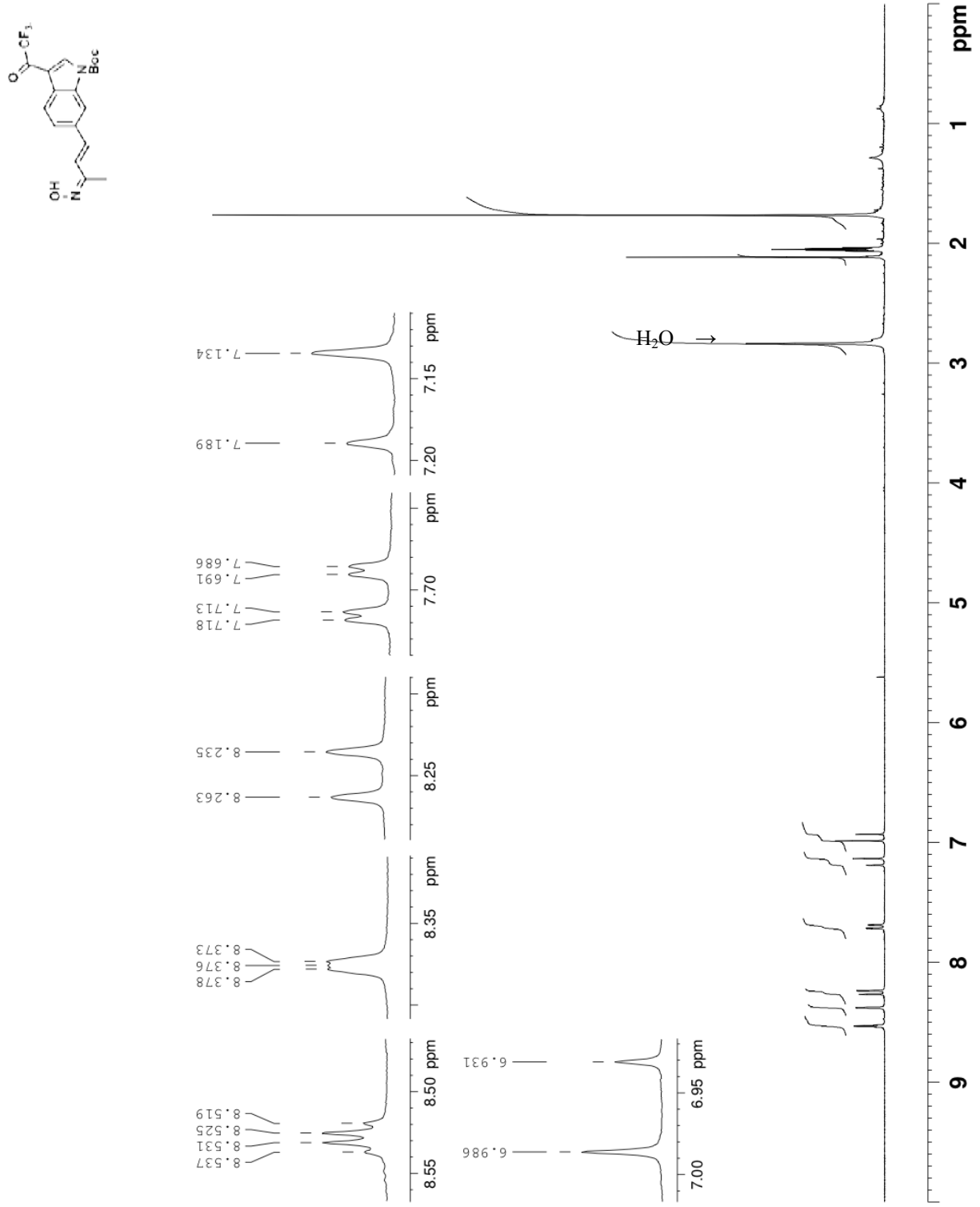

Spectrum 110. ^{1}H NMR spectrum of oxime **3.23** (300 MHz, 1%CD_3OD in acetone-d_6 293K)

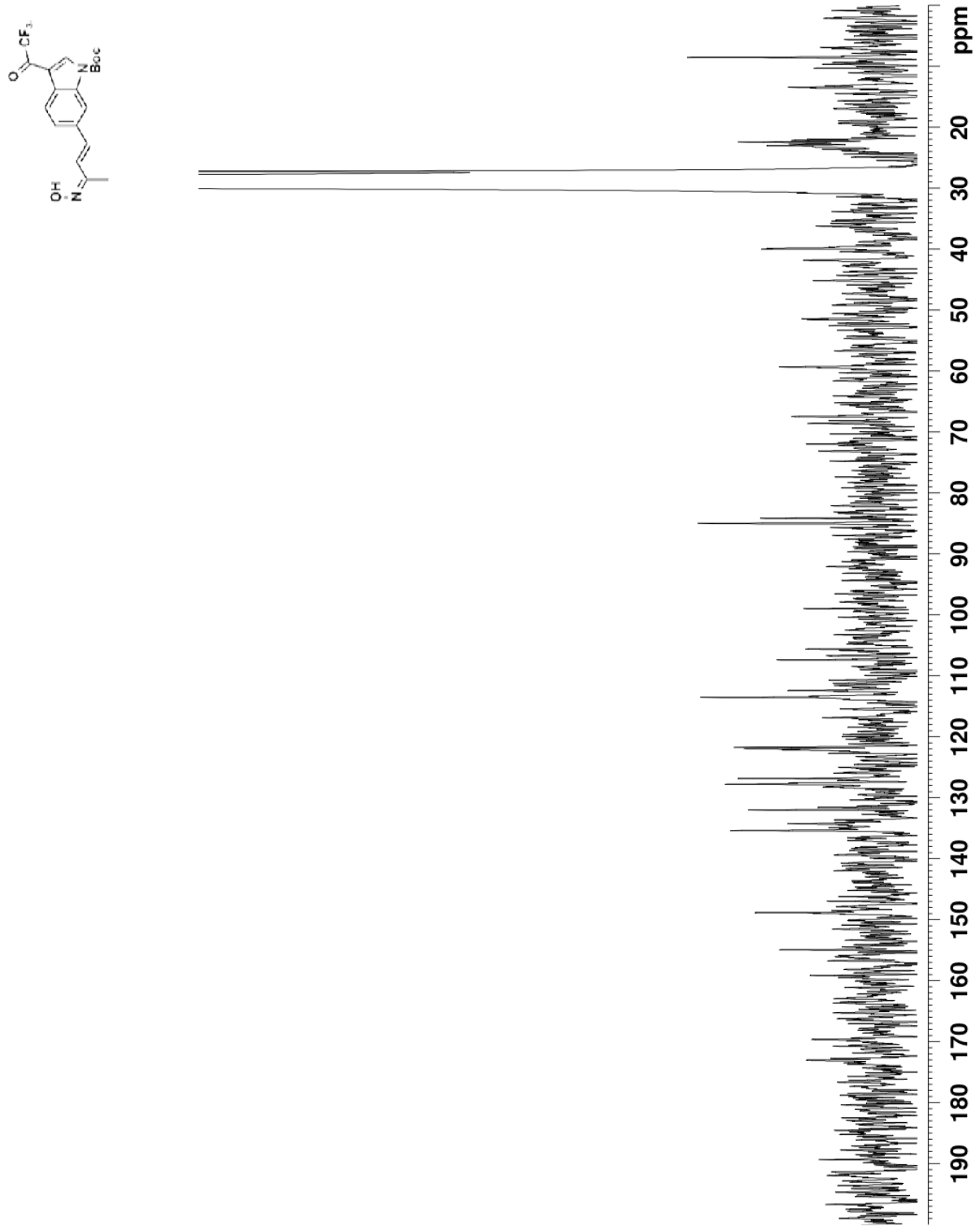

Spectrum 111. ^{13}C NMR spectrum of oxime **3.23** (100 MHz, acetone-d_6, 293K)

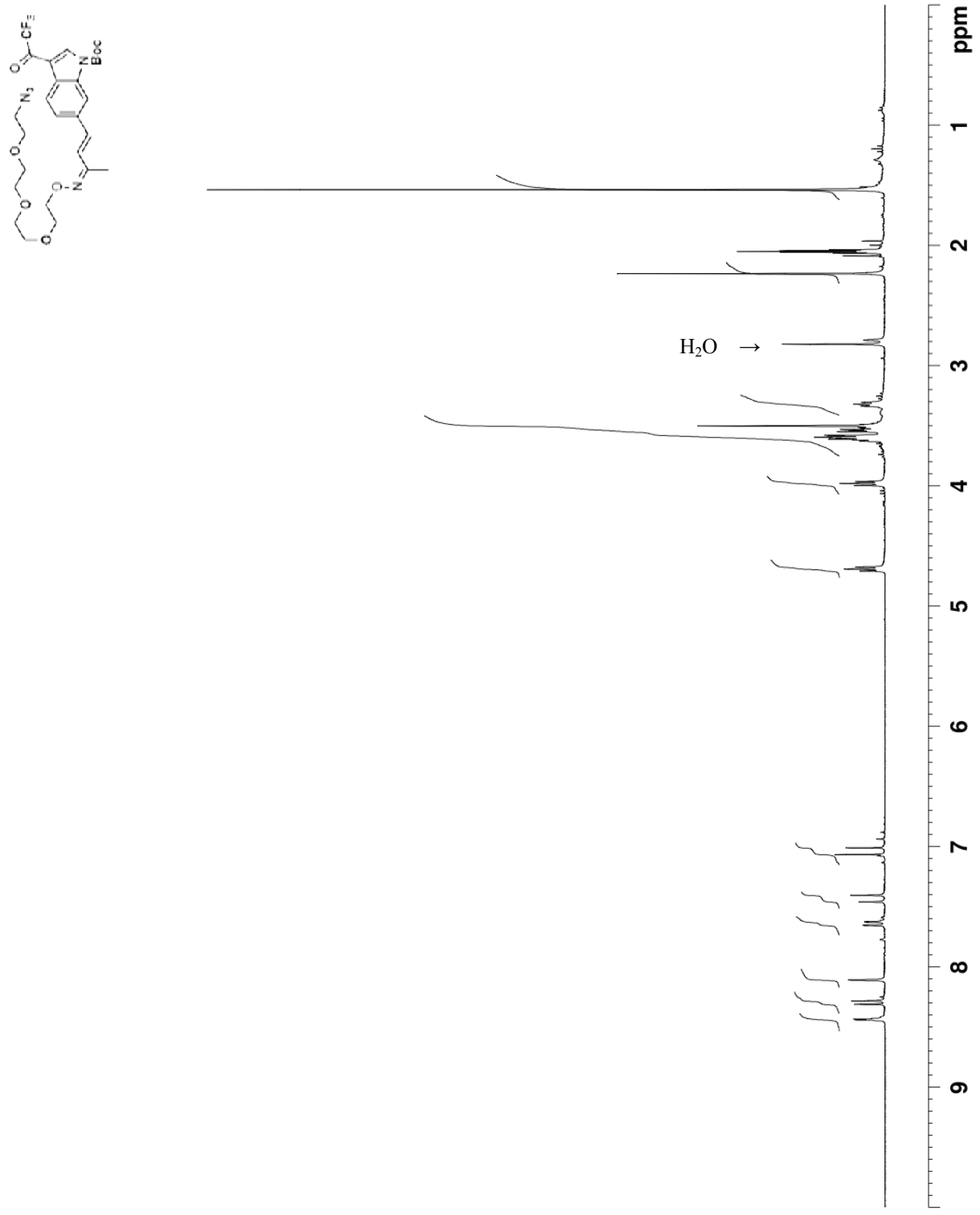

Spectrum 112. ^{1}H NMR spectrum of **3.25** (300 MHz, acetone-d_6, 293K)

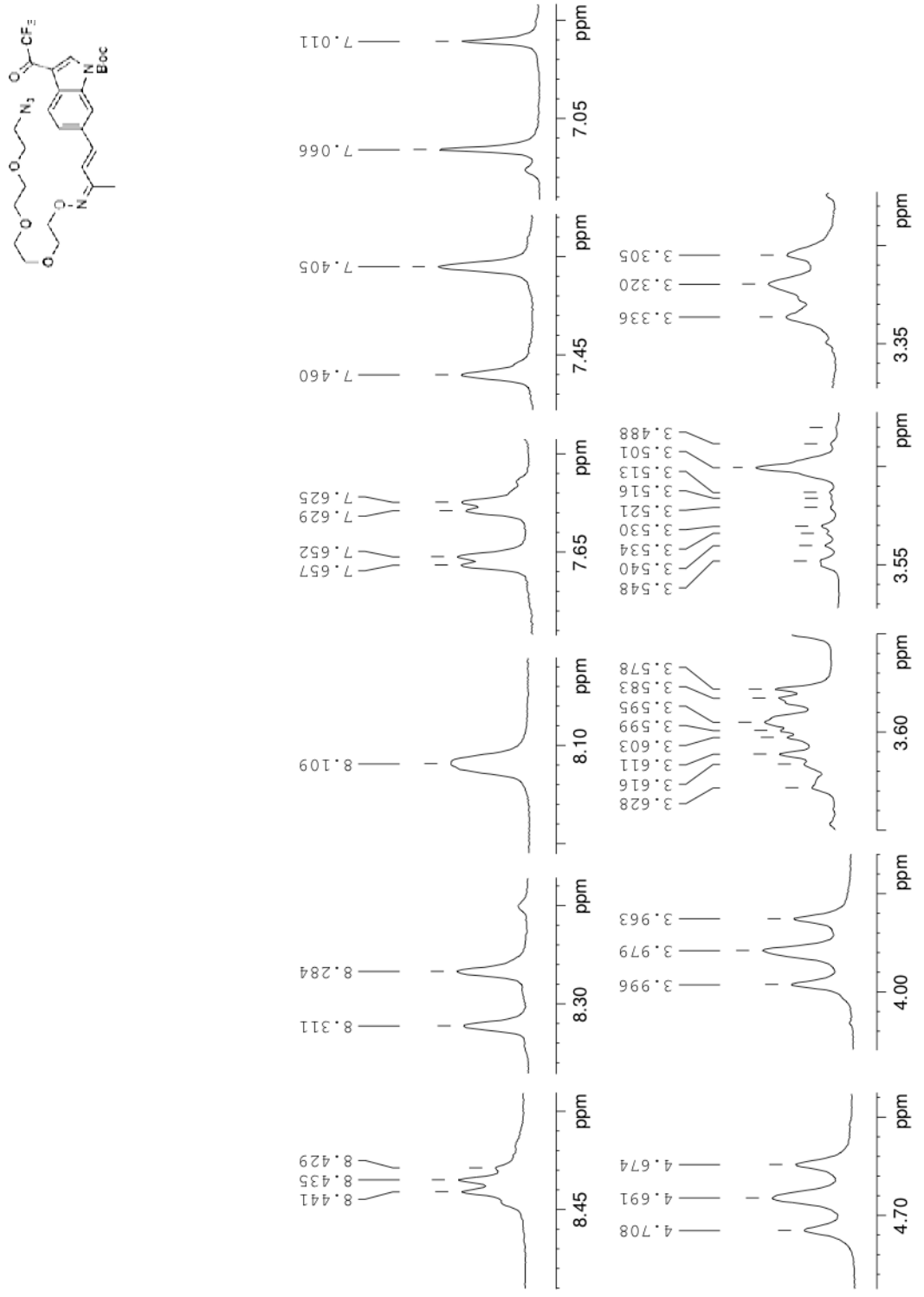

Spectrum 113. ^{1}H NMR spectrum of **3.25** (300 MHz, acetone-d_6, 293K)

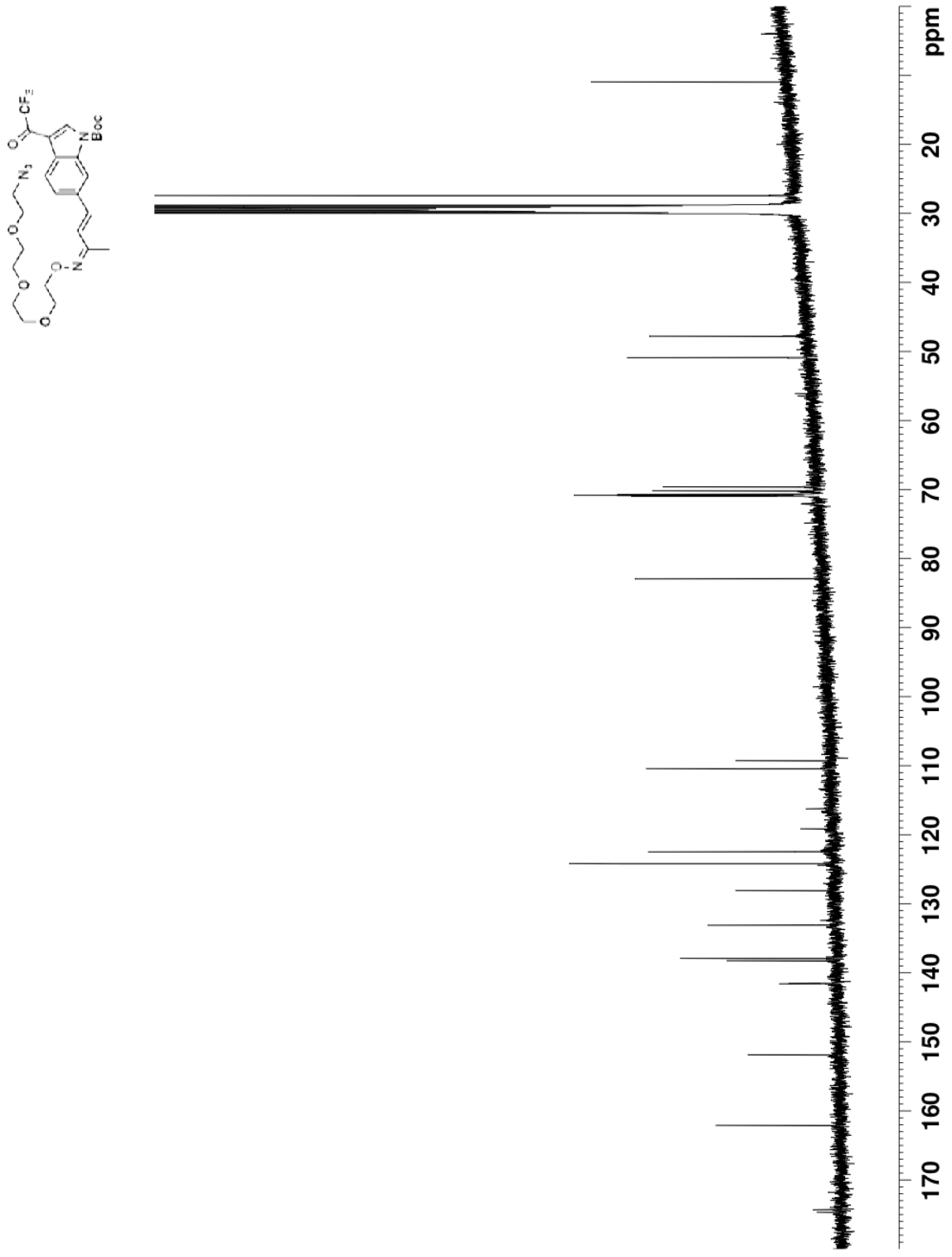

Spectrum 114. ^{13}C NMR spectrum of **3.25** (100 MHz, acetone-d_6, 293K)

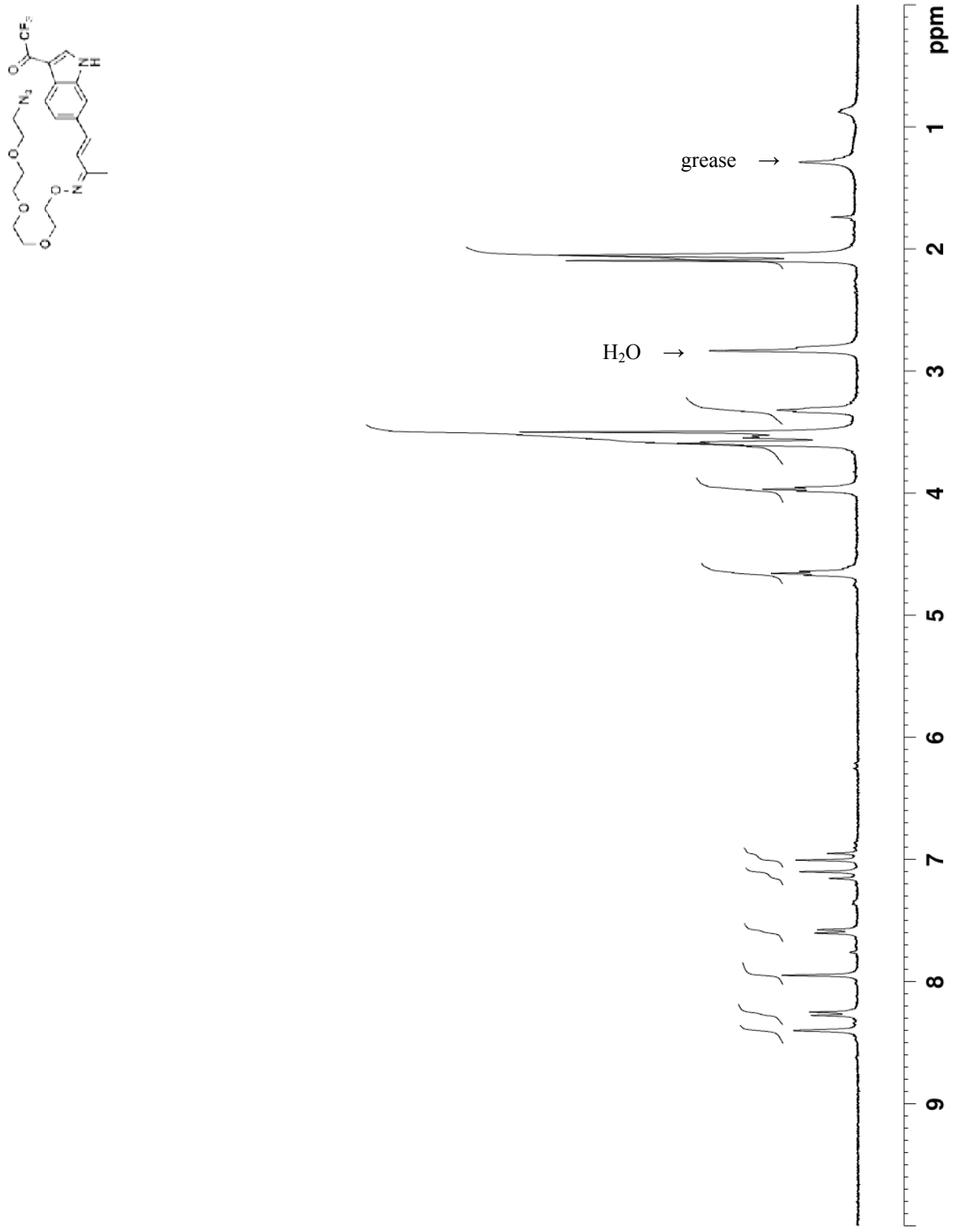

Spectrum 115. ^{1}H NMR spectrum of **3.26** (300 MHz, 1%CD_3OD in acetone-d_6 293K)

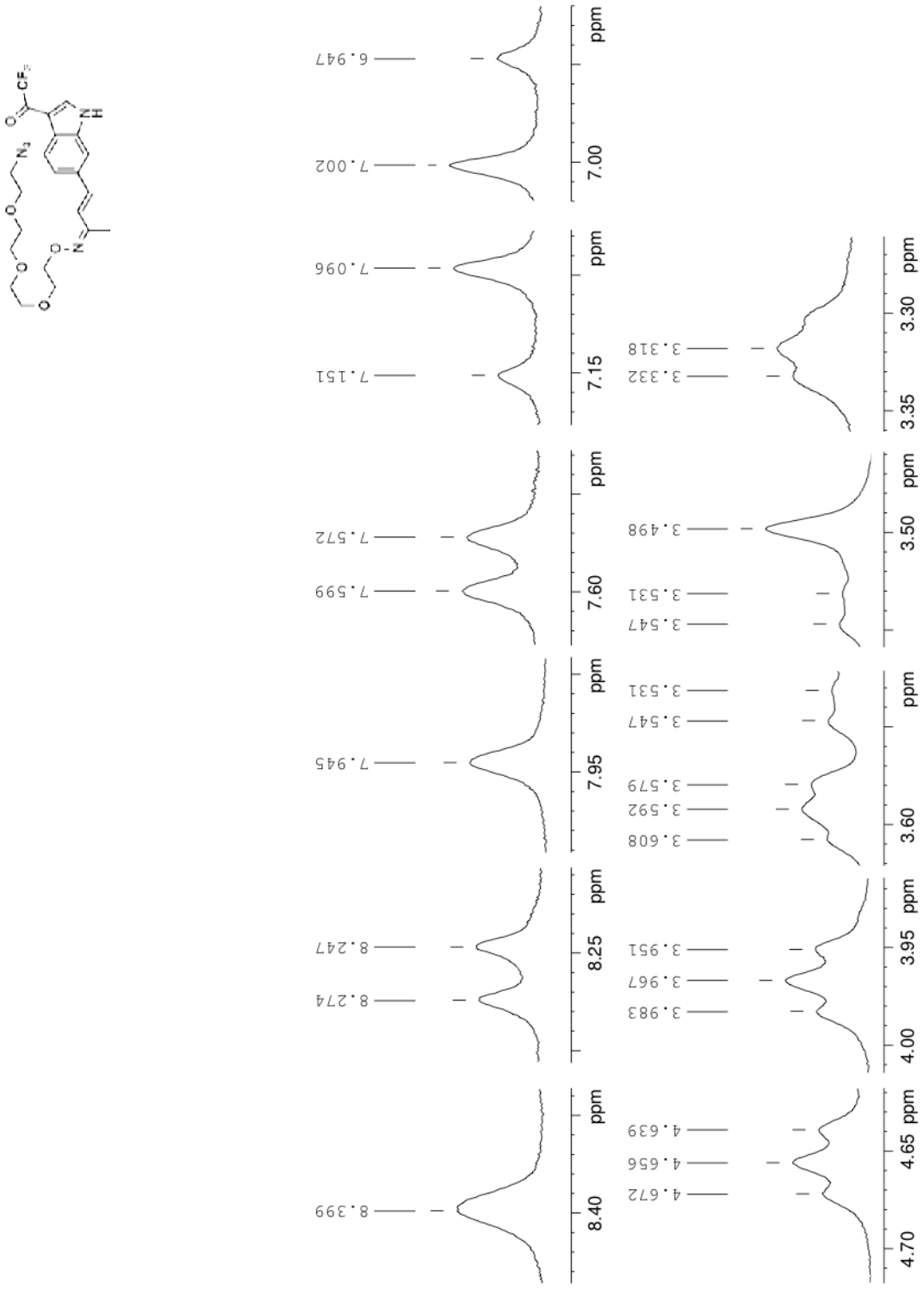

Spectrum 116. ^{1}H NMR spectrum of **3.26** (300 MHz, 1%CD_3OD in acetone-d_6 293K)

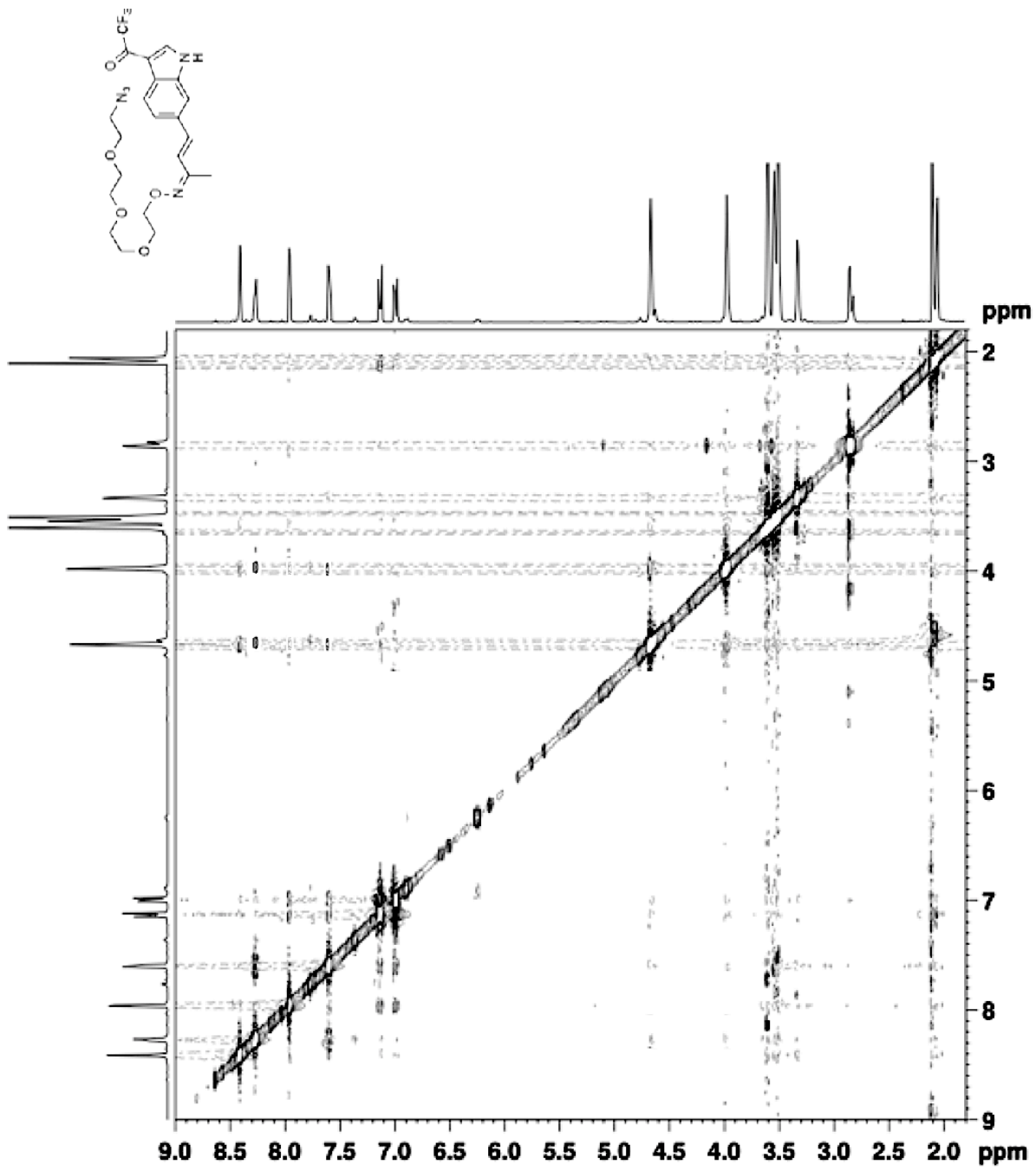

Spectrum 117. NOESY spectrum of **3.26** (600 MHz, 1%CD_3OD in acetone-d_6 293K)

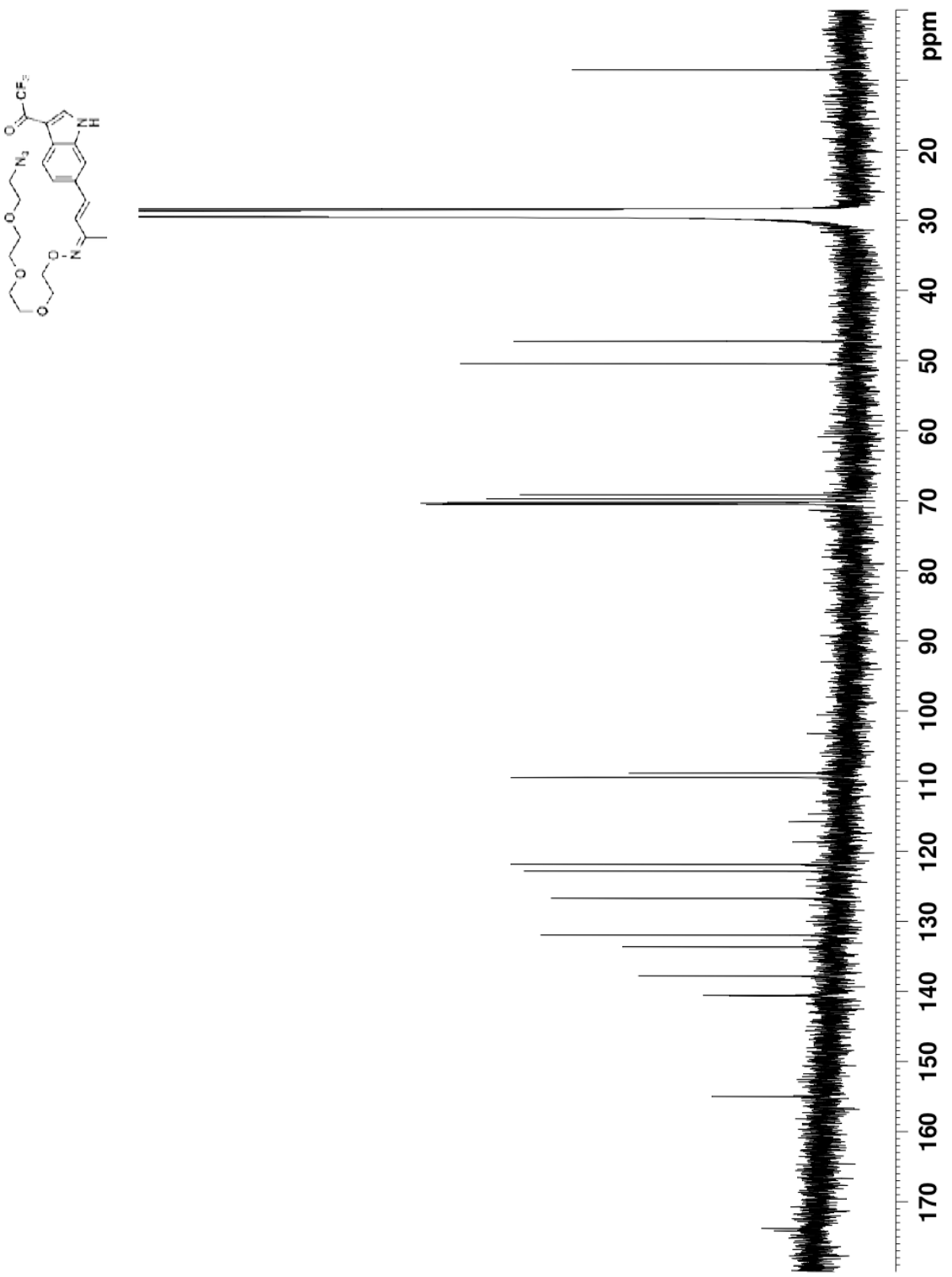

Spectrum 118. ^{13}C NMR spectrum of **3.26** (100 MHz, acetone-d_6, 293K)

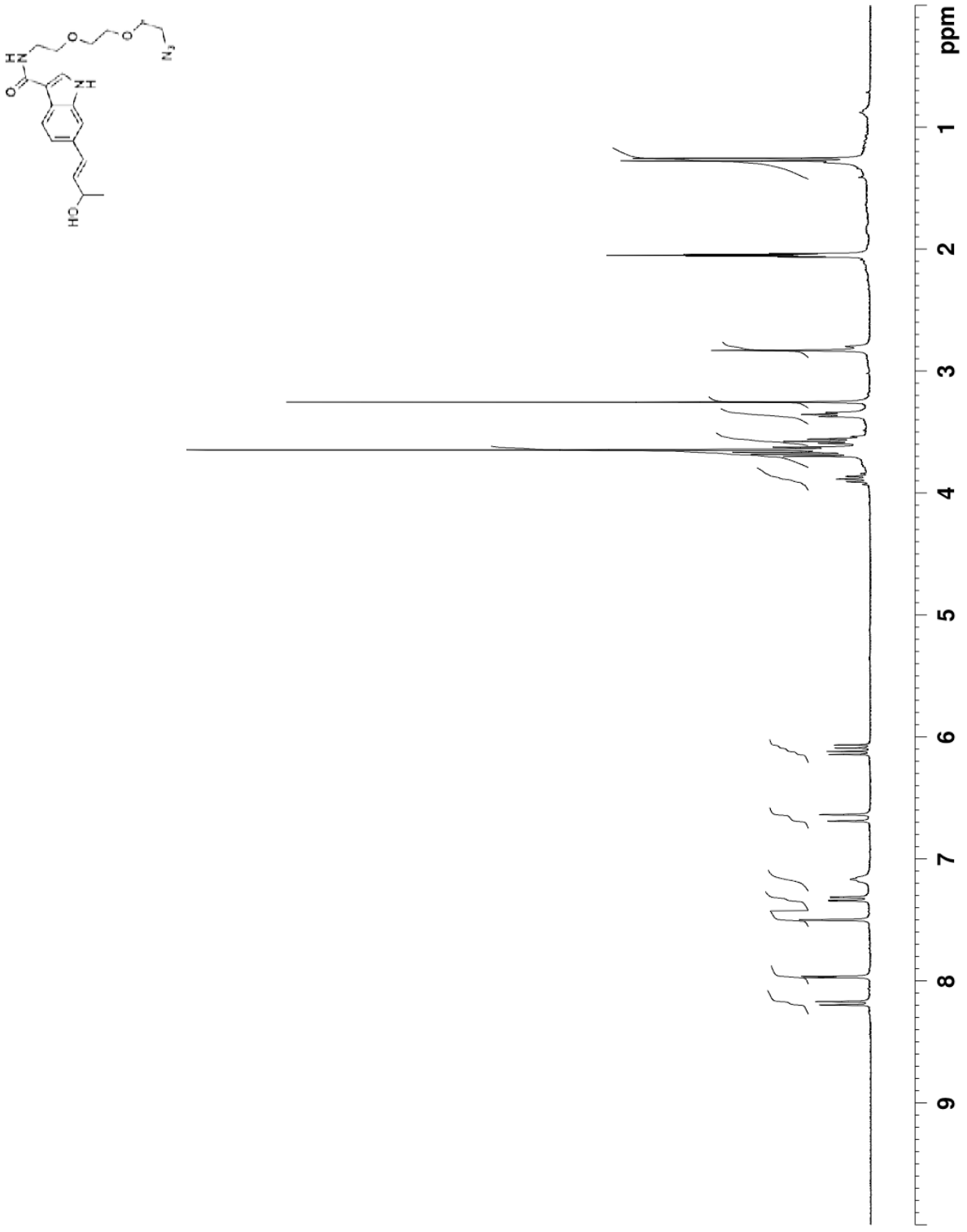

Spectrum 119. ^{1}H NMR spectrum of **3.27** (300 MHz, 1%CD_3OD in acetone-d_6 293K)

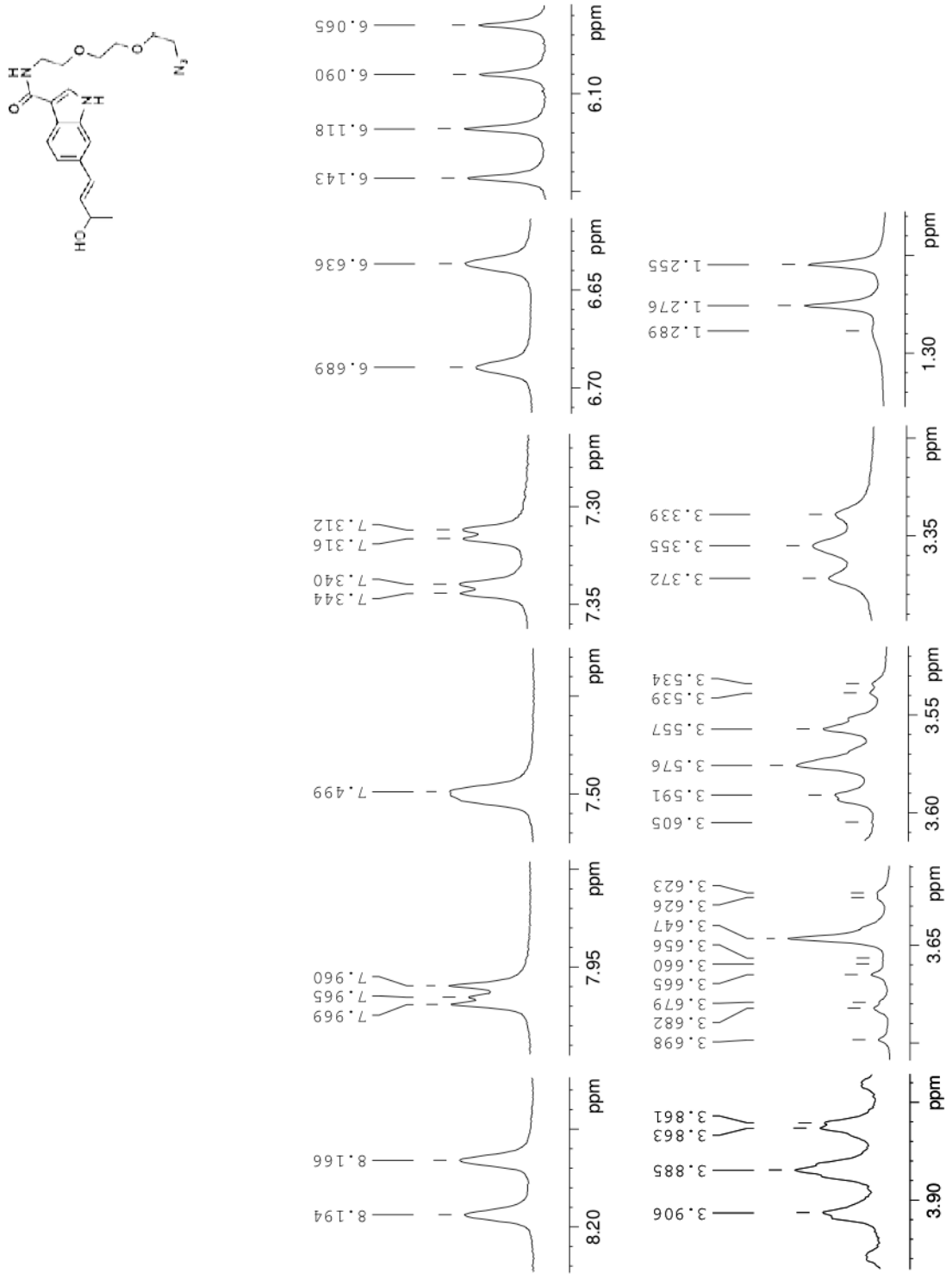

Spectrum 120. ^{1}H NMR spectrum of **3.27** (300 MHz, 1%CD_3OD in acetone-d_6 293K)

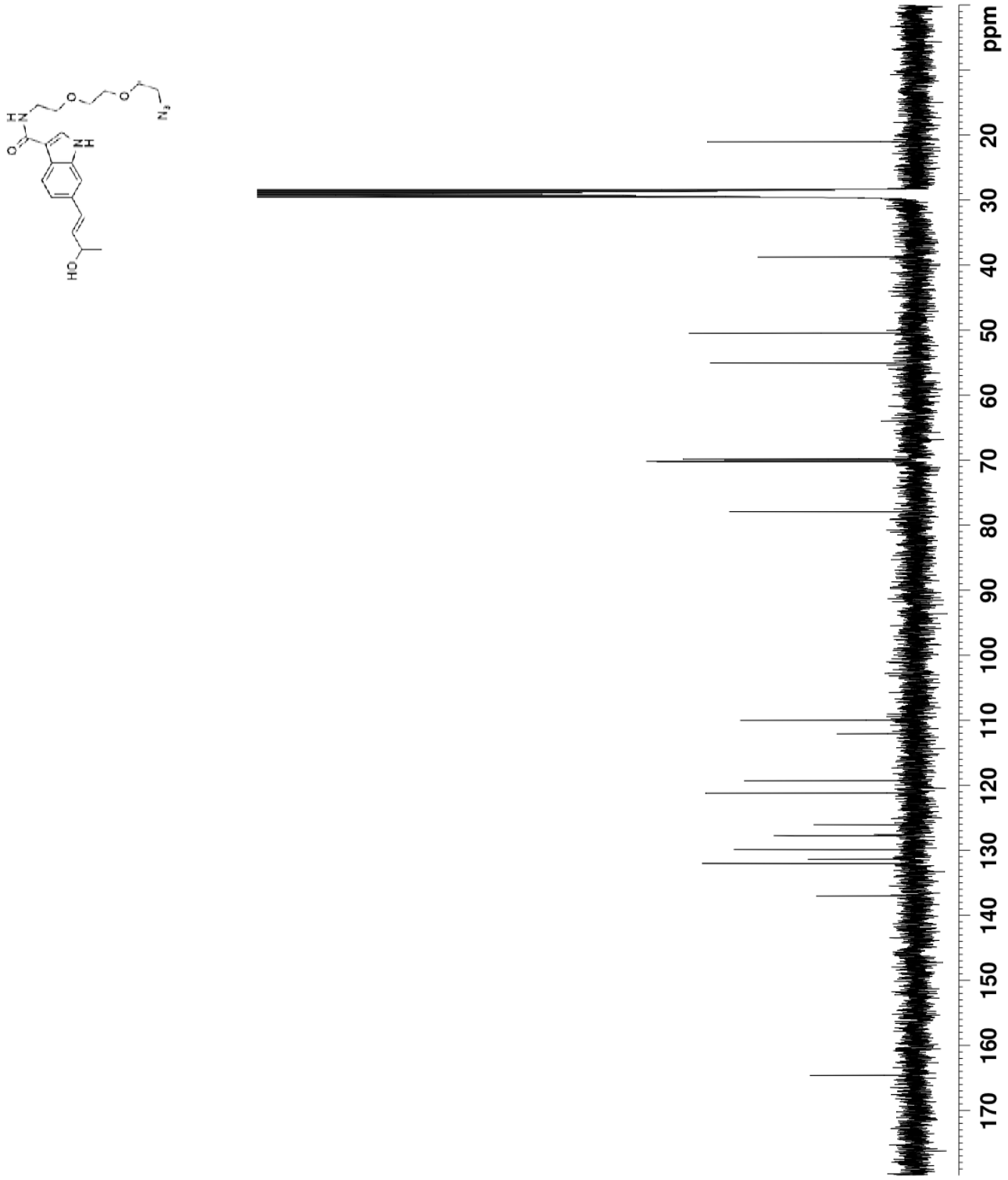

Spectrum 121. ^{13}C NMR spectrum of **3.27** (100 MHz, acetone-d_6, 293K)

BIBLIOGRAPHY

(1) Cooper, T. A.; Wan, L.; Dreyfuss, G. *Cell* **2009**, *136*, 777.

(2) Pilch, B.; Allemand, E.; Facompre, M.; Bailly, C.; Riou, J. F.; Soret, J.; Tazi, J. *Cancer Res.* **2001**, *61*, 6876.

(3) Bakkour, N.; Lin, Y. L.; Maire, S.; Ayadi, L.; Mahuteau-Betzer, F.; Nguyen, C. H.; Mettling, C.; Portales, P.; Grierson, D.; Chabot, B.; Jeanteur, P.; Branlant, C.; Corbeau, P.; Tazi, J. *PLoS Pathog.* **2007**, *3*, 1530.

(4) Lagisetti, C.; Pourpak, A.; Goronga, T.; Jiang, Q.; Cui, X.; Hyle, J.; Lahti, J. M.; Morris, S. W.; Webb, T. R. *J. Med. Chem.* **2009**, *52*, 6979.

(5) Nakajima, H.; Hori, Y.; Terano, H.; Okuhara, M.; Manda, T.; Matsumoto, S.; Shimomura, K. *J. Antibiot.* **1996**, *49*, 1204.

(6) Kotake, Y.; Sagane, K.; Owa, T.; Mimori-Kiyosue, Y.; Shimizu, H.; Uesugi, M.; Ishihama, Y.; Iwata, M.; Mizui, Y. *Nat. Chem. Biol.* **2007**, *3*, 570.

(7) Kaida, D.; Motoyoshi, H.; Tashiro, E.; Nojima, T.; Hagiwara, M.; Ishigami, K.; Watanabe, H.; Kitahara, T.; Yoshida, T.; Nakajima, H.; Tani, T.; Horinouchi, S.; Yoshida, M. *Nat. Chem. Biol.* **2007**, *3*, 576.

(8) Wahl, M. C.; Will, C. L.; Luhrmann, R. *Cell* **2009**, *136*, 701.

(9) Fedorova, L.; Fedorov, A. *Curr. Genomics* **2005**, *6*, 589.

(10) Skotheim, R. I.; Nees, M. *Int. J. Biochem. Cell Biol.* **2007**, *39*, 1432.

(11) Levanon, E. Y. S., R *Targets* **2003**, *2*, 109.

(12) Faustino, N. A.; Cooper, T. A. *Genes Dev.* **2003**, *17*, 419.

(13) van Alphen, R. J.; Wiemer, E. A. C.; Burger, H.; Eskens, F. A. L. M. *Br. J. Cancer* **2009**, *100*, 228.

(14) Laverman, P.; Roosenburg, S.; Gotthardt, M.; Park, J.; Oyen, W. J.; de Jong, M.; Hellmich, M. R.; Rutjes, F. P.; van Delft, F. L.; Boerman, O. C. *Eur. J. Nucl. Med. Mol. Imaging* **2008**, *35*, 386.

(15) Jemal, A.; Siegel, R.; Xu, J.; Ward, E. *CA Cancer J. Clin.* **2010**, *60*, 277.

(16) Koehn, F. E.; Carter, G. T. *Nat. Rev. Drug Discov.* **2005**, *4*, 206.

(17) Nakajima, H.; Sato, B.; Fujita, T.; Takase, S.; Terano, H.; Okuhara, M. *J. Antibiot.* **1996**, *49*, 1196.

(18) Nakajima, H.; Takase, S.; Terano, H.; Tanaka, H. *J. Antibiot.* **1997**, *50*, 96.

(19) Zhang, F.; He, H. Y.; Tang, M. C.; Tang, Y. M.; Zhou, Q.; Tang, G. L. *J. Am. Chem. Soc.* **2011**, *133*, 2452.

(20) Thompson, C. F.; Jamison, T. F.; Jacobsen, E. N. *J. Am. Chem. Soc.* **2001**, *123*, 9974.

(21) Horigome, M. M., H.; Watanabe, H.; Kitahara, T. *Tetrahedron Lett.* **2001**, *42*, 8207.

(22) Albert, B. J.; Sivaramakrishnan, A.; Naka, T.; Koide, K. *J. Am. Chem. Soc.* **2006**, *128*, 2792.

(23) Motoyoshi, H.; Horigome, M.; Ishigami, K.; Yoshida, T.; Horinouchi, S.; Yoshida, M.; Watanabe, H.; Kitahara, T. *Biosci. Biotechnol. Biochem.* **2004**, *68*, 2178.

(24) Osman, S.; Albert, B. J.; Wang, Y.; Li, M.; Czaicki, N. L.; Koide, K. *Chem.–Eur. J.* **2011**, *17*, 895.

(25) Albert, B. J.; Sivaramakrishnan, A.; Naka, T.; Czaicki, N. L.; Koide, K. *J. Am. Chem. Soc.* **2007**, *129*, 2648.

(26) Imamura, Y. O., Y.; Tanaka, H.; Hatakeyama, M.; Manabe, T.; Kawaguchi, H.; Handa, H.; Takahashi, T. *Heterocycles* **2004**, *64*, 51.

(27) Day, B. W.; Magarian, R. A.; Jain, P. T.; Pento, J. T.; Mousissian, G. K.; Meyer, K. L. *J. Med. Chem.* **1991**, *34*, 842.

(28) Corrionero, A.; Minana, B.; Valcarcel, J. *Genes Dev.* **2011**, *25*, 445.

(29) Albert, B. J.; McPherson, P. A.; O'Brien, K.; Czaicki, N. L.; Destefino, V.; Osman, S.; Li, M.; Day, B. W.; Grabowski, P. J.; Moore, M. J.; Vogt, A.; Koide, K. *Mol. Cancer Ther.* **2009**, *8*, 2308.

(30) Sakai, T.; Sameshima, T.; Matsufuji, M.; Kawamura, N.; Dobashi, K.; Mizui, Y. *J. Antibiot.* **2004**, *57*, 173.

(31) Sakai, T.; Asai, N.; Okuda, A.; Kawamura, N.; Mizui, Y. *J. Antibiot.* **2004**, *57*, 180.

(32) Semenza, G. L. *Nat. Rev. Cancer* **2003**, *3*, 721.

(33) Mizui, Y.; Sakai, T.; Iwata, M.; Uenaka, T.; Okamoto, K.; Shimizu, H.; Yamori, T.; Yoshimatsu, K.; Asada, M. *J. Antibiot.* **2004**, *57*, 188.

(34) Kotake, Y. N., J.; Nagai, M.; Okano, K.; Sakai, T.; Yoshida, M.;; Tsuchida, T. N., T.; Dobashi, K.; Mizui, Y.; Shimizu, H.; Uenaka, T.; Iwata,; M.; Asada, M. Y., K. *Clin. Cancer Res.* **2003**, *16*, 6208S.

(35) Kanada, R. M.; Itoh, D.; Nagai, M.; Niijima, J.; Asai, N.; Mizui, Y.; Abe, S.; Kotake, Y. *Angew. Chem. Int. Ed.* **2007**, *46*, 4350.

(36) Eskens, F. A. R., F. J.; Burger, H.; de Jonge, M. J.; Wanders, J. A.; Lopez-Anaya, J.; Baselga, J.; Tabernero, J. *J. Clin. Oncol. (Meeting Abstracts)* **2009**, *27*, 3508.

(37) Kotake, Y. S., K.; Owa, T.; Mimori-Kiyosue, Y.; Shimizu, H.; Uesugi, M.; Ishihama, Y.; Iwata, M.; Mizui, Y. *Nat. Chem. Biol.* **2007**, *3*, 570.

(38) Yokoi, A.; Kotake, Y.; Takahashi, K.; Kadowaki, T.; Matsumoto, Y.; Minoshima, Y.; Sugi, N. H.; Sagane, K.; Hamaguchi, M.; Iwata, M.; Mizui, Y. *FEBS J.* **2011**, *278*, 4870.

(39) http://clinicaltrials.gov/ct2/show/NCT00459823

(40) Isaac, B. G.; Ayer, S. W.; Elliott, R. C.; Stonard, R. J. *J. Org. Chem.* **1992**, *57*, 7220.

(41) Sakai, Y.; Tsujita, T.; Akiyama, T.; Yoshida, T.; Mizukami, T.; Akinaga, S.; Horinouchi, S.; Yoshida, M. *J. Antibiot.* **2002**, *55*, 863.

(42) Sakai, Y.; Yoshida, T.; Ochiai, K.; Uosaki, Y.; Saitoh, Y.; Tanaka, F.; Akiyama, T.; Akinaga, S.; Mizukami, T. *J. Antibiot.* **2002**, *55*, 855.

(43) Hasegawa, M.; Miura, T.; Kuzuya, K.; Inoue, A.; Won Ki, S.; Horinouchi, S.; Yoshida, T.; Kunoh, T.; Koseki, K.; Mino, K.; Sasaki, R.; Yoshida, M.; Mizukami, T. *ACS Chem. Biol.* **2011**, *6*, 229.

(44) Lagisetti, C.; Pourpak, A.; Jiang, Q.; Cui, X.; Goronga, T.; Morris, S. W.; Webb, T. R. *J. Med. Chem.* **2008**, *51*, 6220.

(45) Bissery, M. C.; Guenard, D.; Gueritte-Voegelein, F.; Lavelle, F. *Cancer Res.* **1991**, *51*, 4845.

(46) van Alphen, R. J.; Wiemer, E. A.; Burger, H.; Eskens, F. A. *Br. J. Cancer* **2009**, *100*, 228.

(47) Rymond, B. *Nat. Chem. Biol.* **2007**, *3*, 533.

(48) Yoshida, K.; Sanada, M.; Shiraishi, Y.; Nowak, D.; Nagata, Y.; Yamamoto, R.; Sato, Y.; Sato-Otsubo, A.; Kon, A.; Nagasaki, M.; Chalkidis, G.; Suzuki, Y.; Shiosaka, M.; Kawahata, R.; Yamaguchi, T.; Otsu, M.; Obara, N.; Sakata-Yanagimoto, M.; Ishiyama, K.; Mori, H.; Nolte, F.; Hofmann, W. K.; Miyawaki, S.; Sugano, S.; Haferlach, C.; Koeffler, H. P.; Shih, L. Y.; Haferlach, T.; Chiba, S.; Nakauchi, H.; Miyano, S.; Ogawa, S. *Nature* **2011**, *478*, 64.

(49) Poulikakos, P. I.; Persaud, Y.; Janakiraman, M.; Kong, X. J.; Ng, C.; Moriceau, G.; Shi, H. B.; Atefi, M.; Titz, B.; Gabay, M. T.; Salton, M.; Dahlman, K. B.; Tadi, M.; Wargo, J. A.; Flaherty, K. T.; Kelley, M. C.; Misteli, T.; Chapman, P. B.; Sosman, J. A.; Graeber, T. G.; Ribas, A.; Lo, R. S.; Rosen, N.; Solit, D. B. *Nature* **2011**, *480*, 387.

(50) Papaemmanuil, E.; Cazzola, M.; Boultwood, J.; Malcovati, L.; Vyas, P.; Bowen, D.; Pellagatti, A.; Wainscoat, J. S.; Hellstrom-Lindberg, E.; Gambacorti-Passerini, C.; Godfrey, A. L.; Rapado, I.; Cvejic, A.; Rance, R.; McGee, C.; Ellis, P.; Mudie, L. J.; Stephens, P. J.; McLaren, S.; Massie, C. E.; Tarpey, P. S.; Varela, I.; Nik-Zainal, S.; Davies, H. R.; Shlien, A.; Jones, D.; Raine, K.; Hinton, J.; Butler, A. P.; Teague, J. W.; Baxter, E. J.; Score, J.; Galli, A.; Della Porta, M. G.; Travaglino, E.; Groves, M.; Tauro, S.; Munshi, N. C.; Anderson, K. C.; El-Naggar, A.; Fischer, A.; Mustonen, V.; Warren, A. J.; Cross, N. C.; Green, A. R.; Futreal, P. A.; Stratton, M. R.; Campbell, P. J. *N. Engl. J. Med.* **2011**, *365*, 1384.

(51) Visconte, V.; Makishima, H.; Jankowska, A.; Szpurka, H.; Traina, F.; Jerez, A.; O'Keefe, C.; Rogers, H. J.; Sekeres, M. A.; Maciejewski, J. P.; Tiu, R. V. *Leukemia* **2012**, *26*, 542.

(52) Rowinsky, E. K. *Annu. Rev. Med.* **1997**, *48*, 353.

(53) Schiff, P. B.; Fant, J.; Horwitz, S. B. *Nature* **1979**, *277*, 665.

(54) Bollag, D. M.; McQueney, P. A.; Zhu, J.; Hensens, O.; Koupal, L.; Liesch, J.; Goetz, M.; Lazarides, E.; Woods, C. M. *Cancer Res.* **1995**, *55*, 2325.

(55) O'Brien, K.; Matlin, A. J.; Lowell, A. M.; Moore, M. J. *J. Biol. Chem.* **2008**, *283*, 33147.

(56) Samatov, T. R.; Wolf, A.; Odenwalder, P.; Bessonov, S.; Deraeve, C.; Bon, R. S.; Waldmann, H.; Luhrmann, R. *ChemBioChem* **2012**, *13*, 640.

(57) Berg, M. G.; Wan, L.; Younis, I.; Diem, M. D.; Soo, M.; Wang, C.; Dreyfuss, G. *Mol. Cell. Biol.* **2012**, *32*, 1271.

(58) Kuhn, A. N.; van Santen, M. A.; Schwienhorst, A.; Urlaub, H.; Luhrmann, R. *RNA* **2009**, *15*, 153.

(59) Hertweck, M.; Hiller, R.; Mueller, M. W. *Eur. J. Biochem.* **2002**, *269*, 175.

(60) Stoilov, P.; Lin, C. H.; Damoiseaux, R.; Nikolic, J.; Black, D. L. *Proc. Natl. Acad. Sci. U.S.A.* **2008**, *105*, 11218.

(61) Younis, I.; Berg, M.; Kaida, D.; Dittmar, K.; Wang, C.; Dreyfuss, G. *Mol. Cell Biol.* **2010**, *30*, 1718.

(62) Spahn, C. M.; Prescott, C. D. *J. Mol. Med.* **1996**, *74*, 423.

(63) Parker, A. R.; Steitz, J. A. *RNA* **1997**, *3*, 1301.

(64) Ajuh, P.; Lamond, A. I. *Nucleic Acids Res.* **2003**, *31*, 6104.

(65) Woolard, J.; Vousden, W.; Moss, S. J.; Krishnakumar, A.; Gammons, M. V. R.; Nowak, D. G.; Dixon, N.; Micklefield, J.; Spannhoff, A.; Bedford, M. T.; Gregory, M. A.; Martin, C. J.; Leadlay, P. F.; Zhang, M. Q.; Harper, S. J.; Bates, D. O.; Wilkinson, B. *Chem. Sci.* **2011**, *2*, 273.

(66) Soret, J.; Bakkour, N.; Maire, S.; Durand, S.; Zekri, L.; Gabut, M.; Fic, W.; Divita, G.; Rivalle, C.; Dauzonne, D.; Nguyen, C. H.; Jeanteur, P.; Tazi, J. *Proc. Natl. Acad. Sci. U.S.A.* **2005**, *102*, 8764.

(67) Aartsma-Rus, A.; van Ommen, G. J. *RNA* **2007**, *13*, 1609.

(68) Manzur, A. Y.; Kinali, M.; Muntoni, F. *Arch. Dis. Child* **2008**, *93*, 986.

(69) Wood, M. J.; Gait, M. J.; Yin, H. *Brain* **2010**, *133*, 957.

(70) Gozani, O.; Feld, R.; Reed, R. *Genes Dev.* **1996**, *10*, 233.

(71) Pauling, M. H.; McPheeters, D. S.; Ares, M., Jr. *Mol. Cell. Biol.* **2000**, *20*, 2176.

(72) Tseng, C. K.; Cheng, S. C. *Science* **2008**, *320*, 1782.

(73) Bessonov, S.; Anokhina, M.; Will, C. L.; Urlaub, H.; Luhrmann, R. *Nature* **2008**, *452*, 846.

(74) Kuwasako, K.; Dohmae, N.; Inoue, M.; Shirouzu, M.; Taguchi, S.; Guntert, P.; Seraphin, B.; Muto, Y.; Yokoyama, S. *Proteins* **2008**, *71*, 1617.

(75) Sperling, J.; Azubel, M.; Sperling, R. *Structure* **2008**, *16*, 1605.

(76) Hoskins, A. A.; Friedman, L. J.; Gallagher, S. S.; Crawford, D. J.; Anderson, E. G.; Wombacher, R.; Ramirez, N.; Cornish, V. W.; Gelles, J.; Moore, M. J. *Science* **2011**, *331*, 1289.

(77) Woolard, J. V., W.; Moss, S. J.; Krishnakumar, A.; Gammons, M. V. R.; Nowak, D. G.; Dixon, N.; Micklefield, J.; Spannhoff, A.; Bedford, M. T.; Gregory, M. A.; Martin, C. J.; Leadlay, P. F.; Zhang, M. Q.; Harper, S. J.; Bates, D. O.; Wilkson, B. *Chem. Sci.* **2011**, *2*, 273.

(78) Visconte, V.; Makishima, H.; Jankowska, A.; Szpurka, H.; Traina, F.; Jerez, A.; O'Keefe, C.; Rogers, H. J.; Sekeres, M. A.; Maciejewski, J. P.; Tiu, R. V. *Leukemia* **2012**, *26*, 542.

(79) Furumai, R.; Uchida, K.; Komi, Y.; Yoneyama, M.; Ishigami, K.; Watanabe, H.; Kojima, S.; Yoshida, M. *Cancer Sci.* **2010**, *101*, 2483.

(80) Roybal, G. A.; Jurica, M. S. *Nucleic Acids Res.* **2010**, *38*, 6664.

(81) Groll, M.; Schellenberg, B.; Bachmann, A. S.; Archer, C. R.; Huber, R.; Powell, T. K.; Lindow, S.; Kaiser, M.; Dudler, R. *Nature* **2008**, *452*, 755.

(82) Clerc, J.; Groll, M.; Illich, D. J.; Bachmann, A. S.; Huber, R.; Schellenberg, B.; Dudler, R.; Kaiser, M. *Proc. Natl. Acad. Sci. U.S.A.* **2009**, *106*, 6507.

(83) Wissner, A.; Overbeek, E.; Reich, M. F.; Floyd, M. B.; Johnson, B. D.; Mamuya, N.; Rosfjord, E. C.; Discafani, C.; Davis, R.; Shi, X.; Rabindran, S. K.; Gruber, B. C.; Ye, F.; Hallett, W. A.; Nilakantan, R.; Shen, R.; Wang, Y. F.; Greenberger, L. M.; Tsou, H. R. *J. Med. Chem.* **2003**, *46*, 49.

(84) Weerapana, E.; Wang, C.; Simon, G. M.; Richter, F.; Khare, S.; Dillon, M. B.; Bachovchin, D. A.; Mowen, K.; Baker, D.; Cravatt, B. F. *Nature* **2010**, *468*, 790.

(85) Singh, J.; Petter, R. C.; Baillie, T. A.; Whitty, A. *Nat. Rev. Drug Discovery* **2011**, *10*, 307.

(86) V.i Theodorou, M. G., M. Philippidou, V. Ragoussis, G. Paraskevopoulos, K. Skobridis *Tetrahdron* **2011**, *67*, 5630.

(87) Michrowska, A.; Bujok, R.; Harutyunyan, S.; Sashuk, V.; Dolgonos, G.; Grela, K. *J. Am. Chem. Soc.* **2004**, *126*, 9318.

(88) Osman, S. W., W. R.; Gorman, G. S.; Day, B. W.; Koide, K. *Med. Chem. Commun.* **2011**, *2*, 38.

(89) Zhou, G.; Tsai, C. W.; Liu, J. O. *J. Med. Chem.* **2003**, *46*, 3452.

(90) Basabe, P.; Delgado, S.; Marcos, I. S.; Diez, D.; Diego, A.; De Roman, M.; Urones, J. G. *J. Org. Chem.* **2005**, *70*, 9480.

(91) Miguel Del Corral, J. M.; Gordaliza, M.; Castro, M. A.; Mahiques, M. M.; Chamorro, P.; Molinari, A.; Garcia-Gravalos, M. D.; Broughton, H. B.; San Feliciano, A. *J. Med. Chem.* **2001**, *44*, 1257.

(92) Kanemitsu, T.; Seeberger, P. H. *Org. Lett.* **2003**, *5*, 4541.

(93) de Almeida, S. F.; Grosso, A. R.; Koch, F.; Fenouil, R.; Carvalho, S.; Andrade, J.; Levezinho, H.; Gut, M.; Eick, D.; Gut, I.; Andrau, J. C.; Ferrier, P.; Carmo-Fonseca, M. *Nat. Struct. Mol. Biol.* **2011**, *18*, 977.

(94) Brody, Y.; Neufeld, N.; Bieberstein, N.; Causse, S. Z.; Bohnlein, E. M.; Neugebauer, K. M.; Darzacq, X.; Shav-Tal, Y. *PLoS Biol.* **2011**, *9*.

(95) Quesada, V.; Conde, L.; Villamor, N.; Ordonez, G. R.; Jares, P.; Bassaganyas, L.; Ramsay, A. J.; Bea, S.; Pinyol, M.; Martinez-Trillos, A.; Lopez-Guerra, M.; Colomer, D.; Navarro, A.; Baumann, T.; Aymerich, M.; Rozman, M.; Delgado, J.; Gine, E.; Hernandez, J. M.; Gonzalez-Diaz, M.; Puente, D. A.; Velasco, G.; Freije, J. M. P.; Tubio, J. M. C.; Royo, R.; Gelpi, J. L.; Orozco, M.; Pisano, D. G.; Zamora, J.; Vazquez, M.; Valencia, A.; Himmelbauer, H.; Bayes, M.; Heath, S.; Gut, M.; Gut, I.; Estivill, X.; Lopez-Guillermo, A.; Puente, X. S.; Campo, E.; Lopez-Otin, C. *Nat. Genet.* **2012**, *44*, 47.

(96) Marnef, A.; Weil, D.; Standart, N. *Mol. Biol. Cell* **2012**, *23*, 213.

(97) Kim, S.; Kim, H.; Fong, N.; Erickson, B.; Bentley, D. L. *Proc. Natl. Acad. Sci. U.S.A.* **2011**, *108*, 13564.

(98) Corrionero, A.; Minana, B.; Valcarcel, J. *Gene Dev.* **2011**, *25*, 445.

(99) Kaida, D.; Berg, M. G.; Younis, I.; Kasim, M.; Singh, L. N.; Wan, L.; Dreyfuss, G. *Nature* **2010**, *468*, 664.

(100) Roybal, G. A.; Jurica, M. S. *Nucleic Acids Res.* **2010**, *38*, 6664.

(101) K. C. Nicolaou, C. V. C. P., P. K. Somers, C. K. Hwang *J. Am. Chem. Soc.* **1989**, *111*, 5330.

(102) Walshe, N. D. A. G., G. B. T.; Smith, G. C.; Woodward, F. E. *Org. Synth.* **1993**, *8*, 1.

(103) Mukaiyama, T. N., K.; Banno, K. *Chem. Lett.* **1973**, *2*, 1011.

(104) Kobayashi, S. H., I.; Yamanoi, Y. *Bull. Chem. Soc. Jpn.* **1994**, *67*, 2342.

(105) Lu, X.; Liu, Y.; Sun, B.; Cindric, B.; Deng, L. *J. Am. Chem. Soc.* **2008**, *130*, 8134.

(106) Nemoto, T.; Ohshima, T.; Yamaguchi, K.; Shibasaki, M. *J. Am. Chem. Soc.* **2001**, *123*, 2725.

(107) Liu, Y.; Provencher, B. A.; Bartleson, K. J.; Deng, L. *Chem. Sci.* **2011**, *2*, 1301.

(108) Wu, M. H.; Hansen, K. B.; Jacobsen, E. N. *Angew. Chem. Int., Ed.* **1999**, *38*, 2012.

(109) Lebel, H. J., E. N. *Tetrahedron Lett.* **1999**, *40*, 7303.

(110) Akiyama, T.; Itoh, J.; Fuchibe, K. *Adv. Synth. Catal.* **2006**, *348*, 999.

(111) Zamfir, A.; Schenker, S.; Freund, M.; Tsogoeva, S. B. *Org. Biomol. Chem.* **2010**, *8*, 5262.

(112) Terada, M.; Kanomata, K. *Synlett* **2011**, 1255.

(113) Kirk, O.; Christensen, M. W. *Org. Process Res. Dev.* **2002**, *6*, 446.

(114) Gao, Y.; Hanson, R. M.; Klunder, J. M.; Ko, S. Y.; Masamune, H.; Sharpless, K. B. *J. Am. Chem. Soc.* **1987**, *109*, 5765.

(115) Ley, S. V.; Norman, J.; Griffith, W. P.; Marsden, S. P. *Synthesis* **1994**, 639.

(116) Dess, D. B.; Martin, J. C. *J. Org. Chem.* **1983**, *48*, 4155.

(117) Parikh, J. R.; Doering, W. V. E. *J. Am. Chem. Soc.* **1967**, *89*, 5505.

(118) Mancuso, A. J.; Huang, S. L.; Swern, D. *J. Org. Chem.* **1978**, *43*, 2480.

(119) Zhang, W.; Basak, A.; Kosugi, Y.; Hoshino, Y.; Yamamoto, H. *Angew. Chem., Int. Ed.* **2005**, *44*, 4389.

(120) Cho, J. H.; Kim, B. M. *Org. Lett.* **2003**, *5*, 531.

(121) Ahn, Y. M.; Yang, K.; Georg, G. I. *Org. Lett.* **2001**, *3*, 1411.

(122) Paquette, L. A. S., J.; Efremov, I.; Fabris, F.; Gallou, F.; Mendez-Andino, J.; Yang, J. *Org. Lett.* **2000**, *9*, 1259.

(123) Hanahan, D. W., R. A. *Cell* **2000**, *100*, 57.

(124) Gossen, M. B., H. *Proc. Natl. Acad. Sci. U.S.A.* **1992**, *89*, 5547.

(125) Kistner, A. G., M.; Zimmerman, F.; Jerecic, J.; Ullmer, C.; Hermann, L.; Bujard, H. *Proc. Natl. Acad. Sci. U.S.A.* **1996**, *93*, 10933.

(126) Liberles, S. D.; Diver, S. T.; Austin, D. J.; Schreiber, S. L. *Proc. Natl. Acad. Sci. U.S.A.* **1997**, *94*, 7825.

(127) Nyanguile, O.; Uesugi, M.; Austin, D. J.; Verdine, G. L. *Proc. Natl. Acad. Sci. U.S.A.* **1997**, *94*, 13402.

(128) Kwon, Y.; Arndt, H. D.; Mao, Q.; Choi, Y.; Kawazoe, Y.; Dervan, P. B.; Uesugi, M. *J. Am. Chem. Soc.* **2004**, *126*, 15940.

(129) Minter, A. R.; Brennan, B. B.; Mapp, A. K. *J. Am. Chem. Soc.* **2004**, *126*, 10504.

(130) Liu, B.; Alluri, P. G.; Yu, P.; Kodadek, T. *J. Am. Chem. Soc.* **2005**, *127*, 8254.

(131) Parsons, P. G. H., C.; Fairlie, D. P.; West, M. L.; Danoy, P. A. C.; Sturm, R. A.; Dunn, I. S.; Pedky, J. Ablett, E. M. *Biochem. Pharmacol.* **1997**, *53*, 1719.

(132) Sowa, Y. O., T.; Minamikawa, S.; Nakano, K.; Mizuno, T.; Nomura, H.; Sakai, T. *Biochem. Biophys. Res. Commun.* **1997**, *241*, 142.

(133) Ueda, H. N., H.; Hori, Y.; Fujita, T.; Nishimura, M.; Goto, T.; Okuhara, M. *J. Antibiot.* **1994**, *47*, 301.

(134) Sakai, Y. T., T.; Akiyama, T.; Yoshida, T.; Mizukami, T.; Akinaga, S.; Horinouchi, S.; Yoshida, M.; Yoshida, T. *J. Antibiot.* **2002**, *55*, 863.

(135) Sakai, Y. Y., T.; Ochiai, K.; Uosaki, Y.; Saitoh, Y.; Tanaka, F.; Akiyama, T.; Akinaga, S.; Mizukami, T. *J. Antibiot.* **2002**, *55*, 855.

(136) Nakajima, H.; Hori, Y.; Terano, H.; Okuhara, M.; Manda, T.; Matsumoto, S.; Shimomura, K. *J. Antibiot.* **1996**, *49*, 1204.

(137) Nakajima, H.; Sato, B.; Fujita, T.; Takase, S.; Terano, H.; Okuhara, M. *J. Antibiot.* **1996**, *49*, 1196.

(138) Nakajima, H.; Takase, S.; Terano, H.; Tanaka, H. *J. Antibiot.* **1997**, *50*, 96.

(139) Johnstone, R. W. *Nat. Rev. Drug Discovery* **2002**, *1*, 287.

(140) Furumai, R.; Komatsu, Y.; Nishino, N.; Khochbin, S.; Yoshida, M.; Horinouchi, S. *Proc. Natl. Acad. Sci. U.S.A.* **2001**, *98*, 87.

(141) Vigushin, D. M.; Ali, S.; Pace, P. E.; Mirsaidi, N.; Ito, K.; Adcock, I.; Coombes, R. C. *Clin. Cancer Res.* **2001**, *7*, 971.

(142) Tazi, J.; Durand, S.; Jeanteur, P. *Trends Biochem. Sci.* **2005**, *30*, 469.

(143) Johnson, J. M.; Castle, J.; Garrett-Engele, P.; Kan, Z.; Loerch, P. M.; Armour, C. D.; Santos, R.; Schadt, E. E.; Stoughton, R.; Shoemaker, D. D. *Science* **2003**, *302*, 2141.

(144) Sakurai, M. K., J.; Nishio, M.; Yamamoto, K.; Okuda, T.; Kawano, K.; Nakanishi, N. *J. Antibiot.* **2001**, *54*, 628.

(145) Stille, J. K. *Angew. Chem., Int. Ed.* **1986**, *25*, 508.

(146) Miyaura, N. S., A. *Chem. Rev.* **1995**, *95*, 2457.

(147) Swain, C. J. B., R.; Kneen, C.; Moseley, J.; Saunders, J.; Seward, E. M.; Stevenson, G.; Beer, M.; Stanton, J.; Watling, K. *J. Med. Chem.* **1991**, *34*, 140.

(148) Lane, C. F. K., G. W. *Tetrahedron* **1976**, *32*, 981.

(149) Hilt, G. H., W.; Harms, K. *Org. lett.* **2006**, *8*, 3287.

(150) Ferreira, E. M. S., B. M. *Tetrahedron Lett.* **2006**, *47*, 8579.

(151) Aksela, R. O., A. C. *Tetrahedron* **1991**, *47*, 1163.

(152) Barbero, A. P., F. J. *Chem. Soc. Rev.* **2005**, *34*, 913.

(153) Mudry, C. A. F., A. R. *Tetrahedron* **1973**, *29*, 603.

(154) Nkunya, M. H. H. M., J. J.; Jonker, S. A.; *Nat. Prod. Res.* **2004**, *18*, 253.

(155) Heck, R. F. N., J. P. *J. Org. Chem.* **1972**, *37*, 2320.

(156) Eferl, R. W., E. F. *Nat. Rev. Cancer* **2003**, *3*, 859.